plants

Special Issue Reprint

New Insights into Plant Signaling Mechanisms in Biotic and Abiotic Stress

Edited by
Hamdy Kashtoh, Kwang-Hyun Baek and Muhammad Fazle Rabbee

mdpi.com/journal/plants

MDPI

New Insights into Plant Signaling Mechanisms in Biotic and Abiotic Stress

New Insights into Plant Signaling Mechanisms in Biotic and Abiotic Stress

Guest Editors

Hamdy Kashtoh
Kwang-Hyun Baek
Muhammad Fazle Rabbee

MDPI

Basel • Beijing • Wuhan • Barcelona • Belgrade • Novi Sad • Cluj • Manchester

Guest Editors

Hamdy Kashtoh
Department of Biotechnology
Yeungnam University
Gyeongsan
Republic of Korea

Kwang-Hyun Baek
Department of Biotechnology
Yeungnam University
Gyeongsan
Republic of Korea

Muhammad Fazle Rabbee
Department of Biotechnology
Yeungnam University
Gyeongsan
Republic of Korea

Editorial Office
MDPI AG
Grosspeteranlage 5
4052 Basel, Switzerland

This is a reprint of the Special Issue, published open access by the journal *Plants* (ISSN 2223-7747), freely accessible at: https://www.mdpi.com/journal/plants/special_issues/1CVE8G8180.

For citation purposes, cite each article independently as indicated on the article page online and as indicated below:

Lastname, A.A.; Lastname, B.B. Article Title. *Journal Name* **Year**, *Volume Number*, Page Range.

ISBN 978-3-7258-5813-2 (Hbk)
ISBN 978-3-7258-5814-9 (PDF)
https://doi.org/10.3390/books978-3-7258-5814-9

Contents

About the Editors

Hamdy Kashtoh

Hamdy Kashtoh serves as an international Research Professor in the Department of Biotechnology, at Yeungnam University, Republic of Korea. He obtained his Master's degree in Biomolecular Sciences, Institute of Molecular Cell Biology, Vrije Universiteit of Amsterdam, The Netherlands. He obtained his PhD in Biochemistry at King Abdulaziz University, Jeddah, Kingdom of Saudi Arabia, and he worked as a postdoctoral fellow at the Institute of Genetics and Developmental Biology, Chinese Academy of Sciences, Beijing, Republic of China. Dr. Hamdy Kashtoh's research focuses on the molecular mechanism of regulation of plant ion channels, abiotic stress, plant extracts, and bioactive compounds for different therapeutic strategies. He is also a member of several academic societies, an international reviewer, and an editorial board member. He has been awarded various research prizes, excellence awards, special honors, and medals from international organizations.

Kwang-Hyun Baek

Kwang-Hyun Baek serves as a Full Professor in the Department of Biotechnology at Yeungnam University, Republic of Korea. He obtained a Ph.D. in Crop and Soil Sciences at Washington State University, Pullman, WA, U.S.A., and he has worked as an Assistant, Associate, and full professor at Yeungnam University. Professor Kwang-Hyun Baek's research focuses on the development of nanocomposites for antibiotics, secondary metabolites, and plant extracts, and elucidation of natural compounds for natural antibiotics. He has served as an editorial board member for top-ranked International journals in MDPI, *Plant Pathology Journal*, and *Applied Biological Chemistry*, and as a committee member for the Korea Research Funding Allocation.

Muhammad Fazle Rabbee

Muhammad Fazle Rabbee serves as an international Research Professor in the Department of Biotechnology at Yeungnam University, Republic of Korea, where he also obtained his PhD. Dr. Muhammad Fazle Rabbee's research focuses on endophytes, bioactive compounds from endophytes, antibacterial resistance, plant–pathogen interaction, and plant defense against pathogens.

plants

MDPI

Editorial

New Insights into Plant Signaling Mechanisms in Biotic and Abiotic Stress

Hamdy Kashtoh, Muhammad Fazle Rabbee and Kwang-Hyun Baek *

Department of Biotechnology, Yeungnam University, Gyeongsan 38541, Republic of Korea; hamdy_kashtoh@ynu.ac.kr (H.K.); rabbi_biotech@ynu.ac.kr (M.F.R.)
* Correspondence: khbaek@ynu.ac.kr; Tel.: +82-53-810-3029

Plants are constantly challenged by their environments, including both biotic and abiotic stress factors. As a result, plants have developed complex signaling pathways in response to various challenges, allowing them to adapt and survive [1]. To detect and react to pathogen attacks, herbivore feeding, and symbiotic interactions in the case of biotic stress, plants use a complex network of signaling molecules, including phytohormones, reactive oxygen species (ROS), and secondary metabolites [2,3]. These signaling cascades cause the activation of systemic acquired resistance, the synthesis of antimicrobial chemicals, the reinforcement of physical barriers, and genes involved in defense. When plants are exposed to abiotic stress, such as extreme temperatures, drought, salinity, and nutrient deficiencies, they use different signaling pathways to adapt [4,5]. Abscisic acid, ethylene, jasmonic acid, calcium ions (Ca^{2+}), and other signaling molecules are involved in these pathways [6]. These signaling molecules coordinate cellular responses such as stomatal closure, osmotic correction, and the activation of stress-responsive genes. Understanding the mechanisms of plant signaling networks involved in biotic and abiotic stress responses is essential for developing crop plants that are resilient to changing environmental conditions [7]. This Special Issue aims to present recent contributions to developing our understanding of the mechanisms involved in plant responses to biotic and abiotic stress. It features ten papers, comprising four reviews and six research studies that address the aforementioned aspects.

In this Special Issue, four articles discussed the tolerance mechanisms that plants exert to adapt to stress and highlighted their stress signaling networks. One study summarized the challenges faced by rice (*Oryza sativa* L.) due to global climate change, which induces various abiotic stresses that detrimentally affect rice grain quality and yield. The study highlighted the defensive strategies rice plants employ to deal with abiotic stressors, particularly drought, salinity, submergence, extreme temperatures, and heavy metal toxicity, which significantly influence key morphological, chemical, and metabolic processes. Furthermore, it also outlined approaches for developing rice cultivars that can endure multiple abiotic stresses [8]. Another article addressed the issue of microbial pathogens that impede the growth of plants and their productivity. It described how plants identify pathogens, effectors, and microbe-associated molecular patterns (PAMPs or MAMPs) as imminent danger signals and initiate various immune responses like effector-triggered immunity (ETI) and PAMP-triggered immunity (PTI) [9]. Additionally, it also discussed the roles of autophagy, RNA silencing, and systemic acquired immunity as dynamic host-mediated defensive responses against pathogens. Moreover, it underlined the initial biochemical signaling processes, including ROS, Ca^{2+}, and hormones, that activate various plant immune response mechanisms.

Two manuscripts provided a comprehensive analysis of stress signaling molecules and their role in plant stress adaptation. One of them elaborated on the importance of the

role of plant heterotrimeric G protein signaling in maintaining a balance between normal growth and stress adaptation. It illustrated the signaling pathways by which heterotrimeric G proteins assist plants in regulating growth, while also adapting to immune challenges and thermomorphogenesis [10]. The second article discussed another signaling molecule that has a pivotal role in stress signaling networks, the plant-specific protein kinase, sucrose non-fermenting-1-related protein kinase 2 (SnRK2). This kinase plays a crucial part in helping plants adapt to stress by phosphorylating downstream targets, which in turn influences gene expression and physiological responses [11]. This article explored the substrates that SnRK2 phosphorylates in *Arabidopsis thaliana*, providing a comprehensive understanding of their roles in stress signaling and developmental processes. Furthermore, it described various post-translational modifications (PTMs) that SnRK2 undergoes, which collectively fine-tune its stability, activity, and intracellular dynamics, demonstrating an intricate feedback system that manages the activation and attenuation of the kinase.

Six manuscripts covered a variety of topics, including plants' responses to salt, alkaline, high-temperature stress, and pathogen infection, using different analytical tools such as genomics, transcriptomics, proteomics, and metabolomics approaches to understand such responses. One interesting article discussed the modulating roles of MYC2 and BBX21 transcriptional factors (TFs) in the flavonoid network in plants [12]. The study suggested that MYC2 has a dual role (activator/repressor) in regulating the anthocyanin pathway, depending on the cellular environment. Additionally, there is a possibility that BBX21 plays a similar role in the regulation of the *BAN* gene within the proanthocyanidin pathway in both *O. sativa* and *Arabidopsis thaliana*. Another article investigated the way in which wheat plants manage root exudation in response to alkali stress, employing a metabolomics method to detect and quantify root exudates generated in these circumstances. The research concentrated on transcriptional and metabolic processes, particularly alkali stress-induced secreted metabolites (AISMs) [13]. The findings suggested that when wheat plants are under alkali stress, the release of multiple metabolites containing a –COOH group plays a vital role in pH regulation. In response to alkali stress, wheat plants increase the synthesis of fatty acids, glycolysis, and phenolic acid production, which will supply additional energy and substrates for root exudation. Similarly, another study conducted on celery (*Apium graveliens* L.) investigated the synergistic effects of aspartic acid (Asp) and silicon (Si) in mitigating salt stress. The study showed that salt toxicity, which is identified via an altered nutritious status, hindered photosynthetic ability, reduced plant growth, and disrupted internal ion balance, and that an activated antioxidant defense system (indicated by higher levels of antioxidant enzymes and lower ROS accumulation) was ameliorated through the use of Si, Asp, or a combination of both [14]. Importantly, the combined application of Si and Asp was found to be more effective in minimizing salt stress compared to applying either of them individually. In summary, the exogenous application of Si and Asp aided in alleviating salt stress and enhanced the salt tolerance of celery.

Another interesting article described how a plant systemically responds to stress or stimulus by means of variation potential (VP). The study focused on the mechanisms that influence the specificity of VP in response to different local stimuli, including heating, burning, and wounding, which all result in distinct VP parameters [15]. It suggested that the varying functions of hydraulic and chemical signals determine the distinct characteristics of these VP parameters. The phenomenon by which VP triggers systemic responses is likely linked to variations in the concentration of ions, such as Ca^{2+} and H^{+}, that occur during the generation of VP. Overall, these findings indicated that the specificity of VP in response to stimuli stems from the unique properties of the chemical and hydraulic signals that create it, which may additionally impact variations in ion concentrations.

To study plant–pathogen interactions and their effects on plant growth, Li et al. investigated how *GhSTR1*, a member of the ABCG subfamily of ATP-binding cassette (ABC) transporters, mediates the defense mechanisms of cotton (*Gossypium hirsutum*) plants against various pathogens [16]. The study suggested that *GhSTR1* plays a role in cotton's defense against Verticillium wilt and Fusarium wilt, which are caused by the fungal pathogens *Verticillium dahliae* and *Fusarium oxysporum.* These fungi infect the plant's vascular system, resulting in wilting, yellowing, and often plant death. The study also suggested that *GhSTR1* mediates the plant's vegetative and reproductive development, seemingly balancing the trade-off between defending against pathogens and promoting plant growth.

Expression analysis is a powerful tool for deciphering the regulatory mechanisms of different genes during plants' environmental stress responses. In this Special Issue, one study examined the *PIN* gene family, auxin efflux transporter proteins, and identified nine members of the *CsPIN* gene family in the cucumber (*Cucumis sativus* L.) genome [17]. Furthermore, it investigated the expression levels of *CsPIN* genes in both leaves and roots when subjected to different abiotic stresses and hormone treatments. Different *CsPIN* genes showed varied response patterns to abiotic stresses like NaCl, high temperature, and PEG, as well as to different hormone signals, aiding in the regulation of auxin balance and facilitating plant adaptation to environmental changes.

In summary, this Special Issue features a series of research studies that deepen our knowledge of the fundamental mechanisms underlying plant responses to different stresses. Gaining insight into these defense mechanisms contributes to the development of effective strategies aimed at boosting plant resilience and productivity in harsh conditions.

Author Contributions: Conceptualization, H.K.; Writing—original draft preparation, H.K.; Writing—review and editing, H.K., M.F.R., and K.-H.B.; Funding acquisition, K.-H.B. All authors have read and agreed to the published version of the manuscript.

Funding: This research was carried out with the support of the funding (RS-2025-02223124) of the Cooperative Research Program for Agriculture Science and Technology Development, RDA, Republic of Korea.

Acknowledgments: As Guest Editors of the Special Issue "New Insights into Plant Signaling Mechanisms in Biotic and Abiotic Stress," we extend our sincere gratitude to all the authors whose valuable publications have contributed to the success of this Special Issue edition.

Conflicts of Interest: The authors declare no conflicts of interest.

References

1. Suzuki, N.; Rivero, R.M.; Shulaev, V.; Blumwald, E.; Mittler, R. Abiotic and biotic stress combinations. *New Phytol.* **2014**, *203*, 32–43. [CrossRef] [PubMed]
2. Rejeb, I.; Pastor, V.; Mauch-Mani, B. Plant Responses to Simultaneous Biotic and Abiotic Stress: Molecular Mechanisms. *Plants* **2014**, *3*, 458–475. [CrossRef] [PubMed]
3. Demidchik, V. Mechanisms of oxidative stress in plants: From classical chemistry to cell biology. *Environ. Exp. Bot.* **2015**, *109*, 212–228. [CrossRef]
4. Kashtoh, H.; Baek, K.-H. Structural and Functional Insights into the Role of Guard Cell Ion Channels in Abiotic Stress-Induced Stomatal Closure. *Plants* **2021**, *10*, 2774. [CrossRef] [PubMed]
5. Deng, Y.; Kashtoh, H.; Wang, Q.; Zhen, G.; Li, Q.; Tang, L.; Gao, H.; Zhang, C.; Qin, L.; Su, M. Structure and activity of SLAC1 channels for stomatal signaling in leaves. *Proc. Natl. Acad. Sci. USA* **2021**, *118*, e2015151118. [CrossRef] [PubMed]
6. Zhang, H.; Zhu, J.; Gong, Z.; Zhu, J.-K. Abiotic stress responses in plants. *Nat. Rev. Genet.* **2022**, *23*, 104–119. [CrossRef] [PubMed]
7. Cramer, G.R.; Urano, K.; Delrot, S.; Pezzotti, M.; Shinozaki, K. Effects of abiotic stress on plants: A systems biology perspective. *BMC Plant Biol.* **2011**, *11*, 163. [CrossRef] [PubMed]
8. Sarma, B.; Kashtoh, H.; Lama Tamang, T.; Bhattacharyya, P.N.; Mohanta, Y.K.; Baek, K.H. Abiotic Stress in Rice: Visiting the Physiological Response and Its Tolerance Mechanisms. *Plants* **2023**, *12*, 3948. [CrossRef] [PubMed]

9. Ali, S.; Tyagi, A.; Mir, Z.A. Plant Immunity: At the Crossroads of Pathogen Perception and Defense Response. *Plants* **2024**, *13*, 1434. [CrossRef] [PubMed]
10. Lee, H. Trade-Off Regulation in Plant Growth and Stress Responses Through the Role of Heterotrimeric G Protein Signaling. *Plants* **2024**, *13*, 3239. [CrossRef] [PubMed]
11. Wei, Y.; Peng, L.; Zhou, X. SnRK2s: Kinases or Substrates? *Plants* **2025**, *14*, 1171. [CrossRef] [PubMed]
12. Li, N.; Xu, Y.; Lu, Y. A Regulatory Mechanism on Pathways: Modulating Roles of MYC2 and BBX21 in the Flavonoid Network. *Plants* **2024**, *13*, 1156. [CrossRef] [PubMed]
13. Wang, H.; Zhao, S.; Qi, Z.; Yang, C.; Ding, D.; Xiao, B.; Wang, S.; Yang, C. Regulation of Root Exudation in Wheat Plants in Response to Alkali Stress. *Plants* **2024**, *13*, 1227. [CrossRef] [PubMed]
14. Song, J.; Yang, J.; Jeong, B.R. Synergistic Effects of Silicon and Aspartic Acid on the Alleviation of Salt Stress in Celery (*Apium graveliens* L.) "Si Ji Xiao Xiang Qin". *Plants* **2024**, *13*, 2072. [CrossRef] [PubMed]
15. Mudrilov, M.; Ladeynova, M.; Vetrova, Y.; Vodeneev, V. Analysis of the Mechanisms Underlying the Specificity of the Variation Potential Induced by Different Stimuli. *Plants* **2024**, *13*, 2896. [CrossRef] [PubMed]
16. Cheng, G.; Li, X.; Fernando, W.G.D.; Bibi, S.; Liang, C.; Bi, Y.; Liu, X.; Li, Y. Fatty Acid ABCG Transporter GhSTR1 Mediates Resistance to Verticillium dahliae and Fusarium oxysporum in Cotton. *Plants* **2025**, *14*, 465. [CrossRef] [PubMed]
17. Zhang, Y.; Zhu, K.; Shen, W.; Cui, J.; Miao, C.; Lu, P.; Wu, S.; Zhu, C.; Jin, H.; Zhang, H.; et al. The PIN Gene Family in Cucumber (*Cucumis sativus* L.): Genome-Wide Identification and Gene Expression Analysis in Phytohormone and Abiotic Stress Response. *Plants* **2025**, *14*, 1566. [CrossRef] [PubMed]

plants

MDPI

Article

The *PIN* Gene Family in Cucumber (*Cucumis sativus* L.): Genome-Wide Identification and Gene Expression Analysis in Phytohormone and Abiotic Stress Response

Yongxue Zhang [1,†], Kaili Zhu [1,2,†], Weiyao Shen [1,3], Jiawei Cui [1], Chen Miao [1], Panling Lu [1], Shaofang Wu [1], Cuifang Zhu [1], Haijun Jin [1], Hongmei Zhang [1], Liying Chang [4] and Xiaotao Ding [1,*]

[1] Shanghai Key Laboratory of Protected Horticulture Technology, Horticultural Research Institute, Shanghai Academy of Agricultural Science, Shanghai 201403, China; zhangyongxue@saas.sh.cn (Y.Z.); z18253926832@163.com (K.Z.); 19542816801@163.com (W.S.); cuijiawei@saas.sh.cn (J.C.); miaochen@saas.sh.cn (C.M.); lpl2245@163.com (P.L.); sfwu@saas.sh.cn (S.W.); zhucuifang1996@163.com (C.Z.); jinhaijun@saas.sh.cn (H.J.); zhanghongmei@saas.sh.cn (H.Z.)
[2] College of Ecological Technology and Engineering, Shanghai Institute of Technology, Shanghai 201418, China
[3] College of Life Sciences, Shanghai Normal University, Shanghai 200234, China
[4] School of Agriculture and Biology, Shanghai Jiao Tong University, Shanghai 200240, China; changly@sjtu.edu.cn
* Correspondence: dingxiaotao@saas.sh.cn
† These authors contributed equally to this work.

Abstract: The auxin efflux transporter PIN protein plays a crucial role in the asymmetric distribution of auxin on the plasma membrane, influencing the growth and development of plant organs. In this study, we identified nine members of the *PIN* gene family in the cucumber genome, which could be classified into five phylogenetic groups. These genes have diverse structures but conserved transmembrane domains. Analysis of cis-acting elements in the promoters revealed that *CsPINs* contain 48 types of cis-acting elements, predominantly light-responsive elements and plant hormone response elements. In addition, PIN proteins may interact with a variety of auxin-related proteins (including auxin response factor, auxin binding protein, mitogen-activated protein kinase PINOID, etc.) to jointly regulate the auxin synthesis and metabolic pathways. We analyzed the expression profiles of *PIN* genes in 23 tissues of cucumber using the CuGenDB database, and further investigated the expression levels of *PIN* genes in leaves and roots in response to different abiotic stresses and hormone treatments by qRT-PCR. This study provides a theoretical basis for clarifying the regulatory mechanism of the cucumber *PIN* gene family during environmental stress processes.

Keywords: PIN; auxin; cucumber; hormone; abiotic stress

1. Introduction

Auxin, as a small signaling molecule in plants, mainly exists in the form of indole-3-acetic acid (IAA). Auxin is widely distributed in various plant tissues and organs and participates in multiple biological functions, such as establishing the apical–basal polarity during embryogenesis, forming apical and axillary meristems, promoting fruit ripening, shaping root system architecture, and influencing plant tropisms [1,2]. Auxin is mainly synthesized in the apical meristem, rapidly generating a concentration gradient and is transported to different organs through polar auxin transport mechanisms [3]. The polar transport of auxin between plant cells is mainly mediated by three transporter families,

including the auxin resistance 1/auxin-like 1 (AUX/LAX), the ATP-binding cassette B/P-glycoprotein (ABCB), and the PIN-forming (PIN) influx carrier [4]. Members of these gene families control the influx and efflux of auxin, forming a complex auxin regulatory network that regulates growth and development and responses to environmental stimuli [5–7].

With the advancement of next-generation sequencing technology [8], PIN family members have been identified in multiple plant species. Specifically, 8, 10, 10, 11, 11, 11, 12, 14, 15, 17, 20, and 23 *PIN* family members have been identified in the genomes of *Arabidopsis* [9], pepper (*Capsicum annuum*) [10], potato (*Solanum tuberosum*) [11], maize (*Zea mays* L.) [12], *Medicago truncatula* [13], *Sorghum bicolor* [14], grapes (*Vitis vinifera*) [15], pear (*Pyrus bretschneideri*) [16], poplar (*Populus trichocarpa*) [17], cotton (*Gossypium hirsutum*) [18], tobacco (*Nicotiana tabacum*) [19], and soybeans (*Glycine max*) [20], respectively.

To date, the gene functions of several members of the *PIN* family have been characterized in specific crop species. Plasma membrane (PM)-localized AtPIN1-4/7 mediate directional auxin transport through long central hydrophilic loops [21,22], whereas endoplasmic reticulum (ER)-localized AtPIN5/8 regulate intracellular homeostasis via short loops [23–25]. AtPIN6 uniquely dual-localizes to PM/ER, indicating that it may be involved in both intercellular auxin transport and homeostasis regulation [26,27]. Key *Arabidopsis* PIN proteins orchestrate developmental processes through specialized functions: AtPIN1/8 regulate floral development via embryonic auxin gradients (AtPIN1) and pollen-specific gametogenesis (AtPIN8) [23,28–30]. AtPIN2-5 mediate root architecture, with AtPIN2 governing meristem elongation, AtPIN3/4 coordinating apical hook formation, and AtPIN5 driving lateral root initiation [6,25,30–32]. AtPIN6 uniquely modulates multi-tissue development, including apical dominance and nectar formation [26,33,34]. AtPIN7 establishes embryonic polarity through basal PM-localized auxin maxima [35]. These regulators establish auxin distribution patterns critical for organogenesis. OsPIN1a/b regulate root system development, with overexpression enhancing lateral root formation [36]. OsPIN2 modulates shoot-to-root auxin redistribution [37], while OsPIN9/10s potentially drive adventitious root initiation [38]. ZmPIN1a/b mediate auxin transport during maize embryogenesis and endosperm development, with ZmPIN1a exhibiting sustained upregulation throughout stem maturation [39,40]. In addition, under drought, salt, and cold stress, most *ZmPIN* genes are induced to express in the stems of maize, while their expression is inhibited in the roots [41].

Cucumber (*Cucumis sativus* L.) is one of the most economically important vegetable crops worldwide. However, genome-wide information on *CsPIN* family members has not been reported. Auxin polar transport forms concentration gradients and local differences through the synergistic effect of synthetic and metabolic pathways, thereby achieving precise regulation of plant growth and development, tropism, and responses to endogenous and exogenous signals. In this study, we identified nine *CsPIN* genes and classified them into five groups. Furthermore, the physicochemical properties, phylogenetic relationship, chromosome localization, collinearity analysis, gene structure, cis-acting elements, and protein interaction prediction were comprehensively analyzed. The transcriptional levels of *CsPIN* genes in various tissues/organs and under abiotic stress conditions were analyzed through gene expression profiling and qRT-PCR. The results of this study will provide a theoretical basis for analyzing the function of the *PIN* gene in cucumbers and lay the foundation for the breeding of new high-quality cucumber varieties.

2. Results

2.1. Genome-Wide Identification and Phylogenetic Analysis of PIN Proteins in Cucumber

Using eight PIN protein sequences of *Arabidopsis* as the queries, a local Blastp (E-value 1×10^{-5}) search was performed in the cucumber genome, and 68 protein sequences were

obtained initially. A total of 15 candidate genes were identified according to conserved domain (PF03547). After the combined sequences were duplicated, 73 candidate genes remained. Then, SMART and CDD databases were used to predict the domains of candidate genes, and nine *CsPIN* genes were eventually identified. Moreover, gene locus, chromosome location, open reading frame length, and physical and chemical properties of *PIN* gene family members were analyzed, as shown in Table 1. The gene members have a length of 356 to 645 amino acids (aa), molecular weights ranging from 38.98 to 70.83 kDa, and a theoretical isoelectric point (pI) in the range of 7.04 to 9.59. Aliphatic index and hydrophilicity predicted that CsPIN is a mostly hydrophobic protein. CsPINs are multiple transmembrane proteins, which are mainly predicted to be located in PM and ER.

Table 1. Characteristics of the putative PIN-FORMED (PIN) proteins in cucumber.

Gene Name	Gene Locus	Chromosome Location	ORF Length (bp)	No. of AA	MW (kDa)	pI	Aliphatic Index	GRAVY	TMHs	Subcellular Localization #
CsPIN1	CsaV3_1G007160.1	chr1:4542181–4546111(−)	1857	618	67.44	9.13	89.61	0.077	9	PM
CsPIN1b	CsaV3_4G029470.1	chr4:19012575–19015651(+)	1791	596	63.70	8.77	96.71	0.264	9	ER
CsPIN1c	CsaV3_1G004350.1	chr1:2730713–2734038(−)	1827	608	66.63	9.09	90.90	0.098	8	PM
CsPIN1d	CsaV3_2G009700.1	chr2:6188991–6193716(+)	1191	396	43.04	7.57	112.75	0.494	5	ER
CsPIN2	CsaV3_1G032010.1	chr1:19030115–19033521(+)	1938	645	70.83	9.29	85.46	0.017	9	PM
CsPIN3	CsaV3_5G028620.1	chr5:23739663–23744519(−)	1911	636	69.46	7.12	91.42	0.111	9	PM
CsPIN5	CsaV3_2G009610.1	chr2:6112103–6116586(+)	1116	371	40.37	7.04	112.24	0.675	9	ER
CsPIN7	CsaV3_5G013380.1	chr5:9982996–9987398(−)	1890	629	68.48	8.50	92.62	0.137	9	PM
CsPIN8	CsaV3_3G041710.1	chr3:34023847–34026847(+)	1071	356	38.98	9.59	129.61	0.692	8	ER

(+): forward strand; (−): reverse strand; bp: base pair; AA: amino acid; MW: molecular weight, kDa: kilodalton; pI: isoelectric point; GRAVY: grand average of hydropathicity; TMHs: transmembrane helices; #: based on the prediction of the LocTree3 website; PM: plasma membrane; ER: endoplasmic reticulum membrane.

2.2. Phylogenetic Relationship Analysis of Cucumber PINs

To further understand the phylogenetic relationship between the *CsPIN* gene family of cucumber and *PIN* genes of other species, we constructed a phylogenetic tree using PIN protein sequences of *Arabidopsis* (8), wheat (44), soybean (23), rice (12), and cucumber (Figure 1). They were divided into five subgroups based on sequence similarity and labeled with different colors. Group II contained one *CsPIN5* gene. The third group contains two genes, *CsPIN1d* and *CsPIN2*. Groups IV and V each contained three cucumber PIN family members (*CsPIN1/1b/1c* and *CsPIN3/7/8*). The aggregation of PIN protein sequences into five groups indicates that they have similar functional or subfunctional roles in species-dependent development. In group IV, cucumber *PIN* genes were clustered with *Arabidopsis* homologs (e.g., PIN3, PIN7, PIN8). In Arabidopsis, PIN3 has been shown to regulate hypocotyl gravitropism by redistributing auxin in root columella cells [42], while PIN7 mediates light-induced phototropism through asymmetric auxin transport in hypocotyls [43]. Additionally, *pin8* exhibits impaired root gravitropic bending and shoot phototropic responses [44]. These results suggest that PIN family proteins are evolutionarily conserved and play a key role in mediating auxin-dependent tropism responses.

2.3. Chromosomal Distribution of Cucumber PIN Genes

Chromosome density information was obtained from the genome using the TBtools v 2.119 software, and the positions of the *CsPIN* genes on the chromosomes were located (Figure 2A). The results indicated that nine *CsPIN* genes were unevenly distributed on five chromosomes (Chr1 to Chr5). The chromosome with the highest gene distribution was Chr1 (three genes), followed by Chr2 and Chr5 (two genes each). *CsPIN1d* and *CsPIN5* on Chr2 formed a cluster. Each of Chr3 and Chr4 had one gene.

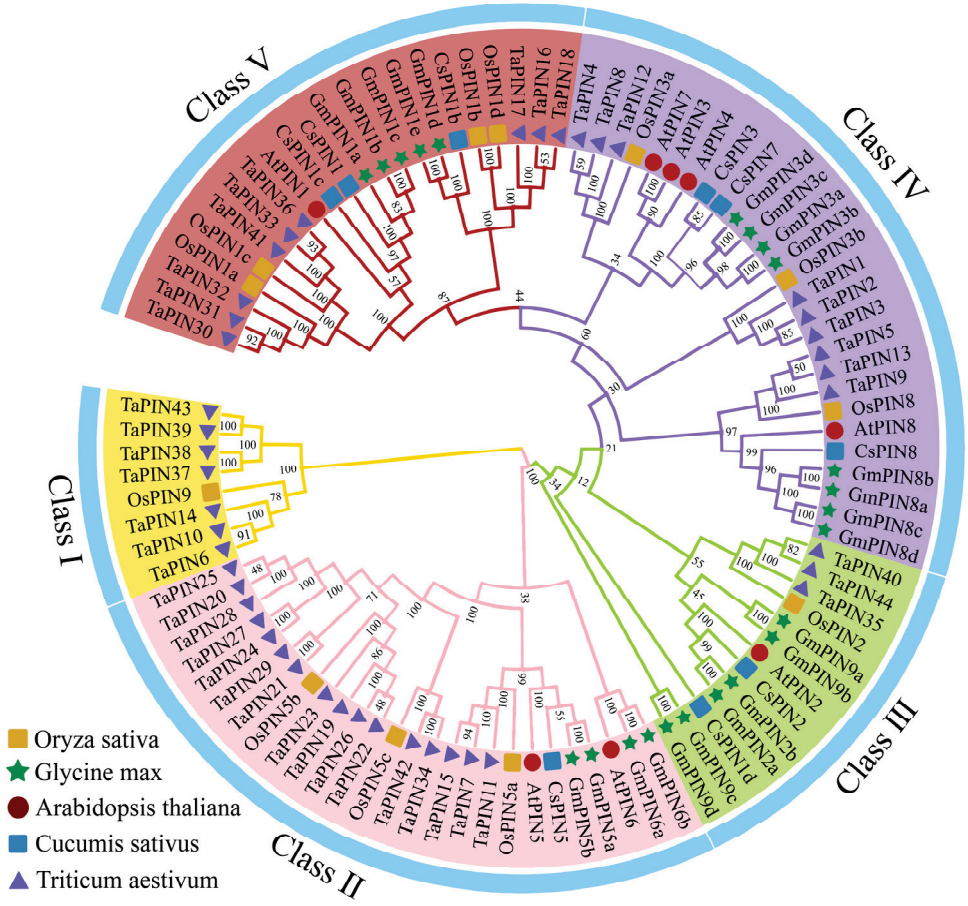

Figure 1. The phylogenetic tree of the PIN proteins from five species. The subgroups were designated through comparative analysis with *O. sativa* (12, yellow squares), *G. max* (23, green stars), *Arabidopsis* (8, red circles), and *T. aestivum* (44, purple triangles).

To further investigate the potential evolutionary relationship of the *CsPIN* genes in cucumber, collinearity analysis was conducted between cucumber and *Arabidopsis*, *G. max*, *Cucumis melo*, and tomato (*Solanum lycopersicum*) (Figure 2B). The results demonstrated that most *CsPIN* genes had at least three pairs of homologous genes in the genomes of other plants. Specifically, *CsPIN1* exhibited the highest number of homologous pairs (seven pairs), followed by *CsPIN1c* (six pairs), *CsPIN1b*, *CsPIN3*, and *CsPIN9* (five pairs each), *CsPIN7* (four pairs), *CsPIN2* and *CsPIN5* (three pairs each), and *CsPIN1d* (one pair). These results indicate that the *PIN* genes in cucumber share a common ancestor with those in other species.

2.4. The Conserved Domains and Gene Structure of Cucumber PIN Genes

We further analyzed the conserved domains, gene structure, and exon/intron structure patterns of *CsPINs* (Figure 3). The results revealed that the motif distribution patterns of CsPIN proteins within groups were similar (Figure 3A,B). There are six CsPIN members that contain ten motifs, including CsPIN1, CsPIN1b, CsPIN1c, CsPIN2, CsPIN3, and CsPIN7; CsPIN5 and CsPIN8 contain seven motifs, while CsPIN1d contains six motifs. All nine CsPIN members contain motifs 1, 2, 3, 4, 6, and 8. These results suggest that these motifs are relatively conserved, and some unique motifs may be related to specific functions of the genes.

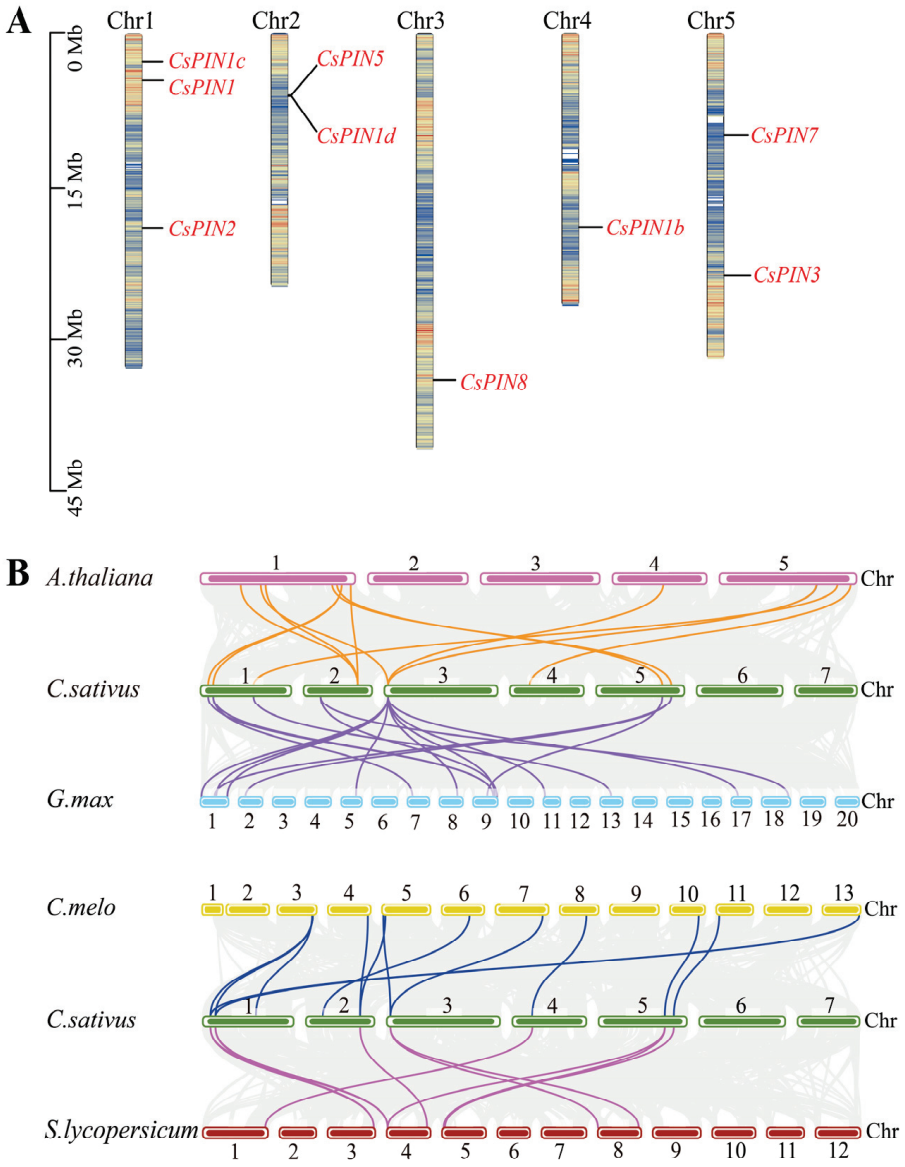

Figure 2. Chromosomal mapping and colinearity analysis of *CsPIN* genes. (**A**) Chromosomal localization. Mb: megabase. The different colors on the chromosome represent the gene density. (**B**) Collinearity analysis. Highlight lines: syntenic *PIN* gene pairs; Gray: collinear blocks.

The Mem_transfamily functional domain was found in the CsPIN family members (Figure 3C). On the other hand, most *CsPIN* genes with similar structures had a similar number of exons/introns but differed in arrangement and length (Figure 3D). For instance, *CsPIN1c* and *CsPIN2* have the largest number of exons, both containing seven exons; *CsPIN1*, *CsPIN1b*, *CsPIN3*, *CsPIN5*, and *CsPIN7* all contain six exons; *CsPIN8* contains five exons; *CsPIN1d* contains the fewest number of exons, with four exons. *CsPIN1d* only contains the upstream non-translated region, excluding the downstream non-translated region. The remaining eight *CsPIN* members all contain 5′ untranslated regions and 3′ untranslated regions. The results indicated that the *CsPIN* genes were relatively conserved during evolution, which ensured the integrity of their gene structure and resulted in minimal functional changes.

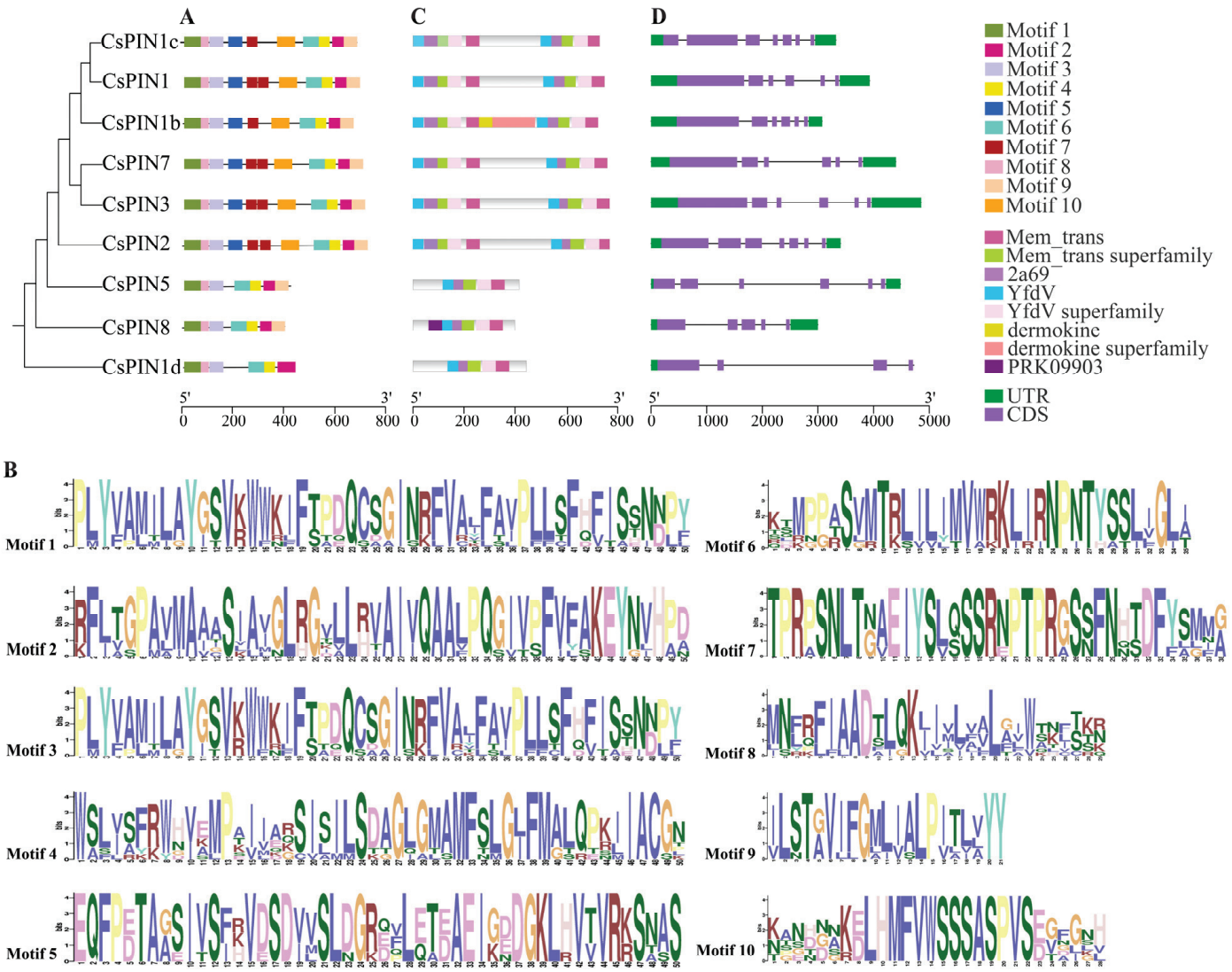

Figure 3. Conserved motifs (**A**,**B**), gene structure (**C**), and exon–intron structure (**D**) of *CsPINs*. Colored boxes of different lengths represent different conserved motifs, and letters in different colors mean the sequences of the conserved motifs.

2.5. Analysis of Cis-Acting Elements Prediction in CsPIN Promoters

The promoter sequence of the *CsPIN* genes located 2000 bp upstream of coding sequences was analyzed to predict their cis-acting elements (Figure 4A). The results showed that nine *CsPIN* members predicted a total of 48 CAREs, including light response (17), plant hormones (14) (including auxins, gibberellins, salicylic acid, abscisic acid, methyl jasmonate, ethylene), plant growth and development (10), low temperature (2), high temperature (2), drought (1), and anaerobic conditions (1). Among them, cis-acting elements such as light (G-box, GT1 motif, and TCT motif), plant hormones (ABRE, AAGAA motif, and TATC box), and plant growth and development (MYB and MYC) account for the largest proportion in *CsPINs*. *CsPIN7* contains the most light-responsive elements (17) and plant growth and development-related elements (19). *CsPIN1* contained the largest number of elements, with the largest number of plant hormone-related elements (Figure 4B,C). These results indicate that the *CsPIN* gene family is mainly regulated by light and plant hormones.

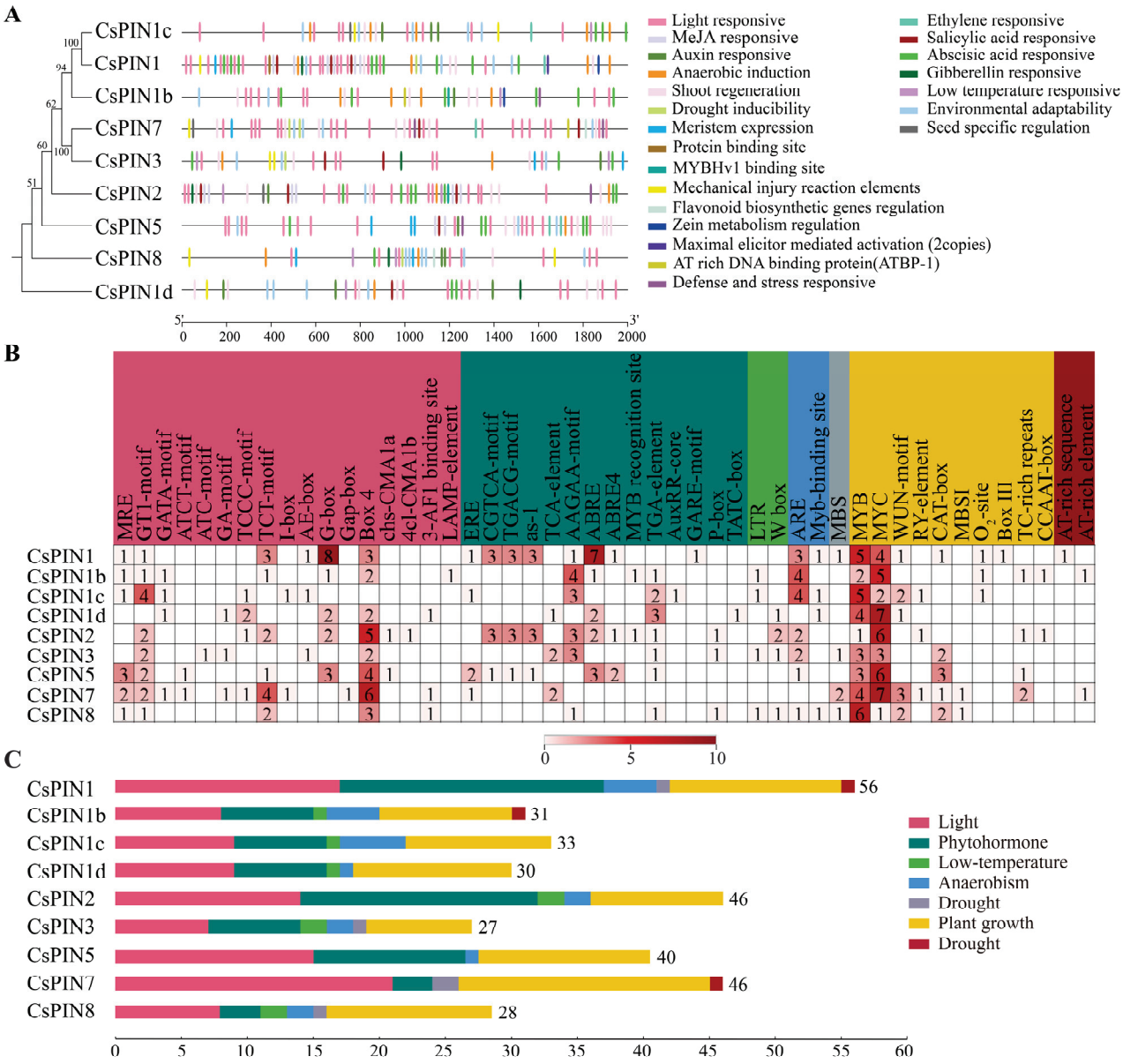

Figure 4. Analysis of cis-acting regulatory elements of the *CsPIN* genes. (**A**) The cis-acting elements distribution in the promoters of *CsPINs*. (**B**,**C**) The names and numbers of cis-acting elements in the promoters of each *CsPIN* gene.

2.6. Interaction Network of CsPIN Proteins

To predict the interaction between PIN and other proteins in cucumber, we constructed an interaction network using the STRING database (Figure 5). According to the prediction results, we identified eight CsPINs that interact with 34 distinct cucumber proteins. CsPIN may interact with multiple auxin-related proteins, including auxin response factor (ARF), auxin-binding protein (ABP), auxin-induced protein (AUX), serine/threonine protein kinase PINOID (PID), indole-3-pyruvate monooxygenase (YUC), etc. These transcription factors, growth hormone receptors, and auxin transporter proteins work together to participate in the expression of auxin genes, auxin biosynthesis, and transport, and are essential for the formation of tissues and organs such as flowers, stems, and roots.

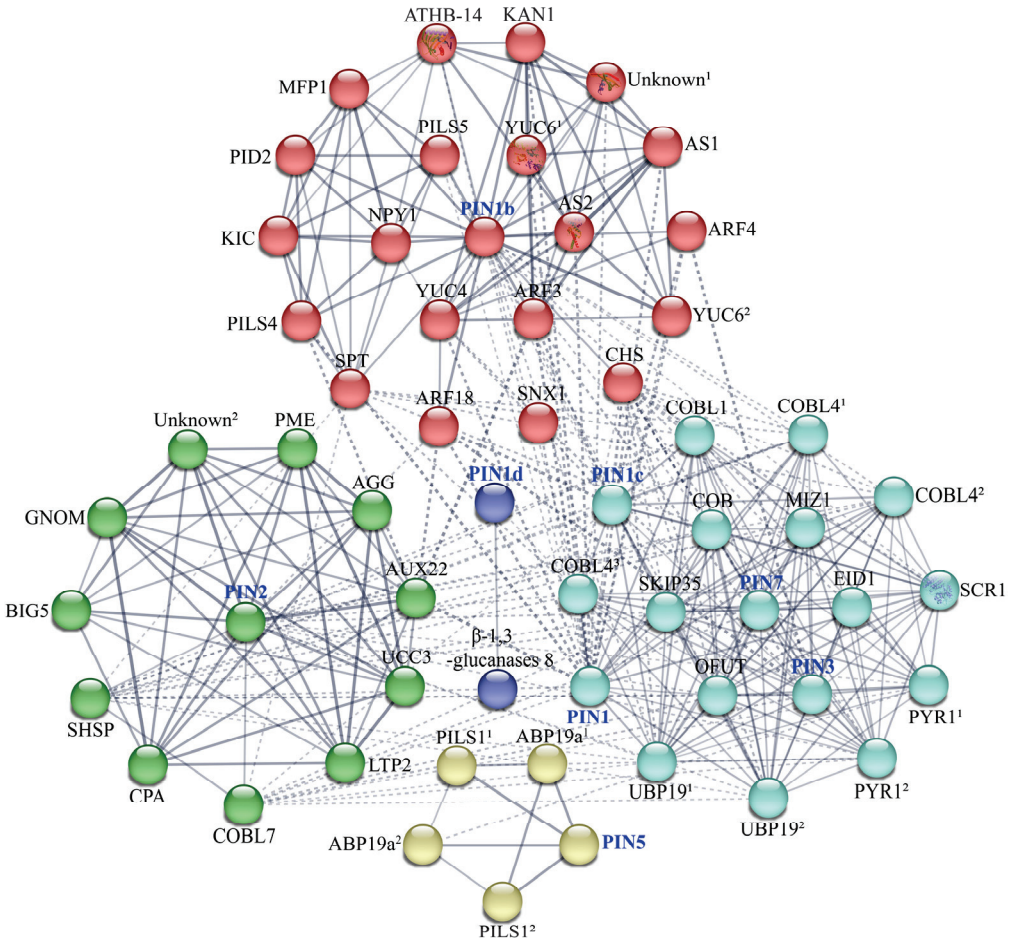

Figure 5. Protein–protein interaction analysis of CsPINs proteins. Abbreviations: ABP19a: auxin-binding protein ABP19a; AGG: agglutinin domain-containing protein; ARF: auxin response factor; AS1: transcription factor AS1; AS2: protein ASYMMETRIC LEAVES 2; ATHB-14: homeobox-leucine zipper protein ATHB-14; AUX22: auxin-induced protein AUX22-like; BIG5: brefeldin A-inhibited guanine nucleotide-exchange protein 5 isoform X1; β-1,3-glucanases 8: glucan endo-1,3-beta-glucosidase 8; CHS: chalcone synthase; COB: protein COBRA; COBL: COBRA-like protein; CPA: F-actin-capping protein subunit alpha; EID1: phytochrome A-associated F-box protein; GNOM: ARF guanine-nucleotide exchange factor GNOM; KAN1: transcription repressor KAN1 isoform X1; KIC: calcium-binding protein KIC; LTP2: non-specific lipid-transfer protein 2; MFP1: MFP1 attachment factor 1; MIZ1: protein MIZU-KUSSEI 1; NPY1: BTB/POZ domain-containing protein NPY1; OFUT: O-fucosyltransferase family protein; PILS: auxin transporter-like protein; PID2: protein kinase PINOID 2; PME: pectinesterase; PYR1: abscisic acid receptor PYR1; SCR1: protein SCARECROW 1; SHSP: SHSP domain-containing protein; SKIP35: ankyrin repeat protein SKIP35; SNX1: sorting nexin 1; SPT: sugar phosphate transporter domain-containing protein; UBP19: ubiquitin-specific protease family C19-related protein; UCC3: uclacyanin-3; Unknown: uncharacterized protein; YUC: indole-3-pyruvate monooxygenase YUCCA. Protein names marked with numbers were assigned based on BLAST alignments (NCBI) to identify entries with identical names but distinct gene IDs.

CsPIN1 and CsPIN1b may interact with transcription factor AS1 (AS1), protein ASYMMETRIC LEAVES 2 (AS2), and transcription repressor KAN1 (KAN1). AS1, a MYB-type transcriptional repressor, regulates leaf development by modulating KNOX gene expression [45]. AS2 is a negative regulator of cell proliferation in the adaxial side of leaves, regulating the formation of the symmetrical lamina and the establishment of venation patterns [46]. It has been reported that AS2 can directly interact with AS1, synergistic with RH10 or RID2 to inhibit the expression of abaxial genes such as ARF3, ARF4, KAN1, and KAN2, and promote adaxial development in leaf primordia at shoot apical meristem

under high temperatures, thereby participating in the establishment of leaf polarity [47,48]. Therefore, PIN proteins in cucumber may also regulate the development of narrow leaves by interacting with AS1, AS2, or KAN1.

2.7. Expression Profiles of CsPIN Genes in Different Tissues and Organs

To elucidate the role of *CsPIN* genes in cucumber growth and development, we obtained RNA sequencing data for *CsPIN* gene expression profiles across 23 distinct tissues from the CuGenDB database v2.0 (biological project PRJNA312872) available at the website (http://cucurbitgenomics.org). As shown in Figure 6, except for *CsPIN1d*, the other eight *CsPIN* genes were all up-regulated in roots, among which *CsPIN1* had the highest expression level in roots. Except for *CsPIN1b*, *CsPIN1d*, *CsPIN2,* and *CsPIN5*, the other five *CsPIN* genes were expressed in all 23 different tissues. *CsPIN1b* was not expressed in the male flowers and pericarp of 2-week-old fruits. *CsPIN1d* was specifically expressed in the stem, male flowers, female flowers, unpollinated ovaries, 2-week-old fruit flesh, and 3-week-old fruit flesh. *CsPIN2* was specifically expressed in the roots, male flowers, male flower buds, female flowers, hypocotyls, and roots of 4-week-old seedlings. *CsPIN5* was specifically expressed in the roots, old leaves, and roots of 4-week-old seedlings. *CsPIN7* was highly expressed in all 23 tissues. Except for *CsPIN1d* and *CsPIN5*, the expression levels of all *CsPIN* genes in young leaves were higher than those in old leaves, indicating that *CsPIN* plays an important role in the early growth and development of leaves. These results indicate that the expression of *CsPIN* genes shows obvious tissue specificity.

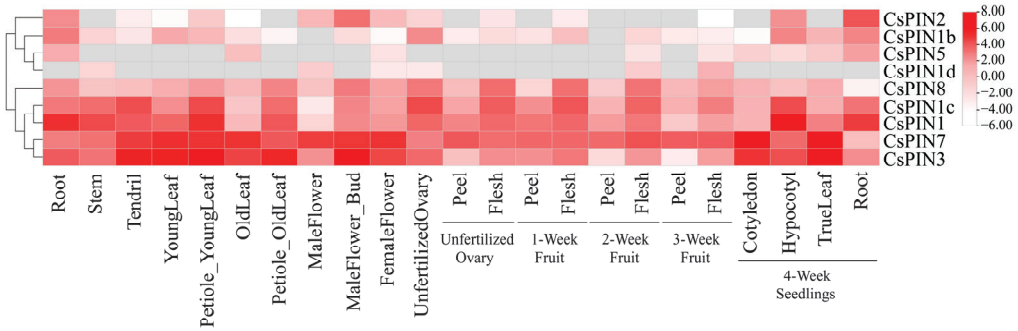

Figure 6. The expression profiles of *CsPIN* genes. The public transcriptome data of 23 cucumber tissues were downloaded, and the *CsPIN* genes heat map were drawn based on the FPKM values of log2.

2.8. Expression Analysis of CsPIN Genes Under Different Stress Conditions

To explore the expression patterns of *CsPIN* genes under abiotic stresses (NaCl, HT, and PEG) and hormone stresses (SA, IAA, and ABA), we conducted qRT-PCR analysis on cucumber leaves and roots. The results indicated that the expression patterns of *CsPIN* gene family members under different stress conditions were significantly different (Figure 7). Under NaCl treatment, *CsPIN1d* had the highest expression level in leaves, while *CsPIN1b*, *CsPIN1c*, *CsPIN5*, *CsPIN7,* and *CsPIN8* had relatively low expression levels in leaves. Under HT treatment, the expression levels of *CsPIN1*, *CsPIN2*, *CsPIN1b*, *CsPIN3,* and *CsPIN7* were increased in leaves. The expression of *CsPIN5* was suppressed in the roots under NaCl and HT. Under PEG stress treatment, the expression levels of *CsPIN1c*, *CsPIN2*, and *CsPIN5* in leaves were increased; *CsPIN1c*, *CsPIN1d*, and *CsPIN7* were significantly induced in the roots; whereas the the expression levels of *CsPIN1*, *CsPIN1b*, *CsPIN2*, *CsPIN3*, and *CsPIN8* in roots were not significant, with similar patterns of change.

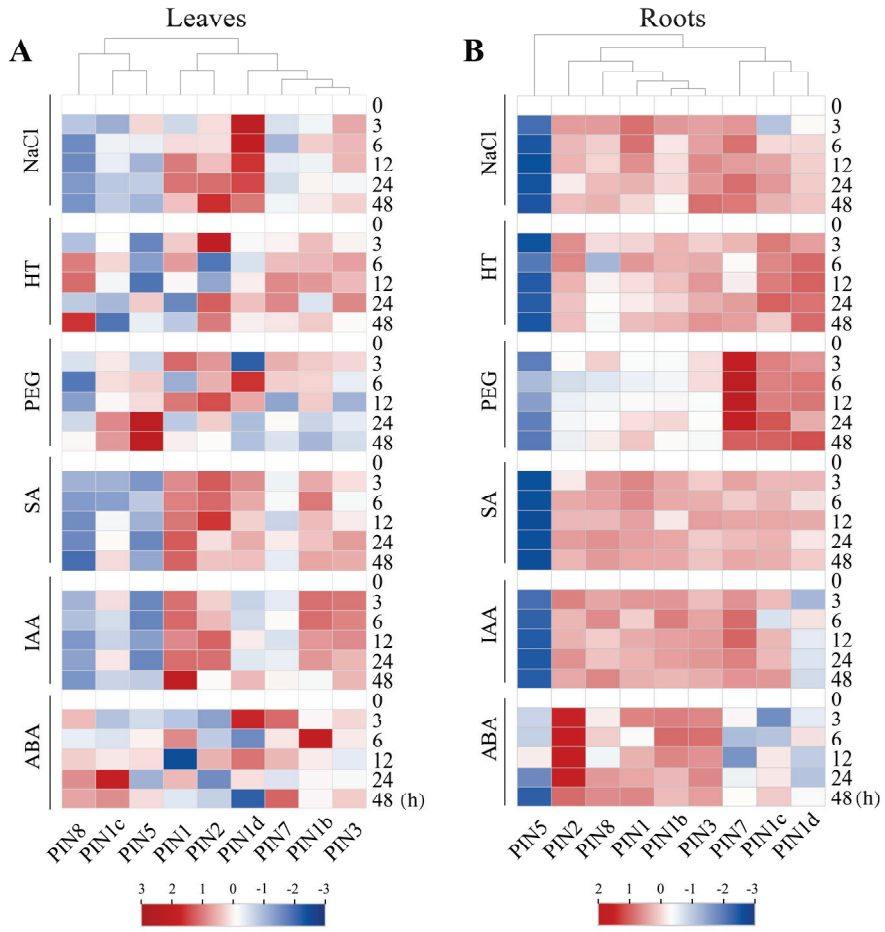

Figure 7. Heatmap of qPCR-based expression patterns of CsPIN genes in cucumber leaves and roots under abiotic stress and hormone treatment. The relative expression level was calculated by $2^{-\Delta\Delta CT}$ method compared with EF1 alpha (CsaV3_2G011610) as a reference gene.

Under SA and IAA hormone stress, the expression patterns of most *CsPIN* genes were similar. In leaves, *CsPIN1* was significantly induced, while *CsPIN1c*, *CsPIN5*, *CsPIN7*, and *CsPIN8* were inhibited; *CsPIN5* was inhibited in roots. After ABA treatment, the expression pattern of the *CsPIN2* gene in leaves and roots showed opposite trends; the expression levels of *CsPIN1b*, *CsPIN1c*, *CsPIN1d*, *CsPIN3*, and *CsPIN8* in leaves increased; *CsPIN1*, *CsPIN1b*, *CsPIN3*, *CsPIN2*, *CsPIN5*, and *CsPIN8* in roots were up-regulated. Under the three hormone treatments, the relative expression levels of most *CsPIN* genes in roots increased. *CsPIN2*, *CsPIN5*, and *CsPIN8* were extremely sensitive to SA, IAA, and ABA. These results indicate that members of the *CsPIN* gene family have different adaptive responses under different abiotic stresses and hormone treatments.

3. Discussion

3.1. Identification and Evolution of CsPIN Gene Family in Cucumber

Currently, *PIN* gene family members have been identified in multiple species using whole-genome approaches, and the number of the PIN family members varies among different plants. The *PIN* gene family members are quite diverse, with the fewest being four in the with the least number of four members in *Marchantia polymorpha* [49], and relatively large numbers in soybean and wheat [20,50]. In this study, we identified nine *CsPINs* in the cucumber genome (Table 1); this number of *PIN* genes is similar to that in *Arabidopsis* and tomato, suggesting that some *PINs* may have originated from one or more common genes. The expansion of the *PIN* gene family in different species might be attributed to genomic

duplication events [16]. Phylogenetic analysis of PIN proteins from five plants classified these proteins into five sub-families (Figure 1), and *CsPINs* have the closest evolutionary relationship with the genes of the dicotyledonous plants soybean and *Arabidopsis*. Multiple gene pairs were also identified with dicotyledonous plants in the collinearity analysis. These findings indicate that these genes likely descended from a common ancestor, and the specific differences of the genes in different species could be attributed to the evolutionary process of plants.

Chromosome mapping analysis revealed that the *CsPIN* genes were significantly unevenly distributed on five chromosomes of cucumber (Figure 2A). Chr3 and Chr4 each had one gene, Chr2 and Chr5 each had two genes, and Chr1 had three genes. Chr2 contained a pair of tandemly duplicated genes, *CsPIN5* and *CsPIN1d*. In addition, *CsPIN1* and *CsPIN1c* were highly similar in gene structure and motifs, indicating that they may have similar functions (Figure 3A). In rice, *OsPIN1a-1d*, *OsPIN3a-3b*, and *OsPIN5a-5c* sequences were similar, suggesting that the *PIN* gene family was generated through chromosomal segment duplication [51]. Maize and wheat also have three and fifteen pairs of repeated genes, respectively [12,50]. The replication and specific amplification of gene fragments throughout the genome have played a significant role in the process of evolution.

To compare the structures of CsPIN proteins, we identified the conserved motifs and domains of CsPIN (Figure 3B,C). We found that all CsPIN proteins contain six conserved motifs (Motif 1-4, Motif 6, Motif 8) and a conserved domain Men_Trans (PF03547). PIN proteins are connected by a heterogeneous central hydrophilic loop between the two highly conserved hydrophobic fragments at the N-terminal and C-terminal [52]. This hydrophilic loop contains four highly conserved sequences (HC1-HC4), among which the long central hydrophilic loop is approximately 300 amino acids, while the short one is about 50–100 amino acids (Figure S1). According to the length of the central hydrophilic loop, PIN proteins can be classified into long or typical PINs, short or atypical PINs, and semi-typical PINs [24,26,53]. In this study, the long and typical members of the cucumber *PIN* gene family include *CsPIN1*, *CsPIN1b*, *CsPIN1c*, *CsPIN2*, *CsPIN3*, and *CsPIN7*; short or atypical PINs are *CsPIN1d*, *CsPIN5*, and *CsPIN8*. Similar to the reported PIN family members in rice, maize, and wheat [12,50,51], there is no homologous gene to *AtPIN6* in cucumber. This result indicates that short or atypical *PINs* evolved independently of long or typical *PINs*. This difference is directly related to the presence or absence of certain motifs in the protein. In *Arabidopsis*, antagonistic interactions between the PID kinase and protein phosphatase 2A (PP2A) dynamically regulate the apical–basal polarity of PIN proteins by modulating their phosphorylation status [54]. PID-mediated phosphorylation of conserved residues within the central hydrophilic loop of PIN proteins (e.g., Ser337/Thr340 in PIN1) promotes their apical membrane localization, whereas PP2A-catalyzed dephosphorylation redirects PINs to the basal membrane [54]. Notably, phylogenetic analysis reveals that all long hydrophilic loop-containing PIN homologs in cucumber retain the conserved Ser337 residue. Furthermore, both CsPIN1 and CsPIN1c exhibit conservation at the Thr340 position (Figure S1), suggesting their potential functional conservation with AtPIN1 in phosphorylation-dependent polar targeting mechanisms.

The diversification of exon–intron structure is believed to have played a significant role in the evolution of certain gene families. The presence of introns promotes exon shuffling, driving gene evolution, allowing the production of multiple proteins from a single gene through alternative splicing, and playing a key role in gene regulation. Through the analysis of the exon–intron structure of nine *CsPIN* gene members, we found that seven of them contain more than six exons (Figure 3D). Homologous genes in the same phylogenetic branch, such as *CsPIN1*/*CsPIN1b* and *CsPIN3*/*CsPIN7*, have similar exon–intron structures. Except for *CsPIN1d*, which shows a significantly different exon–intron structure, the gene

structures of other members are relatively conserved. Therefore, we hypothesize that throughout the evolutionary history of cucumbers, *PIN* genes have experienced a series of intron deletions, insertions, and gene duplication events, which may have triggered changes in gene expression patterns and protein functions.

Cis-acting regulatory elements refer to non-coding DNA sequences located in the promoter region of genes. The distribution patterns of different types of cis-acting regulatory elements in the promoter region may reveal differences in gene regulatory mechanisms and functions [55]. In this study, we identified a total of 48 elements, which are mainly involved in light response, hormone response, abiotic stress response, as well as growth and development regulation (Figure 4). Among the nine *CsPIN* genes, there are a total of 60 cis-acting elements related to light response, including MRE, GT1 motif, GATA motif, ATCT motif, ATC motif, GA motif, TCCC motif, TCT motif, etc. At the same time, the *PIN* family also has hormone-induced elements such as auxin, salicylic acid, jasmonic acid, abscisic acid, ethylene, and gibberellin, suggesting that the members of the *PIN* gene family may not only have the biological activity of transporting auxin but also may be involved in the synergistic or antagonistic pathways of different plant hormones and auxin [22]. Similar to the cis-acting elements identified in the promoter region of the coffee PIN gene [56], the promoter regions of *CsPINs* also contain multiple abiotic stress elements, such as LTR and W-box (cold response), myb binding sites (hypoxia induction), MBS (drought induction) elements, etc. These findings suggest that the cucumber *PIN* gene family may play extensive roles in plant responses to abiotic stress; however, further experimental validation is required to confirm their precise regulatory mechanisms.

3.2. Protein–Protein Interaction Network of CsPIN

Numerous studies have found that protein–protein interactions can accurately predict the cellular functions of uncharacterized proteins [57]. In this study, eight CsPIN proteins were predicted to interact with 34 kinds of proteins (Figure 5). We predicted that CsPIN2 in cucumber might interact with GNOM and BIG5 (BEN1). We also found that five CsPIN protein members (PIN1, PIN1b, PIN1c, PIN2, and PIN3) in cucumber may interact with ARF and USP19 (Figure 5). In *Arabidopsis*, GNOM, as a membrane-associated guanine nucleotide exchange factor on ADP-ribosylation factor G protein (ARF GEF), regulates the vesicle transport required for the polar localization of auxin efflux carriers, thereby determining the direction of auxin flow [58]. It has been reported that GNOM mediates the sorting of PIN1 from endosomal compartments to the basal PM and the polarization of PIN3 to the bottom side of hypocotyl endodermal cells in the hypocotyl [59,60]. BEN1 and BEN2 play essential roles in the polar localization of PIN, dynamic repolarization events, and the establishment of auxin activity gradients [61]. These processes are vital for various developmental mechanisms, such as embryonic pattern formation, organogenesis, and vascular venation pattern formation [61]. It has been reported that four VvPIN protein members in grape may interact with ARF to regulate plant growth and development processes by controlling auxin response genes [15]. It has been reported that auxin can regulate the transcription of multiple AtPIN proteins in a tissue-specific manner through the TIR1-Aux/IAA-ARF pathway [62]; at the same time, auxin may also regulate the protein stability of AtPIN2 through the mechanisms of ubiquitination and proteasome activity [63]. In this study, CsPIN1b may interact with CsPID2, and at the same time, CsPIN1 and CsPIN1b may interact with multiple proteins involved in leaf morphology (transcription factor AS1, ASYMMETRIC LEAVES 2, and transcription repressor KAN1) (Figure 5). PID has been reported to be capable of catalyzing the phosphorylation of PIN and plays a key role in regulating the apical–basal PIN polarity [64]. In wheat, TaPIN8 and TaPIN9 may interact with TaPID under drought and heat stress conditions, influencing

the localization and polar auxin transport of TaPIN by regulating the phosphorylation state [50]. Auxin is also crucial for regulating leaf development. Under warm conditions, the photoreceptor phytochrome-interacting factor 4 (PIF4) directly activates the protein kinase PID, promoting auxin production in leaves and leading to auxin accumulation in petioles [65]. At the same time, PID polarizes the auxin transporter PIN3 to the outer membrane of petiole cells through phosphorylation. Moreover, AS1 mainly regulates the induced expression of PID on the back of the petiole, indicating that the polar transport of auxin is a key biochemical event in the process of leaf temperature regulation [65]. The triple mutants of ospin1c ospin1d ospid have also been reported to have serious defects in leaf morphogenesis in rice [66]. While these findings advance our understanding of auxin-mediated co-regulation of PIN polar transport in cucumber, future studies should employ co-immunoprecipitation (Co-IP) and yeast two-hybrid (Y2H) assays to experimentally map the interaction networks among these signaling components.

3.3. Role of the CsPIN Genes in Plant Growth and Development

The gene functions of the *PIN* gene family members exhibit tissue specificity, and this differentiated expression pattern plays a significant role in the growth and development of cucumbers. In this study, we obtained RNA-Seq data for 23 different cucumber tissue expression profiles from the CuGenDB database and examined the transcriptional levels of nine *CsPIN* genes. The results showed that *CsPIN* genes from different phylogenetic branches exhibited multiple expression patterns in different organs (Figure 6). In Group I, *CsPIN2*, *CsPIN1b*, and *CsPIN5* had similar expression patterns, mainly expressed in roots. *CsPIN1d* was expressed in stems but not in other organs. The five genes (*CsPIN1*, *CsPIN1c*, *CsPIN3*, *CsPIN7*, and *CsPIN8*) in Group II were highly expressed in roots, stems, tendrils, and petioles of new leaves. Among them, *CsPIN1* had the highest expression levels in mature roots and four-week-old hypocotyls, and weak expression in male flowers and old leaves, while *CsPIN3* and *CsPIN7* were highly expressed in male flowers, four-week-old cotyledons, and true leaves. Similar expression patterns have also been found in other species. In *Arabidopsis*, *AtPIN1* and *AtPIN3* display substantial expression levels in root tissues, influencing the dimensions of the primary root meristem and the growth rate of the primary root [67]. *GbPIN1*, *GbPIN2*, and *GbPIN3* exhibit substantial expression levels in the roots and stems of cotton but are nearly absent in leaves [68]. *PbPIN3-1*, *PbPIN3-2*, *PbPIN3-3*, and *PbPIN4* display similar expression patterns across various organs in both dwarfing (QN101) and vigorous (OHF51) pear rootstocks, suggesting functional redundancy among these genes [16]. In rice, *OsPIN5a* and *OsPIN5c* show high expression in leaves, shoot tips, and panicles, whereas *OsPIN5b* is predominantly expressed in young panicles [38]. *TaPIN5*, *9*, *13*, *21*, and *28* are highly expressed in wheat stems, while *TaPIN31*, *32*, *35*, *40*, and *44* exhibit elevated expression levels in grains [50]. In maize, most *PIN* gene members are highly expressed in embryos, roots, and stems, with *ZmPIN1b* showing significant expression during female inflorescence development [41]. In tobacco, multiple *NtPIN* genes are highly expressed in stems, and *NtPIN5a* and *NtPIN5b* have higher expression levels in flowers [19]. The above research results indicate that roots, axillary buds, and young stems are the main regulatory targets of PIN proteins [69]. Members of the *PIN* gene family regulate the distribution of auxin through a coordinated and redundant mechanism, playing a crucial role in the normal growth and development of plants [14,18].

The *PIN* gene facilitates plant adaptation to adverse environmental conditions through the regulation of auxin distribution. In cucumber leaves, the transcription levels of *CsPIN* genes under abiotic stress and hormone treatments were significantly different (Figure 7). Among them, *CsPIN1*, *CsPIN1d*, *CsPIN2*, and *CsPIN3* were all induced under NaCl treatment. The expression levels of *CsPIN1c* and *CsPIN5* under PEG treatment were significantly

higher than those of other *CsPIN* genes. Four genes (*CsPIN1*, *CsPIN1b*, *CsPIN2*, and *CsPIN3*) were significantly induced under SA and IAA treatments. Meanwhile, the above- and below-ground parts had opposite expression patterns. Except for *CsPIN5*, most *CsPIN* genes in roots were induced under both abiotic and hormone stresses. *CsPIN2* and *CsPIN7* were sensitive to PEG and ABA treatments, respectively. Several *PIN* genes in grapes, soybeans, and maize respond to different abiotic or hormone stresses [15,20,41]. *VvPIN7* and *VvPIN9* are sensitive to PEG treatment [15]; *GmPIN* genes can be induced by various abiotic stresses and plant hormones, among which the expression level of *GmPIN5a* is inhibited after IAA treatment [20]; the expression levels of *ZmPIN5c*, *ZmPIN15*, and *ZmPIN10b* are all up-regulated under NaCl treatment [41]. *PIN* genes are highly expressed in cotton plants under drought, salt, and dehydration treatments [18]. These findings suggest that by modulating the expression levels of *PIN* genes, the dynamic equilibrium of auxin in various tissues and organs is maintained, thereby contributing to tissue and organ formation and differentiation. Future studies employing CRISPR/Cas9 knockout technology will be essential to elucidate the precise spatiotemporal roles of *CsPIN* genes in developmental processes such as phyllotaxis and root gravitropism.

4. Materials and Methods

4.1. Identification and Physicochemical Properties of PIN Genes in Cucumber

To identify the *PIN* genes in cucumber (Chinese Long), the whole genome sequences were retrieved from the Cucurbit Genomics Database (CuGenDBv2) website (http://cucurbitgenomics.org/v2/, accessed on 8 October 2024). *Arabidopsis* PIN protein sequences were obtained from TAIR 10 (https://www.arabidopsis.org/, accessed on 8 October 2024). Next, the Hidden Markov Model (HMM) of the PIN domain (PF03547) was obtained from the Pfam database (http://pfam.xfam.org/, accessed on 8 October 2024), and the HMMER 3.0 software was used to search for candidate *PIN* genes. Then, redundant sequences were removed to ensure only unique candidate *CsPIN* genes were retained. Using ExPASy online (https://web.expasy.org/protparam/, accessed on 19 October 2024) program to analyze the physicochemical properties of cucumber PIN protein. Subcellular locations of CsPIN proteins were predicted using the LocTree3 server (https://rostlab.org/services/loctree3/, accessed on 24 October 2024).

4.2. Phylogenetic Analysis of Cucumber PIN Gene Family

MEGA6 software was used to perform multiple sequence alignment of PIN protein sequences in cucumber, *Arabidopsis*, wheat, soybean, and rice species. And the multi-sequence alignment result file was converted into meg format for PIN protein phylogenetic analysis.

4.3. Chromosome Localization and Gene Duplication Analysis

TBtools v 2.119 software was used to obtain chromosome density information from genome annotation, and the chromosomal distribution, length, and the start and end positions of *CsPIN* genes were screened for and located as *CsPINs* according to their distribution on chromosomes. Then the visualization analysis was performed using the Gene Location Visualize from the GTF/ TFF function. Gene annotation files and genome files for *Arabidopsis*, *G. max*, *C. melo*, and *S. lycopersicum* were downloaded using the Ensembl Plants database (https://plants.ensembl.org/index.html, accessed on 22 November 2024).

Used one-step McScanx-super-fast to map chromosome location. The results of the blast were simplified by using the Text merge for MCScanX function, and TBtools Multiple Synteny Plot function was used to highlight the identified PIN collinear pairs and their collinear pairs with the other four species.

4.4. The Conserved Motifs, Gene Structure, Function Domain, Putative Cis-Acting Elements Analysis

The gff3 annotation file (ChineseLong_v3.gff3.gz), the genome file (ChineseLong_genome_v3.fa.gz), the gene CDS sequence file (Chinese Long_CDS_v3.fa.gz), and the protein sequence file (ChineseLong_pep_v3.fa.gz) were downloaded from the cucumber database. The MEME website (https://meme-suite.org/meme/, accessed on 21 November 2024) was used on the cucumber PIN family to predict the conservative base sequence of the protein sequence; the largest number of motifs was set to 10, and the rest of the parameter was set to the default value. Through a CD search on the NCBI website (https://www.ncbi.nlm.nih.gov/cdd, accessed on 26 November 2024), conservative domain analysis of the cucumber PIN protein sequence was performed. Exon–intron structure prediction and gene structure analysis of *CsPIN* genes were performed at the GSDS online website (https://gsds.gao-lab.org/, accessed on 25 November 2024). Ultimately, they were further visualized through the Gene Structure View function in TBtools.

The promoter sequences (2000 bp before the start codon of a gene) were extracted from the cucumber genome database. These sequences were subsequently submitted to PlantCARE (http://bioinformatics.psb.ugent.be/webtools/plantcare/html/, accessed on 7 November 2024). The cis-acting elements were analyzed, and the predicted results were submitted to the TB tool software for visual analysis.

4.5. Protein–Protein Interaction Network

The functional interaction network model of CsPIN proteins was established by using the STRING database (https://cn.string-db.org/, accessed on 10 November 2024) to predict the relationship between CsPIN proteins and other related proteins. The species was designated as Cucumis sativus, with confidence parameters set to a threshold of 0.40 and disconnected nodes hidden in the network.

4.6. Analysis of Expression Profiles of CsPINs Genes in Different Tissues

To examine the tissue-specific expression patterns of *CsPIN* genes, we retrieved expression data with accession number PRJNA312872 from the Cucurbit Genomics Database (http://cucurbitgenomics.org/v2/download, accessed on 11 November 2024). A total of 23 different tissues and organs of cucumber were downloaded with FPKM transcriptome data, including roots, stems, tendrils, young leaves, young leaf petioles, old leaves, old leaf petioles, male flowers, male flower buds, female flowers, unfertilized ovary, unfertilized ovary peels, unfertilized ovary fleshes, one week fruit peels, one week fruit flesh, two week fruit peels, two week fruit flesh, three week fruit peels, three week fruit flesh, four week old cotyledon, four week old hypocotyls, four week old true leaves, and four week old roots. Meanwhile, the FPKM values were converted using the log2 method, and the *CsPIN* gene expression heatmap was drawn using TBtools software.

4.7. Plant Materials and Treatment

The cucumber cultivar "Chunqiu Wang No. 3" was used as an experimental material and planted in the Chongming Base of National Engineering Research Center for Facility Agriculture, Shanghai Academy of Agricultural Sciences (Shanghai, China). Cucumber seedlings were grown in a plant growth chamber (26 °C/18 °C day/night condition, 14/10 h (light/darkness) photoperiod, 75% relative humidity). When the seedlings reached a true leaf stage, the root of plantlets was soaked in a hydroponic nutrient solution, and an oxygen pump was added to the basin containing the nutrient solution to ensure an adequate oxygen supply. Uniformly grown three-week-old cucumber seedlings were selected and treated according to previously published concentrations for plant hormones and abiotic stresses [11,15,50,70,71], including 1 mmol/L IAA, 5 mmol/L SA, 100 μmol/L

ABA, 150 mmol/L NaCl, 5% PEG 6000, and high temperature (35 °C). Leaf and root samples were collected at 0, 3, 6, 12, 24, and 48 h after treatment. All samples were immediately immersed in liquid nitrogen and stored at −80 °C. Three biological replicates were set for each treatment.

4.8. RNA Extraction and Quantitative qRT-PCR Analysis

Total RNA was extracted from the treated and control samples in the leaves and roots of cucumber using a high-purity total RNA rapid extraction kit (Takara Biomedical Technology Co., Beijing, China). The quality and concentration of different RNA samples were quantified using a NanoDrop (ND-1000, NanoDrop Technologies, Wilmington, DE, USA), followed by reverse transcription using Prime Script RT reagent kit (Takara, Beijing, China) according to the manufacturer's instructions. The qRT-PCR reactions were performed using the QuantStudio 6 Flex Real-Time PCR System (Thermo Fisher Scientific, Waltham, MA, USA). Gene-specific primer pairs for all *CsPIN* genes were designed using NCBI Primer-BLAST with default parameters (Table S1). The amplification was carried out as follows: 95 °C for 5 min, 45 cycles at 95 °C for 10 s, 55 °C for 20 s, and 72 °C for 20 s, followed by a dissociation stage. The relative expression levels of CsPINs were calculated using the $2^{-\Delta\Delta CT}$ method. All the expression analyses included three biological replicates and three technical replicates.

5. Conclusions

In general, this study identified nine *CsPIN* family members and systematically analyzed their genomic locations, phylogenetic relationships, conserved domains, gene structures, protein interactions, and gene expression levels. Meanwhile, *CsPIN* genes were significantly differentially expressed during the development of various cucumber tissues, with specific members playing leading roles in regulating root polarity development and leaf morphogenesis. In response to abiotic stresses such as NaCl, HT, and PEG, as well as various hormone stimuli, different *CsPIN* genes exhibited diverse response patterns, coordinating the dynamic balance of auxin to adapt to environmental changes. However, the details of functional redundancy among cucumber *PIN* genes and their complex interaction networks require further elucidation. In the future, we plan to utilize single-cell sequencing and gene editing technologies to further explore the functions of *CsPIN* genes, providing key targets for molecular breeding and targeted genetic improvement of cucumber growth and development.

Supplementary Materials: The following supporting information can be downloaded at https://www.mdpi.com/article/10.3390/plants14111566/s1, Figure S1: Multiple sequence alignments of PIN domains. Table S1: Primers for RT-qPCR analysis of *PIN* genes in cucumber.

Author Contributions: Conceptualization, Y.Z., K.Z. and X.D.; methodology, Y.Z. and W.S.; software, Y.Z. and K.Z.; validation, K.Z., H.Z. and X.D.; formal analysis, Y.Z., K.Z. and J.C.; investigation, Y.Z., K.Z. and C.M.; resources, Y.Z. and P.L.; data curation, Y.Z., K.Z. and H.J.; writing—original draft preparation, Y.Z.; writing—review and editing, L.C. and X.D.; visualization, S.W.; supervision, C.Z.; project administration, X.D.; funding acquisition, X.D. All authors have read and agreed to the published version of the manuscript.

Funding: This research was funded by the Excellent Team Program of the Shanghai Academy of Agricultural Sciences (grant No. [2022]022) and Shanghai Key Laboratory of Protected Horticulture Technology Open Project (grant No. KF202405).

Data Availability Statement: The original contributions presented in this study are included in the article/Supplementary Material. Further inquiries can be directed to the corresponding author.

Conflicts of Interest: The authors declare no conflicts of interest.

Abbreviations

The following abbreviations are used in this manuscript:

ABA	Abscisic acid
HT	High temperature
IAA	Indole-3-acetic acid
NaCl	Sodium chloride
PEG	Polyethylene glycol
SA	Salicylic acid
qRT-PCR	Quantitative real-time polymerase chain reaction

References

1. Vanneste, S.; Friml, J. Auxin: A Trigger for Change in Plant Development. *Cell* **2009**, *136*, 1005–1016. [CrossRef] [PubMed]
2. Zhao, Y.D. Essential Roles of Local Auxin Biosynthesis in Plant Development and in Adaptation to Environmental Changes. *Annu. Rev. Plant Biol.* **2018**, *69*, 417–435. [CrossRef] [PubMed]
3. Gomes, G.L.B.; Scortecci, K.C. Auxin and its role in plant development: Structure, signalling, regulation and response mechanisms. *Plant Biol.* **2021**, *23*, 894–904. [CrossRef]
4. Swarup, R.; Kargul, J.; Marchant, A.; Zadik, D.; Rahman, A.; Mills, R.; Yemm, A.; May, S.; Williams, L.; Millner, P.; et al. Structure-function analysis of the presumptive Arabidopsis auxin permease AUX1. *Plant Cell* **2004**, *16*, 3069–3083. [CrossRef]
5. Petrásek, J.; Mravec, J.; Bouchard, R.; Blakeslee, J.J.; Abas, M.; Seifertová, D.; Wisniewska, J.; Tadele, Z.; Kubes, M.; Covanová, M.; et al. PIN proteins perform a rate-limiting function in cellular auxin efflux. *Science* **2006**, *312*, 914–918. [CrossRef]
6. Cho, M.; Lee, S.H.; Cho, H.T. P-glycoprotein4 displays auxin efflux transporter-like action in Arabidopsis root hair cells and tobacco cells. *Plant Cell* **2007**, *19*, 3930–3943. [CrossRef]
7. Barbez, E.; Kubes, M.; Rolcík, J.; Béziat, C.; Pencík, A.; Wang, B.J.; Rosquete, M.R.; Zhu, J.S.; Dobrev, P.I.; Lee, Y.; et al. A novel putative auxin carrier family regulates intracellular auxin homeostasis in plants. *Nature* **2012**, *485*, 119-U155. [CrossRef]
8. Lee, I. A showcase of future plant biology: Moving towards next-generation plant genetics assisted by genome sequencing and systems biology. *Genome Biol.* **2014**, *15*, 305. [CrossRef]
9. Krecek, P.; Skupa, P.; Libus, J.; Naramoto, S.; Tejos, R.; Friml, J.; Zazímalová, E. The PIN-FORMED (PIN) protein family of auxin transporters. *Genome Biol.* **2009**, *10*, 249. [CrossRef]
10. Zhang, C.; Dong, W.; Huang, Z.A.; Cho, M.; Yu, Q.; Wu, C.; Yu, C. Genome-wide identification and expression analysis of the CaLAX and CaPIN gene families in pepper (*Capsicum annuum* L.) under various abiotic stresses and hormone treatments. *Genome* **2018**, *61*, 121–130. [CrossRef]
11. Yang, C.; Wang, D.; Zhang, C.; Kong, N.; Ma, H.; Chen, Q. Comparative Analysis of the PIN Auxin Transporter Gene Family in Different Plant Species: A Focus on Structural and Expression Profiling of PINs in Solanum tuberosum. *Int. J. Mol. Sci.* **2019**, *20*, 3270. [CrossRef] [PubMed]
12. Forestan, C.; Farinati, S.; Varotto, S. The Maize PIN Gene Family of Auxin Transporters. *Front. Plant Sci.* **2012**, *3*, 16. [CrossRef]
13. Sańko-Sawczenko, I.; Łotocka, B.; Czarnocka, W. Expression Analysis of PIN Genes in Root Tips and Nodules of Medicago truncatula. *Int. J. Mol. Sci.* **2016**, *17*, 1197. [CrossRef]
14. Shen, C.; Bai, Y.; Wang, S.; Zhang, S.; Wu, Y.; Chen, M.; Jiang, D.; Qi, Y. Expression profile of PIN, AUX/LAX and PGP auxin transporter gene families in Sorghum bicolor under phytohormone and abiotic stress. *FEBS J.* **2010**, *277*, 2954–2969. [CrossRef]
15. Gou, H.; Nai, G.; Lu, S.; Ma, W.; Chen, B.; Mao, J. Genome-wide identification and expression analysis of PIN gene family under phytohormone and abiotic stresses in *Vitis vinifera* L. *Physiol. Mol. Biol. Plants* **2022**, *28*, 1905–1919. [CrossRef]
16. Qi, L.; Chen, L.; Wang, C.; Zhang, S.; Yang, Y.; Liu, J.; Li, D.; Song, J.; Wang, R. Characterization of the Auxin Efflux Transporter PIN Proteins in Pear. *Plants* **2020**, *9*, 349. [CrossRef]
17. Liu, B.; Zhang, J.; Wang, L.; Li, J.; Zheng, H.; Chen, J.; Lu, M. A survey of Populus PIN-FORMED family genes reveals their diversified expression patterns. *J. Exp. Bot.* **2014**, *65*, 2437–2448. [CrossRef]
18. He, P.; Zhao, P.; Wang, L.; Zhang, Y.; Wang, X.; Xiao, H.; Yu, J.; Xiao, G. The PIN gene family in cotton (*Gossypium hirsutum*): Genome-wide identification and gene expression analyses during root development and abiotic stress responses. *BMC Genom.* **2017**, *18*, 507. [CrossRef]
19. Xie, X.; Qin, G.; Si, P.; Luo, Z.; Gao, J.; Chen, X.; Zhang, J.; Wei, P.; Xia, Q.; Lin, F.; et al. Analysis of Nicotiana tabacum PIN genes identifies NtPIN4 as a key regulator of axillary bud growth. *Physiol. Plant* **2017**, *160*, 222–239. [CrossRef]
20. Wang, Y.; Chai, C.; Valliyodan, B.; Maupin, C.; Annen, B.; Nguyen, H.T. Genome-wide analysis and expression profiling of the PIN auxin transporter gene family in soybean (Glycine max). *BMC Genom.* **2015**, *16*, 951. [CrossRef]
21. Friml, J. Auxin transport—Shaping the plant. *Curr. Opin. Plant Biol.* **2003**, *6*, 7–12. [CrossRef] [PubMed]
22. Adamowski, M.; Friml, J. PIN-dependent auxin transport: Action, regulation, and evolution. *Plant Cell* **2015**, *27*, 20–32. [CrossRef]

23. Ding, Z.; Wang, B.; Moreno, I.; Dupláková, N.; Simon, S.; Carraro, N.; Reemmer, J.; Pěnčík, A.; Chen, X.; Tejos, R.; et al. ER-localized auxin transporter PIN8 regulates auxin homeostasis and male gametophyte development in Arabidopsis. *Nat. Commun.* **2012**, *3*, 941. [CrossRef]
24. Bennett, T.; Brockington, S.F.; Rothfels, C.; Graham, S.W.; Stevenson, D.; Kutchan, T.; Rolf, M.; Thomas, P.; Wong, G.K.; Leyser, O.; et al. Paralogous radiations of PIN proteins with multiple origins of noncanonical PIN structure. *Mol. Biol. Evol.* **2014**, *31*, 2042–2060. [CrossRef]
25. Mravec, J.; Skůpa, P.; Bailly, A.; Hoyerová, K.; Krecek, P.; Bielach, A.; Petrásek, J.; Zhang, J.; Gaykova, V.; Stierhof, Y.D.; et al. Subcellular homeostasis of phytohormone auxin is mediated by the ER-localized PIN5 transporter. *Nature* **2009**, *459*, 1136–1140. [CrossRef]
26. Simon, S.; Skůpa, P.; Viaene, T.; Zwiewka, M.; Tejos, R.; Klíma, P.; Čarná, M.; Rolčík, J.; De Rycke, R.; Moreno, I.; et al. PIN6 auxin transporter at endoplasmic reticulum and plasma membrane mediates auxin homeostasis and organogenesis in Arabidopsis. *New Phytol.* **2016**, *211*, 65–74. [CrossRef]
27. Ganguly, A.; Lee, S.H.; Cho, M.; Lee, O.R.; Yoo, H.; Cho, H.T. Differential auxin-transporting activities of PIN-FORMED proteins in Arabidopsis root hair cells. *Plant Physiol.* **2010**, *153*, 1046–1061. [CrossRef]
28. Benková, E.; Michniewicz, M.; Sauer, M.; Teichmann, T.; Seifertová, D.; Jürgens, G.; Friml, J. Local, efflux-dependent auxin gradients as a common module for plant organ formation. *Cell* **2003**, *115*, 591–602. [CrossRef]
29. Mudgett, M.; Shen, Z.; Dai, X.; Briggs, S.P.; Zhao, Y. Suppression of pinoid mutant phenotypes by mutations in PIN-FORMED 1 and PIN1-GFP fusion. *Proc. Natl. Acad. Sci. USA* **2023**, *120*, e2312918120. [CrossRef]
30. Li, K.; Kamiya, T.; Fujiwara, T. Differential Roles of PIN1 and PIN2 in Root Meristem Maintenance Under Low-B Conditions in Arabidopsis thaliana. *Plant Cell Physiol.* **2015**, *56*, 1205–1214. [CrossRef]
31. Chen, Q.; Liu, Y.; Maere, S.; Lee, E.; Van Isterdael, G.; Xie, Z.; Xuan, W.; Lucas, J.; Vassileva, V.; Kitakura, S.; et al. A coherent transcriptional feed-forward motif model for mediating auxin-sensitive PIN3 expression during lateral root development. *Nat. Commun.* **2015**, *6*, 8821. [CrossRef] [PubMed]
32. Friml, J.; Benková, E.; Blilou, I.; Wisniewska, J.; Hamann, T.; Ljung, K.; Woody, S.; Sandberg, G.; Scheres, B.; Jürgens, G.; et al. AtPIN4 mediates sink-driven auxin gradients and root patterning in Arabidopsis. *Cell* **2002**, *108*, 661–673. [CrossRef]
33. Cazzonelli, C.I.; Vanstraelen, M.; Simon, S.; Yin, K.; Carron-Arthur, A.; Nisar, N.; Tarle, G.; Cuttriss, A.J.; Searle, I.R.; Benkova, E.; et al. Role of the Arabidopsis PIN6 auxin transporter in auxin homeostasis and auxin-mediated development. *PLoS ONE* **2013**, *8*, e70069. [CrossRef]
34. Ditengou, F.A.; Gomes, D.; Nziengui, H.; Kochersperger, P.; Lasok, H.; Medeiros, V.; Paponov, I.A.; Nagy, S.K.; Nádai, T.V.; Mészáros, T.; et al. Characterization of auxin transporter PIN6 plasma membrane targeting reveals a function for PIN6 in plant bolting. *New Phytol.* **2018**, *217*, 1610–1624. [CrossRef]
35. Xiong, F.; Liu, H.H.; Duan, C.Y.; Zhang, B.K.; Wei, G.; Zhang, Y.; Li, S. Arabidopsis JANUS Regulates Embryonic Pattern Formation through Pol II-Mediated Transcription of WOX2 and PIN7. *iScience* **2019**, *19*, 1179–1188. [CrossRef]
36. Xu, M.; Zhu, L.; Shou, H.; Wu, P. A PIN1 family gene, OsPIN1, involved in auxin-dependent adventitious root emergence and tillering in rice. *Plant Cell Physiol.* **2005**, *46*, 1674–1681. [CrossRef]
37. Chen, Y.; Fan, X.; Song, W.; Zhang, Y.; Xu, G. Over-expression of OsPIN2 leads to increased tiller numbers, angle and shorter plant height through suppression of OsLAZY1. *Plant Biotechnol. J.* **2012**, *10*, 139–149. [CrossRef] [PubMed]
38. Wang, J.R.; Hu, H.; Wang, G.H.; Li, J.; Chen, J.Y.; Wu, P. Expression of PIN genes in rice (*Oryza sativa* L.): Tissue specificity and regulation by hormones. *Mol. Plant* **2009**, *2*, 823–831. [CrossRef]
39. Carraro, N.; Forestan, C.; Canova, S.; Traas, J.; Varotto, S. ZmPIN1a and ZmPIN1b encode two novel putative candidates for polar auxin transport and plant architecture determination of maize. *Plant Physiol.* **2006**, *142*, 254–264. [CrossRef]
40. Gallavotti, A.; Yang, Y.; Schmidt, R.J.; Jackson, D. The Relationship between auxin transport and maize branching. *Plant Physiol.* **2008**, *147*, 1913–1923. [CrossRef]
41. Yue, R.; Tie, S.; Sun, T.; Zhang, L.; Yang, Y.; Qi, J.; Yan, S.; Han, X.; Wang, H.; Shen, C. Genome-wide identification and expression profiling analysis of ZmPIN, ZmPILS, ZmLAX and ZmABCB auxin transporter gene families in maize (*Zea mays* L.) under various abiotic stresses. *PLoS ONE* **2015**, *10*, e0118751. [CrossRef] [PubMed]
42. Roychoudhry, S.; Sageman-Furnas, K.; Wolverton, C.; Grones, P.; Tan, S.; Molnár, G.; De Angelis, M.; Goodman, H.L.; Capstaff, N.; Lloyd, J.P.B.; et al. Antigravitropic PIN polarization maintains non-vertical growth in lateral roots. *Nat. Plants* **2023**, *9*, 1500–1513. [CrossRef] [PubMed]
43. Shibata, A.; Yumoto, G.; Shimizu, H.; Honjo, M.N.; Kudoh, H. Flower movement induced by weather-dependent tropism satisfies attraction and protection. *Nat. Commun.* **2025**, *16*, 4132. [CrossRef]
44. Ung, K.L.; Winkler, M.; Schulz, L.; Kolb, M.; Janacek, D.P.; Dedic, E.; Stokes, D.L.; Hammes, U.Z.; Pedersen, B.P. Structures and mechanism of the plant PIN-FORMED auxin transporter. *Nature* **2022**, *609*, 605–610. [CrossRef]
45. Byrne, M.E.; Barley, R.; Curtis, M.; Arroyo, J.M.; Dunham, M.; Hudson, A.; Martienssen, R.A. Asymmetric leaves1 mediates leaf patterning and stem cell function in Arabidopsis. *Nature* **2000**, *408*, 967–971. [CrossRef]

46. Semiarti, E.; Ueno, Y.; Tsukaya, H.; Iwakawa, H.; Machida, C.; Machida, Y. The ASYMMETRIC LEAVES2 gene of Arabidopsis thaliana regulates formation of a symmetric lamina, establishment of venation and repression of meristem-related homeobox genes in leaves. *Development* **2001**, *128*, 1771–1783. [CrossRef]
47. Luo, M.; Yu, C.W.; Chen, F.F.; Zhao, L.; Tian, G.; Liu, X.; Cui, Y.; Yang, J.Y.; Wu, K. Histone deacetylase HDA6 is functionally associated with AS1 in repression of KNOX genes in arabidopsis. *PLoS Genet.* **2012**, *8*, e1003114. [CrossRef]
48. Matsumura, Y.; Ohbayashi, I.; Takahashi, H.; Kojima, S.; Ishibashi, N.; Keta, S.; Nakagawa, A.; Hayashi, R.; Saéz-Vásquez, J.; Echeverria, M.; et al. A genetic link between epigenetic repressor AS1-AS2 and a putative small subunit processome in leaf polarity establishment of Arabidopsis. *Biol. Open* **2016**, *5*, 942–954. [CrossRef]
49. Fisher, T.J.; Flores-Sandoval, E.; Alvarez, J.P.; Bowman, J.L. PIN-FORMED is required for shoot phototropism/gravitropism and facilitates meristem formation in Marchantia polymorpha. *New Phytol.* **2023**, *238*, 1498–1515. [CrossRef]
50. Kumar, M.; Kherawat, B.S.; Dey, P.; Saha, D.; Singh, A.; Bhatia, S.K.; Ghodake, G.S.; Kadam, A.A.; Kim, H.U.; Manorama; et al. Genome-Wide Identification and Characterization of PIN-FORMED (PIN) Gene Family Reveals Role in Developmental and Various Stress Conditions in *Triticum aestivum* L. *Int. J. Mol. Sci.* **2021**, *22*, 7396. [CrossRef]
51. Miyashita, Y.; Takasugi, T.; Ito, Y. Identification and expression analysis of PIN genes in rice. *Plant Sci.* **2010**, *178*, 424–428. [CrossRef]
52. Bennett, T. PIN proteins and the evolution of plant development. *Trends Plant Sci.* **2015**, *20*, 498–507. [CrossRef] [PubMed]
53. Viaene, T.; Delwiche, C.F.; Rensing, S.A.; Friml, J. Origin and evolution of PIN auxin transporters in the green lineage. *Trends Plant Sci.* **2013**, *18*, 5–10. [CrossRef]
54. Michniewicz, M.; Zago, M.K.; Abas, L.; Weijers, D.; Schweighofer, A.; Meskiene, I.; Heisler, M.G.; Ohno, C.; Zhang, J.; Huang, F.; et al. Antagonistic regulation of PIN phosphorylation by PP2A and PINOID directs auxin flux. *Cell* **2007**, *130*, 1044–1056. [CrossRef]
55. Hu, S.; Liu, X.; Xuan, W.; Mei, H.; Li, J.; Chen, X.; Zhao, Z.; Zhao, Y.; Jeyaraj, A.; Periakaruppan, R.; et al. Genome-wide identification and characterization of PIN-FORMED (PIN) and PIN-LIKES (PILS) gene family reveals their role in adventitious root development in tea nodal cutting (*Camellia sinensis*). *Int. J. Biol. Macromol.* **2023**, *229*, 791–802. [CrossRef]
56. Huang, X.; Bai, X.; Guo, T.; Xie, Z.; Laimer, M.; Du, D.; Gbokie, T., Jr.; Zhang, Z.; He, C.; Lu, Y.; et al. Genome-Wide Analysis of the PIN Auxin Efflux Carrier Gene Family in Coffee. *Plants* **2020**, *9*, 1061. [CrossRef]
57. Brun, C.; Chevenet, F.; Martin, D.; Wojcik, J.; Guénoche, A.; Jacq, B. Functional classification of proteins for the prediction of cellular function from a protein-protein interaction network. *Genome Biol.* **2003**, *5*, R6. [CrossRef]
58. Geldner, N.; Anders, N.; Wolters, H.; Keicher, J.; Kornberger, W.; Muller, P.; Delbarre, A.; Ueda, T.; Nakano, A.; Jürgens, G. The Arabidopsis GNOM ARF-GEF mediates endosomal recycling, auxin transport, and auxin-dependent plant growth. *Cell* **2003**, *112*, 219–230. [CrossRef]
59. Steinmann, T.; Geldner, N.; Grebe, M.; Mangold, S.; Jackson, C.L.; Paris, S.; Gälweiler, L.; Palme, K.; Jürgens, G. Coordinated polar localization of auxin efflux carrier PIN1 by GNOM ARF GEF. *Science* **1999**, *286*, 316–318. [CrossRef]
60. Rakusová, H.; Gallego-Bartolomé, J.; Vanstraelen, M.; Robert, H.S.; Alabadí, D.; Blázquez, M.A.; Benková, E.; Friml, J. Polarization of PIN3-dependent auxin transport for hypocotyl gravitropic response in Arabidopsis thaliana. *Plant J.* **2011**, *67*, 817–826. [CrossRef]
61. Tanaka, H.; Kitakura, S.; Rakusová, H.; Uemura, T.; Feraru, M.I.; De Rycke, R.; Robert, S.; Kakimoto, T.; Friml, J. Cell polarity and patterning by PIN trafficking through early endosomal compartments in Arabidopsis thaliana. *PLoS Genet.* **2013**, *9*, e1003540. [CrossRef] [PubMed]
62. Baster, P.; Robert, S.; Kleine-Vehn, J.; Vanneste, S.; Kania, U.; Grunewald, W.; De Rybel, B.; Beeckman, T.; Friml, J. SCF(TIR1/AFB)-auxin signalling regulates PIN vacuolar trafficking and auxin fluxes during root gravitropism. *Embo J.* **2013**, *32*, 260–274. [CrossRef]
63. Abas, L.; Benjamins, R.; Malenica, N.; Paciorek, T.; Wiśniewska, J.; Moulinier-Anzola, J.C.; Sieberer, T.; Friml, J.; Luschnig, C. Intracellular trafficking and proteolysis of the Arabidopsis auxin-efflux facilitator PIN2 are involved in root gravitropism. *Nat. Cell Biol.* **2006**, *8*, 249–256. [CrossRef]
64. Kleine-Vehn, J.; Huang, F.; Naramoto, S.; Zhang, J.; Michniewicz, M.; Offringa, R.; Friml, J. PIN auxin efflux carrier polarity is regulated by PINOID kinase-mediated recruitment into GNOM-independent trafficking in Arabidopsis. *Plant Cell* **2009**, *21*, 3839–3849. [CrossRef]
65. Park, Y.J.; Lee, H.J.; Gil, K.E.; Kim, J.Y.; Lee, J.H.; Lee, H.; Cho, H.T.; Vu, L.D.; De Smet, I.; Park, C.M. Developmental Programming of Thermonastic Leaf Movement. *Plant Physiol.* **2019**, *180*, 1185–1197. [CrossRef]
66. Liu, J.; Shi, X.; Zhong, T.; Jie, W.; Xu, R.; Ding, Y.; Ding, C. PINOID and PIN-FORMED Paralogous Genes Are Required for Leaf Morphogenesis in Rice. *Plant Cell Physiol.* **2023**, *64*, 1146–1158. [CrossRef]
67. Omelyanchuk, N.A.; Kovrizhnykh, V.V.; Oshchepkova, E.A.; Pasternak, T.; Palme, K.; Mironova, V.V. A detailed expression map of the PIN1 auxin transporter in *Arabidopsis thaliana* root. *BMC Plant Biol.* **2016**, *16* (Suppl. S1), 5. [CrossRef]

68. Long, Y.; Chen, Q.; Qu, Y.; Liu, P.; Jiao, Y.; Cai, Y.; Deng, X.; Zheng, K. Identification and functional analysis of PIN family genes in *Gossypium barbadense*. *PeerJ* **2022**, *10*, e14236. [CrossRef]
69. Barbosa, I.C.R.; Hammes, U.Z.; Schwechheimer, C. Activation and Polarity Control of PIN-FORMED Auxin Transporters by Phosphorylation. *Trends Plant Sci.* **2018**, *23*, 523–538. [CrossRef]
70. Hu, L.; Wang, P.; Long, X.; Wu, W.; Zhang, J.; Pan, Y.; Cheng, T.; Shi, J.; Chen, J. The PIN gene family in relic plant L. chinense: Genome-wide identification and gene expression profiling in different organizations and abiotic stress responses. *Plant Physiol. Biochem.* **2021**, *162*, 634–646. [CrossRef]
71. Zhu, K.; Zhang, Y.; Shen, W.; Yu, L.; Li, D.; Zhang, H.; Miao, C.; Ding, X.; Jiang, Y. Genome-Wide Analysis and Expression Profiling of Glyoxalase Gene Families Under Abiotic Stresses in Cucumber (*Cucumis sativus* L.). *Int. J. Mol. Sci.* **2024**, *25*, 11294. [CrossRef] [PubMed]

plants

MDPI

Article

Fatty Acid ABCG Transporter *GhSTR1* Mediates Resistance to *Verticillium dahliae* and *Fusarium oxysporum* in Cotton

Guanfu Cheng [1,†], Xiuqing Li [1,†,‡], W. G. Dilantha Fernando [2], Shaheen Bibi [2], Chunyan Liang [1], Yanqing Bi [1], Xiaodong Liu [1] and Yue Li [1,*]

[1] Key Laboratory of Biological Ecological Adaptation and Evolution in Extreme Environments, College of Life Science, Xinjiang Agricultural University, Urumqi 830001, China; cgfyouxi@163.com (G.C.); 15099389419@163.com (X.L.); lcyiang060723@163.com (C.L.); b916228271@126.com (Y.B.); xiaodongliu75@aliyun.com (X.L.)

[2] Department of Plant Science, University of Manitoba, Winnipeg, MB CAR3T2N2, Canada; dilantha.fernando@umanitoba.ca (W.G.D.F.); shaheen.bibi@umanitoba.ca (S.B.)

* Correspondence: liyue6905@126.com

† These authors contributed equally to this work.

‡ Current address: School of Information Management, Xinjiang University of Finance and Economics, Urumqi 830012, China.

Abstract: Verticillium wilt and Fusarium wilt cause significant losses in cotton (*Gossypium hirsutum*) production and have a significant economic impact. This study determined the functional role of *GhSTR1*, a member of the ABCG subfamily of ATP-binding cassette (ABC) transporters, that mediates cotton defense responses against various plant pathogens. We identified *GhSTR1* as a homolog of *STR1* from *Medicago truncatula* and highlighted its evolutionary conservation and potential role in plant defense mechanisms. Expression profiling revealed that *GhSTR1* displays tissue-specific and spatiotemporal dynamics under stress conditions caused by *Verticillium dahliae* and *Fusarium oxysporum*. Functional validation using virus-induced gene silencing (VIGS) showed that silencing *GhSTR1* improved disease resistance, resulting in milder symptoms, less vascular browning, and reduced fungal growth. Furthermore, the *AtSTR1* loss-of-function mutant in *Arabidopsis thaliana* exhibited similar resistance phenotypes, highlighting the conserved regulatory role of *STR1* in pathogen defense. In addition to its role in disease resistance, the mutation of *AtSTR1* in *Arabidopsis* also enhanced the vegetative and reproductive growth of the plant, including increased root length, rosette leaf number, and plant height without compromising drought tolerance. These findings suggest that *GhSTR1* mediates a trade-off between defense and growth, offering a potential target for optimizing both traits for crop improvement. This study identifies *GhSTR1* as a key regulator of plant–pathogen interactions and growth dynamics, providing a foundation for developing durable strategies to enhance cotton's resistance and yield under biotic and abiotic stress conditions.

Keywords: *GhSTR1*; ABCG transporter; cotton disease resistance; Verticillium wilt and Fusarium wilt; growth–defense trade-off

1. Introduction

Cotton (*Gossypium hirsutum*) is an economically important crop that plays a key role in the global textile industry [1]. However, vascular diseases, mainly Verticillium wilt and Fusarium wilt, significantly affect its production. These diseases have resulted in 10–35% annual yield losses in cotton production and reduced fiber quality [2]. Verticillium wilt and Fusarium wilt are caused by the soil-borne pathogens *Verticillium dahliae* and

Fusarium oxysporum, respectively. These two pathogens are significant issues in cotton production in China, especially in Xinjiang province [3]. Both pathogens invade plants through the roots and establish infection in the vascular tissue, thus disrupting water transport and inducing symptoms, such as leaf chlorosis and systemic wilt [2,4]. Cultural practices and fungicide applications have been used to mitigate these diseases. However, these methods are not entirely effective in managing pathogens, and using fungicides often leads to fungicide resistance, high costs, and high environmental risks [5]. Plant breeding, which focuses on genetic resistance, has emerged as a promising alternative to the traditional methods for mitigating these diseases. Genetic resistance is more effective for cotton production and promotes environmentally sustainable agricultural practices [6]. However, candidate resistance resources are limited for genetic resistance in Cotton against *Verticillium dahliae* and *Fusarium oxysporum* [3,7]. Given the substantial economic and agricultural impact of these diseases, it is essential to identify more genes related to cotton defense and use them for cotton breeding and resistance [8].

Plants can prevent pathogen invasion and limit their growth through innate immunity, where the immune system relies on signal transduction pathways [9]. Innate immunity initiates a regulatory mechanism that overcomes pathogen invasion. Plants enhance their resistance to pathogen invasion by fortifying the cell wall, reprogramming metabolic pathways, and activating signal transduction cascades that restrict pathogen colonization and dissemination [10,11]. Pathogens deploy effector proteins and toxins to inhibit host defense mechanisms. This approach enables pathogens to establish infections and use their carbon and energy resources to support pathogen multiplication [12]. Fatty acids, the key energy reserve structural components in plants, serve as a resource for competition between plants and pathogens [13]. During pathogen infection, plants enhance their disease resistance through the stringent use of these resources [14]. However, pathogens often counteract these defenses by activating host fatty acid transporters, enabling them to "hijack" fatty acids directly from plant cells for their growth and infection processes [15]. In addition to their function in plant–pathogen interactions, fatty acids play a significant role in symbiotic relationships. For example, arbuscular mycorrhizal fungi (AMF) depend on their symbiotic association with host plants to obtain fatty acids as their primary carbon source [16,17]. This dual role of fatty acid transport makes them key constituents for plant defense mechanisms against pathogens and as a regulatory element in maintaining plant–microbe symbiosis.

Fatty acid transport proteins, particularly ATP-binding cassette (ABC) transporters, have been shown to play a vital role in facilitating transmembrane fatty acid movement, which regulates the spatial and temporal distribution of fatty acids and maintains the equilibrium between plant growth and defense requirements [18,19]. Among the ABC transporters, the ABCG subfamily is the most functionally diverse. This subfamily includes transporters involved in transporting signaling molecules, defensive metabolites, and hormones across membranes [20–22]. Research has shown that ABCG transporters play a critical role in disease response. In *Arabidopsis thaliana*, AtPDR12/AtABCG40 enables the transport of abscisic acid (ABA), thereby regulating stomatal closure and limiting pathogen entry [23,24]. PEN3/AtABCG36/AtPDR8 in *Arabidopsis thaliana* facilitates the efflux of defensive metabolites, increases callose deposition, and strengthens the physical barriers against pathogen invasion [25]. In *Nicotiana benthamiana*, NbABCG1 and NbABCG2 secrete antifungal diterpenoids while limiting the biosynthesis of pathogen-supportive metabolites, such as eugenol, during *Phytophthora infestans* infection [26]. In rice (*Oryza sativa*), OsABCG31 mediates the movement of resistance-related metabolites, thereby protecting *Magnaporthe oryzae* and *Rhizoctonia solani* [27]. In wheat (*Triticum aestivum*), Lr34 offers broad-spectrum resistance to fungal pathogens by transporting sinapyl alcohol, a precursor

of cell wall lignification [28]. These findings demonstrate the functional diversity of ABCG transporters and their critical roles in plant disease resistance through the transport of metabolites and hormones.

Despite these significant studies on the roles of ABCG transporters in plant disease resistance, their specific functions in cotton, particularly in response to Verticillium wilt and Fusarium wilt, have not been studied thoroughly. Recent studies have identified stunted arbuscule (STR) and STR2 as fatty acid ABCG transporters in *Medicago truncatula*. These transporters facilitate the transport of plastid-synthesized fatty acids to the extracellular space and provide carbon sources for arbuscular mycorrhizal fungi [29]. Additionally, AP2/ERF, the key transcription factor in *Medicago*, is shown to regulate fatty acid transport by binding to the AW-box cis-regulatory element in the STR/STR2 promoter and activating its expression [30]. Based on these studies, this study aimed to understand the role of the homologous *GhSTR1* gene in Cotton. Using the amino acid sequence of *Medicago STR1* as a reference, the homologous *GhSTR1* gene was identified in cotton via sequence similarity analysis using BlastP. The expression of *GhSTR1* was found to be induced upon infection with *Verticillium dahliae* and *Fusarium oxysporum*. Functional analysis using virus-induced gene silencing (VIGS) indicated that *GhSTR1* is a negative regulator of disease resistance in cotton. To further validate its role, the homologous *AtSTR1* gene in *Arabidopsis* was deleted using T-DNA insertional mutagenesis (*Atstr1*). Loss of *AtSTR1* significantly increased the resistance to both Verticillium wilt and Fusarium wilt, further validating our findings in cotton. These findings indicate the functional role of *GhSTR1* as a negative regulator of cotton defense against Verticillium wilt and Fusarium wilt. Understanding *GhSTR1's* role broadens our knowledge of ABCG transporters in plant–pathogen interactions in cotton and provides a novel approach to enhance disease resistance in cotton.

2. Results

2.1. Cloning and Bioinformatics Analysis of GhSTR1

Based on the *MtSTRI* function in interaction with arbuscular fungi, as indicated by many studies, a homologous protein in *Gossypium hirsutum* (cotton), designated as Gohir.A12G270100, was identified through homology searches in the Phytozome database and named *GhSTR1*. Using cDNA from the leaves of the cotton cultivar Junmian 1 as a template, the *GhSTR1* coding sequence (CDS) was successfully amplified via PCR, yielding a fragment of 2454 bp (Figure 1a). Bioinformatic analysis revealed that *GhSTR1* encodes a protein comprising 817 amino acids, predicted to be basic, hydrophilic, and unstable, with subcellular localization at the cell membrane. Using a homology-based approach, AtSTR1, a protein from Arabidopsis thaliana, was selected as a reference. Structural predictions using the SMART7 platform indicated that GhSTR1, MtSTR1, and AtSTR1 possess conserved ATPases associated with a variety of cellular activities and transmembrane helices, which are key characteristics of the ABCG subfamily of ABC transporters (Figure 1b). According to the HUGO (Human Genome Organization) nomenclature, ABC transporters are classified into eight subfamilies (ABCA–ABCH), with the ABCH subfamily absent in plants [21]. To examine the evolutionary relationship of GhSTR1, sequences from other plant ABC transporter gene families, including *Carya illinoinensis* (pecan), *Juglans regia* (walnut), *Alnus glutinosa* (alder), *Theobroma cacao* (cacao), *Citrus* x *clementina* (clementine), *Prunus avium* (cherry), and *Ricinus communis* (castor bean), were retrieved from GenBank. A phylogenetic tree was constructed using MEGA11 that revealed that GhSTR1 shares the closest evolutionary relationship with MtSTR1 and AtSTR1, with sequence similarities of 70.14% and 63.27%, respectively (Figure 1c). By integrating phylogenetic analysis and protein structural predictions, GhSTR1 was classified as a member of the ABCG subfamily, which is consistent with the classification of MtSTR1 and AtSTR1.

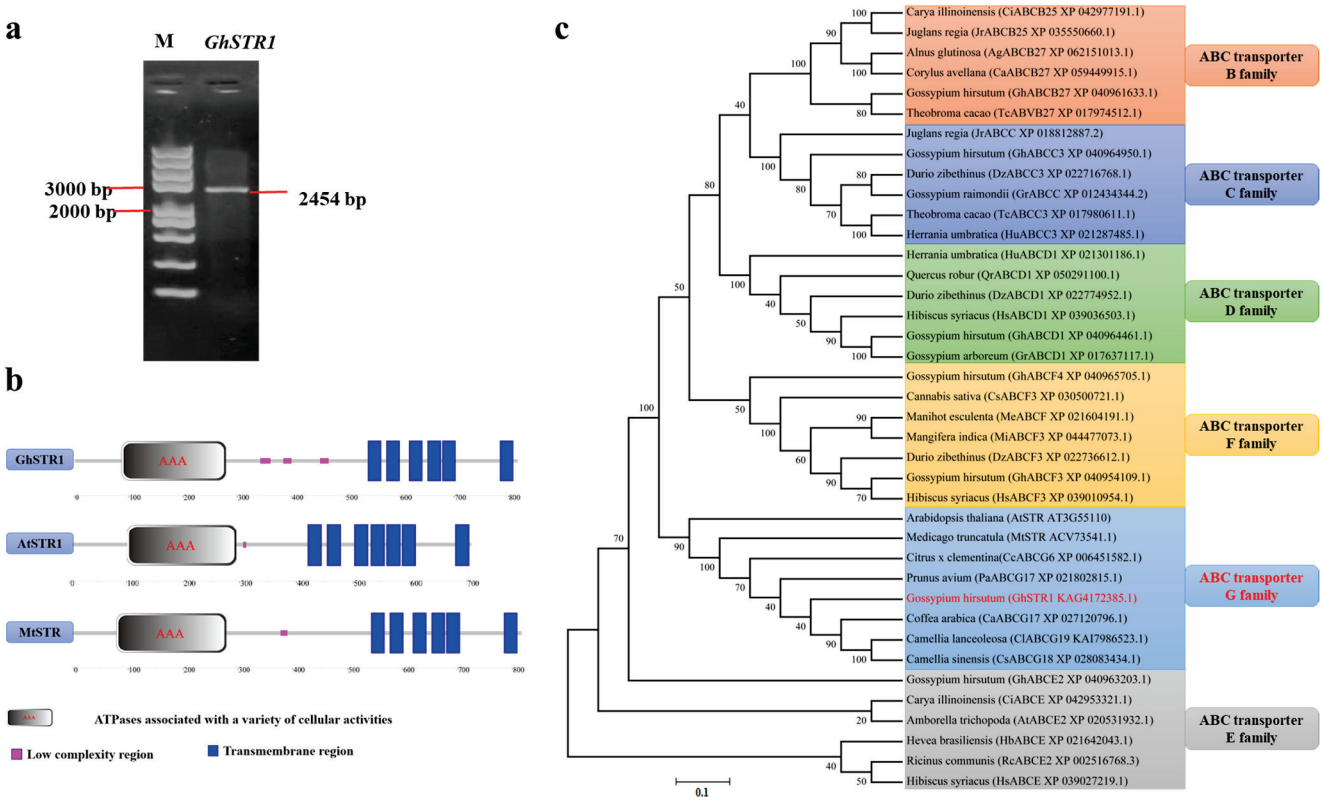

Figure 1. Cloning, structural analysis, and phylogenetic relationships of *GhSTR1*. (**a**) PCR amplification of the *GhSTR1* gene. The red arrow indicates the target band at the expected size of 2454 bp, confirming the successful cloning of the *GhSTR1* coding sequence (CDS). (**b**) Protein domain comparison. SMART-based domain predictions showed that *GhSTR1*, *MtSTR1*, and *AtSTR1* share a conserved AAA ATPase domain (red oval) and transmembrane helices (blue rectangles), which are characteristic features of the ABCG subfamily. (**c**) The phylogenetic analysis of GhSTR1 was conducted using MEGA11 to study the primary ABC transporter proteins from *Carya illinoinensis* (pecan), *Juglans regia* (walnut), *Alnus glutinosa* (alder), *Theobroma cacao* (cacao), *Citrus x clementina* (clementine), *Prunus avium* (cherry), and *Ricinus communis* (castor bean). The evolutionary relationships among these major ABC transporter proteins were analyzed using the Neighbor-Joining (NJ) method and the JTT substitution model in MEGA11 software (The red section of the figure illustrates the cotton proteins and their corresponding protein families analyzed in this study). Bootstrap analyses with 1000 replications were performed on the nodes of the phylogenetic tree to evaluate their statistical support. As shown in Figure 1c, the statistical support for key nodes confirms the robustness of the inferred evolutionary relationships. The phylogenetic tree indicates that GhSTR1 is closely related to MtSTR1 and AtSTR1, confirming its classification within the ABCG subfamily.

2.2. Expression Analysis of GhSTR1 Under V991 and St89 Stress

To investigate the expression pattern of the *GhSTR1* gene in cotton under stress from *V. dahliae* V991 (Verticillium wilt) and *F. oxysporum* St89 (Fusarium wilt), 15-day-old seedlings were inoculated using the root-dipping method [31]. Samples were collected from roots and true leaves at 0, 12, 24, 48, 72, 96, and 120 h post-inoculation (hpi). Water-treated plants (CK group) served as controls for analyzing the spatiotemporal expression characteristics of *GhSTR1* under these stress conditions. Under *V. dahliae* stress, *GhSTR1* expression in the leaves and roots showed dynamic variability. In leaves, the expression was significantly downregulated at 24 h and 96 h, followed by significant upregulation at 120 h ($p < 0.05$) (Figure 2a). In the roots, the expression followed a "rise–fall–rise–fall" pattern, with significant upregulation at 72 h and downregulation at 120 h ($p < 0.05$). No significant changes were observed at other time points (Figure 2b). Under *F. oxysporum* stress, a similar fluctuating expression pattern of *GhSTR1* was observed in both the leaves and roots. In

leaves, significant downregulation occurred at 48 h, followed by considerable upregulation at 72 h and 120 h ($p < 0.05$) (Figure 2c). In the roots, expression was significantly upregulated at 96 h and downregulated at 120 h ($p < 0.05$), with no significant differences at other time points (Figure 2d). In the uninfected control cotton tissues (roots, stems, and true leaves), *GhSTR1* exhibited distinct tissue-specific expression patterns (Supplementary Figure S1). The expression levels in stems were significantly higher than those in roots and leaves, suggesting a potential role in stem-specific physiological processes. These findings revealed that *GhSTR1* shows a notable spatiotemporal and tissue-specific expression pattern when subjected to *V. dahliae* and *F. oxysporum* stress, suggesting its potential involvement in the dynamic modulation of disease resistance mechanisms in cotton.

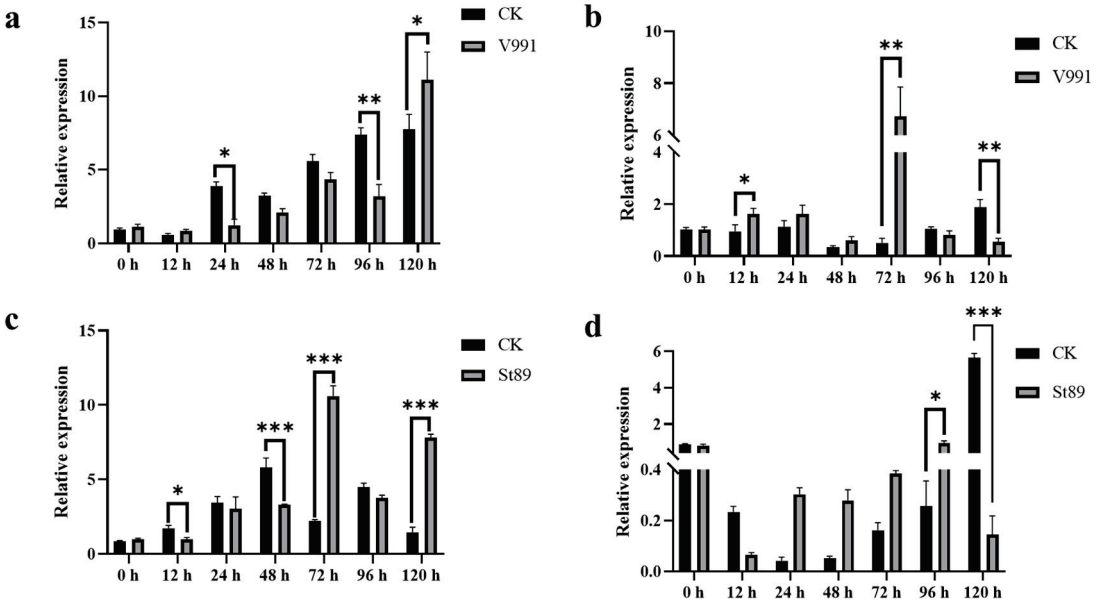

Figure 2. Transcript levels of *GhSTR1* under *Verticillium dahliae* V991 and *Fusarium oxysporum* St89 stress. (**a**,**c**) Relative expression levels of *GhSTR1* in leaves under stress from *V. dahliae* V991 and *F. oxysporum* St89, respectively. (**b**,**d**) Relative expression levels of *GhSTR1* in roots under stress from *V. dahliae* V991 and *F. oxysporum* St89, respectively. Data are expressed as the mean ± standard error ($n = 3$) and normalized to the control group (CK, sterile water treatment). Statistical analysis was conducted using the *t*-test, with significance indicated as follows: * $p < 0.05$, ** $p < 0.01$, and *** $p < 0.001$.

2.3. Construction of the GhSTR1 VIGS Vector and Verification of Silencing Efficiency

A VIGS targeting *GhSTR1* was successfully constructed where a 416 bp target fragment of *GhSTR1* was amplified by PCR and cloned into the TRV vector (Figure 3a). To confirm the cloning of the fragment, the TRV vector was digested with *Eco*RI and *Kpn*I, which yielded fragments of the expected sizes (Figure 3b). To confirm the accuracy of the TRV vector insert, we sequenced the cloned 416 bp fragment of *GhSTR1*. The sequencing data verified that the inserted fragment matches the *GhSTR1* target sequence without errors.

Cotyledons from cotton plants were infiltrated with the resuspended VIGS vector solution, and inoculated plants were kept in a growth chamber for 15 days at the conditions outlined in the methods. In the positive control plants carrying pTRV2::*GhCLA1*, a bleaching phenotype was observed (Figure 3c), demonstrating effective gene silencing. The expression levels of *GhCLA1* and *GhSTR1* were quantified by qRT-PCR. *GhCLA1* expression was significantly reduced in the leaves of pTRV2:: *GhCLA1* plants compared to pTRV2::*00* control, while *GhSTR1* expression was markedly downregulated in both roots and leaves of pTRV2::*GhSTR1* plants (Figure 3d,e). In summary, the TRV-based VIGS system effectively silenced *GhSTR1*, thus providing a reliable tool for its functional analysis.

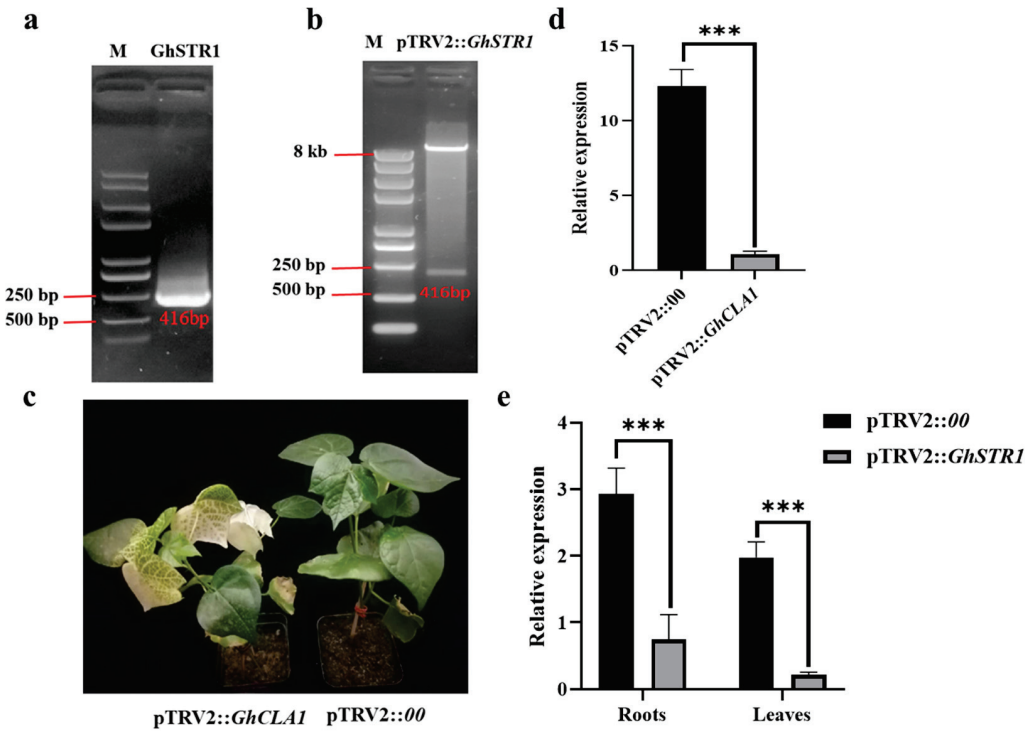

Figure 3. Silencing efficiency of the *GhSTR1* gene. (**a**) PCR amplification of the *GhSTR1* target fragment. (**b**) Restriction digestion of the TRV vector, confirming successful vector construction. (**c**) The bleaching phenotype observed in pTRV2::*GhCLA1*-silenced cotton plants, demonstrating effective gene silencing. (**d**,**e**) Relative expression levels of *GhCLA1* and *GhSTR1* in pTRV2::*00* and pTRV2::*GhSTR1* plants, respectively. Data are presented as the mean ± standard error (n = 3). Statistical significance is indicated as follows: *** $p < 0.001$.

2.4. Knockdown of GhSTR1 Enhances Cotton Resistance to V. dahliae and F. oxysporum

The role of *GhSTR1* in cotton resistance against *V. dahliae* (V991) and *F. oxysporum* (St89) was further investigated by using *GhSTR1*-silenced plants (pTRV2::*GhSTR1*), negative control plants (pTRV2::*00*), and wild-type (WT) plants. Following pathogen inoculation, phenotypic observations, disease index measurements, vascular browning assessments, and fungal biomass quantification were performed over a 20-day infection period. Silencing *GhSTR1* significantly enhanced cotton resistance to both pathogens. Compared to pTRV2::*00* and WT plants, the pTRV2::*GhSTR1* plants exhibited reduced symptoms of leaf chlorosis, wilting, and desiccation (Figure 4a,f). In particular, vascular browning in stems, which serves as an indicator of pathogen invasion severity, was markedly less severe in pTRV2::*GhSTR1* plants (Figure 4b,g). Disease index analysis showed a 50% reduction in disease severity in pTRV2::*GhSTR1* plants compared to that in controls (Figure 4c,h). Fungal biomass quantification confirmed these results, with fungal accumulation in pTRV2::*GhSTR1* plants reduced by over twofold compared to control plants for both *V. dahliae* and *F. oxysporum* (Figure 4d,i). Culturing of pathogens from stems further confirmed that fungal hyphal growth was significantly inhibited in pTRV2::*GhSTR1* plants compared to that in controls (Figure 4e,j). In summary, silencing *GhSTR1* significantly enhanced cotton resistance to *V. dahliae* and *F. oxysporum*, suggesting that *GhSTR1* functions as a negative regulator in disease resistance pathways.

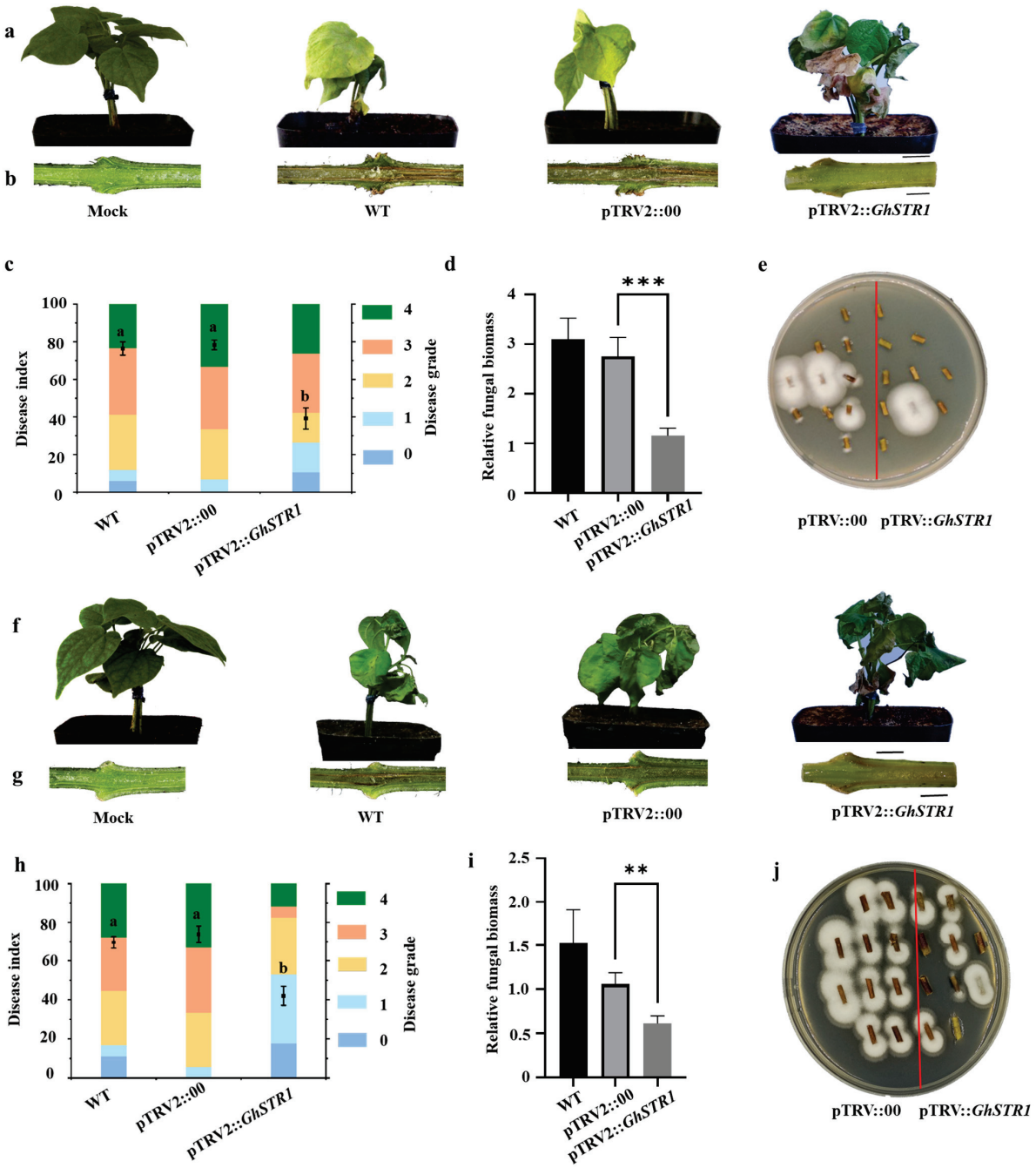

Figure 4. Effects of *GhSTR1* gene silencing in cotton resistance to *V. dahliae* V991 and *F. oxysporum* St89. (**a**,**f**) Leaves of pTRV2::*GhSTR1* plants exhibited more severe chlorosis, wilting, and lesions following infection with *V. dahliae* (V991) and *F. oxysporum* (St89) compared to WT and pTRV2::*00* controls, respectively. Scale bar = 2 cm. (**b**,**g**) Longitudinal sections of infected stems showed more pronounced vascular browning in pTRV2::*GhSTR1* plants, indicating greater pathogen invasion. Scale bar = 0.2 cm. (**c**,**h**) Disease index analysis at 20 dpi revealed significantly higher indices in pTRV2::*GhSTR1* plants than WT and pTRV2::*00* control. (**d**,**i**) qRT-PCR analysis showed significantly higher fungal biomass in pTRV2::*GhSTR1* plants than in the controls. (**e**,**j**) Fungal hyphal growth in stem sections (1 cm above the cotyledonary node) cultured on PDA medium was significantly greater in pTRV2::*GhSTR1* plants than in the controls. Scale bar = 0.2 cm. Each group included ≥30 plants with 3 replicates to ensure result reliability. Data are expressed as the mean ± standard error (n = 3). Statistical significance was assessed using analysis of variance (ANOVA), followed by Duncan's multiple comparison test. The significance levels are indicated as follows: ** $p < 0.01$, and *** $p < 0.001$. Different groups with different letters represent statistically significant differences ($p < 0.05$).

2.5. Identification and Expression Analysis of the AtSTR1 T-DNA Insertion Homozygous Mutant

Based on the information in the database (http://signal.salk.edu/tdnaprimers.2.html) (accessed on 12 June 2024), the *AtSTR1* gene, located on chromosome 3 of *Arabidopsis thaliana*, consists of a single exon, with the T-DNA insertion site in the exon region of the SALK_129014 mutant (Figure 5a). Genotyping was conducted using SALK_129014-LP, SALK_129014-RP, and the T-DNA border primer, LBa1. PCR analysis indicated that the wild-type plants (Col-0) amplified a 1170 bp fragment with LP/RP primers, but no product was amplified with LBa1/RP primers. The homozygous mutant produced a 523–823 bp T-DNA fragment with LBa1/RP primers but no LP/RP product. The heterozygous mutant exhibited both bands. Plants 1 through 8 exclusively amplified the T-DNA fragment, confirming their homozygous status for *AtSTR1* (Figure 5b). To verify the loss of *AtSTR1* expression, the transcription levels in plant 1 (*Atstr1*) and wild-type plants were analyzed using SqRT-PCR and qRT-PCR. Both methods confirmed a significant reduction in *AtSTR1* expression in the mutant, with stable expression of the reference gene *Actin2* (Figure 5c,d). In conclusion, plant 1 (*Atstr1*) was characterized as a homozygous T-DNA insertion mutant, thus providing a robust model for investigating *AtSTR1* function.

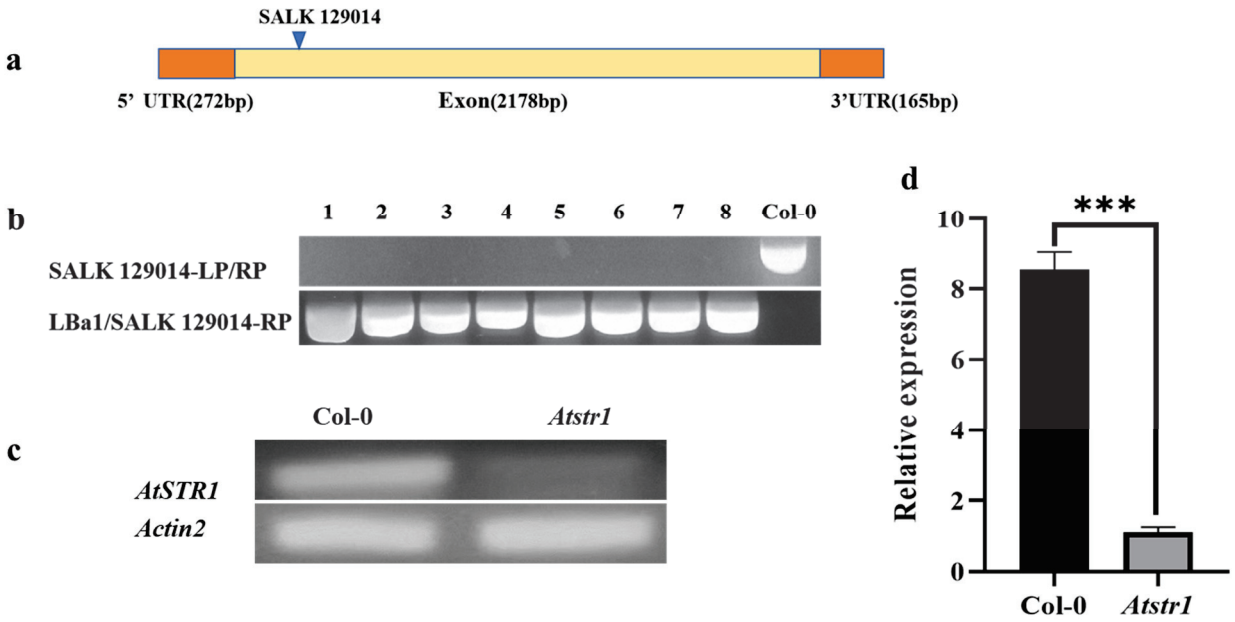

Figure 5. Genotypic validation and expression analysis of *AtSTR1* T-DNA insertion mutant in *Arabidopsis thaliana*. (**a**) Schematic representation of *AtSTR1* gene structure in the SALK_129014 mutant. The promoter is shown as an orange rectangle, the single exon as a yellow rectangle, and the T-DNA insertion site as a blue inverted triangle. (**b**) Genotyping results for the homozygous SALK_129014 mutant. Homozygous plants lacked amplification with LP/RP primers but showed a T-DNA-specific fragment with LBa1/RP primers. (**c**) SqRT-PCR showed reduced *AtSTR1* expression in the *Atstr1* mutant compared to that in the wild-type plants. *Actin2* was used as the reference gene for normalization. (**d**) qRT-PCR confirmed significantly reduced *AtSTR1* expression in the *Atstr1* mutant relative to the wild-type plants. Data are presented as mean ± standard error ($n = 3$), with statistical significance indicated as follows: *** $p < 0.001$.

2.6. Atstr1 Mutant Enhances Resistance to V. dahliae (V991) and F. oxysporum (St89) in Arabidopsis thaliana

To evaluate the role of *STR1* genes in disease resistance, the *Atstr1* mutant of *Arabidopsis thaliana* was tested against *V. dahliae* (V991) and *F. oxysporum* (St89). Following 15 days of infection, the *Atstr1* mutant showed significantly enhanced resistance compared to wild-type (Col-0) plants. The mutant showed decreased chlorosis, wilting, and growth

inhibition (Figure 6a,e). Disease index analysis also confirmed a substantial reduction in disease severity within the mutant (Figure 6c,g). Stem cross-sections revealed moderate vascular browning in the *Atstr1* mutant compared to the severe browning observed in wild-type plants (Figure 6b,f). qRT-PCR analysis further attested to these findings by determining significantly lower fungal biomass in mutant than wild-type plants (Figure 6d,h). These findings indicate that the *AtSTR1* gene negatively influences disease resistance in *Arabidopsis*, implying a potentially conserved role of *STR1* genes in plant defense mechanisms. This research offers significant contributions to our understanding of the regulatory pathways underlying plant–pathogen interactions.

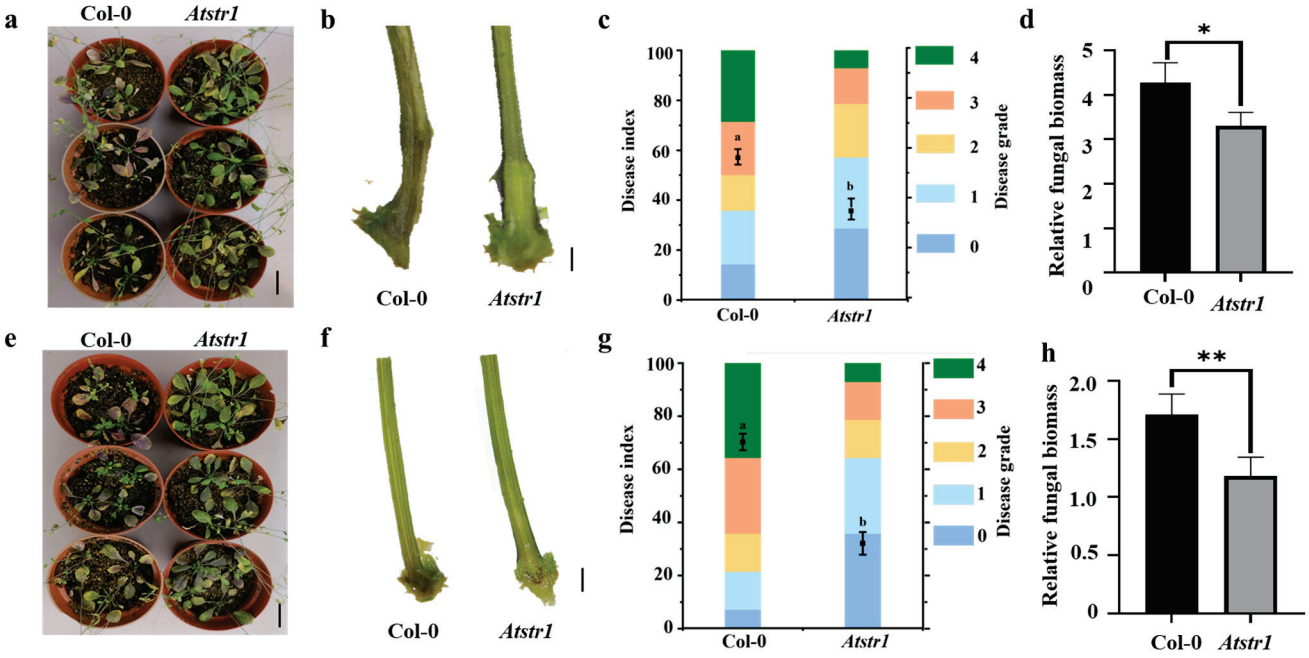

Figure 6. Enhanced resistance of *Atstr1* mutant to *V. dahliae* (V991) and *F. oxysporum* (St89). (**a**,**e**) Phenotypic comparison of *Arabidopsis thaliana* Col-0 wild-type and *Atstr1* mutant 15 days post-infection (dpi) with *V. dahliae* (V991) and *F. oxysporum* (St89), respectively. *Atstr1* mutant displayed reduced wilting and chlorosis compared to the wild-type plants. Scale bar = 1 cm. (**b**,**f**) Stem longitudinal sections 1 cm above the tillering node, showing vascular browning at 15 dpi with V991 and St89. *Atstr1* mutant exhibited milder vascular browning compared to the wild-type plants. Scale bar = 0.2 cm. (**c**,**g**) Disease index values at 15 dpi. *Atstr1* mutant showed significantly lower disease indices than the wild-type plants for both V991 and St89 infections. (**d**,**h**) qRT-PCR analysis of the fungal biomass at 15 dpi. *Atstr1* mutant exhibited significantly reduced fungal biomass compared to wild-type plants. Data are expressed as mean ± standard error (n = 3). Statistical significance was assessed using analysis of variance (ANOVA), followed by Duncan's multiple comparison test. Significance levels are indicated as follows: * $p < 0.05$, ** $p < 0.01$. Groups with different letters represent statistically significant differences at $p < 0.05$.

2.7. AtSTR1 Mutant Enhances Growth and Development in Arabidopsis thaliana

Plants with increased stress resistance often exhibit reduced growth, posing a challenge for resistance breeding [32]. To evaluate the effects of the *AtSTR1* mutation (*Atstr1*) on the growth and development of *Arabidopsis thaliana*, we recorded key morphological characteristics during the early growth phase (15 days) and reproductive stage (45 days). Phenotypic analysis indicated that the *Atstr1* mutant showed improved growth compared to wild-type (Col-0) plants (Figure 7a). The mutant demonstrated increased root elongation (Figure 7b), expanded rosette leaf size (Figure 7c,d), and a greater number of rosette leaves (Figure 7e) at the 15-day mark. By day 45, the *Atstr1* mutant showed accelerated bolting (Figure 7f), an overall great plant height (Figure 7g), and an increased number of bolting

branches and siliques relative to the wild-type specimens (Figure 7h,i). These observations suggest that the absence of *AtSTR1* considerably enhanced both the vegetative and reproductive developmental traits. In conclusion, the functional loss of *AtSTR1* promoted growth vigor and development efficiency in *Arabidopsis*, highlighting its key role as a negative regulator of plant growth. These findings suggest the potential of targeting *AtSTR1* for improving growth traits in breeding programs.

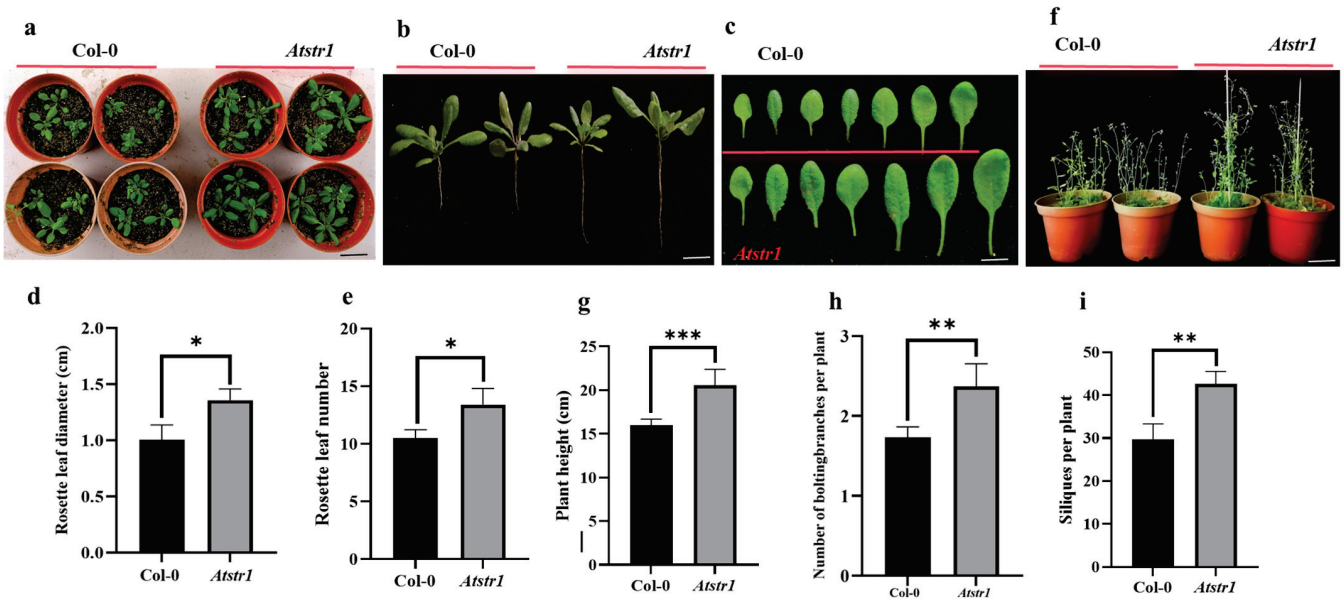

Figure 7. Growth and development phenotype analysis of *Atstr1* mutant in *Arabidopsis thaliana*. (**a**) Overall developmental state of the wild-type (Col-0) and *Atstr1* mutant during the 15-day growth stage. Scale bar = 5 cm. (**b**) Root length measurements during the 15-day growth period. Scale bar = 1 cm. (**c**) Leaf size of the wild-type and *Atstr1* mutant during the 15-day growth stage. Scale bar = 2 mm. (**d**) Rosette leaf diameter during the 15-day growth stage. The average diameter was measured at the widest point of the leaf blade across all rosette leaves of the plant. (**e**) Rosette leaf number during the 15-day growth stage. (**f**) Overall developmental state of the wild-type and *Atstr1* mutant during the 45-day growth stage. Scale bar = 5 cm. (**g**) Plant height during the 45-day growth stage. (**h**) Number of bolted branches per plant during the 45-day growth stage. (**i**) Number of siliques per plant during the 45-day growth stage. Forty plants were analyzed for each treatment. Data are presented as the mean ± standard error (SEM; $n = 3$). The statistical significance is as follows: * $p < 0.05$, ** $p < 0.01$, and *** $p < 0.001$.

2.8. Phenotypic Analysis of Atstr1 Mutant Under Drought Stress

To assess the effect of *AtSTR1* deletion on drought tolerance, wild-type (Col-0) and *Atstr1* mutant plants were grown in nutrient-rich soil for 25 days and then subjected to drought stress by withholding water. After 10 days of drought treatment, both genotypes showed typical drought symptoms, including leaf wilting, desiccation, curling, and slow growth, with no significant phenotypic differences observed between *Atstr1* mutant and wild-type plants (Figure 8a). Plants that were rated for survival following 8 days of rehydration also showed no significant differences between the two genotypes (Figure 8b), indicating that *AtSTR1* deletion does not affect drought tolerance in *Arabidopsis*. Water loss rate analysis further confirmed these findings. Across the eight time points, no significant differences in water retention patterns were detected between *Atstr1* mutant and wild-type plants (Figure 8c). These results align with those of the survival rate analysis, demonstrating that the loss of *AtSTR1* has no significant impact on drought tolerance in *Arabidopsis*. These findings suggest that *AtSTR1* may not play a critical role in drought stress responses, although it does have a key involvement in other abiotic stress.

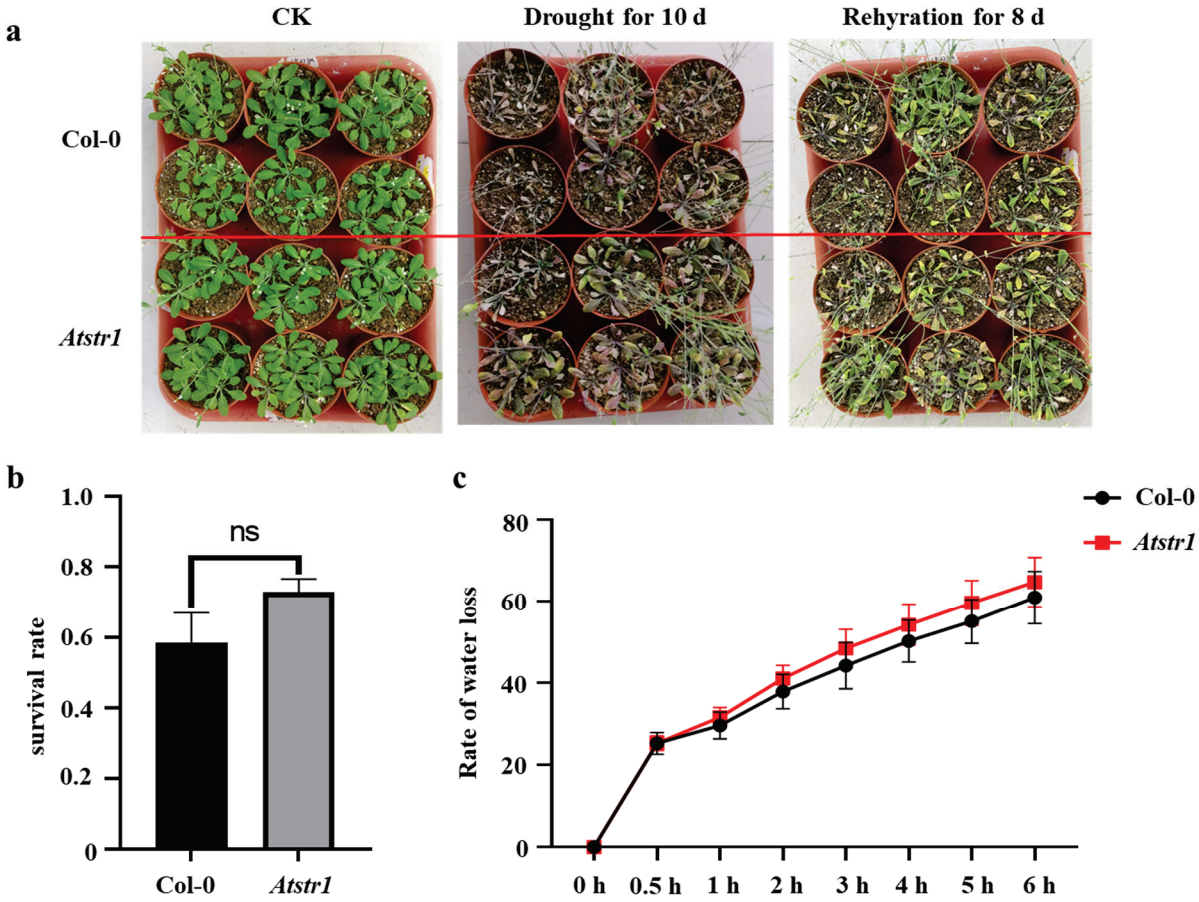

Figure 8. Phenotypic and physiological analysis of *Atstr1* mutant under drought stress. (**a**) Phenotypic comparison of *Arabidopsis thaliana* Col-0 wild-type and *Atstr1* mutant plants before drought treatment, after 10 days of drought stress, and following 8 days of rehydration. (**b**) Survival rate analysis of Col-0 and *Atstr1* mutant plants after drought stress and rehydration. (**c**) Water loss rate curves comparing Col-0 and *Atstr1* mutant plants during drought stress. A total of 40 plants were analyzed per treatment. Data are presented as mean ± standard error (SEM; $n = 3$). Statistical significance is as follows: ns: no significant difference.

3. Discussion

Verticillium wilt and Fusarium wilt significantly affect cotton production in China and drastically impact crop yield and quality. While current management strategies have shown some effectiveness, their use is limited due to their economic costs and environmental impact. Therefore, it is crucial to develop resistance in cotton plants using molecular breeding.

Previous studies have revealed that pathogen virulence is influenced by the availability of sugar and fatty acids provided by the host plant. This provides a novel approach to enhance plant resistance by regulating the nutrient supply from the host to the pathogen, thus restricting the pathogen [33]. For example, researchers have significantly improved plant resistance and disease reduction in maize smut, rice sheath blight, and cotton Verticillium wilt by silencing SWEET sugar transporter genes [33–35]. Previous research has also shown that fatty acids are the primary carbon source transferred from host plants to arbuscular mycorrhizal fungi [16,36]. In *Medicago truncatula*, the *STR*/*STR2* genes regulate lipid transport and play a crucial role in the formation of mycorrhizae [29].

Based on these studies and information on the *STR1* gene associated with fatty acid transport proteins, we identified its homologous gene in *Gossypium hirsutum* cv. Junmian1 using BlastP. The gene homologous to *STR1* was amplified using PCR. Bioinformatics analysis revealed that *GhSTR1* encodes a protein consisting of 817 amino acids. We characterized

the gene and found it to be basic, hydrophilic, and unstable, and predicted to be localized to the cell membrane. SMART and phylogenetic analyses indicated that *GhSTR1* contains ATPase domain (AAA) associated with various cellular activities and six transmembrane domains, classifying it in the same ABCG subfamily as *MtSTR1* and *AtSTR1 (*Figure 1).

Previous studies have demonstrated that ABCG transporters are essential for plant resistance. Several examples from across different plant species have provided evidence to support this claim. In Arabidopsis thaliana, AtPDR12 [23] and AtABCG36 [24] have been shown to play a significant role in plant immunity. Similarly, NbABCG1 and NbABCG2 in tobacco [26], OsABCG31 in rice [27], and Lr34 in wheat [28] have been shown to regulate plant defense. These transporters move metabolites or signaling molecules, thereby controlling the response of plants to pathogens. However, the role of these transporters has not been explored deeply in cotton.

Given that these transporters are less studied in cotton, we investigated the expression patterns of *GhSTR1* in *Gossypium hirsutum* cv Junmian1 in response to *Verticillium dahliae* V991 and *Fusarium oxysporum* St89 inoculation. Our results from the study revealed that *GhSTR1* expression under pathogen-induced stress exhibited notable tissue specificity and temporal variations, following either "rise–fall–rise–fall" or "fall–rise–fall" patterns (Figure 2). These fluctuating gene expressions suggest that the plants use a multistage regulatory approach to combat pathogen invasion. The initial decrease in expression suggests that the plant restricts fatty acid transport to the pathogen to limit its growth. Conversely, the increase in gene expression indicates that the plant might be regulating its metabolic balance to enhance its defense. Furthermore, the tissue-specific expression observed in roots and leaves might be associated with infection routes and localized defense needs, implying that *GhSTR1* contributes to localized and systemic defense responses.

Recently, virus-induced gene silencing (VIGS) technology has been widely used to study gene function in cotton, owing to its high efficiency [37]. VIGS has been used to demonstrate the role of *GhPLP2* in regulating fatty acid metabolism and the Jasmonic acid signaling pathway, as well as its function in regulating resistance to Verticillium wilt [38]. In this study, we used VIGS to understand the role of the fatty acid transporter gene *GhSTR1* in cotton resistance to Fusarium wilt and Verticillium wilt. The results from our study indicated that silencing the expression of *GhSTR1* significantly increased resistance to both Fusarium wilt and Verticillium wilt. Plants with silenced *GhSTR1* showed reduced disease indices, reduced vascular browning, and decreased fungal biomass, suggesting enhanced resistance (Figure 4).

Although the negative regulatory role of *GhSTR1* has been studied using VIGS technology, the results may be limited by the instability and off-target effects inherent to VIGS. To further validate the function of *GhSTR1*, the role of *AtSTR1* (the homologous gene in *Arabidopsis thaliana*) was studied using T-DNA insertion mutagenesis. Under pathogen stress, the *Atstr1* mutant showed significantly lower disease indices, a reduction in vascular browning, and decreased fungal biomass compared to the wild-type (Col-0), indicating an increase in disease resistance (Figure 6). These findings are consistent with the functional identification of *GhSTR1* using VIGS and further confirm the role of *GhSTR1* in cotton's response to *Verticillium dahliae* and *Fusarium oxysporum*. Interestingly, GhSTR1 is predicted to localize to the cell membrane, whereas its homolog AtSTR1 (also known as ABCG19) has been reported to localize to the vacuole membrane in *Arabidopsis thaliana* [39]. This discrepancy suggests that *STR1* genes may have context-dependent localization or dual roles in fatty acid transport. In the future, we should investigate whether GhSTR1 exhibits dynamic membrane localization under pathogen stress and whether this affects its role in disease resistance.

This research highlights the critical role of resistance genes in enhancing crop resistance to pathogens. However, practical breeding efforts require a comprehensive study of traits such as growth and development, drought tolerance, quality, and yield to ensure stable performance under multiple stress conditions [32]. This study showed that the *Atstr1* mutant showed overall better growth, including leaf area, root area, root length, and plant height, than the wild type (Figure 7). However, in the experiment on drought stress, there were no significant differences between mutant and wild-type plants in terms of survival rate and water loss (Figure 8). These results indicate a possible divergence in the functional roles of *AtSTR1* in disease resistance and drought tolerance.

Developing breeding techniques focused on nutrient delivery for disease resistance has been widely recognized as a practical and durable approach [40]. For example, CRISPR/Cas9 gene editing has been efficiently used to change TALE-binding elements, such as SWEET gene promoters, resulting in broad-spectrum resistance to bacterial blight in rice [41,42]. This research identified a novel modulator of cotton resistance to Fusarium and Verticillium wilts. This finding indicates the functional importance of ABCG transporters in plant–pathogen interactions. Our results suggest that *GhSTR1* is vital for cotton's disease resistance mechanisms, although further research is required for deeper analysis of its function pathways.

Furthermore, *GhSTR1* may interact with other defense-related systems. Exploring these potential cross-regulatory interactions could significantly increase our understanding of cotton's complex networks governing disease resistance. Moreover, gene-editing technologies could precisely control fatty acid transport between cotton and pathogenic fungi, an approach known as "starvation therapy." Targeting the metabolic requirements of pathogens could effectively diminish the pathogen virulence and boost disease resistance in plants.

This study provides theoretical support for improving cotton disease resistance and suggests innovative gene editing and cross-pathway regulation strategies. To maximize their relevance in practical breeding programs, future studies should confirm these findings in multi-gene scenarios and under various environmental conditions.

4. Materials and Methods

4.1. Plant Materials and Growth Conditions

Seeds of *Gossypium hirsutum* cv. "Junmian 1" were surface-sterilized with 75% ethanol and rinsed with sterile water twice. They were soaked in 30% hydrogen peroxide (H_2O_2) at 28 °C for 3 h. Residual H_2O_2 was removed by rinsing the seeds 3 to 5 times with sterile conditions. Seeds were incubated in liquid Murashige and Skoog (MS) medium at 28 °C in the dark for 24–48 h until seed germination. Germinated seeds with uniform radicle lengths were subsequently transplanted to the matrix (the vermiculite and black soil in a volume ratio of 1:2). Sixty plants were used for this experiment. The pots were covered with plastic bags and kept under a 16 h light/8 h dark photoperiod at 28 °C with a light intensity of 120 $\mu E \cdot m^{-2} \cdot s^{-1}$ and relative humidity of 60–70%. The plastic bag was removed 5–7 days post-germination, and seedlings were left to grow in the above-mentioned conditions.

For *Arabidopsis thaliana*, Col-0 wild-type, and T-DNA insertion mutant, the seeds were surface-sterilized with 6% sodium hypochlorite for 5 min and rinsed 5 times with sterile water. The seeds were sown on 1/2 MS solid medium and placed at 4 °C in the dark for 3 days. The plates were kept in a growth chamber at 22 °C under a 16 h light/8 h dark photoperiod with a light intensity of 6000–8000 lx for 7 days. After seedling germination, the germinated plants were transplanted into a sterilized substrate of peat, vermiculite, and perlite (4:3:1, $v/v/v$) and grown at 23 °C in a growth chamber with 16 h light/8 h dark photoperiod.

4.2. Pathogen Growth and Inoculation

The fungal strains *Verticillium dahliae* V991 and *Fusarium oxysporum* St89 were used for plant inoculation. The strains were grown on potato dextrose agar (PDA) plates at 28 °C for 3–5 days. The fungal hyphae were then transferred to Czapek-Dox liquid medium ($NaNO_3$, 0.3% *w*/*v*; KH_2PO_4, 0.1% *w*/*v*; $MgSO_4$, 0.1% *w*/*v*; KCl, 0.1% *w*/*v*; $FeSO_4$, 0.0002% *w*/*v*; and sucrose, 3% *w*/*v*; pH 6.0) and incubated at 28 °C with shaking at 180 rpm for 5–7 days.

Cotton plants were inoculated using the root dip method, as described by Zhang [31]. After 15–20 days of growth, the roots, stems, and fully expanded true leaves were sampled from some plants for tissue-specific expression analysis. At the same time, the seedlings with uniform root growth were selected, where roots were washed with water, and the seedlings were immersed in spore suspensions of *V. dahliae* V991 and *F. oxysporum* St89 at a concentration of 1×10^6–10^7 spores·mL^{-1} for 1 min. Seedlings treated with sterile water served as controls (CK). The roots and true leaves were sampled at 0, 12, 24, 48, 72, 96, and 120 h post-inoculation (hpi) for gene cloning and expression pattern analysis.

4.3. Analysis of GhSTR1 Gene Expression Patterns

Total RNA was extracted from collected leaves and roots sampled at 0, 4, 8, 12, 24, and 48 hpi using the Plant Polysaccharide and Polyphenol RNA Extraction Kit (Tiangen, Beijing, China), following the manufacturer's protocol. First-strand cDNA was synthesized using the 5× All-In-One RT MasterMix kit (ABM, Zhenjiang, China). Quantitative RT-PCR (qRT-PCR) was performed on a LightCycler 480 system (Roche, Basilea Switzerland) using SYBR Premix Ex Taq (Takara, Beijing, China). Relative gene expression levels were calculated using the $2^{-\Delta\Delta Ct}$ method [43], with *GhUBQ7* (DQ116441) as the internal reference gene. Each experimental condition consisted of three biological replicates, each biological replicate including three technical replicates (n = 3 for each level). All the primers used for this analysis are listed in Supplementary Table S1.

4.4. Gene Cloning and Sequence Analysis

The amino acid sequence of *Medicago truncatula MtSTR1* (GenBank accession number: ACV73541.1) was used as a query to identify the homologous gene *GhSTR1* in upland cotton through a BlastP search in the Phytozome database (https://phytozome-next.jgi.doe.gov/) (12 June 2024). Primers specific to the *GhSTR1* sequence were designed using primer 5.0 (Table S1). Amplification of the gene was conducted using Phusion High-Fidelity DNA Polymerase (NEB, Ipswich, MA, USA), following the manufacturer's instructions. PCR amplicons were analyzed on 1% agarose gel electrophoresis, and the target bands were excised and cleaned using the Agarose Gel DNA Recovery Kit (Tiangen, Beijing, China). The purified amplicon fragments were ligated into the pEASY Blunt-Zero cloning vector and transformed into *Escherichia coli* DH5α competent cells (Tiangen, Beijing, China) according to manufacture protocol. The restriction enzyme digestion identified positive clones and sequenced by the Shanghai JieLi Biotechnology Co., Ltd. (Shanghai, China).

4.5. Sequence and Bioinformatics Analysis of GhSTR1

The open reading frame (ORF) of *GhSTR1* was analyzed using DNA Star17.6 software. Physicochemical properties, including the molecular weight, isoelectric point, instability index, and hydrophilicity, were predicted using the EXPASY ProtParam tool (https://web.expasy.org/protparam/) (7 May 2024). Subcellular localization was predicted using the LocTree tool (https://www.rostlab.org/services/loctree2/) (8 May 2024). Functional annotation and protein family classification were performed using Prosite (https://prosite.expasy.org/) (10 May 2024) and SMART tools (http://smart.embl-heidelberg.de/) (11 May

2024) [44]. Sequence alignment was conducted using Clustal X, and a phylogenetic tree was constructed using MEGA11 software [45]. These analyses provided insights into the evolutionary characteristics of *GhSTR1*.

4.6. Construction of Silencing Vectors and VIGS in Cotton

The Tobacco rattle virus (TRV)-mediated VIGS technology is well adapted to study the function of genes in cotton [46]. We used this technology to understand the function of *GhSTR1.* To suppress *GhSTR1* expression, the target sequences were designed using the SGN-VIGS online tool (https://vigs.solgenomics.net/) (12 June 2024). Primers were designed using DNAMAN software with *Eco*R1 and *Kpn*I restriction sites (Table S1). The PCR product was digested with *Eco*R1 and *Kpn*I and then ligated into the pTRV2 vector using T4 DNA ligase. Ligated products were transformed into *E. coli* DH5α competent cells. Positive clones were confirmed by restriction digestion. Verified pTRV2::*GhSTR1* recombinant plasmids, along with pTRV:RNA1 and pTRV:RNA2 plasmids, were transformed into *Agrobacterium tumefaciens* GV3101 cells via electroporation. The *Agrobacterium* cells were injected into the cotyledons of 7-day-old plants using 1 mL syringes. The plants were then grown at 25 °C under 16 h /8 h light/dark cycle, as described by Li [5]. Approximately 15 days post-infection, bleaching of leaves was observed in the positive control group (pTRV2::*GhCLA1*). Root and true leaf samples were collected from the experimental group (pTRV2::*GhSTR1*) and control group (pTRV2::*00*). Silencing efficiency was assessed via qRT-PCR. Each experimental group included more than 60 seedlings, with three biological replicates per condition.

4.7. Genomic DNA Extraction and Homozygous Identification

DNA was extracted from fresh leaves of *Arabidopsis thaliana* seedlings using the EasyPure Plant Genomic DNA Extraction Kit (TransGen Biotech, Beijing, China). Gene-specific primers (LP and RP) and a T-DNA-specific primer (LBa1) were designed based on the T-DNA insertion site information for Salk129014 from the Salk Institute (http://signal.salk.edu/) (14 June 2024). PCR amplification was performed using genomic DNA extracted from Col-0 wild-type plants and mutant lines using the LP/RP and LBa1/RP primer combinations. The reaction conditions followed the EasyTaq DNA Polymerase protocol (TransGen Biotech, Beijing, China).

Total RNA was extracted from the leaves of homozygous *AtSTR1* mutant lines, and that of Col-0 wild-type plants was extracted using the EasyPure RNA Extraction Kit (TransGen Biotech, Beijing, China). RNA was reverse transcribed into cDNA using a Reverse Transcription Kit (TransGen Biotech, Beijing, China). Expression levels of *AtSTR1* were analyzed by qRT-PCR and semi-quantitative PCR (SqRT-PCR), using *Actin2* as the internal reference gene. Primer sequences are provided in Table S1.

4.8. Disease Resistance Evaluation of Arabidopsis Atstr1 Mutant and Cotton VIGS Plants Against Fusarium and Verticillium Wilts

The severity of plant disease symptoms was categorized into four grades, ranging from 0 to 4 as follows. Grade 0: healthy plants with no visible symptoms. Grade 1: 0–25% of leaves show chlorosis or yellow spots. Grade 2: 25–50% of leaves exhibit yellow spots with slight leaf shedding. Grade 3: 50–75% of leaves display yellow or brown spots with moderate shedding. Grade 4: 75–100% of leaves are affected by yellow or brown spots, with significant leaf drop [47]. The Disease Index (DI) was calculated using the following formula:

$$\mathbf{DI = [(Disease\ Grade \times Number\ of\ Infected\ Plants)/(Total\ Number\ of\ Plants \times 4)] \times 100}$$

Next, 3 mm stem pieces were excised 2 cm below the cotyledons from *pTRV::GhSTR1*-silenced and *pTRV::00* control plants after 15 days post-inoculation (dpi) with *Verticillium dahliae* or *Fusarium oxysporum*. These excised sections were sterilized with 75% sodium hypochlorite, rinsed with sterile water, and cultured on PDA medium containing 400 mg/L cefotaxime at 25 °C for 4 days to observe fungal regrowth [5]. DNA extraction was performed using the Plant Genomic DNA Extraction Kit (TransGen Biotech, Beijing, China), and qRT-PCR followed the protocol described by Luchi [48]. Fungal DNA's ITS region was amplified with primers ITS-F and VE1-R, while internal reference genes were used (*UBQ7* for cotton and *Actin2* for *Arabidopsis*). This experiment was independently repeated with three technical and three biological replicates each time.

4.9. Growth and Development Phenotype Observation and Drought Stress Experiment for Arabidopsis Atstr1 Mutant

Wild-type (*Col-0*) and *Atstr1* mutant seedlings were transplanted into nutrient soil (vermiculite and black soil 1:2, *v*/*v*) for phenotype analysis. After 15 days, the plants were observed to determine overall plant morphology, root growth, rosette leaf diameter, and the number of rosette leaves. At 45 days, during the reproductive stage, additional phenotypes were assessed, such as plant height, leaf size, root characteristics, number of bolting branches, and number of siliques. A minimum of 40 plants per group was evaluated to ensure sufficient statistical power.

To assess drought tolerance, *Col-0* and *Atstr1* mutant plants were grown in nutrient-rich soil for 25 days under normal conditions. The plants were exposed to drought conditions by withholding irrigation for 10 days. Following re-watering, phenotypic changes were recorded, and the survival rates were calculated. For the water loss rate (WLR) measurements, 30-day-old plants were selected. The fresh weight (FW) of detached leaves was recorded initially and at 1 h intervals over a 15 h period.

4.10. Statistical Analysis

Results were presented as the mean ± standard deviation (SD) or standard error of the mean (SEM) based on three replicates. Statistical analyses were performed using GraphPad Prism 9.5 software (HM, San Diego, CA, USA). The significance levels were determined using *t*-tests or one-way analysis of variance (ANOVA). The levels of significance were indicated as follows: * $p < 0.05$, ** $p < 0.01$, and *** $p < 0.001$, representing varying degrees of statistical significance.

5. Conclusions

In this study, we determined the functional role of GhSTR1, a member of the ABCG subfamily of ATP-binding cassette (ABC) transporters that mediate cotton defense responses against *V. dahliae* and *F. oxysporum*. We identified *GhSTR1* as a homolog of *STR1* from *Medicago truncatula* and highlighted its evolutionary conservation and potential role in plant defense mechanisms. Expression profiling revealed that *GhSTR1* displays tissue-specific and spatiotemporal dynamics under stress conditions caused by *V. dahliae* and *F. oxysporum*. Functional validation was conducted using virus-induced gene silencing (VIGS), which showed that silencing *GhSTR1* enhanced disease resistance, as indicated by reduced symptom severity, vascular browning, and fungal biomass. Furthermore, *AtSTR1* loss-of-function mutants in *Arabidopsis thaliana* exhibit similar resistance phenotypes, highlighting the conserved regulatory role of *STR1* in pathogen defense. In addition to its role in disease resistance, the mutation of *AtSTR1* in *Arabidopsis* enhances the vegetative and reproductive growth of the plant, including increased root length, rosette leaf number, and plant height without compromising drought tolerance. These findings suggest that

GhSTR1 mediates a trade-off between defense and growth, offering a potential target for optimizing both traits for crop improvement.

Supplementary Materials: The following supporting information can be downloaded at: https://www.mdpi.com/article/10.3390/plants14030465/s1, Figure S1: Relative expression of *GhSTR1* in cotton roots, stems, and leaves as measured by qRT–PCR; Table S1: Primers used in this study.

Author Contributions: G.C.: conceptualization, writing—original draft. X.L. (Xiuqing Li): conceptualization, software. W.G.D.F.: writing—review, supervision. S.B.: writing—review and editing, validation. C.L.: software, validation. Y.B.: software, formal analysis. X.L. (Xiaodong Liu): Data curation, project administration. Y.L.: funding acquisition, supervision, writing—review and editing. All authors have read and agreed to the published version of the manuscript.

Funding: This work was supported by grants from the Xinjiang Uygur Autonomous Region Natural Science Foundation (2023D01E03), the Autonomous Region "Tianshan Talents" Training Program "Three Rural" Backbone Talents–Agricultural Technology Extension Talents Project (2023SNGGNT0630) and the National Natural Science Foundation of China (32160494).

Data Availability Statement: The data that support the findings of this study are available from the corresponding author upon reasonable request.

Acknowledgments: We thank the editors for their expertise in the content of this manuscript.

Conflicts of Interest: The authors declare no conflicts of interest.

References

1. Adeleke, A.A. Technological advancements in cotton agronomy: A review and prospects. *Technol. Agron.* **2024**, *4*, e008. [CrossRef]
2. Man, M.; Zhu, Y.; Liu, L.; Luo, L.; Han, X.; Qiu, L.; Li, F.; Ren, M.; Xing, Y. Defense Mechanisms of Cotton Fusarium and Verticillium Wilt and Comparison of Pathogenic Response in Cotton and Humans. *Int. J. Mol. Sci.* **2022**, *23*, 12217. [CrossRef] [PubMed]
3. Cai, Y.; Xiaohong, H.; Mo, J.; Sun, Q.; Yang, J.; Liu, J. Molecular research and genetic engineering of resistance to Verticillium wilt in cotton A review. *Afr. J. Biotechnol.* **2009**, *8*, 7363–7372.
4. Zhang, Z.; Zhao, J.; Ding, L.; Zou, L.; Li, Y.; Chen, G.; Zhang, T. Constitutive expression of a novel antimicrobial protein, Hcm1, confers resistance to both Verticillium and Fusarium wilts in cotton. *Sci. Rep.* **2016**, *6*, 20773. [CrossRef] [PubMed]
5. Li, Y.; Zhou, Y.; Dai, P.; Ren, Y.; Wang, Q.; Liu, X. Cotton Bsr-k1 modulates lignin deposition participating in plant resistance against Verticillium dahliae and Fusarium oxysporum. *Plant Growth Regul.* **2021**, *95*, 283–292. [CrossRef]
6. Li, T.; Zhang, Q.; Jiang, X.; Li, R.; Dhar, N. Cotton CC-NBS-LRR Gene GbCNL130 Confers Resistance to Verticillium Wilt Across Different Species. *Front. Plant Sci.* **2021**, *12*, 695691. [CrossRef]
7. Gong, Q.; Yang, Z.; Wang, X.; Butt, H.I.; Chen, E.; He, S.; Zhang, C.; Zhang, X.; Li, F. Salicylic acid-related cotton (*Gossypium arboreum*) ribosomal protein GaRPL18 contributes to resistance to *Verticillium dahliae*. *BMC Plant Biol.* **2017**, *17*, 59. [CrossRef]
8. Lacombe, S.; Rougon-Cardoso, A.; Sherwood, E.; Peeters, N.; Dahlbeck, D.; van Esse, H.P.; Smoker, M.; Rallapalli, G.; Thomma, B.P.; Staskawicz, B.; et al. Interfamily transfer of a plant pattern-recognition receptor confers broad-spectrum bacterial resistance. *Nat. Biotechnol.* **2010**, *28*, 365–369. [CrossRef]
9. Yang, Y.; Wu, Y.; Huang, J.; Tang, H.; Gao, H.; Yu, J.; Chen, J.; Ji, H.; Huang, M.; Wan, X.; et al. A novel type III effector RipBU from Ralstonia solanacearum suppresses plant immunity and promotes peanut susceptibility. *Int. J. Biol. Macromol.* **2025**, *284*, 138189. [CrossRef]
10. Zhou, J.M.; Zhang, Y. Plant Immunity: Danger Perception and Signaling. *Cell* **2020**, *181*, 978–989. [CrossRef]
11. Zhu, Y.; Zhao, M.; Li, T.; Wang, L.; Liao, C.; Liu, D.; Zhang, H.; Zhao, Y.; Liu, L.; Ge, X.; et al. Interactions between *Verticillium dahliae* and cotton: Pathogenic mechanism and cotton resistance mechanism to Verticillium wilt. *Front. Plant Sci.* **2023**, *14*, 1174281. [CrossRef] [PubMed]
12. Macho, A.P.; Zipfel, C. Targeting of plant pattern recognition receptor-triggered immunity by bacterial type-III secretion system effectors. *Curr. Opin. Microbiol.* **2015**, *23*, 14–22. [CrossRef] [PubMed]
13. Kuźniak, E.; Gajewska, E. Lipids and Lipid-Mediated Signaling in Plant-Pathogen Interactions. *Int. J. Mol. Sci.* **2024**, *25*, 7255. [CrossRef] [PubMed]
14. Mo, S.; Zhang, Y.; Wang, X.; Yang, J.; Sun, Z.; Zhang, D.; Chen, B.; Wang, G.; Ke, H.; Liu, Z.; et al. Cotton *GhSSI2* isoforms from the stearoyl acyl carrier protein fatty acid desaturase family regulate Verticillium wilt resistance. *Mol. Plant Pathol.* **2021**, *22*, 1041–1056. [CrossRef]

15. Seth, T.; Asija, S.; Umar, S.; Gupta, R. The intricate role of lipids in orchestrating plant defense responses. *Plant Sci.* **2024**, *338*, 111904. [CrossRef]
16. Keymer, A.; Pimprikar, P.; Wewer, V.; Huber, C.; Brands, M.; Bucerius, S.L.; Delaux, P.M.; Klingl, V.; Röpenack-Lahaye, E.V.; Wang, T.L.; et al. Lipid transfer from plants to arbuscular mycorrhiza fungi. *Elife* **2017**, *6*, e29107. [CrossRef]
17. Luginbuehl, L.H.; Menard, G.N.; Kurup, S.; Van Erp, H.; Radhakrishnan, G.V.; Breakspear, A.; Oldroyd, G.E.D.; Eastmond, P.J. Fatty acids in arbuscular mycorrhizal fungi are synthesized by the host plant. *Science* **2017**, *356*, 1175–1178. [CrossRef]
18. Gill, R.A.; Ahmar, S.; Ali, B.; Saleem, M.H.; Khan, M.U.; Zhou, W.; Liu, S. The Role of Membrane Transporters in Plant Growth and Development, and Abiotic Stress Tolerance. *Int. J. Mol. Sci.* **2021**, *22*, 12792. [CrossRef]
19. De Marcos Lousa, C.; van Roermund, C.W.; Postis, V.L.; Dietrich, D.; Kerr, I.D.; Wanders, R.J.; Baldwin, S.A.; Baker, A.; Theodoulou, F.L. Intrinsic acyl-CoA thioesterase activity of a peroxisomal ATP binding cassette transporter is required for transport and metabolism of fatty acids. *Proc. Natl. Acad. Sci. USA* **2013**, *110*, 1279–1284. [CrossRef]
20. Verrier, P.J.; Bird, D.; Burla, B.; Dassa, E.; Forestier, C.; Geisler, M.; Klein, M.; Kolukisaoglu, U.; Lee, Y.; Martinoia, E.; et al. Plant ABC proteins—A unified nomenclature and updated inventory. *Trends Plant Sci.* **2008**, *13*, 151–159. [CrossRef]
21. Dean, M.; Rzhetsky, A.; Allikmets, R. The human ATP-binding cassette (ABC) transporter superfamily. *Genome Res.* **2001**, *11*, 1156–1166. [CrossRef] [PubMed]
22. Huo, X.; Pan, A.; Lei, M.; Song, Z.; Chen, Y.; Wang, X.; Gao, Y.; Zhang, J.; Wang, S.; Zhao, Y.; et al. Genome-Wide Characterization and Functional Analysis of ABCG Subfamily Reveal Its Role in Cutin Formation in Cotton. *Int. J. Mol. Sci.* **2023**, *24*, 2379. [CrossRef] [PubMed]
23. Lee, M.; Lee, K.; Lee, J.; Noh, E.W.; Lee, Y. AtPDR12 contributes to lead resistance in Arabidopsis. *Plant Physiol.* **2005**, *138*, 827–836. [CrossRef]
24. Kuromori, T.; Shinozaki, K. ABA transport factors found in Arabidopsis ABC transporters. *Plant Signal. Behav.* **2010**, *5*, 1124–1126. [CrossRef]
25. Campe, R.; Langenbach, C.; Leissing, F.; Popescu, G.V.; Popescu, S.C.; Goellner, K.; Beckers, G.J.; Conrath, U. ABC transporter PEN3/PDR8/ABCG36 interacts with calmodulin that, like PEN3, is required for Arabidopsis nonhost resistance. *New Phytol.* **2016**, *209*, 294–306. [CrossRef]
26. Shibata, Y.; Ojika, M.; Sugiyama, A.; Yazaki, K.; Jones, D.A.; Kawakita, K.; Takemoto, D. The Full-Size ABCG Transporters Nb-ABCG1 and Nb-ABCG2 Function in Pre- and Postinvasion Defense against *Phytophthora infestans* in *Nicotiana benthamiana*. *Plant Cell* **2016**, *28*, 1163–1181. [CrossRef]
27. Garroum, I.; Bidzinski, P.; Daraspe, J.; Mucciolo, A.; Humbel, B.M.; Morel, J.B.; Nawrath, C. Cuticular Defects in Oryza sativa ATP-binding Cassette Transporter G31 Mutant Plants Cause Dwarfism, Elevated Defense Responses and Pathogen Resistance. *Plant Cell Physiol.* **2016**, *57*, 1179–1188. [CrossRef]
28. Zhang, Y.; Chen, G.; Zang, Y.; Bhavani, S.; Bai, B.; Liu, W.; Zhao, M.; Cheng, Y.; Li, S.; Chen, W.; et al. Lr34/Yr18/Sr57/Pm38 confers broad-spectrum resistance to fungal diseases via sinapyl alcohol transport for cell wall lignification in wheat. *Plant Commun.* **2024**, *5*, 101077. [CrossRef]
29. Jiang, Y.; Xie, Q.; Wang, W.; Yang, J.; Zhang, X.; Yu, N.; Zhou, Y.; Wang, E. Medicago AP2-Domain Transcription Factor WRI5a Is a Master Regulator of Lipid Biosynthesis and Transfer during Mycorrhizal Symbiosis. *Mol. Plant* **2018**, *11*, 1344–1359. [CrossRef]
30. Zhang, Q.; Wang, S.; Xie, Q.; Xia, Y.; Lu, L.; Wang, M.; Wang, G.; Long, S.; Cai, Y.; Xu, L.; et al. Control of arbuscule development by a transcriptional negative feedback loop in Medicago. *Nat. Commun.* **2023**, *14*, 5743. [CrossRef]
31. Zhang, J.; Hu, H.L.; Wang, X.N.; Yang, Y.H.; Zhang, C.J.; Zhu, H.Q.; Shi, L.; Tang, C.M.; Zhao, M.W. Dynamic infection of Verticillium dahliae in upland cotton. *Plant Biol.* **2020**, *22*, 90–105. [CrossRef]
32. Huot, B.; Yao, J.; Montgomery, B.L.; He, S.Y. Growth-defense tradeoffs in plants: A balancing act to optimize fitness. *Mol. Plant* **2014**, *7*, 1267–1287. [CrossRef]
33. Sun, M.; Zhang, Z.; Ren, Z.; Wang, X.; Sun, W.; Feng, H.; Zhao, J.; Zhang, F.; Li, W.; Ma, X.; et al. The GhSWEET42 Glucose Transporter Participates in Verticillium dahliae Infection in Cotton. *Front. Plant Sci.* **2021**, *12*, 690754. [CrossRef]
34. Sosso, D.; van der Linde, K.; Bezrutczyk, M.; Schuler, D.; Schneider, K.; Kämper, J.; Walbot, V. Sugar Partitioning between Ustilago maydis and Its Host Zea mays L during Infection. *Plant Physiol.* **2019**, *179*, 1373–1385. [CrossRef]
35. Gao, Y.; Zhang, C.; Han, X.; Wang, Z.Y.; Ma, L.; Yuan, P.; Wu, J.N.; Zhu, X.F.; Liu, J.M.; Li, D.P.; et al. Inhibition of OsSWEET11 function in mesophyll cells improves resistance of rice to sheath blight disease. *Mol. Plant Pathol.* **2018**, *19*, 2149–2161. [CrossRef]
36. Jiang, Y.; Wang, W.; Xie, Q.; Liu, N.; Liu, L.; Wang, D.; Zhang, X.; Yang, C.; Chen, X.; Tang, D.; et al. Plants transfer lipids to sustain colonization by mutualistic mycorrhizal and parasitic fungi. *Science* **2017**, *356*, 1172–1175. [CrossRef]
37. Rössner, C.; Lotz, D.; Becker, A. VIGS Goes Viral: How VIGS Transforms Our Understanding of Plant Science. *Annu. Rev. Plant Biol.* **2022**, *73*, 703–728. [CrossRef]
38. Zhu, Y.; Hu, X.; Wang, P.; Gao, L.; Pei, Y.; Ge, Z.; Ge, X.; Li, F.; Hou, Y. GhPLP2 Positively Regulates Cotton Resistance to Verticillium Wilt by Modulating Fatty Acid Accumulation and Jasmonic Acid Signaling Pathway. *Front. Plant Sci.* **2021**, *12*, 749630. [CrossRef]

39. Mentewab, A.; Stewart, C.N., Jr. Overexpression of an Arabidopsis thaliana ABC transporter confers kanamycin resistance to transgenic plants. *Nat. Biotechnol.* **2005**, *23*, 1177–1180. [CrossRef]
40. Oliva, R.; Quibod, I.L. Immunity and starvation: New opportunities to elevate disease resistance in crops. *Curr. Opin. Plant Biol.* **2017**, *38*, 84–91. [CrossRef]
41. Eom, J.S.; Luo, D.; Atienza-Grande, G.; Yang, J.; Ji, C.; Thi Luu, V.; Huguet-Tapia, J.C.; Char, S.N.; Liu, B.; Nguyen, H.; et al. Diagnostic kit for rice blight resistance. *Nat. Biotechnol.* **2019**, *37*, 1372–1379. [CrossRef] [PubMed]
42. Oliva, R.; Ji, C.; Atienza-Grande, G.; Huguet-Tapia, J.C.; Perez-Quintero, A.; Li, T.; Eom, J.S.; Li, C.; Nguyen, H.; Liu, B.; et al. Broad-spectrum resistance to bacterial blight in rice using genome editing. *Nat. Biotechnol.* **2019**, *37*, 1344–1350. [CrossRef] [PubMed]
43. Livak, K.J.; Schmittgen, T.D. Analysis of relative gene expression data using real-time quantitative PCR and the 2(-Delta Delta C(T)) Method. *Methods* **2001**, *25*, 402–408. [CrossRef] [PubMed]
44. Letunic, I.; Doerks, T.; Bork, P. SMART 7: Recent updates to the protein domain annotation resource. *Nucleic Acids Res.* **2012**, *40*, D302–D305. [CrossRef] [PubMed]
45. Tamura, K.; Stecher, G.; Kumar, S. MEGA11: Molecular Evolutionary Genetics Analysis Version 11. *Mol. Biol. Evol.* **2021**, *38*, 3022–3027. [CrossRef]
46. Gao, W.; Long, L.; Zhu, L.F.; Xu, L.; Gao, W.H.; Sun, L.Q.; Liu, L.L.; Zhang, X.L. Proteomic and virus-induced gene silencing (VIGS) Analyses reveal that gossypol, brassinosteroids, and jasmonic acid contribute to the resistance of cotton to Verticillium dahliae. *Mol. Cell. Proteom.* **2013**, *12*, 3690–3703. [CrossRef]
47. Wang, P.; Zhou, L.; Jamieson, P.; Zhang, L.; Zhao, Z.; Babilonia, K.; Shao, W.; Wu, L.; Mustafa, R.; Amin, I.; et al. The Cotton Wall-Associated Kinase GhWAK7A Mediates Responses to Fungal Wilt Pathogens by Complexing with the Chitin Sensory Receptors. *Plant Cell* **2020**, *32*, 3978–4001. [CrossRef]
48. Luchi, N.; Santini, A.; Salvianti, F.; Pinzani, P. Early Detection of Fungal Plant Pathogens by Real-Time Quantitative PCR: The Case of Diplodia sapinea on Pine. *Methods Mol. Biol.* **2020**, *2065*, 95–104. [CrossRef]

plants

MDPI

Article

Analysis of the Mechanisms Underlying the Specificity of the Variation Potential Induced by Different Stimuli

Maxim Mudrilov, Maria Ladeynova, Yana Vetrova and Vladimir Vodeneev *

Department of Biophysics, National Research Lobachevsky State University of Nizhny Novgorod, 23 Gagarin Avenue, 603022 Nizhny Novgorod, Russia
* Correspondence: v.vodeneev@mail.ru

Abstract: Plants are able to perceive diverse environmental factors and form an appropriate systemic functional response. Systemic responses are induced by stimulus-specific long-distance signals that carry information about the stimulus. Variation potential is proposed as a candidate for the role of such a signal. Here, we focus on the mechanisms that determine the specificity of the variation potential under the action of different local stimuli. Local stimuli such as heating, burning and wounding cause variation potential, the parameters of which differ depending on the type of stimulus. It was found that the stimulus-specific features of the hydraulic signal monitored by changes in leaf thickness and variation potential, such as a greater amplitude upon heating and burning and a significant amplitude decrement upon burning and wounding, were similar. The main features of these signals are the greater amplitude upon heating and burning, and a significant amplitude decrement upon burning and wounding. Together with the temporal correspondence of signal propagation, this evidence indicates a role for the hydraulic signal in the induction of stimulus-specific variation potential. Experiments using mechanosensitive channel inhibitors have demonstrated that the hydraulic signal contributes more to the induction of the variation potential in the case of rapidly growing stimuli, such as burning and wounding, than in the case of gradual heating. For thermal stimuli (gradual heating and burning), a greater contribution, compared to wounding, of the chemical signal related to reactive oxygen species to the induction of the variation potential was demonstrated. Thus, the specificity of the parameters of the variation potential is determined by the different contributions of hydraulic and chemical signals.

Keywords: abiotic stress; signal transduction; electrical signal; variation potential; hydraulic signal

1. Introduction

To date, sufficient evidence has accumulated that local stimuli trigger systemic functional responses that cover the whole plant body [1,2]. Such responses are known to be stimulus-specific and involve unstimulated parts of the plant. First of all, it is worth noting the stimulus-specific differences in the dynamics of various phytohormones [3–7] and metabolites [4,8], the dynamics of photosynthesis and transpiration responses [3–6], the level of expression of various genes [6–9], etc. Such stimulus-specific systemic responses can only be induced by a stimulus-specific long-distance signal that carries information about the stimulus.

One such signal may be the variation potential (VP), which is a transient depolarization of irregular shape and duration [1,2,10–12]. VP occurs in response to various damaging stimuli [1,2,10,11], and its parameters, such as the amplitude and propagation velocity, may depend on the type of stimulus [5,13] and the area of damage [14]. Experiments on the stimulus specificity of the VP parameters revealed that in the case of rapidly growing stimuli, such as burning and wounding, there is a significant decrement during the VP propagation, whereas in the case of slowly growing stimuli, such as gradual heating, there is almost no decrement [5,13]. Most importantly, it was shown that VP can induce a

stimulus-specific systemic response [1,2]. Thus, VP can potentially regulate the systemic response by changing its parameters.

However, the outstanding question remains: how are VP parameters regulated upon different stimulations? The specificity of VP may be based on the features of its mechanisms of generation and propagation, due to its complex nature: VP is an electrical reaction in response to a hydraulic or chemical signal, or a combination of both [1,2,11,12]. The role of the hydraulic signal is evidenced by data on the induction of VP by artificially increasing intra-vessel fluid pressure [14,15], data on increases in the thickness of leaves or stems preceding the VP [16,17], as well as good agreement with the results of mathematical ing [18,19]. It is assumed that chemical signals may be some wounding substances propagating from the damage site throughout vascular bundles, such as reactive oxygen species (ROS) produced by NADPH oxidases [2,11,20–22], which is supported by the similar dynamics of ROS wave propagation [11,21]. It is proposed that hydraulic and chemical signals activate mechanosensitive and/or ligand-gated Ca^{2+}-permeable channels, respectively, inducing an initial step of membrane potential changes during VP generation [2,11]. An important role in the formation of the specificity of VP parameters can be played by the physical features of the propagation of hydraulic and chemical signals, for example, the higher propagation velocity of hydraulic signals compared to chemical ones [11]. This can lead to the activation of Ca^{2+}-permeable channels of different types and different lag times for their activation, which determines the characteristics of the VP parameters. Thus, differences in the parameters of the VPs caused by various stimuli may be primarily due to the different contributions of chemical and hydraulic signals to the induction of the VP.

However, the precise mechanism of the specificity of VP parameters needs investigation. In summary, the present work aimed to identify the stimulus-specific features of the mechanisms of generation and propagation of VP in wheat plants.

2. Results

2.1. Parameters of Variation Potentials Induced by Different Local Stimuli

Heating, burning and mechanical wounding of the tip of a wheat leaf caused the generation of a long-distance electrical signal in the form of a transient depolarization of irregular shape and duration (Figure 1A), with characteristics corresponding to VP [1,2,11]. In the cases of heating and burning, the VP amplitudes near the site of stimulation (3 cm) were similar (~54.5 $\pm$ 3.5 mV), whereas in the case of wounding it was significantly lower (~32 $\pm$ 3 mV). As VP propagates, its amplitude decreases; the degree of attenuation depends on the type of stimulus. In cases of burning and wounding, the VP amplitude was significantly attenuated: at a distance of 9 cm from the stimulation site, the amplitude was 46% and 19% of the initial amplitude (at 3 cm), respectively. By contrast, the amplitude of the heat-induced VP was attenuated to 83% of the initial amplitude (Figure 1B). These results demonstrate the dependence of VP parameters, such as amplitude and decrement, on the type of stimulus. These findings suggest that there are stimulus-specific differences in the mechanisms of VP generation and propagation.

2.2. The Role of the Hydraulic Wave in the Propagation of Variation Potentials Caused by Different Local Stimuli

Heating, burning and mechanical wounding induced a hydraulic signal that caused an increase in leaf thickness (Figure 2B). The main stimulus-specific features of changes in leaf thickness at a distance of 4.5 cm from the stimulation area will be discussed below. A slight decrease in leaf thickness preceded leaf thickening (Figure 2A,B and Figure S1). In cases of burning and wounding, the amplitude of the thickness reduction phase was small (<5 μm), and its duration did not exceed several seconds. In the case of heating, the amplitude of the thickness reduction phase was several times greater than that upon burning and wounding, and its duration was several minutes (Figure S1).

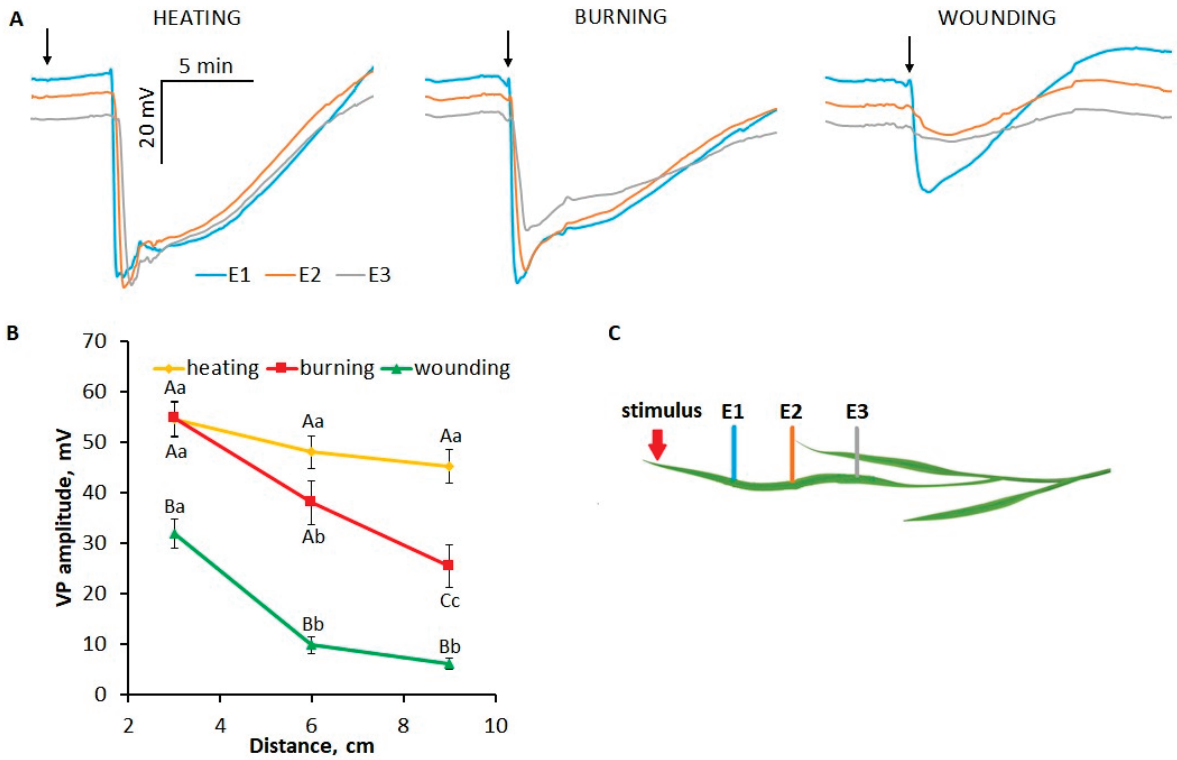

Figure 1. Variation potentials (VPs) induced by local heating, burning or wounding in wheat plants. (**A**) Averaged VP traces. The arrow indicates the moment of mechanical wounding, burning or the beginning of gradual heating of the leaf tip. (**B**) Dependence of the VP amplitude on the distance to the area of local stimulation. Data are means ± SEM. Different uppercase letters indicate statistically significant differences between stimuli; different lowercase letters indicate statistically significant differences between distances within a single stimulus ($p < 0.05$). (**C**) Schematic representation of the experimental design for monitoring surface potentials in wheat plants. E1, E2, E3: surface electrodes.

The amplitude (Figure 2C) and duration (Figure 2D) of the phase of increasing leaf thickness were significantly greater compared to the thickness reduction phase. The amplitude of thickening upon wounding was about 15–20 µm, whereas upon heating and burning it reached 20–30 µm. The duration of the thickening phase, i.e., the time taken from the beginning of an increase in leaf thickness until the thickness reached its maximum, was greatest upon heating compared to other stimuli (Figure 2D). The leaf thickening rate was lowest upon wounding, higher upon heating and highest upon burning (Figure 2E).

It is important to note that the thickening phase began almost simultaneously with the VP generation under the action of stimuli of all types (Figure 2A), suggesting that the hydraulic signal is essential for VP induction.

The thickness change parameters show a dependence on the distance from the stimulation area. The amplitude of the heat-induced increase in leaf thickness decreased slightly with increasing distance from the stimulation site, whereas it greatly decreased in the case of burning and, especially, in the case of wounding (Figure 2C). The ratios of the durations of the thickening phases between stimuli were maintained as the distance from the stimulation area increased (Figure 2D). Thus, hydraulic-signal-induced changes in leaf thickness also depend on the stimulus type in a similar manner to VP parameters.

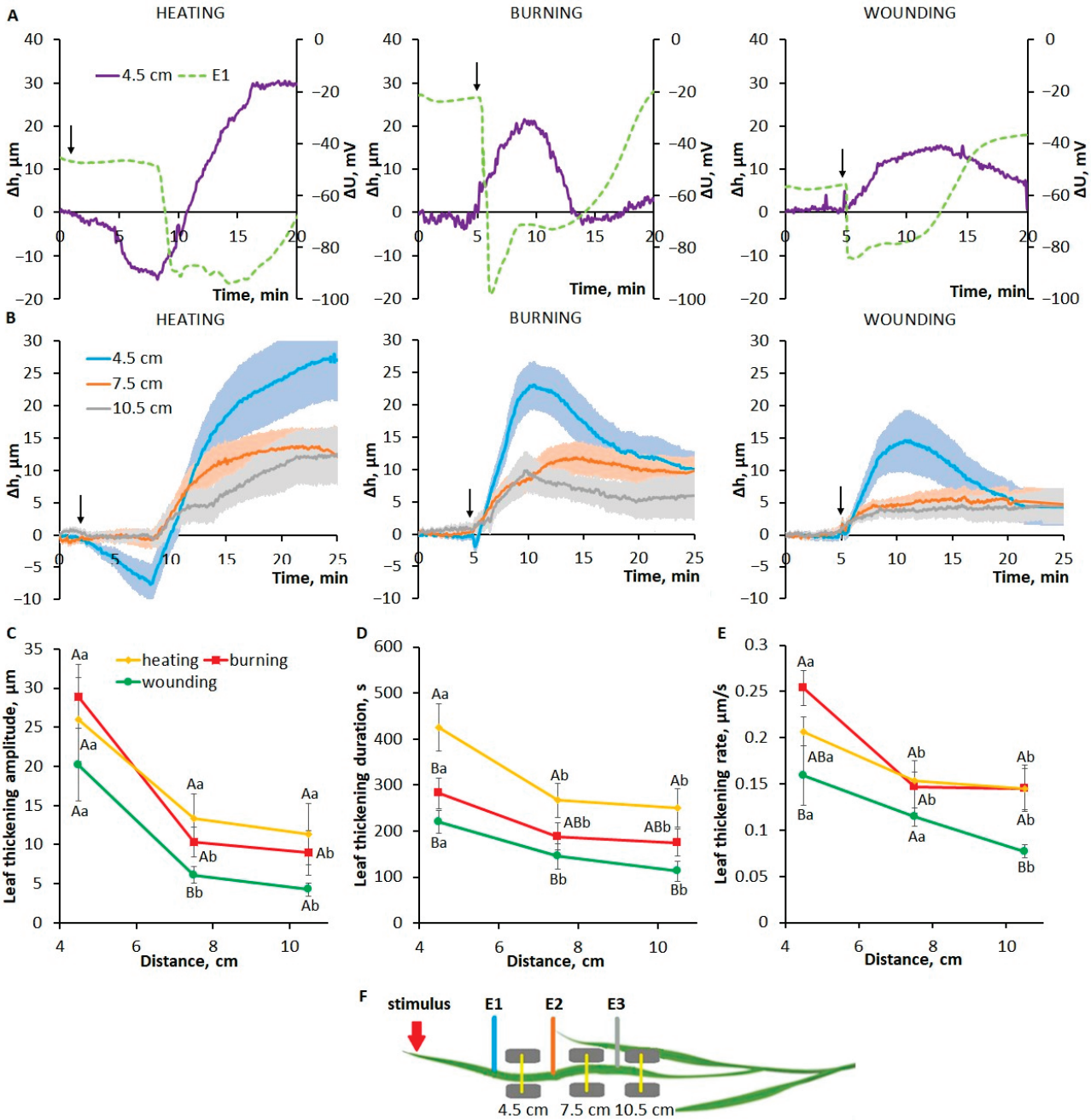

Figure 2. Systemic changes in leaf thickness induced by local heating, burning or wounding in wheat plants. (**A**) Simultaneous representative recordings of leaf thickness changes (Δh, solid lines) and variation potentials (ΔU, dashed lines) at a distance of 4.5 cm and 3 cm, respectively, from the stimulation area. The arrow indicates the moment of mechanical wounding, burning or the beginning of gradual heating of the leaf tip. (**B**) Averaged recordings of leaf thickness changes (Δh); shaded regions (envelopes) represent SEM. The arrow indicates the moment of mechanical wounding, burning or the beginning of gradual heating of the leaf tip. (**C**–**E**) Dependences of the amplitude (**C**), duration (**D**) and rate (**E**) of leaf thickening on the distance to the area of local stimulation. Data are means ± SEM. Different uppercase letters indicate statistically significant differences between stimuli; different lowercase letters indicate statistically significant differences between distances within a single stimulus ($p < 0.05$). (**F**) Schematic representation of the experimental design for simultaneous monitoring of surface potentials and changes in wheat leaf thickness. E1, E2, E3: surface electrodes. Yellow lines are light bands between the sender units and the receiver units of the optical micrometers (gray rectangles).

2.3. Systemic Changes in Stomatal Conductance Induced by Different Local Stimuli

The observed increase in wheat leaf thickness due to the propagation of the hydraulic signal may be associated with changes in water exchange. One of the important components of water exchange is water loss through the stomata. Changes in stomatal conductance (g_S) induced by local heating, burning or mechanical wounding were investigated in the unstimulated part of the wheat leaf. Changes in g_S were biphasic, with an initial slight increase in transpiration rate followed by a significant decrease (Figure 3). Note that the first phase of increasing the transpiration rate either began simultaneously with the VP generation or preceded it by several seconds. The phase of the decrease in transpiration rate was more pronounced and prolonged. The amplitude of g_S changes was the smallest upon wounding (g_S decrease by 1/4 from the resting level), whereas it was significantly greater upon burning and heating.

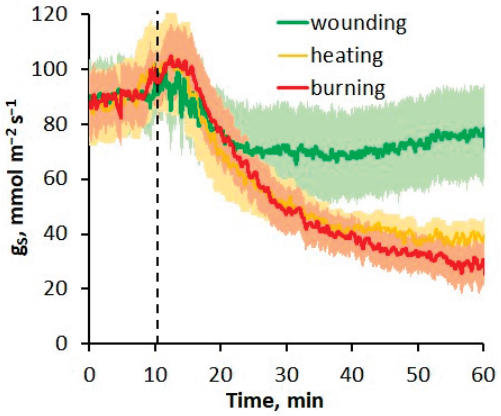

Figure 3. The dynamics of stomatal conductance (g_S) induced by local heating, burning or wounding in the unstimulated part of the wheat plant. Lines are means; shaded regions (envelopes) represent SEM. The dashed line indicates the moment of generation of the variation potential.

2.4. Parameters of Variation Potential and Hydraulic Signal in a Detached Wheat Leaf

The study of stimulus-specific features of the mechanisms of propagation and generation of VP was performed on the basis of inhibitor analysis. Due to the low penetration of inhibitors through the wheat leaf epidermis, experiments with inhibitors were carried out using a detached wheat leaf. To assess the suitability of the detached leaf model, VP parameters in whole plants and detached leaves were compared. The VP in the detached leaves had its own characteristic shape (Figure 4A). VP amplitudes near the stimulation area (3 cm) in whole plants and excised leaves were very similar. However, the VP propagation in the detached leaf was altered: VP amplitude was more attenuated with increasing distance from the stimulation site. The differences were more pronounced in the case of heating. At distances of 6 cm and 9 cm, the amplitudes were reduced to 56% and 25% of the initial amplitude (at 3 cm), respectively (Figure 4B), whereas a decrement was almost not observed in whole plants (Figure 1B). The decrease in amplitude was 47% and 11% at a distance of 6 cm and 34% and 11% at a distance of 9 cm from the initial amplitude upon burning and wounding, respectively (Figure 4B). Notwithstanding, the main stimulus-specific differences between VP parameters were clearly identified using detached leaves as in whole plants.

The effect of leaf detachment on hydraulic signal parameters was also analyzed (Figure 5). A significant decrease in leaf thickening amplitude was found for all stimulus types, both near the stimulation site (4.5 cm) and at a distance of 10.5 cm. However, as for VP, the main stimulus-specific features of the hydraulic signals were also clearly identified in detached leaves, such as the presence of a pronounced and prolonged phase of thickness reduction upon heating, as well as the greatest amplitude of the thickening phase in the case of heating and the smallest in the case of wounding. It can also be noted that the

changes in hydraulic signals caused by the leaf detachment were similar to those for the VP.

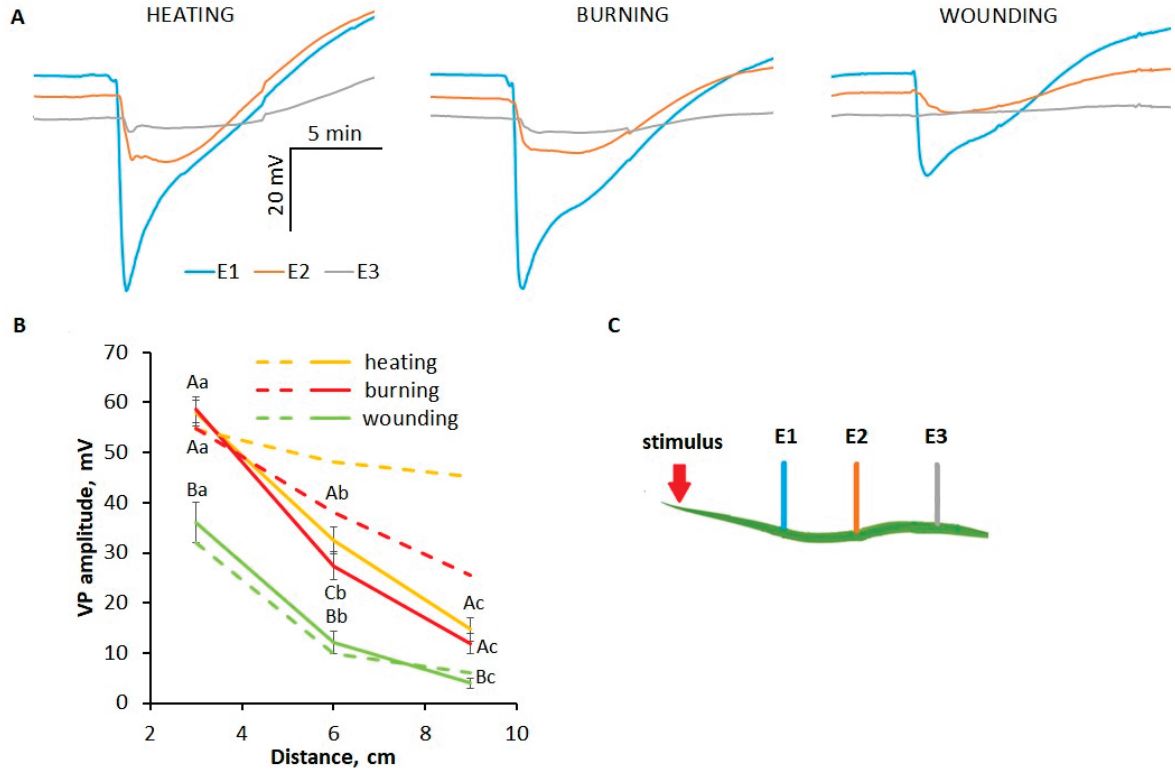

Figure 4. Variation potentials (VPs) induced by local heating, burning or wounding in the detached wheat leaf. (**A**) Averaged VP traces. The arrow indicates the moment of mechanical wounding, burning or the beginning of gradual heating of the leaf tip. (**B**) Comparison of the dependences of the VP amplitude on the distance to the area of local stimulation in detached leaves (solid lines) and whole wheat plants (dashed lines). Data are means ± SEM. For detached leaves only, different uppercase letters indicate statistically significant differences between stimuli; different lowercase letters indicate statistically significant differences between distances within a single stimulus ($p < 0.05$). (**C**) Schematic representation of the experimental design for monitoring surface potentials in wheat plants. E1, E2, E3: surface electrodes.

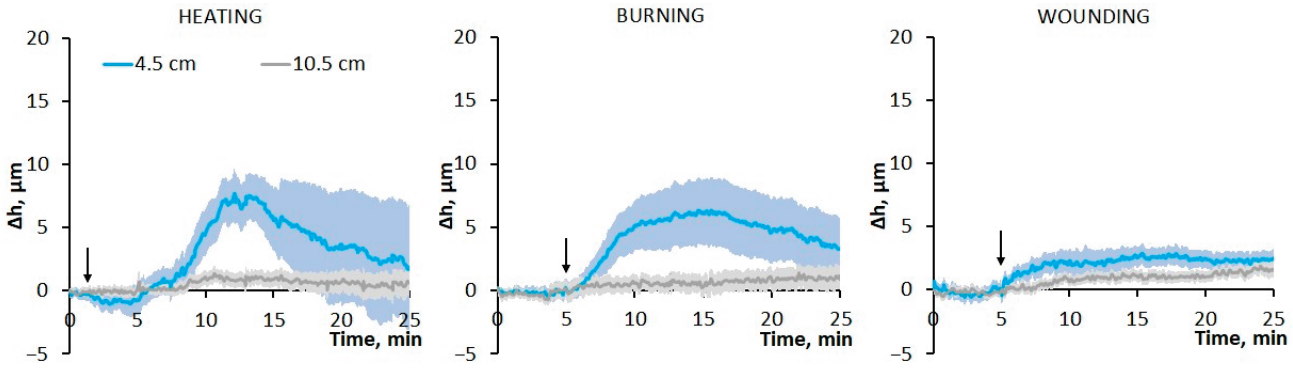

Figure 5. Systemic changes in leaf thickness (Δh) induced by local heating, burning or wounding in the detached wheat leaf. Lines are means; shaded regions (envelopes) represent SEM. The arrow indicates the moment of mechanical wounding, burning or the beginning of gradual heating of the leaf tip.

Similarities in the dependences of the parameters of VP and hydraulic signal on the type of stimulus between whole plants and detached leaves indicate the suitability of the detached leaf model for studying the mechanisms of VP generation and propagation.

2.5. Contribution of Reactive Oxygen Species to the Propagation of Variation Potentials Caused by Different Local Stimuli

In addition to the hydraulic signal, the VP propagation is associated with a chemical signal, the role of which, according to hypotheses in some works [2,11,22], can be played by ROS. The possible contribution of ROS to the VP propagation was evaluated using an ROS scavenger N,N′-dimethylthiourea (DMTU) [23,24]. Treatment with DMTU led to a decrease in the VP amplitude near the site of stimulation (3 cm) under the action of all stimuli (Figure 6). VP propagation was more suppressed upon heating compared to burning and wounding. To determine the ROS sources, the inhibitor of NADPH oxidases diphenyleneiodonium chloride (DPI) [25,26] and salicylhydroxamic acid (SHAM), which inhibits cell wall peroxidases [27] and mitochondrial alternative oxidases [28], were used. These inhibitors slightly reduced the VP amplitude near the stimulation area but significantly suppressed the propagation of heat- and burn-induced VPs. The propagation of the wound-induced VP was less inhibited, especially upon SHAM treatment. The inhibition of ROS production also resulted in a change in VP amplitude decrement, which was more than 75% at a distance of 6 cm from the stimulation area for all stimulus types except SHAM treatment upon wounding. These results suggest that DPI- and SHAM-inhibited oxidases are involved in maintaining the propagation of the heat- and burn-induced VPs through active ROS production [2], whereas they are probably not involved in the propagation of the wound-induced VP.

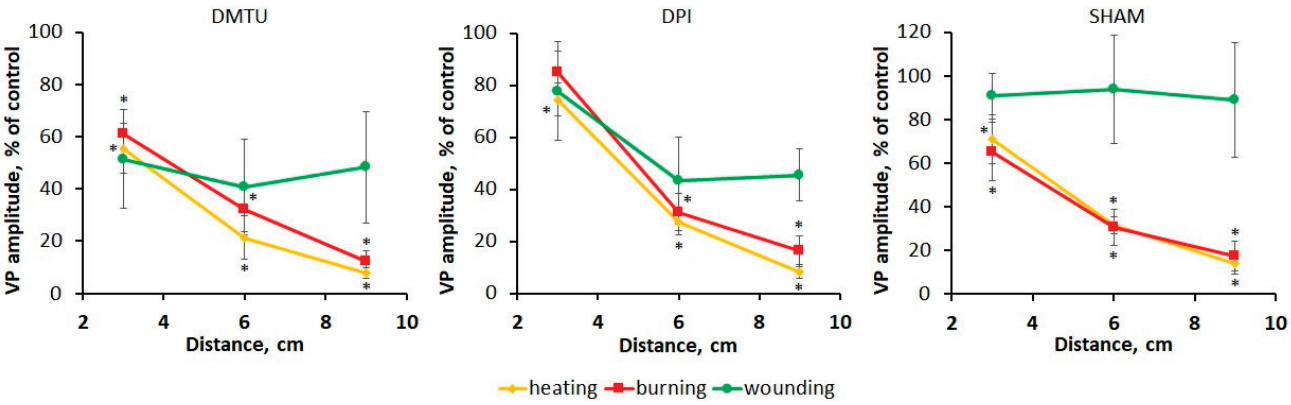

Figure 6. Effects of the reactive oxygen species (ROS) scavenger N,N′-dimethylthiourea (DMTU) and ROS-producing enzyme inhibitors diphenyleneiodonium chloride (DPI) and salicylhydroxamic acid (SHAM) on the amplitudes of the variation potentials (VPs) induced by local heating, burning or wounding in the detached wheat leaf. VP amplitude is represented as the percentage of control, which is the VP amplitude in untreated leaves (without scavengers and inhibitors). Data are means ± SEM. * indicates data significantly different from untreated leaves ($p < 0.05$).

Thus, the different contributions of ROS indicate, first of all, stimulus-specific differences in the parameters of VP propagation, but not differences in the VP amplitude near the stimulation area. Therefore, further studies are needed to determine the stimulus-specific features of the VP generation mechanism.

2.6. Analysis of the Features of the Mechanisms of Generation of Variation Potentials Induced by Different Local Stimuli

To study the features of the VP generation mechanism, an inhibitor analysis using inhibitors of ion transport systems was used. It is known that H^+-ATPase inactivation plays a key role in VP generation [2,10,11,22]. Treatment with an H^+-ATPase inhibitor sodium

orthovanadate resulted in the almost complete suppression of the VP for all types of stimuli; the VP amplitude was less than 10% of the amplitude in untreated leaves (Figure 7B).

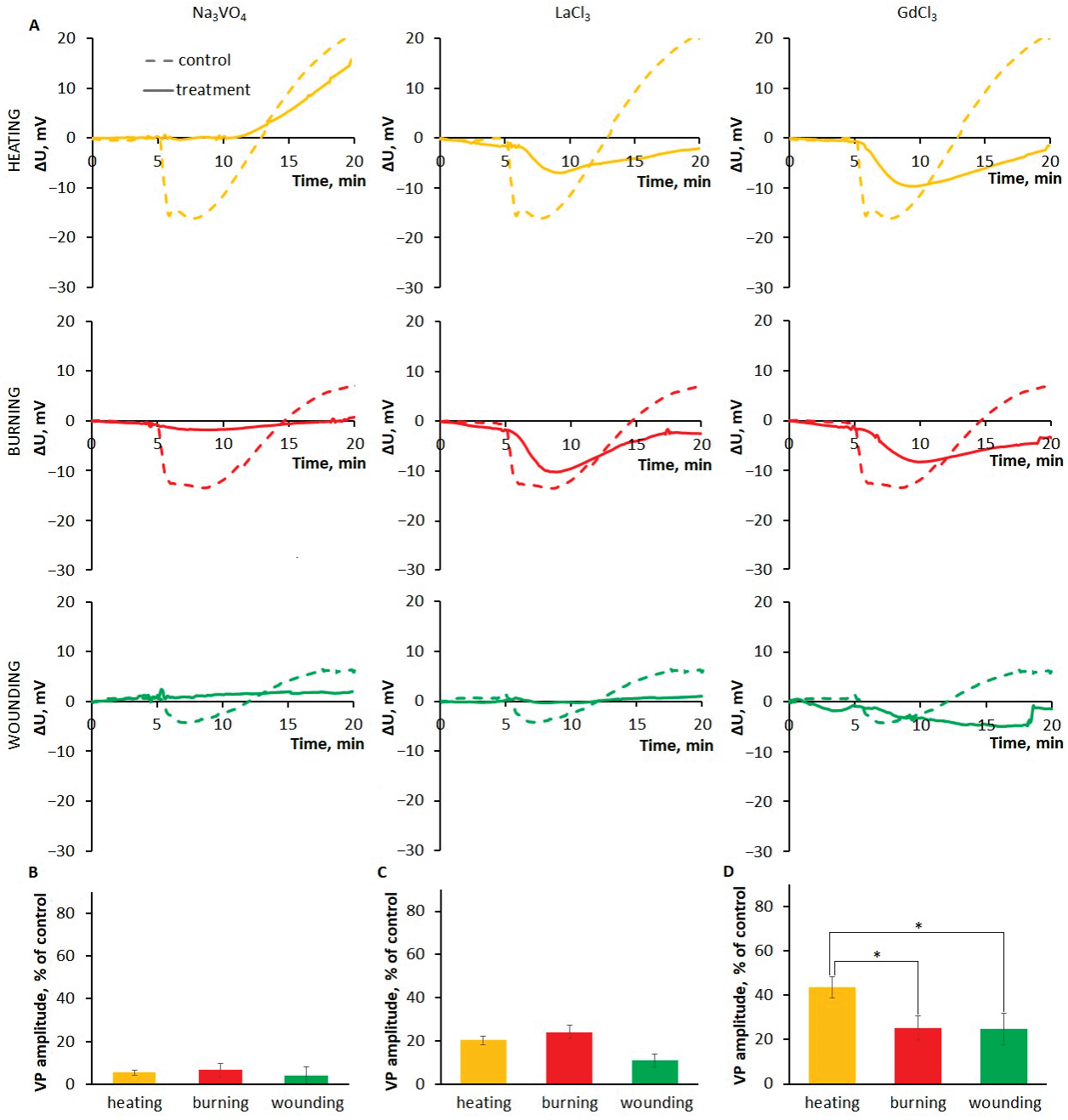

Figure 7. Effects of the H^+-ATPase inhibitor Na_3VO_4, the Ca^{2+}-permeable channel blocker $LaCl_3$ and the mechanosensitive channel inhibitor $GdCl_3$ on the variation potentials (VPs) induced by local heating, burning or wounding in the detached wheat leaf. (**A**) Averaged VP traces observed at a distance of 6 cm from the stimulation area in untreated leaves (dashed lines) or those treated with the inhibitor/blocker (solid lines). (**B**–**D**) VP amplitude at a distance of 6 cm from the area of local stimulation upon treatment with Na_3VO_4 (**B**), $LaCl_3$ (**C**) or $GdCl_3$ (**D**). VP amplitude is represented as the percentage of control, which is the VP amplitude in untreated leaves (without inhibitor). Data are means ± SEM. Statistically significant differences between untreated and treated leaves were found for all stimuli. * indicates significant differences between the stimuli ($p < 0.05$).

Changes in H^+-ATPase activity may be related to an increase in cytosolic Ca^{2+} concentration due to the activation of Ca^{2+}-permeable channels [2,29]. It is proposed that

both mechanosensitive and ROS-activated Ca^{2+}-permeable plasma membrane channels are involved in VP generation [2,11,22,29].

Treatment with the Ca^{2+}-permeable plasma membrane channel blocker $LaCl_3$ led to a significant (more than 50%) decrease in VP amplitude for all stimuli (Figure 7C). It should be noted that, along with the suppression of amplitude, there was a pronounced decrease in the rate of depolarization (Figure 7A).

To analyze the involvement of mechanosensitive channels in the generation of VPs induced by different stimuli, the effects of the inhibitor $GdCl_3$ on the VP parameters were evaluated. It was shown that treatment with the $GdCl_3$ led to a decrease in VP amplitude and depolarization rate for all stimuli, but a greater effect was observed in the cases of burning and wounding, which was expressed as a decrease in amplitude by more than 60% compared to untreated leaves (Figure 7D).

Thus, a greater contribution of mechanosensitive channels to VP generation was revealed in the cases of burning and wounding compared to gradual heating.

3. Discussion

The analysis of the parameters of VPs induced by different local stress stimuli revealed stimulus-specific differences. The smallest amplitude was in the case of wounding, which rapidly attenuated during VP propagation, and the greatest amplitude was near the stimulation area in the cases of heating and burning, which had a pronounced decrement upon burning and a small decrement upon heating (Figure 1). The stimulus-specific features of VPs in wheat plants revealed in this work correspond to those in pea plants [13].

As noted, VP is not a self-propagating signal but is an electrical reaction that is induced by a hydraulic or chemical signal, or a combination of both [1,2,11,12]. It can be proposed that the stimulus-specific features of the electrical reaction at a distance from the stimulation zone are due to the features of these signals, which are discussed below.

3.1. The Role of the Hydraulic Signal in the Formation of the Specificity of Variation Potentials Induced by Different Local Stimuli

To study the role of the hydraulic signal in VP induction, an analysis of systemic changes in leaf thickness in response to different stimuli was performed. The stimulus-induced increase in leaf thickness was several micrometers, lasted for tens of minutes and was preceded by a decrease in leaf thickness of shorter duration and smaller amplitude (Figure 2). Hydraulic signals, monitored by changes in the thickness of leaves or stems or other methods, have been shown in previous works in response to externally applied pressure [15], burning [15,16,30–32], insect feeding [17,30], and mechanical wounding [17,33]. The thickness change parameters from previous studies are in good agreement with the data in this work: a duration of up to tens of minutes, an amplitude of several micrometers [15–17,30,31], and a decrement in amplitude with distance from the stimulation area [16,31]. Stimulus-specific differences in the parameters of changes in leaf thickness have also been shown previously, in particular between burning and insect feeding [30].

This study demonstrated that the stimulus-specific features of VP and leaf thickening parameters were similar (Figures 1 and 2), suggesting a hydraulic signal as a trigger for both leaf thickening and VP. This was also evidenced by the fact that an increase in leaf thickness preceded or coincided with VP generation (Figure 2A) [16,17,32]. VP occurred when the increase in leaf thickness was at the initial stage (Figure 2A), which may indicate a small threshold for VP generation.

The mechanisms of VP induction and the increase in leaf thickness by a hydraulic signal are open questions. Pressure wave propagation or xylem mass flow may be these mechanisms [11,17]. Hydraulic pressure waves propagate in liquid at very high speeds and can cause rapid changes in the size of vessels, which causes deformations of adjacent parenchyma cells [11,19,34]. In the case of hydraulic mass flow, there is a direct fluid translocation through the vessels, propagating at a much lower speed, but also capable of causing a change in both the size of the vessels and the cells surrounding them [11,18,35].

These changes may lead to an increase in leaf thickness [14,18,19] and to VP induction through the activation of mechanosensitive ion channels in the plasma membrane of parenchyma cells adjacent to the xylem [2,11,19]. These channels are activated in response to changes in plasma membrane tension (including sensing membrane tension directed from the outside of the cell), as well as in response to cell turgor changes [36,37] caused by water movement from the xylem during hydraulic mass flow.

First, the role of the hydraulic pressure wave as a possible VP inducer will be discussed. A wave of positive pressure changes originates as a result of wound-induced damage to xylem vessels and the subsequent release of xylem water column tension [11], since under normal conditions, there is negative pressure in the xylem as a result of transpiration [38,39]. This can potentially cause leaf thickness increase and VP generation [32], which is supported by data on the possibility of inducing tissue deformation and VP-like electrical signals by artificially increasing the pressure in the xylem [14,15,40]. Moreover, the amplitudes of VP-like electrical signals depend on the size of the applied pressure steps [14]. The role of the hydraulic pressure wave in VP induction is supported by the dependence of the VP amplitude on the values of the initial negative pressure (tension) in the xylem [14,40], as well as by the fact that VP is not observed when the initial xylem pressure is positive [14,32].

However, there are some contradictory facts regarding the involvement of the hydraulic pressure wave in the VP induction mechanism. First, although there is some flexibility in the cell walls of xylem vessels [41–43], it is unlikely that, under normal conditions, pressure-induced changes in xylem vessel size will be sufficient to cause significant changes in leaf thickness. Moreover, even under severe drought, significant deformations of xylem vessels cause changes in cell diameter not exceeding a few micrometers [41,43]. Secondly, xylem pressure is unlikely to change significantly with increasing distance from the stimulation site, even taking into account the gradient of negative xylem pressure from root to shoot [14,40,44]. Thirdly, due to the high propagation speeds of the pressure wave in the liquid [11,17,34], the observed changes in leaf thickness (Figure 2) should occur almost instantaneously; however, there is a time lag between the moment of stimulation and the phase of increasing leaf thickness.

Another potential mechanism for increasing leaf thickness and VP induction is xylem mass flow, which results in the movement of fluid from the xylem to surrounding cells and an increase in their turgor pressure. An increase in the volume of many parenchyma cells can lead to a significant increase in leaf thickness. In addition, there is evidence of the possibility of VP induction by changing the turgor of the cells surrounding the xylem [14]. Moreover, one study showed that water influx was required for VP propagation upon stem excision [45], i.e., pressure change alone was insufficient to trigger VP, suggesting the involvement of hydraulic mass flow. Finally, hydraulic mass flow can facilitate the propagation of chemical signals that cause the activation of ligand-gated ion channels and VP induction [1,2,18], which is supported by the results of this study (Figure 6). Taken together, the evidence described above is more consistent with the hypothesis of hydraulic mass flow as the main VP inducer.

The next question is about the water supply involved in hydraulic mass flow. The most likely supply of water to the xylem is from the apoplast and damaged cells of the wounded area [16,30,46]. In one study, calculations showed that wound-induced changes in leaf thickness depended on the amount of water available in the stimulation area [30]. It should also be noted that increasing positive pressure in the damage site can promote hydraulic mass flow, as evidenced by the increased xylem flow rate upon wounding [44,47].

In addition to positive pressure changes due to the damage-induced release of xylem tension, water supply may be facilitated by the inhibition of transpiration, which under normal conditions provides an upward flow of fluid [35,39,44]. It is well known that stimuli such as heating [5], burning [5,48] and mechanical damage [49] cause a significant decrease in stomatal conductance and transpiration, which was also shown in this work (Figure 3). This leads to a positive change in xylem pressure and disruption of the normal fluid flow

in the xylem, which probably underlies the dependence of the amplitude and velocity of VP propagation on the transpiration rate [50].

Next, possible mechanisms of stimulus-specific features of the parameters of leaf thickness changes will be discussed. In the case of heating and burning, the greater amplitude of leaf thickening compared to wounding (Figure 2B) could have been caused by heat-driven water expansion [14,17]. In the case of burning, this process was probably faster and more severe due to the higher flame temperature, providing a high rate of increase in leaf thickness compared to heating (Figure 2E). The longer duration of the leaf thickening phase upon heating was likely due to the longer duration of stimulation (Figure 2D), leading to an increased amount of water available for hydraulic mass flow (Figure 2C).

Another factor that determines the greater amplitude and duration of leaf thickening in the case of heating may be the large contribution of changes in transpiration, since leaf thickness reached its maximum 10–15 min after stimulation (Figure 2B), when the transpiration rate decreased significantly (Figure 3). In the case of burning and wounding, the influence of transpiration on changes in leaf thickness was most likely insignificant, since the decrease in stomatal conductance began no earlier than 5 min after stimulation (Figure 3), when the increase in leaf thickness had reached its maximum (Figure 2B).

The rather large decrease in leaf thickness observed during heating, which preceded the VP generation (Figure 2A), can be explained by an increase in the transpiration rate (Figure 3), which led to a tension increase in the xylem sap column (negative pressure) [39,40,44,51] and, as a consequence, to an accelerated efflux of water from systemic tissues to the heated area. The increase in the transpiration rate may be associated with both an increase in temperature [6,52] and with the hydropassive opening of stomata, possibly due to the loss of turgor in the epidermis [5,48].

The role of hydraulic mass flow in VP induction is also supported by the results of experiments on detached leaves, which showed a significant reduction in VP amplitude and an increase in decrement, particularly in the case of heating (Figure 4B). This suggestion is based on the fact that the pressure in the xylem vessels of a detached leaf is more positive compared to the whole plant due to a loss of vessel integrity upon excision [14], which leads to a reduced damage-induced pressure drop, and as a consequence, to impaired hydraulic mass flow and VP propagation. Another reason for the suppression of hydraulic mass flow and VP may be the influence of other plant parts, potentially through two ways: first, by changing the total amount of water available for hydraulic mass flow [30], and second, by altering xylem water column tension (more negative pressure in intact plants due to xylem tension in other leaves and active transpiration) [39,40,51].

3.2. The Role of the Chemical Signal in the Formation of the Specificity of Variation Potentials Induced by Different Local Stimuli

Along with the hydraulic signal, the chemical signal is proposed as a VP inducer, the role of which can be played by ROS [2,11,20–22]. To determine the contribution of ROS to the VP propagation caused by different stimuli, the effects of ROS scavengers and ROS production inhibitors on VP amplitude were evaluated. Treatment with DMTU led to a suppression of VPs, induced by all stimuli (Figure 6). VP suppression was more pronounced at a distance from the stimulation area, supporting the role of ROS in VP propagation. The suppression of the wound-stimulated VP was the smallest, suggesting a smaller contribution of ROS to the induction of wound-stimulated VP compared to other stimuli. This appears to be related to a reduced initial ROS burst in the stimulated area compared to burning and heating due to the lack of thermal exposure [53–55].

In addition to ROS transported by xylem mass flow from the stimulation area, the systemic production of ROS is possible, maintaining the propagation of the ROS wave in unstimulated parts of the plant [2,11,56–58]. These propagating ROS signals appear to be dependent on ROS-producing enzymes, which are inhibited by DPI [25,26] and SHAM [27,28]. This is supported by the significant VP suppression by these inhibitors at a

distance from the stimulation site (Figure 6). According to the literature, the central role in the systemic propagation of ROS waves is played by DPI-inhibited NADPH oxidases, most likely RESPIRATORY BURST OXIDASE HOMOLOGUE D (RBOHD) [8,20,54,57,59]. This is consistent with the results that VPs were more attenuated upon DPI treatment compared to SHAM treatment (Figure 6). Moreover, the results of this work are in good agreement with data from other studies in which VP propagation in systemic tissues was suppressed in loss-of-function *rbohD* mutants, but local membrane potential changes were not suppressed in the *rbohD* mutant [8,33].

It should be noted that the statistically significant VP suppression by inhibitors of ROS production compared to control treatment was observed only upon heating and burning, but not upon wounding (Figure 6). In addition to the aforementioned reduced initial ROS burst, the more attenuated ROS wave upon wounding was possibly due to lower systemic ROS production, which could be related to the different mechanisms of occurrence of this wave upon different stimulations. This is supported by the fact that the regulatory mechanisms and propagation pathways of the ROS wave in Arabidopsis are different in response to the local application of high-light stress on the one hand, and in response to wounding [33] and heating [6] on the other hand, while the function of RBOHD is required in response to all stimuli.

3.3. The Features of Generation of Variation Potentials Induced by Different Stimuli

Inhibitor studies have revealed the universality of the involvement of H^+-ATPase in the generation of VPs caused by different local stimuli. H^+-ATPase is the major contributor to VP generation (Figure 7). However, it should be noted that the suppression of VPs during inhibition of H^+-ATPase may be associated not only with its direct contribution to generation, but also with the dissipation of gradients of other ions [60,61].

The results of this work are consistent with other studies that have demonstrated the involvement of H^+-ATPase in VP generation upon wounding [62,63], burning [5,60,64,65] and heating [5,66,67], including by detecting pH changes during VP generation [5,65,67]. It can be assumed that the absence of differences in VP parameters between stimuli upon inhibitor treatment (Figure 7) is due to a similar main contribution of H^+-ATPase, probably H^+-ATPase 1 (AHA1) [62,63], to the change in membrane potential during VP generation [2,10,11,22,29,56], although limitations of the approach used, inhibitor analysis, cannot be excluded.

The universality of the involvement of Ca^{2+}-permeable plasma membrane channels in the generation of VPs induced by different local stimuli was also demonstrated (Figure 7). Other studies have previously shown the involvement of Ca^{2+}-permeable channels in in VP generation upon heating [66] and burning [64,68], including studies using inhibitors of Ca^{2+}-permeable channels [64,66] and Ca^{2+} chelators [64,66,68]. When Ca^{2+}-permeable channels are inhibited, the VP amplitude is suppressed less than when H^+-ATPase is inhibited (Figure 7), which can be associated with the aforementioned reduction in the electrochemical potential gradient [60,61].

Treatment with the mechanosensitive channel inhibitor $GdCl_3$ led to the suppression of VPs caused by all stimuli (Figure 7), further indicating the involvement of hydraulic signals in the VP generation and propagation. Treatment with $GdCl_3$, like treatment with $LaCl_3$, led to a decrease in the rate of depolarization, which suggests that the mechanosensitive channels are involved in the formation of the rapid depolarization phase for all types of stimuli. These channels appeared to contribute more to the generation and propagation of burn- and wound-induced VPs than heat-induced VPs, as evidenced by a decrease in VP amplitude upon $GdCl_3$ treatment (Figure 7). It is possible that this may be associated with the rate of pressure increase (slope) during the hydraulic signal, which is higher in the case of burning and, partly, wounding, since a dependence of activation on the rate of pressure increase has been demonstrated for mechanosensitive plant channels [69]. The results of this study suggest a greater contribution of mechanosensitive channels to the generation of VPs in the case of burning and wounding.

The molecular identities of the signaling components underlying the specificity of the mechanisms of VP generation and propagation, and the mechanisms of their interplay, are still not clear. ROS-activated Ca^{2+}-permeable plasma membrane channels have been suggested to be involved in VP generation and propagation, but the molecular identity of these channels remains unknown [29,70–72]. To date, ligand-gated Ca^{2+}-permeable cation channels of the GLUTAMATE RECEPTOR-LIKE (GLR) family have been confirmed to be essential to generating VPs [61,70]. Among the channels of the GLR family, the contribution to the VP generation and propagation was experimentally shown for GLR3.3 [33,54,63,73–76], GLR3.6 [33,54,63,73–75], GLR3.1 and GLR3.5 [74,75]. It should be noted that GLR3.3 and GLR3.6 are required for wound-induced systemic Ca^{2+} waves [63,74,76–78], hydraulic waves [33] and RBOHD-mediated ROS waves [33,54,79].

The initial perception of hydraulic waves may be mediated by the stretch-activated anion channel, MECHANOSENSITIVE CHANNEL OF SMALL CONDUCTANCE-LIKE 10 (MSL10), which plays a critical role in the proper formation of VPs through the regulation of GLR3.3 and GLR3.6 activity [80], which links this channels to hydraulic waves. It should be emphasized that for MSL10, the dependence of activation on the rate of pressure increase is shown [69]. It is possible that other mechanosensitive channels may also be involved in VP generation and propagation [61].

It should be noted that the above-mentioned GLR3.3 and GLR3.6 may also be involved in the interplay of various components of the complex plant stress signal—Ca^{2+}, ROS and hydraulic waves—providing crosstalk between the signals. Thus, based on the similar suppression of wound-induced Ca^{2+} waves in the *glr3.3;glr3.6* double mutant and *rbohD* mutants, it can be assumed that RBOHD is involved in the regulation of Ca^{2+} signals [33,54], which in turn provides additional ROS production [11,58]. At the same time, it was shown that wound-induced GLR3.3-mediated calcium waves are RBOHD independent [77]. It has also been shown that GLR3.3 and GLR3.6 are involved in maintaining ROS waves induced by certain stimuli [33]. Thus, wound-induced ROS waves were suppressed in the *glr3.3;glr3.6* double mutant. At the same time, in response to high-light stress, ROS waves were not completely suppressed [33], indicating a different mechanism for ROS wave propagation [6,33] and, in general, the presence of the specificity of this signal caused by different stimuli.

It is important to note that no influence was found of the key ROS wave generator, RBOHD, on the other component of the complex stress signal, which is the hydraulic wave [33]. The mechanism of water transport into cells surrounding the xylem during hydraulic mass flow may involve aquaporins, such as plasma membrane intrinsic protein 2;1 (PIP2;1) [33,81]. Aquaporins are known to play a role in regulating the hydraulic conductance of vascular bundles [81]. The wound-induced systemic hydraulic signal is suppressed in the *pip2;1* mutant. The function of aquaporins is regulated by calcium, likely mediated by the cation channels GLR3.3 and GLR3.6. According to the authors, an increase in cytosolic Ca^{2+} concentration leads to the closure of aquaporins and a subsequent increase in hydraulic pressure in the xylem vessels due to the abolished efflux of water into the cells surrounding the xylem [33]. In addition, aquaporins such as PIP2;1, as well as plasmodesmata (PD)-localized proteins (PDLP) 1 and 5 play key roles in regulating rapid systemic ROS signals [33,82].

Thus, it can be proposed that the mechanisms of stimulus-specific VP induction and propagation are based on the different contributions of the hydraulic and chemical components of VP. Stimulus-induced damage results in the release of xylem water column tension and the release of chemical elicitors such as ROS and water from damaged cells. In the case of thermal stimuli, more ROS are produced compared to mechanical wounding due to thermal exposure. ROS are transported by xylem mass flow. During hydraulic mass flow, water moves into the cells surrounding the xylem, resulting in increased cell turgor and the subsequent activation of mechanosensitive channels, probably MSL10. Mechanosensitive channels contribute more to the induction of burn- and wound-triggered VPs, which is related to more abrupt pressure changes due to instantaneous stimulation,

whereas upon gradual heating, prolonged stimulation causes less abrupt pressure changes. In turn, ROS activate ligand-gated Ca^{2+} channels, either the proposed ROS-activated Ca^{2+}-permeable plasma membrane channel, the molecular identity of which remains unknown, or GLR3.3 and GLR3.6 through the MSL10-dependent regulation of their activity. Increased cytosolic Ca^{2+} levels induce H^+-ATPase inactivation and, as a result, VP generation. In the cases of heating and burning, additional ROS production is mediated by the Ca^{2+}- or ROS-dependent activation of NADPH oxidases, mainly RBOHD. Other factors, such as heat-driven water expansion and transpiration changes upon heating, may also contribute to the mechanism of stimulus-specific VP induction.

4. Materials and Methods

4.1. Plant Material and Growth Conditions

Wheat (*Triticum aestivum* L.) cv. Daria was grown in a growth room at 24 °C under long-day conditions (16 h/8 h light/dark). For all experiments, 14–21-day-old plants, grown in pots with sand as soil, were used. Due to the low penetration of inhibitors through the wheat leaf epidermis, experiments with inhibitors were carried out using a detached wheat leaf (second mature leaf 17 cm long) cut from wheat plants and adapted in a standard solution (1 mM KCl, 0.5 mM $CaCl_2$, 0.1 mM NaCl) for 17 h.

4.2. Local Stimulation

Local stimulation was applied to the tip (~1 cm long) of a second mature wheat leaf. Three types of stimuli were used: (1) gradual heating in a cuvette with water to 60 °C for 5–7 min; (2) burning with a flame for 3 s; (3) mechanical wounding by crushing with a plastic cylinder. One single stimulation experiment was carried out per plant. Before stimulation, wheat plants were removed from the growth room and acclimated for a minimum of 1 h in the recording room at ~24 °C.

4.3. Extracellular Measurements of Electrical Signals

Surface potentials were recorded using Ag^+/AgCl macroelectrodes EVL-1M3 (Gomel Plant of Measuring Devices, Gomel, Belarus) filled with 3 M KCl, a high-impedance three-channel amplifier IPL-113 (Semico, Novosibirsk, Russia) and a personal computer. Three measuring electrodes were placed on the second mature wheat leaf with an inter-electrode distance of 3 cm and a distance of 3 cm between the damage site and the first electrode. The interface between the measuring electrode and the leaf was a cotton thread wetted with a standard solution. A reference electrode was placed in the soil during recordings from whole plants or in a standard solution surrounding the leaf cut during recordings from detached leaves. Surface potential recordings were acquired at 1 Hz.

4.4. Inhibitor Studies

To investigate the features of the mechanisms of generation and propagation of VP induced by different stimuli, inhibitor analysis was performed using the plasma membrane H^+-ATPase inhibitor sodium orthovanadate (2 mM), the plasma membrane Ca^{2+}-permeable channel blocker lanthanum chloride (5 mM), the mechanosensitive channel inhibitor gadolinium chloride (10 mM), the scavenger of ROS DMTU (1 mM) [23,24], the inhibitor of NADPH oxidases DPI (20 μM) [25,26], the cell wall peroxidase inhibitor and the mitochondrial alternative oxidase inhibitor SHAM (1 mM) [27,28]. All chemicals were from Sigma-Aldrich (St. Louis, MO, USA). Solutions for chemical treatments were made in a standard solution. The solutions were loaded into a detached wheat leaf by vacuum infiltration. To do this, the cut of the detached leaf was immersed in a solution of the corresponding compound, and then exposed to one cycle of vacuum infiltration for 5 min at 70 kPa in a vacuum desiccator. Control experiments were carried out in exactly the same way via infiltration with a standard solution. All experiments were carried out 1.5 h after infiltration.

4.5. Monitoring of Leaf Thickness

Changes in wheat leaf thickness were monitored to detect hydraulic signals. The leaf thickness was measured using a system including an OL1 optical micrometer (SICK, Düsseldorf, Germany), an AOD1 evaluation unit (SICK, Düsseldorf, Germany) and LTR12 analog-to-digital converters in the LTR-EU-2-5 crate (L-Card, Moscow, Russia). Changes in leaf thickness were recorded at 10 Hz using L-Card Measurement Studio software (version 1.1.0) (L-Card, Moscow, Russia). A wheat leaf was fixed at an equal distance between the sender unit and the receiver unit so that the shading of the light band by the leaf, recorded by the receiver unit, corresponded to the leaf thickness. Regions of interest (3 mm) were located at distances of 4.5, 7.5 and 10.5 cm from the stimulation area (Figure 1). Simultaneously with the monitoring of leaf thickness, surface electrical potentials were recorded.

4.6. Measurements of Leaf Stomatal Conductance

A GFS-3000 gas analyzer (Heinz Walz GmbH, Effeltrich, Germany) and Dual-PAM gas-exchange Cuvette 3010-Dual common measuring head (Heinz Walz GmbH, Effeltrich, Germany) were used for investigations of leaf stomatal conductance, which was automatically calculated by GFS-Win software (version 3.82) (Heinz Walz GmbH, Effeltrich, Germany). The CO_2 concentration in the measuring cuvette was 360 ppm, the relative humidity was about 70%, and the temperature was 23 °C. Blue actinic light (460 nm, 240 μmol m^{-2} s^{-1}) were used in the experiments. The measuring cuvette was placed on the second mature wheat leaf at a distance of 4.5 cm from the stimulation area. Leaf stomatal conductance recordings were acquired at 1 Hz.

4.7. Statistical Analysis

All experiments with each stimulus type were repeated with at least 10 independent biological replicates. Each replicate was performed on a separate wheat plant. Results are represented as means ± SEM, first-order derivative, typical records of individual measurements. Statistical significance in pair-wise comparisons was evaluated by Student's *t*-test. For multiple comparisons, two-way ANOVA were performed. The level of statistical significance was set at $p < 0.05$. Statistical analysis was performed using Microsoft Excel (version 2409) and GraphPad Prism 6 software (version 6.07) (GraphPad Software, Boston, MA, USA).

5. Conclusions

Thus, the study revealed differences in the parameters of VPs induced by different local stimuli: less of a decrement upon heating compared to burning and wounding, and the smallest amplitude upon wounding. Differences in VP parameters indicate the possibility of the VP-mediated induction of stimulus-specific systemic functional responses [1,2]. These findings suggest that the VP is not only a signal with information about the damaging effect, but also has the potential to encode information about the stimulus. The mechanism of the VP-mediated induction of systemic responses is most likely based on shifts in the concentrations of ions, such as Ca^{2+} and H^+, accompanying VP generation [1,2]. Taken together, these findings suggest that the stimulus specificity of VP originates in the features of the chemical and hydraulic signals that form the VP, which, in turn, can influence changes in ion concentrations.

However, there are outstanding questions about the mechanisms of VP formation and their roles in the regulation of the physiological state of plants. Can hydraulic signals independently perform regulatory functions in plants? What is the molecular identity of ROS-activated Ca^{2+}-permeable channels? What is the precise molecular pathway for VP generation? How do aquaporins play a role in generating VP and hydraulic signals? These and many other questions require further research.

Answers to these questions will facilitate the practical implementation of the acquired knowledge about the mechanisms of specificity of electrical signals in plants, primarily

for solving agricultural problems. One of the priority applications is the identification of critical stressors based on the monitoring of electrical activity. To date, there are more works aimed at identifying the influencing stressor based on the classification of plant electrical signals using machine learning methods [83–85], including herbivore [86] and pathogen attacks [87], early detection of water [88,89] and nitrogen deficiency [90], etc. Another problem is to assess the resistance of plants based on the characteristics of electrical reactions under the influence of various stressors, such as salinity [91], high temperatures [91] and heavy metals [92], which allows the selection of the most resistant varieties at the early stages of selection. Other problems may also be addressed, including the modification of resistance to stressors by regulating the electrical activity of plants.

Supplementary Materials: The following supporting information can be downloaded at: https://www.mdpi.com/article/10.3390/plants13202896/s1, Figure S1: Dependences of the amplitude of leaf thickness reduction on the distance to the area of local stimulation induced by local heating, burning or wounding in wheat plants.

Author Contributions: Conceptualization, M.M. and V.V.; methodology, M.M. and V.V.; validation, M.M. and Y.V.; formal analysis, M.M.; investigation, M.M., M.L. and Y.V.; resources, Y.V. and V.V.; data curation, M.M.; writing—original draft preparation, M.M.; writing—review and editing, M.M., M.L. and V.V.; visualization, M.M.; supervision, V.V.; project administration, V.V.; funding acquisition, V.V. All authors have read and agreed to the published version of the manuscript.

Funding: The research was funded by the Russian Science Foundation (project No. 22-14-00388).

Data Availability Statement: The data that support the findings of this study are available from the corresponding author upon reasonable request.

Conflicts of Interest: The authors declare no conflicts of interest.

References

1. Sukhov, V.; Sukhova, E.; Vodeneev, V. Long-Distance Electrical Signals as a Link between the Local Action of Stressors and the Systemic Physiological Responses in Higher Plants. *Prog. Biophys. Mol. Biol.* **2019**, *146*, 63–84. [CrossRef] [PubMed]
2. Mudrilov, M.; Ladeynova, M.; Grinberg, M.; Balalaeva, I.; Vodeneev, V. Electrical Signaling of Plants under Abiotic Stressors: Transmission of Stimulus-Specific Information. *Int. J. Mol. Sci.* **2021**, *22*, 10715. [CrossRef] [PubMed]
3. Yan, H.; Fu, K.; Li, J.; Li, M.; Li, S.; Dai, Z.; Jin, X. Photosynthesis, Chlorophyll Fluorescence, and Hormone Regulation in Tomato Exposed to Mechanical Wounding. *Plants* **2024**, *13*, 2594. [CrossRef] [PubMed]
4. Krausko, M.; Perutka, Z.; Šebela, M.; Šamajová, O.; Šamaj, J.; Novák, O.; Pavlovič, A. The Role of Electrical and Jasmonate Signalling in the Recognition of Captured Prey in the Carnivorous Sundew Plant *Drosera capensis*. *New Phytol.* **2017**, *213*, 1818–1835. [CrossRef]
5. Mudrilov, M.; Ladeynova, M.; Berezina, E.; Grinberg, M.; Brilkina, A.; Sukhov, V.; Vodeneev, V. Mechanisms of Specific Systemic Response in Wheat Plants under Different Locally Acting Heat Stimuli. *J. Plant Physiol.* **2021**, *258–259*, 153377. [CrossRef]
6. Zandalinas, S.I.; Fichman, Y.; Devireddy, A.R.; Sengupta, S.; Azad, R.K.; Mittler, R. Systemic Signaling during Abiotic Stress Combination in Plants. *Proc. Natl. Acad. Sci. USA* **2020**, *117*, 13810–13820. [CrossRef]
7. Meena, M.K.; Prajapati, R.; Krishna, D.; Divakaran, K.; Pandey, Y.; Reichelt, M.; Mathew, M.K.; Boland, W.; Mithöfer, A.; Vadassery, J. The Ca^{2+} Channel CNGC19 Regulates *Arabidopsis* Defense Against *Spodoptera* Herbivory. *Plant Cell* **2019**, *31*, 1539–1562. [CrossRef]
8. Suzuki, N.; Miller, G.; Salazar, C.; Mondal, H.A.; Shulaev, E.; Cortes, D.F.; Shuman, J.L.; Luo, X.; Shah, J.; Schlauch, K.; et al. Temporal-Spatial Interaction between Reactive Oxygen Species and Abscisic Acid Regulates Rapid Systemic Acclimation in Plants. *Plant Cell* **2013**, *25*, 3553–3569. [CrossRef]
9. Ma, Y.; Flückiger, I.; Nicolet, J.; Pang, J.; Dickinson, J.B.; De Bellis, D.; Emonet, A.; Fujita, S.; Geldner, N. Comparisons of Two Receptor-MAPK Pathways in a Single Cell-Type Reveal Mechanisms of Signalling Specificity. *Nat. Plants* **2024**, *10*, 1343–1362. [CrossRef]
10. Lee, K.; Seo, P.J. Wound-Induced Systemic Responses and Their Coordination by Electrical Signals. *Front. Plant Sci.* **2022**, *13*, 880680. [CrossRef]
11. Huber, A.E.; Bauerle, T.L. Long-Distance Plant Signaling Pathways in Response to Multiple Stressors: The Gap in Knowledge. *J. Exp. Bot.* **2016**, *67*, 2063–2079. [CrossRef] [PubMed]
12. Vodeneev, V.; Akinchits, E.; Sukhov, V. Variation Potential in Higher Plants: Mechanisms of Generation and Propagation. *Plant Signal. Behav.* **2015**, *10*, e1057365. [CrossRef] [PubMed]
13. Vodeneev, V.; Mudrilov, M.; Akinchits, E.; Balalaeva, I.; Sukhov, V. Parameters of Electrical Signals and Photosynthetic Responses Induced by Them in Pea Seedlings Depend on the Nature of Stimulus. *Funct. Plant Biol.* **2018**, *45*, 160. [CrossRef]

14. Stahlberg, R.; Cleland, R.E.; Van Volkenburgh, E. Slow Wave Potentials—A Propagating Electrical Signal Unique to Higher Plants. In *Communication in Plants*; Baluška, F., Mancuso, S., Volkmann, D., Eds.; Springer: Berlin, Heidelberg, Germany, 2006; pp. 291–308, ISBN 978-3-540-28475-8.
15. Stankovic, B.; Zawadzki, T.; Davies, E. Characterization of the Variation Potential in Sunflower. *Plant Physiol.* **1997**, *115*, 1083–1088. [CrossRef]
16. Malone, M. Kinetics of Wound-Induced Hydraulic Signals and Variation Potentials in Wheat Seedlings. *Planta* **1992**, *187*, 505–510. [CrossRef]
17. Kurenda, A.; Nguyen, C.T.; Chételat, A.; Stolz, S.; Farmer, E.E. Insect-Damaged *Arabidopsis* Moves like Wounded *Mimosa pudica*. *Proc. Natl. Acad. Sci. USA* **2019**, *116*, 26066–26071. [CrossRef]
18. Evans, M.J.; Morris, R.J. Chemical Agents Transported by Xylem Mass Flow Propagate Variation Potentials. *Plant J.* **2017**, *91*, 1029–1037. [CrossRef]
19. Sukhova, E.; Akinchits, E.; Gudkov, S.V.; Pishchalnikov, R.Y.; Vodeneev, V.; Sukhov, V. A Theoretical Analysis of Relations between Pressure Changes along Xylem Vessels and Propagation of Variation Potential in Higher Plants. *Plants* **2021**, *10*, 372. [CrossRef]
20. Miller, G.; Schlauch, K.; Tam, R.; Cortes, D.; Torres, M.A.; Shulaev, V.; Dangl, J.L.; Mittler, R. The Plant NADPH Oxidase RBOHD Mediates Rapid Systemic Signaling in Response to Diverse Stimuli. *Sci. Signal.* **2009**, *2*, ra45. [CrossRef]
21. Mittler, R.; Vanderauwera, S.; Suzuki, N.; Miller, G.; Tognetti, V.B.; Vandepoele, K.; Gollery, M.; Shulaev, V.; Van Breusegem, F. ROS Signaling: The New Wave? *Trends Plant Sci.* **2011**, *16*, 300–309. [CrossRef]
22. Farmer, E.E.; Gao, Y.; Lenzoni, G.; Wolfender, J.; Wu, Q. Wound- and Mechanostimulated Electrical Signals Control Hormone Responses. *New Phytol.* **2020**, *227*, 1037–1050. [CrossRef] [PubMed]
23. Arfan, M.; Zhang, D.-W.; Zou, L.-J.; Luo, S.-S.; Tan, W.-R.; Zhu, T.; Lin, H.-H. Hydrogen Peroxide and Nitric Oxide Crosstalk Mediates Brassinosteroids Induced Cold Stress Tolerance in Medicago Truncatula. *Int. J. Mol. Sci.* **2019**, *20*, 144. [CrossRef] [PubMed]
24. Jiang, J.; Su, M.; Wang, L.; Jiao, C.; Sun, Z.; Cheng, W.; Li, F.; Wang, C. Exogenous Hydrogen Peroxide Reversibly Inhibits Root Gravitropism and Induces Horizontal Curvature of Primary Root during Grass Pea Germination. *Plant Physiol. Biochem.* **2012**, *53*, 84–93. [CrossRef]
25. Lee, D.J.; Choi, H.J.; Moon, M.; Chi, Y.; Ji, K.; Choi, D. Superoxide Serves as a Putative Signal Molecule for Plant Cell Division: Overexpression of *CaRLK1* Promotes the Plant Cell Cycle via Accumulation of O_2^- and Decrease in H_2O_2. *Physiol. Plant.* **2017**, *159*, 228–243. [CrossRef]
26. Kai, K.; Kasa, S.; Sakamoto, M.; Aoki, N.; Watabe, G.; Yuasa, T.; Iwaya-Inoue, M.; Ishibashi, Y. Role of Reactive Oxygen Species Produced by NADPH Oxidase in Gibberellin Biosynthesis during Barley Seed Germination. *Plant Signal. Behav.* **2016**, *11*, e1180492. [CrossRef]
27. Khokon, A.R.; Okuma, E.; Hossain, M.A.; Munemasa, S.; Uraji, M.; Nakamura, Y.; Mori, I.C.; Murata, Y. Involvement of Extracellular Oxidative Burst in Salicylic Acid-induced Stomatal Closure in *Arabidopsis*. *Plant Cell Environ.* **2011**, *34*, 434–443. [CrossRef]
28. Vanlerberghe, G. Alternative Oxidase: A Mitochondrial Respiratory Pathway to Maintain Metabolic and Signaling Homeostasis during Abiotic and Biotic Stress in Plants. *Int. J. Mol. Sci.* **2013**, *14*, 6805–6847. [CrossRef]
29. Johns, S.; Hagihara, T.; Toyota, M.; Gilroy, S. The Fast and the Furious: Rapid Long-Range Signaling in Plants. *Plant Physiol.* **2021**, *185*, 694–706. [CrossRef]
30. Alarcon, J.-J.; Malone, M. Substantial Hydraulic Signals Are Triggered by Leaf-Biting Insects in Tomato. *J. Exp. Bot.* **1994**, *45*, 953–957. [CrossRef]
31. Boari, F.; Malone, M. Wound-Induced Hydraulic Signals: Survey of Occurrence in a Range of Species. *J. Exp. Bot.* **1993**, *44*, 741–746. [CrossRef]
32. Mancuso, S. Hydraulic and Electrical Transmission of Wound-Induced Signals in *Vitis vinifera*. *Funct. Plant Biol.* **1999**, *26*, 55. [CrossRef]
33. Fichman, Y.; Mittler, R. Integration of Electric, Calcium, Reactive Oxygen Species and Hydraulic Signals during Rapid Systemic Signaling in Plants. *Plant J.* **2021**, *107*, 7–20. [CrossRef] [PubMed]
34. Lopez, R.; Badel, E.; Peraudeau, S.; Leblanc-Fournier, N.; Beaujard, F.; Julien, J.-L.; Cochard, H.; Moulia, B. Tree Shoot Bending Generates Hydraulic Pressure Pulses: A New Long-Distance Signal? *J. Exp. Bot.* **2014**, *65*, 1997–2008. [CrossRef] [PubMed]
35. Christmann, A.; Grill, E.; Huang, J. Hydraulic Signals in Long-Distance Signaling. *Curr. Opin. Plant Biol.* **2013**, *16*, 293–300. [CrossRef]
36. Basu, D.; Haswell, E.S. Plant Mechanosensitive Ion Channels: An Ocean of Possibilities. *Curr. Opin. Plant Biol.* **2017**, *40*, 43–48. [CrossRef]
37. Hamilton, E.S.; Schlegel, A.M.; Haswell, E.S. United in Diversity: Mechanosensitive Ion Channels in Plants. *Annu. Rev. Plant Biol.* **2015**, *66*, 113–137. [CrossRef]
38. Dainese, R.; Tarantino, A. Measurement of Plant Xylem Water Pressure Using the High-Capacity Tensiometer and Implications for the Modelling of Soil–Atmosphere Interaction. *Géotechnique* **2021**, *71*, 441–454. [CrossRef]
39. Schenk, H.J.; Jansen, S.; Hölttä, T. Positive Pressure in Xylem and Its Role in Hydraulic Function. *New Phytol.* **2021**, *230*, 27–45. [CrossRef]

40. Stahlberg, R.; Cosgrove, D.J. A Reduced Xylem Pressure Altered the Electric and Growth Responses in Cucumber Hypocotyls. *Plant Cell Environ.* **1997**, *20*, 101–109. [CrossRef]
41. Cochard, H.; Froux, F.; Mayr, S.; Coutand, C. Xylem Wall Collapse in Water-Stressed Pine Needles. *Plant Physiol.* **2004**, *134*, 401–408. [CrossRef]
42. Ménard, D.; Blaschek, L.; Kriechbaum, K.; Lee, C.C.; Serk, H.; Zhu, C.; Lyubartsev, A.; Nuoendagula; Bacsik, Z.; Bergström, L.; et al. Plant Biomechanics and Resilience to Environmental Changes Are Controlled by Specific Lignin Chemistries in Each Vascular Cell Type and Morphotype. *Plant Cell* **2022**, *34*, 4877–4896. [CrossRef] [PubMed]
43. Zhang, Y.-J.; Rockwell, F.E.; Graham, A.C.; Alexander, T.; Holbrook, N.M. Reversible Leaf Xylem Collapse: A Potential "Circuit Breaker" against Cavitation. *Plant Physiol.* **2016**, *172*, 2261–2274. [CrossRef] [PubMed]
44. Benkert, R.; Balling, A.; Zimmermann, U. Direct Measurements of the Pressure and Flow in the Xylem Vessels of *Nicotiana Tabacum* and Their Dependence on Flow Resistance and Transpiration Rate. *Bot. Acta* **1991**, *104*, 423–432. [CrossRef]
45. Stahlberg, R.; Cosgrove, D.J. Rapid Alterations in Growth Rate and Electrical Potentials upon Stem Excision in Pea Seedlings. *Planta* **1992**, *187*, 523–531. [CrossRef]
46. Malone, M. Hydraulic Signals. *Phil. Trans. R. Soc. Lond. B* **1993**, *341*, 33–39. [CrossRef]
47. Vodeneev, V.; Orlova, A.; Morozova, E.; Orlova, L.; Akinchits, E.; Orlova, O.; Sukhov, V. The Mechanism of Propagation of Variation Potentials in Wheat Leaves. *J. Plant Physiol.* **2012**, *169*, 949–954. [CrossRef]
48. Kaiser, H.; Grams, T.E.E. Rapid Hydropassive Opening and Subsequent Active Stomatal Closure Follow Heat-Induced Electrical Signals in *Mimosa Pudica**. *J. Exp. Bot.* **2006**, *57*, 2087–2092. [CrossRef]
49. Fromm, J.; Hajirezaei, M.-R.; Becker, V.K.; Lautner, S. Electrical Signaling along the Phloem and Its Physiological Responses in the Maize Leaf. *Front. Plant Sci.* **2013**, *4*, 239. [CrossRef]
50. Stahlberg, R.; Cleland, R.E.; Van Volkenburgh, E. Decrement and Amplification of Slow Wave Potentials during Their Propagation in *Helianthus annuus* L. Shoots. *Planta* **2005**, *220*, 550–558. [CrossRef]
51. Wei, C.; Tyree, M.T.; Steudle, E. Direct Measurement of Xylem Pressure in Leaves of Intact Maize Plants. A Test of the Cohesion-Tension Theory Taking Hydraulic Architecture into Consideration. *Plant Physiol.* **1999**, *121*, 1191–1205. [CrossRef]
52. Sadok, W.; Lopez, J.R.; Smith, K.P. Transpiration Increases under High-temperature Stress: Potential Mechanisms, Trade-offs and Prospects for Crop Resilience in a Warming World. *Plant Cell Environ.* **2021**, *44*, 2102–2116. [CrossRef] [PubMed]
53. Hasanuzzaman, M.; Nahar, K.; Alam, M.M.; Roychowdhury, R.; Fujita, M. Physiological, Biochemical, and Molecular Mechanisms of Heat Stress Tolerance in Plants. *Int. J. Mol. Sci.* **2013**, *14*, 9643–9684. [CrossRef] [PubMed]
54. Lew, T.T.S.; Koman, V.B.; Silmore, K.S.; Seo, J.S.; Gordiichuk, P.; Kwak, S.-Y.; Park, M.; Ang, M.C.-Y.; Khong, D.T.; Lee, M.A.; et al. Real-Time Detection of Wound-Induced H_2O_2 Signalling Waves in Plants with Optical Nanosensors. *Nat. Plants* **2020**, *6*, 404–415. [CrossRef] [PubMed]
55. Li, Z.; Howell, S.H. Heat Stress Responses and Thermotolerance in Maize. *Int. J. Mol. Sci.* **2021**, *22*, 948. [CrossRef]
56. Vega-Muñoz, I.; Duran-Flores, D.; Fernández-Fernández, Á.D.; Heyman, J.; Ritter, A.; Stael, S. Breaking Bad News: Dynamic Molecular Mechanisms of Wound Response in Plants. *Front. Plant Sci.* **2020**, *11*, 610445. [CrossRef]
57. Suda, H.; Toyota, M. Integration of Long-Range Signals in Plants: A Model for Wound-Induced Ca^{2+}, Electrical, ROS, and Glutamate Waves. *Curr. Opin. Plant Biol.* **2022**, *69*, 102270. [CrossRef]
58. Choi, W.-G.; Hilleary, R.; Swanson, S.J.; Kim, S.-H.; Gilroy, S. Rapid, Long-Distance Electrical and Calcium Signaling in Plants. *Annu. Rev. Plant Biol.* **2016**, *67*, 287–307. [CrossRef]
59. Fichman, Y.; Miller, G.; Mittler, R. Whole-Plant Live Imaging of Reactive Oxygen Species. *Mol. Plant* **2019**, *12*, 1203–1210. [CrossRef]
60. Yudina, L.; Sherstneva, O.; Sukhova, E.; Grinberg, M.; Mysyagin, S.; Vodeneev, V.; Sukhov, V. Inactivation of H^+-ATPase Participates in the Influence of Variation Potential on Photosynthesis and Respiration in Peas. *Plants* **2020**, *9*, 1585. [CrossRef]
61. Mudrilov, M.A.; Ladeynova, M.M.; Kuznetsova, D.V.; Vodeneev, V.A. Ion Channels in Electrical Signaling in Higher Plants. *Biochem. Mosc.* **2023**, *88*, 1467–1487. [CrossRef]
62. Kumari, A.; Chételat, A.; Nguyen, C.T.; Farmer, E.E. *Arabidopsis* H^+-ATPase AHA1 Controls Slow Wave Potential Duration and Wound-Response Jasmonate Pathway Activation. *Proc. Natl. Acad. Sci. USA* **2019**, *116*, 20226–20231. [CrossRef] [PubMed]
63. Shao, Q.; Gao, Q.; Lhamo, D.; Zhang, H.; Luan, S. Two Glutamate- and pH-Regulated Ca^{2+} Channels Are Required for Systemic Wound Signaling in *Arabidopsis*. *Sci. Signal.* **2020**, *13*, eaba1453. [CrossRef] [PubMed]
64. Katicheva, L.; Sukhov, V.; Akinchits, E.; Vodeneev, V. Ionic Nature of Burn-Induced Variation Potential in Wheat Leaves. *Plant Cell Physiol.* **2014**, *55*, 1511–1519. [CrossRef] [PubMed]
65. Sukhov, V.; Sherstneva, O.; Surova, L.; Katicheva, L.; Vodeneev, V. Proton Cellular Influx as a Probable Mechanism of Variation Potential Influence on Photosynthesis in Pea. *Plant Cell Environ.* **2014**, *37*, 2532–2541. [CrossRef]
66. Julien, J.L.; Desbiez, M.O.; De Jaegher, G.; Frachisse, J.M. Characteristics of the Wave of Depolarization Induced by Wounding in *Bidens pilosa* L. *J. Exp. Bot.* **1991**, *42*, 131–137. [CrossRef]
67. Ladeynova, M.; Kuznetsova, D.; Pecherina, A.; Vodeneev, V. pH Change Accompanying Long-Distance Electrical Signal Controls Systemic Jasmonate Biosynthesis. *J. Plant Physiol.* **2024**, *296*, 154225. [CrossRef]
68. Vodeneev, V.A.; Akinchits, E.K.; Orlova, L.A.; Sukhov, V.S. The Role of Ca^{2+}, H^+, and Cl^- Ions in Generation of Variation Potential in Pumpkin Plants. *Russ. J. Plant Physiol.* **2011**, *58*, 974–981. [CrossRef]

69. Maksaev, G.; Haswell, E.S. MscS-Like10 Is a Stretch-Activated Ion Channel from *Arabidopsis thaliana* with a Preference for Anions. *Proc. Natl. Acad. Sci. USA* **2012**, *109*, 19015–19020. [CrossRef]
70. Demidchik, V.; Shabala, S.; Isayenkov, S.; Cuin, T.A.; Pottosin, I. Calcium Transport across Plant Membranes: Mechanisms and Functions. *New Phytol.* **2018**, *220*, 49–69. [CrossRef]
71. Pei, Z.-M.; Murata, Y.; Benning, G.; Thomine, S.; Klüsener, B.; Allen, G.J.; Grill, E.; Schroeder, J.I. Calcium Channels Activated by Hydrogen Peroxide Mediate Abscisic Acid Signalling in Guard Cells. *Nature* **2000**, *406*, 731–734. [CrossRef]
72. Zhang, W.; Jeon, B.W.; Assmann, S.M. Heterotrimeric G-Protein Regulation of ROS Signalling and Calcium Currents in Arabidopsis Guard Cells. *J. Exp. Bot.* **2011**, *62*, 2371–2379. [CrossRef] [PubMed]
73. Mousavi, S.A.R.; Chauvin, A.; Pascaud, F.; Kellenberger, S.; Farmer, E.E. GLUTAMATE RECEPTOR-LIKE Genes Mediate Leaf-to-Leaf Wound Signalling. *Nature* **2013**, *500*, 422–426. [CrossRef] [PubMed]
74. Nguyen, C.T.; Kurenda, A.; Stolz, S.; Chételat, A.; Farmer, E.E. Identification of Cell Populations Necessary for Leaf-to-Leaf Electrical Signaling in a Wounded Plant. *Proc. Natl. Acad. Sci. USA* **2018**, *115*, 10178–10183. [CrossRef] [PubMed]
75. Salvador-Recatalà, V. New Roles for the *GLUTAMATE RECEPTOR-LIKE 3.3*, *3.5*, and *3.6* Genes as on/off Switches of Wound-Induced Systemic Electrical Signals. *Plant Signal. Behav.* **2016**, *11*, e1161879. [CrossRef]
76. Yan, C.; Gao, Q.; Yang, M.; Shao, Q.; Xu, X.; Zhang, Y.; Luan, S. Ca^{2+}/Calmodulin-Mediated Desensitization of Glutamate Receptors Shapes Plant Systemic Wound Signalling and Anti-Herbivore Defence. *Nat. Plants* **2024**, *10*, 145–160. [CrossRef]
77. Bellandi, A.; Papp, D.; Breakspear, A.; Joyce, J.; Johnston, M.G.; De Keijzer, J.; Raven, E.C.; Ohtsu, M.; Vincent, T.R.; Miller, A.J.; et al. Diffusion and Bulk Flow of Amino Acids Mediate Calcium Waves in Plants. *Sci. Adv.* **2022**, *8*, eabo6693. [CrossRef]
78. Toyota, M.; Spencer, D.; Sawai-Toyota, S.; Jiaqi, W.; Zhang, T.; Koo, A.J.; Howe, G.A.; Gilroy, S. Glutamate Triggers Long-Distance, Calcium-Based Plant Defense Signaling. *Science* **2018**, *361*, 1112–1115. [CrossRef]
79. Zandalinas, S.I.; Mittler, R. Vascular and Nonvascular Transmission of Systemic Reactive Oxygen Signals during Wounding and Heat Stress. *Plant Physiol.* **2021**, *186*, 1721–1733. [CrossRef]
80. Moe-Lange, J.; Gappel, N.M.; Machado, M.; Wudick, M.M.; Sies, C.S.A.; Schott-Verdugo, S.N.; Bonus, M.; Mishra, S.; Hartwig, T.; Bezrutczyk, M.; et al. Interdependence of a Mechanosensitive Anion Channel and Glutamate Receptors in Distal Wound Signaling. *Sci. Adv.* **2021**, *7*, eabg4298. [CrossRef]
81. Sade, N.; Shatil-Cohen, A.; Moshelion, M. Bundle-Sheath Aquaporins Play a Role in Controlling *Arabidopsis* Leaf Hydraulic Conductivity. *Plant Signal. Behav.* **2015**, *10*, e1017177. [CrossRef]
82. Fichman, Y.; Myers, R.J.; Grant, D.G.; Mittler, R. Plasmodesmata-Localized Proteins and ROS Orchestrate Light-Induced Rapid Systemic Signaling in *Arabidopsis*. *Sci. Signal.* **2021**, *14*, eabf0322. [CrossRef] [PubMed]
83. Buss, E.; Aust, T.; Wahby, M.; Rabbel, T.-L.; Kernbach, S.; Hamann, H. Stimulus Classification with Electrical Potential and Impedance of Living Plants: Comparing Discriminant Analysis and Deep-Learning Methods. *Bioinspir. Biomim.* **2023**, *18*, 025003. [CrossRef] [PubMed]
84. Costa, Á.V.L.; Oliveira, T.F.D.C.; Posso, D.A.; Reissig, G.N.; Parise, A.G.; Barros, W.S.; Souza, G.M. Systemic Signals Induced by Single and Combined Abiotic Stimuli in Common Bean Plants. *Plants* **2023**, *12*, 924. [CrossRef]
85. Bhadra, N.; Chatterjee, S.K.; Das, S. Multiclass Classification of Environmental Chemical Stimuli from Unbalanced Plant Electrophysiological Data. *PLoS ONE* **2023**, *18*, e0285321. [CrossRef]
86. Najdenovska, E.; Dutoit, F.; Tran, D.; Plummer, C.; Wallbridge, N.; Camps, C.; Raileanu, L.E. Classification of Plant Electrophysiology Signals for Detection of Spider Mites Infestation in Tomatoes. *Appl. Sci.* **2021**, *11*, 1414. [CrossRef]
87. Simmi, F.Z.; Dallagnol, L.J.; Ferreira, A.S.; Pereira, D.R.; Souza, G.M. Electrome Alterations in a Plant-Pathogen System: Toward Early Diagnosis. *Bioelectrochemistry* **2020**, *133*, 107493. [CrossRef]
88. Tran, D.; Dutoit, F.; Najdenovska, E.; Wallbridge, N.; Plummer, C.; Mazza, M.; Raileanu, L.E.; Camps, C. Electrophysiological Assessment of Plant Status Outside a Faraday Cage Using Supervised Machine Learning. *Sci. Rep.* **2019**, *9*, 17073. [CrossRef]
89. De Toledo, G.R.A.; Reissig, G.N.; Senko, L.G.S.; Pereira, D.R.; Da Silva, A.F.; Souza, G.M. Common Bean under Different Water Availability Reveals Classifiable Stimuli-Specific Signatures in Plant Electrome. *Plant Signal. Behav.* **2024**, *19*, 2333144. [CrossRef]
90. González, I.; Juclà, D.; Najdenovska, E.; Dutoit, F.; Raileanu, L.E. Detecting Stress Caused by Nitrogen Deficit Using Deep Learning Techniques Applied on Plant Electrophysiological Data. *Sci. Rep.* **2023**, *13*, 9633. [CrossRef]
91. Qin, X.-H.; Wang, Z.-Y.; Yao, J.-P.; Zhou, Q.; Zhao, P.-F.; Wang, Z.-Y.; Huang, L. Using a One-Dimensional Convolutional Neural Network with a Conditional Generative Adversarial Network to Classify Plant Electrical Signals. *Comput. Electron. Agric.* **2020**, *174*, 105464. [CrossRef]
92. Kenderešová, L.; Staňová, A.; Pavlovkin, J.; Ďurišová, E.; Nadubinská, M.; Čiamporová, M.; Ovečka, M. Early Zn^{2+}-Induced Effects on Membrane Potential Account for Primary Heavy Metal Susceptibility in Tolerant and Sensitive Arabidopsis Species. *Ann. Bot.* **2012**, *110*, 445–459. [CrossRef] [PubMed]

plants

MDPI

Article

Synergistic Effects of Silicon and Aspartic Acid on the Alleviation of Salt Stress in Celery (*Apium graveliens* L.) "Si Ji Xiao Xiang Qin"

Jinnan Song [1,*], Jingli Yang [1] and Byoung Ryong Jeong [2,*]

[1] Shandong Provincial University Laboratory for Protected Horticulture, Weifang University of Science and Technology, Shouguang 262700, China; yangmiaomiaode@gmail.com
[2] Division of Horticultural Science, College of Agriculture and Life Sciences, Gyeongsang National University, Jinju 52828, Republic of Korea
* Correspondence: jinnansong93@gmail.com (J.S.); brjeong@gnu.ac.kr (B.R.J.); Tel.: +86-156-216-21721 (J.S.); +82-55-772-1913 (B.R.J.)

Abstract: Salinity is one of the primary abiotic stresses that seriously hampers plant quality and productivity. It is feasible to reduce or reverse the negative effects of salt through the supplementation of silicon (Si) and aspartic acid (Asp). However, the question of how exogenous Si and Asp induce salt tolerance in celery remains incipient. Thus, this study was performed to determine the synergistic effects of Si and Asp on the alleviation of salt stress in celery. To this end, the celery plants were cultivated in a controlled regime (light for 14 h at 22 °C; darkness for 10 h at 16 °C) and treated with one of five treatments (CK, 100 mM NaCl, 100 mM NaCl + 75 mg/L Si, 100 mM NaCl + 100 mg/L Asp, and 100 mM NaCl + 75 mg/L Si + 100 mg/L Asp). Results showed that solely NaCl-treated celery plants developed salt toxicity, as characterized by decreased growth, declined photosynthetic ability, disturbed nutritious status and internal ion balance, and a boosted antioxidant defense system (Improved antioxidant enzymes and reduced ROS accumulation). In contrast, these adverse effects of NaCl were ameliorated by the additions of Si and Asp, regardless of Si, Asp, or both. Moreover, the mitigatory impacts of the co-application of Si and Asp on salt stress were more pronounced compared to when one of them was solely applied. Collectively, exogenous Si and Asp alleviate the degree of salt stress and thereby improve the salt tolerance of celery.

Keywords: plant biomass; photosynthesis; ion uptake; nutritious status; antioxidants

1. Introduction

Agricultural sustainability and productivity are being threatened by multiple negative influences on crops, such as climate change [1], together with plant homeostatic instability by global warming and water and nutrient limitation [2,3]. Moreover, indisposed irrigations are increasing soil salinity levels; salinity is one of the predominant harmful abiotic factors that restrict a plant's growth, quality, and yield worldwide [4]. Intuitively, salinity soils account for 20% of the worldwide agricultural land, and approximately 800 million hectares of soil globally are being highly affected by a high salt content [5,6]. Soil salinization is considered a major cause of land degradation in both arid and semiarid regions [7].

Meanwhile, salt stress could disturb a plant's growth and development in all stages [8]. According to previous reports, the most common adverse effects of salinity on plants are an interrupted reactive oxygen species (ROS) detoxification system, thereby causing impaired redox homeostasis, membrane damage, plasmolysis, and even nutritional disturbances and toxicity [6,9–11]. Physiologically, the plant's growth regarding its roots, shoots, and leaves were notably inhibited [6,12]. Morphologically, the plants were subjected to being stunted [8,13]. Metabolically, the cellular homeostasis regarding multiple biomolecules, such as lipids, chlorophylls, proteins, and nutrition ions, was severely damaged [8,13–15].

Higher plants have developed sophisticated mechanisms to cope with the toxic influences of salt stresses. For instance, plants will activate the ROS scavenge mechanism by enhancing the antioxidant defense system for a reduction in ROS [16]. Usually, the synthesis and accumulation of osmoprotectants or suitable osmolytes are common mechanisms where plants can overcome abiotic stresses [17,18]. A plant's antioxidant defense system is composed of a nonenzymatic antioxidant system and an antioxidative enzymatic system [19], such as the antioxidant enzymes regarding superoxide dismutase (SOD), peroxidase (POD), and catalase (CAT) [20].

Celery (*Apium graveliens* L.). is an annual or perennial old herb belonging to the *Apiaceae* family and is widely distributed nationwide [21]. As a salad vegetable, it has been ranked second in global consumption due to the following reasons [22]: Environmentally, celery was adopted in a drainage solution reuse system for the reduction in pollutants by wastewater and excrescent chemicals [23]. Medicinally, celery can prevent liver and lien diseases, jaundice, and cardiovascular diseases due to the fact that it contains abundant nutrients regarding the apigenin coumarins, vitamins, carotene, volatile oil, flavonoids, etc. [24–26]. Most of the previous studies on celery have focused on its therapeutic roles [27], celery food chemistry [28], cultivation regime [29], and abiotic stress effects on celery development [21,30–32], neglecting the effective approach to the alleviation of stresses, in particular of salt stress. And the yield and quality of celery were severely restricted by salt stress.

To reduce the salt damages on the plant quality and production, attempts have been made to mitigate soil salinization and improve plant salt tolerances [33,34]. For instance, researchers implemented leaching and flushing to reduce the salt in the soil, which is time-consuming and labor-intensive [35]. Phytoremediation is another way, and it has been shown to be eco-friendly but not effective [33,35]. Moreover, applying exogenous substances, such as silicon (Si) [36] and amino acid (AA) [32], is a method to promote the salt tolerance of plants. And this approach, which is associated with agronomical means, remains the most reliable avenue for minimizing the adverse impacts of salinity.

Silicon (Si) is one of the most abundant elements in the Earth's crust and was recently considered a "quasi-essential" element, according to the International Plant Nutrition Institute [37]. Although Si is not listed as an essential element, supplementation of Si has been suggested as beneficial for plant growth regarding multiple aspects, such as improved yield ability and enhanced resistance against disease and abiotic stresses [38]. More specifically, Si is often used as an attenuator to reduce the adverse impacts of salinity, and moreover, its promotion of a plant's salt tolerance could be ascribed to many physiological improvements. The amorphous Si could be deposited on the leaf epidermis, regulating the stomatal conductance and transpiration rate, which favors photosynthesis [39]. Si participates in the rigidity of cell walls, constituting a better leaf architecture and leaf area and greater light interception, which also increases the net photosynthetic rate [39,40]. Meanwhile, Si has been shown to interact with certain cations, such as Na^+ and K^+; thus, the important role of Si in the alleviation of salt toxicity is the reduction in Na^+ accumulation and facilitating Na^+ exclusion [38]. In addition, previous reports disclosed that the application of Si can decrease lipid peroxidation and maintain redox homeostasis by reinforcing the antioxidant defense system [40,41]. Therefore, Si is believed to be an effective method to improve the salt tolerance and quality of plants.

Aspartic acid (Asp), also known as Aspartate, is a basic constituent of proteins and plays an important role in metabolic energy production and equivalent reductions [42,43]. Asp participates in the plant metabolism pathway for the synthesis of important molecules, such as organic acids, nucleotides, and hormones [43]. Meanwhile, considerable reports have shown that Asp is required in the regulation process when facing adverse conditions, particularly regarding salinity [42,44]. In high salt environments, Asp has been found to accumulate with proline in osmotic adjustments and membrane stability on the basis of the physiological responses, even though the underlying metabolic mechanism remains unclear [18,44,45]. Thus, these beneficial influences on plant growth and development

conferred by exogenous Asp have encouraged more researchers to apply Asp to other plants, especially for salt-sensitive crops.

However, the synergistic effects of Si and Asp on the alleviation of salt stress in celery have rarely been reported. Therefore, the main objective of the study undertaken herein on celery is to (1) investigate whether exogenous Si or Asp is able to reduce the salt stress degree in celery; concomitantly, to (2) assess the combined effects of Si and Asp on the physiology, morphology, photosynthesis, nutrition status, and antioxidant defense system in salt-stressed celery.

2. Materials and Methods

2.1. Plant Material and Growing Conditions

The celery seeds "Si Ji Xiao Xiang Qin" were purchased from LuTong Seed Company., Ltd. (Handan, China) with a mean germination ratio of over 70%. The celery seeds were planted in 128-cell plug trays containing a mini-K substrate (Klasmann-Deilmann GmbH Company, Geeste, Germany) and moistened with running tap water. The celery seeds germinated 7 days after sowing (DAS) in an air-conditioned environment at 20 °C and a relative humidity of 80%. Then, the germinated seedlings were watered with MNS (multiple nutrition solutions, pH = 6.0), according to our previous reports [46]. The seedlings were cultured in a controlled alternating diurnal regime with 14 h light (white LED at 800 μmol m^{-2} s^{-1} PPFD) and 10 h dark, at 22 °C and 16 °C, respectively, and the relative humidity was 70% [32]. The celery seedlings were allowed to grow for another 7 days (14 DAS) until they turned into two true leaves and one heart. The seedlings with uniform size and similar morphology but without mechanical flaws were monitored, selected, and transferred to new 128-cell plug trays.

2.2. Treatments and Experimental Design

Subsequently, the transferred celery seedlings were equally divided into 5 parts and treated with the following 5 combinations: CK (0 mM NaCl + 0 mg/L Si + 0 mg/L Asp), NaCl (100 mM NaCl + 0 mg/L Si + 0 mg/L Asp), NaCl + Si (100 mM NaCl + 75 mg/L Si + 0 mg/L Asp), NaCl + Asp (100 mM NaCl + 0 mg/L Si + 100 mg/L Asp), and NaCl + Si + Asp (100 mM NaCl + 75 mg/L Si + 100 mg/L Asp). NaCl was directly dissolved in the MNS, and Si was sourced from K_2SiO_3; thus, the excessive introduced potassium was reduced by KNO_3, and the resultant losses of nitrate were balanced by nitric acid [46]. The optimized level of K_2SiO_3 was at 75 mg/L, following our previous finding [47]. All the plants were watered with the treatment solutions only, and all the treatment solutions were irrigated every alternative day until harvest. The Asp solution at 100 mg/L was foliar sprayed twice with a 7-day interval (on 15 DAS and 22 DAS) [18].

This experiment is laid out in a completely randomized design with three biological replications. For each replicate, 16 celery seedlings underpinning one treatment were adopted.

2.3. Measurement of Growth Parameters and Destructive Sampling

The celery plants were harvested until they showed distinct appearances (39 DAS). During the harvest, the plant growth parameters from different treatments were individually determined. The whole plant weights in terms of fresh weight and whole dry mass (kept in an air-force oven at 60 °C for 72 h) were determined by an electronic balance. The stem diameter was measured using a Vernier caliper (SJ-455520, ShangJiang Instrument Co., Ltd., Haining, China). The shoot length, leaf length and width, and tap root length were recorded with a metal ruler. The celery plants from different treatments were individually sampled, immediately frozen in liquid N_2, and stored in a refrigerator at −80 °C until further experiments.

2.4. Estimation of Net Photosynthesis, Transpiration Rates, Stomatal Conductance, and Chlorophylls

The net photosynthesis (*P*n), transpiration rates (*T*r), and stomatal conductance (g_s) were determined with a hand-held photosynthesis measurement system (TARGAS-1, PP Systems, Amesbury, MA, USA). Briefly, these parameters were measured on the three topmost fully expanded leaves, and the measurement per leaf was conducted three times. The leaf temperature was about 23 °C, and the environment during measuring was identical with that previously set when growing celery.

The chlorophyll contents (chlorophyll a and b) were measured following Arnon's reports with minor modifications [48]. Briefly, 0.1 g of fresh celery leaves was mixed with a 2 mL extraction buffer (45% v/v acetone, 45% v/v ethanol, and 10% v/v H_2O) and kept at 4 °C overnight. A mild shaking was carried out with a rotator (AG, FINEPCR, Seoul, Republic of Korea) during the incubation. After the incubation, the supernatant was transferred and spectrophotometrically read at 645 nm, 663 nm, and 440 nm with a spectrophotometer (UV3200, OptoSky, Xiamen, China). Afterwards, the contents of chlorophyll a and chlorophyll b, together with the carotenoids, were individually calculated with the following formulae:

$$\text{Chlorophyll a} = \frac{(12.72 \times \text{OD}_{663} - 2.59 \times \text{OD}_{645}) \times \text{V}}{\text{Sample fresh weight}}$$

$$\text{Chlorophyll b} = \frac{(22.88 \times \text{OD}_{645} - 4.67 \times \text{OD}_{663}) \times \text{V}}{\text{Sample fresh weight}}$$

$$\text{Carotenoids} = \frac{4.7 \times \text{OD}_{440} - 0.27 \times (\text{Chl a} + \text{Chl b})}{\text{Sample fresh weight}}$$

where 'V' refers to the volume used of the extraction buffer ('V' was 2 mL herein), and the chlorophyll content is quantified by milligrams per gram of fresh-weight leaves.

2.5. Determination of Soluble Sugar, Starch, and Soluble Protein

The soluble sugar and starch contents were determined following an anthrone–sulfuric acid colorimetry approach according to McCready's reports with minor modifications [49].

Briefly, 0.5 g of finely ground celery leaf powder was vigorously mixed with 25 mL deionized water and incubated in a 90 °C water bath for 40 min. Then, the mixture was subjected to centrifugation (6500 rpm, 10 min, RT) to collect the supernatant. A total of 0.1 mL of the supernatant was mixed with distilled water and 2% (w/v) anthrone (dissolved in ethyl acetate) at 1.9 mL and 1 mL, respectively. A total of 5 mL concentrated H_2SO_4 was slowly added to the mixture and was subjected to a 90 °C water bath for 10 min. Finally, the absorbance was recorded at 630 nm, and the soluble sugar content was calculated on the basis of a standard soluble sugar curve. The residue after centrifugation from the previous steps was collected for the determination of starch; the detailed procedure can be found in our previous publication [50].

The soluble protein contents were determined with a Bradford reagent [51].

2.6. Quantifications of Na, K, Ca, and Mg

The celery leaf samples from each treatment were harvested and washed with distilled water to remove foreign particles. Then, they were placed in an oven at 70 °C until they had a constant weight. All the samples were finely ground into powder and wet-ashed to break all the organic matrix, leaving only the minerals for analysis. The ion contents (Na, K, Ca, and Mg) in the digested transparent solution were determined with Atomic Absorption Spectrophotometry. The detailed digesting method, decoction method, and calibration procedure can be found in Sahito's report [52].

2.7. Determination of Antioxidant Enzyme Activities and ROS ($O_2^{\cdot-}$, H_2O_2) Contents

The antioxidant enzyme activities, herein consisting of SOD, POD, CAT, and APX, were calculated on the basis of the determined soluble protein contents mentioned above. The SOD concentration was determined according to the nitro blue tetrazolium (NBT) inhibition method [53]. POD activity was determined by adopting the guaiacol oxidation reaction [54]. CAT activity was measured based on the H_2O_2 decomposition [55]. APX activity was determined on the basis of the H_2O_2 scavenging degree [56]. The mentioned antioxidant enzyme activities were all spectrophotometrically determined with a spectrophotometer (UV3200, OptoSky, Xiamen, China).

A principle of hydroxylamine oxidization was used for measuring the superoxide ($O_2^{\cdot-}$) level according to a protocol by Wu [57]. The Hydrogen Peroxide (H_2O_2) content was determined following a rapid and sensitive approach, as presented by Uchida [58].

2.8. Statistics and Graphing

All the displayed data in this experiment are the means ± SE of no less than three biological replicates ($n \geq 3$). The obtained data were subjected to a one-way ANOVA following Duncan's multiple comparison range test at $p = 0.05$ with SAS statistical software 8.2, and the significant differences are shown by different lowercase letters over bars. The bar graphs were created with GraphPad Prism 8.2 software. The correlation heat map was plotted in an Origin 2022 procedure.

3. Results

3.1. The Celery Growth Parameters as Affected by NaCl, Si, and Asp

The celery plants showed distinct changes in response to the salt stress, exogenous Si, and Asp treatments (Figure 1). The growth and morphology were notably inhibited when treated with NaCl compared to CK. However, the supplementation of Si or Asp significantly promoted the growth compared to CK. Solely Si- or Asp-treated celery plants displayed similar morphology to CK, while the co-application of Si and Asp dramatically increased the growth and morphology.

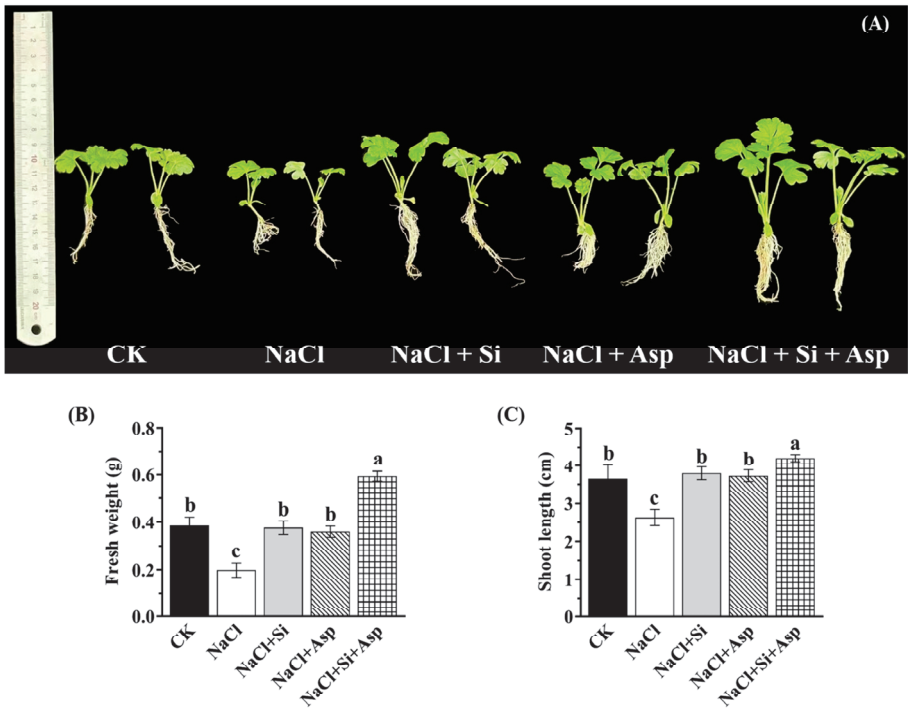

Figure 1. Effect of exogenous Si and Asp on the (**A**) morphology and growth parameters regarding (**B**) fresh weight and (**C**) shoot length of celery plants under salt stress. Data are means ± SE generated

from n = 6 biological replicates. The significant differences among treatments were determined according to Duncan's multiple comparison range test when p = 0.05 (One-way ANOVA) and shown by different lowercase letters over bars.

In a large number of celery plants, the fresh weight and shoot length could directly reflect the plant's growth ability. As depicted in Figure 1B,C, salt treatment significantly decreased the fresh weight and shoot length by 38.8% and 27.9%, respectively, when compared with CK (Figure 1B,C). However, the supplementation of Si or Asp alone markedly improved the fresh weight by 90.4% and 81.8%, respectively, while the co-application of Si and Asp significantly improved this parameter by 1.98-fold when compared with that cultured with NaCl (Figure 1B). Similarly, the shoot length in the 'NaCl + Si + Asp' regime significantly improved by 60.5% relative to that treated with NaCl (Figure 1C).

3.2. Other Main Growth Parameters as Affected by NaCl, Si, and Asp

Consistent with the growth status depicted in Figure 1, other major investigated parameters regarding the tap root length, leaf length and width, whole dry weight, and stem diameter were also determined. These parameters were all reduced in response to the NaCl treatment, while no significant differences were conferred among CK, NaCl + Si, and NaCl + Asp (Figure 2; Table 1).

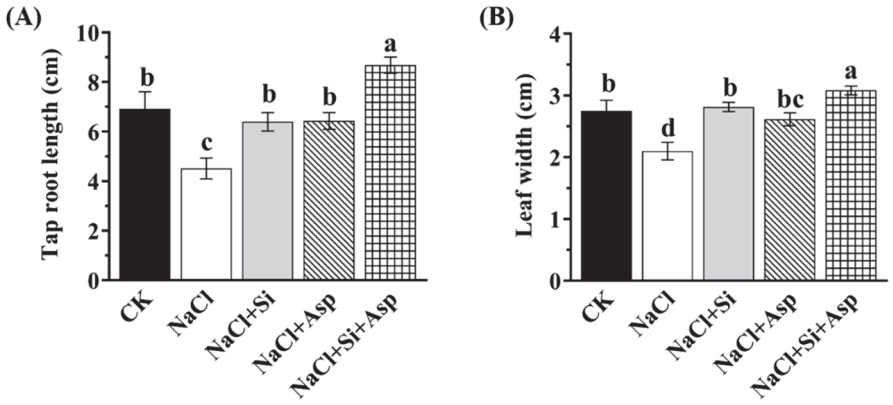

Figure 2. Effect of exogenous Si and Asp on the (**A**) tap root length and (**B**) leaf width of celery plants under salt stress. Data are means ± SE generated from n = 6 biological replicates. The significant differences among treatments were determined according to Duncan's multiple comparison range test when p = 0.05 (One-way ANOVA) and shown by different lowercase letters over bars.

Table 1. The whole dry weight, leaf length, and stem diameter of celery as affected by 5 treatments.

Treatment	Whole Dry Weight (mg)	Leaf Length (cm)	Stem Diameter (mm)
CK	50.1 b	2.00 b	0.23 bc
NaCl	28.0 c	1.63 c	0.12 d
NaCl + Si	52.7 b	2.07 b	0.23 b
NaCl + Asp	49.2 b	2.02 b	0.20 bc
NaCl + Si + Asp	86.0 a	2.35 a	0.32 a

The displayed data are the means ± SE by n = 6 replicates. The different accompanied lowercase letters indicate the significant differences according to Duncan's multiple comparison range test (One-way ANOVA) at $p \leq 0.05$.

However, conspicuously, compared with the celery plants treated with NaCl, the supplementation of either Si or Asp or co-application of both substances significantly improved these determined parameters (Figure 2; Table 1). As the most important finding, the collegial use of Si and Asp further dramatically increased these parameters compared with that treated with Si or Asp alone (Figure 2; Table 1).

3.3. The Photosynthetic Responses to the NaCl, Si, and Asp

The photosynthetic ability in terms of certain major parameters, such as the net photosynthesis (*P*n), transpiration rates (*T*r), and stomatal conductance (g_s), was determined herein when the celery was cultured in different regimes. We found that all the recorded traits were significantly decreased in response to NaCl treatment (Figure 3). Regarding the more affected parameters, the net photosynthesis rate and the transpiration rates of NaCl-spiked celery plants were significantly decreased by 27.2% and 39.6%, respectively, compared with CK (Figure 3A,B). However, both Si and Asp remarkedly ameliorated the photosynthetic ability, regardless of the determined specific parameters. For instance, the supplementation of Si and Asp significantly improved the stomatal conductance (g_s) by 81.74% and 89.06%, respectively, in comparison with that in the salt-stressed celery (Figure 3C). Similar trends could be found in the modulations of chlorophyll a and b (Figure 3D,E).

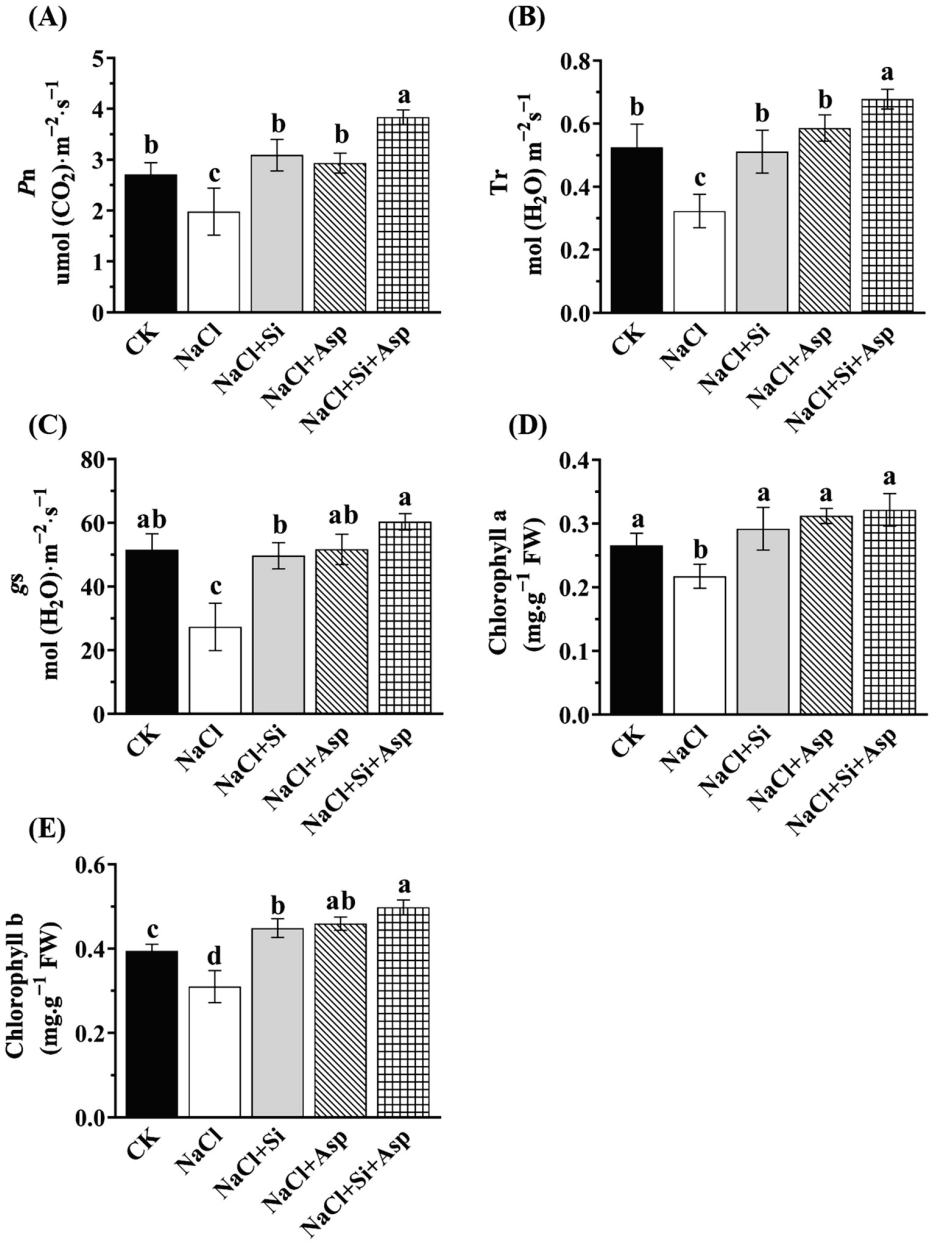

Figure 3. Effect of exogenous Si and Asp on the photosynthetic capacity regarding (**A**) the net photosynthesis (*P*n), (**B**) transpiration rates (*T*r), (**C**) the stomatal conductance (g_s), (**D**) chlorophyll

a content, and (**E**) chlorophyll b content of celery plants under salt stress. Data are means ± SE generated from n = 6 biological replicates. The significant differences among treatments were determined according to Duncan's multiple comparison range test when p = 0.05 (One-way ANOVA) and shown by different lowercase letters over bars.

3.4. Contents of Soluble Sugar, Starch, Soluble Protein, and Carotenoids as Affected by NaCl, Si, and Asp

Certain celery internal parameters, such as the soluble sugar, starch, soluble protein, and carotenoids, were determined to reflect the plant's nutritional status herein (Figure 4). As compared with the CK, the salt-treated celery plants exhibited significant diminishments of the starch content, soluble protein content, and carotenoids. Notably, the soluble sugar content in salt-spiked plants displayed a significant improvement of 104% compared with that in CK (Figure 4A). In contrast, the starch content, soluble protein content, and carotenoids markedly decreased by 28.6%, 28.1%, and 27.3%, respectively (Figure 4B–D).

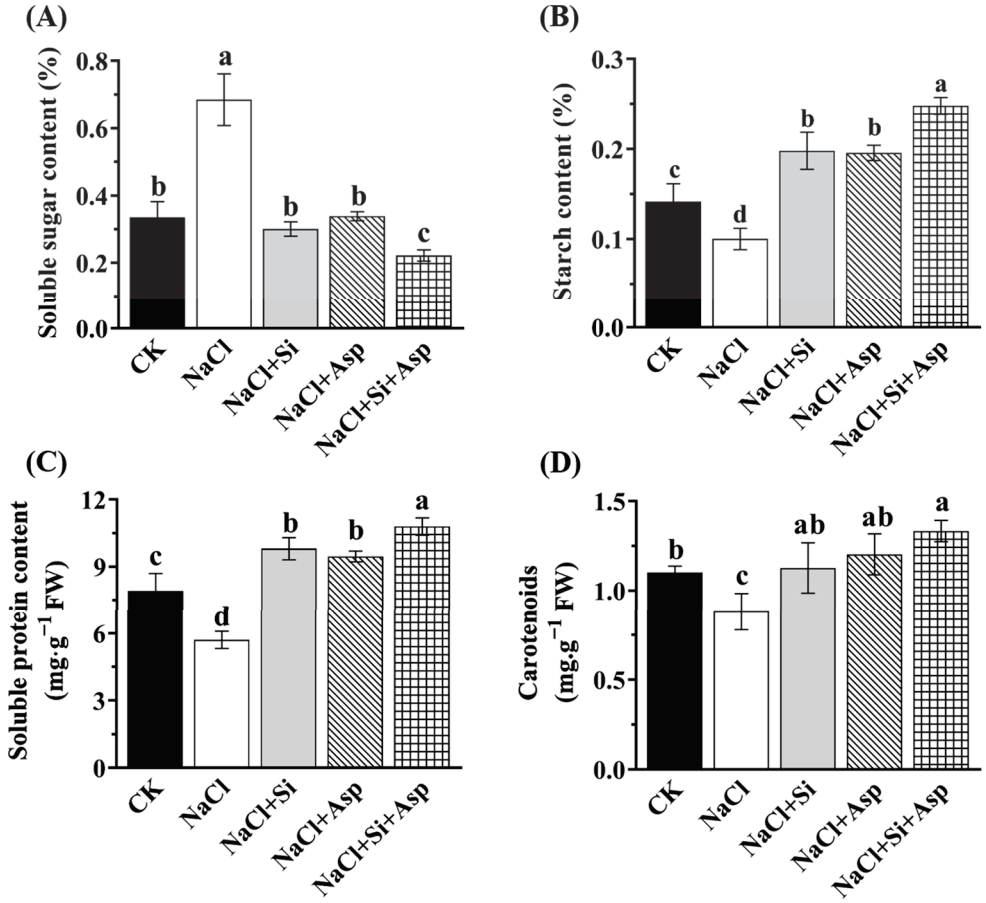

Figure 4. Effect of exogenous Si and Asp on the nutrition parameters regarding (**A**) soluble sugar content, (**B**) starch content, (**C**) soluble protein content, and (**D**) carotenoids content of celery plants under salt stress. Data are means ± SE generated from n = 6 biological replicates. The significant differences among treatments were determined according to Duncan's multiple comparison range test when p = 0.05 (One-way ANOVA) and shown by different lowercase letters over bars.

However, irrespective of the spraying exogenous substances, both Si and Asp significantly upsurged the level of starch, soluble protein, and carotenoids compared with that cultured in the NaCl regime (Figure 4B–D). Moreover, compared with the salt-stressed celery plants, the co-application of Si and Asp considerably improved the starch content, soluble protein content, and carotenoids by 1.5-fold, 89.0%, and 51.1%, respectively (Figure 4). However, we noticed that both Si and Asp significantly declined the soluble

sugar content compared to the salt-stressed plants (Figure 4A). In addition, we found that the co-application of Si and Asp significantly increased the starch content and soluble protein content more than Si or Asp used alone (Figure 4B,C).

3.5. Na, K, Ca, and Mg Concentration as Affected by NaCl, Si, and Asp

In order to figure out the modulation of internal ion homeostasis when the celery plants were under salt stress and concomitantly determine the correlations among the main ions subjected to five treatments, we further investigated the Na, K, Ca, and Mg contents and assessed the correlations among them.

As is apparent in Figure 5, the salt-spiked celery plants exhibited a higher Na content while decreasing the concentrations of K, Ca, and Mg. In other words, the Na in celery plants grew in the NaCl regime significantly by 65.8% compared with CK (Figure 5A); however, the K, Ca, and Mg in that regime significantly decreased by 26.8%, 71.8%, and 62.4%, respectively (Figure 5B–D). By contrast, the added Si and Asp remarkably diminished the Na content while improving the internal level of K, Ca, and Mg. In particular, regarding the co-applications of Si and Asp, the Na level in the 'NaCl + Si + Asp' group was 31.01% lower relative to that solely treated with NaCl (Figure 5A).

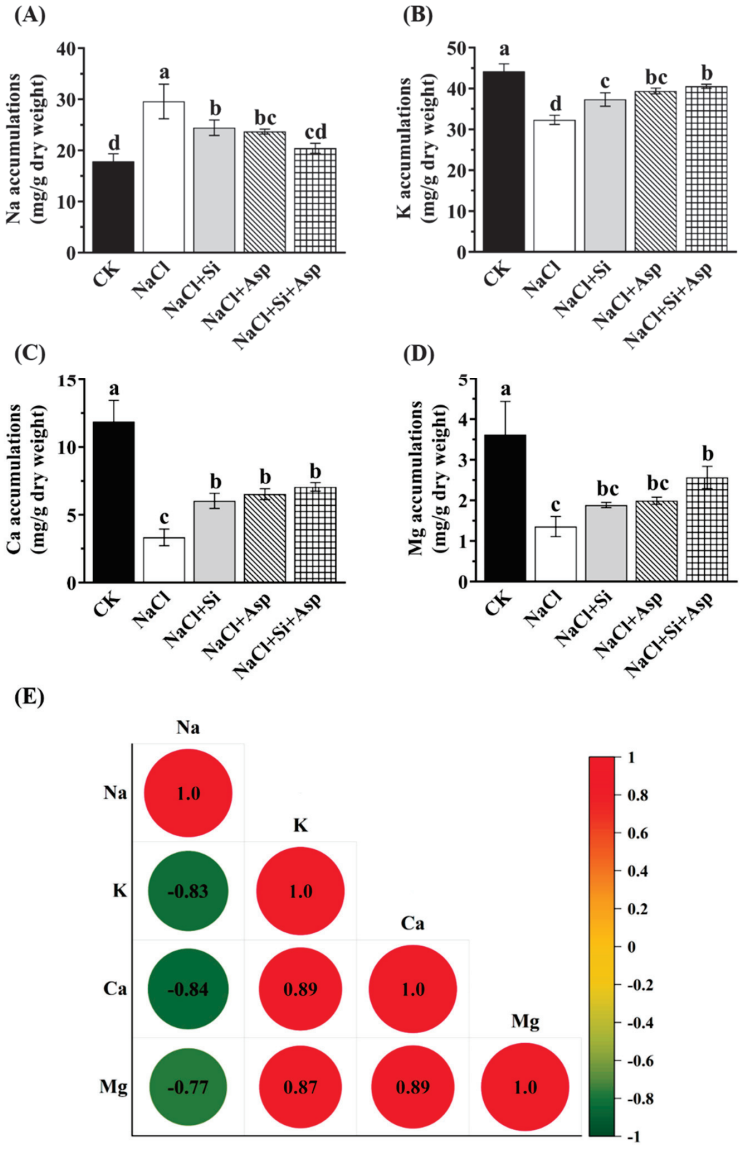

Figure 5. Effect of exogenous Si and Asp on the ion concentration regarding (**A**) Na, (**B**) K, (**C**) Ca, and (**D**) Mg of celery plants under salt stress. Multivariate data analysis of a (**E**) heatmap showing

the correlations among these studied ions. Data are means ± SE generated from n = 3 biological replicates. The significant differences among treatments were determined according to Duncan's multiple comparison range test when p = 0.05 (One-way ANOVA) and shown by different lowercase letters over bars.

Consistently, we noticed that the Na content was negatively correlated with K, Ca, and Mg. On the contrary, positive relations among K, Ca, and Mg were monitored (Figure 5E).

3.6. Responses of Antioxidant Enzymes Activities to NaCl, Si, and Asp

The oxidative protective system was triggered when the celery plants suffered from salt stress. During this process, the antioxidant capacity, such as the antioxidant enzymes, was improved to reduce the degree of stress. We, therefore, investigated the activities of the main defense antioxidant enzymes regarding SOD, CAT, POD, and APX.

As compared with CK, the salt-stressed celery plants significantly decreased the CAT, POD, and APX by 44.4%, 1.24-fold, and 56%, respectively (Figure 6B–D). Irrespective of Si or Asp, both of them notably improved these four antioxidant enzymes when compared with those in the salt-spiked celery plants. The co-application of Si and Asp remarkably enhanced SOD, CAT, POD, and APX by 62.5%, 1-fold, 1.97-fold, and 1.4-fold, respectively (Figure 6). In addition, the co-application of Si and Asp significantly improved SOD activity by 10.2% and 8.6%, respectively, than when Si and Asp were used alone (Figure 6A).

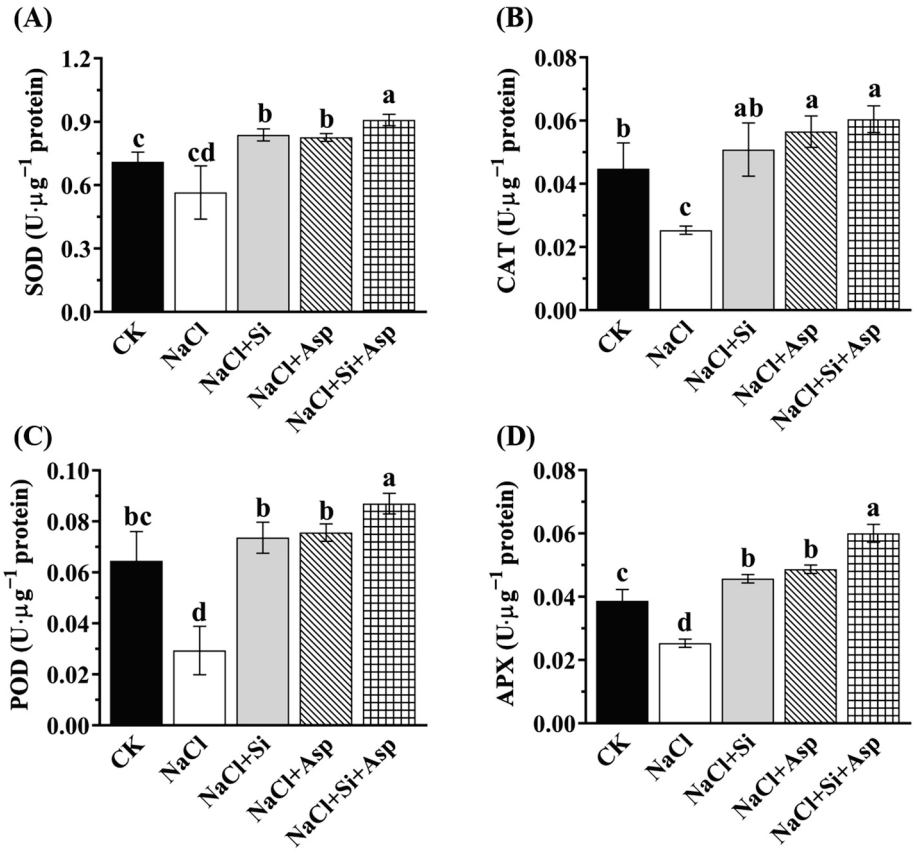

Figure 6. Effect of exogenous Si and Asp on the concentrations of antioxidant enzymes regarding (**A**) SOD, (**B**) CAT, (**C**) POD, and (**D**) APX of celery plants under salt stress. Data displayed are means ± SE generated from n = 6 biological replicates. The significant differences among treatments were determined according to Duncan's multiple comparison range test when p = 0.05 (One-way ANOVA) and shown by different lowercase letters over bars.

3.7. Oxidative Damage as Affected by NaCl, Si, and Asp

The oxidative damage could further reflect the antioxidant ability of celery plants, while the former, herein consisting of $O_2^{\cdot-}$ and H_2O_2 levels, were determined.

Consistent with the above, the celery plants treated with NaCl rapidly increased the accumulations of $O_2^{\cdot-}$ and H_2O_2 by 43.3% and 28.01%, respectively, compared with CK (Figure 7). As expected, both $O_2^{\cdot-}$ and H_2O_2 were significantly diminished after the supplementation of Si and Asp. For instance, the added Si and Asp to the salt-treated celery plants rapidly reduced the $O_2^{\cdot-}$ content by 31.84% and 31.11%, respectively (Figure 7A).

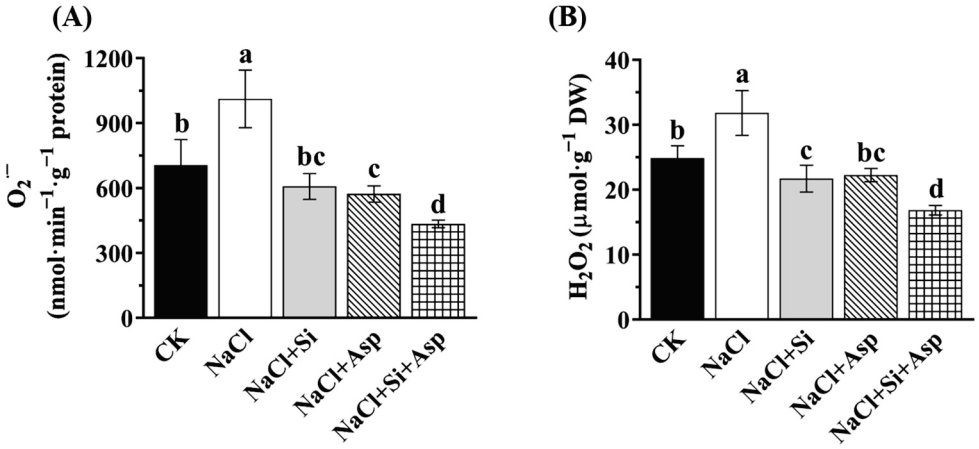

Figure 7. Effect of exogenous Si and Asp on the ROS contents regarding (**A**) $O_2^{\cdot-}$ and (**B**) H_2O_2 of celery plants under salt stress. Data displayed are means ± SE generated from $n = 6$ biological replicates. The significant differences among treatments were determined according to Duncan's multiple comparison range test when $p = 0.05$ (One-way ANOVA) and shown by different lowercase letters over bars.

More importantly, the co-application of Si and Asp dramatically decreased the production of ROS compared with when one of them was solely applied (Figure 7). The H_2O_2 content in the 'NaCl + Si + Asp' group was significantly lower by 22.34% and 24.26%, compared with that in 'NaCl + Si' and 'NaCl + Asp', respectively (Figure 7B).

4. Discussion

A high salt-spiked supply could inevitably instigate the uptake of Na^+ by plants, resulting in the imbalance of ions and the inhibition of the plant's growth ability. This was believed to be the primary cause of salt toxicity [59]. In fact, Si- and Asp-induced alleviations on salt stress have been extensively studied in many plant species, such as pepper [60], rice [41], and wheat [18]. Moreover, Gao recently presented the effects of salt stress on celery and successfully reduced the degree of salt toxicity by using the other amino acid proline [32]. However, the influence of the co-application of Si and Asp on salt-stressed celery has been less understood. Thus, we aimed to confirm the alleviatory effects of Si and Asp on salt-stressed celery plants and concomitantly unveil the associated mechanisms that are responsible for it.

Plant growth and morphology can be adversely affected by high salt content, which has been shown in many plant species, oscillating from crops to vegetables [10–12,18]. We also confirmed that the normal growth ability of celery plants was severely disturbed by NaCl (100 mM) treatment (Figures 1 and 2), which is in agreement with Gao's report [32]. However, this adverse effect was notably mitigated by Si and Asp in terms of the morphology and growth parameters (Figures 1 and 2). Several reports have demonstrated that the application of Si could remarkably reduce the degree of salt toxicity. In addition, the supplementation of Si considerably promoted plant growth and development [41,46,60,61]. Indeed, using Si was solely found to alleviate the salt-stressed degree in celery, as evidenced by the ameliorated whole biomass and multiple main growth traits (Figures 1 and 2). It

is worth noting that the water content of plants significantly influenced the uptake and accumulation of Si, showing quadratic behavior [36,38]. However, this effect is minor for the obtained outcome due to the identical water scheme and irrigation frequency. These findings were not only in corroboration with the report by Rohanipoor but also suggest the beneficial effects conferred by Si, in particular for the plants at risk of salt stress [62]. Likewise, the elevation of salt tolerance by the addition of Asp has been found in wheat [18], tomato [11], and onion [42]. And the results shown by this study are in line with these earlier reports: the growth of salt-stressed celery notably increased after the addition of Asp (Figures 1 and 2). Moreover, the growth parameters of salt-stressed celery plants were more promoted when Si and Asp were simultaneously applied than when one of them was solely used, illustrating the synergistic effects between them.

Photosynthetic performance was regarded as one of the most important processes modulating the overall yield ability of plants [63]. Salt toxicity would firstly over-produce the ROS, resulting in oxidative damage and eventually the membrane's instability, together with the decline of its photosynthetic capacity [41,63,64]. Indeed, our study showed that the investigated photosynthesis-related parameters of salt-stressed celery plants were significantly decreased compared with CK (Figure 3). The net photosynthetic rate (*P*n) is correlated with plant growth and carbohydrate demand, which could directly refer to the accumulation of organic matter [65]. Similarly, as a basic physiological activity, transpiration is associated with heat transfer and directly determines the photosynthesis and yield of crops [66]. In addition, Sakoda noted that a high photosynthetic rate is usually accompanied by a high stomatal conductance (positive correlation) [67]. This phenomenon could probably be attributed to the finding that plants with more stomata tend to have a higher net CO_2 assimilation rate [67,68]. Meanwhile, photosynthesis is also an intricate mechanism pertaining to the synthesis of photosynthetic pigments. Some studies underpinning various plant species disclosed that the chlorophyll contents were positively correlated with the photosynthetic ability [40,46,69,70]. Consistently, these parameters were significantly improved after the addition of Si and Asp compared with the salt-stressed celery (Figure 3).

Soluble sugar is the primary product of photosynthesis, and it plays a pivotal role as a building block of many indispensable macromolecules that regulate plant growth and development [71]. Also, sugar in plants is believed to be a candidate target of the osmoregulation system in response to salt stress [72]. Thus, it can be enriched when plants are subjected to salinity, in particular salt-tolerant genotypes [73]. Moreover, soluble sugar acts as a chelating agent, trapping the Na^+ within starch granules for detoxification [73,74]. Furthermore, starch could play a critical role in detoxifying toxic ions by acting as a Na^+-starch-binding granule [74]. In this study, the soluble sugar content in salt-stressed celery leaves was notably higher compared with that in CK (Figure 4A), which agrees with the findings by Gao [32] and Yin [73]. On the contrary, starch content strongly declined when NaCl was applied (Figure 4B), which is in line with the results in rice (both sensitive and tolerant genotypes against salt) [73,75,76]. Similarly, the salt stress resulted in reductions in both soluble protein and carotenoids, suggesting that the physiological status of celery was severely affected. Similar results of soluble protein were also reported in *Phaseolus vulgaris* [77] and *Lycopersicon esculentum* [78]. Several previous reports showed that the total carotenoids were increased, as affected by the salt stresses in many plants, due to the fact that the carotenoids played a protective role against oxidative damages [79,80]. Nevertheless, the carotenoids were clearly decreased in salt-stressed celery leaves in this study (Figure 4C), which is probably because of the photo-damage as a result of the loss of chlorophyll due to light absorbance. Our data are in line with the findings in wheat [81] and tomato [82]. Interestingly, the application of Si and Asp significantly reduced these detrimental influences caused by high salt content. Therefore, Si and Asp could synergistically alleviate the degree of salt stress in terms of nutritional status.

The external solution containing a high salt concentration inevitably instigated the ion imbalance or disturbances of ion homeostasis [1,4]. It has been established that there

existed a competition between Na^+ and K^+, and thereby, the internal K^+ declined under a high external NaCl environment, causing the K^+ deficiency and, eventually, plant growth inhibition and ionic toxicity [83,84]. Indeed, solely NaCl-treated celery plants herein promoted the enhancement of Na^+ while decreasing the internal K^+ (Figure 5A,B). And we clearly detected a negative correlation ($r = -0.83$) between the Na^+ and K^+ (Figure 5E). Similar to K^+, salt-stressed celery also showed lower tissue retention of Ca^{2+} and Mg^{2+} (Figure 5C,D), suggesting that Na^+ was still negatively correlated with Ca^{2+} and Mg^{2+}. This finding was further evidenced by Figure 5E, and the coefficient between Na^+ and Ca^{2+} and Na^+ and Mg^{2+} was -0.84 and -0.77, respectively. However, the addition of Si and Asp significantly ameliorated the reductions in K^+, Ca^{2+}, and Mg^{2+} (Figure 5). The Si-related alleviation of ionic toxicity during salt stress has been widely reported: the mechanism beyond it is that Si can restrict the uptake and transportation of Na^+ and even mediate the compartmentalization of Na^+ [85]. On the other hand, pioneering researchers found that exogenous amino acids could incite the stomatal opening and further modulate the ion's transportation across the membrane, thereby improving salt tolerance [86]. Accordingly, the beneficial impacts of Si and Asp on the reduction in the ionic toxicity degree by salinity have been confirmed again.

It has been well-established that the addition of Si could regulate the defense system against oxidative stresses [37,38,41,60]. The stimulation of antioxidant enzyme activities by the supplementation of Si was frequently observed, rendering a protective role against oxidative damage on the cell membrane [40,41,46,47]. In this work, exogenous Si on salt-treated celery plants dramatically improved the concentration of SOD, POD, CAT, and APX (Figure 6), and we noticed that ROS accumulations ($O_2^{\cdot -}$ and H_2O_2) declined accordingly (Figure 7). It can, therefore, be concluded that the salt toxicity that induced excess oxidative injuries was mitigated by the supplementation of Si. The data regarding the triggered antioxidant machinery of this study are in line with numerous previous studies [41,87]. Meanwhile, the leaf spraying of amino acids like Asp and proline improved the antioxidant enzyme activities under abiotic stresses, in accordance with the literature [18,32,83]. The amino acid per se is one of the important components of an antioxidant system in higher plants, and its actions involve not only the scavenging of free radicals but also osmoprotection and stress response [88,89]. Our results regarding the spraying of Asp and its influences on antioxidant enzymes and ROS content support these research findings (Figures 6 and 7). As expected, the effect of the co-application of Si and Asp on the antioxidant defense system was the most pronounced. Succinctly, Si and Asp could reinforce antioxidant enzyme activities and concomitantly decrease antioxidative damages, especially in salt-stressed celery.

5. Conclusions

To sum up, this study first showed that 100 mM of NaCl-spiked celery "Si Ji Xiao Xiang Qin" developed salt toxicity. This phenomenon mainly included the following: seriously decreased plant growth parameters (whole plant biomass, shoot length, stem diameter, leaf length and width, and tap root length), declined photosynthetic capacity (Pn, Tr, g_s, and chlorophylls), disturbed nutritional status (soluble sugar, starch, soluble protein, and carotenoids), interrupted ion uptake (Na, K, Ca, and Mg), and a diminished antioxidant defense system (antioxidant enzymes and ROS).

Conversely, the supplementation of Si and Asp, regardless of Si, Asp, or both, significantly reduced the degree of salt stress. Si and Asp may attribute this mitigation potential to the ameliorated parameters mentioned above.

Overall, exogenously applied Si and Asp could be an effective fertilization strategy in the alleviation of salt stress for celery cultivation.

Author Contributions: Conceptualization, J.S.; methodology, B.R.J. and J.S.; software, J.S.; validation, B.R.J.; formal analysis, B.R.J. and J.S.; investigation, J.S. and J.Y.; resources, J.S. and B.R.J.; data curation, J.S.; writing—original draft preparation, J.S.; writing—review and editing, B.R.J. and J.S.;

supervision, B.R.J.; project administration, J.S.; funding acquisition, J.S. All authors have read and agreed to the published version of the manuscript.

Funding: This work was supported by young researcher project (KJRC2023018) from Weifang University of Science and Technology, Shouguang, China.

Data Availability Statement: Data sharing is not applicable to this article.

Conflicts of Interest: The authors declare no conflicts of interest.

References

1. Hurtado, A.C.; Chiconato, D.A.; de Mello Prado, R.; da Silveira Sousa Junior, G.; Viciedo, D.O.; Díaz, Y.P.; Calzada, K.P.; Gratão, P.L. Silicon alleviates sodium toxicity in sorghum and sunflower plants by enhancing ionic homeostasis in roots and shoots and increasing dry matter accumulation. *Silicon* **2021**, *13*, 475–486. [CrossRef]
2. Viciedo, D.O.; de Mello Prado, R.; Martínez, C.A.; Habermann, E.; de Cássia Piccolo, M. Short-term warming and water stress affect Panicum maximum *Jacq*. stoichiometric homeostasis and biomass production. *Sci. Total Environ.* **2019**, *681*, 267–274. [CrossRef] [PubMed]
3. Peña Calzada, K.; Olivera Viciedo, D.; Habermann, E.; Calero Hurtado, A.; Lupino Gratão, P.; De Mello Prado, R.; Lata-Tenesaca, L.F.; Martinez, C.A.; Ajila Celi, G.E.; Rodríguez, J.C. Exogenous application of amino acids mitigates the deleterious effects of salt stress on soybean plants. *Agronomy* **2022**, *12*, 2014. [CrossRef]
4. Song, J.; Yang, J.; Xu, X.; Wang, Z.; Yang, C.; Zhang, K.; Yang, H.-B. A novel Tartary buckwheat gene FtIST1, associated with salt tolerance, was isolated and identified via over-expression and VIGS. *S. Afr. J. Bot.* **2023**, *161*, 202–210. [CrossRef]
5. Kalanaki, M.; Ritzema, H.; Bamshad, R.; Jones, E.; Fazilatnia, M. Application of bio-desalinization for reclamation of salt-affected soil under composted cow manure and deficit irrigation with saline water. *Paddy Water Environ.* **2020**, *18*, 469–479. [CrossRef]
6. Acosta-Motos, J.R.; Ortuño, M.F.; Bernal-Vicente, A.; Diaz-Vivancos, P.; Sanchez-Blanco, M.J.; Hernandez, J.A. Plant responses to salt stress: Adaptive mechanisms. *Agronomy* **2017**, *7*, 18. [CrossRef]
7. Karim, S.; Hussain, E.; Khan, J.A.; Hameed, A.; Ougahi, J.H.; Iqbal, F. Spatiotemporal investigation of soil salinity using geospatial techniques: A case study of Tehsil Toba Tek Singh. *Commun. Soil Sci. Plan.* **2022**, *53*, 1960–1978. [CrossRef]
8. Wang, L.; Li, G.; Wei, S.; Li, L.; Zuo, S.; Liu, X.; Gu, W.; Li, J. Effects of exogenous glucose and sucrose on photosynthesis in triticale seedlings under salt stress. *Photosynthetica* **2019**, *57*, 286–294. [CrossRef]
9. Meloni, D.A.; Oliva, M.A.; Martinez, C.A.; Cambraia, J. Photosynthesis and activity of superoxide dismutase, peroxidase and glutathione reductase in cotton under salt stress. *Environ. Exp. Bot.* **2003**, *49*, 69–76. [CrossRef]
10. Alharbi, B.M.; Elhakem, A.H.; Alnusairi, G.S.; Soliman, M.H.; Hakeem, K.R.; Hasan, M.M.; Abdelhamid, M.T. Exogenous application of melatonin alleviates salt stress-induced decline in growth and photosynthesis in *Glycine max* (L.) seedlings by improving mineral uptake, antioxidant and glyoxalase system. *Plant Soil Environ.* **2021**, *67*, 208–220. [CrossRef]
11. Akladious, S.A.; Abbas, S.M. Alleviation of sea water stress on tomato plants by foliar application of aspartic acid and glutathione. *Bangladesh J. Bot.* **2013**, *42*, 31–44. [CrossRef]
12. Stoeva, N.; Kaymakanova, M. Effect of salt stress on the growth and photosynthesis rate of bean plants (*Phaseolus vulgaris* L.). *J. Cent. Eur. Agric.* **2008**, *9*, 385–391.
13. Nawaz, K.; Hussain, K.; Majeed, A.; Khan, F.; Afghan, S.; Ali, K. Fatality of salt stress to plants: Morphological, physiological and biochemical aspects. *Afr. J. Biotechnol.* **2010**, *9*, 5475–5480.
14. Patel, M.K.; Kumar, M.; Li, W.; Luo, Y.; Burritt, D.J.; Alkan, N.; Tran, L.-S.P. Enhancing salt tolerance of plants: From metabolic reprogramming to exogenous chemical treatments and molecular approaches. *Cells* **2020**, *9*, 2492. [CrossRef] [PubMed]
15. Singh, M.; Singh, A.; Prasad, S.M.; Singh, R.K. Regulation of plants metabolism in response to salt stress: An omics approach. *Acta Physiol. Plant.* **2017**, *39*, 48. [CrossRef]
16. Singhal, R.K.; Saha, D.; Skalicky, M.; Mishra, U.N.; Chauhan, J.; Behera, L.P.; Lenka, D.; Chand, S.; Kumar, V.; Dey, P. Crucial cell signaling compounds crosstalk and integrative multi-omics techniques for salinity stress tolerance in plants. *Front. Plant Sci.* **2021**, *12*, 670369. [CrossRef] [PubMed]
17. Mostafa, M.R.; Mervat, S.S.; Safaa, R.E.-L.; Ebtihal, M.A.E.; Magdi, T.A. Exogenous α-tocopherol has a beneficial effect on *Glycine max* (L.) plants irrigated with diluted sea water. *J. Hortic. Sci. Biotechnol.* **2015**, *90*, 195–202. [CrossRef]
18. Sadak, M.S.; Sekara, A.; Al-Ashkar, I.; Habib-ur-Rahman, M.; Skalicky, M.; Brestic, M.; Kumar, A.; Sabagh, A.E.; Abdelhamid, M.T. Exogenous aspartic acid alleviates salt stress-induced decline in growth by enhancing antioxidants and compatible solutes while reducing reactive oxygen species in wheat. *Front. Plant Sci.* **2022**, *13*, 987641. [CrossRef]
19. Sharma, P.; Dubey, R. Involvement of oxidative stress and role of antioxidative defense system in growing rice seedlings exposed to toxic concentrations of aluminum. *Plant Cell Rep.* **2007**, *26*, 2027–2038. [CrossRef]
20. Abogadallah, G.M. Insights into the significance of antioxidative defense under salt stress. *Plant Signal. Behav.* **2010**, *5*, 369–374. [CrossRef]
21. Ma, J.-Z.; Zhang, M.; Liu, Z.-G.; Wang, M.; Sun, Y.; Zheng, W.-K.; Lu, H. Copper-based-zinc-boron foliar fertilizer improved yield, quality, physiological characteristics, and microelement concentration of celery (*Apium graveolens* L.). *Environ. Pollut. Bioavailab.* **2019**, *31*, 261–271. [CrossRef]

22. Malhotra, S.K. *Handbook of Herbs and Spices*; Woodhead Publishing: Cambridge, UK, 2006; Volume 3, pp. 317–336.
23. Pardossi, A.; Bagnoli, G.; Malorgio, F.; Campiotti, C.; Tognoni, F. NaCl effects on celery (*Apium graveolens* L.) grown in NFT. *Sci. Hortic.* **1999**, *81*, 229–242. [CrossRef]
24. Duan, A.-Q.; Yang, X.-L.; Feng, K.; Liu, J.-X.; Xu, Z.-S.; Xiong, A.-S. Genome-wide analysis of NAC transcription factors and their response to abiotic stress in celery (*Apium graveolens* L.). *Comput. Biol. Chem.* **2020**, *84*, 107186. [CrossRef] [PubMed]
25. Zhu, L.-H.; Bao, T.-H.; Deng, Y.; Li, H.; Chen, L.-X. Constituents from Apium graveolens and their anti-inflammatory effects. *J. Asian Nat. Prod. Res.* **2017**, *19*, 1079–1086. [CrossRef]
26. Kooti, W.; Daraei, N. A review of the antioxidant activity of celery (*Apium graveolens* L.). *J. Evid-Based Complement. Altern. Med.* **2017**, *22*, 1029–1034. [CrossRef] [PubMed]
27. Hedayati, N.; Bemani Naeini, M.; Mohammadinejad, A.; Mohajeri, S.A. Beneficial effects of celery (*Apium graveolens*) on metabolic syndrome: A review of the existing evidences. *Phytother. Res.* **2019**, *33*, 3040–3053. [CrossRef]
28. Consentino, B.B.; Virga, G.; La Placa, G.G.; Sabatino, L.; Rouphael, Y.; Ntatsi, G.; Iapichino, G.; La Bella, S.; Mauro, R.P.; D'Anna, F. Celery (*Apium graveolens* L.) performances as subjected to different sources of protein hydrolysates. *Plants* **2020**, *9*, 1633. [CrossRef]
29. Bruznican, S.; De Clercq, H.; Eeckhaut, T.; Van Huylenbroeck, J.; Geelen, D. Celery and celeriac: A critical view on present and future breeding. *Front. Plant Sci.* **2020**, *10*, 491122. [CrossRef]
30. Sun, M.; Xu, Q.-Y.; Zhu, Z.-P.; Liu, P.-Z.; Yu, J.-X.; Guo, Y.-X.; Tang, S.; Yu, Z.-F.; Xiong, A.-S. *AgMYB5*, an MYB transcription factor from celery, enhanced β-carotene synthesis and promoted drought tolerance in transgenic *Arabidopsis*. *BMC Plant Biol.* **2023**, *23*, 151. [CrossRef]
31. Li, M.; Zhou, J.; Du, J.; Li, X.; Sun, Y.; Wang, Z.; Lin, Y.; Zhang, Y.; Wang, Y.; He, W. Comparative physiological and transcriptomic analyses of improved heat stress tolerance in celery (*Apium graveolens* L.) caused by exogenous melatonin. *Int. J. Mol. Sci.* **2022**, *23*, 11382. [CrossRef]
32. Gao, Y.; Zhang, J.; Wang, C.; Han, K.; Hu, L.; Niu, T.; Yang, Y.; Chang, Y.; Xie, J. Exogenous proline enhances systemic defense against salt stress in celery by regulating photosystem, phenolic compounds, and antioxidant system. *Plants* **2023**, *12*, 928. [CrossRef]
33. Arora, S.; Singh, A.K.; Sahni, D. Bioremediation of salt-affected soils: Challenges and opportunities. In *Bioremediation of Salt Affected Soils: An Indian Perspective*; Springer: Cham, Switzerland, 2017; pp. 275–301.
34. Shahbaz, M.; Ashraf, M.; Al-Qurainy, F.; Harris, P.J. Salt tolerance in selected vegetable crops. *Crit. Rev. Plant Sci.* **2012**, *31*, 303–320. [CrossRef]
35. Fedeli, R.; Vannini, A.; Djatouf, N.; Celletti, S.; Loppi, S. Can lettuce plants grow in saline soils supplemented with biochar? *Heliyon* **2024**, *10*, 4. [CrossRef]
36. Lamsaadi, N.; El Moukhtari, A.; Oubenali, A.; Farissi, M. Exogenous silicon improves salt tolerance of Fenugreek (*Trigonella foenum-graecum* L.) during seed germination and early seedling stages. *Biologia* **2022**, *77*, 2023–2036. [CrossRef]
37. Thakral, V.; Raturi, G.; Sudhakaran, S.; Mandlik, R.; Sharma, Y.; Shivaraj, S.; Tripathi, D.K.; Sonah, H.; Deshmukh, R. Silicon, a quasi-essential element: Availability in soil, fertilizer regime, optimum dosage, and uptake in plants. *Plant Physiol. Biochem.* **2024**, *208*, 108459. [CrossRef] [PubMed]
38. Thorne, S.J.; Hartley, S.E.; Maathuis, F.J. Is silicon a panacea for alleviating drought and salt stress in crops? *Front. Plant Sci.* **2020**, *11*, 1221. [CrossRef] [PubMed]
39. Shah, A.A.; Yasin, N.A.; Akram, K.; Ahmad, A.; Khan, W.U.; Akram, W.; Akbar, M. Ameliorative role of Bacillus subtilis FBL-10 and silicon against lead induced stress in *Solanum melongena*. *Plant Physiol. Biochem.* **2021**, *158*, 486–496. [CrossRef]
40. Song, J.; Yang, J.; Jeong, B.R. Silicon mitigates ammonium toxicity in cabbage (*Brassica campestris* L. ssp. *pekinensis*) 'Ssamchu'. *Front. Sus. Food Syst.* **2022**, *6*, 922666. [CrossRef]
41. Farooq, M.; Saqib, Z.; Akhtar, J.; Bakhat, H.; Pasala, R.; Dietz, K. Protective role of SILICON (Si) against combined stress of salinity and Boron (B) toxicity by improving antioxidant enzymes activity in rice. *Silicon* **2019**, *11*, 2193–2197. [CrossRef]
42. Çavuşoğlu, K.; Dinçtürk, İ.; Çavuşoğlu, D. The effects of aspartic acid on some physiological and cytogenetical parameters in *Allium cepa* L. seeds germinated under salt stress. *Bulg. J. Crop Sci.* **2020**, *57*, 66–72.
43. Han, M.; Zhang, C.; Suglo, P.; Sun, S.; Wang, M.; Su, T. L-aspartate: An essential metabolite for plant growth and stress acclimation. *Molecules* **2021**, *26*, 1887. [CrossRef] [PubMed]
44. Farhangi-Abriz, S.; Ghassemi-Golezani, K. Improving amino acid composition of soybean under salt stress by salicylic acid and jasmonic acid. *J. Appl. Bot. Food Qual.* **2016**, *89*, 243–248.
45. Hayat, S.; Hayat, Q.; Alyemeni, M.N.; Wani, A.S.; Pichtel, J.; Ahmad, A. Role of proline under changing environments: A review. *Plant Signal. Behav.* **2012**, *7*, 1456–1466. [CrossRef] [PubMed]
46. Song, J.; Yang, J.; Jeong, B.R. Alleviation of ammonium toxicity in salvia splendens 'Vista Red' with silicon supplementation. *Toxics* **2022**, *10*, 446. [CrossRef] [PubMed]
47. Hu, J.; Li, Y.; Jeong, B.R. Silicon alleviates temperature stresses in poinsettia by regulating stomata, photosynthesis, and oxidative damages. *Agronomy* **2020**, *10*, 1419. [CrossRef]
48. Amnon, D. Copper enzymes in isolated chloroplasts. *Plant Physiol.* **1949**, *24*, x1–x15.
49. McCready, R.; Guggolz, J.; Silviera, V.; Owens, H. Determination of starch and amylose in vegetables. *Anal. Chem.* **1950**, *22*, 1156–1158. [CrossRef]

50. Song, J.; Yang, J.; Jeong, B.R. Root GS and NADH-GDH play important roles in enhancing the ammonium tolerance in three bedding plants. *Int. J. Mol. Sci.* **2022**, *23*, 1061. [CrossRef]
51. Bradford, M.M. A rapid and sensitive method for the quantitation of microgram quantities of protein utilizing the principle of protein-dye binding. *Anal. Biochem.* **1976**, *72*, 248–254. [CrossRef]
52. Sahito, S.B.; Jatoi, W.B.; Shaar, G.Q.; Mahar, K.P.; Makhija, P.M.; Kazi, T.G. Determination and evaluation of mineral constituents of medicinal plants used for the treatment of asthma and other ailments by atomic absorption spectrophotometry. *Pak. J. Anal. Environ. Chem.* **2013**, *14*, 7.
53. Giannopolitis, C.N.; Ries, S.K. Superoxide dismutases: I. Occurrence in higher plants. *Plant Physiol.* **1977**, *59*, 309–314. [CrossRef] [PubMed]
54. Amako, K.; Chen, G.-X.; Asada, K. Separate assays specific for ascorbate peroxidase and guaiacol peroxidase and for the chloroplastic and cytosolic isozymes of ascorbate peroxidase in plants. *Plant Cell Physiol.* **1994**, *35*, 497–504.
55. Cakmak, I.; Marschner, H. Magnesium deficiency and high light intensity enhance activities of superoxide dismutase, ascorbate peroxidase, and glutathione reductase in bean leaves. *Plant Physiol.* **1992**, *98*, 1222–1227. [CrossRef] [PubMed]
56. Nakano, Y.; Asada, K. Hydrogen peroxide is scavenged by ascorbate-specific peroxidase in spinach chloroplasts. *Plant Cell Physiol.* **1981**, *22*, 867–880.
57. Wu, Y.-X.; von Tiedemann, A. Impact of fungicides on active oxygen species and antioxidant enzymes in spring barley (*Hordeum vulgare* L.) exposed to ozone. *Environ. Pollut.* **2002**, *116*, 37–47. [CrossRef] [PubMed]
58. Uchida, A.; Jagendorf, A.T.; Hibino, T.; Takabe, T.; Takabe, T. Effects of hydrogen peroxide and nitric oxide on both salt and heat stress tolerance in rice. *Plant Sci.* **2002**, *163*, 515–523. [CrossRef]
59. Yadav, S.; Irfan, M.; Ahmad, A.; Hayat, S. Causes of salinity and plant manifestations to salt stress: A review. *J. Environ. Biol.* **2011**, *32*, 667.
60. Abdelaal, K.A.; Mazrou, Y.S.; Hafez, Y.M. Silicon foliar application mitigates salt stress in sweet pepper plants by enhancing water status, photosynthesis, antioxidant enzyme activity and fruit yield. *Plants* **2020**, *9*, 733. [CrossRef]
61. Laifa, I.; Hajji, M.; Farhat, N.; Elkhouni, A.; Smaoui, A.; M'nif, A.; Hamzaoui, A.H.; Savouré, A.; Abdelly, C.; Zorrig, W. Beneficial effects of silicon (Si) on sea barley (*Hordeum marinum* Huds.) under salt stress. *Silicon* **2021**, *13*, 4501–4517. [CrossRef]
62. Rohanipoor, A.; Norouzi, M.; Moezzi, A.; Hassibi, P. Effect of silicon on some physiological properties of maize (*Zea mays*) under salt stress. *J. Biol. Environ. Sci.* **2013**, *7*, 71–79.
63. Sharma, A.; Kumar, V.; Shahzad, B.; Ramakrishnan, M.; Singh Sidhu, G.P.; Bali, A.S.; Handa, N.; Kapoor, D.; Yadav, P.; Khanna, K. Photosynthetic response of plants under different abiotic stresses: A review. *J. Plant Growth Regul.* **2020**, *39*, 509–531. [CrossRef]
64. Parida, A.K.; Das, A.B. Salt tolerance and salinity effects on plants: A review. *Ecotox. Environ. Saf.* **2005**, *60*, 324–349. [CrossRef] [PubMed]
65. Wu, T.; Zhang, W.; Wu, S.; Cheng, M.; Qi, L.; Shao, G.; Jiao, X. Retrieving rice (*Oryza sativa* L.) net photosynthetic rate from UAV multispectral images based on machine learning methods. *Front. Plant Sci.* **2023**, *13*, 1088499. [CrossRef] [PubMed]
66. Zhu, Y.; Cheng, Z.; Feng, K.; Chen, Z.; Cao, C.; Huang, J.; Ye, H.; Gao, Y. Influencing factors for transpiration rate: A numerical simulation of an individual leaf system. *Therm. Sci. Eng. Prog.* **2022**, *27*, 101110. [CrossRef]
67. Sakoda, K.; Yamori, W.; Shimada, T.; Sugano, S.S.; Hara-Nishimura, I.; Tanaka, Y. Higher stomatal density improves photosynthetic induction and biomass production in Arabidopsis under fluctuating light. *Front. Plant Sci.* **2020**, *11*, 589603. [CrossRef]
68. Xu, Z.; Zhou, G. Responses of leaf stomatal density to water status and its relationship with photosynthesis in a grass. *J. Exp. Bot.* **2008**, *59*, 3317–3325. [CrossRef] [PubMed]
69. Cho, J.-W.; Park, H.-W.; Kim, M.-J.; Kim, H.-H.; Choi, J.-E. Photosynthetic, morphological and growing characteristics by shading materials in *Panax ginseng* CA Meyer. *Korean J. Crop Sci.* **2008**, *53*, 256–260.
70. Jang, I.-B.; Lee, D.-Y.; Yu, J.; Park, H.-W.; Mo, H.-S.; Park, K.-C.; Hyun, D.-Y.; Lee, E.-H.; Kim, K.-H.; Oh, C.-S. Photosynthesis rates, growth, and ginsenoside contents of 2-yr-old *Panax ginseng* grown at different light transmission rates in a greenhouse. *J. Ginseng Res.* **2015**, *39*, 345–353. [CrossRef] [PubMed]
71. Boriboonkaset, T.; Theerawitaya, C.; Yamada, N.; Pichakum, A.; Supaibulwatana, K.; Cha-Um, S.; Takabe, T.; Kirdmanee, C. Regulation of some carbohydrate metabolism-related genes, starch and soluble sugar contents, photosynthetic activities and yield attributes of two contrasting rice genotypes subjected to salt stress. *Protoplasma* **2013**, *250*, 1157–1167. [CrossRef] [PubMed]
72. Rosa, M.; Hilal, M.; Gonzalez, J.A.; Prado, F.E. Low-temperature effect on enzyme activities involved in sucrose–starch partitioning in salt-stressed and salt-acclimated cotyledons of quinoa (*Chenopodium quinoa* Willd.) seedlings. *Plant Physiol. Bioch.* **2009**, *47*, 300–307. [CrossRef]
73. Yin, Y.-G.; Kobayashi, Y.; Sanuki, A.; Kondo, S.; Fukuda, N.; Ezura, H.; Sugaya, S.; Matsukura, C. Salinity induces carbohydrate accumulation and sugar-regulated starch biosynthetic genes in tomato (*Solanum lycopersicum* L. cv. 'Micro-Tom') fruits in an ABA-and osmotic stress-independent manner. *J. Exp. Bot.* **2010**, *61*, 563–574. [CrossRef] [PubMed]
74. Kanai, M.; Higuchi, K.; Hagihara, T.; Konishi, T.; Ishii, T.; Fujita, N.; Nakamura, Y.; Maeda, Y.; Yoshiba, M.; Tadano, T. Common reed produces starch granules at the shoot base in response to salt stress. *New Phytol.* **2007**, *176*, 572–580. [CrossRef] [PubMed]
75. Djanaguiraman, M.; Sheeba, J.A.; Shanker, A.K.; Devi, D.D.; Bangarusamy, U. Rice can acclimate to lethal level of salinity by pretreatment with sublethal level of salinity through osmotic adjustment. *Plant Soil* **2006**, *284*, 363–373. [CrossRef]
76. Chen, H.-J.; Chen, J.-Y.; Wang, S.-J. Molecular regulation of starch accumulation in rice seedling leaves in response to salt stress. *Acta Physiol. Plant.* **2008**, *30*, 135–142. [CrossRef]

77. Yurekli, F.; Porgali, Z.B.; Turkan, I. Variations in abscisic acid, indole-3-acetic acid, gibberellic acid and zeatin concentrations in two bean species subjected to salt stress. *Acta Biol. Cracov. Bot.* **2004**, *46*, 201–212.
78. Porgali, Z.; Yurekli, F. Salt stress-induced alterations in proline accumulation, relative water content and superoxide dismutase (SOD) activity in salt sensitive *Lycopersicon esculentum* and salt-tolerant *L. pennellii*. *Acta Bot. Hung.* **2005**, *47*, 173–182. [CrossRef]
79. Lim, J.-H.; Park, K.-J.; Kim, B.-K.; Jeong, J.-W.; Kim, H.-J. Effect of salinity stress on phenolic compounds and carotenoids in buckwheat (*Fagopyrum esculentum* M.) sprout. *Food Chem.* **2012**, *135*, 1065–1070. [CrossRef] [PubMed]
80. Borghesi, E.; González-Miret, M.L.; Escudero-Gilete, M.L.; Malorgio, F.; Heredia, F.J.; Meléndez-Martínez, A.J. Effects of salinity stress on carotenoids, anthocyanins, and color of diverse tomato genotypes. *J. Agric. Food Chem.* **2011**, *59*, 11676–11682. [CrossRef] [PubMed]
81. Sienkiewicz-Cholewa, U.; Sumisławska, J.; Sacała, E.; Dziągwa-Becker, M.; Kieloch, R. Influence of silicon on spring wheat seedlings under salt stress. *Acta Physiol. Plant.* **2018**, *40*, 54. [CrossRef]
82. Muneer, S.; Park, Y.G.; Manivannan, A.; Soundararajan, P.; Jeong, B.R. Physiological and Proteomic Analysis in Chloroplasts of *Solanum lycopersicum* L. under Silicon Efficiency and Salinity Stress. *Int. J. Mol. Sci.* **2014**, *15*, 21803–21824. [CrossRef]
83. Kaya, C.; Tuna, A.L.; Ashraf, M.; Altunlu, H. Improved salt tolerance of melon (*Cucumis melo* L.) by the addition of proline and potassium nitrate. *Environ. Exp. Bot.* **2007**, *60*, 397–403. [CrossRef]
84. Zhang, M.; Fang, Y.; Ji, Y.; Jiang, Z.; Wang, L. Effects of salt stress on ion content, antioxidant enzymes and protein profile in different tissues of *Broussonetia papyrifera*. *S. Afr. J. Bot.* **2013**, *85*, 1–9. [CrossRef]
85. Zhu, Y.-X.; Gong, H.-J.; Yin, J.-L. Role of Silicon in Mediating Salt Tolerance in Plants: A Review. *Plants* **2019**, *8*, 147. [CrossRef] [PubMed]
86. Rai, V. Role of amino acids in plant responses to stresses. *Biol. Plant.* **2002**, *45*, 481–487. [CrossRef]
87. Talaat, N.B.; Todorova, D. Antioxidant machinery and glyoxalase system regulation confers salt stress tolerance to wheat (*Triticum aestivum* L.) plants treated with melatonin and salicylic Acid. *J. Soil Sci. Plant Nut.* **2022**, *22*, 3527–3540. [CrossRef]
88. Hildebrandt, T.M.; Nesi, A.N.; Araújo, W.L.; Braun, H.-P. Amino acid catabolism in plants. *Mol. Plant* **2015**, *8*, 1563–1579. [CrossRef]
89. Teixeira, W.F.; Fagan, E.B.; Soares, L.H.; Umburanas, R.C.; Reichardt, K.; Neto, D.D. Foliar and seed application of amino acids affects the antioxidant metabolism of the soybean crop. *Front. Plant Sci.* **2017**, *8*, 245273. [CrossRef]

plants

MDPI

Article

Regulation of Root Exudation in Wheat Plants in Response to Alkali Stress

Huan Wang [1,†], Shuting Zhao [1,†], Zexin Qi [1,†], Changgang Yang [2], Dan Ding [1], Binbin Xiao [3], Shihong Wang [2,*] and Chunwu Yang [3]

[1] Department of Agronomy, Jilin Agricultural University, Changchun 130118, China; angelfuture@163.com (H.W.); 20232052@mails.jlau.edu.cn (S.Z.); 20232053@mails.jlau.edu.cn (Z.Q.); aubunuri@163.com (D.D.)
[2] Wheat Research Institute, Gansu Academy of Agricultural Sciences, Lanzhou 730070, China; cgyang1985@126.com
[3] Key Laboratory of Molecular Epigenetics of Ministry of Education, Northeast Normal University, Changchun 130024, China; xiaobb663@nenu.edu.cn (B.X.); yangcw809@nenu.edu.cn (C.Y.)
* Correspondence: wangshh0811@163.com
† These authors contribute equally to this work.

Abstract: Soil alkalization is an important environmental factor limiting crop production. Despite the importance of root secretion in the response of plants to alkali stress, the regulatory mechanism is unclear. In this study, we applied a widely targeted metabolomics approach using a local MS/MS data library constructed with authentic standards to identify and quantify root exudates of wheat under salt and alkali stresses. The regulatory mechanism of root secretion in alkali-stressed wheat plants was analyzed by determining transcriptional and metabolic responses. Our primary focus was alkali stress-induced secreted metabolites (AISMs) that showed a higher secretion rate in alkali-stressed plants than in control and salt-stressed plants. This secretion was mainly induced by high-pH stress. We discovered 55 AISMs containing –COOH groups, including 23 fatty acids, 4 amino acids, 1 amino acid derivative, 7 dipeptides, 5 organic acids, 9 phenolic acids, and 6 others. In the roots, we also discovered 29 metabolites with higher levels under alkali stress than under control and salt stress conditions, including 2 fatty acids, 3 amino acid derivatives, 1 dipeptide, 2 organic acids, and 11 phenolic acids. These alkali stress-induced accumulated carboxylic acids may support continuous root secretion during the response of wheat plants to alkali stress. In the roots, RNAseq analysis indicated that 5 6-phosphofructokinase (glycolysis rate-limiting enzyme) genes, 16 key fatty acid synthesis genes, and 122 phenolic acid synthesis genes have higher expression levels under alkali stress than under control and salt stress conditions. We propose that the secretion of multiple types of metabolites with a –COOH group is an important pH regulation strategy for alkali-stressed wheat plants. Enhanced glycolysis, fatty acid synthesis, and phenolic acid synthesis will provide more energy and substrates for root secretion during the response of wheat to alkali stress.

Keywords: wheat; pH regulation; root secretion; respiration; carboxylic acid

1. Introduction

As the ecological environment continues to deteriorate through unreasonable development and use, the global area of saline land has increased yearly [1–5]. The harmful salts in saline soils mainly include NaCl, Na_2SO_4, $NaHCO_3$, and Na_2CO_3. About 46% of saline soils contain only neutral salts, NaCl, and Na_2SO_4, but the remaining 54% contain both neutral salts and alkaline salts [6]. The stress type exerted by NaCl and/or Na_2SO_4 is defined as salt stress, whereas the stress type exerted by $NaHCO_3$ and/or Na_2CO_3 is defined as alkali stress [7,8]. Previous studies have verified that the destructive effect of alkaline salt stress on plants is significantly stronger than that of neutral salt stress at the same salinity [7–9]. Soil alkalization has caused serious environmental problems in

some areas of the world. For example, in northeastern China, about 50% of grassland is threatened by soil alkalization [10]. Soil pH in the alkalized area even reaches above 10.5. Only a few alkali-resistant halophytes can survive under such heavily alkaline conditions, and no crop can survive extreme alkalinity. Therefore, further research on soil alkalization and alkali stress is warranted.

Salt stress produces negative effects on plants through osmotic stress and ion toxicity. However, in addition to osmotic stress and ion toxicity, alkali stress produces high-pH stress. High pH caused by alkali stress can lead to the precipitation of Ca^{2+}, Mg^{2+}, Fe^{2+}, Mn^{2+}, Cu^{2+}, Zn^{2+}, and $PO_4{}^{3-}$ to surrounding roots, which induces a reduction in the bioavailability of nutrient elements [2,9]. Additionally, a proton gradient across root plasma membranes is the driving force for mineral ion uptake. $HCO_3{}^-$ or $CO_3{}^{2-}$ from alkaline soils will neutralize the proton outside the root plasma membrane, thus breaking the proton gradient and inhibiting the uptake of mineral ions. The plants living in alkaline soils must regulate rhizosphere pH to alleviate nutrient stress. Therefore, the pH regulation of the roots is essential for alkali tolerance in plants.

In the past 30 years, great progress has been made in several areas of salt stress study, such as ion homeostasis, signal transduction, and hormone regulation [11–15]. To date, multilevel signal networks mediating salt tolerance and Na^+ compartmentalization mechanisms at the subcellular level have been elucidated [11–16]. However, relatively few studies have focused on plant alkali tolerance [3,4,17–28]. Important progress in research on plant alkali tolerance has been made in Arabidopsis [21], maize [25], and wheat [27], in which H^+-ATPase was demonstrated to play an important role in alkali tolerance.

Our group and other researchers have found that root secretion is the main pH regulation pathway of plants under alkali stress [29–31]. Root exudates usually include amino acids, phenolics, fatty acids, organic acids, and carbohydrates [22,32]. Secretion of organic acids induced by alkali stress has been reported in many plants, such as *P. tenuiflora* [30,33], grape plants [31], and *Chloris virgata* [29]. However, the physiological and molecular mechanisms underlying root secretion regulation during the response of plants to alkali stress are poorly understood. Wheat provides about 20% of the calories consumed by humans [34]. Soil alkalization is an important factor limiting wheat production in northern China. To explore the specific effects of high pH caused by alkali stress on root secretion, we applied salt stress and alkali stress treatments at the same Na^+ concentration and total salt concentration but with different pH values. Thus, differences in plant root secretion in response to the two stress conditions were mainly attributed to pH differences. In this study, we identified and quantified root exudates of wheat under salt and alkali stresses. To ascertain the regulatory mechanism of root secretion in wheat under alkali stress, we also analyzed the transcriptional and metabolic responses of wheat roots to alkali stress.

2. Results

2.1. Components of Root Exudates

We used a high throughput metabolomic method to detect metabolites in the root exudates (Figure 1A) and root tissues of wheat plants (Figure 1B). Collectively, we detected 443 root exudates in wheat plants under three conditions (Figure 1A), including 75 fatty acids, 52 lipids, 27 organic acids, 31 amino acids or amino acid derivatives, 81 phenolic acids, 28 nucleotides or nucleotide derivatives, 54 flavonoids, 38 alkaloids, 7 terpenoids, 18 carbohydrates, 8 vitamins, 7 lignans or coumarins, and 17 others (Table S1). In wheat plants, 326 root exudates were detected under control conditions, 437 under salt stress, and 431 under alkali stress (Table S1 and Figure 1A). We particularly focused on alkali stress-induced secreted metabolites (AISMs), which were found at a higher root secretion rate under alkali stress condition than under control and salt stress conditions. The number of AISMs for each type of metabolite is displayed in Figure 2A,B. In Figure 2A, salt stress did not affect the secretion rate of the metabolites, but alkali stress enhanced the secretion rate. Conversely, in Figure 2B, both salt stress and alkali stress enhanced the secretion rate of the

metabolites, with greater enhancement in alkali stress than in salt stress. We discovered 105 AISMs in wheat root exudates, including 27 fatty acids, 6 amino acids, 1 amino acid derivative, 7 dipeptides, 5 organic acids, 19 phenolic acids, 9 nucleotides or nucleotide derivatives, 6 flavonoids, 1 lignan or coumarin, 11 alkaloids, 2 carbohydrates, 1 terpenoid, 6 lipids, and 4 vitamins (Figures 1C and 2). Of 105 AISMs, 55 AISMs contained the –COOH group, including 23 fatty acids, 4 amino acids, 1 amino acid derivative, 7 dipeptides, 5 organic acids, 9 phenolic acids, 3 alkaloids, 1 terpenoid, and 2 others (Figures 3–7). These data revealed that fatty acids, amino acids, dipeptides, and phenolic acids were dominant AISMs for alkali-stressed wheat plants. Some plant "hub" fatty acids, such as γ-linolenic acid, arachidonic acid, α-linolenic acid, linoleic acid, and palmitoleic acid also showed higher root secretion rates under alkali stress conditions than under control and salt stress conditions (Figures 4 and 5). All of the three aromatic amino acids (tryptophan, tyrosine, and phenylalanine) were discovered in the list of AISMs (Figure 3).

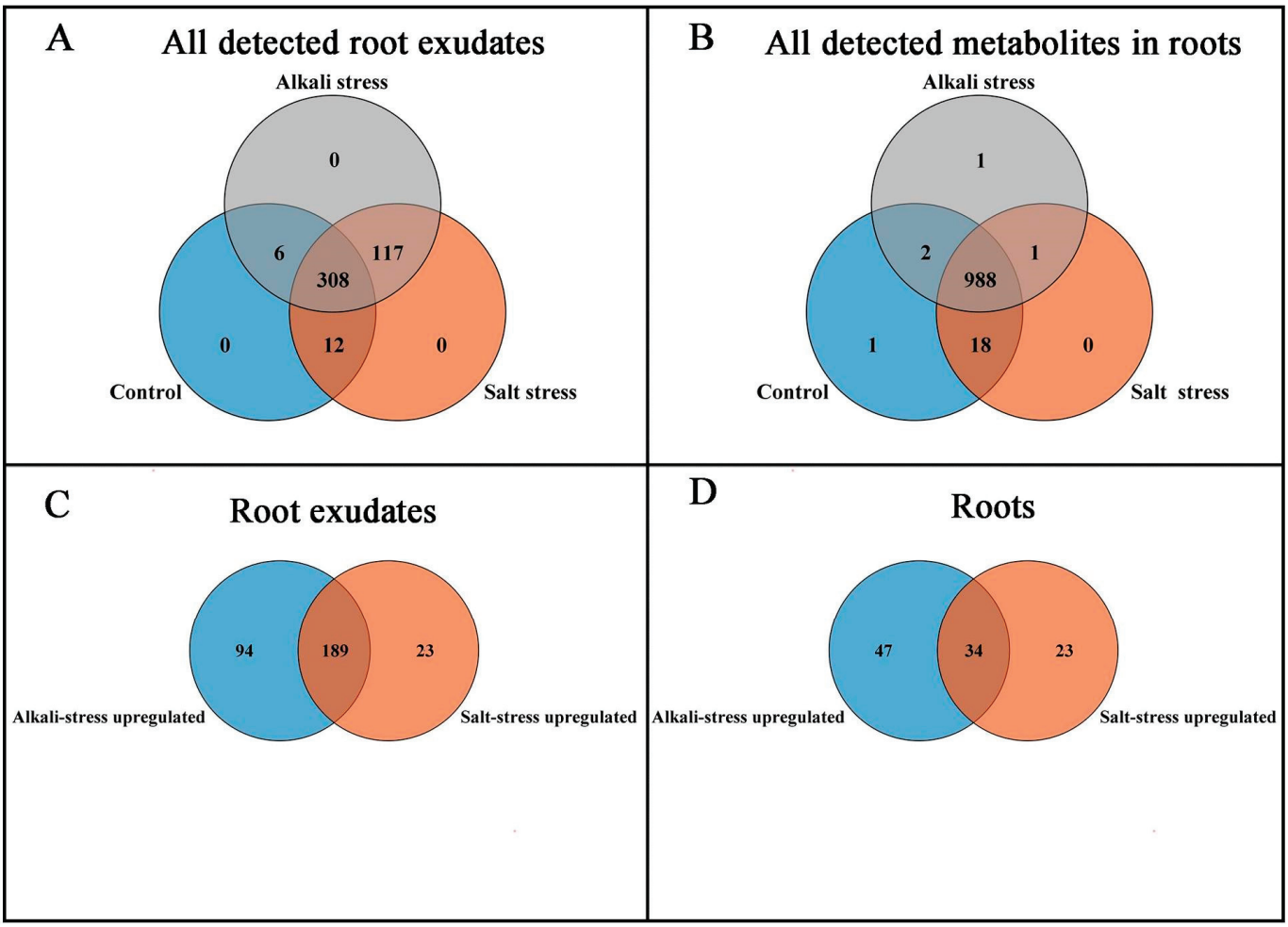

Figure 1. Comparison of metabolite components in root exudates and roots of wheat plants under control, salt stress, and alkali stress conditions. (**A**) Number of all detected root exudates; (**B**) number of all detected metabolites in roots; (**C**) number of the metabolites with enhanced root secretion rate; (**D**) number of the metabolites with upregulated accumulation in roots. The 30-day-old wheat seedlings were treated with salt (88 mM Na^+ and pH 6.7) and alkali (88 mM Na^+ and pH 8.8) solutions for 3 days. Three biological replicates were used for each treatment.

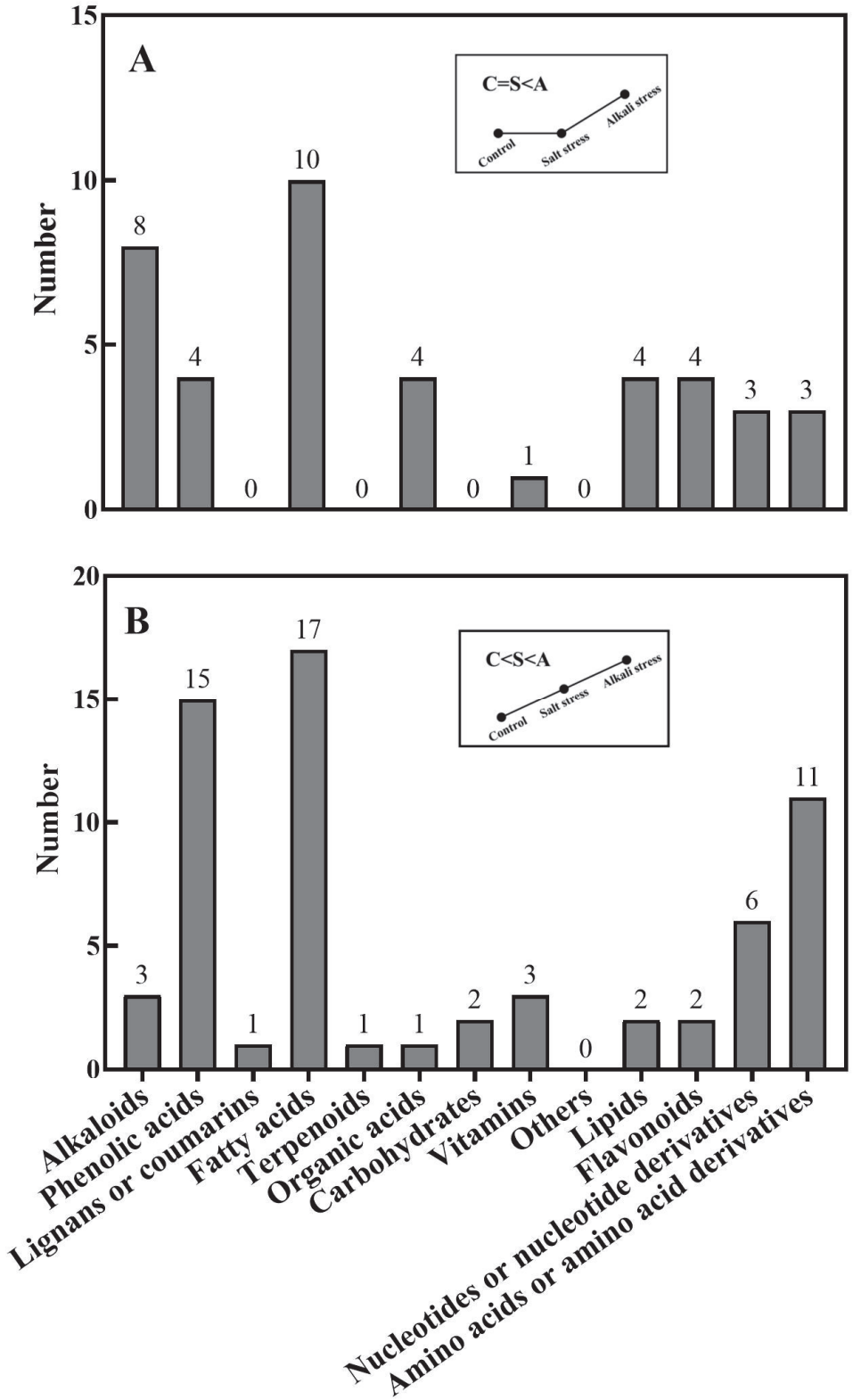

Figure 2. Alkali stress-induced secreted metabolites. The number of metabolites for each type of metabolite was displayed. (**A**) Control and salt-stressed plants showed a similar secretion rate for each metabolite, with a lower secretion rate than that in alkali-stressed plants; (**B**) alkali-stressed plants > salt-stressed plants > control plants in the secretion rate of metabolites. The 30-day-old wheat seedlings were treated with salt (88 mM Na^+ and pH 6.7) and alkali (88 mM Na^+ and pH 8.8) solutions for 3 days. Three biological replicates were used for each treatment.

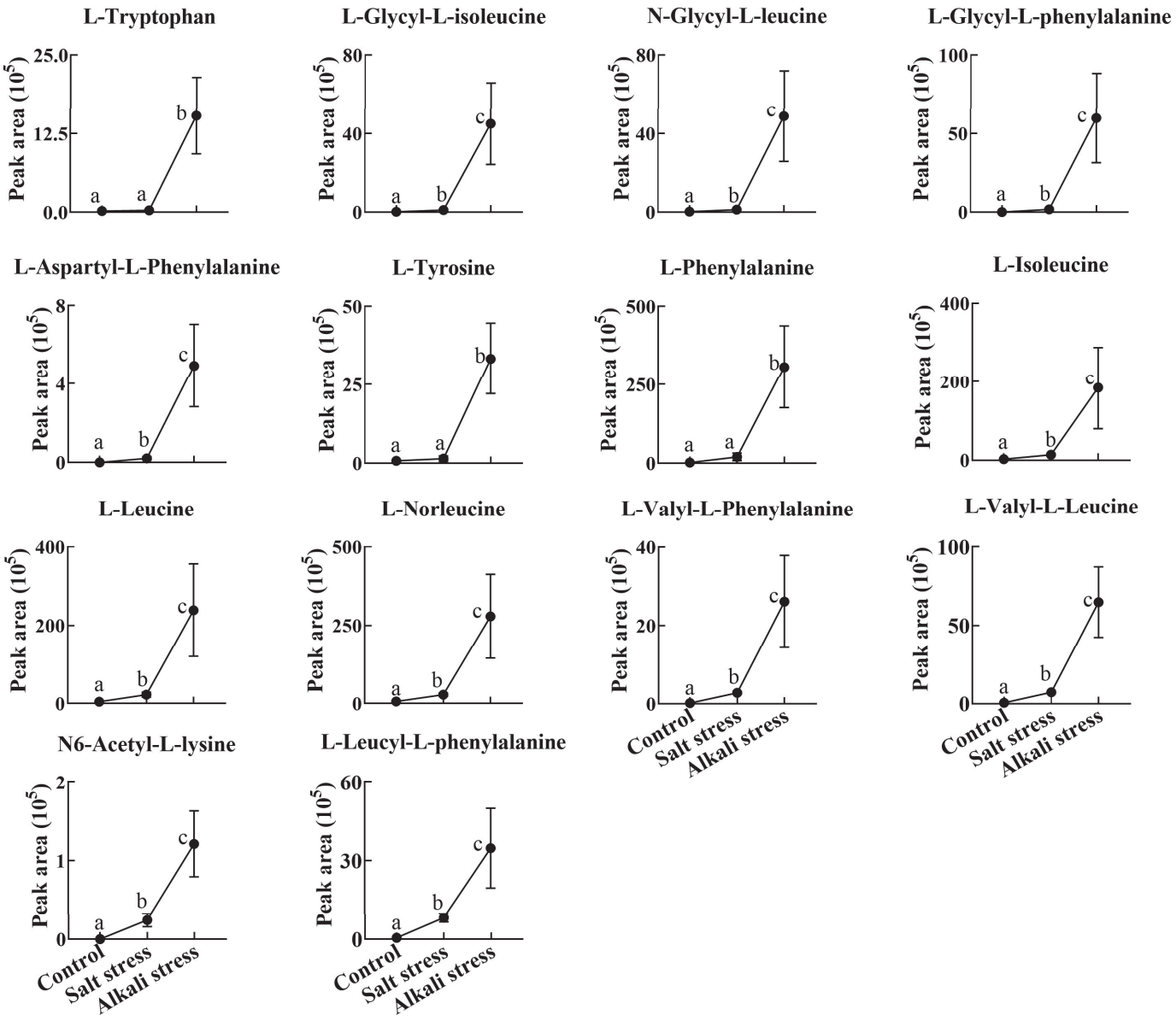

Figure 3. Comparative effects of salt and alkali stresses on the secretion of amino acids and amino acid derivatives in wheat plants. Alkali stress-induced secreted amino acids or amino acid derivatives are displayed. The 30-day-old wheat seedlings were treated with salt stress (88 mM Na^+ and pH 6.7) and alkali stress (88 mM Na^+ and pH 8.8) solutions for 3 days. Three biological replicates were used for each treatment. Different letters above the bar indicate significant differences.

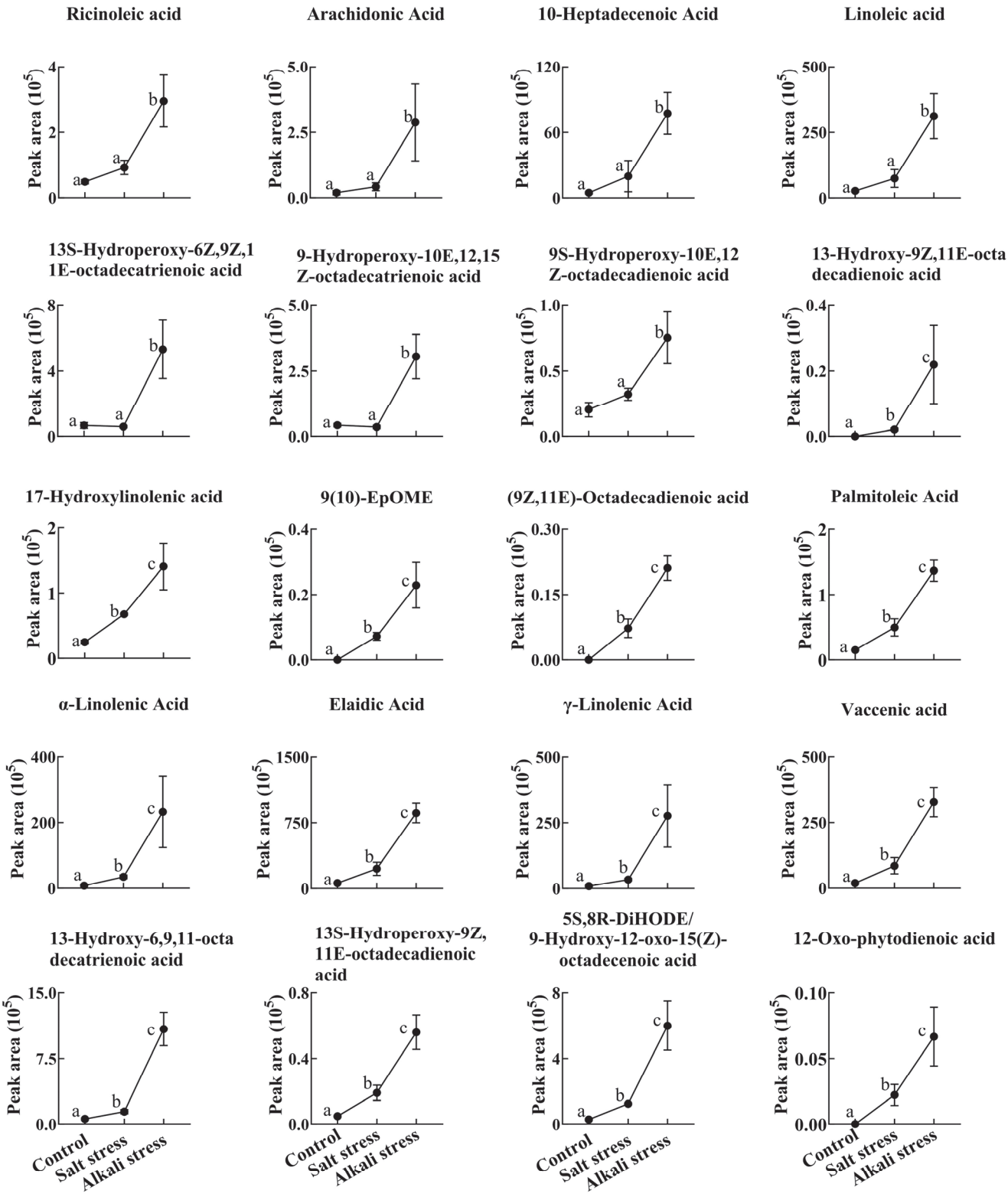

Figure 4. Comparative effects of salt and alkali stresses on the secretion of unsaturated fatty acids in wheat plants. Alkali stress-induced secreted unsaturated fatty acids are displayed. The 30-day-old wheat seedlings were treated with salt (88 mM Na^+ and pH 6.7) and alkali (88 mM Na^+ and pH 8.8) solutions for 3 days. Three biological replicates were used for each treatment. Different letters above the bar indicate significant differences.

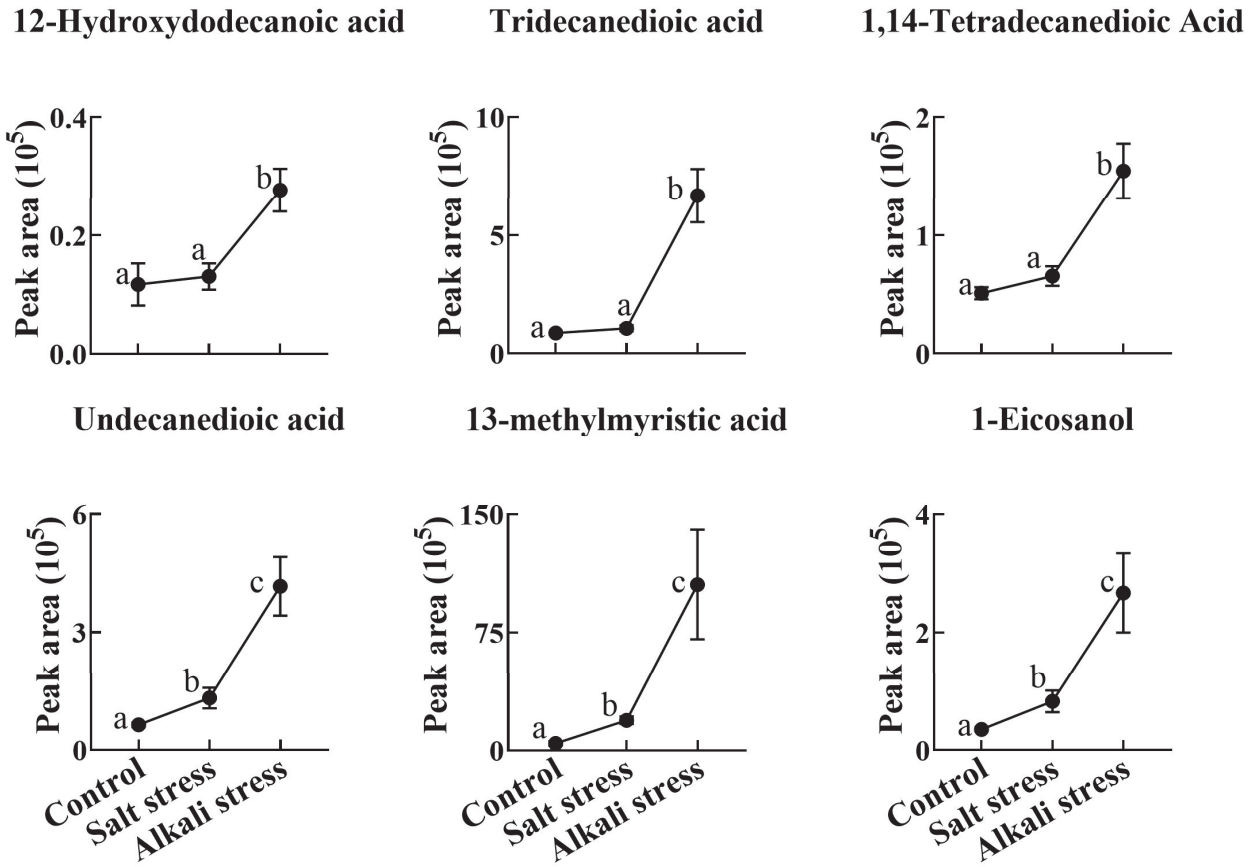

Figure 5. Comparative effects of salt and alkali stresses on the secretion of saturated fatty acids in wheat plants. Alkali stress-induced secreted saturated fatty acids are displayed. The 30-day-old wheat seedlings were treated with salt stress (88 mM Na^+ and pH 6.7) and alkali stress (88 mM Na^+ and pH 8.8) solutions for 3 days. Three biological replicates were used for each treatment. Different letters above the bar indicate significant differences.

2.2. Metabolic Profiling of the Roots

In wheat roots, we collectively detected 1011 metabolites, including 91 fatty acids, 93 lipids, 81 organic acids, 97 amino acids or amino acid derivatives, 164 phenolic acids, 71 nucleotides or nucleotide derivatives, 128 flavonoids, 111 alkaloids, 22 terpenoids, 64 carbohydrates, 16 vitamins, 44 lignans or coumarins, 5 quinones, and 24 others (Figure 1B,D and Table S2). Of these metabolites, 106 metabolites displayed different concentrations under control and salt stress conditions, 224 metabolites displayed different concentrations under control and alkali stress conditions, and 144 metabolites were differentially accumulated under salt stress and alkali stress conditions. We displayed alkali stress-induced accumulated metabolites (AIAMs), which were found at a higher concentration in the roots under alkali stress conditions than under control and salt stress conditions (Figure 8). The number of AIAMs for each type of metabolite is shown in Figure 8A,B. In Figure 8A, salt stress did not affect the accumulation of the metabolites, but alkali stress enhanced the accumulation. In Figure 8B, both salt stress and alkali stress enhanced the concentration of the metabolites, with greater enhancement in alkali stress than in salt stress. We discovered 29 AIAMs in wheat roots, including 2 fatty acids (γ-linolenic acid and α-linolenic acid), 3 amino acid derivatives, 1 dipeptide, 2 organic acids (shikimic acid and muconic acid), 11 phenolic acids, 2 flavonoids, 1 lipid, 1 terpenoid, and 6 alkaloids (Figure 8 and Table S3). Integrated analysis of root exudates and root metabolome data showed higher levels of γ-linolenic acid and α-linolenic acid in alkali-stressed roots than in control and salt-stressed roots, as well as a faster secretion rate in alkali-stressed roots than in control and salt-stressed roots.

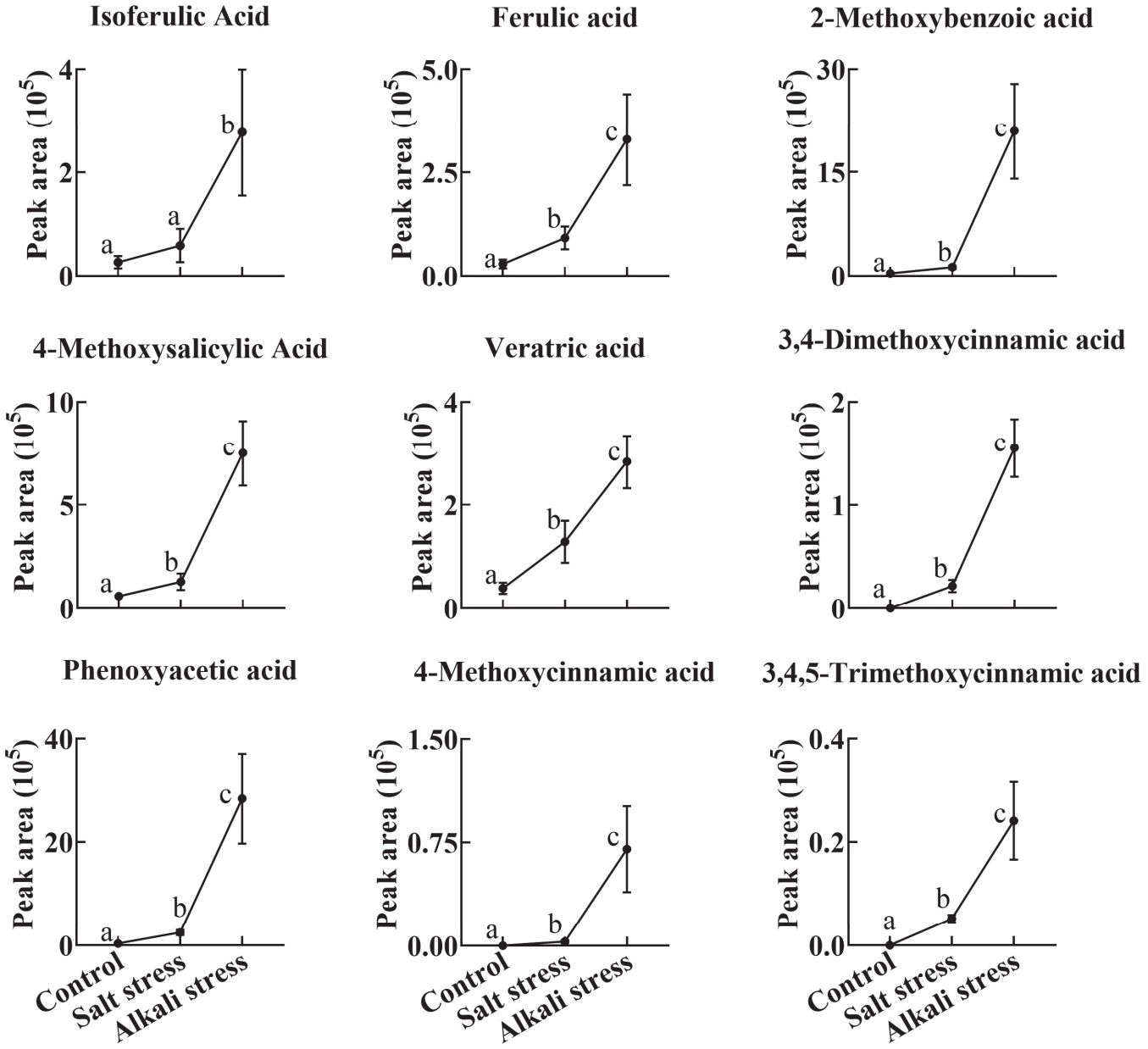

Figure 6. Comparative effects of salt and alkali stresses on the secretion of phenolic acids with a –COOH group in wheat plants. Alkali stress-induced secreted phenolic acids are displayed. The 30-day-old wheat seedlings were treated with salt stress (88 mM Na^+ and pH 6.7) and alkali stress (88 mM Na^+ and pH 8.8) solutions for 3 days. Three biological replicates were used for each treatment. Different letters above the bar indicate significant differences.

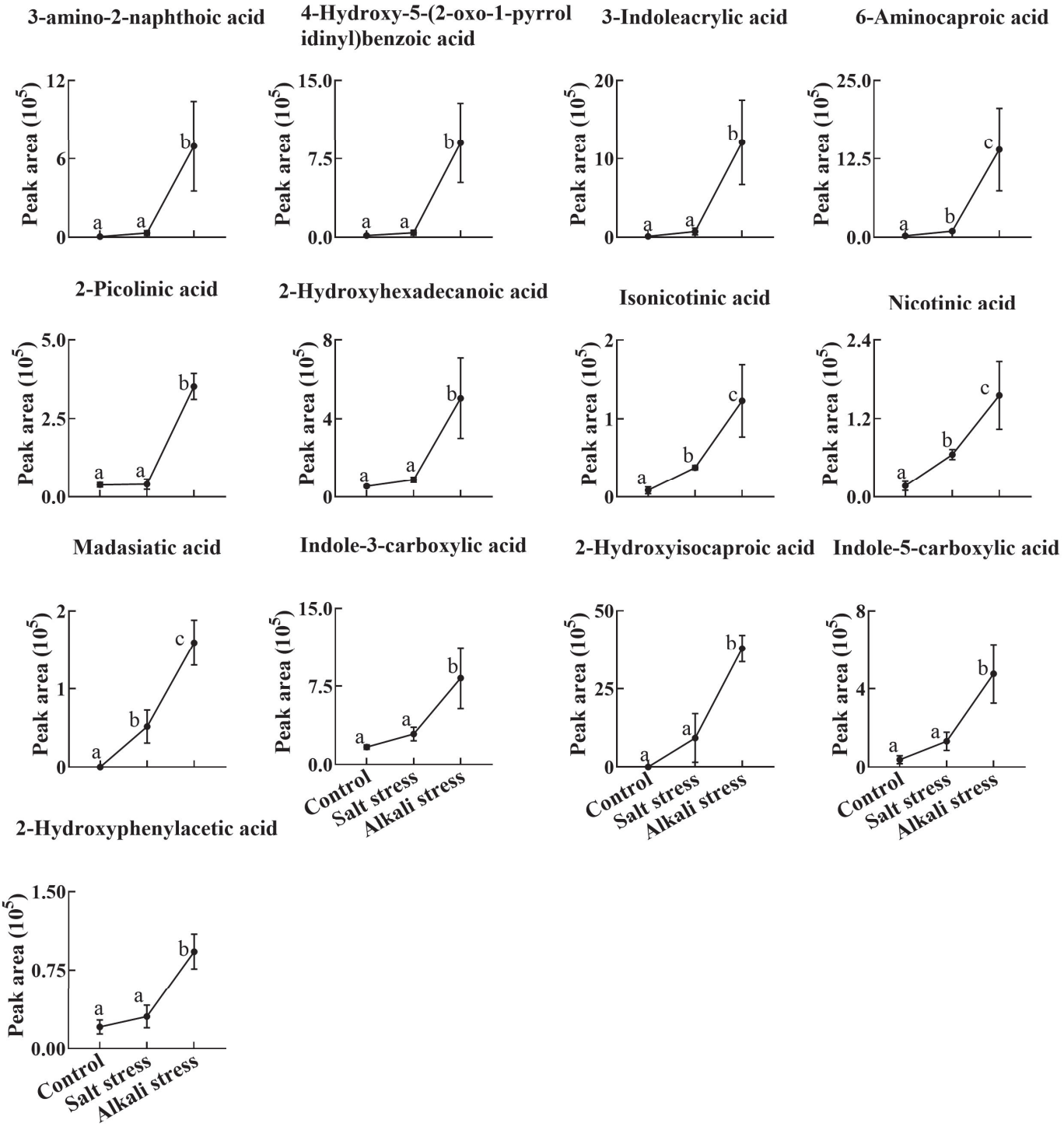

Figure 7. Comparative effects of salt and alkali stresses on the secretion of other carboxylic acids in wheat plants. The 30-day-old wheat seedlings were treated with salt stress (88 mM Na^+ and pH 6.7) and alkali stress (88 mM Na^+ and pH 8.8) solutions for 3 days. Three biological replicates were used for each treatment. Different letters above the bar indicate significant differences.

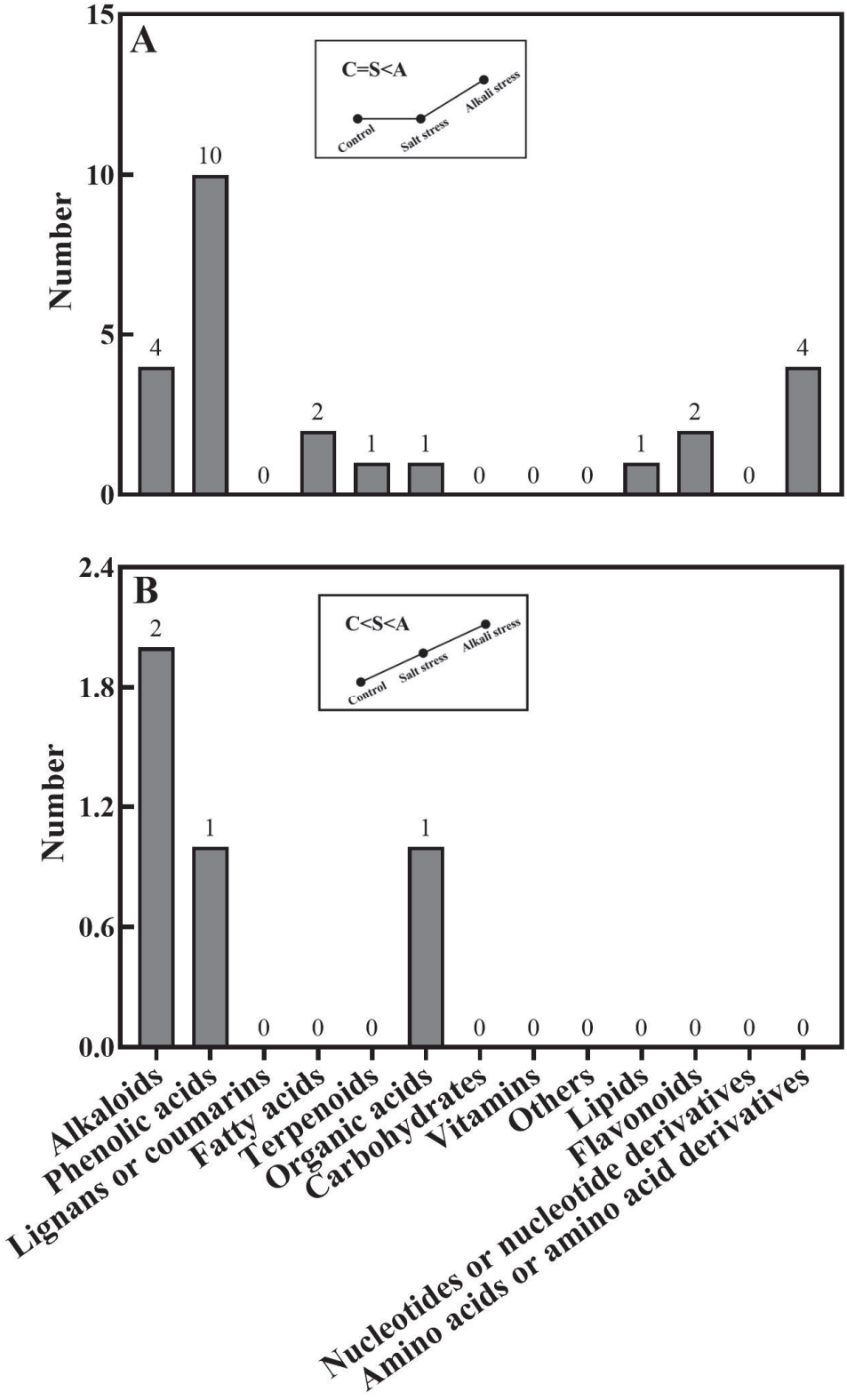

Figure 8. Alkali stress-induced accumulated metabolites in wheat roots. The number of metabolites in each type is displayed. (**A**) Control and salt-stressed plants showed similar levels for each metabolite, with lower levels than those in alkali-stressed plants; (**B**) alkali-stressed plants > salt-stressed plants > control plants in levels of metabolites. The 30-day-old wheat seedlings were treated with salt stress (88 mM Na^+ and pH 6.7) and alkali stress (88 mM Na^+ and pH 8.8) solutions for 3 days. Three biological replicates were used for each treatment.

2.3. Gene Expression Response in the Roots

The results of the RNAseq were validated with real-time quantitative PCR (qRT-PCR) (Table S4). In 10 of the 12 randomly selected genes, the fold changes of the RNAseq experiment were similar to those of the qRT-PCR experiment, indicating that the results of the RNAseq experiment were reliable (Table S4). Compared with the control, salt stress upregulated the expression of 2108 genes and downregulated the expression of 1470 genes, whereas alkali stress upregulated the expression of 8542 genes and downregulated the expression of 6764 genes. The expression level of 5967 genes was higher in alkali-stressed roots than in salt-stressed roots, and 8147 genes displayed a lower level of expression in alkali-stressed roots than in salt-stressed roots. Alkali stress-induced genes (AIGs) were considered those with an expression level higher in alkali-stressed plants than in control and salt-stressed plants. We discovered 5764 AIGs, which were exposed to KEGG enrichment. The AIGs were enriched in phenylpropanoid biosynthesis, amino acid metabolism, nitrogen metabolism, amino acid-related enzymes, phenylalanine metabolism, flavonoid biosynthesis, alpha-linolenic acid metabolism, and other pathways (Table S5). AIGs involved in alkali tolerance are shown in Figures S1–S6. The AIGs included 18 NRT1/PTR FAMILY (*NPF*) genes, 22 *NRT* genes (Figure S1), 11 1-aminocyclopropane-1-carboxylate (ACC) oxidase genes, and 38 ethylene-responsive transcription factor genes (Figure S2). In the AIG list, we also discovered 29 glycolysis/gluconeogenesis genes including 5 glycolysis rate-limiting enzyme (6-phosphofructokinase) genes, and 16 key fatty acid synthesis genes (4 *FabG* genes, 1 *FabF* gene, 1 medium-chain acyl-[acyl-carrier-protein] hydrolase gene and 4 long-chain acyl-CoA synthetase genes) (Figure S3). Additionally, we also found 122 phenolic acid synthesis genes in the list of AIGs (Table S5), including 4 phenylalanine ammonia-lyase (*PAL*, phenolic acid synthesis rate-limiting enzyme) genes, 7 4-coumarate-CoA ligase (*4CL*) genes, and 2 trans-cinnamate 4-monooxygenase genes (Figure S4). The expression level of 22 peptide transporter genes, 3 oligopeptide transporter genes, 6 protease genes, 1 ubiquitin-conjugating enzyme gene, and 13 E3 ubiquitin-protein ligase genes was also higher in alkali-stressed roots than in control and salt-stressed roots (Figures S5 and S6).

3. Discussion

Root secretion has a vital role in the tolerance of plants to abiotic stresses, such as phosphorus deficiency, heavy metal pollution, aluminum toxicity, and alkali stress [22,32]. The roles of organic acid secretion in pH regulation under alkali stress have been reported in grapevine roots [35], grape plants [31], and *C. virgata* plants [29]. High pH caused by alkali stress can precipitate various mineral element ions at the rhizosphere, leading to nutrient deficiency [28]. High pH can also induce the over-accumulation of Na^+ and enhance ion toxicity [28]. Thus, the regulation of pH at the rhizosphere or within roots is vital for plant survival under high alkali conditions. In this study, we detected a diverse array of metabolites covering most types of metabolites in the root exudates of alkali-stressed wheat plants. We particularly focused on secreted metabolites induced by alkali stress (high-pH). We discovered 55 AISMs contained a –COOH group, including 23 fatty acids, 4 amino acids, 1 amino acid derivative, 7 dipeptides, 5 organic acids, 9 phenolic acids, 3 alkaloids, 1 terpenoid, and 2 others. We propose that the secretion of multiple types of metabolites with the –COOH group may be an important pH regulation strategy for wheat roots under alkali stress. Recently, root exudates of a halophyte *Puccinellia tenuiflora* under alkali stress were also analyzed by a metabolomics approach [33]. In *P. tenuiflora* plants, 75 AISMs with the –COOH group were discovered, including 42 fatty acids, 3 amino acid derivatives, 22 phenolic acids, and 8 organic acids [33]. Our recently published work revealed that halophyte *Leymus chinensis* responded to alkali stress via the secretion of phenolic acids, free fatty acids, organic acids, and amino acids [36]. However, that study did not apply salt stress treatment, so the root secretion response of *L. chinensis* to a high pH was not explored. The above data demonstrated that the secretion of fatty acids, phenolic acids, and organic acids was the common response of plants to alkali stress. However, amino acids and dipeptides were discovered in AISMs of wheat and not in *P. tenuiflora*. This suggests

that wheat and the halophyte *P. tenuiflora* have different pH regulation strategies under alkali stress. The secretion of amino acids and dipeptides may play more important roles in wheat alkali tolerance.

Glycolysis provides the reducing power (ATP and NADH) and carbon source for metabolisms and the root secretion process. In the wheat roots, five 6-phosphofructokinase (glycolysis rate-limiting enzyme) genes displayed higher expression levels under alkali stress than under control and salt stress conditions (Figure S3). Enhanced glycolysis will provide more reducing power and carbon sources for the synthesis of fatty acids, phenolic acids, and organic acids to support their secretion into the rhizosphere during the response of wheat to alkali stress. We also focused on metabolites with a higher level in alkali-stressed wheat roots than in control and salt-stressed wheat roots, including 2 fatty acids, 3 amino acid derivatives, 1 dipeptide, 2 organic acids, 11 phenolic acids, 2 flavonoids, 1 lipid, 1 terpenoid, and 6 alkaloids. These alkali stress-induced accumulated carboxylic acids not only have roles in osmotic regulation but also directly or indirectly support root secretion during the response of wheat to alkali stress. The enhanced accumulation of carboxylic acids (e.g., amino acids, fatty acids, and organic acids) has also been observed in alkali-stressed rice [19], alfalfa [9], and sunflower [37]. RNAseq analysis showed that 16 key fatty acid synthesis genes and 122 phenolic acid synthesis genes (including rate-limiting enzyme genes *PAL*) have a higher expression level in wheat roots under alkali stress conditions than under control and salt stress conditions (Figure S4), indicating a strategy for the regulation of gene expression for the accumulation and secretion of fatty acids and phenolic acids during the response of wheat roots to alkali stress. Additionally, the expression level of 18 *NPF* genes and 25 peptide transporter genes was higher in alkali-stressed wheat roots than in control and salt-stressed wheat roots (Figure S1). The NPF family can transport multiple substrates, including chloride, potassium, carboxylate, plant hormones, peptides, nitrate, and metabolites containing a –COOH group [38]. The upregulated expression of the *NPF* genes may accelerate the secretion of metabolites containing the –COOH group and facilitate rhizosphere pH regulation in alkali-stressed wheat. Although we have identified some candidate genes that can mediate root secretion of wheat plants under alkali stress, some important questions remain, such as which genes mediate the co-expression of 19 *NPF* genes and 25 peptide transporter genes under alkali stress and what mechanism coordinates the production and secretion of AISMs. In wheat plants, alkali stress-induced secreted dipeptides and amino acids may be produced from protein degradation, while other secreted carboxylic acids may be generated from continuous biosynthesis. The upregulation of E3 ubiquitin-protein ligase genes, ubiquitin-conjugating enzyme genes, and protease genes facilitates the protein degradation that generates oligopeptides or amino acids (Figure S6), which provides materials for the secretion of dipeptides and amino acids by wheat roots under alkali stress. In wheat roots, the expression of 11 key ethylene synthesis genes and 38 ethylene-responsive transcription factor genes was particularly upregulated under alkali stress condition, suggesting that ethylene may mediate the response of wheat roots to alkali stress. It has been reported that ethylene plays a beneficial role in enhancing the salt tolerance of plants [39]. Ethylene may exert important effects in mediating the production and secretion of carboxylic acids and dipeptides during the response of wheat roots to alkali stress, which warrants further investigations.

4. Materials and Methods

4.1. Stress Treatment and Root Exudate Collection

Xiaobingmai33, a spring wheat variety widely cultivated in Northeast China, was selected as the test organism. The wheat seeds were provided by Prof. Jinsong Pang from Northeast Normal University, China. The seeds were sown in plastic pots containing sand. All pots (15 seedlings per pot; pot size height 19 cm and diameter 18.5 cm) were watered with half-strength Hoagland nutrient solution for 30 days in a greenhouse (23–25 °C day and 17–20 °C night, 16 h light). The experiment was conducted from mid-April to mid-May in Changchun, China. Based on the pH and salinity levels of moderate soda salt-alkaline

in Northeast China, $NaHCO_3$ and Na_2CO_3 were added at a 9:1 molar ratio (80 mM total salt concentration, 88 mM Na^+ concentration, and pH 8.8) to mimic alkali stress conditions in the moderate soda salt–alkaline soil. To explore the specific effects of high-pH, NaCl and Na_2SO_4 were added at a 9:1 molar ratio (80 mM total salt concentration, 88 mM Na^+ concentration, and pH 6.7) for the salt stress treatment. The control was cultured with a half-strength Hoagland nutrient solution (pH 6.6). The final pH values of the salt stress and alkali stress treatment solutions were determined after adding the nutrient solution. Wheat plants can finish their life cycle under such stress conditions. The pots with uniform wheat seedlings were treated with salt or alkali treatment solution containing nutrient components for three days, and then root exudates were collected and stored at −80 °C according to a method by Li et al. [33]. After root exudate collection, the root samples were collected and freeze-dried, and RNA samples were collected and stored at −80 °C. Ten plants were pooled as a biological replicate, with three biological replicates for metabolome analysis and RNA sequencing.

4.2. Metabolome Analysis

Metabolites in root exudates and root tissues were qualified and quantified using a widely targeted metabolomics approach based on a local MS-MS data library constructed with authentic standards [40]. The secretion rate of each metabolite was expressed as the relative amount (peak area) of g^{-1} root DW. Metabolites in root exudates and root tissues were measured according to Li et al. [33]. Briefly, freeze-dried root samples and freeze-dried root exudates were treated with 70% methanol, and then the extracts were loaded onto an LC–MS/MS system (QTRAP, AB SCIEX). A mixed sample of all extracts in equal volumes was loaded onto an LC–MS/MS system (QTRAP, AB SCIEX) to construct an MS2 spectral tag library. Retention time, m/z ratio, and fragmentation information were applied to identify each metabolite through an in-house database (MWDB, https://www.metware.cn accessed on 11 December 2021). All the metabolites identified were quantified using the MRM method [40]. We defined differentially accumulated metabolite (DAM) or differentially secreted metabolite (DSM) as VIP > 1, p value (t test) < 0.05, and |Log2(Fold change)| > 1.

4.3. RNAseq and qRT-PCR

Conventional methods were applied to conduct RNAseq experiments and data analyses [2]. Total RNA samples were used as input material for library construction. The prepared libraries were sequenced on an Illumina platform. Wheat reference genome and gene model annotation files were downloaded from the Ensembl Plants website (http://plants.ensembl.org/Triticum_aestivum/Info/Index accessed on 20 December 2021). The paired-end clean reads were mapped to the reference genome using Hisat2 v2.0.5. Differentially expressed genes (DEGs) were identified using the DESeq2 R package 1.20.0 (adjusted p value ≤ 0.05 and |log2fold change| ≥ 1) [41]. We applied the TBtools program to conduct GO and KEGG enrichments for DEGs [42]. The reliability of the RNAseq analysis was validated using qRT-PCR. *RLI*, *Actin 2*, *Actin 7*, and *β-tubulin* were selected as internal control genes. The expression level of the genes was calculated using the ΔΔCt method [43].

5. Conclusions

The secretion of multiple types of metabolites with a –COOH group is an important pH regulation strategy for alkali-stressed wheat plants. Enhanced glycolysis, fatty acid synthesis, and phenolic acid synthesis will provide more energy and substrates for root secretion during the response of wheat to alkali stress. In wheat plants, alkali stress-induced secreted dipeptides and amino acids may be produced from protein degradation, while other secreted carboxylic acids may be generated from continuous biosynthesis. Some *NPF* genes and peptide transporter genes may play important roles in the pH regulation of alkali-stressed wheat plants.

Supplementary Materials: The following supporting information can be downloaded at: https://www.mdpi.com/article/10.3390/plants13091227/s1. Table S1: Mass spectrum information of all detected metabolites in root exudates of wheat plants. Table S2: Mass spectrum information of all detected metabolites in wheat roots. Table S3: Mass spectrum information of accumulated metabolites induced by alkali stress in wheat roots. Table S4: Results of qPCR. Table S5: KEGG enrichment for alkali stress-induced genes. Figure S1: Comparative effects of salt and alkali stresses on the expression of NPF genes. The 30-day-old wheat seedlings were treated with salt (88 mM Na^+ and pH 6.7) and alkali (88 mM Na^+ and pH 8.8) solutions for 3 days. Three biological replicates were used for each treatment. Different letters above the bars indicate significant differences. In the figures, each gene ID represents different members of a gene family. Figure S2: Comparative effects of salt and alkali stresses on the expression of genes involved in ethylene signal transduction. The 30-day-old wheat seedlings were treated with salt (88 mM Na^+ and pH 6.7) and alkali (88 mM Na^+ and pH 8.8) solutions for 3 days. Three biological replicates were used for each treatment. Different letters above the bars indicate significant differences. In the figures, each gene ID represents different members of a gene family. Figure S3: Comparative effects of salt and alkali stresses on the expression of the genes involved in glycolysis and fatty acid synthesis. The 30-day-old wheat seedlings were treated with salt (88 mM Na^+ and pH 6.7) and alkali (88 mM Na^+ and pH 8.8) solutions for 3 days. Each treatment had three biological replicates. Different letters above the bars indicate significant differences. In the figures, each gene ID represents different members of a gene family. Figure S4: Comparative effects of salt and alkali stresses on the expression of genes involved in phenolic acid synthesis. The 30-day-old wheat seedlings were treated with salt (88 mM Na^+ and pH 6.7) and alkali (88 mM Na^+ and pH 8.8) solutions for 3 days. Three biological replicates were used for each treatment. Different letters above the bars indicate significant differences. In the figures, each gene ID represents different members of a gene family. Figure S5: Comparative effects of salt and alkali stresses on the expression of peptide transporter genes. The 30-day-old wheat seedlings were treated with salt (88 mM Na^+ and pH 6.7) and alkali (88 mM Na^+ and pH 8.8) solutions for 3 days. Each treatment had three biological replicates. Different letters above the bars indicate significant differences. In the figures, each gene ID represents different members of a gene family. Figure S6: Comparative effects of salt and alkali stresses on the expression of the genes involved in protein degradation. The 30-day-old wheat seedlings were treated with salt (88 mM Na^+ and pH 6.7) and alkali (88 mM Na^+ and pH 8.8) solutions for 3 days. Three biological replicates were used for each treatment. Different letters above the bars indicate significant differences. In the figures, each gene ID represents different members of a gene family.

Author Contributions: Conceptualization: H.W. and S.W.; formal analysis: S.Z., Z.Q., C.Y. (Changgang Yang), D.D., B.X. and C.Y. (Chunwu Yang); investigation: H.W., S.Z., Z.Q., D.D. and B.X.; methodology: S.Z., Z.Q., D.D. and B.X.; project administration: S.W.; supervision: H.W. and S.W.; writing—original draft: H.W., S.Z., Z.Q. and S.W. All authors have read and agreed to the published version of the manuscript.

Funding: This work was supported by the Technology Development Plan of the Jilin Provincial Government (No. 20220202006NC), National Natural Science Foundation of China (Regional Science Fund) (No. 32360505), Basic construction funding (Innovation Capacity construction) of the Jilin Province budget for 2023 (No. 2023C035-7), Fundamental Research Funds for the Central Universities (No. CGZH202202), and Research Condition Construction and Achievement Transformation Project of Gansu Academy of Agricultural Sciences (No. 2021GAAS03).

Data Availability Statement: All RNA sequencing raw data are deposited at NCBI (Accession number PRJNA970414). The datasets used and/or analyzed during the current study are available from the corresponding author upon reasonable request.

Conflicts of Interest: The authors have no conflicts of interest.

References

1. Liu, B.; Hu, Y.; Wang, Y.; Xue, H.; Li, Z.; Li, M. Effects of saline-alkali stress on bacterial and fungal community diversity in *Leymus chinensis* rhizosphere soil. *Environ. Sci. Pollut. Res.* **2022**, *29*, 70000–70013. [CrossRef] [PubMed]
2. Xiao, B.; Lu, H.; Li, C.; Bhanbhro, N.; Cui, X.; Yang, C. Carbohydrate and plant hormone regulate the alkali stress response of hexaploid wheat (*Triticum aestivum* L.). *Environ. Exp. Bot.* **2020**, *175*, 104053. [CrossRef]

3. Yan, H.; Liu, B.; Cui, Y.; Wang, Y.; Sun, S.; Wang, J.; Tan, M.; Wang, Y.; Zhang, Y. LpNAC6 reversely regulates the alkali tolerance and drought tolerance of *Lilium pumilum*. *J. Plant Physiol.* **2022**, *270*, 153635. [CrossRef]
4. Zhang, G.; Peng, Y.; Zhou, J.; Tan, Z.; Jin, C.; Fang, S.; Zhong, S.; Jin, C.; Wang, R.; Wen, X. Genome-Wide Association Studies of Salt-Alkali Tolerance at Seedling and Mature Stages in *Brassica napus*. *Front. Plant Sci.* **2022**, *13*, 857149. [CrossRef] [PubMed]
5. Liu, B.; Li, M.; Wang, Y.; Li, J.; Xue, H. Effects of saline-alkali stress on the functional traits and physiological characteristics of *Leymus chinensis* leaves. *Grassl. Sci.* **2022**, *68*, 336–342. [CrossRef]
6. Tanji, K.K. Salinity in the soil environment. In *Salinity: Environment-Plants-Molecules*; Tanji, K.K., Ed.; Kluwer Academic Publishers: Dordrecht, The Netherlands, 2002; pp. 21–51.
7. Shi, D.; Sheng, Y. Effect of various salt–alkaline mixed stress conditions on sunflower seedlings and analysis of their stress factors. *Environ. Exp. Bot.* **2005**, *54*, 8–21. [CrossRef]
8. Shi, D.; Wang, D. Effects of various salt-alkaline mixed stresses on *Aneurolepidium chinense* (Trin.) Kitag. *Plant Soil.* **2005**, *271*, 15–26. [CrossRef]
9. Guo, R.; Zhou, Z.; Cai, R.; Liu, L.; Wang, R.; Sun, Y.; Wang, D.; Yan, Z.; Guo, C. Metabolomic and physiological analysis of alfalfa (*Medicago sativa* L.) in response to saline and alkaline stress. *Plant Physiol. Biochem.* **2024**, *207*, 108338. [CrossRef] [PubMed]
10. Yao, R. Characteristics and agro-biological management of saline-alkalized land in the Northeast China. *Soils* **2006**, *38*, 256–262.
11. Maryum, Z.; Luqman, T.; Nadeem, S.; Khan, S.M.U.D.; Wang, B.; Ditta, A.; Khan, M.K.R. An overview of salinity stress, mechanism of salinity tolerance and strategies for its management in cotton. *Front. Plant Sci.* **2022**, *13*, 907937. [CrossRef]
12. Guo, M.; Wang, X.-S.; Guo, H.-D.; Bai, S.-Y.; Khan, A.; Wang, X.-M.; Gao, Y.-M.; Li, J.-S. Tomato salt tolerance mechanisms and their potential applications for fighting salinity: A review. *Front. Plant Sci.* **2022**, *13*, 949541. [CrossRef] [PubMed]
13. Price, L.; Han, Y.; Angessa, T.; Li, C. Molecular pathways of WRKY genes in regulating plant salinity tolerance. *Int. J. Mol. Sci.* **2022**, *23*, 10947. [CrossRef] [PubMed]
14. Rasheed, F.; Anjum, N.A.; Masood, A.; Sofo, A.; Khan, N.A. The key roles of salicylic acid and sulfur in plant salinity stress tolerance. *J. Plant Growth Regul.* **2020**, *41*, 1891–1904. [CrossRef]
15. Chen, T.; Shabala, S.; Niu, Y.; Chen, Z.-H.; Shabala, L.; Meinke, H.; Venkataraman, G.; Pareek, A.; Xu, J.; Zhou, M. Molecular mechanisms of salinity tolerance in rice. *Crop. J.* **2021**, *9*, 506–520. [CrossRef]
16. Munns, R.; Tester, M. Mechanisms of salinity tolerance. *Annu. Rev. Plant Biol.* **2008**, *59*, 651–681. [CrossRef] [PubMed]
17. Zhou, Y.; Xu, K.; Gao, H.; Yao, W.; Zhang, Y.; Zhang, Y.; Azhar Hussain, M.; Wang, F.; Yang, X.; Li, H. Comparative proteomic analysis of two wild Soybean (*Glycine soja*) genotypes reveals positive regulation of saline-alkaline stress tolerance by tonoplast transporters. *J. Agric. Food Chem.* **2023**, *71*, 14109–14124. [CrossRef] [PubMed]
18. Zhao, Z.; Liu, J.; Jia, R.; Bao, S.; Chen, X. Physiological and TMT-based proteomic analysis of oat early seedlings in response to alkali stress. *J. Proteom.* **2019**, *193*, 10–26. [CrossRef] [PubMed]
19. Qian, G.; Wang, M.; Wang, X.; Liu, K.; Li, Y.; Bu, Y.; Li, L. Integrated Transcriptome and Metabolome Analysis of Rice Leaves Response to High Saline–Alkali Stress. *Int. J. Mol. Sci.* **2023**, *24*, 4062. [CrossRef]
20. Xu, W.; Jia, L.; Shi, W.; Balu¡ ka, F.E.; Kronzucker, H.J.; Liang, J.; Zhang, J. The tomato 14-3-3 protein TFT4 modulates H^+ efflux, basipetal auxin transport, and the PKS5-J3 pathway in the root growth response to alkaline stress. *Plant Physiol.* **2013**, *163*, 1817–1828. [CrossRef] [PubMed]
21. Yang, Y.; Wu, Y.; Ma, L.; Yang, Z.; Dong, Q.; Li, Q.; Ni, X.; Kudla, J.; Song, C.; Guo, Y. The Ca^{2+} sensor SCaBP3/CBL7 modulates plasma membrane H^+-ATPase activity and promotes alkali tolerance in Arabidopsis. *Plant Cell* **2019**, *31*, 1367–1384. [CrossRef] [PubMed]
22. Wang, N.Q.; Kong, C.H.; Wang, P.; Meiners, S.J. Root exudate signals in plant–plant interactions. *Plant Cell Environ.* **2021**, *44*, 1044–1058. [CrossRef] [PubMed]
23. Mei, S.; Zhang, G.; Jiang, J.; Lu, J.; Zhang, F. Combining genome-wide association study and gene-based haplotype analysis to identify candidate genes for alkali tolerance at the germination stage in rice. *Front. Plant Sci.* **2022**, *13*, 887239. [CrossRef]
24. Que, T.; Wang, H.; Yang, W.; Wu, J.; Hou, C.; Pei, S.; Wu, Q.; Li, L.M.; Wei, S.; Xie, X. The reference genome and transcriptome of the limestone langur, *Trachypithecus leucocephalus*, reveal expansion of genes related to alkali tolerance. *BMC Biol.* **2021**, *19*, 67. [CrossRef] [PubMed]
25. Cao, Y.; Zhang, M.; Liang, X.; Li, F.; Shi, Y.; Yang, X.; Jiang, C. Natural variation of an EF-hand Ca^{2+}-binding-protein coding gene confers saline-alkaline tolerance in maize. *Nat. Commun.* **2020**, *11*, 186. [CrossRef] [PubMed]
26. Guo, R.; Yang, Z.; Li, F.; Yan, C.; Zhong, X.; Liu, Q.; Xia, X.; Li, H.; Zhao, L. Comparative metabolic responses and adaptive strategies of wheat (*Triticum aestivum*) to salt and alkali stress. *BMC Plant Biol.* **2015**, *15*, 170. [CrossRef] [PubMed]
27. Cui, M.; Li, Y.; Li, J.; Yin, F.; Chen, X.; Qin, L.; Wei, L.; Xia, G.; Liu, S. Ca^{2+}-dependent TaCCD1 cooperates with TaSAUR215 to enhance plasma membrane H^+-ATPase activity and alkali stress tolerance by inhibiting PP2C-mediated dephosphorylation of TaHA2 in wheat. *Mol. Plant* **2023**, *16*, 571–587. [CrossRef] [PubMed]
28. Wang, H.; Ahan, J.; Wu, Z.; Shi, D.; Liu, B.; Yang, C. Alteration of nitrogen metabolism in rice variety 'Nipponbare' induced by alkali stress. *Plant Soil.* **2012**, *355*, 131–147. [CrossRef]
29. Yang, C.; Guo, W.; Shi, D. Physiological roles of organic acids in alkali-tolerance of the alkali-tolerant halophyte *Chloris virgata*. *Agron. J.* **2010**, *102*, 1081–1089. [CrossRef]
30. Guo, L.; Shi, D.; Wang, D. The key physiological response to alkali stress by the alkali-resistant halophyte *Puccinellia tenuiflora* is the accumulation of large quantities of organic acids and into the rhyzosphere. *J. Agron. Crop Sci.* **2010**, *196*, 123–135. [CrossRef]

31. Guo, S.-H.; Niu, Y.-J.; Zhai, H.; Han, N.; Du, Y.-P. Effects of alkaline stress on organic acid metabolism in roots of grape hybrid rootstocks. *Sci. Hortic.-Amst.* **2018**, *227*, 255–260. [CrossRef]
32. Chen, Y.-T.; Wang, Y.; Yeh, K.-C. Role of root exudates in metal acquisition and tolerance. *Curr. Opin. Plant Biol.* **2017**, *39*, 66–72. [CrossRef] [PubMed]
33. Li, H.; Xu, C.; Han, L.; Li, C.; Xiao, B.; Wang, H.; Yang, C. Extensive secretion of phenolic acids and fatty acids facilitates rhizosphere pH regulation in halophyte *Puccinellia tenuiflora* under alkali stress. *Physiol. Plant* **2022**, *174*, e13678. [CrossRef] [PubMed]
34. Dubcovsky, J.; Dvorak, J. Genome plasticity a key factor in the success of polyploid wheat under domestication. *Science* **2007**, *316*, 1862–1866. [CrossRef] [PubMed]
35. Xiang, G.; Ma, W.; Gao, S.; Jin, Z.; Yue, Q.; Yao, Y. Transcriptomic and phosphoproteomic profiling and metabolite analyses reveal the mechanism of $NaHCO_3$-induced organic acid secretion in grapevine roots. *BMC Plant Biol.* **2019**, *19*, 383. [CrossRef] [PubMed]
36. Wang, H.; Zhao, S.; Sun, B.; Osman, F.M.; Qi, Z.; Ding, D.; Liu, X.; Ding, J.; Zhang, Z. Carboxylic acid accumulation and secretion contribute to the alkali-stress tolerance of halophyte *Leymus chinensis*. *Front. Plant Sci.* **2024**, *15*, 1366108. [CrossRef] [PubMed]
37. Lu, H.; Wang, Z.; Xu, C.; Li, L.; Yang, C. Multiomics analysis provides insights into alkali stress tolerance of sunflower (*Helianthus annuus* L.). *Plant Physiol. Biochem.* **2021**, *166*, 66–77. [CrossRef] [PubMed]
38. Kanstrup, C.; Nour-Eldin, H.H. The emerging role of the nitrate and peptide transporter family: NPF in plant specialized metabolism. *Curr. Opin. Plant Biol.* **2022**, *68*, 102243. [CrossRef] [PubMed]
39. Lin, Y.; Yang, L.; Zhao, X.; Tang, Z. Effects of increased endogenous ethylene on plant salt tolerance in Arabidopsis seedlings under saline condition. *Bull. Bot. Res.* **2010**, *30*, 703–707.
40. Chen, W.; Gong, L.; Guo, Z.; Wang, W.; Zhang, H.; Liu, X.; Yu, S.; Xiong, L.; Luo, J. A novel integrated method for large-scale detection, identification, and quantification of widely targeted metabolites: Application in the study of rice metabolomics. *Mol. Plant* **2013**, *6*, 1769–1780. [CrossRef] [PubMed]
41. Love, M.I.; Huber, W.; Anders, S. Moderated estimation of fold change and dispersion for RNA-seq data with DESeq2. *Genome Biol.* **2014**, *15*, 1–21. [CrossRef]
42. Chen, C.; Chen, H.; Zhang, Y.; Thomas, H.R.; Frank, M.H.; He, Y.; Xia, R. TBtools: An integrative toolkit developed for interactive analyses of big biological data. *Mol. Plant* **2020**, *13*, 1194–1202. [CrossRef] [PubMed]
43. Livak, K.J.; Schmittgen, T.D. Analysis of relative gene expression data using real-time quantitative PCR and the $2^{-\Delta\Delta CT}$ method. *Methods* **2001**, *25*, 402–408. [CrossRef] [PubMed]

plants

MDPI

Article

A Regulatory Mechanism on Pathways: Modulating Roles of MYC2 and BBX21 in the Flavonoid Network

Nan Li [1,2], Yunzhang Xu [1,2,3] and Yingqing Lu [1,2,*]

[1] State Key Laboratory of Systematic and Evolutionary Botany, Institute of Botany, Chinese Academy of Sciences, Beijing 100093, China; linan90633@163.com (N.L.); yunzhangxu@qhu.edu.cn (Y.X.)
[2] University of Chinese Academy of Sciences, Beijing 100049, China
[3] State Key Laboratory of Plateau Ecology and Agriculture, Qinghai University, Xining 810016, China
* Correspondence: yqlu@ibcas.ac.cn

Abstract: Genes of metabolic pathways are individually or collectively regulated, often via unclear mechanisms. The anthocyanin pathway, well known for its regulation by the MYB/bHLH/WDR (MBW) complex but less well understood in its connections to MYC2, BBX21, SPL9, PIF3, and HY5, is investigated here for its direct links to the regulators. We show that MYC2 can activate the structural genes of the anthocyanin pathway but also suppress them (except *F3′H*) in both *Arabidopsis* and *Oryza* when a local MBW complex is present. BBX21 or SPL9 can activate all or part of the structural genes, respectively, but the effects can be largely overwritten by the local MBW complex. HY5 primarily influences expressions of the early genes (*CHS*, *CHI*, and *F3H*). TF-TF relationships can be complex here: PIF3, BBX21, or SPL9 can mildly activate *MYC2*; MYC2 physically interacts with the bHLH (GL3) of the MBW complex and/or competes with strong actions of BBX21 to lessen a stimulus to the anthocyanin pathway. The dual role of MYC2 in regulating the anthocyanin pathway and a similar role of BBX21 in regulating *BAN* reveal a network-level mechanism, in which pathways are modulated locally and competing interactions between modulators may tone down strong environmental signals before they reach the network.

Keywords: pathway regulation; light signaling; molecular competition; BBX21; *F3′H* activation

1. Introduction

Metabolic pathways are major machineries governed by the genomes to coordinate cellular activities under various internal and external environments. They also bridge genomes and phenotypes of individuals, providing a biochemical basis for phenotypic plasticity. A major gap in understanding pathway regulation is the frequent lack of knowledge of the methods of perception of environmental signals by individual pathways. An example in plants is the relatively well-studied anthocyanin pathway. Anthocyanins generated from the pathway are part of flavonoids synthesized in plants, which include also proanthocyanidins, flavonols, flavones, aurones, and others from different branches of the flavonoid network. In *Arabidopsis thaliana* [1], transiently enhanced accumulation of the anthocyanin pigments is regularly seen in seedlings between day three and day six after seed germination under normal physiological conditions, and the phenotype can also be induced under adverse conditions [2]. The transient pigmentation of leaf and stem, commonly observed in other species [3–5] as well, is considered beneficial to plants for protection against stressful environments [6,7]. The molecular mechanism behind the phenotype, however, remains ambiguous. The clearly reversible phenotypes (i.e., pigmented and non-pigmented) imply an involvement of on-and-off signals in plant cells. At least three types of cellular signals have been implicated so far—light signaling [8,9], hormones such as jasmonate [10,11], gibberellin [10,12], brassinoids [13], or abscisic acid [10], and organ development [14,15]. It is puzzling how the anthocyanin pathway responds to the

myriad of signals. To search for mechanical details of the response, we interrogated several transcription factors (TFs) previously studied or implicated in *A. thaliana*.

The primary regulators documented for the anthocyanin pathway include PAP1, GL3 (or EGL3), and TTG1, which can form a protein complex to strongly activate structural genes of the anthocyanin pathway in shoots of *A. thaliana* [9,16,17], while another complex of similar components, formed by TT2, TT8, and TTG1, regulates synthesis of proanthocyanidins in the seed coat [18,19]. These complexes can regulate, in varied efficiencies, structural genes including *CHS*, *CHI*, *F3H*, *DFR*, and *ANS* that encode enzymes commonly used by the anthocyanin and proanthocyanidin pathways [20]. For simplicity, the regulatory assembly that involves members of three gene families—*MYB* (PAP1 or TT2), *bHLH* (GL3, EGL3, or TT8), and *WDR* (TTG1)—for the pathways have been dubbed MBW complexes [21]. Except in a few cases shown below, not much has been reported on relationships of an MBW complex with other TFs. Even less is known about how the complex is connected to various sources of signaling in cells. In general, signals may each take either a specific course to reach a pathway or converge with one another at certain points to rely on common modulator(s) to relay the signals to a pathway. For the anthocyanin pathway, it is unclear how multiple signals are interpreted with or without the MBW complex. A major goal here is to evaluate which of the scenarios above is closer to the in vivo process of pathway regulation.

Several classes of TFs have been studied or implicated in anthocyanin production. One is the light-responsive gene family BBX (B-box proteins) genes. BBX21 (or STH2) can activate *CHI* [22] and respond to red/far red and blue light (reviewed by [23]), and over-expression of *BBX21* causes high accumulation of anthocyanins in *Arabidopsis* [24]. Its homolog (PpBBX18) in the pear (*Pyrus pyrifolia*) can activate *PpMYB10*, an MYB component of the pear's MBW complex [25]. In the apple (*Malus x domestica*), a homolog of *Arabidopsis* BBX22 (MdCOL11) can activate *MdMYBA* [26]. When introduced into the potato, *Arabidopsis* BBX21 can elevate photosynthetic rate to show enhanced anthocyanin accumulation and tuber growth [24]. Other regulators in light-signaling pathways, such as HY5 [27] and PIF3 [28], were also implicated [29]. HY5, in particular, can suppress expression of *MYBL2* [30], which encodes a repressor of the anthocyanin pathway [31]. PIF3 is sensitive to the environment through mutually destructive interactions with phytochrome B [32–34] and A [28], whereas *HY5* can be activated by UV-B light [35] and BBX21 [36]. Besides being sensitive to red and blue light, BBX21 can also be stabilized by UV-B exposure [37], functioning as a light detector of the outer environment.

Besides light, anthocyanin accumulation can also be influenced by internal hormones such as jasmonate [38,39], abscisic acid [40–42], and gibberellin [43], or indirectly by ethylene [44] through sugar metabolism [10] or by brassinosteroids via crosstalk interactions [13]. Here, *MYC2* (initially known as JASMONATE-INSENSITIVE1 [45], or rd22BP1 [46]) plays a central role. MYC2 not only positively regulates signaling of abscisic acid [46] and sesquiterpene-synthase genes of gibberellin signaling [47], but also activates synthesis of jasmonate ZIM-domain proteins (JAZs) and other regulators in jasmonate signaling [48–51]. It can serve as a negative regulator for JA-responsive genes in pathogen defense (reviewed in [52]). JAZs can interact with GL3/EGL3 and PAP1, causing reduced output of the pathway [39]. Without MYC2, *myc2* shows enhanced pigmentation under blue or far-red light [53] but reduced expressions of *PAP1* and *EGL3* when jasmonate was externally supplied [54]. Nevertheless, whether or not MYC2 directly interacts with the anthocyanin pathway has not been shown.

Another class of implicated regulators is development-stage associated SPLs (SQUAMOSA PROMOTER BINDING PROTEIN-LIKE). For SPL9 [55–57] and its regulator *mir156*, over-expressing *mir156* presumably reduced SPL9, reportedly causing enhanced accumulation of anthocyanins and high expression of *DFR*, a gene encoding the dihydroflavonol reductase of the anthocyanin pathway [14]. Since mir156 can also target *mir172* [56] and multiple *SPL*s [58,59], it is uncertain how much of the enhanced pigmentation in over-expression lines of *mir156* is due to reduced SPL9 alone. More importantly, since the anthocyanin

pathway is primarily under the activation of an MBW complex for an enhanced output, how the other regulators act in concert with MBW during plant development and/or stimuli needs to be articulated.

Through gathering genetic and molecular data, which target some of the missing aspects of the regulators above, we show previously undiscovered interactions between BBX21 and MYC2 and their methods of influencing genes of the flavonoid network. For MYC2 in particular, MYC2 of *Arabidopsis* modulates the local anthocyanin pathway much as its ortholog (Os10g42430), *OsMYC2* [60], does in *Oryza sativa*. A high-level molecular mechanism is revealed here (at least in part), which connects multiple signals to flavonoid pathways, emerging as a likely molecular basis for dynamic accumulation of anthocyanins in plants.

2. Results

2.1. MYC2 Plays a Dual Role in Regulation of the Anthocyanin Pathway

Transient pigmentation of *A. thaliana* was compared between *myc2*, its complementary lines (35S::*MYC2*-1 & 35S::*MYC2*-2) of *MYC2* (Figure S1), and Col in 3-d old seedlings. A darker coloration was shown in the mutant and complementary lines than in the wild-type (Figures 1A and S2A,B). Dynamic accumulation of anthocyanins in the seedlings was explored in two sets of whole-plant samples, which were collected under the same growth conditions at 4 pm after the seeds had imbibed water for 48 and 72 h, respectively. The 48-h set was sampled at a 4-h interval over the next 24-h period for profiling pigmentation process. The 72-h set was sampled once for analysis of gene expression. Data of the 48-h set indicate an earlier accumulation of anthocyanins in *myc2* and its complementary lines than that in Col (Figure 1B), which is consistent with the phenotypes observed in Figure 1A. For the 72-h sample set, quantifications of transcripts show significantly more *MYC2* copies in 35S::*MYC2*-1 than in 35S::*MYC2*-2 (one tailed *t*-test, $p = 0.01$) and both lines expressed more copies of *MYC2* than *myc2*; but the transcript levels in the complementary lines were lower than that of Col (Figure 1C). Since *MYC2* is rhythmically expressed and peaks before dusk in Col [61], whereas the 35S-driven promoter leads to presumably constant transcription of *MYC2* in the complementary lines, the comparisons above reflect mostly point differences between the peak-level transcription of *MYC2* in Col and the average *MYC2* expression in the complementary line instead of the total difference over a periodic cycle between the lines. The latter is more relevant to protein levels of MYC2. This assessment was supported by estimation of transcript levels of *JAZ1*, a known target of MYC2, across lines. The complementary lines had more *JAZ1* transcripts than *myc2*, as expected; and the level in 35S::*MYC2*-1 surpassed that of Col (Figure 1C), which indicates that the in vivo expression of *MYC2* is likely higher in 35S::*MYC2*-1 than in Col (also see Figure S2C). Nonetheless, neither expression of *JAZ1* nor that of *MYC2* alone can account for the variation of transient pigmentation across lines (Figure 1B). It appears that over-expression of MYC2 or deficient transcripts of MYC2 can both lead to enhanced pigmentation in seedlings (Figures 1B and S2).

To probe the molecular basis of the transient pigmentation shown above, the impact of MYC2 was examined directly on a promoter region of the anthocyanin pathway gene via transient dual LUC assays using leaf protoplasts of Col. Reporters, each carrying the 5′ region (~1 kb) of a specific gene (Figure S3), were tested by MYC2-containg effectors under the same experimental conditions. The 5′ regions of *CHS*, *CHI*, *F3H*, *F3′H*, *DFR*, and *3GT* (except *ANS*) react positively to addition of MYC2 to cells (Figure 1D). The positive activation of *F3′H* came as a surprise, as the same promoter did not respond to the PAP1/GL3 (EGL3)/TTG1 complex [20]. Additional tests were pursued on 5′ region of *PAP1*, *GL3*, or *TTG1* (Figure S4). Little response of *GL3* or *TTG1* to MYC2 can be seen but a moderate yet significant activation of *PAP1* is evident (Figure 1E). Consistently, the in vivo transcript levels of *PAP1* in the complementary lines (35S::*MYC2*-1 and 35S::*MYC2*-2) are also higher than the mutant (Figure 1F) and in accordance with the elevated *MYC2* transcripts (Figure 1C).

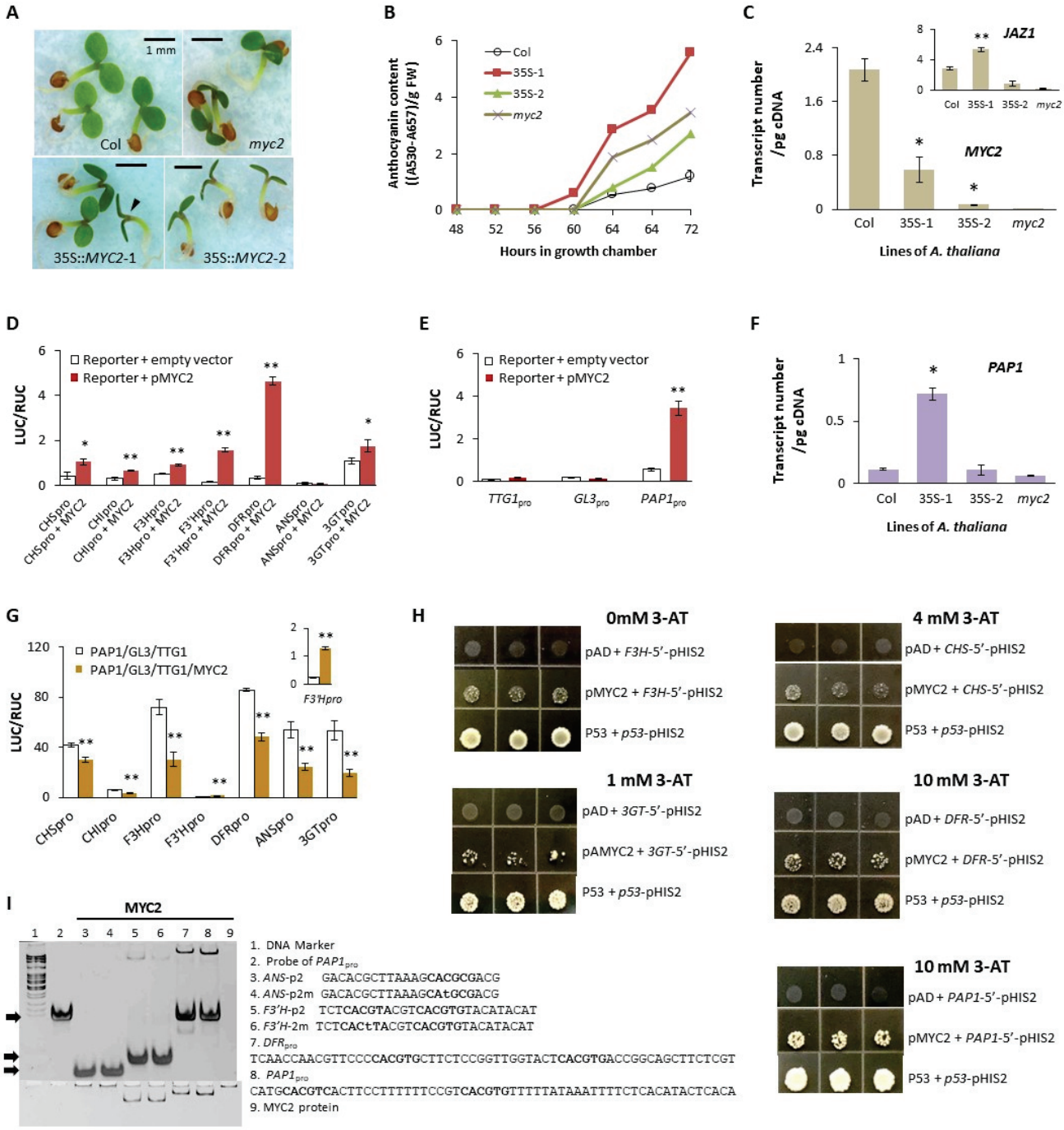

Figure 1. Effects of MYC2 on the anthocyanin pathway of *A. thaliana*. (**A**) Phenotypes of mutant *myc2* and its complementary lines at day 3. The control line is Columbia (Col). The bar is 1 mm. (**B**) Accumulation of anthocyanins in seedlings. The lines in (**A**) were quantified for anthocyanin content during 48–72 h of growth. The unit is arbitrary and weighted by the fresh weight (FW) of seedlings. Each data point has two replicates, with each replicate containing 20–30 plants. 35S-1 is for 35S::MYC2-1, and 35S-2 for 35S::MYC2-2. The difference between 35S-1 and Col at 72 h is highly significant (*t*-test, one-tailed, $p = 0.002$), and that between 35S-2 and *myc2* is also significant (*t*-test, one-tailed, $p = 0.03$). (**C**) Real-time expressions of *MYC2* and *JAZ1* across the lines at day 3. Data are shown as mean ± standard error. Each mean is based on three biological replicates ($n = 3$) at the same sampling time, and each replicate was measured at least twice. The transcript levels of two complementary lines are significantly higher than that of *myc2* (one-tailed *t*-tests; *, $p < 0.02$; **, $p < 0.01$). (**D**) Activations of genes by MYC2 in dual LUC assays. Reporter is indicated by the *x*-axis,

containing 5′ region of the target gene and designated by CHSpro for CHS_{pro}, etc., introduced along with pMYC2 (4 μg each). The promoter activity was measured by LUC/RUC. The background activity (blank) of each gene was shown by the treatment of reporters and empty effectors (4 μg each). The standard error bars include three to five biological replicates. Data were normalized. Compared to the reporter's background level, the treatment of pMYC2 was significant for all reporters (one-tailed *t*-tests; *, $p < 0.05$; **, $p < 0.01$) except that of ANS ($p = 0.40$). (**E**) Effect of MYC2 on transcriptions of the MBW genes. Effectors and reporters (1:1) were mixed in 4 μg each for $PAP1_{pro}$ and 5–10 μg each for $GL3_{pro}$ or $TTG1_{pro}$. Each test had at least two biological replicates. Activation of $PAP1_{pro}$ is highly significant per the *t*-test (one-tailed, **, $p < 0.001$, $n = 28$). (**F**) Transcript numbers of *PAP1* in the lines of (**A**) at day 3. Three biological replicates were taken. Format follows (**C**). (**G**) Combined effect of MYC2 and MBW on structural genes in dual LUC assays. Adding MYC2 caused significantly altered activity for all reporters (two-tailed *t*-tests; **, $p < 0.002$ in all cases). Data were normalized across tests ($n \geq 3$). (**H**) Interactions of MYC2 with promoters of anthocyanin genes in Y1H. Each test had at least three biological replicates, with the interaction between P53 and the original pHIS2 as the positive control and the combination of empty pAD and a reporter vector as the negative one. (**I**) Interactions of MYC2 with probes based on 5′ regions of anthocyanin genes in EMSAs. Each of the probes with the sequences (5′ → 3′) listed by the numbers to the right was mixed with MYC2 (~10 μg) to test its binding capacity. The upper panel shows the DNA binding and the lower one the protein binding of the same gel (non-denaturing 8% polyacrylamide). The free probes are indicated by the black arrows. The expected *cis* elements are in bold and mutated ones in lower case.

Since the anthocyanin pathway is activated strongly by an MBW complex, we re-examined the role of MYC2 in the presence of PAP1, GL3, and TTG1 (Figure S1). In dual luciferase assays as above, we measured the activity of a reporter (2 μg) driven by the MBW complex (pPAP1, pGL3, and pTTG1 in 2 μg each) as a base line and compared it to that of the same reporter and complex but with pMYC2 (2 μg) added. With the exception of *F3′H*, all enzyme genes, including *3GT* (AT5G17050), responded positively to the MBW complex but decreased their transcription levels significantly when pMYC2 was added (Figure 1G). The negative impact of MYC2 largely holds true when GL3 is replaced by EGL3 (Figure S5). These results suggest that MYC2 turns suppressive in the presence of an anthocyanin-related MBW complex, and the largest reduction of transcription varied from 64% in *3GT* for PAP1/GL3/TTG1 to 58% in *F3H* for PAP1/EGL3/TTG1. Here *3GT*, which differs from one (AT5G54060) tested before [20], can be regulated similarly as other genes of the pathway. The function of 3GT has been tested in prokaryotic cells [62]. These complementary results confirm its membership in the anthocyanin pathway of *A. thaliana*.

To make sure that in vivo activations by MYC2 above indeed operate at promoters of anthocyanin genes, we examined bindings of MYC2 to the promoters with Y1H as well as EMSAs. In Y1H, when MYC2 is the only effector, the histidine-based reporter (pHIS2), which takes the 5′ region of *CHS*, *F3H*, *ADFR*, *3GT*, or *PAP1* (Figure S3) as its own 5′ region, can be activated (Figure 1H) under the appropriate concentration of 3-amino-1,2,4-triazole (3-AT); a high auto-activation associated with the reporter of *F3′H* or *ANS*, however, obscured the signal of their possible interactions with MYC2. In EMSAs, MYC2 can directly bind to probes based on the proximal 5′ sequences of *F3′H*, *DFR*, and *PAP1*, respectively; binding to a probe based on *F3′H* with modified site of the suspected *cis* element (CACGTA → CACTTA) causes little change in the presence of CACGTG, which suggests no or little affinity of MYC2 to CACGTA. Probes with a G-box variant based on *ANS* or a mutated version of the variant also failed to interact with MYC2 under the same condition (Figure 1I). Taken together, MYC2 can physically interact with promoters of targeted genes (barring *ANS* here) to influence their transcriptions in *Arabidopsis*.

2.2. The Dual Role of MYC2 in Oryza Sativa

The dual role of MYC2 in regulating the anthocyanin pathway was previously unknown, thus its specificity needs to be evaluated in a different species. In rice (*Oryza sativa* L.), we cloned a homolog of *MYC2*, *OsMYC2*, from the leaf cDNAs of cultivar Heidao.

The sequence is identical to that of Nipponbare (Os10g42430.1). Since microarray data have been reported for Nipponbare [63], we examined the leaf expression of *OsMYC2* and observed a rhythmic pattern of gene expression (Figure S6). Two effects of OsMYC2 were subsequently tested in leaf protoplasts of rice. One is its single activations of *PAP1* ortholog and structural genes (particularly *OsF3′H* and *OsDFR*), and the other is its negative impact on the structural genes when acting along with a local MBW complex. Since a known MBW complex is OsC1/OsB2/OsTTG1 in rice leaves [64], we built effectors pOsC1, pOsB2, and pOsTTG1 using appropriate primers (Table S2). The reporters included $pOsC1_{pro}$, $pOsCHS_{pro}$, $pOsCHI_{pro}$, $pOsF3H_{pro}$, $pOsF3'H_{pro}$, $pOsDFR_{pro}$, and $pOsANS_{pro}$, with primers (Table S2) targeting the 5′ regions of *OsC1*, *OsCHS*, *OsCHI*, *OsF3H*, *OsF3′H*, *OsDFR*, or *OsANS1* (Figure S7), respectively. Here, *OsC1* is a homolog of *C1* in maize [64] and *PAP1* in *A. thaliana*. The tests were conducted in protoplasts of a white-rice material (which was known to have little native expression of *OsB2*). Significant activations by pOsMYC2 were seen for reporters carrying $OsC1_{pro}$, $OsCHS_{pro}$, $OsCHI_{pro}$, $OsF3'H_{pro}$, $OsDFR_{pro}$, or $OsANS1_{pro}$ but not $OsF3H_{pro}$ (Figure 2A). When OsMYC2 was introduced along with OsC1/OsB2/OsTTG1 as effectors, $OsCHS_{pro}$, $OsCHI_{pro}$, $OsF3H_{pro}$, and $OsANS_{pro}$ displayed significantly reduced transcriptions, and $OsF3'H_{pro}$ showed enhanced activation (Figure 2B), similarly to the responses of their counter-parts in *A. thaliana*.

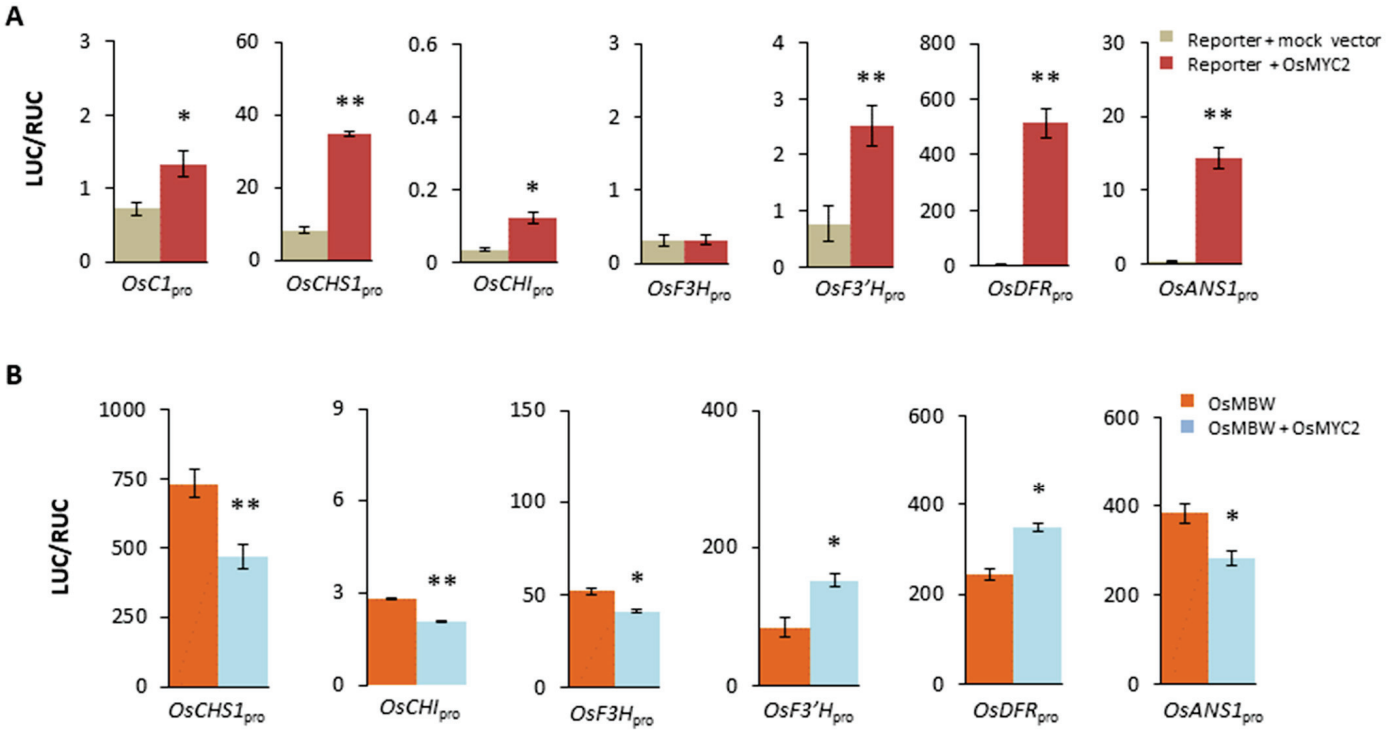

Figure 2. Dual roles of *OsMYC2* in regulation of the anthocyanin pathway of *Oryza sativa*. (**A**) Activations of the local anthocyanin genes by OsMYC2 in living protoplasts of rice. In each treatment, a reporter (pOsC1pro, pOsCHSpro, pOsCHIpro, pOsF3Hpro, pOsF3′Hpro, pOsDFRpro, or pOsANSpro, 4 μg/each) was introduced along with 4 μg mock vectors (empty effectors) or pOsMYC2 to test background activation of *LUC* (corrected by RUC as inner reference) or the effect of OsMYC2, respectively. One standard error bar includes two to seven biological replicates. Data were normalized. The significant differences between the reporter background and the OsMYC2 treatment are shown (one-tailed *t*-tests; *, $p < 0.05$; **, $p < 0.01$). (**B**) Effects of OsMYC2 on the anthocyanin genes in the presence of OsC1/OsB2/OsTTG1. For each test, 2 μg reporter was introduced along with the OsMBW (2 μg of each component) in two biological replicates or further with 2 μg pOsMYC2 in three biological replicates. The format follows (**A**).

Unlike MYC2 in *A. thaliana*, OsMYC2 alone can cause a significant expression of *OsANS1* (Figure 2A) and the impact turns negative when the MBW complex is present (Figure 2B), the latter part of which agrees with the response of *ANS* in *A. thaliana*. Meanwhile, OsMYC2 is such a strong activator of *OsDFR* (Figure 2A) that it outshines the effect of OsC1/OsB2/OsTTG1 (Figure 2B). Consequently, activation of OsDFR due to the combination of the local MBW complex and OsMYC2 is lower than that due to OsMYC2 alone, likely from the negative impact of OsMYC2 at the presence of the complex, but the activation level itself is still higher than that initiated by the complex alone (Figure 2B).

2.3. MYC2 Reduces Function of MBW Complex via Interactions with GL3

Since bHLH proteins can form a heterodimer with each other (e.g., [65]), we explored possible in vivo interaction between MYC2 and GL3 (Figure S1), both of which are bHLHs, to know whether MYC2 interacts with the MBW complex to exert its negative impact. In Y2H, we observed a dubious signal due to strong auto-activation of pBD-MYC2 or pBD-GL3 in yeast cells (Figure S8A). Meanwhile, no interaction was found between MYC2 and TTG1 when MYC2 was fused with pAD (Figure S8B). A probable MYC2-GL3 interaction was re-examined in co-IP, with MYC2 labeled by MYC-tag and GL3 by HA-tag. Following verifications of fused proteins expressed in leaf cells of *Nicotiana benthamiana*, a clear protein-protein interaction was detected in vivo between MYC2 and GL3 (Figure 3A). In the same experiment, no interaction was seen between MYC2 and PAP1, though expressions and function of the TFs were both confirmed (Figure 3A). Further in vivo interaction between MYC2 and GL3 was shown in BiFC, and the interaction signals focused primarily on the nucleus (Figure 3B). Collectively, the results here suggest that GL3 is the only MYC2-interacting factor in the complex of PAP1/GL3/TTG1.

Given the reported affinity of MYC2 or GL3 to G-box [54,66], probable competition between MYC2 and GL3 for the same *cis* element was suspected and subsequently tested at the 5′ region of *DFR* (Figure S3). The region has two G-boxes; one is farther away from the starting site of transcription and the other (#2) closer to it (Figure 3C). To seek evidence for DNA-recognition competition between MYC2 and GL3, we alternately mutated G-boxes to test a possible location effect of G-box on transcription of *DFR* in dual LUC assays. The results indicate that both TFs prefer the G-box located further away from the transcription starting site (Figure 3C), which leads to potential interference when MYC2 and GL3 accumulate simultaneously in cells. In EMSAs, we further compared associations of MYC2 and GL3 to variants of G-box, finding evidence for the binding of MYC2 to AACGTG and CTCGTG but not CAAGTG, and the weak binding of GL3 to AACGTG only but not CTCGTG and CAAGTG (Figure 3D). These results suggest that competitive binding between MYC2 and GL3 extends to variants of G-box (e.g., AACGTG). Since variants of G-boxes are frequently seen at promoters of anthocyanin genes (Figure S3), competitive binding between GL3 and MYC2 is expected to happen, causing degrees of in vivo interference at targeted promoters.

To visualize the competition between MYC2 and GL3, varied quantities of MYC2 (of its whole coding region) were supplied, along with the fixed quantity of GL3 (of its DNA-binding domain only), in EMSAs to show their interactions with the same quantity of probe of known *cis* elements (Figure 3D). The binding signals indicate that increasing the quantity of MYC2 weakens the binding capacity of GL3 (Figure 3E). Altogether, interaction and interference between MYC2 and GL3 reveals a mechanism by which MYC2 modulates in vivo transcriptions of the structural genes of the anthocyanin pathway.

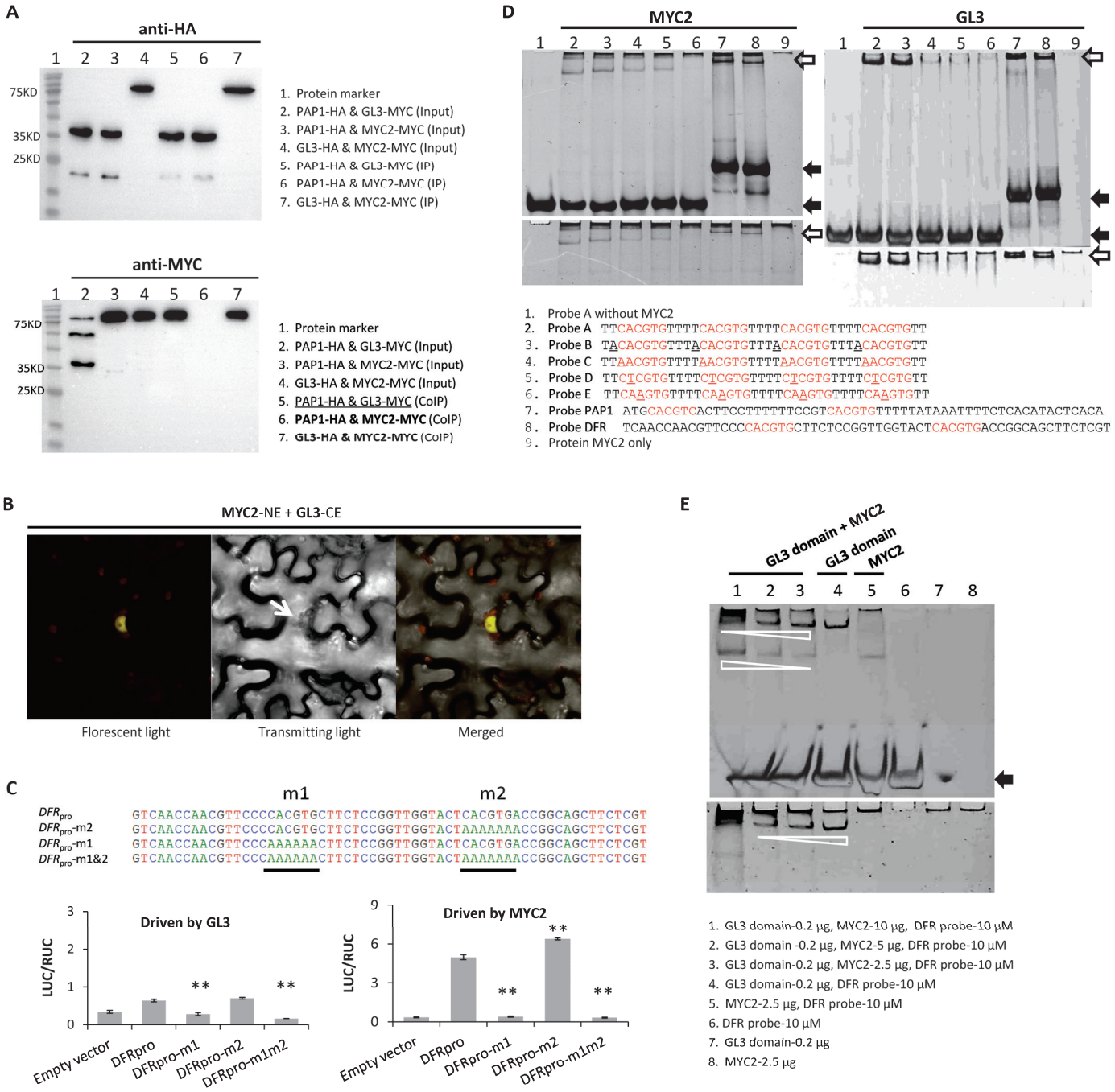

Figure 3. Interaction and competition between MYC2 and GL3. (**A**) Protein interaction between MYC2 and GL3 in co-IP. The upper panel shows expressed proteins (HA-labeled) detected by mouse antibodies (anti-HA) in input solution (Input) or from HA-agarose beads (IP). The lower panel shows the detections of MYC-label proteins in the same input (Input) and IP solutions (CoIP) by mouse anti-MYC. Only interacting proteins are present in CoIP. The known interaction (underlined) is shown as positive control and the targeted interaction in bold. The results had at least two biological duplicates ($n \geq 2$). (**B**) Interaction of MYC2 and GL3 in BiFC. The nucleus indicated by the arrow emits yellow fluorescence as a result of the physical interaction of NE-labeled MYC2 and CE-labeled GL3. Pictures were taken of the epidermis of *N. benthamiana* under visible or fluorescent lights. No signal was detected in co-transformations of pMYC2-NE and pUC-SPYCE (in place of pGL3-CE). (**C**) Responses of MYC2 and GL3 to mutated G-boxes in dual LUC assays. Four reporters hosting the promoter of *DFR* (DFR_{pro}) and its mutated versions (–m1, –m2, and –m1&2), as shown in partial sequences here

($5' \rightarrow 3'$), were driven by effectors pGL3 or pMYC2. Each treatment had three biological replicates, shown in the standard error bar. Significant changes in promoter activity are shown (two-tailed *t*-tests; **, $p < 0.01$). (**D**) Binding preferences between MYC2 and GL3 in EMSAs. Probes were labeled by numbers, with sequences shown ($5' \rightarrow 3'$). The known *cis* element is in red, and mutated sites are underlined. A non-denaturing polyacrylamide gel (10%) was used. The upper gel shows results of DNA-binding, while the lower one shows protein-binding. (**E**) Competition of MYC2 with GL3 in DNA binding in EMSAs. The probe is *DFR*-based. Different quantities of MYC2, shown by the lane numbers (1–3), were mixed with the same quantity (0.2 μg) of GL3 (bHLH domain) and exposed to the same quantity of probe. Controls are in lanes 5–8. A non-denaturing polyacrylamide (8%) gel was used. The black arrow indicates free probes. The white arrows indicate the strengths of binding under different quantities of MYC2. The binding tests were duplicated and results were the same.

2.4. MYC2 Can Work with BBX21 and SPL9 to Activate PAP1, TT2, MYBL2, and HY5

Since seedlings of *bbx21* accumulate a less quantity of anthocyanins [67], *BBX22* can promote anthocyanin-related MYB [26], and SPL9 was suspected to be a negative regulator of anthocyanin synthesis [14], we compared the impacts of BBX21, BBX22, and SPL9 as well as the previously mentioned PIF3 and HY5 on the promoter of *PAP1* ($PAP1_{pro}$) in dual LUC assays, relative to that of MYC2. Results show that $PAP1_{pro}$ can be activated by PIF3, SPL9, BBX21, and BBX22, but only negligibly by HY5 (Figure 4A). In comparison, PIF3 is a weaker activator of $PAP1_{pro}$ than BBX21, MYC2, and SPL9 (Figure 4A). Relative to BBX21, BBX22 is also a much weaker activator of $PAP1_{pro}$ (Figures 4A and S9), thus was omitted in the subsequent investigation.

The tests above were extended to *MYBL2* and *TT2* (Figure S10), showing activations of $MYBL2_{pro}$ (Figure 4B) and $TT2_{pro}$ (Figure 4C) by MYC2, BBX21, and SPL9 individually or collectively. Magnitudes of the activations, however, are much lower than those observed on $PAP1_{pro}$ under the same testing condition (*t*-tests, all $p < 0.001$). As BBX21 and MYC2 can activate *HY5* [68,69], we further assessed the influence of SPL9 on $HY5_{pro}$ (Figure S10) and observed its low but positive impact singly or with MYC2 (Figure 4D). Unlike $PAP1_{pro}$, the combined activation of $HY5_{pro}$ by BBX21 and SPL9 can be largely dampened by adding pHY5 (Figure 4D), which agrees with the negative feedback on *HY5* reported before [70,71]. The activating function of MYC2 on $HY5_{pro}$ also concurs with a lowered transcription of *HY5* in *myc2* (Figure 4E). The same activation patterns by MYC2, BBX21, and SPL9 on four genes above led us to inspect possible protein interactions among MYC2, BBX21, and SPL9 to interpret their regulation, as recruitment of partners to the promoters of regulated genes may occur if protein interaction exists between TFs.

Possible protein-protein interactions were examined in co-IP tests. After functional confirmations of tested proteins, no interactions could be detected between MYC2 and SPL9 (Figure 4F), between MYC2 and BBX21 (Figure 4G), or between SPL9 and BBX21 (Figure 4H). Thus, the regulation by MYC2, BBX21, or SPL9 is basically free-lanced at protein level, without recruitment mechanism. Consistently, unlike the synergistic activation by the MBW complex on the structural genes, regulation by MYC2, BBX21, and SPL9 has little synergy on their targets (Figure 4A–D). Since little expressions of $pGL3_{pro}$ and $pTTG1_{pro}$ can be initiated by effector pMYC2, pBBX21, pSPL9, pPIF3, or pHY5 in dual LUC assays, the MYB (encoded by *PAP1* or *TT2*) is the only component of an MBW complex influenced by MYC2, BBX21, and SPL9.

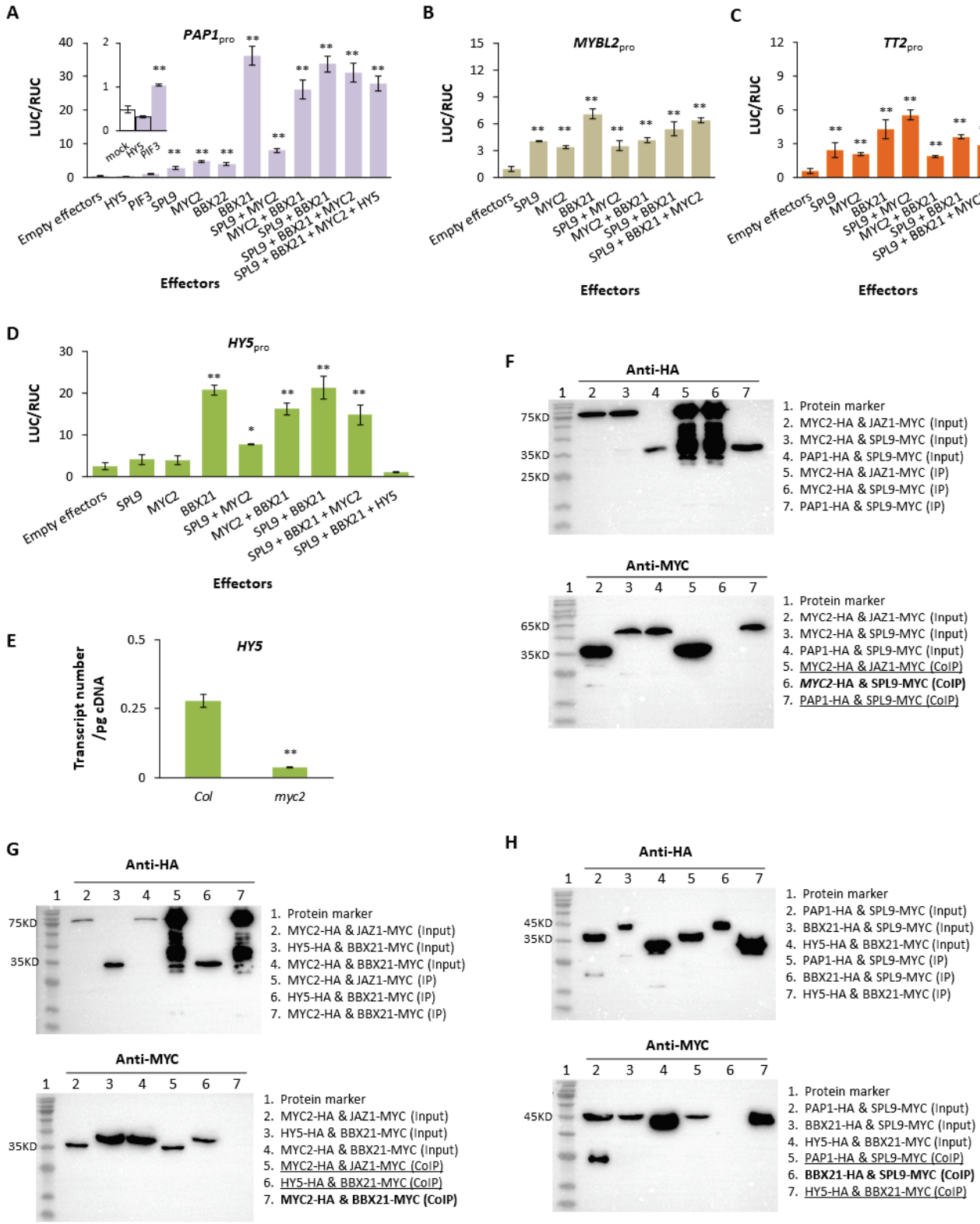

Figure 4. Features of regulations of *MYB*s and *HY5* by MYC2, BBX21, and SPL9. (**A**) Responses of the reporter (pPAP1$_{pro}$) to TF effectors in dual LUC assays. The *Y*-axis shows the background activity (PAP1$_{pro}$) of the reporter with empty effectors (4 µg, as mock) co-transformed (1:1) and activities of the same reporter co-transformed with effectors (4 µg/each) as indicated. The standard error bars are based on biological replicates varying from 2 (PIF3 or HY5) to 27 (BBX21 + MYC2). Data were normalized. All effectors are significant (*t*-tests; **, $p < 0.005$), except HY5. (**B**) Activation of *MYBL2*

by MYC2, BBX21, and SPL9. The experimental conditions and data format followed (**A**) and the standard error bars represent at least three biological replicates per treatment. (**C**) Activation of *TT2* by MYC2, SPL9, and BBX21. The format follows (**B**) and the standard error bars contain at least two biological replicates per trial. (**D**) Activation of *HY5* by MYC2, SPL9, and BBX21. As in (**B**), the standard error bar contains at least three biological replicates (one-tailed *t*-tests; *, $p < 0.05$; **, $p < 0.01$). (**E**) Quantifications of *HY5* transcripts. Transcript copy number estimated for *myc2* is significantly smaller than that of Col for day-3 seedlings, with three biological replicates (one-tailed *t*-tests; **, $p = 0.004$). (**F**) Co-IP tests on possible protein interaction between SPL9 and MYC2. As in Figure 3A, confirmed protein functions are underlined and the interaction at focus is in bold. (**G**) Co-IP tests on possible interaction between BBX21 and MYC2. Proteins are labeled as in (**F**). (**H**) Co-IP tests on possible interaction between BBX21 and SPL9. Presentation follows (**F**).

2.5. Direct Impacts of BBX21 and SPL9 on the Pathways of the Flavonoid Network

Though BBX21 can significantly activate expressions of *PAP1* and *MYBL2*, its direct interaction with the structural genes (other than the previously reported *CHI*) of flavonoid pathways in the presence of an MBW complex has not been reported for *A. thaliana*. Our dual LUC assays indicate that BBX21 can single-handedly stimulate expressions of all structural genes of the anthocyanin pathway, with *CHS*, *F3H*, and *3GT* particularly responsive (Figure 5A). Unlike MYC2, however, the role of BBX21 becomes far less visible in the presence of PAP1/GL3/TTG1 (Figure 5B). BBX21 interacts with neither GL3, PAP1 (Figure S11A,B), nor TTG1 (Figure S11C). The lack of interaction between BBX21 and the MBW complex suggests an independent regulation of BBX21, and its impact can be overwritten by a stronger activation of PAP1/GL3/TTG1.

Under the same condition as above, SPL9 can mildly but significantly activate *F3H* and *3GT* when acting alone in dual LUC assays (Figure 5C). With the MBW complex, however, SPL9's effect is largely obscured and visible only at *F3H* (Figure 5D). SPL9 interacts with PAP1 [14] but not with GL3 in co-IP (Figure S12A) or with TTG1 in Y2H (Figure S12B). It shows a dosage effect on *PAP1's* transcription (Figure S12C). These patterns indicate a positive effect of SPL9 in terms of its direct action on the anthocyanin pathway; however, this effect can hardly explain the enhanced pigmentation of *spl9* relative to Col (Figure 5E), which reaches a level milder than that of *myc2* (Figure 5F).

Since the proanthocyanidin pathway is also under the regulation of an MBW complex (TT2/TT8/TTG1 [18]), we examined probable effects of MYC2, BBX21, and SPL9 on the 5′ region of *BAN* (*BANYULS* or *ANR*) gene of the pathway. In dual LUC assays using the same conditions as above, a significantly activating effect of BBX21, but not SPL9 or MYC2, was documented on BAN_{pro} (Figures 5G and S12D). In the presence TT2/TT8/TTG1, BBX21 shows a significantly repressive effect for the activation of *BAN* whereas SPL9 has no effect (Figure 5G) and MYC2 has a dubious effect (Figure S12D) that requires further verification.

2.6. Dynamic Relationships among MYC2, BBX21, and SPL9

More evidence emerged in this study, showing that regulatory relationships of MYC2, BBX21, and SPL9 with the anthocyanin pathway are dynamic within the cellular environment. Since the *cis* element (NNGTAC) recognized by SBP domain TFs [72], which include SPL9, differs from those (G-box and some of its variants) by MYC2 [54], SPL9 may regulate additively with MYC2 for their common targets. The supporting evidence was seen on $PAP1_{pro}$ when the effectors were present in the same (Figure 4A) or different quantities (Figure 6A). Because BBX21 also recognizes G-box-like elements [68], a possible competitive relationship between MYC2 and BBX21 was tested and confirmed at $PAP1_{pro}$ (Figure 6B). In dual LUC assays, when testing with multiple effectors in large quantities, vector overloading may bring in reduced activation of a promoter [73]. This artificial effect was indeed detected here when 8 μg empty vectors were introduced along with 8 μg reporter and effectors per transformation reaction; however, the reduced reporter activity caused by pMYC2 was significantly lower than the overloading effect (Figure 6B). The results therefore suggest competition between MYC2 and BBX21 at $PAP1_{pro}$.

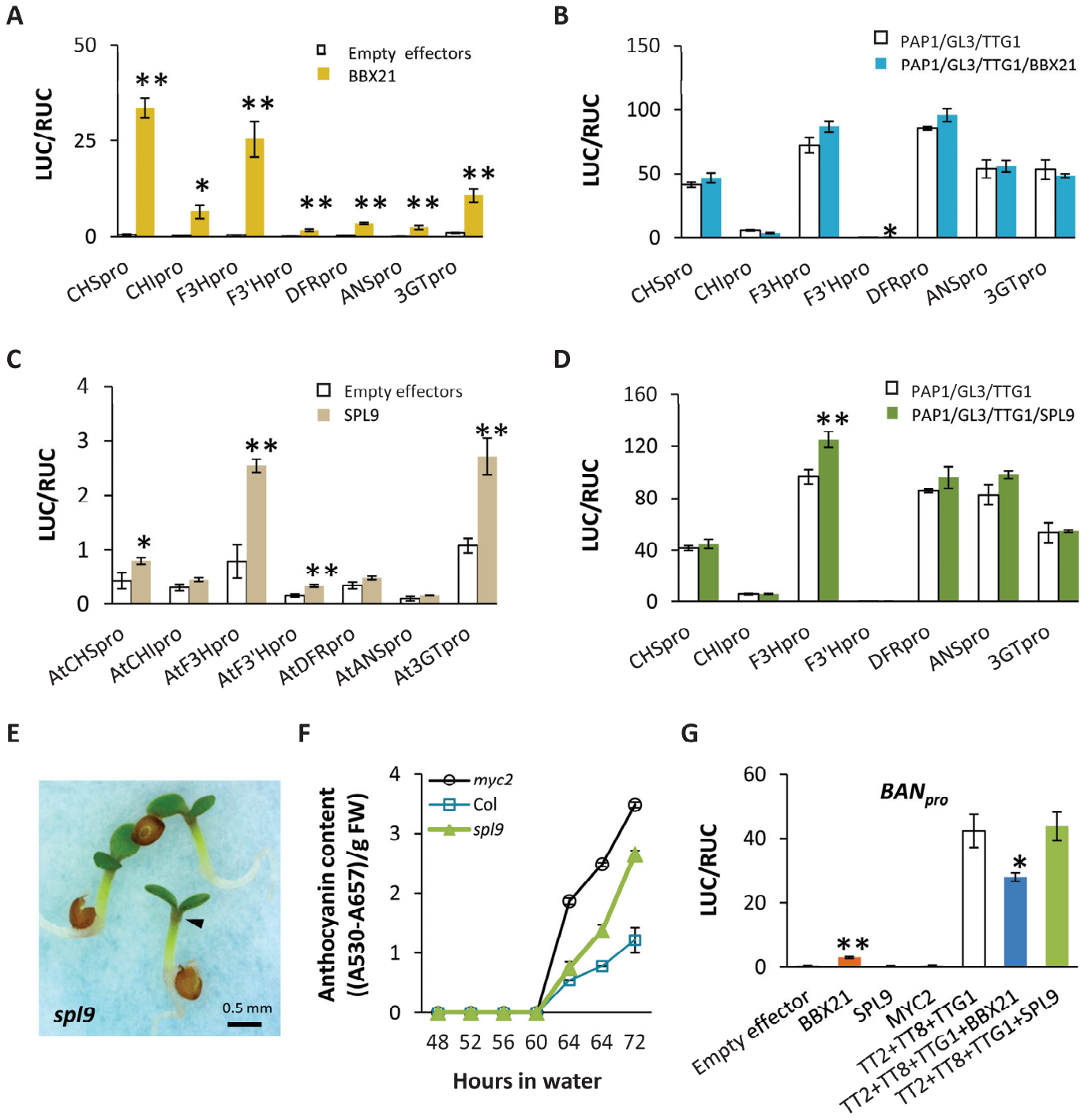

Figure 5. Regulations of BBX21 and SPL9 on structural genes of the flavonoid network with or without an MBW complex in *A. thaliana*. (**A**) Single effects of BBX21 in dual LUC assays. Each test (4 µg/each vector) was done with at least three biological replicates, shown by the standard error. Data were normalized. Significant activations (relative to empty effectors) are shown (one-tailed *t*-tests; *, $p < 0.05$; **, $p < 0.01$). (**B**) Combined regulation of BBX21 with the MBW complex. All vectors were introduced in 2 µg, with at least three biological replicates performed. Only reporter of *F3′H* shows a significantly lower activity for combined regulation than for BBX21 only (one-tailed *t*-test, *, $p = 0.007$). (**C**) Single effects of SPL9 in dual LUC assays. The format follows those in (**A**). (**D**) Regulation of SPL9 with the MBW complex. The tests follow those in (**B**), with *F3H* showing a higher activation by combined regulation than by SPL9 alone (one-tailed *t*-test, **, $p = 0.004$). (**E**) Phenotype of *spl9* at day 3. Pigmentation is indicated by the arrow. The control line is Columbia

(Col) shown in Figure 1A. (**F**) Anthocyanin content of seedlings from day 2 to day 3. The protocol follows Figure 1B. (**G**) Effects of BBX21, SPL9, and MYC2 on promoter of *BAN*. The activation by BBX21 is significant relative to the background (empty effectors) by one-tailed *t*-test (**, $p = 0.006$). The activation of TT2/TT8/TTG1 complex is significantly lower when BBX21 is present (one-tailed *t*-test, *, $p = 0.049$), following settings of (**A**,**B**) here. Sample sizes are at least two biological replicates per treatment.

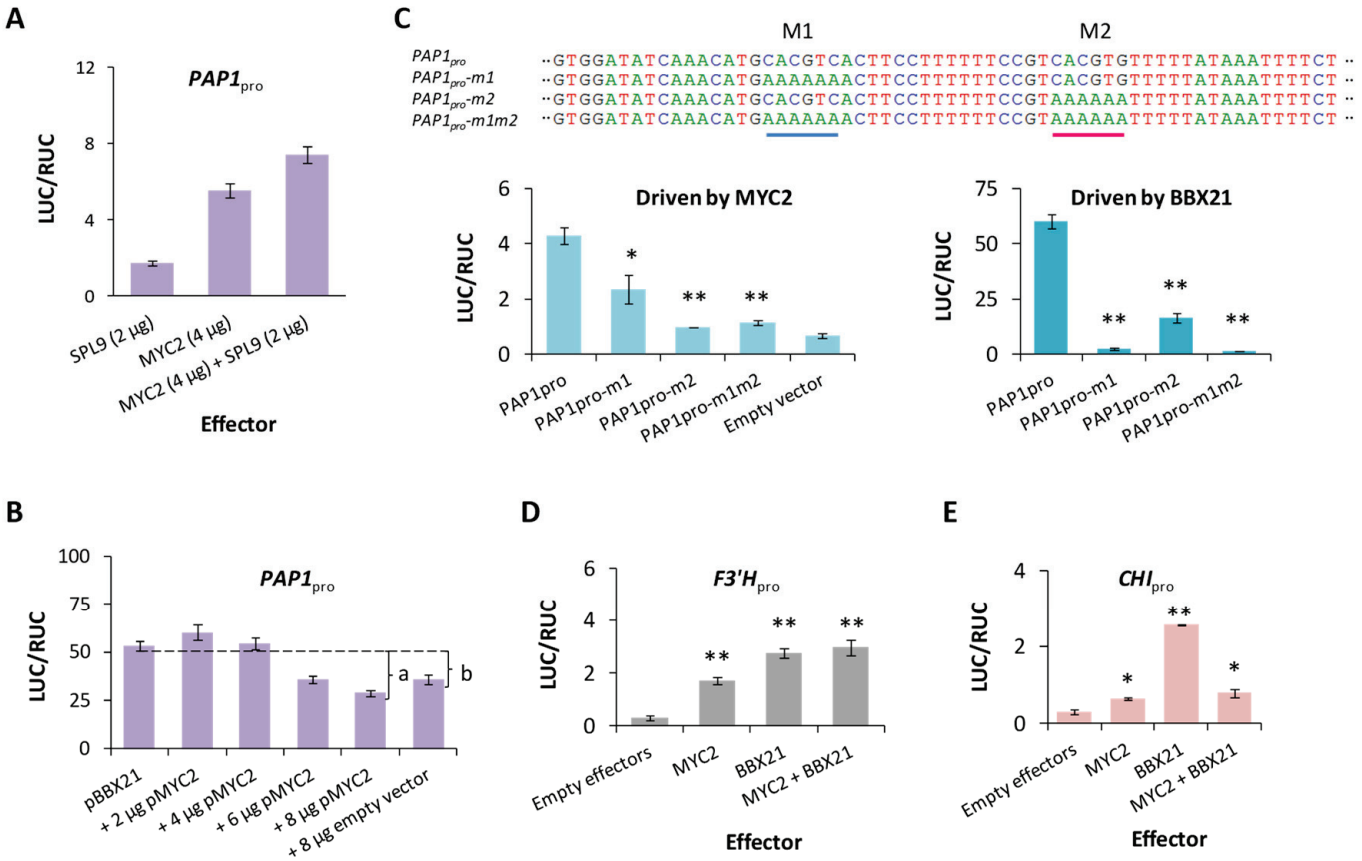

Figure 6. Interactive relationships of MYC2 with SPL9 and BBX21 in dual LUC assays in *A. thaliana* leaf cells. (**A**) Additive relationship between SPL9 and MYC2 in activation of *PAP1*. Results are shown as mean ± standard error, based on three biological replicates ($n = 3$). (**B**) Competition test between BBX21 and MYC2 at $PAP1_{pro}$. The effectors are indicated by the *x*-axis, with pBBX21 (4 µg) in every trial and varied amounts of pMYC2 shown after + sign across trials. The same reporter ($pPAP1_{pro}$) in 4 µg is provided across tests. The standard error bar includes at least three biological replicates. The comparison between treatments (a and b) is significant (one-tailed *t*-test, $p = 0.016$, $n = 12$). (**C**) Tests of effects of *cis* elements of $PAP1_{pro}$ on regulations of BBX21 and MYC2. Four reporters are shown in the upper panel with mutations (M1 & M2) indicated in the partial sequences. Their activations were examined under effector pMYC2 or pBBX21 (4 µg/each), with standard error bars shown ($n = 3$). Significant reductions in promoter activity are shown (one-tailed *t*-tests; *, $p < 0.05$; **, $p < 0.01$). (**D**) Competition between BBX21 and MYC2 at $F3'H_{pro}$. Effectors and reporters (4 µg each) were provided as 1:1 for each test ($n = 3$). Significant activations (relative to empty effectors) are shown (one-tailed *t*-tests; **, $p < 0.01$). (**E**) Competition between BBX21 and MYC2 at CHI_{pro}. Significant activations (relative to empty effectors) are shown (one-tailed *t*-tests; *, $p < 0.05$; **, $p < 0.01$). Data were normalized.

To seek further evidence for the inferred competition between MYC2 and BBX21 above, we analyzed two *cis* elements (CACGTC and CACGTG) of $PAP1_{pro}$ using site mutagenesis and dual LUC assays (Figure 6C). Responses of MYC2 and BBX21 to mutations at *cis* sites of the promoter differ from each other: MYC2 favors CACGTG over CACGTC, whereas

BBX21 does the opposite. Nonetheless, both TFs can recognize these *cis* elements and may simultaneously approach these sites, potentially causing interference. This may explain the decreased transcriptive capacity of BBX21 when MYC2 is more abundant in the cellular environment. The competition is not specific to $PAP1_{pro}$; it operates on $TT2_{pro}$, $MYBL2_{pro}$, and $HY5_{pro}$, as shown in Figure 4. It also acts on structural genes such as $F3'H_{pro}$ (Figure 6D) or CHI_{pro} (Figure 6E). These cases suggest that the competition is not dependent on other factors, thus broadly seen across genes.

2.7. Indirect Relationships of HY5 and PIF3 with the Anthocyanin Pathway

To discern the roles of HY5 and PIF3 in regulation of the anthocyanin pathway [29], we examined their direct impacts in dual LUC assays. HY5 generally imposes a small impact under daylight on the promoters of structural genes when acting alone (Figure S13A), and PIF3 alone shows similarly low impacts on the genes (Figure S13B). When the MBW complex is present, HY5 can significantly reduce its impact at *CHS*, *CHI*, and *F3H*, but not as much for the downstream genes (*DFR*, *ANS*, *3GT*) of the pathway (Figure 7A). Though over-expression of *HY5* can lead to pigmentation of seedlings [74], few anthocyanins are accumulated and detected in *hy5* (Figure 7B), as previously known [75]. To look for possible causes of this phenomenon, we first estimated the transcript level of *MYBL2* in *hy5* and expected its high expression, given negative action of HY5 on *MYBL2*'s expression [30]. Surprisingly, compared to Col, the increase of *MYBL2*'s transcription in *hy5* was barely significant (Figure 7C) at the point of estimation. The path, by which HY5 regulates the anthocyanin pathway via MYBL2, appears unlikely to be the major one due to lack of anthocyanins in *hy5*. When quantifications of structural gene expression were carried out for *hy5* and Col, *CHS* and *F3H* were much less expressed in *hy5* than in the wild type (Figure 7D), which forms the direct reason for low synthesis of anthocyanins in *hy5*. It is unclear, however, why the early steps of anthocyanin synthesis are strongly influenced by the absence of HY5. To seek more clues, we quantified other TF transcripts in *hy5* and witnessed significantly higher transcriptions of *MYC2*, *BBX21*, and *PAP1* than their counterparts in Col, along with a slight increase of *SPL9* and non-significant changes of *PIF3* (Figure 7E). The role of HY5 in expressions of *SPL9* and *BBX21* was subsequently evaluated in dual-LUC assays. HY5-carrying effectors can significantly suppress transcriptions of both *SPL9* (Figure 7F) and *BBX21* (Figure 7G) under daylight condition. These relationships can account for (at least in part) the higher transcript levels of *SPL9* and *BBX21* in *hy5* but not for reduced transcripts for the early enzymes. It remains to be understood how HY5 specifically influences *CHS*, *CHI*, and *F3H*.

Compared to HY5, PIF3 can repress $SPL9_{pro}$ (Figure 7F) without much affecting $BBX21_{pro}$ (Figure 7G). In contrast to *hy5*, *pif3* exhibits intense accumulation of anthocyanins at day 3 (Figure 7H). The phenotype is congruent with not only an earlier onset of anthocyanin accumulation during the plant development (Figure 7I), but also higher transcripts of *SPL9*, *BBX21*, *PAP1*, *GL3* (Figure 7J) and the structural genes (Figure 7K) than ones in the wild type. Though PIF3 can impose a small but positive effect on $PAP1_{pro}$ (Figure 4A), the action alone is inadequate to explain the high level of *PAP1* transcripts detected in *pif3*. By contrast, the high transcript levels of *BBX21* and *SPL9* are more compatible with *PAP1*'s transcripts in *pif3*. Given that expression of *PIF3* peaks at night in the wild type [76] and the anthocyanin pathway is active mainly during the day [9], the overall influence of *PIF3* on the anthocyanin pathway is expected to be indirect. Collectively, little evidence has been found for *PIF3* or *HY5* to serve as a significant modulator for the anthocyanin pathway.

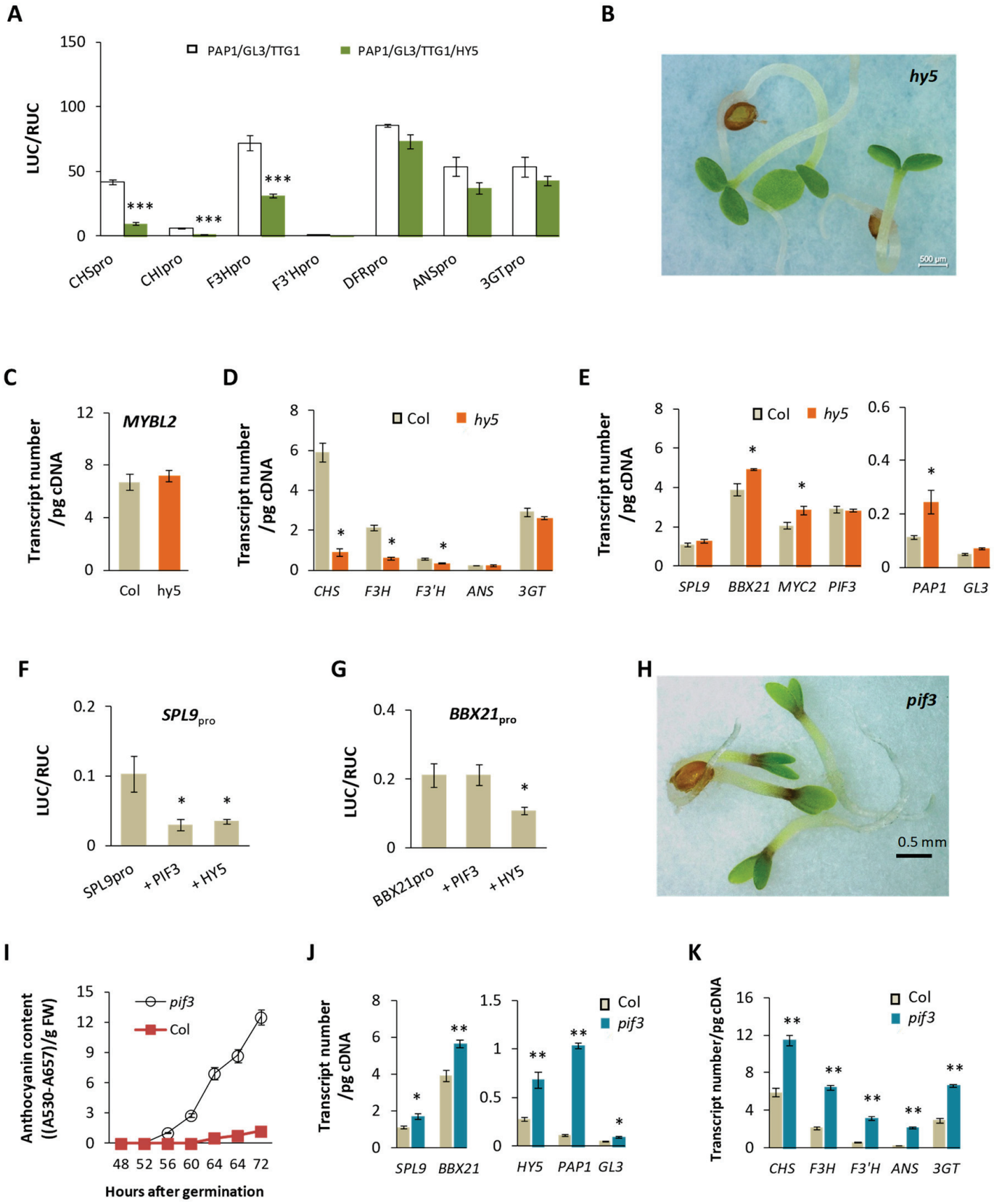

Figure 7. Effects of HY5 and PIF3 on the anthocyanin pathway and related genes. (**A**) Impact of HY5 on the anthocyanin genes with MBW. Dual LUC assays show the activations of the promoter regions when exposed to two sets of effectors in at least two biological replicates. Effector and reporter were provided in the same ratio (2 µg/each). Data were normalized. Significantly reduced activity was

shown for CHS_{pro}, CHI_{pro}, and $F3H_{pro}$ (one-tailed *t*-tests; ***, $p < 0.0001$ in all cases). (**B**) Phenotype of *hy5* at day 3 in water. The bar is for 0.5 mm. The control line is Columbia (Col) shown in Figure 1A. The anthocyanin content was undetectable using the same protocol as in Figure 1B. (**C**) Quantifications of transcript copy numbers of *MYBL2* between lines of day-3 seedlings. The difference is not significant between the wild type (Col) and *hy5* (two-tailed *t*-test, $p = 0.56$). (**D**) Transcript levels of structural genes between Col and *hy5*. Significant differences between lines are based on one-tailed *t*-tests after Bonferroni's correction for multiple comparisons (experimental error rate $\alpha = 0.05$, * $p < 0.05$). (**E**) Transcript levels of regulators between Col and *hy5*. Standard errors are based on three biological replicates ($n = 3$). Significant differences (*) are based on one-tailed *t*-tests ($p = 0.04$ for *BBX21* and $p = 0.03$ for *MYC2*). (**F**) Responses of $pSPL9_{pro}$ to pHY5 or pPIF3 in dual LUC assays. Results show activities of the reporter $pSPL9_{pro}$ with 4 μg empty TF-vector (SPL9pro, $n = 4$), 4 μg pPIF3 (+PIF3pro, $n = 6$), or 4 μg pHY5 (+HY5pro, $n = 6$). Significantly reduced responses (*) are shown (one-tailed *t*-tests; $p < 0.04$ for both TF effectors). (**G**) Response of $pBBX21_{pro}$ to pHY5 or pPIF3 in dual LUC assays. As in (**F**), results show the activity of reporter with empty effectors ($n = 3$), PIF3 (+PIF, $n = 6$), or HY5 (+HY5, $n = 6$). One-tailed *t*-test is significant for HY5 only ($p = 0.04$). (**H**) Phenotype of *pif3* at day 3. The control line is Columbia (Col) shown in Figure 1A. (**I**) Accumulation of anthocyanins in *pif3* seedlings over 24-h period from day 2 to day 3. Format follows that of Figure 1B. (**J**) Transcript levels of TF genes between line Col and line *pif3*. TF transcripts increased significantly in *pif3* (one-tailed *t*-tests; *, $p < 0.05$; **, $p < 0.05$). (**K**) Transcript levels of structural genes between Col and *pif3*. Significantly increased transcripts are shown (one-tailed *t*-tests; all ** $p < 0.002$; after Bonferroni's correction, ** $p < 0.05$).

2.8. MYC2 Moderates Responses of the Anthocyanin Pathway to Light, Hormone, or Developmental Signaling

Given significantly lowered transcriptions of *MYC2* in *pif3* (Figure 8A), we explored possible influences of PIF3, SPL9, or BBX21 in expression of *MYC2*. In dual LUC assays, mild but significant responses of $MYC2_{pro}$ to effectors carrying *SPL9*, *PIF3*, or *BBX21* were identified (Figure 8B). When pMYC2 was further provided in the cellular environment, activation of $MYC2_{pro}$ by SPL9 and BBX21 was significantly reduced (Figure 8B). A feedback loop and/or interference between MYC2 and BBX21 possibly operates during *MYC2*'s expression.

MYC2's dual influence on transcription of *PAP1* (Figure 4A) and its activation of *MYBL2* (Figure 4B), the latter of which is also supported by patterns of *MYBL2*'s transcripts across *myc2* and the complementary lines (Figure 8C), signal a way of balancing the positive and negative MYBs on the anthocyanin pathway. In short, a low level of MYC2 can lead to a higher efficiency of the MBW complex and less available MYBL2, both of which can boost output of the anthocyanin pathway; an excessive MYC2 may promote expression of *F3′H* and engage in multiple interactions with other regulators (BBX21, HY5, JAZ1, etc.). Though future enquires are pending to fill gaps here, the collective impact is shown by the phenotype of *35S*::*MYC2-1* (Figures 1A,B and S2), which also connects with enhanced production of anthocyanins. Clearly, *MYC2*'s role in regulation of the anthocyanin pathway hinges on its own expression and those of other regulators in a molecular mechanism that starts to emerge here (Figure 8D).

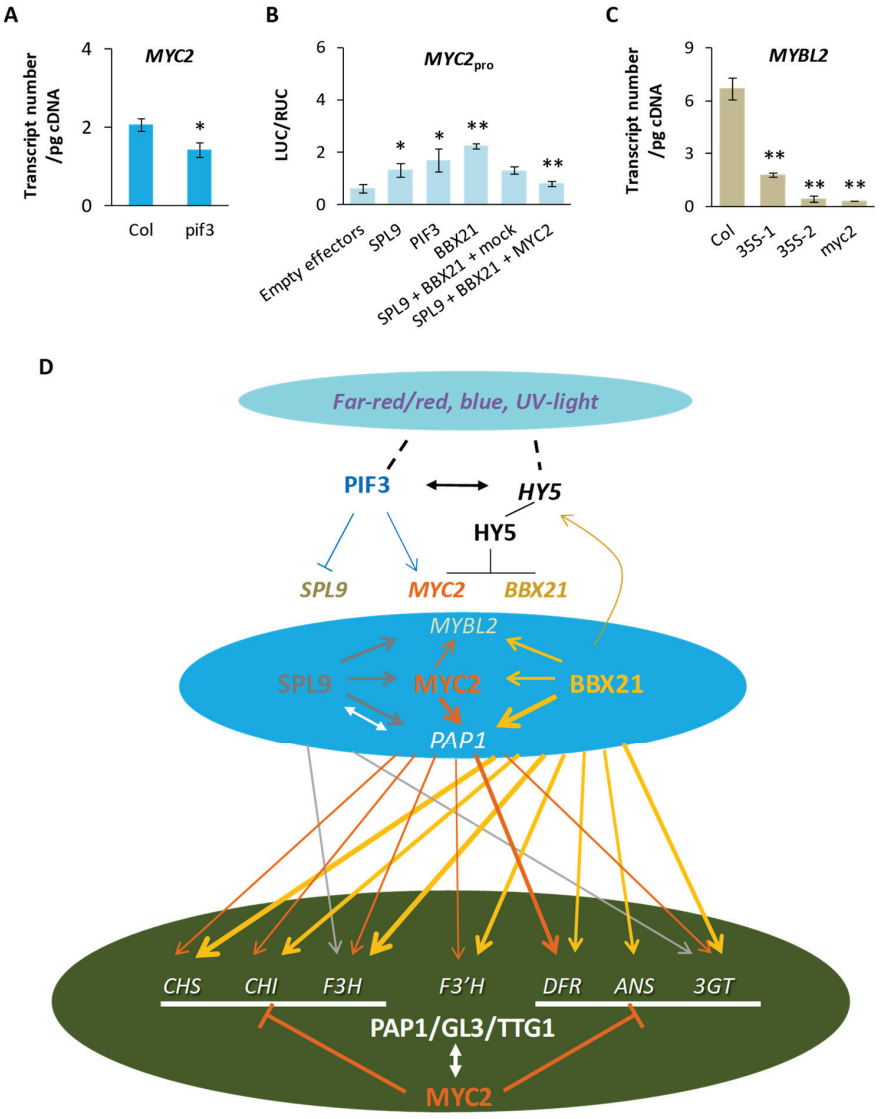

Figure 8. *MYC2* as a modulator for the anthocyanin pathway. (**A**) Transcript levels of *MYC2* between lines. The estimated numbers of transcripts are from day-3 seedlings and the standard errors from three biological replicates. The mutant lines contain fewer transcript copies than Col (one-tailed *t*-test, *, $p < 0.03$). (**B**) Activation of $MYC2_{pro}$ by different regulators in dual LUC assays. Results are based on four to eight biological replicates for each treatment. The activation effect of SPL, PIF3, or BBX21 is significant (one-tailed *t*-test, $n = 5–8$; *, $p < 0.03$, **, $p < 0.001$). The difference between a (with empty effectors added) and b is also significant (one-tailed *t*-test, $p = 0.005$, $n = 12$). Data were normalized. (**C**) Transcript levels of *MYBL2* across lines of day-3 seedlings. Details of the lines follow Figure 1C. The lines of 35S-MYC2 and *myc2* have significantly fewer copies of *MYBL2* transcripts than Col (one-tailed *t*-tests; **, $p < 0.01$). (**D**) A summary of major relationships among the regulators and the anthocyanin pathway. The upper plate is for environmental signals, which regulate PIF3 and *HY5* (black lines show inferences from literature), which in turn regulate *SPL9*, *MYC2*, and *BBx21* (colored lines having evidence from this study). Actions of SPL9, MYC2, and BBx21 on *MYB* genes (*PAP1* and *MYBL2*) are indicated in the middle plate and their regulations of the structural genes in the bottom plate. A single activation (without MBW) is presented by an arrow in the color of the regulator in the middle plate, thickness of which roughly indicates activation strength. Double arrows indicate protein-protein interactions. White bars in the bottom plate designate the scope of genes under the regulation of the PAP1/GL3/TTG1 complex, which is also suppressed by MYC2 when coupling with the complex.

3. Discussion

3.1. Regulation of the Anthocyanin Pathway by a High-Level Network Involving MYC2

Transient pigmentation of plant organs from leaf to stem, widely seen in nature, primarily comes from products of the anthocyanin pathway [8,77]. The paths connecting various signals to the anthocyanin pathway emerge as the tip of the iceberg here. One path involves *MYC2*. Although long noted in JA, ABA, and light signaling [52–54,78], MYC2 was not suspected to directly modulate response of the anthocyanin pathway. Its new role disclosed here, along with that of BBX21 in the proanthocyanidin pathway, reveals that some TFs can accommodate influxes of stimuli from inner and outer environments via interactions and pathway-specific modulations to facilitate output of a metabolic pathway kept at a physiologically desirable level.

MYC2 is rhythmically expressed ([76]; Figure S6) and interacts with components located at multiple paths of signaling [52]. These features may assist its interception with an unexpected impetus of the outer or inner environment. The rhythmic expression of *MYC2* is clearly important to its modulating function in the anthocyanin pathway, since non-rhythmic (constant and varied) expression of *MYC2* in the complementary lines here clearly signals a stress, leading to an early activation of the anthocyanin pathway in seedlings of *A. thaliana* (Figure 1B). These newly documented actions of MYC2 on the anthocyanin pathway make the phenotype of pigmentation interpretable in many cases. For instance, repressor DELLA proteins of gibberellin signaling can interact with MYC2 [47], JAZs [79–81], and MYBL2 [82]. Their mutants show enhanced pigmentation [82], which is possibly due to more MYC2 being available in cells in the absence of the interactions. Repressor JAZs of jasmonate signaling also interact with MYC2 [48–50], showing enhanced anthocyanins in their mutants as well [83]. Even in the case of protoplasmic injury, where altered expression of *MYC2* was recently documented [84], enhanced accumulation of anthocyanins, as previously reported in damaged leaves of *Pseudowintera colorata* [85], agrees with the documented impact of MYC2 here.

For light signaling, *MYC2* responds to blue and far-red light [53] and interacts with blue-light responsive proteins such as GBF1 [86]. Here, the response of *MYC2* to far-red light can be partly interpreted by the mild activation of *MYC2* by PIF3 (Figure 8B). Meanwhile, stability of MYC2 can be influenced by red/far red light ratio via JAZ repressors [87]. While negative impacts of HY5 on transcriptions of *MYC2* [88] and *BBX21* may form feedback loops on *HY5*'s expression, UV-B light can promote *HY5*'s expression [35] and stabilize BBX21 [37], causing enhanced accumulation of anthocyanins in plants exposed to the light [9,89]. By relating to HY5, PIF3, BBX21, SPL9, and other regulators/transducers of various paths of signaling, *MYC2* is clearly well positioned to modulate external and internal influences on the anthocyanin pathway.

Besides the connections mentioned above, the modulating function of MYC2 also relies on its opposing effects on the anthocyanin pathway under different circumstances (Figure 8D). The positive ones include activations of *PAP1* and structural genes (particularly *F3′H*). The negative ones consist of one or more of the following: suppression of an anthocyanin-specific MBW complex, mild activation of the repressor gene *MYBL2*, and competitions with BBX21 at different gene promoters. These effects may be somewhat balanced under normal physiological conditions when MYC2 is at the equilibrium level, so the overall production of the anthocyanin pathway remains steady. When a stimulus takes effect, extra MYC2 or lack of MYC2 can cause more enzyme production or less interference, respectively, and both can bring enhanced production of anthocyanins thus darker pigmentation. Here, less attention was paid to EGL3 and none was given to PAP2, since EGL3 is less responsible to anthocyanin accumulation under nitrogen deletion [90], and *PAP2* hardly responds to UV-B light while *PAP1* does [9]. During promoter competition, MYC2 can form a tetramer when interacting with a DNA helix [91], which helps its binding ability when competing with BBX21 or GL3 at mutually recognized *cis* elements. When *BBX21* is highly expressed, which may happen at least under red and blue light [92], MYC2 may compete with BBX21 in activating *PAP1* (Figure 5B), in effect reducing the stimulating

impact brought by BBX21 on *PAP1*; when BBX21 is at a low level, MYC2 can act additively with it to maintain the transcript level of *PAP1*. Collectively, a steady supply of PAP1 keeps the operation of the anthocyanin pathway less susceptible to environmental impulses.

Under a physiologically harsh environment, transiently increased anthocyanins can be naturally selected due to possible benefits to plants. For instance, under high light conditions, cells frequently generate an overload of reactive oxygen species, which anthocyanins can neutralize [7]. A level higher than equilibrium of anthocyanins is expected to eliminate the overload, and the equilibrium level can then be restored once the stimulus disappears, which is in part credited to the modulating effect of MYC2.

3.2. HY5 and PIF3 Are Upper-Level Factors to the Anthocyanin Pathway

The opposite phenotypes of *pif3* (strong pigmentation) and *hy5* (no visible pigmentation) clearly implicate PIF3 and HY5 in the pigmentation process, but evidence here does not support their direct participation in regulating the structural genes. Though PIF3 can bind to a G-box motif (CACGTG) in promoters of several genes [93], its direct impact was shown here on the promoters of *MYC2* (Figure 8B) and SPL9 (Figure 7F) but not BBX21 (Figure 7G). Nonetheless, transcripts of *SPL9*, *BBX21*, and anthocyanin structural genes are all up-regulated and *MYC2* down-regulated in *pif3*. Though the transcription patterns are fully compatible with the pigmentation of *pif3* (Figure 7H), it remains unclear why *BBX21* is transcribed at a higher level in *pif3* than in the wild type.

We have shown that *hy5* has low transcript numbers of *CHS* and *F3H*, which encode enzymes located at the early steps shared by different branches of the flavonoid network, including pathways to flavonols, anthocyanins, and proanthocyanidins [19,20]. A halting (or lowering) of anthocyanin production can cause the long-noted pale phenotype of *hy5* seedlings, possibly due to an unidentified and indirect regulation of HY5 on these genes. For instance, HY5 might suppress an unknown repressor of the branch to flavonols, as it does to *MYBL2*. If so, when HY5 is absent, the unknown repressor may impose its negative influence on the early genes. This analysis is extended below. Given that *hy5* is lacking in anthocyanins and *myc2* has enhanced anthocyanins, the phenotype of the double mutant *myc2*/*hy5*, which shows a higher anthocyanin accumulation than the wild type [88], suggests that MYC2 may operate downstream of HY5's action to cause the pigmented phenotype.

Collective evidence suggests that PIF3 and HY5 influence plant pigmentation primarily by activating or suppressing other regulators (e.g., SPL9, MYC2, and BBX21). As an upper-level TF, PIF3 is suppressed by phytochromes under red light [32,94], whereas expression of *HY5* is enhanced by blue light [95], UV-B light [35], BBX21 [68], MYC2 [69], and SPL9 but reduced by some BBXs (e.g., BBX24, 25, 28). We show that transcription of *HY5* is enhanced in *pif3* (Figure 7J), whereas *PIF3′s* transcription remains essentially unchanged in *hy5* (Figure 7E). Elevated *HY5* transcripts in *pif3* can be partly ascribed to higher expressions of *BBX21* and *SPL9* during the daytime (Figure 7J) and their activations of *HY5* (Figure 4D). PIF3′s physical interaction with HY5 [96] appears to have little effect on the transcription of *PIF3* itself here. As the number of *HY5* transcripts is much smaller than those of *BBX21* and *SPL9* in *pif3* (Figure 7J), suppression of HY5 on *BBX21* and *SPL9* is expected to be limited in *pif3* and incapable of reversing the positive responses of *PAP1* to abundant BBX21 and SPL9. With plentiful enzyme activities provided for the anthocyanin pathway, seedlings of *pif3* become darkly pigmented due to plentiful anthocyanins (Figure 7H). The genic relationships revealed here suggest that in cascade, light signals to PIF3 and HY5 can penetrate through expressions of *MYC2* (via PIF3 and HY5), *BBX21* (via HY5), and *SPL9* (via PIF3 and HY5) to the anthocyanin pathway (Figure 8D).

TF-TF relationships can be interactive and/or hierarchical. MYC2's interaction with HY5 may suppress $HY5_{pro}$ under blue light [88]; a mild and positive role of MYC2 alone was observed on $HY5_{pro}$ under white light ([69,97]; Figure 4D), which may account for lowered transcription of *HY5* in *myc2* (Figure 4E). Two feedback loops, one between *HY5* and *BBX21* (Figures 4D and 7G), which has been documented for orthologs of tomato [98], and another

between *HY5* and *MYC2* (Figures 4D and 8B) observed here, presumably assist transmission of signals in a controlled manner. In addition, HY5 and PIF3 can suppress collaboratively the transcriptions of *miR156*s [99], which may reduce the availability of *SPL9*-targeted mirRNAs and in effect increase the quantity of SPL9. These TF-TF relationships start to emerge as part of a broader web of regulation, which connects the flavonoid network to other physiological processes in plants.

3.3. Coordinated Regulation of Pathways via MYC2, BBX21, and SPL9

For the flavonoid network, previously unknown activations of *TT2* and *MYBL2* by MYC2, BBX21, and SPL9 (in addition to *PAP1*) are clearly part of the high-level regulation that targets both activator and repressor MYBs of flavonoid branches [20] while associating with multiple signals including hormones, light, or development. When a given TF (e.g., BBX21) simultaneously interacts with two pathways, a typical situation is that none of the pathways can gain unlimited supplies (e.g., enzymes) within cells to outcompete another pathway. A higher contingency of the scenario can be seen when pathways additionally share several enzymes before they branch off, as in the cases of the anthocyanin pathway and the proanthocyanidin pathway of the flavonoid network [20]. A coordinated regulation of the two pathways becomes necessary. The situation also applies to transcriptive outputs of specific regulators. For instance, certain members (BBX24, BBX25, BBX28) of the BBX family suppress *HY5* [100–102] but BBX21, along with BBX20 [98], clearly activates *HY5* [36,68]. This activation, however, can be attenuated when MYC2 is abundantly available, based on what we learnt in this study. If the MYC2-BBX21 interaction influences transcription of *PAP1* at the same time, transcriptions of *HY5* and *PAP1* would have to be co-regulated to some degree to enable both processes.

In high-level regulation, hierarchical relationships among *MYC2*, *BBX21*, and *SPL9* (e.g., activations of *MYC2* by BBX21 and SPL9) may cause the phenotype of *spl9* (or *bbx21*) seedlings to be confounded, thus partly mimicking *myc2* seedlings. Given that *SPL9* is involved in developmental transitions from vegetative to reproductive growth [103], its changed expression may affect *MYC2*, leading to a transient pigmentation of the plant. Our results (Figure 8D) further suggest that a base-line function of the anthocyanin pathway may exist in the absence of a local MBW complex, since MYC2 and BBX21 can together activate all structural genes including *F3′H* and *3GT* (AT5G17050) at a level collectively lower than that of the MBW. Finally, the *3GT* in *A. thaliana* is experimentally confirmed here as the formal member of the anthocyanin pathway.

Although the proanthocyanidin pathway was less studied here than the anthocyanin pathway, the significantly activated promoter of *BAN* by BBX21 (rather than MYC2) and reduced activation capacity of the TT2/TT8/TTG1 complex in the presence of BBX21 clearly resemble the dual actions of MYC2 on genes of the anthocyanin pathway. While additional analysis is pending on details of BBX21's regulation of the proanthocyanidin pathway, MYC2's competition with BBX21 is expected to play a significant role in coordination of the pathways. Finally, as the dual role of MYC2 and BBX21 is not seen in other TFs investigated here, we designate them the modulators of the anthocyanin pathway and proanthocyanidin pathway, respectively, to recognize their specific functions in the network-level regulation of flavonoids.

4. Materials and Methods

4.1. Plant Materials and Growth Conditions

For phenotypic and gene-expression analyses, seeds of *myc2* (SALK_017005C), *spl9* (CS67866), *hy5* (SALK_096651C), and *pif3* (CS66042) were obtained from *Arabidopsis* Biological Resource Center (ABRC) and examined at genotypic level before further tests. Complementary lines were made for *myc2* only. All seeds, along with the wild-type Columbia (Col), were cleaned and soaked in distilled water in petri dishes with moist filter paper, placed in a growth chamber (8 h/16 h light/dark; 23 °C/20 °C; 40–60% relative humidity, 1000–4000 lux white light) before sampling. For protein-protein interactions,

healthy seeds of *Nicotiana benthamiana* were placed on rich and moist soil and cultivated under conditions of 8 h 25 °C light and 16 h 22 °C dark until leaves were larger than 3 cm in width before transformation. For *Oryza sativa*, grains of a white-grain accession (B16–44) were steeped in water overnight and spread on water-soaked cotton under growth conditions (8 h/16 h light/dark; 32 °C/28 °C; 40–60% relative humidity, ~1500 lux white light) for about 10 days prior to leaf sampling.

4.2. Plasmid Constructions

The coding region of *MYC2* was obtained via PCR from leaf cDNA of the Col ecotype using primers incorporating cutting sites for restriction enzymes BglII and PstI (Table S1). The product was cut with the enzymes (New England Biolabs, Ipswich, MA, USA) and inserted in frame into pCAMBIA1301 (Abcam, Cambridge, UK) to make vector pCAM-MYC2 for complementary test in *myc2*. pET-MYC2 for protein expression was similarly built, based on pET-30a (Novagen, Merckmillipore, Burlington, MA, USA) with primers MYC2-BglII-F and MYC2-NcoI-R (Table S1). For BiFC experiments, pMYC2-NE was constructed from pUC-SPYNE (HonorGene, Changsha, China) with primers MYC2-ClaI-5f and MYC2-KpnI-3r (Table S1). Similarly, GL3 were obtained in the cDNA above using primers GL3-XbaI-F and GL3-BamHI-3r (Table S1) and inserted into pUC-SPYCE (HonorGene) to make pGL3-CE. All vectors above are driven by the CaMV 35S (35S) promoter and ended by NOS terminator. For expressing the binding domain (Figure S1) of GL3, pCOLD-GL3 was made from pCOLD-vector (Takara, Shiga, Japan) with primers (GL3-KpnI-F and GL3-SalI-R: Figure S1), driven by *cspA* promoter and the terminator.

For dual luciferase assays, the coding sequence of a TF (e.g., MYC2) was inserted in frame after the double 35S promoter of pJIT163 [104] to make an effecter (e.g., pMYC2). By replacing the 35S promoter of pJIT163 by the 5′ region (including (at least partial) promoter and 5′ UTR) of a gene using primers listed (Table S1), a reporter was prepared for expressing firefly luciferase (LUC) and labeled after the promoter region of the gene (e.g., $pMYC2_{pro}$, $pBAN_{pro}$). Effectors and reporters of *Os* genes were also pJIT16-based, using allele-specific primers (Table S2). The reference reporter on the same backbone has 35S-driven renilla luciferase (RUC). For Y2H tests, pAD- and pBD-vectors of HybriZAP 2.1 (Stratagene, San Diego, CA, USA) were used, along with its control vectors. The pAD-TF vector was further used in Y1H, along with pHIS2 vector (Clontech, Mountain View, CA, USA) as the reporter, which hosted the 5′ region of a tested gene (amplified using primers listed in Table S1) and yeast *HIS3* as reporter gene. Constructs for Co-IP tests were built by inserting the coding sequence of *MYC2*, *SPL9*, *BBX21*, *HY5*, *PAP1*, or *GL3* in frame into pCAMBIA1302 (Abcam) with appropriate primers (Table S1).

4.3. Complementary Lines

Vector pCAM-MYC2 was introduced into competent cells of *Agrobacteria tumefaciens* (strain LBA4404). Floral buds of *myc2* of *A. thaliana* were then infected by transformed *Agrobacteria*, following the method of Clough and Bent [105]. Seeds of the T_0 transformants were selected at MS medium with 50 mg/mL hygromycin B. At T_1 generation, transformants following 3:1 segregation were selected and gave rise to T_2 seeds, which were stored at 4 °C before analysis.

4.4. Anthocyanin Measurements

Stratified T_2 seeds were cultivated in the growth chamber above. The whole plants were sampled at 4 pm at 72 h (about 4 h before night cycle). Some of the samples were photographed under a 3D digital microscope (Leica DVM6, Leica Microsystems, Wetzlar, Germany). Others were weighted and frozen in liquid nitrogen before extraction. Ground seedlings (~0.2 g) were dissolved in 0.2 mL extraction solution (methanol with 1% HCL (*w*/*v*)), which was gently rocked at 4 °C for 24 h. Absorption of the clean supernatant was measured under 530 nm and 657 nm using a spectrophotometer (Evolution, ThermoFisher, Waltham, MA, USA), as described in [106].

4.5. Dual-LUC Assays

Co-transformations were carried out using the reported protocol [73] for handling of leaf protoplasts of *Arabidopsis thaliana*. Typically, effector was provided in the same quantity as that of reporter (1:1). When multiple trials were needed, a positive reference was included in each trial, which consisted of reporter $pDFR_{pro}$ and effectors pPAP1, pGL3, and pTTG1, to allow data normalization. The tests with leaf protoplasts of *Oryza sativa* adopted a modified version of the protocol above, with a filter of 400 μm for protoplast collection and incubating the protoplasts at 28 °C. The positive control consisted of reporter $pOsF3'H_{pro}$ and effectors pOsC1, pOsB2, and pOsTTG1. Fluorescent levels of reporter enzymes were measured in a dual-Luciferase reporter assay system using the dual-glow protocol implemented in a Glomax 20/20 luminometer (Promega, Madison, WI, USA). Promoter activity was expressed as the ratio of fluorescent levels of LUC and RUC.

4.6. Yeast Two-Hybrids (Y2H)

The entire coding region of *MYC2*, *BBX21*, *SPL9*, *PAP1*, *GL3*, or *TTG1* was inserted in frame into pAD-GAL4 2.1 or pBD-GAL4 Cam using HybriZAP-2.1 yeast two-hybrid system (Stratagene). The vectors were introduced into the YRG-2 yeast strain and the culture was screened in SD medium deficient in leucine and histidine to ensure double transformations. The positive clones were then examined for possible protein interaction at the promoter of *HIS3* on the three-deficient medium (SD/-Leu-His-Trp), which was added with or without 3-amino-1,2,4-triazole (3-AT) in appropriate quantity to contain the background growth due to leaking production of histidine.

4.7. Yeast One-Hybrid (Y1H)

Effectors from Y2H were paired with a pHIS2-based reporter, which contained 5′ regions of a targeted gene in the place of the original 5′ region (*p53*). TF and reporter vectors were introduced into yeast strain Y187 using the PEG-LiAc (TE:LiAc:50%PEG = 1:1:8) method shown by the manufacturer (Clontech). The transformed cultures were cultivated on two-deficient medium (SD/-leu-his) first. Colonies from the medium were further selected on the three-deficient medium (SD/-Leu-His-Trp) with a variable amount of 3-AT for detection of a possible protein-DNA interaction.

4.8. Bimolecular Fluorescence Complementation Assay (BiFC)

The coding region of *MYC2* or *GL3* was fused with part of a fluorescent protein (YFP) to make pMYC2-NE or pGL3-CE vectors, which were introduced into *Agrobacteria tumefaciens* (strain EHA105). The transformant solutions (each about 0.5 OD) were then mixed in 1:1 and injected into fresh leaves of *N. benthamiana* for in vivo expressions of the TF proteins. Interaction of the proteins was examined under fluorescent light and transmitting light with a two-photon fluorescence microscope (Olympus, Tokyo, Japan) and photographed at about 100×.

4.9. Co-Immunoprecipitation (Co-IP)

For co-transformations of plant cells, healthy leaves of *N. benthamiana* were infiltrated with a mixture of two solutions (1:1) from differently infected *A. tumefaciens* (EHA105), which carried protein expression vectors with a HA- or MYC-label. Vectors included pMYC2-HA/pMYC2-MYC, pBBX21-MYC, pSPL9-MYC, pGL3-MYC/pGL3-HA, pPAP1-HA, and pHY5-HA. Infected plants were grown under the long day condition in dim light and their leaves were sampled 40 h later and frozen in liquid nitrogen. Total proteins were extracted from ground leaves (~2 g) placed in 1 mL lysis buffer (50 mM Tris-HCl (pH = 7.5), 150 mM NaCl, 1 mM EDTA, 10% glycerol, 0.05% Tween20 (*v*/*v*), 1× protease inhibitor cocktail (Lablead, Hangzhou, China), 1 mM phenylmethylsulfonyl fluoride, 10 mM DTT, and 50 μM MG132 (Sigma-Aldrich, St. Louis, MO, USA) and set at 4 °C for 1 h. Part of the supernatant was then taken as input, and the rest was added to HA-agarose beads following the manufacturer's instructions (Lablead). The cleaned beads were placed in

1× SDS loading buffer and boiled for 10 min to release proteins. An SDS-PAGE gel (12%) was used to separate proteins. Proteins were transferred to a PVDF membrane (Millipore, Carrigtwohill, Ireland) and stained (1:10,000) with anti-HA or anti-MYC mouse antibodies (Lablead). The second antibody (1:10,000) was horseradish peroxidase (HRP)-conjugated goat anti-mouse IgG (Bioeasytech, Beijing, China). Detection of protein interaction was via chemiluminescent signal derived from HRP-substrate interaction using an ECL kit (Mei5 Biotech, Beijing, China). A photo was taken with Tanon Imaging System (Tanon 5200, Shanghai, China).

4.10. Electrophoretic Mobility Shift Assays (EMSAs)

Protein expression vectors pCOLD-GL3 (bHLH domain) and pET-MYC2 were separately expressed in bacteria strain DE3 (Transetta, Beijing, China). Protein extraction was through a column of Ni Sepharose (GE Healthcare, Chicago, IL, USA). Probe-protein interaction was in a 10 μL binding solution (E33075), which was loaded into a non-denaturing gel of 8–10% polyacrylamide to separate the bound probe from the unbound one following the instructions (Invitrogen, Waltham, MA, USA). Signals for bound DNA and protein were taken under different UV lights, as previously reported [107].

4.11. Real-Time Quantification of Gene Expression

Seedlings of Col, two *MYC2*-complementary lines, *myc2*, *spl9*, *hy5*, and *pif3* were harvested at 4 pm after seeds had spent 3 days in water in a growth chamber. Total RNAs were extracted from each sample that contained about 10–25 mg fresh seedlings of each material and reversely transcribed to obtain the first strand cDNAs. Concentrations of cDNAs were estimated in triplets, as were standard references prepared from coding sequences of targeted genes, as previously described [108]. Reactions of qPCR (20-μL/each) were carried out in duplicates with Premix ExTag (Takara, San Jose, CA, USA) and internal reference dye (ROX), taking 10–30 ng cDNA as template and gene-specific primers (Table S1) on StepOne-PLUS Real-time PCR systems (Applied Biosystems, Foster City, CA, USA).

4.12. Statistical Analysis

Standard *t*-tests were performed in Excel 2016. Bonferroni's correction was applied when needed, taking the experimental error rate at $\alpha = 0.05$. The microarray-based expression data of *O. sativa* [63] were corrected for background signal and normalized using quantile method ([109]) prior to being averaged over three biological replicates. Means of the replicates were used for profiling *OsMYC2*'s expression.

5. Conclusions

Environmentally induced active production of the anthocyanin pathway can cause temporary pigmentation of plants via a molecular mechanism of network-level coordination of environment-sensitive transcription factors. Here, we identified two such TFs, showing strong evidence for the modulating role of MYC2 as an activator or a repressor for primarily the anthocyanin pathway in different cellular environments, and some evidence for a similar role of *BBX21* in regulating the *BAN* gene of the proanthocyanidin pathway. This high-level regulatory mechanism connects multiple TFs (e.g., PIF3, HY5, BBX21, MYC2, and SPL9) of signaling to the anthocyanin pathway via both hierarchical and interactive relationships that vary from transcriptive (e.g., *MYC2* by PIF3, BBX21, and SPL9), protein-protein interactions (e.g., MYC2 and GL3), to protein-protein competitions (e.g., MYC2 and BBX21) for DNA binding at the targeted promoters. HY5's impact primarily focuses on the early genes (*CHS*, *CHI*, and *F3H*) of the flavonoid network, while each of MYC2, BBX21, and SPL9 can be a significant activator not only for *HY5* but also for *PAP1*, *TT2*, and *MYBL2* (the latter MYBs are known to specifically regulate parts of the flavonoid network). The mechanism is capable of explaining changes in pigmentation under a wide range of circumstances and may include additional components in future studies. While this investigation was mainly focused on *A. thaliana*, MYC2's dual role in modulating the

anthocyanin pathway was also demonstrated here in *Oryza sativa*. Clearly, this previously unknown high-level regulatory mechanism is largely conserved between plant species.

Supplementary Materials: The following supporting information can be downloaded at: https://www.mdpi.com/article/10.3390/plants13081156/s1, Table S1: Primers for genes of *A. thaliana*. Table S2: Primers for genes of *O. sativa*. Figure S1: Coding regions of regulatory genes examined in this study. Figure S2: Phenotype of transformation of *myc2* in 2021. Figure S3: 5′ regions of the anthocyanin-pathway genes in *Arabidopsis thaliana* examined in this study. Figure S4: 5′ regions of the MBW genes examined in dual LUC assays. Figure S5: Effects of MYC2 on the structural genes in the presence of PAP1/EGL3/TTG1 complex in dual LUC assays. Figure S6: Expression pattern of *OsMYC2* in leaves of *O. sativa* Nipponbare. Figure S7: 5′ regions of the anthocyanin-pathway genes of *O. sativa* tested in this study. Figure S8: Detection of protein interactions of MYC2 with GL3 and TTG1 in Y2H. Figure S9: Impacts of BBX21 and BBX22 on transcriptions of anthocyanin genes in dual-LUC assays. Figure S10: 5′ regions of TF genes examined in this study. Figure S11: Lack of interactions of BBX21 with PAP1, GL3, or TTG1 in Co-IP or Y2H. Figure S12: Relationships of SPL9 with GL3, TTG1, and MYC2. Figure S13: Single effects of HY5 and PIF3 on anthocyanin genes in dual LUC assays.

Author Contributions: Conceptualization, N.L. and Y.L.; methodology, N.L., Y.X. and Y.L.; validation, N.L. and Y.L.; formal analysis, N.L. and Y.L.; investigation, N.L., Y.X. and Y.L.; resources, Y.L.; data curation, N.L. and Y.L.; writing—original draft preparation, Y.L. and N.L.; writing—review and editing, N.L., Y.X. and Y.L.; visualization, N.L., Y.X. and Y.L.; supervision, Y.L.; project administration, N.L. and Y.L.; funding acquisition, Y.L. All authors have read and agreed to the published version of the manuscript.

Funding: This work was supported in part by National Natural Science Foundation of China (grant no. 91331116) and Chinese Academy of Sciences (grant no. XDA08020204).

Data Availability Statement: The data that support the findings of this study are available from the corresponding author upon reasonable request.

Acknowledgments: The authors would like to thank Shan Guan for help in bioinformatics and State Key Laboratory of Systematic and Evolutionary Botany for logistic support.

Conflicts of Interest: The authors declare no conflicts of interest.

References

1. Shi, M.-Z.; Xie, D.-Y. Biosynthesis and metabolic engineering of anthocyanins in *Arabidopsis thaliana*. *Recent Pat. Biotechnol.* **2014**, *8*, 47–60. [CrossRef] [PubMed]
2. Kitashova, A.; Adler, S.O.; Richter, A.S.; Eberlein, S.; Dziubek, D.; Klipp, E.; Nagele, T. Limitation of sucrose biosynthesis shapes carbon partitioning during plant cold acclimation. *Plant Cell Environ.* **2023**, *46*, 464–478. [CrossRef] [PubMed]
3. Motten, A.F.; Stone, J.L. Heritability of stigma position and the effect of stigma-anther separation on outcrossing in a predominantly self-fertilizing weed, *Datura stramonium* (Solanaceae). *Am. J. Bot.* **2000**, *87*, 339–347. [CrossRef] [PubMed]
4. Lan, J.X.; Li, A.L.; Chen, C.X. Effect of transient accumulation of anthocyanin on leaf development and photoprotection of *Fagopyrum dibotrys* mutant. *Biol. Plant.* **2011**, *55*, 766–770. [CrossRef]
5. Luo, H.H.; Li, W.J.; Zhang, X.; Deng, S.F.; Xu, Q.C.; Hou, T.; Pang, X.Q.; Zhang, Z.Q.; Zhang, X.L. In planta high levels of hydrolysable tannins inhibit peroxidase mediated anthocyanin degradation and maintain abaxially red leaves of *Excoecaria cochinchinensis*. *BMC Plant Biol.* **2019**, *19*, 20. [CrossRef] [PubMed]
6. Chalker-Scott, L. Environmental significance of anthocyanins in plant stress responses. *Photochem. Photobiol.* **1999**, *70*, 1–9. [CrossRef]
7. Gould, K.S. Nature's Swiss army knife: The diverse protective roles of anthocyanins in leaves. *J. Biomed. Biotechnol.* **2004**, *2004*, 314–320. [CrossRef] [PubMed]
8. Kubasek, W.L.; Shirley, B.W.; McKillop, A.; Goodman, H.M.; Briggs, W.; Ausubel, F.M. Regulation of flavonoid biosynthetic genes in germinating *Arabidopsis* seedlings. *Plant Cell* **1992**, *4*, 1229–1236. [CrossRef] [PubMed]
9. Cominelli, E.; Gusmaroli, G.; Allegra, D.; Galbiati, M.; Wade, H.K.; Jenkins, G.I.; Tonelli, C. Expression analysis of anthocyanin regulatory genes in response to different light qualities in *Arabidopsis thaliana*. *J. Plant Physiol.* **2008**, *165*, 886–894. [CrossRef]
10. Loreti, E.; Povero, G.; Novi, G.; Solfanelli, C.; Alpi, A.; Perata, P. Gibberellins, jasmonate and abscisic acid modulate the sucrose-induced expression of anthocyanin biosynthetic genes in *Arabidopsis*. *New Phytol.* **2008**, *179*, 1004–1016. [CrossRef]
11. Shan, X.Y.; Zhang, Y.S.; Peng, W.; Wang, Z.L.; Xie, D.X. Molecular mechanism for jasmonate-induction of anthocyanin accumulation in *Arabidopsis*. *J. Exp. Bot.* **2009**, *60*, 3849–3860. [CrossRef] [PubMed]

12. Jiang, C.F.; Gao, X.H.; Liao, L.; Harberd, N.P.; Fu, X.D. Phosphate starvation root architecture and anthocyanin accumulation responses are modulated by the gibberellin-DELLA signaling pathway in *Arabidopsis*. *Plant Physiol.* **2007**, *145*, 1460–1470. [CrossRef] [PubMed]
13. Peng, Z.H.; Han, C.Y.; Yuan, L.B.; Zhang, K.; Huang, H.M.; Ren, C.M. Brassinosteroid enhances jasmonate-induced anthocyanin accumulation in *Arabidopsis* seedlings. *J. Integr. Plant Biol.* **2011**, *53*, 632–640. [CrossRef] [PubMed]
14. Gou, J.Y.; Felippes, F.F.; Liu, C.J.; Weigel, D.; Wang, J.W. Negative regulation of anthocyanin biosynthesis in *Arabidopsis* by a miR156-targeted SPL transcription factor. *Plant Cell* **2011**, *23*, 1512–1522. [CrossRef] [PubMed]
15. Cui, L.G.; Shan, J.X.; Shi, M.; Gao, J.P.; Lin, H.X. The *miR156-SPL9-DFR* pathway coordinates the relationship between development and abiotic stress tolerance in plants. *Plant J.* **2014**, *80*, 1108–1117. [CrossRef] [PubMed]
16. Zhang, F.; Gonzalez, A.; Zhao, M.Z.; Payne, C.T.; Lloyd, A. A network of redundant bHLH proteins functions in all TTG1-dependent pathways of *Arabidopsis*. *Development* **2003**, *130*, 4859–4869. [CrossRef]
17. Gonzalez, A.; Zhao, M.; Leavitt, J.M.; Lloyd, A.M. Regulation of the anthocyanin biosynthetic pathway by the TTG1/bHLH/Myb transcriptional complex in *Arabidopsis* seedlings. *Plant J.* **2008**, *53*, 814–827. [CrossRef]
18. Baudry, A.; Heim, M.A.; Dubreucq, B.; Caboche, M.; Weisshaar, B.; Lepiniec, L. TT2, TT8, and TTG1 synergistically specify the expression of BANYULS and proanthocyanidin biosynthesis in *Arabidopsis thaliana*. *Plant J.* **2004**, *39*, 366–380. [CrossRef] [PubMed]
19. Yu, K.J.; Song, Y.S.; Lin, J.X.; Dixon, R.A. The complexities of proanthocyanidin biosynthesis and its regulation in plants. *Plant Commun.* **2023**, *4*, 16. [CrossRef]
20. Zhu, Z.; Wang, H.; Wang, Y.; Guan, S.; Wang, F.; Tang, J.; Zhang, R.; Xie, L.; Lu, Y. Characterization of the *cis* elements in the proximal promoter regions of the anthocyanin pathway genes reveals a common regulatory logic that governs pathway regulation. *J. Exp. Bot.* **2015**, *66*, 3775–3789. [CrossRef]
21. Hichri, I.; Barrieu, F.; Bogs, J.; Kappel, C.; Delrot, S.; Lauvergeat, V. Recent advances in the transcriptional regulation of the flavonoid biosynthetic pathway. *J. Exp. Bot.* **2011**, *62*, 2465–2483. [CrossRef]
22. Datta, S.; Hettiarachchi, C.; Johansson, H.; Holm, M. SALT TOLERANCE HOMOLOG2, a B-Box protein in *Arabidopsis* that activates transcription and positively regulates light-mediated development. *Plant Cell* **2007**, *19*, 3242–3255. [CrossRef]
23. Yadav, A.; Ravindran, N.; Singh, D.; Rahul, P.V.; Datta, S. Role of *Arabidopsis* BBX proteins in light signaling. *J. Plant Biochem. Biotechnol.* **2020**, *29*, 623–635. [CrossRef]
24. Crocco, C.D.; Ocampo, G.G.; Ploschuk, E.L.; Mantese, A.; Botto, J.F. Heterologous expression of *AtBBX21* enhances the rate of photosynthesis and alleviates photoinhibition in *Solanum tuberosum*. *Plant Physiol.* **2018**, *177*, 369–380. [CrossRef] [PubMed]
25. Bai, S.L.; Tao, R.Y.; Yin, L.; Ni, J.B.; Yang, Q.S.; Yan, X.H.; Yang, F.P.; Guo, X.P.; Li, H.X.; Teng, Y.W. Two B-box proteins, PpBBX18 and PpBBX21, antagonistically regulate anthocyanin biosynthesis via competitive association with *Pyrus pyrifolia* ELONGATED HYPOCOTYL 5 in the peel of pear fruit. *Plant J.* **2019**, *100*, 1208–1223. [CrossRef]
26. Bai, S.L.; Saito, T.; Honda, C.; Hatsuyama, Y.; Ito, A.; Moriguchi, T. An apple B-box protein, MdCOL11, is involved in UV-B- and temperature-induced anthocyanin biosynthesis. *Planta* **2014**, *240*, 1051–1062. [CrossRef] [PubMed]
27. Oyama, T.; Shimura, Y.; Okada, K. The *Arabidopsis HY5* gene encodes a bZIP protein that regulates stimulus-induced development of root and hypocotyl. *Genes Dev.* **1997**, *11*, 2983–2995. [CrossRef] [PubMed]
28. Ni, M.; Tepperman, J.M.; Quail, P.H. PIF3, a phytochrome-interacting factor necessary for normal photoinduced signal transduction, is a novel basic helix-loop-helix protein. *Cell* **1998**, *95*, 657–667. [CrossRef]
29. Shin, J.; Park, E.; Choi, G. PIF3 regulates anthocyanin biosynthesis in an HY5-dependent manner with both factors directly binding anthocyanin biosynthetic gene promoters in *Arabidopsis*. *Plant J.* **2007**, *49*, 981–994. [CrossRef]
30. Wang, Y.L.; Wang, Y.Q.; Song, Z.Q.; Zhang, H.Y. Repression of *MYBL2* by both microRNA858a and HY5 leads to the activation of anthocyanin biosynthetic pathway in *Arabidopsis*. *Mol. Plant.* **2016**, *9*, 1395–1405. [CrossRef]
31. Matsui, K.; Umemura, Y.; Ohme-Takagi, M. AtMYBL2, a protein with a single MYB domain, acts as a negative regulator of anthocyanin biosynthesis in *Arabidopsis*. *Plant J.* **2008**, *55*, 954–967. [CrossRef] [PubMed]
32. Ni, M.; Tepperman, J.M.; Quail, P.H. Binding of phytochrome B to its nuclear signalling partner PIF3 is reversibly induced by light. *Nature* **1999**, *400*, 781–784. [CrossRef] [PubMed]
33. Jiang, B.C.; Shi, Y.T.; Peng, Y.; Jia, Y.X.; Yan, Y.; Dong, X.J.; Li, H.; Dong, J.; Li, J.G.; Gong, Z.Z.; et al. Cold-induced CBF-PIF3 interaction enhances freezing tolerance by stabilizing the phyB thermosensor in *Arabidopsis*. *Mol. Plant.* **2020**, *13*, 894–906. [CrossRef] [PubMed]
34. Hernando, C.E.; Murcia, M.G.; Pereyra, M.E.; Sellaro, R.; Casal, J.J. Phytochrome B links the environment to transcription. *J. Exp. Bot.* **2021**, *72*, 4068–4084. [CrossRef] [PubMed]
35. Yang, Y.; Liang, T.; Zhang, L.B.; Shao, K.; Gu, X.X.; Shang, R.X.; Shi, N.; Li, X.; Zhang, P.; Liu, H.T. UVR8 interacts with WRKY36 to regulate *HY5* transcription and hypocotyl elongation in *Arabidopsis*. *Nat. Plants* **2018**, *4*, 98–107. [CrossRef] [PubMed]
36. Xu, D.Q.; Jiang, Y.; Li, J.; Holm, M.; Deng, X.W. The B-Box domain protein BBX21 promotes photomorphogenesis. *Plant Physiol.* **2018**, *176*, 2365–2375. [CrossRef] [PubMed]
37. Podolec, R.; Wagnon, T.B.; Leonardelli, M.; Johansson, H.; Ulm, R. *Arabidopsis* B-box transcription factors BBX20-22 promote UVR8 photoreceptor-mediated UV-B responses. *Plant J.* **2022**, *111*, 422–439. [CrossRef]
38. Franceschi, V.R.; Grimes, H.D. Induction of soybean vegetative storage proteins and anthocyanins by low-level atmospheric methyl jasmonate. *Proc. Natl. Acad. Sci. USA* **1991**, *88*, 6745–6749. [CrossRef]

39. Qi, T.C.; Song, S.S.; Ren, Q.C.; Wu, D.W.; Huang, H.; Chen, Y.; Fan, M.; Peng, W.; Ren, C.M.; Xie, D.X. The jasmonate-zim-domain proteins interact with the WD-repeat/bHLH/MYB complexes to regulate jasmonate-mediated anthocyanin accumulation and trichome initiation in *Arabidopsis thaliana*. *Plant Cell* **2011**, *23*, 1795–1814. [CrossRef]
40. Kataoka, I.; Sugiura, A.; Utsunomiya, N.; Tomana, T. Effect of abscisic-acid and defoliation on anthocyanin accumulation in Kyoho grapes (*Vitis vinifera* L x *V*. *labruscana* BAILEY). *Vitis* **1982**, *21*, 325–332.
41. Jeong, S.T.; Goto-Yamamoto, N.; Kobayashi, S.; Esaka, A. Effects of plant hormones and shading on the accumulation of anthocyanins and the expression of anthocyanin biosynthetic genes in grape berry skins. *Plant Sci.* **2004**, *167*, 247–252. [CrossRef]
42. Samkumar, A.; Jones, D.; Karppinen, K.; Dare, A.P.; Sipari, N.; Espley, R.V.; Martinussen, I.; Jaakola, L. Red and blue light treatments of ripening bilberry fruits reveal differences in signalling through abscisic acid-regulated anthocyanin biosynthesis. *Plant Cell Environ.* **2021**, *44*, 3227–3245. [CrossRef] [PubMed]
43. Ilan, A.; Dougall, D.K. The effect of growth retardants on anthocyanin production in carrot cell suspension cultures. *Plant Cell Rep.* **1992**, *11*, 304–309. [CrossRef] [PubMed]
44. Jeong, S.W.; Das, P.K.; Jeoung, S.C.; Song, J.Y.; Lee, H.K.; Kim, Y.K.; Kim, W.J.; Park, Y.I.; Yoo, S.D.; Choi, S.B.; et al. Ethylene suppression of sugar-induced anthocyanin pigmentation in *Arabidopsis*. *Plant Physiol.* **2010**, *154*, 1514–1531. [CrossRef] [PubMed]
45. Berger, S.; Bell, E.; Mullet, J.E. Two methyl jasmonate-insensitive mutants show altered expression of *AtVsp* in response to methyl jasmonate and wounding. *Plant Physiol.* **1996**, *111*, 525–531. [CrossRef] [PubMed]
46. Abe, H.; YamaguchiShinozaki, K.; Urao, T.; Iwasaki, T.; Hosokawa, D.; Shinozaki, K. Role of *Arabidopsis* MYC and MYB homologs in drought- and abscisic acid-regulated gene expression. *Plant Cell* **1997**, *9*, 1859–1868. [PubMed]
47. Hong, G.J.; Xue, X.Y.; Mao, Y.B.; Wang, L.J.; Chen, X.Y. *Arabidopsis* MYC2 interacts with DELLA proteins in regulating sesquiterpene synthase gene expression. *Plant Cell* **2012**, *24*, 2635–2648. [CrossRef] [PubMed]
48. Chini, A.; Fonseca, S.; Fernandez, G.; Adie, B.; Chico, J.M.; Lorenzo, O.; Garcia-Casado, G.; Lopez-Vidriero, I.; Lozano, F.M.; Ponce, M.R.; et al. The JAZ family of repressors is the missing link in jasmonate signaling. *Nature* **2007**, *448*, 666–671. [CrossRef]
49. Melotto, M.; Mecey, C.; Niu, Y.; Chung, H.S.; Katsir, L.; Yao, J.; Zeng, W.Q.; Thines, B.; Staswick, P.; Browse, J.; et al. A critical role of two positively charged amino acids in the Jas motif of *Arabidopsis* JAZ proteins in mediating coronatine- and jasmonoyl isoleucine-dependent interactions with the COI1F-box protein. *Plant J.* **2008**, *55*, 979–988. [CrossRef]
50. Chung, H.S.; Howe, G.A. A critical role for the TIFY motif in repression of jasmonate signaling by a stabilized splice variant of the JASMONATE ZIM-domain protein JAZ10 in *Arabidopsis*. *Plant Cell* **2009**, *21*, 131–145. [CrossRef]
51. Niu, Y.J.; Figueroa, P.; Browse, J. Characterization of JAZ-interacting bHLH transcription factors that regulate jasmonate responses in *Arabidopsis*. *J. Exp. Bot.* **2011**, *62*, 2143–2154. [CrossRef]
52. Kazan, K.; Manners, J.M. MYC2: The master in action. *Mol. Plant.* **2013**, *6*, 686–703. [CrossRef]
53. Yadav, V.; Mallappa, C.; Gangappa, S.N.; Bhatia, S.; Chattopadhyay, S. A basic helix-loop-helix transcription factor in *Arabidopsis*, MYC2, acts as a repressor of blue light-mediated photomorphogenic growth. *Plant Cell* **2005**, *17*, 1953–1966. [CrossRef] [PubMed]
54. Dombrecht, B.; Xue, G.P.; Sprague, S.J.; Kirkegaard, J.A.; Ross, J.J.; Reid, J.B.; Fitt, G.P.; Sewelam, N.; Schenk, P.M.; Manners, J.M.; et al. MYC2 differentially modulates diverse jasmonate-dependent functions in *Arabidopsis*. *Plant Cell* **2007**, *19*, 2225–2245. [CrossRef]
55. Schwarz, S.; Grande, A.V.; Bujdoso, N.; Saedler, H.; Huijser, P. The microRNA regulated SBP-box genes *SPL9* and *SPL15* control shoot maturation in *Arabidopsis*. *Plant Mol.Biol.* **2008**, *67*, 183–195. [CrossRef] [PubMed]
56. Wu, G.; Park, M.Y.; Conway, S.R.; Wang, J.W.; Weigel, D.; Poethig, R.S. The sequential action of mir156 and mir172 regulates developmental timing in *Arabidopsis*. *Cell* **2009**, *138*, 750–759. [CrossRef]
57. He, J.; Xu, M.; Willmann, M.R.; McCormick, K.; Hu, T.; Yang, L.; Starker, C.G.; Voytas, D.F.; Meyers, B.C.; Poethig, R.S. Threshold-dependent repression of SPL gene expression by miR156/miR157 controls vegetative phase change in *Arabidopsis thaliana*. *PLoS Genet.* **2018**, *14*, e1007337. [CrossRef] [PubMed]
58. Wu, G.; Poethig, R.S. Temporal regulation of shoot development in *Arabidopsis thaliana* by *miR156* and its target *SPL3*. *Development* **2006**, *133*, 3539–3547. [CrossRef] [PubMed]
59. Xing, S.P.; Salinas, M.; Hohmann, S.; Berndtgen, R.; Huijser, P. miR156-targeted and nontargeted SBP-box transcription factors act in concert to secure male fertility in *Arabidopsis*. *Plant Cell* **2010**, *22*, 3935–3950. [CrossRef]
60. Cai, Q.; Yuan, Z.; Chen, M.J.; Yin, C.S.; Luo, Z.J.; Zhao, X.X.; Liang, W.Q.; Hu, J.P.; Zhang, D.B. Jasmonic acid regulates spikelet development in rice. *Nat. Commun.* **2014**, *5*, 13. [CrossRef]
61. Shin, J.; Heidrich, K.; Sanchez-Villarreal, A.; Parker, J.E.; Davis, S.J. TIME FOR COFFEE represses accumulation of the MYC2 transcription factor to provide time-of-day regulation of jasmonate signaling in *Arabidopsis*. *Plant Cell* **2012**, *24*, 2470–2482. [CrossRef]
62. Cress, B.F.; Leitz, Q.D.; Kim, D.C.; Amore, T.D.; Suzuki, J.Y.; Linhardt, R.J.; Koffas, M.A.G. CRISPRi-mediated metabolic engineering of *E*. coli for O-methylated anthocyanin production. *Microb. Cell. Fact.* **2017**, *16*, 14.
63. Sato, Y.; Takehisa, H.; Kamatsuki, K.; Minami, H.; Namiki, N.; Ikawa, H.; Ohyanagi, H.; Sugimoto, K.; Antonio, B.A.; Nagamura, Y. RiceXPro Version 3.0: Expanding the informatics resource for rice transcriptome. *Nucleic Acids Res.* **2013**, *41*, D1206–D1213. [CrossRef]
64. Zheng, J.; Wu, H.; Zhu, H.B.; Huang, C.Y.; Liu, C.; Chang, Y.S.; Kong, Z.C.; Zhou, Z.H.; Wang, G.W.; Lin, Y.J.; et al. Determining factors, regulation system, and domestication of anthocyanin biosynthesis in rice leaves. *New Phytol.* **2019**, *223*, 705–721. [CrossRef]

65. Fernandez-Calvo, P.; Chini, A.; Fernandez-Barbero, G.; Chico, J.M.; Gimenez-Ibanez, S.; Geerinck, J.; Eeckhout, D.; Schweizer, F.; Godoy, M.; Franco-Zorrilla, J.M.; et al. The *Arabidopsis* bHLH transcription factors MYC3 and MYC4 are targets of JAZ repressors and act additively with MYC2 in the activation of jasmonate responses. *Plant Cell* **2011**, *23*, 701–715. [CrossRef]
66. Shangguan, X.X.; Xu, B.; Yu, Z.X.; Wang, L.J.; Chen, X.Y. Promoter of a cotton fibre *MYB* gene functional in trichomes of *Arabidopsis* and glandular trichomes of tobacco. *J. Exp. Bot.* **2008**, *59*, 3533–3542. [CrossRef]
67. Datta, S.; Johansson, H.; Hettiarachchi, C.; Irigoyen, M.L.; Desai, M.; Rubio, V.; Holm, M. LZF1/SALT TOLERANCE HOMOLOG3, an *Arabidopsis* B-Box protein involved in light-dependent development and gene expression, undergoes COP1-mediated ubiquitination. *Plant Cell* **2008**, *20*, 2324–2338. [CrossRef]
68. Xu, D.Q.; Jiang, Y.; Li, J.G.; Lin, F.; Holm, M.; Deng, X.W. BBX21, an *Arabidopsis* B-box protein, directly activates *HY5* and is targeted by COP1 for 26S proteasome-mediated degradation. *Proc. Natl. Acad. Sci. USA* **2016**, *113*, 7655–7660. [CrossRef]
69. Ortigosa, A.; Fonseca, S.; Franco-Zorrilla, J.M.; Fernandez-Calvo, P.; Zander, M.; Lewsey, M.G.; Garcia-Casado, G.; Fernandez-Barbero, G.; Ecker, J.R.; Solano, R. The JA-pathway MYC transcription factors regulate photomorphogenic responses by targeting *HY5* gene expression. *Plant J.* **2020**, *102*, 138–152. [CrossRef]
70. Abbas, N.; Maurya, J.P.; Senapati, D.; Gangappa, S.N.; Chattopadhyay, S. *Arabidopsis* CAM7 and HY5 physically interact and directly bind to the *HY5* promoter to regulate its expression and thereby promote photomorphogenesis. *Plant Cell* **2014**, *26*, 1036–1052. [CrossRef]
71. Binkert, M.; Kozma-Bognar, L.; Terecskei, K.; De Veylder, L.; Nagy, F.; Ulm, R. UV-B-responsive association of the *Arabidopsis* bZIP transcription factor ELONGATED HYPOCOTYL5 with target genes, including its own promoter. *Plant Cell* **2014**, *26*, 4200–4213. [CrossRef]
72. Liang, X.W.; Nazarenus, T.J.; Stone, J.M. Identification of a consensus DNA-binding site for the *Arabidopsis thaliana* SBP domain transcription factor, AtSPL14, and binding kinetics by surface plasmon resonance. *Biochemistry* **2008**, *47*, 3645–3653. [CrossRef]
73. Yoo, S.D.; Cho, Y.H.; Sheen, J. *Arabidopsis* mesophyll protoplasts: A versatile cell system for transient gene expression analysis. *Nat. Protoc.* **2007**, *2*, 1565–1572. [CrossRef]
74. Bhagat, P.K.; Verma, D.; Sharma, D.; Sinha, A.K. HY5 and ABI5 transcription factors physically interact to fine tune light and ABA signaling in *Arabidopsis*. *Plant Mol.Biol.* **2021**, *107*, 117–127. [CrossRef]
75. Ang, L.H.; Deng, X.W. Regulatory hierarchy of photomorphogenic loci-allele-specific and light-dependent interaction between the *HY5* and *COP1* loci. *Plant Cell* **1994**, *6*, 613–628.
76. Soy, J.; Leivar, P.; Gonzalez-Schain, N.; Sentandreu, M.; Prat, S.; Quail, P.H.; Monte, E. Phytochrome-imposed oscillations in PIF3 protein abundance regulate hypocotyl growth under diurnal light/dark conditions in *Arabidopsis*. *Plant J.* **2012**, *71*, 390–401. [CrossRef]
77. Weiss, M.R. Floral color change—a widespread functional convergence. *Am. J. Bot.* **1995**, *82*, 167–185. [CrossRef]
78. Abe, H.; Urao, T.; Ito, T.; Seki, M.; Shinozaki, K.; Yamaguchi-Shinozaki, K. *Arabidopsis* AtMYC2 (bHLH) and AtMYB2 (MYB) function as transcriptional activators in abscisic acid signaling. *Plant Cell* **2003**, *15*, 63–78. [CrossRef]
79. Hou, X.L.; Lee, L.Y.C.; Xia, K.F.; Yen, Y.Y.; Yu, H. DELLAs modulate jasmonate signaling via competitive binding to JAZs. *Dev. Cell* **2010**, *19*, 884–894. [CrossRef]
80. Yang, D.L.; Yao, J.; Mei, C.S.; Tong, X.H.; Zeng, L.J.; Li, Q.; Xiao, L.T.; Sun, T.P.; Li, J.G.; Deng, X.W.; et al. Plant hormone jasmonate prioritizes defense over growth by interfering with gibberellin signaling cascade. *Proc. Natl. Acad. Sci. USA* **2012**, *109*, E1192–E1200. [CrossRef]
81. Wild, M.; Daviere, J.M.; Cheminant, S.; Regnault, T.; Baumberger, N.; Heintz, D.; Baltz, R.; Genschik, P.; Achard, P. The *Arabidopsis* DELLA RGA-LIKE3 is a direct target of MYC2 and modulates jasmonate signaling responses. *Plant Cell* **2012**, *24*, 3307–3319. [CrossRef]
82. Xie, Y.; Tan, H.J.; Ma, Z.X.; Huang, J.R. DELLA proteins promote anthocyanin biosynthesis via sequestering MYBL2 and JAZ suppressors of the MYB/bHLH/WD40 complex in *Arabidopsis thaliana*. *Mol. Plant.* **2016**, *9*, 711–721. [CrossRef]
83. Liu, B.; Seong, K.; Pang, S.A.; Song, J.Q.; Gao, H.; Wang, C.L.; Zhai, J.Q.; Zhang, Y.; Gao, S.; Li, X.D.; et al. Functional specificity, diversity, and redundancy of *Arabidopsis* JAZ family repressors in jasmonate and COI1-regulated growth, development, and defense. *New Phytol.* **2021**, *231*, 1525–1545. [CrossRef]
84. Son, S.; Kwon, M.; Im, J.H. A new approach for wounding research: *MYC2* gene expression and protein stability in wounded *Arabidopsis* protoplasts. *Plants-Basel* **2021**, *10*, 1518. [CrossRef]
85. Gould, K.S.; McKelvie, J.; Markham, K.R. Do anthocyanins function as antioxidants in leaves? Imaging of H_2O_2 in red and green leaves after mechanical injury. *Plant Cell Environ.* **2002**, *25*, 1261–1269. [CrossRef]
86. Maurya, J.P.; Sethi, V.; Gangappa, S.N.; Gupta, N.; Chattopadhyay, S. Interaction of MYC2 and GBF1 results in functional antagonism in blue light-mediated *Arabidopsis* seedling development. *Plant J.* **2015**, *83*, 439–450. [CrossRef]
87. Chico, J.M.; Fernandez-Barbero, G.; Chini, A.; Fernandez-Calvo, P.; Diez-Diaz, M.; Solano, R. Repression of jasmonate-dependent defenses by shade involves differential regulation of protein stability of MYC transcription factors and their JAZ repressors in *Arabidopsis*. *Plant Cell* **2014**, *26*, 1967–1980. [CrossRef]
88. Chakraborty, M.; Gangappa, S.N.; Maurya, J.P.; Sethi, V.; Srivastava, A.K.; Singh, A.; Dutta, S.; Ojha, M.; Gupta, N.; Sengupta, M.; et al. Functional interrelation of MYC2 and HY5 plays an important role in *Arabidopsis* seedling development. *Plant J.* **2019**, *99*, 1080–1097. [CrossRef]

89. Reddy, V.S.; Goud, K.V.; Sharma, R.; Reddy, A.R. Ultraviolet-B-responsive anthocyanin production in a rice cultivar is associated with a specific phase of phenylalanine ammonia-lyase biosynthesis. *Plant Physiol.* **1994**, *105*, 1059–1066. [CrossRef]
90. Feyissa, D.N.; Lovdal, T.; Olsen, K.M.; Slimestad, R.; Lillo, C. The endogenous *GL3*, but not *EGL3*, gene is necessary for anthocyanin accumulation as induced by nitrogen depletion in *Arabidopsis* rosette stage leaves. *Planta* **2009**, *230*, 747–754. [CrossRef]
91. Lian, T.F.; Xu, Y.P.; Li, L.F.; Su, X.D. Crystal structure of tetrameric *Arabidopsis* MYC2 reveals the mechanism of enhanced interaction with DNA. *Cell Rep.* **2017**, *19*, 1334–1342. [CrossRef]
92. Kang, X.J.; Xu, G.; Lee, B.; Chen, C.; Zhang, H.N.; Kuang, R.; Ni, M. HRB2 and BBX21 interaction modulates *Arabidopsis ABI5* locus and stomatal aperture. *Plant Cell Environ.* **2018**, *41*, 1912–1925. [CrossRef]
93. Martinez-Garcia, J.F.; Huq, E.; Quail, P.H. Direct targeting of light signals to a promoter element-bound transcription factor. *Science* **2000**, *288*, 859–863. [CrossRef]
94. Cheng, M.C.; Kathare, P.K.; Paik, I.; Huq, E. Phytochrome signaling networks. In *Annual Review of Plant Biology*; Merchant, S.S., Ed.; Annual Reviews: Palo Alto, CA, USA, 2021; Volume 72, pp. 217–244.
95. Hajdu, A.; Dobos, O.; Domijan, M.; Balint, B.; Nagy, I.; Nagy, F.; Kozma-Bognar, L. ELONGATED HYPOCOTYL 5 mediates blue light signalling to the *Arabidopsis* circadian clock. *Plant J.* **2018**, *96*, 1242–1254. [CrossRef]
96. Chen, D.Q.; Xu, G.; Tang, W.J.; Jing, Y.J.; Ji, Q.; Fei, Z.J.; Lin, R.C. Antagonistic basic helix-loop-helix/bZIP transcription factors form transcriptional modules that integrate light and reactive oxygen species signaling in *Arabidopsis*. *Plant Cell* **2013**, *25*, 1657–1673. [CrossRef]
97. Yi, R.; Yan, J.B.; Xie, D.X. Light promotes jasmonate biosynthesis to regulate photomorphogenesis in *Arabidopsis*. *Sci. China-Life Sci.* **2020**, *63*, 943–952. [CrossRef]
98. Yang, G.Q.; Zhang, C.L.; Dong, H.X.; Liu, X.R.; Guo, H.C.; Tong, B.Q.; Fang, F.; Zhao, Y.Y.; Yu, Y.J.; Liu, Y.; et al. Activation and negative feedback regulation of *SlHY5* transcription by the SlBBX20/21-SlHY5 transcription factor module in UV-B signaling. *Plant Cell* **2022**, *34*, 2038–2055. [CrossRef]
99. Xie, Y.R.; Liu, Y.; Wang, H.; Ma, X.J.; Wang, B.B.; Wu, G.X.; Wang, H.Y. Phytochrome-interacting factors directly suppress *MIR156* expression to enhance shade-avoidance syndrome in *Arabidopsis*. *Nat. Commun.* **2017**, *8*, 348. [CrossRef]
100. Gangappa, S.N.; Crocco, C.D.; Johansson, H.; Datta, S.; Hettiarachchi, C.; Holm, M.; Botto, J.F. The *Arabidopsis* B-BOX protein BBX25 interacts with HY5, negatively regulating *BBX22* expression to suppress seedling photomorphogenesis. *Plant Cell* **2013**, *25*, 1243–1257. [CrossRef]
101. Lin, F.; Jiang, Y.; Li, J.; Yan, T.T.; Fan, L.M.; Liang, J.S.; Chen, Z.J.; Xu, D.Q.; Deng, X.W. B-BOX DOMAIN PROTEIN28 negatively regulates photomorphogenesis by repressing the activity of transcription factor HY5 and undergoes COP1-mediated degradation. *Plant Cell* **2018**, *30*, 2006–2019. [CrossRef]
102. Job, N.; Yadukrishnan, P.; Bursch, K.; Datta, S.; Johansson, H. Two B-Box proteins regulate photomorphogenesis by oppositely modulating HY5 through their diverse C-terminal domains. *Plant Physiol.* **2018**, *176*, 2963–2976. [CrossRef]
103. Xu, M.L.; Hu, T.Q.; Zhao, J.F.; Park, M.Y.; Earley, K.W.; Wu, G.; Yang, L.; Poethig, R.S. Developmental functions of miR156-regulated *SQUAMOSA PROMOTER BINDING PROTEIN-LIKE* (SPL) genes in *Arabidopsis thaliana*. *PLoS Genet.* **2016**, *12*, e1006263. [CrossRef]
104. Guerineau, F.; Lucy, A.; Mullineaux, P. Effect of 2 consensus sequences preceding the translation initiator codon on gene-expression in plant-protoplasts. *Plant Mol.Biol.* **1992**, *18*, 815–818. [CrossRef]
105. Clough, S.J.; Bent, A.F. Floral dip: A simplified method for *Agrobacterium*-mediated transformation of *Arabidopsis thaliana*. *Plant J.* **1998**, *16*, 735–743. [CrossRef]
106. Neff, M.M.; Chory, J. Genetic interactions between phytochrome A, phytochrome B, and cryptochrome 1 during *Arabidopsis* development. *Plant Physiol.* **1998**, *118*, 27–36. [CrossRef]
107. Wang, H.L.; Guan, S.; Zhu, Z.X.; Wang, Y.; Lu, Y.Q. A valid strategy for precise identifications of transcription factor binding sites in combinatorial regulation using bioinformatic and experimental approaches. *Plant Methods* **2013**, *9*, 34. [CrossRef]
108. Lu, Y.Q.; Xie, L.L.; Chen, J.N. A novel procedure for absolute real-time quantification of gene expression patterns. *Plant Methods* **2012**, *8*, 9. [CrossRef]
109. Bolstad, B.M.; Irizarry, R.A.; Åstrand, M.; Speed, T.P. A comparison of normalization methods for high density oligonucleotide array data based on variance and bias. *Bioinformatics* **2003**, *19*, 185–193. [CrossRef]

plants

MDPI

Review

SnRK2s: Kinases or Substrates?

Yunmin Wei [1,*], Linzhu Peng [2] and Xiangui Zhou [2,*]

[1] Key Laboratory of Plant Genetics and Molecular Breeding, Zhoukou Normal University, Zhoukou 466001, China
[2] College of Life Sciences and Oceanography, Shenzhen University, Shenzhen 518000, China; 2021300070@email.szu.edu.cn
* Correspondence: weiym1024@163.com (Y.W.); xgzhou@szu.edu.cn (X.Z.); Tel.: +86-134-3996-9956 (X.Z.)

Abstract: Throughout their life cycle, plants persistent through environmental adversities that activate sophisticated stress-signaling networks, with protein kinases serving as pivotal regulators of these responses. The sucrose non-fermenting-1-related protein kinase 2 (SnRK2), a plant-specific serine/threonine kinase, orchestrates stress adaptation by phosphorylating downstream targets to modulate gene expression and physiological adjustments. While SnRK2 substrates have been extensively identified, the existing literature lacks a systematic classification of these components and their functional implications. This review synthesizes recent advances in characterizing SnRK2-phosphorylated substrates in *Arabidopsis thaliana*, providing a mechanistic framework for their roles in stress signaling and developmental regulation. Furthermore, we explore the understudied paradigm of SnRK2 undergoing multilayered post-translational modifications (PTMs), including phosphorylation, ubiquitination, SUMOylation, S-nitrosylation, sulfation (S-sulfination and tyrosine sulfation), and N-glycosylation. These PTMs collectively fine-tune SnRK2 stability, activity, and subcellular dynamics, revealing an intricate feedback system that balances kinase activation and attenuation. By integrating substrate networks with regulatory modifications, this work highlights SnRK2's dual role as both a phosphorylation executor and a PTM-regulated scaffold, offering new perspectives for engineering stress-resilient crops through targeted manipulation of SnRK2 signaling modules.

Keywords: phosphorylation; post-translational modification; substrates; SnRK2

1. Introduction

Drought, high salinity, osmotic stress, cold, heat, and heavy metals are the primary environmental factors limiting plant growth and agricultural productivity. To adapt to these adverse conditions, plants have evolved a series of physiological and molecular mechanisms over evolutionary timescales. Among these, protein phosphorylation and dephosphorylation play pivotal roles in signal transduction during plant responses to abiotic stressors [1]. Protein phosphorylation is a reversible process mediated by two antagonistic enzymes: protein kinases and phosphatases. Protein kinases perceive diverse environmental signals and activate distinct phosphorylation cascades to regulate the downstream expression of the target gene, thereby enhancing plant resilience against various abiotic stresses. Key plant protein kinase families include receptor-like protein kinases (RLKs), mitogen-activated protein kinases (MAPKs), calcium-dependent protein kinases (CDPKs), and sucrose non-fermenting-1-related protein kinases (SnRKs).

Arabidopsis thaliana contains ten SnRK2 kinases, which are classified into three subfamilies: subfamily I (SnRK2.1, SnRK2.4, SnRK2.5, SnRK2.9, SnRK2.10), subfamily II (SnRK2.7,

SnRK2.8), and subfamily III (SnRK2.2, SnRK2.3, OST1/SnRK2.6) [2–6]. Kinases in subfamily I exhibit no sensitivity to abscisic acid (ABA), kinases in subfamily II show weak or no induction by ABA, whereas kinases in subfamily III are strongly induced by ABA. Notably, SnRK2.2, SnRK2.3, and SnRK2.6 are key components of ABA signaling pathways [7–9]. In the absence of ABA, type-A protein phosphatases PP2Cs (e.g., ABI1) inhibit the kinase activity of SnRK2.2/2.3/2.6 [10–13]. Upon stress exposure, ABA accumulates and binds to PYRAB-ACTIN RESISTANCE1 (PYR1)/PYR1-LIKE (PYL)/REGULATORY COMPONENT OF ABA RECEPTOR (RCAR) receptors, forming a complex that interacts with PP2Cs to relieve their inhibitory effects on SnRK2.2/2.3/2.6. Activated SnRK2 kinases subsequently phosphorylate downstream substrates, positively regulating ABA-responsive pathways [11–14]. These three kinases exhibit functional redundancy; for example, the *snrk2.2/2.3/2.6* triple mutant displays stronger ABA insensitivity compared to single or double mutants [2,6,15]. While *snrk2.2/2.3* mutants exhibit strong resistance to ABA during seed germination and root growth, they show no significant difference in stomatal movement compared to wild-type plants. Conversely, the *snrk2.6* single mutant demonstrates ABA insensitivity in stomatal regulation, accompanied by increased water loss from detached leaves and heightened drought sensitivity. In the *snrk2.2/2.3/2.6* triple mutant, nearly all ABA-responsive downstream genes fail to be activated, resulting in severe ABA insensitivity during seed dormancy, germination, root growth, and stomatal movement. These findings underscore the central regulatory role of subfamily III SnRK2 kinases in ABA signaling [2,10].

Despite extensive studies on ABA-induced activation mechanisms of SnRK2.2/2.3/2.6, the functions and substrates of ABA-independent SnRK2s remain relatively underexplored. This gap is partly due to the high degree of functional redundancy within the SnRK2 kinase family. Single mutants often exhibit minimal developmental phenotypes, complicating the efforts to elucidate the physiological roles of individual members. Fujii et al. generated an *Arabidopsis* decuple mutant (*snrk2.1/2.3/3.4/4.5/5.6/6.7/7.8/8.9/9.10*) and demonstrated that SnRK2s are the primary protein kinases responding to osmotic stress in plants [16]. However, the precise mechanisms underlying the activation of these kinases by osmotic stress remain unclear [11], including potential interactions with known or unknown osmotic stress receptors/sensors. Addressing these questions represents a critical direction for future research.

In this review, we systematically summarize the target proteins of SnRK2s and classify them based on their biological functions, including ABA/stomatal movement, drought, osmotic stress, and cold stress. Additionally, we synthesize existing reports on post-translational modifications of SnRK2s mediated by other proteins.

2. SnRK2 and ABA

The phosphorylation and dephosphorylation of proteins serve as the switches for ABA responses, and the SnRK2 represents a key core component in ABA signal transduction. As a protein kinase, SnRK2 mainly classifies the target proteins it regulates in ABA signaling into two categories: transcription factors and ion channels. Research has demonstrated that downstream transcription factors such as ABF1 [9], ABF2/AREB1 [9,17,18], ABF3 [19], ABF4/AREB2 [17], and ABI5 [9,15] can all be directly phosphorylated by SnRK2, and they are among the earliest and, undoubtedly, one of the most classic and important components of ABA signaling (Table 1).

Numerous studies have demonstrated that the transcription factor RAV1 is a member of the RAV (related to ABI3/VP1) subfamily within the AP2/ERF (APETALA2/Ethylene responsive factor) transcription factor superfamily. RAV1 directly binds to the promoters of *ABI3*, *ABI4*, and *ABI5* to downregulate their expression. The SnRK2.2/2.3/2.6 kinases

interact with and phosphorylate RAV1, thereby reducing RAV1's inhibitory effect on *ABI5* [20].

ABA-responsive kinase substrate 1 (AKS1) is a basic helix-loop-helix (bHLH) transcription factor that typically forms multimeric complexes with DNA. Upon phosphorylation and exposure to ABA, AKS1 undergoes monomerization, which consequently diminishes its transcriptional activation activity [21]. Subsequent studies have indicated that AKS1, as an endogenous phosphorylation substrate, would be phosphorylated by SnRK2s in *Arabidopsis* guard cells in response to ABA [22]. SnRK2.6 can interact with RAP2.6 and phosphorylating it. RAP2.6 can directly bind to the GCC or DREs of *RD29A* and *COR15A*, thereby facilitating their expression [23].

Recent research has shown that SnRK2s play a role in stomatal precursor development and directly phosphorylate SPCH (the main transcription factor for stomatal initiation). SnRK2.2/2.3/2.6 kinases act on specific amino acid residues of SPCH, which mediate the inhibition of SPCH by ABA/drought and the suppression of stomatal formation [24].

In the ion channel aspect, the slow anion channel protein SLAC1 [25–28] and the quick anion channel protein QUAC1 [29] that are closely related to stomatal movement, as well as the potassium ion channel KAT1 [30] and chloride channels AtCLCa [31], are all regulated by SnRK2.6. Additionally, SnRK2.2 phosphorylates AHA2, a PLASMA MEMBRANE PROTON ATPASE [32].

In the recent years, new targets downstream of SnRK2 have been discovered. SnRK2.6 phosphorylates PIP2;1, regulating the stomatal response to ABA [33]. SnRK2.6 can interact with an ATPase in chromatin remodeling complex BRM (BRAHMA) and phosphorylate it in vivo, thereby activating the downstream transcription factor ABI5 [34]. Interestingly, BRM can also interact with the negative regulator of ABA-signaling PP2C, and further studies show that the phosphorylation of BRM by SnRK2.6 is inhibited by PP2C [34]. Additionally, Group C Raf-like protein kinase Raf36/Raf22 can also be phosphorylated by SnRK2.6, serving as a brake for ABA signaling in the downstream of SnRK2 [35].

The ABA-activated calcium channels in the guard cell plasma membrane of *Arabidopsis thaliana* are primarily composed of four members of the CNGC family: CNGC5, CNGC6, CNGC9, and CNGC12 (collectively referred to as CNGC5/6/9/12). ABA activates these CNGC proteins to generate cytosolic calcium signals, thereby inducing stomatal closure [36]. SnRK2.6 directly interacts with CNGC5/6/9/12, targeting their N-terminal regions. Researchers identified a conserved serine residue at the N-terminus of CNGC proteins as the phosphorylation site using proteomics and in vitro protein phosphorylation techniques. Further studies, using point mutations combined with electrophysiology and intracellular Ca^{2+} imaging, demonstrated that an S-to-A mutation at this conserved serine residue significantly inhibits the Ca^{2+} channel activity of CNGC5/6/9/12, while an S-to-D mutation significantly enhances it. Subsequent in vivo experiments revealed that in response to drought and ABA stimulation, plants activate the Ca^{2+} channel activity of CNGCs through SnRK2.6-mediated phosphorylation of the conserved N-terminal serine residue, leading to extracellular Ca^{2+} influx and regulation of cytosolic Ca^{2+} oscillations in guard cells, ultimately controlling stomatal movement. This study elucidates a Ca^{2+}-dependent ABA signaling pathway and demonstrates that this pathway is coupled with another non-Ca^{2+}-dependent signaling branch via SnRK2.6, forming an integrated ABA signal network [37].

The Zhu Jiankang team employed quantitative phosphorylated proteomics to identify multiple targets of SnRK2.6. The researchers compared the overall changes in phosphorylated peptides in WT and *snrk2.2/2.3/2.6* triple mutant seedlings after ABA treatment. ABA increased the phosphorylation of 166 peptides in WT seedlings and decreased the phosphorylation of 117 peptides. In the *snrk2.2/2.3/2.6* triple mutant, 84 of the 166 pep-

tides (representing 58 proteins) failed to be phosphorylated or had a reduced degree of phosphorylation in ABA treatment. In vitro kinase experiments indicated that these 58 proteins could act as substrates for SnRK2s. SnRK2 substrates encompass proteins involved in flower timing regulation, RNA and DNA binding, miRNA and epigenetic regulation, signal transduction, chloroplast function, and numerous other cellular processes. Among them, seven proteins (enhancing the rich level of late embryogenesis abundant (EEL), small conductance mechanosensitive channel 9 (MSL9), superoxide dismutase 2 (FSD2), AREB3, flowering basic helix-loop-helix transcription factor 3 (FBH3), binding to tomato mosaic virus RNA 1 long chain (BTR1L), and chloroplast outer membrane translocon complex 159 (TOC159)) might be phosphorylated by reconstructed SnRK2.6, while another two (arginine/serine-rich Splicing factor 41 (RSP41) and histone deacetylase 2B (HD2B)) could not. These results imply that most of the 58 SnRK2.2/2.3/2.6-dependent phosphorylated proteins are direct substrates of SnRK2s [38]. Moreover, the team reported that SnRK2.6 can phosphorylate thousands of peptide segments in ABA signaling [39]. Similarly, Kazuo Shinozaki's research group identified multiple substrates, including MPK1, SnRK2-substrate 1 (SNS1) [40]. This suggests that phosphoproteomic analysis can identify multiple potential substrates of SnRK2; however, the biological significance of these phosphorylated substrates requires further experimental validation.

Table 1. The substrate proteins that are phosphorylated and regulated by SnRK2 in the ABA signaling pathway.

Substrates	Locus	Phosphorylation Sites	Kinases	Description	Reference
ABF1	AT1G49720	Not determined	SnRK2.2/2.3	bZIP transcription factor	[8]
ABF2/AREB1	AT1G45249	Ser26, Ser86, Ser94	SnRK2.2/2.3/2.6/2.7/2.8	bZIP transcription factor	[8,17,18]
ABF3	AT4G34000	Thr145	SnRK2.6	bZIP transcription factor	[19]
ABF4/AREB2	AT3G19290	Ser39	SnRK2.2/2.3/2.6	bZIP transcription factor	[17]
ABI5	AT2G36270	Not determined	SnRK2.2/2.3/2.6	bZIP transcription factor	[9,15]
RAV1	AT1G13260	Not determined	SnRK2.2/2.3/2.6	AP2/B3 domain transcription factor	[20]
AKS1	AT1G51140	Ser284, Ser288, Ser290	SnRK2.2/2.3/2.7	bHLH transcription factor	[22]
RAP2.6	AT1G43160	Not determined	SnRK2.6	ERF/AP2 transcription factor	[23]
SPCH	AT5G53210	Ser240, Ser271	SnRK2.2/2.3/2.6	bHLH transcription factor	[24]
SLAC1	AT1G12480	Ser59, Ser86, Ser113, Ser120	SnRK2.6	Anion channel	[25–28]
QUAC1	AT4G17970	Not determined	SnRK2.6	Anion channel	[29]

Table 1. *Cont.*

Substrates	Locus	Phosphorylation Sites	Kinases	Description	Reference
KAT1	AT1G04710	Thr306, Thr308	SnRK2.6	Potassium channel	[30]
AtCLCa	AT5G40890	Thr38	SnRK2.6	Chloride channel	[31]
AHA2	AT4G30190	Thr947	SnRK2.2	P-type ATPase	[32]
PIP2;1	AT3G53420	Ser121	SnRK2.6	Aquaporin	[33]
BRM	AT2G46020	Ser1760, Ser1762	SnRK2.6	Chromatin-Remodeling ATPase	[34]
Raf22	AT2G24360	Ser81	SnRK2.6	MAP kinase kinase kinase	[35]
Raf36	AT5G58950	Ser145	SnRK2.6	MAP kinase kinase kinase	[35]
CNGC5	AT5G57940	Ser20	SnRK2.6	Ca^{2+} channel	[37]
CNGC6	AT2G23980	Ser27	SnRK2.6	Ca^{2+} channel	[37]
CNGC9	AT4G30560	Ser26	SnRK2.6	Ca^{2+} channel	[37]
CNGC12	AT2G46450	Ser13	SnRK2.6	Ca^{2+} channel	[37]
EEL	AT2G41070	Not determined	SnRK2.6	Transcription factor	[38]
MSL9	AT5G19520	Not determined	SnRK2.6	Mechanosensitive ion channel	[38]
FSD2	AT5G51100	Not determined	SnRK2.6	Fe superoxide dismutase	[38]
AREB3	AT3G56850	Not determined	SnRK2.6	bZIP transcription factor	[38]
FBH3	AT1G51140	Not determined	SnRK2.6	bHLH transcription factor	[38]
BTR1L	AT5G04430	Not determined	SnRK2.6	Binding to tomv RNA 1L	[38]
TOC159	AT4G02510	Not determined	SnRK2.6	GTPase	[38]
MPK1	AT1G10210	Not determined	SnRK2.6	MAP kinase	[40]
SNS1	AT1G26470	Ser43	SnRK2.6	Chromatin modification-like protein	[40]

3. SnRK2 and Drought

Drought has a significant impact on plant growth and crop yields. The ABA signaling pathway serves as the central hub enabling plants to respond to drought stress. It enhances drought tolerance through a multifaceted approach, including rapid stomatal regulation, gene reprogramming, and morphological adaptation. Single mutants of SnRK2.6 and double mutants of SnRK2.2/2.3 are highly sensitive to drought stress, hence, SnRK2.2/2.3/2.6 exert positive regulation in drought stress response. Multiple substrates have been identified to participate in SnRK2-mediated drought stress response.

K^+ uptake transporter 6 (KUP6) is positively regulated by drought stress. SnRK2.6 interacts with KUP6 and phosphorylates its C-terminal region, enhancing its function under drought conditions [41] (Table 2). NTL6, a plant-specific NAC (NAM/ATAF1/2/CUC2) transcription factor, undergoes proteolytic cleavage in response to biotic stress, which is mediated by abscisic acid. NTL6 directly interacts with SnRK2.8, which primarily phosphorylates Ser-142 of NTL6, thereby modulating its activity. The drought resistance mediated by NTL6 is dependent on the interaction with SnRK2.8 [42]. Additionally, OST1 regulates

ABA-mediated stomatal closure through proteins other than ion channels. The ubiquitin ligase RAFP34 (ring zinc-finger protein34)/CHYR1 (CHY zinc-finger and ring protein1 [CHYR1]) is regulating the ABA-induced stomatal closure, active oxygen production, and drought resistance process. CHCY1 is mainly expressed in the vascular tissue and guard cells. SnRK2.2/2.3/2.6 interacts with CHYR1 and phosphorylates the Ser-178 of CHYR1 protein. The *chyr1* mutant seed germination and stomatal closure are insensitive to ABA and have increased sensitivity to drought. Overexpression of CHYR1T178A or CHYR1T178D show drought-sensitive and drought-resistant phenotypes, respectively. This indicates that OST1 can regulate the ubiquitin ligase activity of CHYR1 through phosphorylation, thereby positively regulating the role of ABA signaling in stomatal closure [43].

In addition to the ABF family of transcription factors, researchers have identified AtHAT1, a HD-ZIP class transcription factor in *Arabidopsis*, as a substrate of SnRK2.3. HAT1 functions as a negative regulator of ABA biosynthesis and drought stress responses in *Arabidopsis*. Overexpression of AtHAT1 suppresses ABA synthesis and consequently diminishes plant drought tolerance. Phosphorylation of HAT1 by SnRK2.3 reduces its activity, thereby alleviating its negative regulatory effects on ABA signaling and drought response pathways [44].

ABA and cytokinin exert antagonistic effects in numerous developmental processes and environmental stress responses of plants. SnRK2.2, SnRK2.3, and SnRK2.6 directly interact with type A response regulator 5 (ARR5), a negative regulator of the cytokinin signaling pathway, and phosphorylate it. The phosphorylation of serine residues on the ARR5 protein by the SnRK2s enhances its stability. Consequently, plants with overexpression of ARR5 display ABA sensitivity and drought resistance. Additionally, B-type ARRs ARR1, ARR11, and ARR12 physically interact with the SnRK2s and inhibit the kinase activity of SnRK2.6. The *arr1/11/12* triple mutants are sensitive to ABA. Genetic analysis indicates that the SnRK2s are upstream of ARR5 and downstream of ARR1, ARR11, and ARR12, playing an important role in regulating ABA responses and drought resistance [45].

Researchers identified a drought-tolerant mutant, *ppd5-2*, from a T-DNA insertion mutant library of nuclear-encoded chloroplast protein in *Arabidopsis thaliana* through a screening method. Further studies disclosed that PPD5 interacts with and is phosphorylated by OST1. The phosphorylation of PPD5 by OST1 increases its protein stability, but does not influence its chloroplast localization [46].

SnRK2.6/OST1 mediates microtubule disassembly during ABA-induced stomatal closure in *Arabidopsis thaliana*. Researchers have identified MAP SPIRAL1 (SPR1) as a substrate of OST1. OST1 interacts with and phosphorylates SPR1 at Ser-6, promoting the dissociation of SPR1 from microtubules and driving microtubule disassembly. Compared to wild-type plants, *spr1* mutants exhibit significantly increased water loss and reduced ABA responses, including impaired stomatal closure and microtubule disassembly in guard cells. These phenotypes were restored by introducing the phosphorylated active form of SPR1. SPR1 positively regulates microtubule disassembly during ABA-induced stomatal closure, which is dependent on OST1-mediated phosphorylation. These results reveal a critical role for SPR1 in ABA signaling and highlight the specific interaction between ABA signaling components and microtubule-associated proteins (MAPs) [47].

RAF22 [(Rapidly Accelerated Fibrosarcoma)-like mitogen-activated protein kinase kinase kinase 22] physically interacts with ABI1 (ABA insensitive 1) and phosphorylates the Ser-416 residue of ABI1 to enhance its phosphatase activity. Additionally, ABI1 can also dephosphorylate to enhance the activity of RAF22, thereby inhibiting ABA signal transduction and maintaining plant growth under normal conditions. Under drought stress conditions, SnRK2.6/OST1 activated by ABA phosphorylates the Ser-81 residue of RAF22 to inhibit its kinase activity and thereby inhibit its enhancement of ABI1 activity [48].

SNF1-related protein kinase 2 (SnRK2) substrate 1 (SNS1) is a negative regulator of ABA and drought stress and can be phosphorylated by SnRK2 in vivo [40,49,50]. We have noticed that VARICOSE (VCS), an mRNA decapping activator, serves as a substrate for multiple peptide segments of SnRK2.2/2.3/2.6 [40]. Subsequently, two independent research groups have verified that VCS is a target protein of the SnRK2 Group I family members [51,52]. Under drought stress conditions, multiple members of the SnRK2 Group I phosphorylate VCS, and the knockdown plants of VCS reduces its tolerance to drought stress [51]. Another research revealed that VCS and varicose-related (VCR) are both interactors and phosphorylation targets of SnRK2.5, SnRK2.6, and SnRK2.10. These three protein kinases phosphorylate VCS at Ser-645 and Ser-1156, and SnRK2.6 and SnRK2.10 also phosphorylate VCR at Ser-692 and Ser-680. The SnRK2 proteins of the Group I family, VCS, and XRN4 are involved in the regulation of root growth under normal conditions and the modulation of root morphology under salt stress [52].

Non-ABA-activated *Arabidopsis* SnRK2s (SnRK2.10) not only regulate the plant's response to salt stress but also modulate its sensitivity to dehydration. Through phosphoproteomic analysis, several potential SnRK2.10 substrates were identified, including dehydrins ERD10 and ERD14. In vitro experiments confirmed that SnRK2.10 phosphorylates ERD14 and Ser-79 of ERF14, altering its subcellular localization [53,54]. Additionally, non-ABA-dependent SnRK2.4 phosphorylates the water channel protein PIP2;1 at Ser-121 [55].

Furthermore, numerous proteins such as MLP43, SASP, and PIA1 can interact with one or more members of the SnRK2 family; however, there is a dearth of direct evidence regarding whether they serve as direct phosphorylation substrates of SnRK2s in the drought stress response [56–58].

Table 2. The substrate proteins that are phosphorylated and regulated by SnRK2 in the drought stress tolerance.

Substrates	Locus	Phosphorylation Sites	Kinases	Description	Reference
KUP6	AT1G70300	Thr-759	SnRK2.6	K^+ uptake transporter	[41]
NTL6	AT3G49530	Thr-142	SnRK2.8	Transcription factor	[42]
CHYR1	AT5G22920	Thr-178	SnRK2.6	Ubiquitin E3 ligase	[43]
HAT1	AT4G17460	Not determined	SnRK2.3	Transcription factor	[44]
ARR5	AT3G48100	Ser-21, Ser-33, Ser-72, and Ser-117	SnRK2.2/2.3/2.6	Transcription repressor	[45]
PPD5	AT5G11450	Thr-283	SnRK2.6	PsbP-domain proteins	[46]
SPR1	AT2G03680	Ser-6	SnRK2.6	MAP SPIRAL1	[47]
Raf22	AT2G24360	Ser-81	SnRK2.6	MAP Kinase Kinase Kinase	[48]
SNS1	AT1G26470	Ser-43	SnRK2.6	Chromatin modification-like protein	[49]
VCS	AT3G13300	Not determined	SnRK2.4/2.10/2.1/2.5	VARICOSE	[51]
VCS	AT3G13300	Thr-644, Thr-645, Ser-1156	SnRK2.5	VARICOSE	[52]
VCS	AT3G13300	Thr-644, Thr-645, Ser-692, Ser-1156	SnRK2.6	VARICOSE	[52]
VCS	AT3G13300	Thr-645, Ser-692, Ser-1155, Ser-1156	SnRK2.10	VARICOSE	[52]
ERD10	AT1G20450	Ser-22/23/61/65/106/107/208, Thr-49/213/214/221	SnRK2.10	Dehydrin protein	[53]
ERD14	AT1G76180	Ser-21, Thr-26, Ser-78, Ser-79, Ser-136	SnRK2.10	Dehydrin protein	[53]
PIP2;1	AT3G53420	Ser-121	SnRK2.4/2.10/2.1/2.5	Aquaporin	[55]

4. SnRK2 and Cold

Apart from its significant role in drought and osmotic stress, the SnRK2 kinase also exerts a considerable influence in cold stress. The C-repeat (CRT)-binding factors (CBFs) or dehydration-responsive element (DRE)-binding protein (DREB) can bind to the cis-

element of CRT/DRE and trigger the transcription of downstream COR genes, thereby enhancing cold tolerance [59–61]. ICE1 is the core transcription factor in cold stress and positively regulates the expression of CBFs. OST1 phosphorylates ICE1 at position Ser-278 and enhances the protein stability and transcription activation ability of ICE1 during cold stress, thereby strengthening plant cold tolerance [62,63] (Table 3). Meanwhile, MPK3/6 negatively regulates the protein stability of ICE1, thus reducing plant cold tolerance [64]. Subsequently, the research group reported that BTF3/BTF3L, PUB25/PUB26, ANN1, and PP2CG1 are also phosphorylation substrates of OST1 [65–67].

Table 3. The substrate proteins that are phosphorylated and regulated by SnRK2 in the cold stress tolerance.

Substrates	Locus	Phosphorylation Sites	Kinases	Description	Reference
ICE1	AT3G26744	Ser-278	SnRK2.6	Transcription factor	[62]
BTF3	AT1G17880	Not determined	SnRK2.6	NAC transcription factor	[65]
BTF3L	AT1G73230	Ser-50	SnRK2.6	NAC transcription factor	[65]
PUB25	AT3G19380	Thr-95	SnRK2.6	E3 ligase	[66]
PUB26	AT1G49780	Thr-94	SnRK2.6	E3 ligase	[66]
ANN1	AT1G35720	Ser-289	SnRK2.6	Calcium transporter	[67]
EGR2	AT5G27930	Not determined	SnRK2.6	E growth-regulating 2	[68]
PP2CG1	AT2G33700	Ser-365	SnRK2.6	Protein phosphatase 2C	[69]

BTF3 and BTF3L (BTF3-like), the β-subunits of the nascent polypeptide-associated complex (NAC), are phosphorylated at position Ser-50 by OST1, and OST1 enhances the interaction between BTF3 and CBFs under cold stress [65]. Two U-box type E3 ubiquitin ligases, PUB25/26, plays a crucial role in cold stress responses. In the *pub25 pub26* double mutant, the levels of CBFs are significantly reduced compared to wild-type plants, leading to increased cold sensitivity. Further studies have shown that PUB25/26 interacts with MYB15 and participates in its degradation during the early stages of cold treatment. Additionally, the Thr-94 and Thr-95 sites of PUB25/26 serve as target sites of OST1. Cold-activated OST1 phosphorylates PUB25/26 at these sites, enhancing its E3 ligase activity and promoting the ubiquitination and degradation of MYB15. This process positively regulates the induction of CBFs under cold stress and contributes to plant cold tolerance [66].

Yang Shu-hua's research group utilized biochemical, molecular genetics, and electrophysiological approaches to discover that the calcium ion transporter protein AtANN1 plays a crucial role in low-temperature-induced calcium signaling. Their findings indicate that in the atann1 knockout mutant, the low-temperature-induced $[Ca^{2+}]_{cyt}$ is significantly reduced compared to wild-type plants. Additionally, the expression levels of key cold-responsive transcription factors CBFs and their downstream target genes COR are decreased, leading to diminished cold tolerance in Arabidopsis. These results suggest that AtANN1 influences the influx of low-temperature-mediated calcium signals, thereby regulating the CBF-COR-dependent cold signaling pathway and positively modulating plant cold tolerance. Furthermore, low-temperature-activated OST1 phosphorylates Ser-289 of the AtANN1 protein, enhancing its calcium transport activity and calcium binding affinity, which in turn regulates the generation of low-temperature-induced calcium signals [67].

Additionally, the kinase activity of OST1 in cold stress can be inhibited by the phosphatases EGR2 and PP2CG1 [68,69]. EGR2, a phosphatase localized to the cell membrane, interacts with OST1 and weakens its kinase activity, negatively regulating cold stress [68]. Simultaneously, low temperature induces OST1 to phosphorylate Ser-365 of PP2CG1, resulting in a decrease in the protein phosphatase activity of PP2CG1 and significantly affecting plant cold tolerance [69].

Therefore, OST1 is a core protein kinase in the cold stress response, regulating its activity through phosphorylation to enhance protein stability and positively regulate the cold stress response.

5. SnRK2 and Other Vital Biological Processes

In addition to positively regulating responses to drought and cold stress, the SnRK2 kinase family is also extensively implicated in various other biological processes, such as salt stress tolerance, pathogen defense, reactive oxygen species (ROS) generation, cell wall biosynthesis, and microRNAs biogenesis. The following sections will address each of these functions in detail.

Plants have evolved sophisticated signaling mechanisms to redirect growth away from adverse environmental conditions that compromise yield. Root gravitropism, characterized by sodium ion gradient-dependent directional growth, plays a pivotal role in salt stress adaptation. Despite its early discovery, the molecular basis of gravitropic responses under saline conditions remained elusive. Recent studies demonstrate that abscisic acid (ABA)-mediated root curvature governs *Arabidopsis* gravitropism through SnRK2.6 kinase activation. ABA-activated SnRK2.6 phosphorylates SP2L at Ser-406 induce asymmetric cell expansion in the root transition zone via cortical microtubule reorganization. Salt stress initiates SP2L-dependent reorientation of cell wall microtubules, which template cellulose microfibril deposition patterns. These structural modifications drive anisotropic cell wall extension, determining root tip curvature orientation. This molecular cascade elucidates how microtubule-guided microfibril alignment mediates differential cellular expansion, establishing a mechanistic framework for root salt-avoidance behavior. Crucially, salt stress triggers ABA-dependent SnRK2.6 activation, which phosphorylates the microtubule-associated protein SP2L to regulate microtubule array dynamics. This post-translational modification ultimately controls cellulose synthesis directionality and cellular expansion polarity in the root transition zone, enabling directional root growth away from saline substrates [70] (Table 4).

The MYB transcription factor NIGT1.4 is an important component in maintaining root growth under salt stress. T-DNA knockout mutation and functional complementation experiments have verified that NIGT1.4 functions in promoting the growth of the main root under salt stress. NaCl treatment induces the expression of NIGT1.4 in roots in an ABA-dependent manner. SnRK2.2 and SnRK2.3 interact with NIGT1.4 and phosphorylate it. The main root growth phenotype of the *snrk2.2/2.3/2.6* triple plant is like that of the *nigt1.4* mutant which both demonstrating salt stress sensitivity [71].

In plants the site infected by pathogens will exhibit necrotic lesions, and subsequently induce systemic acquired resistance (SAR) in distant tissues. NPR1 is a key regulator of SAR induced by SA. SnRK2.8 phosphorylates NPR1 and is indispensable for NPR1 to enter the nucleus. In *Arabidopsis*, the development of systemic immunity is mediated by SA signaling and SnRK2.8-mediated phosphorylation, which synergistically activate NPR1 in a double-reaction manner [72]. Later, it was confirmed that SnRK2.8-mediated phosphorylation of NPR1 is also necessary for NPR1 to enter the nucleus at low temperatures [73]. Besides phosphorylating NPR1, SnRK2.8 can also phosphorylate the effector protein AvrPtoB. SnRK2.8 interacts with AvrPtoB in yeast and plants. SnRK2.8 is essential for the virulence functions of AvrPtoB,

including promoting bacterial colonization, inhibiting pectin deposition, and targeting plant defense regulatory factors NPR1 and receptor FLS2 [74].

Previous studies have shown that SnRK2.6/OST1 directly interacts with RBOHD and RBOHF [75]. OST1 phosphorylates Ser13 and Ser174 of AtRBOHF, triggering the production of ROS in guard cells, leading to stomatal closure and enhanced plant tolerance to drought and salt stress [76]. The activity of AtRBOHF can also be regulated by phosphorylation by CIPK11 and CIPK26 [77]. Similarly, Ser-343 and Ser-347 of AtRBOHD are targets of OST1, which are crucial for plant cell-to-cell active oxygen signaling under high light stress [78,79].

NRT1.1/NPF6.3/chlorate-resistant 1 (CHL1) is the first identified nitrate transporter, and it is surprising that SnRK2.2/2.3/2.6 interacts with NRT1.1 in vitro and in vivo, and phosphorylates Ser-585 of NRT1.1. Phosphorylation of NRT1.1 by SnRK2s leads to a significant reduction in nitrate uptake and affects root growth [80].

In *Arabidopsis*, the formation of plant secondary cell wall (SCW) is reduced due to genetic blockage of ABA synthesis and perception. SnRK2.2/2.3/2.6 can interact with AtNST1 and phosphorylate it, where AtNST1 is a master regulatory factor that enhances SCW formation and lignin deposition in the stem fiber region. SnRK2-mediated phosphorylation mutations at the regulatory sites of AtNST1 would eliminate the regulatory function of this transcription factor [81].

MicroRNA (miRNA), a 20–24 nucleotide non-coding RNA ubiquitous in eukaryotes, regulates mRNA splicing/translation and governs plant developmental processes and stress responses. The miRNA biogenesis machinery relies on core components including DCL1 (type III ribonuclease), SE (zinc finger protein), and HYL1 (dsRNA-binding protein). While phytohormone ABA and osmotic stress signaling are known to modulate miRNA accumulation, their mechanistic interplay remained unclear. The Zhu Jiankang research group revealed that SnRK2 kinases—central regulators of ABA and osmotic stress pathways—directly orchestrate miRNA synthesis by phosphorylating core biogenesis components. *snrk2.2/2.3/2.6* mutants exhibited reduced miR160 and related miRNAs, accompanied by elevated pri-miRNA levels and target gene expression. Notably, HYL1 protein abundance declined in snrk2 triple/decuple mutants. Phosphorylation assays further implicated HYL1 and SE as SnRK2 substrates. This work elucidates SnRK2-mediated phosphorylation as a molecular bridge linking ABA/osmotic stress to miRNA biogenesis regulation [82].

Table 4. The substrate proteins that are phosphorylated and regulated by SnRK2 in the stress network.

Substrates	Locus	Phosphorylation Sites	Kinases	Description	Reference
SP2L	AT1G50890	Ser-406	SnRK2.6	Microtubule associated protein	[70]
NIGT1.4	AT1G13300	Not determined	SnRK2.2/2.3	MYB transcription factor	[71]
NPR1	AT1G64280	Ser-589, Thr-373	SnRK2.8	NONEXPRESSER OF PR GENES 1	[72]
AvrPtoB		Ser-258	SnRK2.8	*Pseudomonas* effector	[74]
RBOHD	AT5G47910	Ser-163	SnRK2.6	NADPH oxidase	[76]
RBOHF	AT1G64060	Ser-13, Ser-174	SnRK2.6	NADPH oxidase	[76]
RBOHD	AT5G47910	Ser-343, Ser-347	SnRK2.6	NADPH oxidase	[78]
NRT1.1	AT1G12110	Ser-585	SnRK2.2/2.3/2.6	Nitrate transporter	[80]
NST1	AT2G46770	Ser-316	SnRK2.2/2.3/2.6	NAC transcription factor	[81]
HYL1	AT1G09700		SnRK2.4/2.6	Hyponastic leaves 1	[82]
SE	AT2G27100		SnRK2.4/2.6	Serrate	[82]

6. Post-Translational Modification of SnRK2

SnRK2s not only serves as a substrate for protein kinase phosphorylation, but it can also act as a target and present various post-translational modifications, including phosphorylation, SUMOylation, ubiquitination, S-nitrosylation, sulfation, and glycosylation.

6.1. Phosphorylation

In the same year, research groups led by Wang Pengcheng in China, Julian Schroeder in the United States, and Yamaguchi-Shinozaki in Japan published research papers in Nature Communications, revealing that the B subfamily of RAF protein kinases mediates the phosphorylation and activation of SnRK2 [83,84]. Wang Pengcheng's research group discovered that some B2/3 subfamily RAF protein kinases phosphorylate and activate SnRK2.2/2.3/2.6, while the B4 subfamily RAF protein kinases phosphorylate and activate the other six ABA-independent SnRK2s [83]. The Yamaguchi-Shinozaki's research group discovered that three B4 Raf-like MAPKKKs (RAF18, RAF20, and RAF24) in *Arabidopsis* can interact with Group I SnRK2 proteins and phosphorylate and activate the Group I SnRK2s that are not responsive to ABA in stress conditions, but these three B4 Raf-like MAPKKKs are not activated by ABA and do not participate in the activation of Group III SnRK2s [84]. Julian Schroeder's research group discovered that three B3 Raf-like MAPKKKs (MAPKKK δ1, MAPKKK δ6, and MAPKKK δ7) can phosphorylate the Ser-171 residue of SnRK2.6, which cannot be self-phosphorylated to activate it, to reactivate SnRK2.6 [85]. These three studies jointly disclose the crucial role of the RAF-SnRK2 kinase cascade in osmotic stress and ABA signaling pathways. Other reported RAF kinases involved in the phosphorylation of SnRK2 encompass ARK1/2/3 and Raf10 [86,87]. The RAF family of kinases pertains to the MAP kinase kinase kinase, and RAF mediates the self-activation of SnRK2 through phosphorylation to commence the activation process of SnRK2. These studies connect the MAPK cascade and SnRK2 kinases, suggesting that the regulation among different kinases might be a universal mechanism within cells.

Furthermore, it has been reported that the protein kinases involved in the phosphorylation of the SnRK2 complex encompass BAK1, BIN2, ARK, HT1, and so on. BAK1 forms a complex with other lysine-rich repeat receptor-like kinases (LRR-RLKs), such as FLS2 and EFR1, which are implicated in plant basal immune responses triggered by flg22 and elf18 or elf26 [88,89]. Researchers have discovered that the BRI1-associated Receptor Kinase 1 (BAK1) mutant loses water more rapidly than the wild type and is insensitive to ABA-induced stomatal movement. ABA treatment fails to induce the expression of OST1 and the production of ROS in the *bak1* mutant. The overexpression of OST1 cannot complementation for the insensitivity of *bak1* to ABA. BAK1 forms a complex with OST1 and phosphorylates it, and ABA treatment leads to an increase in the BAK1/OST1 complex, thereby enhancing downstream signaling. This suggests that BAK1 mediates the ABA-induced stomatal movement process via OST1 [90].

The research group led by Gong Zhizhong identified that the *Arabidopsis* BRI1-associated Receptor Kinase 1 (BAK1) loss-of-function mutant, *bak1*, exhibits hypersensitivity to ABA in seed germination and primary root growth. Specifically, the ABA-induced OST1 activity in the *bak1-4* mutant is significantly higher than in the wild type, accompanied by elevated transcription levels of downstream ABA-responsive genes. These findings suggest that BAK1 negatively regulates core ABA signaling output. This conclusion contrasts with the earlier report, which indicated that BAK1 promotes OST1 activity [89]. Moreover, the *bak1* mutant displays distinct responses to ABA in seed germination and primary root growth compared to the wild type. Activated BAK1 can phosphorylate OST1 at the Thr-146 site, directly inhibiting its kinase activity. Additionally, BAK1 can phosphorylate

ABI1 within the PYR1-ABA-ABI1 complex, releasing inhibited ABI1 and further negatively regulating core ABA signaling [91].

Arabidopsis thaliana Glycogen synthase kinase 3 (GSK3)-like kinases exert significant roles in plant growth and development, as well as in stress responses. BIN2 interacts with the members of Group III subfamily of SnRK2 kinases and phosphorylates SnRK2.2 at Thr-181 and Thr180 of SnRK2.3, and enhances the kinase activity of SnRK2.3, thereby exerting a positive regulatory effect in ABA signaling [92].

Casein kinase 2 (CK2) regulates the SnRK2 kinase by phosphorylating several conserved serines in the ABA box of the SnRK2 protein, enhancing its interaction with the negative regulatory factor PP2C in the core ABA signaling module [93].

HT1 (high leaf temperature 1) 13 and carbonic anhydrase (CA) 17 are two constituents that seemingly are specifically involved in the carbon dioxide sensing pathway. The *HT1* gene encodes a protein kinase primarily expressed in guard cells and functions as a major negative regulator of CO_2-induced stomatal closure. Intriguingly, HT1, a negative regulator of CO_2-induced stomatal closure, is capable of phosphorylating OST1 and inhibiting the phosphorylation of SLAC1 by OST1 [94].

SnRK2s also partake in the response to high Mg^{2+} concentration stress. CIPK26 (CBL-Interacting Protein Kinase 26) was identified through immunoprecipitation and liquid chromatography-tandem mass spectrometry analysis as a protein interacting with SnRK2.2. CIPK3, CIPK9, and CIPK23 also interact with SnRK2.2 in vivo. In vitro experiments demonstrated that CIPK26 can phosphorylate and activate SnRK2.2. Under high Mg^{2+} conditions, both the *snrk2.2/2.3/2.6* triple mutant and the *cipk26/3/9/23* quadruple mutant present similar phenotypes of shorter aboveground parts [95].

Terrestrial plants employ evolutionarily conserved osmostress adaptation mechanisms, including the activation of SnRK2s, ABA accumulation, and ABA-dependent signaling. As osmotic stress responses often antagonize growth, these pathways are suppressed under non-stress conditions through clade A protein phosphatase 2Cs (PP2Cs), which act as negative regulators by constitutively binding to SnRK2s. PP2Cs maintain SnRK2s in an inactive state via dephosphorylation of conserved serine residues in their activation loops and steric obstruction of catalytic sites. During osmotic stress or ABA signaling, PP2C-mediated inhibition must be relieved to enable SnRK2 activation. The Zhao Yang group demonstrated that *Arabidopsis* receptor-like cytoplasmic kinase BIK1 orchestrates this regulatory switch by phosphorylating SnRK2.6. While the dominant *abi1-1* mutation (G180D) disrupts PYL-PP2C interactions and impairs PYL-mediated SnRK2 release, BIK1 bypasses this defect by directly phosphorylating SnRK2.6 at two critical tyrosine residues (Tyr-163/182). This phosphorylation event likely disrupts PP2C binding by interfering with the tryptophan "lock-and-key" interface between PP2Cs and SnRK2.6. Phenotypic analysis revealed that *bik1* mutants exhibit compromised SnRK2 activation, attenuated stress-responsive gene expression, reduced ABA biosynthesis, impaired growth homeostasis, and accelerated water loss under osmotic challenge [96].

Osmotic stress perception and signaling involve intricate mechanisms, with transient cytosolic Ca^{2+} elevation and rapid SnRK2 kinase activation representing primary early responses. Leveraging wild-type Arabidopsis (Col-0) and a *pyl* duodecuple mutant deficient in ABA receptors, Zhao Yang's team employed quantitative phosphoproteomics to identify 19 putative early-responsive kinases under osmotic challenge. Among these, CPK3/4/6/11/27 emerged as Ca^{2+}-dependent decoders of osmotic stress, exhibiting activation upon mannitol treatment or dehydration. Functional analyses revealed enhanced SnRK2 activation in CPK3/4/6/11/27 overexpression lines versus impaired responses in *cpk3/4/6/11/27* loss-of-function mutants. Mechanistically, CPKs phosphorylate seven conserved residues (S164/S166/S167/S171/S175/T176/T179) within SnRK2's activation loop,

with mutational studies confirming these phosphorylation events as essential for SnRK2.6 catalytic activity and physiological function. These findings establish CPK3/4/6/11/27 as critical mediators linking Ca^{2+} signaling to SnRK2 activation through multisite phosphorylation during osmotic stress adaptation [97].

6.2. Ubiquitination

A research team has discovered that SnRK2.3 can be ubiquitinated and degraded by AtPP2-B11, an F-BOX protein that is part of the SKP1/Cullin/F-BOX E3 ubiquitin ligase complex. The expression of *AtPP2-B1* is induced by ABA, and mutants with downregulated *AtPP2-B11* expression show hypersensitivity to ABA during seed germination and seedling growth. Overexpression of *AtPP2-B11* suppresses the ABA-hypersensitive phenotype of SnRK2.3 overexpression plants. This suggests that AtPP2-B11 can specifically degrade SnRK2.3 to negatively regulate plant responses to ABA [98]. Subsequently, researchers have also revealed that HOS15 (high osmotic stress 15) can facilitate the ubiquitination of SnRK2.6, leading to its degradation by the 26S proteasome. HOS15 is a substrate-receiving protein within the CUL4-DDB1 E3 ubiquitin ligase complex. The *hos15* mutants exhibit enhanced stability of the OST1 protein and are hypersensitive to ABA, showing strong tolerance to drought stress. The absence of OST1 function can significantly restrain the drought-sensitive phenotype of *hos15*. Simultaneously, ABA inhibits the interaction between HOS15 and OST1, thereby enhancing the stability of OST1. Moreover, ABI1 and ABI2 can promote the interaction between HOS15 and OST1 by dephosphorylating OST1 and subsequently facilitating its ubiquitination and degradation [99]. In later reports, there is direct evidence indicating that ubiquitin can interact directly with SnRK2.2/2.3 and inhibit their kinase activity [100].

6.3. SUMOylation

In 2022, two independent research groups almost concurrently reported that the SUMO protease ESD4 and its interacting protein NUA (nuclear pore anchor) regulate the stability of SnRK2.6/OST1 through deSUMOylation, thereby negatively modulating the ABA signaling pathway. In vitro SUMOylation experiments demonstrated that the SnRK2.6 protein can undergo SUMOylation, while ESD4 reduces the SUMOylation level of SnRK2.6. Hence, NUA and ESD4 might be capable of reducing protein stability by means of deSUMOylation [101,102]. Meanwhile, SnRK2.6/OST1 is also degraded by the HOS15 ubiquitin ligase via ubiquitination. Thus, it is hypothesized that SUMOylation is likely to enhance protein stability by competing with ubiquitin for binding to lysine residues on the protein.

6.4. S-Nitrosylation

ABA induces the generation of nitric oxide (NO) in guard cells, and the 137th cysteine residue near the kinase catalytic site of the OST1 protein can be sulfhydryl nitrosylated. The loss of function of the glutathione S-transferase omega (GSNOR) would give rise to the accumulation of nitric oxide in *gsnor1–3* mutant guard cells, leading to constitutive sulfhydryl nitrosylation of OST1 and ultimately blocking ABA-induced stomatal closure. Transforming the 137th cysteine residue of OST1 to serine and introducing it into the *gsnor1–2 ost1–3* double mutant can partially restrain the phenotype of *gsnor1–2* mutant guard cells that fail to close their stomata in response to ABA treatment. This indicates that nitric oxide can inhibit the kinase activity of OST1 via the sulfhydryl nitrosylation mechanism, thereby participating in ABA-mediated stomatal closure [103,104].

6.5. S-Persulfidation

Hydrogen sulfide (H_2S), a water-soluble gas, plays a crucial role in regulating plant responses to environmental stress and growth. The formation of excessive sulfhydryl

groups (with the conversion of Cys-SH to Cys-SSH), caused by the post-translational modification (PTM) of Cys residues and known as persulfidation, is directly regulated by H_2S. Protein persulfidation proteomics data indicate that the SnRK2.6 protein undergoes persulfidation modification. Two persulfidation modification sites have been identified in SnRK2.6, and it has been discovered that these two Cys residues are exposed on the surface of SnRK2.6 and are adjacent to the catalytic ring and a key phosphorylation site of the kinase. Research reveals that when these two Cys residues are persulfidation-modified, they enhance the activity of SnRK2.6 and its interaction with downstream transcription factors of the ABA signal transduction. Furthermore, when Cys131, Cys137, or both were partially or completely replaced with serine in SnRK2.6C131S, SnRK2.6C137S, or SnRK2.6C131SC137S, these partially or fully substituted proteins were unable to restore the *ost1–3* mutant phenotype, displayed a reduced sensitivity to ABA and H_2S-induced stomatal closure and Ca^{2+} influx, increased water loss, and decreased drought tolerance. The persulfidation reaction of SnRK2.6 has been demonstrated to positively regulate ABA signal transduction in guard cells. Therefore, this study proposed a novel mechanism for regulating the ABA signaling pathway, where H_2S positively regulates ABA signal transduction in guard cells through persulfidation of SnRK2.6 [105]. In the subsequent year, the research group reported that hydrogen sulfide (H_2S)-mediated S-persulfidation can modify the structure of the key kinase protein SnRK2.6 in the ABA signaling pathway, thereby enhancing its efficiency in transferring ATP-γ-phosphate groups and leading to increased kinase activity. The study also demonstrated that the phosphorylation level at critical sites of the SnRK2.6 protein positively regulates H_2S-mediated S-sulfhydration [106]. The proposed mechanism of interaction between post-translational modifications not only provides novel insights into the field of protein post-translational modification but also offers theoretical support for understanding plant drought tolerance mechanisms [107,108].

6.6. Tyrosine Sulfation

In recent reports, a novel mechanism for ABA signal transduction "brake/desensitization" via tyrosine sulfation modification has been disclosed. Tyrosylprotein sulfotransferase (TPST) catalyzes the sulfhydryl (-SO_3H) modification of the tyrosine residue (Y) in the substrate protein, thereby regulating the activity, stability, and protein–protein interactions of the substrate protein. There is only one TPST member in the *Arabidopsis* genome, and this study found that *Arabidopsis tpst* mutants are hypersensitive to ABA and that the ABA signal transduction pathway is overly activated in these mutants. Further studies demonstrated that TPST interacts with and sulfhydrylates the key kinase SnRK2.2/2.3/2.6 in the ABA signal transduction pathway, resulting in a significant reduction in the stability of the sulfhydrylated SnRK2.2/2.3/2.6 proteins and their rapid degradation through the 26S proteasome pathway, thereby reducing the intensity of ABA signal transduction and preventing ABA signals from being overly activated for an extended period of time [109].

6.7. N-Glycosylation

The most recent research outcomes indicate that SnRK2s can also undergo N-glycosylation modification. Through mutant screening, researchers found that mutant enzymes for N-glycosylation modification display a sensitive phenotype when exposed to exogenous ABA. They further discovered that the expression of N-glycosylation modification enzymes increased when plants were treated with ABA for an extended period. Subsequently, by employing molecular biology and cell biology techniques, they determined that prolonging the ABA treatment time enables N-glycosylation modification enzymes to bind to SnRK2.2/2.3 and carry out N-glycosylation modification on them. SnRK2.2/2.3 is a key factor in the ABA signal transduction pathway. When plants are

treated with ABA for a short duration, SnRK2.2/2.3 mainly localizes in the nucleus of cells, activating the expression of ABA response genes and rapidly enhancing plant tolerance to stress. When the ABA treatment time is prolonged, SnRK2.2/2.3 undergoes N-glycosylation modification and gradually transitions from a nuclear localization to a peroxisome localization [110].

7. Conclusions and Future Prospects

The SnRK2 kinase family serves as a central regulatory node governing plant responses to abiotic and biotic stresses as well as developmental processes. This review comprehensively analyzes the known phosphorylation targets of SnRK2 kinases, establishing a functional framework wherein these kinases orchestrate diverse physiological outcomes through substrate-specific phosphorylation cascades (Figure 1). Notably, current research disproportionately focuses on ABA-responsive members (SnRK2.2/2.3/2.6), leaving seven ABA-independent isoforms largely uncharacterized. Given their established importance in osmotic stress adaptation, systematic investigation of these understudied kinases is imperative to elucidate their potential roles in alternative signaling networks.

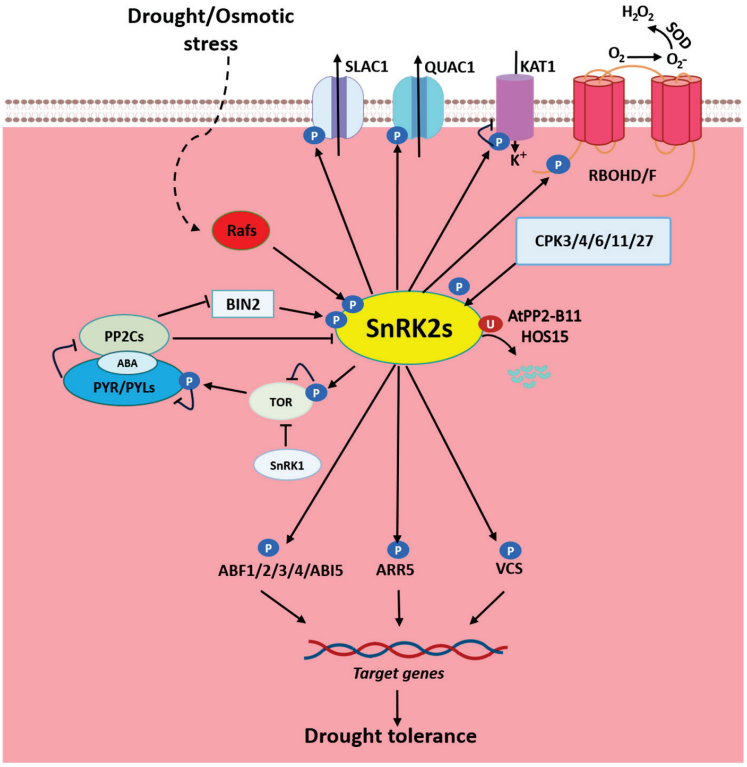

Figure 1. Mechanism of SnRK2 as the core protein kinase in ABA signaling during drought stress. Under ABA-absent conditions, the PP2C phosphatase inhibits the activity of the SnRK2 kinase via dephosphorylation, maintaining SnRK2 in an inactive state. Upon ABA binding, the affinity of PYL receptors for PP2C is enhanced, leading to the formation of the ABA-PYL-PP2C ternary complex. This complex directly suppresses the phosphatase activity of PP2C, thereby relieving its inhibition of SnRK2. Once freed from PP2C suppression, SnRK2 is activated through autophosphorylation or phosphorylation by other kinases (e.g., Raf, CPK, BIN2). The activated, phosphorylated SnRK2 translocates into the nucleus, where it phosphorylates the transcription factors (e.g., ABF1/2/3/4, ABI5, ARR5) and the P-BODY component VCS, driving the expression of stress-responsive genes to enhance plant drought tolerance. Simultaneously, SnRK2 phosphorylates ion channel proteins such as SLAC1, QUAC1, KAT1 (regulating stomatal closure) and RBOHD/F (modulating ROS production). Additionally, SnRK2 activity is regulated by post-translational modifications, including ubiquitination mediated by HOS15 and PP2-B11. This integrated mechanism coordinates gene expression, ion transport, and ROS signaling to bolster plant adaptation to drought stress.

Emerging evidence suggests SnRK2 kinases as master regulators of stress signaling, stomatal dynamics, redox homeostasis, and developmental plasticity. The ABA-SnRK2 axis exhibits extensive crosstalk with various phytohormone pathways including auxin, cytokinin, ethylene, and brassinosteroid signaling. Future studies should prioritize mapping these interactive networks to decode SnRK2's multifaceted regulatory potential beyond canonical osmotic stress responses. While transcription factors dominate the current substrate inventories, critical gaps persist in characterizing SnRK2-mediated phosphorylation of major TF families (WRKY, ERF, MYB, NAC, bHLH). Systematic validation of candidate targets identified through phosphoproteomics, using orthogonal approaches like in vitro kinase assays and site-directed mutagenesis, will clarify their functional relevance in both ABA-dependent and independent contexts.

Intriguingly, SnRK2 proteins undergo complex post-translational modifications, revealing layered regulatory mechanisms that fine-tune kinase activity. SUMOylation enhances the stability of SnRK2 kinase, mitigates its degradation risk, and modulates its nucleocytoplasmic shuttling, thereby facilitating interactions between SnRK2 and nuclear targets such as transcription factors. Conversely, ubiquitination restricts excessive accumulation of SnRK2, preventing energy depletion or cellular damage caused by prolonged activation. Glycosylation further enables SnRK2 to integrate carbon metabolism with stress signaling, thus maintaining a dynamic equilibrium between growth and stress responses. The concerted action of multiple post-translational modifications establishes a "modification code", equipping SnRK2 with the capacity to discern diverse signal inputs, including drought, salt stress, ABA signaling, and ROS. Leveraging this knowledge, gene editing technologies can be employed to target SnRK2 post-translational modification sites (e.g., enhancing SUMOylation for stability or inhibiting ubiquitination to reduce degradation), offering innovative strategies for developing drought-resistant and salt-tolerant crops.

In summary, the diverse post-translational modifications of SnRK2 kinases form an intricate regulatory network, enabling plants to exhibit rapid, precise, and reversible responses to changing environments. Future studies should focus on elucidating the spatiotemporal dynamics of these modifications, the mechanisms underlying their crosstalk, and their potential applications in enhancing stress resilience in crops.

Author Contributions: Conceptualization and writing—original draft preparation, Y.W. Writing, review, editing, drawing figures and tables, L.P. Review and editing, and supervision, X.Z. All authors have read and agreed to the published version of the manuscript.

Funding: This research was funded by Projects of the Joint Fund of Henan Province's Science and Technology Research and Development Program (2251016100540).

Acknowledgments: We would like to thank Dan He (Shenzhen Institute of Advanced Technology, Chinese Academy of Sciences) for her useful discussion and suggestions.

Conflicts of Interest: The authors declare no conflicts of interest.

References

1. Zhang, W.J.; Zhou, Y.; Zhang, Y.; Su, Y.H.; Xu, T. Protein phosphorylation: A molecular switch in plant signaling. *Cell Rep.* **2023**, *42*, 112729. [CrossRef] [PubMed]
2. Fujii, H.; Zhu, J.K. Arabidopsis mutant deficient in 3 abscisic acid-activated protein kinases reveals critical roles in growth, reproduction, and stress. *Proc. Natl. Acad. Sci. USA* **2009**, *106*, 8380–8385. [CrossRef] [PubMed]
3. Fujita, Y.; Nakashima, K.; Yoshida, T.; Katagiri, T.; Kidokoro, S.; Kanamori, N.; Umezawa, T.; Fujita, M.; Maruyama, K.; Ishiyama, K.; et al. Three SnRK2 Protein Kinases are the Main Positive Regulators of Abscisic Acid Signaling in Response to Water Stress in Arabidopsis. *Plant Cell Physiol.* **2009**, *50*, 2123–2132. [CrossRef] [PubMed]

4. Umezawa, T.; Sugiyama, N.; Mizoguchi, M.; Hayashi, S.; Myouga, F.; Yamaguchi-Shinozaki, K.; Ishihama, Y.; Hirayama, T.; Shinozaki, K. Type 2C protein phosphatases directly regulate abscisic acid-activated protein kinases in *Arabidopsis*. *Proc. Natl. Acad. Sci. USA* **2009**, *106*, 17588–17593. [CrossRef]
5. Boudsocq, M.; Barbier-Brygoo, H.; Lauriere, C. Identification of nine sucrose nonfermenting 1-related protein kinases 2 activated by hyperosmotic and saline stresses in *Arabidopsis thaliana*. *J. Biol. Chem.* **2004**, *279*, 41758–41766. [CrossRef]
6. Fujita, Y.; Yoshida, T.; Yamaguchi-Shinozaki, K. Pivotal role of the AREB/ABF-SnRK2 pathway in ABRE-mediated transcription in response to osmotic stress in plants. *Physiol. Plant* **2013**, *147*, 15–27. [CrossRef]
7. Mustilli, A.C.; Merlot, S.; Vavasseur, A.; Fenzi, F.; Giraudat, J. Arabidopsis OST1 protein kinase mediates the regulation of stomatal aperture by abscisic acid and acts upstream of reactive oxygen species production. *Plant Cell* **2002**, *14*, 3089–3099. [CrossRef]
8. Yoshida, R.; Hobo, T.; Ichimura, K.; Mizoguchi, T.; Takahashi, F.; Aronso, J.; Ecker, J.R.; Shinozaki, K. ABA-activated SnRK2 protein kinase is required for dehydration stress signaling in *Arabidopsis*. *Plant Cell Physiol.* **2002**, *43*, 1473–1483. [CrossRef]
9. Fujii, H.; Verslues, P.E.; Zhu, J.K. Identification of two protein kinases required for abscisic acid regulation of seed germination, root growth, and gene expression in *Arabidopsis*. *Plant Cell* **2007**, *19*, 485–494. [CrossRef]
10. Fujii, H.; Chinnusamy, V.; Rodrigues, A.; Rubio, S.; Antoni, R.; Park, S.Y.; Cutler, S.R.; Sheen, J.; Rodriguez, P.L.; Zhu, J.K. *In vitro* reconstitution of an abscisic acid signalling pathway. *Nature* **2009**, *462*, 660–664. [CrossRef]
11. Zhu, J.K. Abiotic Stress Signaling and Responses in Plants. *Cell* **2016**, *167*, 313–324. [CrossRef] [PubMed]
12. Chen, K.; Li, G.J.; Bressan, R.A.; Song, C.P.; Zhu, J.K.; Zhao, Y. Abscisic acid dynamics, signaling, and functions in plants. *J. Integr. Plant Biol.* **2020**, *62*, 25–54. [CrossRef] [PubMed]
13. Gong, Z.; Xiong, L.; Shi, H.; Yang, S.; Herrera-Estrella, L.R.; Xu, G.; Chao, D.Y.; Li, J.; Wang, P.Y.; Qin, F.; et al. Plant abiotic stress response and nutrient use efficiency. *Sci. China Life Sci.* **2020**, *63*, 635–674. [CrossRef] [PubMed]
14. Chen, X.X.; Ding, Y.L.; Yang, Y.Q.; Song, C.P.; Wang, B.S.; Yang, S.H.; Guo, Y.; Gong, Z.Z. Protein kinases in plant responses to drought, salt, and cold stress. *J. Integr. Plant Biol.* **2021**, *63*, 53–78. [CrossRef]
15. Nakashima, K.; Fujita, Y.; Kanamori, N.; Katagiri, T.; Umezawa, T.; Kidokoro, S.; Maruyama, K.; Yoshida, T.; Ishiyama, K.; Kobayashi, M.; et al. Three Arabidopsis SnRK2 protein kinases, SRK2D/SnRK2.2, SRK2E/SnRK2.6/OST1 and SRK2I/SnRK2.3, involved in ABA signaling are essential for the control of seed development and dormancy. *Plant Cell Physiol.* **2009**, *50*, 1345–1363. [CrossRef]
16. Fujii, H.; Verslues, P.E.; Zhu, J.K. *Arabidopsis* decuple mutant reveals the importance of SnRK2 kinases in osmotic stress responses *in vivo*. *Proc. Natl. Acad. Sci. USA* **2011**, *108*, 1717–1722. [CrossRef]
17. Furihata, T.; Maruyama, K.; Fujita, Y.; Umezawa, T.; Yoshida, R.; Shinozaki, K.; Yamaguchi-Shinozaki, K. Abscisic acid-dependent multisite phosphorylation regulates the activity of a transcription activator AREB1. *Proc. Natl. Acad. Sci. USA* **2006**, *103*, 1988–1993. [CrossRef]
18. Sridharamurthy, M.; Kovach, A.; Zhao, Y.; Zhu, J.K.; Xu, H.E.; Swaminathan, K.; Melcher, K. H_2O_2 inhibits ABA-signaling protein phosphatase HAB1. *PLoS ONE* **2014**, *9*, e113643. [CrossRef]
19. Sirichandra, C.; Davanture, M.; Turk, B.E.; Zivy, M.; Valot, B.; Leung, J.; Merlot, S. The Arabidopsis ABA-activated kinase OST1 phosphorylates the bZIP transcription factor ABF3 and creates a 14-3-3 binding site involved in its turnover. *PLoS ONE* **2010**, *5*, e13935. [CrossRef]
20. Feng, C.Z.; Chen, Y.; Wang, C.; Kong, Y.H.; Wu, W.H.; Chen, Y.F. Arabidopsis RAV1 transcription factor, phosphorylated by SnRK2 kinases, regulates the expression of *ABI3*, *ABI4*, and *ABI5* during seed germination and early seedling development. *Plant J.* **2014**, *80*, 654–668. [CrossRef]
21. Takahashi, Y.; Kinoshita, T.; Matsumoto, M.; Shimazaki, K. Inhibition of the *Arabidopsis* bHLH transcription factor by monomerization through abscisic acid-induced phosphorylation. *Plant J.* **2016**, *87*, 559–567. [CrossRef] [PubMed]
22. Takahashi, Y.; Ebisu, Y.; Shimazaki, K. Reconstitution of Abscisic Acid Signaling from the Receptor to DNA via bHLH Transcription Factors. *Plant Physiol.* **2017**, *174*, 815–822. [CrossRef] [PubMed]
23. Zhu, Y.; Huang, P.; Guo, P.; Chong, L.; Yu, G.; Sun, X.; Hu, T.; Li, Y.; Hsu, C.C.; Tang, K.; et al. CDK8 is associated with RAP2.6 and SnRK2.6 and positively modulates abscisic acid signaling and drought response in *Arabidopsis*. *New Phytol.* **2020**, *228*, 1573–1590. [CrossRef]
24. Yang, X.; Gavya, S.L.; Zhou, Z.M.; Urano, D.; Lau, O.S. Abscisic acid regulates stomatal production by imprinting a SnRK2 kinase-mediated phosphocode on the master regulator SPEECHLESS. *Sci. Adv.* **2022**, *8*, eadd2063. [CrossRef]
25. Lee, S.C.; Lan, W.Z.; Buchanan, B.B.; Luan, S. A protein kinase-phosphatase pair interacts with an ion channel to regulate ABA signaling in plant guard cells. *Proc. Natl. Acad. Sci. USA* **2009**, *106*, 21419–21424. [CrossRef]
26. Geiger, D.; Scherzer, S.; Mumm, P.; Marten, I.; Ache, P.; Matschi, S.; Liese, A.; Wellmann, C.; Al-Rasheid, K.A.; Grill, E.; et al. Guard cell anion channel SLAC1 is regulated by CDPK protein kinases with distinct Ca^{2+} affinities. *Proc. Natl. Acad. Sci. USA* **2010**, *107*, 8023–8028. [CrossRef]

27. Vahisalu, T.; Puzorjova, I.; Brosche, M.; Valk, E.; Lepiku, M.; Moldau, H.; Pechter, P.; Wang, Y.S.; Lindgren, O.; Salojarvi, J.; et al. Ozone-triggered rapid stomatal response involves the production of reactive oxygen species, and is controlled by SLAC1 and OST1. *Plant J.* **2010**, *62*, 442–453. [CrossRef]
28. Brandt, B.; Brodsky, D.E.; Xue, S.; Negi, J.; Iba, K.; Kangasjarvi, J.; Ghassemian, M.; Stephan, A.B.; Hu, H.; Schroeder, J.I. Reconstitution of abscisic acid activation of SLAC1 anion channel by CPK6 and OST1 kinases and branched ABI1 PP2C phosphatase action. *Proc. Natl. Acad. Sci. USA* **2012**, *109*, 10593–10598. [CrossRef]
29. Imes, D.; Mumm, P.; Bohm, J.; Al-Rasheid, K.A.; Marten, I.; Geiger, D.; Hedrich, R. Open stomata 1 (OST1) kinase controls R-type anion channel QUAC1 in Arabidopsis guard cells. *Plant J.* **2013**, *74*, 372–382. [CrossRef]
30. Sato, A.; Sato, Y.; Fukao, Y.; Fujiwara, M.; Umezawa, T.; Shinozaki, K.; Hibi, T.; Taniguchi, M.; Miyake, H.; Goto, D.B.; et al. Threonine at position 306 of the KAT1 potassium channel is essential for channel activity and is a target site for ABA-activated SnRK2/OST1/SnRK2.6 protein kinase. *Biochem. J.* **2009**, *424*, 439–448. [CrossRef]
31. Wege, S.; De Angeli, A.; Droillard, M.J.; Kroniewicz, L.; Merlot, S.; Cornu, D.; Gambale, F.; Martinoia, E.; Barbier-Brygoo, H.; Thomine, S.; et al. Phosphorylation of the vacuolar anion exchanger AtCLCa is required for the stomatal response to abscisic acid. *Sci. Signal* **2014**, *7*, ra65. [CrossRef]
32. Planes, M.D.; Ninoles, R.; Rubio, L.; Bissoli, G.; Bueso, E.; Garcia-Sanchez, M.J.; Alejandro, S.; Gonzalez-Guzman, M.; Hedrich, R.; Rodriguez, P.L.; et al. A mechanism of growth inhibition by abscisic acid in germinating seeds of *Arabidopsis thaliana* based on inhibition of plasma membrane H^+-ATPase and decreased cytosolic pH, K^+, and anions. *J. Exp. Bot.* **2015**, *66*, 813–825. [CrossRef] [PubMed]
33. Grondin, A.; Rodrigues, O.; Verdoucq, L.; Merlot, S.; Leonhardt, N.; Maurel, C. Aquaporins Contribute to ABA-Triggered Stomatal Closure through OST1-Mediated Phosphorylation. *Plant Cell* **2015**, *27*, 1945–1954. [CrossRef]
34. Peirats-Llobet, M.; Han, S.K.; Gonzalez-Guzman, M.; Jeong, C.W.; Rodriguez, L.; Belda-Palazon, B.; Wagner, D.; Rodriguez, P.L. A Direct Link between Abscisic Acid Sensing and the Chromatin-Remodeling ATPase BRAHMA via Core ABA Signaling Pathway Components. *Mol. Plant* **2016**, *9*, 136–147. [CrossRef]
35. Kamiyama, Y.; Hirotani, M.; Ishikawa, S.; Minegishi, F.; Katagiri, S.; Rogan, C.J.; Takahashi, F.; Nomoto, M.; Ishikawa, K.; Kodama, Y.; et al. *Arabidopsis* group C Raf-like protein kinases negatively regulate abscisic acid signaling and are direct substrates of SnRK2. *Proc. Natl. Acad. Sci. USA* **2021**, *118*, e2100073118. [CrossRef]
36. Tan, Y.Q.; Yang, Y.; Shen, X.; Zhu, M.; Shen, J.; Zhang, W.; Hu, H.; Wang, Y.F. Multiple cyclic nucleotide-gated channels function as ABA-activated Ca^{2+} channels required for ABA-induced stomatal closure in Arabidopsis. *Plant Cell* **2023**, *35*, 239–259. [CrossRef]
37. Yang, Y.; Tan, Y.-Q.; Wang, X.; Li, J.-J.; Du, B.-Y.; Zhu, M.; Wang, P.; Wang, Y.-F. OPEN STOMATA 1 phosphorylates CYCLIC NUCLEOTIDE-GATED CHANNELs to trigger Ca^{2+} signaling for abscisic acid-induced stomatal closure in Arabidopsis. *Plant Cell* **2024**, *36*, 2328–2358. [CrossRef]
38. Wang, P.; Xue, L.; Batelli, G.; Lee, S.; Hou, Y.J.; Van Oosten, M.J.; Zhang, H.; Tao, W.A.; Zhu, J.K. Quantitative phosphoproteomics identifies SnRK2 protein kinase substrates and reveals the effectors of abscisic acid action. *Proc. Natl. Acad. Sci. USA* **2013**, *110*, 11205–11210. [CrossRef]
39. Wang, P.; Hsu, C.C.; Du, Y.; Zhu, P.; Zhao, C.; Fu, X.; Zhang, C.; Paez, J.S.; Macho, A.P.; Tao, W.A.; et al. Mapping proteome-wide targets of protein kinases in plant stress responses. *Proc. Natl. Acad. Sci. USA* **2020**, *117*, 3270–3280. [CrossRef]
40. Umezawa, T.; Sugiyama, N.; Takahashi, F.; Anderson, J.C.; Ishihama, Y.; Peck, S.C.; Shinozaki, K. Genetics and phosphoproteomics reveal a protein phosphorylation network in the abscisic acid signaling pathway in *Arabidopsis thaliana*. *Sci. Signal* **2013**, *6*, rs8. [CrossRef]
41. Osakabe, Y.; Arinaga, N.; Umezawa, T.; Katsura, S.; Nagamachi, K.; Tanaka, H.; Ohiraki, H.; Yamada, K.; Seo, S.U.; Abo, M.; et al. Osmotic stress responses and plant growth controlled by potassium transporters in *Arabidopsis*. *Plant Cell* **2013**, *25*, 609–624. [CrossRef] [PubMed]
42. Kim, M.J.; Park, M.J.; Seo, P.J.; Song, J.S.; Kim, H.J.; Park, C.M. Controlled nuclear import of the transcription factor NTL6 reveals a cytoplasmic role of SnRK2.8 in the drought-stress response. *Biochem. J.* **2012**, *448*, 353–363. [CrossRef] [PubMed]
43. Ding, S.; Zhang, B.; Qin, F. Arabidopsis RZFP34/CHYR1, a Ubiquitin E3 Ligase, Regulates Stomatal Movement and Drought Tolerance via SnRK2.6-Mediated Phosphorylation. *Plant Cell* **2015**, *27*, 3228–3244. [CrossRef] [PubMed]
44. Tan, W.; Zhang, D.; Zhou, H.; Zheng, T.; Yin, Y.; Lin, H. Transcription factor HAT1 is a substrate of SnRK2.3 kinase and negatively regulates ABA synthesis and signaling in Arabidopsis responding to drought. *PLoS Genet.* **2018**, *14*, e1007336. [CrossRef]
45. Huang, X.; Hou, L.; Meng, J.; You, H.; Li, Z.; Gong, Z.; Yang, S.; Shi, Y. The Antagonistic Action of Abscisic Acid and Cytokinin Signaling Mediates Drought Stress Response in *Arabidopsis*. *Mol. Plant* **2018**, *11*, 970–982. [CrossRef]
46. Hong, Y.; Wang, Z.; Liu, X.; Yao, J.; Kong, X.; Shi, H.; Zhu, J.K. Two Chloroplast Proteins Negatively Regulate Plant Drought Resistance Through Separate Pathways. *Plant Physiol.* **2020**, *182*, 1007–1021. [CrossRef]
47. Wang, P.; Qi, S.; Wang, X.; Dou, L.; Jia, M.A.; Mao, T.; Guo, Y.; Wang, X. The OPEN STOMATA1-SPIRAL1 module regulates microtubule stability during abscisic acid-induced stomatal closure in Arabidopsis. *Plant Cell* **2023**, *35*, 260–278. [CrossRef]

48. Sun, Z.; Feng, Z.; Ding, Y.; Qi, Y.; Jiang, S.; Li, Z.; Wang, Y.; Qi, J.; Song, C.; Yang, S.; et al. RAF22, ABI1 and OST1 form a dynamic interactive network that optimizes plant growth and responses to drought stress in *Arabidopsis*. *Mol. Plant* **2022**, *15*, 1192–1210. [CrossRef]
49. Katagiri, S.; Kamiyama, Y.; Yamashita, K.; Iizumi, S.; Suzuki, R.; Aoi, Y.; Takahashi, F.; Kasahara, H.; Kinoshita, T.; Umezawa, T. Accumulation of Phosphorylated SnRK2 Substrate 1 Promotes Drought Escape in *Arabidopsis*. *Plant Cell Physiol.* **2024**, *65*, 259–268. [CrossRef]
50. Shavrukov, Y. Pathway to the Molecular Origins of Drought Escape and Early Flowering Illuminated via the Phosphorylation of SnRK2-Substrate 1 in *Arabidopsis*. *Plant Cell Physiol.* **2024**, *65*, 179–180. [CrossRef]
51. Soma, F.; Mogami, J.; Yoshida, T.; Abekura, M.; Takahashi, F.; Kidokoro, S.; Mizoi, J.; Shinozaki, K.; Yamaguchi-Shinozaki, K. ABA-unresponsive SnRK2 protein kinases regulate mRNA decay under osmotic stress in plants. *Nat. Plants* **2017**, *3*, 16204. [CrossRef] [PubMed]
52. Kawa, D.; Meyer, A.J.; Dekker, H.L.; Abd-El-Haliem, A.M.; Gevaert, K.; Van De Slijke, E.; Maszkowska, J.; Bucholc, M.; Dobrowolska, G.; De Jaeger, G.; et al. SnRK2 Protein Kinases and mRNA Decapping Machinery Control Root Development and Response to Salt. *Plant Physiol.* **2020**, *182*, 361–377. [CrossRef] [PubMed]
53. Maszkowska, J.; Debski, J.; Kulik, A.; Kistowski, M.; Bucholc, M.; Lichocka, M.; Klimecka, M.; Sztatelman, O.; Szymanska, K.P.; Dadlez, M.; et al. Phosphoproteomic analysis reveals that dehydrins ERD10 and ERD14 are phosphorylated by SNF1-related protein kinase 2.10 in response to osmotic stress. *Plant Cell Env.* **2019**, *42*, 931–946. [CrossRef] [PubMed]
54. Klimecka, M.; Bucholc, M.; Maszkowska, J.; Krzywinska, E.; Goch, G.; Lichocka, M.; Szczegielniak, J.; Dobrowolska, G. Regulation of ABA-Non-Activated SNF1-Related Protein Kinase 2 Signaling Pathways by Phosphatidic Acid. *Int. J. Mol. Sci.* **2020**, *21*, 4984. [CrossRef]
55. Shahzad, Z.; Tournaire-Roux, C.; Canut, M.; Adamo, M.; Roeder, J.; Verdoucq, L.; Martiniere, A.; Amtmann, A.; Santoni, V.; Grill, E.; et al. Protein kinase SnRK2.4 is a key regulator of aquaporins and root hydraulics in Arabidopsis. *Plant J.* **2024**, *117*, 264–279. [CrossRef]
56. Wang, Y.; Yang, L.; Chen, X.; Ye, T.; Zhong, B.; Liu, R.; Wu, Y.; Chan, Z. *Major. latex protein-like protein 43* (MLP43) functions as a positive regulator during abscisic acid responses and confers drought tolerance in *Arabidopsis thaliana*. *J. Exp. Bot.* **2016**, *67*, 421–434. [CrossRef]
57. Wang, Q.; Guo, Q.; Guo, Y.; Yang, J.; Wang, M.; Duan, X.; Niu, J.; Liu, S.; Zhang, J.; Lu, Y.; et al. Arabidopsis subtilase *SASP* is involved in the regulation of ABA signaling and drought tolerance by interacting with OPEN STOMATA 1. *J. Exp. Bot.* **2018**, *69*, 4403–4417. [CrossRef]
58. Huang, Y.; Yang, R.; Luo, H.; Yuan, Y.; Diao, Z.; Li, J.; Gong, S.; Yu, G.; Yao, H.; Zhang, H.; et al. Arabidopsis Protein Phosphatase PIA1 Impairs Plant Drought Tolerance by Serving as a Common Negative Regulator in ABA Signaling Pathway. *Plants (Basel)* **2023**, *12*, 2716. [CrossRef]
59. Liu, Q.; Kasuga, M.; Sakuma, Y.; Abe, H.; Miura, S.; Yamaguchi-Shinozaki, K.; Shinozaki, K. Two transcription factors, DREB1 and DREB2, with an EREBP/AP2 DNA binding domain separate two cellular signal transduction pathways in drought- and low-temperature-responsive gene expression, respectively, in Arabidopsis. *Plant Cell* **1998**, *10*, 1391–1406. [CrossRef]
60. Stockinger, E.J.; Gilmour, S.J.; Thomashow, M.F. *Arabidopsis thaliana CBF1* encodes an AP2 domain-containing transcriptional activator that binds to the C-repeat/DRE, a cis-acting DNA regulatory element that stimulates transcription in response to low temperature and water deficit. *Proc. Natl. Acad. Sci. USA* **1997**, *94*, 1035–1040. [CrossRef]
61. Thomashow, M.F. Plant cold acclimation: Freezing tolerance genes and regulatory mechanisms. *Annu. Rev. Plant Physiol. Plant Mol. Biol.* **1999**, *50*, 571–599. [CrossRef] [PubMed]
62. Ding, Y.; Li, H.; Zhang, X.; Xie, Q.; Gong, Z.; Yang, S. OST1 kinase modulates freezing tolerance by enhancing ICE1 stability in *Arabidopsis*. *Dev. Cell* **2015**, *32*, 278–289. [CrossRef] [PubMed]
63. Lang, Z.; Zhu, J. OST1 phosphorylates ICE1 to enhance plant cold tolerance. *Sci. China Life Sci.* **2015**, *58*, 317–318. [CrossRef] [PubMed]
64. Li, H.; Ding, Y.; Shi, Y.; Zhang, X.; Zhang, S.; Gong, Z.; Yang, S. MPK3- and MPK6-Mediated ICE1 Phosphorylation Negatively Regulates ICE1 Stability and Freezing Tolerance in *Arabidopsis*. *Dev. Cell* **2017**, *43*, 630–642.e4. [CrossRef]
65. Ding, Y.; Jia, Y.; Shi, Y.; Zhang, X.; Song, C.; Gong, Z.; Yang, S. OST1-mediated BTF3L phosphorylation positively regulates CBFs during plant cold responses. *EMBO J.* **2018**, *37*, e98228. [CrossRef]
66. Wang, X.; Ding, Y.; Li, Z.; Shi, Y.; Wang, J.; Hua, J.; Gong, Z.; Zhou, J.M.; Yang, S. PUB25 and PUB26 Promote Plant Freezing Tolerance by Degrading the Cold Signaling Negative Regulator MYB15. *Dev. Cell* **2019**, *51*, 222–235.e5. [CrossRef]
67. Liu, Q.; Ding, Y.; Shi, Y.; Ma, L.; Wang, Y.; Song, C.; Wilkins, K.A.; Davies, J.M.; Knight, H.; Knight, M.R.; et al. The calcium transporter ANNEXIN1 mediates cold-induced calcium signaling and freezing tolerance in plants. *EMBO J.* **2021**, *40*, e104559. [CrossRef]
68. Ding, Y.; Lv, J.; Shi, Y.; Gao, J.; Hua, J.; Song, C.; Gong, Z.; Yang, S. EGR2 phosphatase regulates OST1 kinase activity and freezing tolerance in *Arabidopsis*. *EMBO J.* **2019**, *38*, e99819. [CrossRef]

69. Lv, J.; Liu, J.; Ming, Y.; Shi, Y.; Song, C.; Gong, Z.; Yang, S.; Ding, Y. Reciprocal regulation between the negative regulator PP2CG1 phosphatase and the positive regulator OST1 kinase confers cold response in *Arabidopsis*. *J. Integr. Plant Biol.* **2021**, *63*, 1568–1587. [CrossRef]
70. Yu, B.; Zheng, W.; Xing, L.; Zhu, J.K.; Persson, S.; Zhao, Y. Root twisting drives halotropism via stress-induced microtubule reorientation. *Dev. Cell* **2022**, *57*, 2412–2425.e6. [CrossRef]
71. Hu, Y.; Zeng, L.; Lv, X.; Guo, J.; Li, X.; Zhang, X.; Wang, D.; Wang, J.; Bi, J.; Julkowska, M.M.; et al. NIGT1.4 maintains primary root elongation in response to salt stress through induction of *ERF1* in Arabidopsis. *Plant J.* **2023**, *116*, 173–186. [CrossRef] [PubMed]
72. Lee, H.J.; Park, Y.J.; Seo, P.J.; Kim, J.H.; Sim, H.J.; Kim, S.G.; Park, C.M. Systemic Immunity Requires SnRK2.8-Mediated Nuclear Import of NPR1 in Arabidopsis. *Plant Cell* **2015**, *27*, 3425–3438. [CrossRef] [PubMed]
73. Olate, E.; Jimenez-Gomez, J.M.; Holuigue, L.; Salinas, J. NPR1 mediates a novel regulatory pathway in cold acclimation by interacting with HSFA1 factors. *Nat. Plants* **2018**, *4*, 811–823. [CrossRef] [PubMed]
74. Lei, L.; Stevens, D.M.; Coaker, G. Phosphorylation of the Pseudomonas Effector AvrPtoB by *Arabidopsis* SnRK2.8 Is Required for Bacterial Virulence. *Mol. Plant* **2020**, *13*, 1513–1522. [CrossRef]
75. Acharya, B.R.; Jeon, B.W.; Zhang, W.; Assmann, S.M. Open Stomata 1 (OST1) is limiting in abscisic acid responses of Arabidopsis guard cells. *New Phytol.* **2013**, *200*, 1049–1063. [CrossRef]
76. Sirichandra, C.; Gu, D.; Hu, H.C.; Davanture, M.; Lee, S.; Djaoui, M.; Valot, B.; Zivy, M.; Leung, J.; Merlot, S.; et al. Phosphorylation of the Arabidopsis AtrbohF NADPH oxidase by OST1 protein kinase. *FEBS Lett.* **2009**, *583*, 2982–2986. [CrossRef]
77. Han, J.P.; Koster, P.; Drerup, M.M.; Scholz, M.; Li, S.; Edel, K.H.; Hashimoto, K.; Kuchitsu, K.; Hippler, M.; Kudla, J. Fine-tuning of RBOHF activity is achieved by differential phosphorylation and Ca^{2+} binding. *New Phytol.* **2019**, *221*, 1935–1949. [CrossRef]
78. Fichman, Y.; Zandalinas, S.I.; Peck, S.; Luan, S.; Mittler, R. HPCA1 is required for systemic reactive oxygen species and calcium cell-to-cell signaling and plant acclimation to stress. *Plant Cell* **2022**, *34*, 4453–4471. [CrossRef]
79. Zhang, X.; Zhang, D.; Zhong, C.; Li, W.; Dinesh-Kumar, S.P.; Zhang, Y. Orchestrating ROS regulation: Coordinated post-translational modification switches in NADPH oxidases. *New Phytol.* **2025**, *245*, 510–522. [CrossRef]
80. Su, H.; Wang, T.; Ju, C.; Deng, J.; Zhang, T.; Li, M.; Tian, H.; Wang, C. Abscisic acid signaling negatively regulates nitrate uptake via phosphorylation of NRT1.1 by SnRK2s in *Arabidopsis*. *J. Integr. Plant Biol.* **2021**, *63*, 597–610. [CrossRef]
81. Liu, C.; Yu, H.; Rao, X.; Li, L.; Dixon, R.A. Abscisic acid regulates secondary cell-wall formation and lignin deposition in *Arabidopsis thaliana* through phosphorylation of NST1. *Proc. Natl. Acad. Sci. USA* **2021**, *118*, e2010911118. [CrossRef] [PubMed]
82. Yan, J.; Wang, P.; Wang, B.; Hsu, C.C.; Tang, K.; Zhang, H.; Hou, Y.J.; Zhao, Y.; Wang, Q.; Zhao, C.; et al. The SnRK2 kinases modulate miRNA accumulation in *Arabidopsis*. *PLoS Genet.* **2017**, *13*, e1006753. [CrossRef] [PubMed]
83. Lin, Z.; Li, Y.; Wang, Y.; Liu, X.; Ma, L.; Zhang, Z.; Mu, C.; Zhang, Y.; Peng, L.; Xie, S.; et al. Initiation and amplification of SnRK2 activation in abscisic acid signaling. *Nat. Commun.* **2021**, *12*, 2456. [CrossRef] [PubMed]
84. Soma, F.; Takahashi, F.; Suzuki, T.; Shinozaki, K.; Yamaguchi-Shinozaki, K. Plant Raf-like kinases regulate the mRNA population upstream of ABA-unresponsive SnRK2 kinases under drought stress. *Nat. Commun.* **2020**, *11*, 1373. [CrossRef]
85. Takahashi, Y.; Zhang, J.; Hsu, P.K.; Ceciliato, P.H.O.; Zhang, L.; Dubeaux, G.; Munemasa, S.; Ge, C.; Zhao, Y.; Hauser, F.; et al. MAP3Kinase-dependent SnRK2-kinase activation is required for abscisic acid signal transduction and rapid osmotic stress response. *Nat. Commun.* **2020**, *11*, 12. [CrossRef]
86. Katsuta, S.; Masuda, G.; Bak, H.; Shinozawa, A.; Kamiyama, Y.; Umezawa, T.; Takezawa, D.; Yotsui, I.; Taji, T.; Sakata, Y. Arabidopsis Raf-like kinases act as positive regulators of subclass III SnRK2 in osmostress signaling. *Plant J.* **2020**, *103*, 634–644. [CrossRef]
87. Nguyen, Q.T.C.; Lee, S.J.; Choi, S.W.; Na, Y.J.; Song, M.R.; Hoang, Q.T.N.; Sim, S.Y.; Kim, M.S.; Kim, J.I.; Soh, M.S.; et al. Arabidopsis Raf-Like Kinase Raf10 Is a Regulatory Component of Core ABA Signaling. *Mol. Cells* **2019**, *42*, 646–660.
88. Chinchilla, D.; Zipfel, C.; Robatzek, S.; Kemmerling, B.; Nurnberger, T.; Jones, J.D.; Felix, G.; Boller, T. A flagellin-induced complex of the receptor FLS2 and BAK1 initiates plant defence. *Nature* **2007**, *448*, 497–500. [CrossRef]
89. Roux, M.; Schwessinger, B.; Albrecht, C.; Chinchilla, D.; Jones, A.; Holton, N.; Malinovsky, F.G.; Tor, M.; de Vries, S.; Zipfel, C. The *Arabidopsis* leucine-rich repeat receptor-like kinases BAK1/SERK3 and BKK1/SERK4 are required for innate immunity to hemibiotrophic and biotrophic pathogens. *Plant Cell* **2011**, *23*, 2440–2455. [CrossRef]
90. Shang, Y.; Dai, C.; Lee, M.M.; Kwak, J.M.; Nam, K.H. BRI1-Associated Receptor Kinase 1 Regulates Guard Cell ABA Signaling Mediated by Open Stomata 1 in *Arabidopsis*. *Mol. Plant* **2016**, *9*, 447–460. [CrossRef]
91. Deng, J.; Kong, L.; Zhu, Y.; Pei, D.; Chen, X.; Wang, Y.; Qi, J.; Song, C.; Yang, S.; Gong, Z. BAK1 plays contrasting roles in regulating abscisic acid-induced stomatal closure and abscisic acid-inhibited primary root growth in *Arabidopsis*. *J. Integr. Plant Biol.* **2022**, *64*, 1264–1280. [CrossRef] [PubMed]
92. Cai, Z.; Liu, J.; Wang, H.; Yang, C.; Chen, Y.; Li, Y.; Pan, S.; Dong, R.; Tang, G.; Barajas-Lopez Jde, D.; et al. GSK3-like kinases positively modulate abscisic acid signaling through phosphorylating subgroup III SnRK2s in *Arabidopsis*. *Proc. Natl. Acad. Sci. USA* **2014**, *111*, 9651–9656. [CrossRef] [PubMed]

93. Vilela, B.; Najar, E.; Lumbreras, V.; Leung, J.; Pages, M. Casein Kinase 2 Negatively Regulates Abscisic Acid-Activated SnRK2s in the Core Abscisic Acid-Signaling Module. *Mol. Plant* **2015**, *8*, 709–721. [CrossRef]
94. Tian, W.; Hou, C.; Ren, Z.; Pan, Y.; Jia, J.; Zhang, H.; Bai, F.; Zhang, P.; Zhu, H.; He, Y.; et al. A molecular pathway for CO(2) response in *Arabidopsis* guard cells. *Nat. Commun.* **2015**, *6*, 6057. [CrossRef]
95. Mogami, J.; Fujita, Y.; Yoshida, T.; Tsukiori, Y.; Nakagami, H.; Nomura, Y.; Fujiwara, T.; Nishida, S.; Yanagisawa, S.; Ishida, T.; et al. Two distinct families of protein kinases are required for plant growth under high external Mg^{2+} concentrations in Arabidopsis. *Plant Physiol.* **2015**, *167*, 1039–1057. [CrossRef]
96. Li, G.J.; Chen, K.; Sun, S.; Zhao, Y. Osmotic signaling releases PP2C-mediated inhibition of *Arabidopsis* SnRK2s via the receptor-like cytoplasmic kinase BIK1. *EMBO J.* **2024**, *43*, 6076–6103. [CrossRef]
97. Li, Q.; Hu, T.; Lu, T.; Yu, B.; Zhao, Y. Calcium-dependent protein kinases CPK3/4/6/11 and 27 respond to osmotic stress and activate SnRK2s in *Arabidopsis*. *Dev. Cell* **2025**, in press. [CrossRef]
98. Cheng, C.; Wang, Z.; Ren, Z.; Zhi, L.; Yao, B.; Su, C.; Liu, L.; Li, X. SCFAtPP2-B11 modulates ABA signaling by facilitating SnRK2.3 degradation in *Arabidopsis thaliana*. *PLoS Genet.* **2017**, *13*, e1006947. [CrossRef]
99. Ali, A.; Kim, J.K.; Jan, M.; Khan, H.A.; Khan, I.U.; Shen, M.; Park, J.; Lim, C.J.; Hussain, S.; Baek, D.; et al. Rheostatic Control of ABA Signaling through HOS15-Mediated OST1 Degradation. *Mol. Plant* **2019**, *12*, 1447–1462. [CrossRef]
100. Shao, Z.; Yang, S.; Gu, Y.; Guo, Y.; Zhou, H.; Yang, Y. Ubiquitin negatively regulates ABA responses by inhibiting SnRK2.2 and SnRK2.3 kinase activity in Arabidopsis. *J. Exp. Bot.* **2023**, *74*, 5394–5404. [CrossRef]
101. Chang, Y.N.; Wang, Z.J.; Ren, Z.Y.; Wang, C.H.; Wang, P.C.; Zhu, J.K.; Li, X.; Duan, C.G. NUCLEAR PORE ANCHOR and EARLY IN SHORT DAYS 4 negatively regulate abscisic acid signaling by inhibiting Snf1-related protein kinase2 activity and stability in *Arabidopsis*. *J. Integr. Plant Biol.* **2022**, *64*, 2060–2074. [CrossRef] [PubMed]
102. Cui, X.A.; Lv, M.Y.; Cao, Y.Y.; Li, Z.W.; Liu, Y.; Ren, Z.Z.; Zhang, H.R. NUA and ESD4 negatively regulate ABA signaling during seed germination. *Stress Biol.* **2022**, *2*, 38. [CrossRef]
103. Wang, P.; Du, Y.; Hou, Y.J.; Zhao, Y.; Hsu, C.C.; Yuan, F.; Zhu, X.; Tao, W.A.; Song, C.P.; Zhu, J.K. Nitric oxide negatively regulates abscisic acid signaling in guard cells by S-nitrosylation of OST1. *Proc. Natl. Acad. Sci. USA* **2015**, *112*, 613–618. [CrossRef]
104. Lang, Z.; Zuo, J. Say "NO" to ABA signaling in guard cells by S-nitrosylation of OST1. *Sci. China Life Sci.* **2015**, *58*, 313–314. [CrossRef]
105. Chen, S.; Jia, H.; Wang, X.; Shi, C.; Wang, X.; Ma, P.; Wang, J.; Ren, M.; Li, J. Hydrogen Sulfide Positively Regulates Abscisic Acid Signaling through Persulfidation of SnRK2.6 in Guard Cells. *Mol. Plant* **2020**, *13*, 732–744. [CrossRef]
106. Chen, S.; Wang, X.; Jia, H.; Li, F.; Ma, Y.; Liesche, J.; Liao, M.; Ding, X.; Liu, C.; Chen, Y.; et al. Persulfidation-induced structural change in SnRK2.6 establishes intramolecular interaction between phosphorylation and persulfidation. *Mol. Plant* **2021**, *14*, 1814–1830. [CrossRef]
107. Siodmak, A.; Hirt, H. Stomatal regulation: Role of H(2)S-induced persulfidation in ABA signaling. *Mol. Plant* **2021**, *14*, 858–860. [CrossRef]
108. Chen, J.; Zhou, H.; Xie, Y. SnRK2.6 phosphorylation/persulfidation: Where ABA and H(2)S signaling meet. *Trends Plant Sci.* **2021**, *26*, 1207–1209. [CrossRef]
109. Wang, J.; Wang, C.; Wang, T.; Zhang, S.; Yan, K.; Yang, G.; Wu, C.; Zheng, C.; Huang, J. Tyrosylprotein sulfotransferase suppresses ABA signaling via sulfation of SnRK2.2/2.3/2.6. *J. Integr. Plant Biol.* **2023**, *65*, 1846–1851. [CrossRef]
110. Lu, J.; Li, N.; Li, G.; Tian, Z.; Shi, L.; Wang, Y.; Cai, Y.; Zhang, K.; Sun, W.; Wang, D.; et al. N-glycosylation of SnRK2s affects NADPH maintenance in peroxisomes during prolonged ABA signalling. *Nat. Commun.* **2024**, *15*, 6630. [CrossRef]

plants

MDPI

Review

Trade-Off Regulation in Plant Growth and Stress Responses Through the Role of Heterotrimeric G Protein Signaling

Horim Lee

Department of Biotechnology, Duksung Women's University, Seoul 01369, Republic of Korea; hrlee1375@duksung.ac.kr; Tel.: +82-2-901-8753

Abstract: Unlike animals, plants are sessile organisms that cannot migrate to more favorable conditions and must constantly adapt to a variety of biotic and abiotic stresses. Therefore, plants exhibit developmental plasticity to cope, which is probably based on the underlying trade-off mechanism that allocates energy expenditure between growth and stress responses to achieve appropriate growth and development under different environmental conditions. Plant heterotrimeric G protein signaling plays a crucial role in the trade-off involved in the regulation of normal growth and stress adaptation. This review examines the composition and signaling processes of heterotrimeric G proteins in plants, detailing how they balance growth and adaptive responses in plant immunity and thermomorphogenesis through recent advances in the field. Understanding the trade-offs associated with plant G protein signaling will have significant implications for agricultural innovation, particularly in the development of crops with improved resilience and minimal growth penalties under environmental stress.

Keywords: heterotrimeric G protein; developmental plasticity; trade-off; plant immunity; thermomorphogenesis

1. Introduction

Unlike animals, plants cannot actively select optimal environmental conditions for growth and development. Therefore, plants must exist in constant interactions with a wide range of biotic and abiotic stresses that they are exposed to in the confined place they live throughout their lifespan. Thus, the impact of adverse stress environments on plant growth is an important scientific problem for an integrated understanding of fundamental growth and development under ever-changing environmental conditions. In addition, the impact of adverse stresses on plant growth is a critical issue for agriculture and food security, particularly in response to the extreme environmental challenges expected in the future (e.g., climate change) [1]. Plants can enhance certain traits during growth and development while restricting other traits. Hence, plants under stress conditions exhibit developmental plasticity [2], which is associated with a very active allocation of energy use between growth and stress response (Figure 1). Under optimal growth conditions, plants normally suppress the stress response programs, including abscisic acid (ABA)-mediated morphogenesis and gene expression, which is necessary for resistance or adaptation to biotic and abiotic stresses to avoid unnecessary energy expenditure for normal growth and development [3]. In contrast, plants under stress conditions relatively reduce the energy expenditure required for normal growth and development to use energy for adaptation against various stresses. These plastic growth phenomena are generally observed in the active growth retardation associated with stress tolerance based on the energy allocation in plants exposed to stress environments [4] or in an overexpression of stress-responsive genes in transgenic plants [5,6]. Therefore, stress-induced developmental plasticity is likely linked to the underlying trade-off mechanism that selectively allocates the available energy/nutrient resources to plants in response to environmental changes.

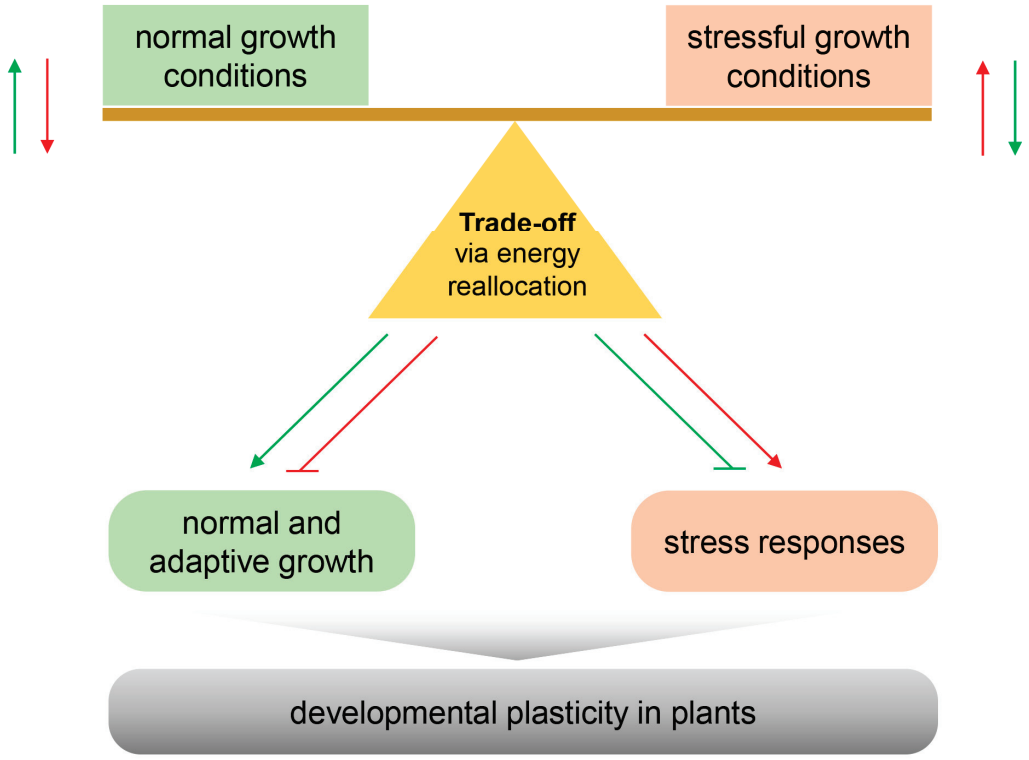

Figure 1. Hypothetical model of the relationship between trade-off and developmental plasticity. As sessile organisms, plants must respond to normal and stressful growth conditions. In general, plants under adverse stress show plastic deformation in growth and development through the underlying mechanism of trade-off between growth and stress responses, including changes in ROS, MAPKs, and gene expression. The green and red lines indicate the corresponding behavior under normal and stressful growth conditions, respectively.

Heterotrimeric G proteins (referred to as G proteins), a complex comprising Gα, Gβ, and Gγ, are an important signaling system that interacts with G protein-coupled receptors (GPCRs) to sense a variety of stimuli, such as nutrients and hormones, and contributes to the regulation of the physiological balance between healthy and stressed conditions in animals [7]. In contrast, although heterotrimeric G protein complexes also exist in plants, their simpler composition and lack of GPCR suggest that plant G protein signaling mechanisms are likely to be regulated differently from those in animals [8,9]. Nevertheless, plant G protein signaling has been shown to be similarly involved in the physiological responses to external stimuli, such as biotic and abiotic stresses, as well as in basic growth and development based on studies using G protein component mutants, such as *gpa1* (loss of function of the Gα subunit), *agb1* (l-o-f of the Gβ subunit), and *agg1/2/3* (l-o-f of the Gγ subunits) [8,10]. Recent findings have revealed alleviated growth inhibition under biotic stress and thermomorphogenesis induced by high ambient temperature in l-o-f *Arabidopsis* G protein component mutants [11], suggesting the significant role of G protein signaling in regulating the trade-off between growth and stress response for developmental plasticity. Fundamentally, G protein-mediated growth inhibition under stress conditions is ultimately associated with the underlying cellular behavior, including cell proliferation and death [12,13]. This cell survival mechanism under nutrient starvation conditions is also regulated by the key trade-off modulator target of rapamycin (TOR) kinase [14]. Here, this review provides an overview of the molecular processes and roles of G protein signaling in plant growth, development, and stress responses. In addition, this review discusses the recent advances in understanding the function of G protein signaling in the trade-off associated with plant immunity and thermomorphogenesis and provides a perspective potentially in connection to trade-off modulators.

2. Heterotrimeric G Protein Signaling Acts to Balance Growth and Stress Responses in Plants

2.1. Heterotrimeric G Protein Subunits in Plants

Compared to vast numbers of G protein subunits in animals [15], most plants show relatively simple compositions of canonical G protein signaling components. For example, *Arabidopsis* has one Gα, one Gβ, and three Gγ subunits [16–20], and rice has one Gα, one Gβ, and five Gγ subunits [21]. Although several Gγ subunits are found in plants, the canonical Gγ prototype that contains the isoprenylation motif at the C-terminus to anchor the plasma membrane in animals is revealed as two *AGG1* and *AGG2* in *Arabidopsis* and one *RGG1* in rice [9,21,22]. Other types of Gγ subunits lack the isoprenylation motif or have extended C-terminal domains with highly enriched cysteine residues [21]. In addition, most plants have non-canonical plant-specific Gα subunits such as the extra-large GTP-binding protein (XLG), which contain the C-terminal domains homologous with canonical Gα subunits and the extensive N-terminal region including a nuclear localization signal, a nuclear export signal, and a cysteine-rich sequence [8,23,24]. The l-o-f triple mutants for all three genes, *XLG1*, *XLG2*, and *XLG3*, encoded in the *Arabidopsis* genome showed similar phenotypes for ABA/sugar sensitivity, defense response, and root-wave response like those in the *agb1* mutant, indicating the associated roles of XLGs with canonical G protein signaling [25,26]. Although mammals have XLGs in addition to five major types of Gα subunits, including $G\alpha_s$, $G\alpha_i$, $G\alpha_{q/11}$, $G\alpha_{12/13}$, and $G\alpha_v$ [27], they are produced by alternative splicing from canonical Gα genes unlike unique genes in plants [23].

Despite the additional non-canonical Gα and Gγ subunits, plants have a relatively limited diversity of combinations to form ternary complexes compared to those in animals, which contain almost 40 Gαβγ components [15]. Nevertheless, G protein signaling in plants affects diverse biological processes ranging from fundamental growth and development to adaptive responses to biotic and abiotic stresses [8,9,28]. Thus, the ability to perform multiple functions with such a low level of combinatorial complexity suggests that plant G protein signaling may be involved in simple and common processes that regulate growth under optimal or stressful conditions. Although the stresses are diverse, the phenomenon resulting from trade-off regulation is commonly found as growth inhibition for proper growth and development under adverse stress conditions.

2.2. Molecular Processes of Heterotrimeric G Protein Signaling in Plants

Most GDP-bound Gαβγ trimeric complexes are activated by GPCRs sensing exogenous signal ligands through the conventional mechanism of G protein signaling in animals [29]. The intrinsic exchange rate from the inactive GDP-bound Gα subunit to the active GTP-bound Gα subunit is very slow. Therefore, GPCRs acting as guanosine exchange factors (GEFs) are required to induce G protein signaling, allowing the trimeric complexes to separate into active Gα and active Gβγ to interact with the downstream effectors, e.g., adenylyl cyclase and ion channels, respectively. Once G protein signaling is activated, the deactivation process occurs through the spontaneous intrinsic GTP hydrolysis of the Gα subunit or GTPase-accelerating proteins (GAPs), also known as a regulator of G protein signaling (RGS) proteins, to terminate G protein signaling [29,30]. In contrast to animals, activation of the Gα subunit is not a rate-limiting step in plants because the GDP from the Gα subunit is released and exchanged spontaneously with GTP without the effort of GEFs [31,32]. Interestingly, the exchange rate of the plant Gα subunit is similar to that of the constitutively active version of the animal Gα mutant subunit [33]. Furthermore, the GPCR that activates the Gα subunit in animals has not been identified in plants [32], suggesting that plant G protein signaling is probably self-activated in a GPCR-independent manner. Instead, the deactivation process is the rate-limiting step in plant G protein signaling in contrast to animals because the Gα subunit has an intrinsically slow activity of GTP hydrolysis [32,34]. Therefore, the function of RGS proteins as GAPs to promote GTP hydrolysis is essential for deactivating the active plant Gα subunits. Another distinctive feature of plant RGS proteins acting as a GTPase is that they contain a seven-transmembrane (7TM)

domain in the N-terminal region, similar to the animal metabotropic glutamate GPCR subfamily [34–36]. The catalytic domain of RGS is located in the cytoplasmic C-terminal region, which is homologous to the animal RGS protein GAP [34,35]. In the active/inactive cycle of G protein signaling, the critical rate-limiting step differs according to the intrinsic catalytic properties and is critically regulated by GPCRs and RGS proteins in animals and plants, respectively, to overcome the impaired catalytic activities.

The purified C-terminal RGS-box domain in *Arabidopsis* 7TM-RGS protein, known as AtRGS1, has been reported to be able to accelerate the GTPase activity of GPA1 in vitro [34,35,37]. In addition, genetic analysis showed that the *gpa1* mutant has a shorter hypocotyl length, whereas *atrga1* and constitutively active *GPA1* increased hypocotyls in the dark [35]. Hence, AtRGS1 negatively regulates the activity of GTP-bound GPA1, which is involved in cell elongation and proliferation. Moreover, the 7TM AtRGS1 protein is a putative receptor for glucose ligands [35,38,39]. Several findings showed that glucose triggers the endocytosis of its receptor AtRGS1 from the plasma membrane to activate Gα signaling through physical uncoupling between GPA1 and its inhibitor AtRGS1 [34,40,41]. The effects of glucose on G protein signaling are supported by genetic analyses. For example, the seedling growth arrest induced by high glucose concentrations was alleviated in the *atrgs1* mutant. In addition, hypersensitive growth arrest was exhibited in *gpa1* and *atrgs1 gpa1* mutant seedlings or transgenic plants overexpressing *AtRGS1* [34], suggesting that *AtRGS1* and *GPA1* are involved in glucose signaling in the same genetic pathway for plant growth and that G protein signaling is vital for sugar signaling.

2.3. Heterotrimeric G Protein Signaling in Plant Immunity

Under biotic stress conditions, plants directly respond to pathogen attacks (e.g., bacteria, fungi, and oomycetes) via microbe-associated molecular pattern (MAMP)-triggered immunity (MTI) as an innate immune system [42,43]. Pathogen signals, MAMPs, are recognized by the pattern recognition receptors (PRRs) on the cell surface [42]. One of the best-characterized plant MAMP signals is the flg22 peptide derived from bacterial flagellin, which is recognized by the PRR flagellin-insensitive 2 (FLS2) receptor, a member of the receptor-like kinase (RLK) family (Figure 2) [42]. Upon the perception of flg22, FLS2 forms a heterodimer complex with the co-receptor BRI1-associated kinase 1 (BAK1) to initiate the downstream immune responses, including mitogen-activated protein kinase (MAPK) activation, reactive oxygen species (ROS) production, and immune gene expression [42,44]. Lu et al. [45] reported that botrytis-induced kinase 1 (BIK1), which encodes the receptor-like cytoplasmic kinase (RLCK), plays an important role in transducing intracellular signals from the flg22-mediated FLS2-BAK1 receptor complex to downstream responses. Accordingly, BIK1 was phosphorylated rapidly by flg22 via BAK1 and activated BIK1 reciprocally phosphorylated FLS2 and BAK1 for positive propagation of the flg22 signaling pathway [45].

Plant G protein signaling is also known to be involved in innate immunity. Liang et al. [46] reported that G protein complexes, including XLG2 and AGB1 with AGG1 or AGG2, are required for FLS2-mediated immunity. They showed that non-canonical Gα XLG2, but not canonical Gα GPA1, is critical for the flg22-mediated response through direct interactions with the FLS2 and BIK1 complex [46]. In l-o-f *xlg2* mutant leaves, increased *Pseudomonas syringae* pv *tomato* (*Pst*) DC3000 growth and reduced ROS production were observed under flg22-infiltrated conditions compared to the water-infiltrated control [46], suggesting the resistance function of *XLG2* against *Pst* DC3000 via flg22-mediated ROS production. After the perception of flg22, XLG2 dissociated from AGB1 was phosphorylated at the N-terminus by activated BIK1, and phosphorylated XLG2 enhanced the activity of NADPH oxidase RbohD, which produces ROS [46]. In addition, BIK1 activated by flg22 also phosphorylated RGS1 at Ser428 and Ser431 to activate the GTP-bound Gα subunit through the dissociation from the FLS2–G protein complex [47]. Previous studies have shown that *AGB1*, *AGG1*, and *AGG2* are involved in pathogen resistance and ROS production [48,49],

suggesting that the XLG2-AGB1-AGG1/2 G protein signaling module is required for FLS2-mediated immunity.

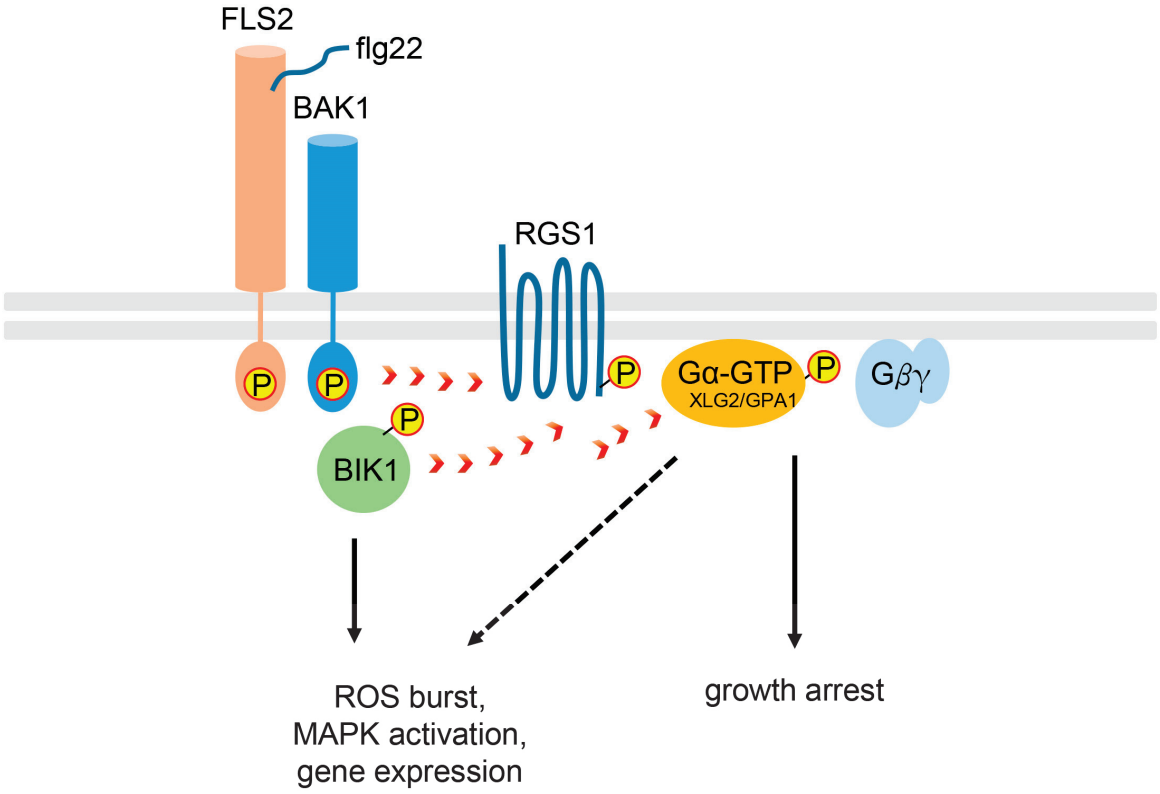

Figure 2. Schematic diagram of plant immune responses via heterotrimeric G protein signaling. Upon perception of flg22 signals, immune complexes, including receptors, cytoplasmic components, RGS1, and inactive G protein trimers, are dissociated. Activated kinases such as receptor BAK1 and cytoplasmic BIK1 phosphorylate 7TM-RGS1 and the Gα subunit to activate them (red arrowheads). A phosphorylated GTPase RGS1 is dissociated from the Gα subunit by endocytosis and the self-activating Gα subunit is activated by spontaneous exchange of GDP to GTP. Flg22 induces ROS burst, MAPK activation, and immune gene expression as an early response and growth arrest is likely to be mediated mainly by G protein signaling as a late response (solid arrows). Based on current data, G protein signaling is partly involved in the immune response for adaptation in response to biotic stress (dotted arrow).

Previous studies have shown that the canonical Gα GPA1 is not essential for flg22-induced ROS production and resistance, as the *gpa1* mutant showed similar susceptibility to different pathogenic *P. syringae* strains compared to the wild type (WT) [48,49]. Although GPA1 does not appear to be involved in FLS2-mediated basal immunity based on these observations, it has been shown to play an important role in FLS2-mediated stomatal resistance [50]. Stomatal opening is critical for pathogen entry [51], and GPA1 is required for stomatal closure due to flg22 treatment [52]. Although the susceptibility of *Pst* DC300 was not indistinguishable between WT and *gpa1* [48,49], the *gpa1* mutant showed increased susceptibility, similar to that of the *fls2* mutant, to the COR-deficient *Pst* DC3000 mutants, which have a defect in stomatal reopening [50]. Moreover, GPA1 and AGG1/2 interact with another defense-related RLK, chitin elicitor receptor kinase 1 (CERK1), but not FLS2, through yeast split ubiquitin and bimolecular fluorescence complementation (BiFC) assays [53]. These reports suggest that GPA1 is likely involved in plant immunity through a distinct signaling module with Gβγ subunits to different RLKs.

Interestingly, recent studies reported that the positive function of the conventional Gα GPA1 instead of XLG2 mediates the responses of flg22 in plant immunity through

different experimental conditions. Xue et al. [54] reported that the bacterial growth of the less virulent *P. syringae* pv. *Maculicola* ES4326, but not *Pst* DC3000, was higher in the flg22-treated *gpa1* mutants than in the WT, indicating compromised flg22-mediated immunity in *gpa1*. In addition, the *gpa1* mutant showed slightly lower ROS production upon flg22 treatment than the WT. Similarly, enhanced bacterial growth and susceptibility in *gpa1* as well as *agb1* and *agg1 agg2* in response to diverse host and nonhost *Pseudomonas* pathogens has been reported [55]. Moreover, an increase in the overall phosphorylation in GPA1 was also induced by flg22, and GPA1 phosphorylation was abolished in the *bak1* null mutant [54,56]. These results suggest that flg22 triggers the downstream immune responses, including GPA1, via BAK1, which probably acts as a kinase for GPA1. Additional in vitro analysis revealed RGS1 phosphorylation upon flg22 perception through defense-related RLKs, including BAK1. This phosphorylated RGS1 induced the dissociation of the FLS2-BAK1-GPA1-AGB1 complex to activate G protein signaling [54,56,57], proposing a similar role of RLKs in plants to that of GPCRs in animals to trigger the self-activation of the Gα subunit. Overall, these data suggest that complex and diverse G protein signaling modules, including GPA1 or XLGs, are involved in plant immunity.

2.4. Trade-Off Regulation Between Plant Growth and Defense via Heterotrimeric G Protein Signaling

In addition to the MAMP-mediated early responses (within 30 min), including ion fluxes, oxidative burst, MAPK activation, receptor endocytosis, and gene expression, plants also have late responses (hours to days), including seedling growth inhibition [42]. The inhibition of plant growth by MAPMs, such as flg22, usually appears to be the result of a trade-off to modulate energy use from normal growth to enhance pathogen resistance [58]. Recently, the *agb1* mutant was almost insensitive to growth inhibition under biotic stress conditions but not *gpa1* [11]. Yang et al. [11] reported that an flg22 treatment severely reduced the primary root length of WT and *gpa1* seedlings. In contrast, the root growth inhibsition of *agb1* single- and *agb1 gpa1* double-mutant seedlings was almost abolished. Consistent with previous studies [49,54,59], early responses, such as MAPK activation and immune gene expression, induced by flg22 were unaffected in *gpa1* and *agb1* mutants compared to WT [11]. Therefore, the flg22-mediated early and late responses are likely to be uncoupled processes. Moreover, G protein signaling is likely to be important for growth regulation associated with plant immunity by modulating energy use. On the other hand, no growth inhibition was observed in *gpa1* compared to *agb1* [11]. Therefore, two possible scenarios for these results can be inferred based on previous reports. First, activated Gβγ complexes, including AGB1, that dissociate from the inactive form of the heterotrimeric complex after flg22 induction may function primarily in growth regulation related to the immune response. Second, the atypical Gα XLG2-mediated G protein signaling module may be important for growth regulation instead of GPA1.

The *Arabidopsis* Gα and Gβ subunits are also involved in regulating shoot apical meristem (SAM) development through the CLAVATA (CLV)-WUSCHEL (WUS) signaling pathway [60,61]. For example, *agb1* was isolated from suppressor mutant screens using *clv2* because it exhibited an enhanced phenotype of an enlarged *clv2* SAM size, and AGB1 controlled SAM maintenance through protein–protein interactions with RECEPTOR-LIKE PROTEIN KINASE 2 (RPK2) [60]. Similarly, the maize Gα subunit COMPACT PLANT2 (CT2) was also reported to interact with the CLV2 ortholog FASCIATED EAR 2 (FEA2) to control SAM size [62]. Recently, maize *XLGs* and *ZmGB1*, which encode atypical Gα and Gβ subunits in maize, respectively, play important roles in SAM development according to CRISPR-Cas9 analysis [63,64]. Unlike *Arabidopsis*, the null mutant of *ZmGB1* showed a seedling-lethal phenotype similar to that of rice [65], suggesting that the monocot Gβ subunit is crucial for growth and survival. Interestingly, Wu et al. [64] reported that the lethal phenotype of *ZmGB1* was caused by an autoimmune response but not by growth arrest. They showed high levels of trypan blue and DAB accumulation, which indicate cell death and H_2O_2 production, respectively. Moreover, immune marker genes, such

as *PATHOGENESIS-RELATED PROTEIN* (*PR1*) and *PR5*, are strongly expressed in the CRISPR/Cas9-mediated knockout mutant of *ZmGB1* (*Zmgb1*^{CR}), suggesting a correlation between seedling death and autoimmunity. In addition, through suppressor analysis by crossing *Zmgb1*^{CR} with a tropical maize line CML103, they reported that suppressed mutants derived from *Zmgb1*^{CR} exhibited reduced *PR* gene expression and an enlarged SAM size [64]. These data suggest that the trade-off regulation between growth and immunity depends on the activity of the Gβ subunit.

2.5. Trade-Off Regulation by Heterotrimeric G Protein Signaling in Thermomorphogenesis

Temperature is one of the most critical abiotic and environmental factors for plastic growth and development in plants. Compared to the normal growth temperature (22–23 °C) of *Arabidopsis*, the high temperature affecting growth and development can mainly be divided into two types [66]. The first type is extremely high temperatures, which are recognized as heat stress (>40 °C), which may cause immediate cell death [67]. *Arabidopsis* plants can sometimes acquire thermotolerance by being exposed to moderately high temperatures (<37 °C) as a heat acclimation process [67,68]. Heat stress suppresses plant growth and development, including seed germination, seedling growth, and pollination. Under this pressure, plants have developed evolutionarily to acquire adaptive priming mechanisms for thermotolerance responses [69], in which the trade-off modulating the re-distribution of energy allocation between growth and stress responses is regulated by heat shock transcription factors (HSFs) and plant hormones, such as gibberellins, brassinosteroids, ABA, and salicylic acid [70]. In addition, the function of TOR has been reported to act as a modulator of the trade-off between growth and heat stress [71]. Sharma et al. [71] reported that glucose–TOR signaling plays a vital role in the adaptation to heat stress responses by reprograming the expression profiles and epigenetic regulation. As a result, the seedlings overexpressing *TOR* showed a significantly enhanced growth phenotype, whereas the *tor* mutant showed a sensitive phenotype.

The second type of high temperature is associated with warmer and relatively non-stressful conditions, known as high ambient temperatures (27–32 °C), which can also affect the morphological and developmental changes known as thermomorphogenesis, including the inhibition of seed germination, enhanced hypocotyl/petiole elongation, and induced leaf thermonasty and early flowering at high ambient temperature, mainly through the PHYTOCHROM-INTERACTING FACTOR 4 (PIF4)-mediated pathways [66,72]. PIFs, including PIF4, are accumulated under high ambient temperature by inhibiting phytochrome B [73], accelerating the expression of auxin biosynthetic genes, such as *YUCCA8* (*YUC8*) and *TRYPTOPHAN AMINOTRANSFERASE OF ARABIDOPSIS1* (*TAA1*), increasing auxin levels and increasing cell elongation in hypocotyls [74,75]. Recently, the LONG HYPOCOTYL5 (HY5)-PIF signaling module was reported to function in the developmental trade-off to balance shoot and root growth at high ambient temperatures [76]. Overall, survival against or thermomorphogenic responses to a wide range of elevated environmental temperatures may be accompanied by different sets of trade-off regulations for plastic growth and development in plants [77].

FLOWERING CONTROL LOCUS A (*FCA*) acts in an autonomous pathway by repressing the floral repressor *FLOWERING LOCUS C* (*FLC*) and plays a significant role in the ambient temperature (thermosensory) pathway through the floral activator *FLOWERING LOCUS T* (*FT*) for flowering [78]. In addition to its role in floral induction, *FCA* was implicated in thermomorphogenesis through the epigenetic regulation of PIF4 activity because the *fca* mutant showed enhanced hypocotyl elongation compared to WT in response to the high-ambient-temperature treatment following normal-temperature conditions (23 °C for four days and then 28 °C for three days) [79]. Interestingly, the different experimental conditions, such as the continuous treatment of high ambient temperature (28 °C) from germination, led to different thermal responses in the *fca* mutant, such as severe seedling growth arrest by regulating the chlorophyll biosynthetic enzymes PROTOCHLOROPHYLLIDE OXIDOREDUCTASES (PORs), which control autotrophic development for plant

growth [80]. Yang et al. [11] reported that the growth inhibition shown in the *fca* mutant was almost entirely rescued in the *gpa1 fca* but not in the *agb1 fca* double mutant under continuous high-ambient-temperature conditions. In addition, the reduced number of dividing cells in root meristems of the *fca* mutant was recovered in *gpa1 fca* but not *agb1 fca*. Interestingly, these rescued phenotypes shown in the *gpa1 fca* double mutant disappeared in the *gpa1 agb1 fca* triple mutant like the *fca* single mutant [11], suggesting that the epistatic relationship between *GPA1* and *AGB1* is essential for thermal adaptation. Therefore, these data suggest that G protein signaling plays a crucial role in the developmental trade-off associated with *FCA*-mediated thermomorphogenesis through cell proliferation.

2.6. Perspective on the Role of Heterotrimeric G Protein Signaling with Trade-Off Modulators

In plants and animals, SNF1/AMPK-related protein kinases (SnRKs) and TOR act as critical modulators in regulating the trade-off between growth and stress responses [4,81]. Plant SnRK1s, including *KIN10* and *KIN11* genes, are most closely related to yeast sucrose non-fermentable 1 (SNF1) and animal AMP-activated protein kinase (AMPK) [4,82]. They are activated in response to the changes in energy status caused by stressful conditions such as nutrient deprivation, darkness, inhibition of photosynthesis, and hypoxia [83]. An l-o-f *kin10 kin11* knockdown mutant showed a growth defect. In contrast, plants overexpressing *KIN10* showed enhanced starvation tolerance and delayed developmental senescence [83], suggesting that SnRK1s are important for growth and development and plant adaptation to stresses associated with energy homeostasis. TOR also plays an evolutionarily conserved role in sensing energy and nutrient status to regulate cell proliferation and overall plant growth [84]. Therefore, null mutations of *TOR* result in embryonic lethality [85]. Even inducible *tor* knockdown- or TOR kinase inhibitor-treated seedlings exhibit severe growth inhibition [86]. In addition to nutrient signals, TOR activity is negatively regulated in response to cold and osmotic stress signals, reflecting the stress status in terms of plastic plant growth and development [87,88]. Previous studies suggested that SnRKs and TOR mainly function in the trade-off for plants to adapt to environmental stress while ensuring maximum survival chances with minimal resources because SnRKs and TOR function antagonistically under normal and stress growth conditions [4,81].

In addition to the roles of plant G protein signaling in normal growth and development [61], phenotypic analyses using G protein component mutants have shown that G proteins are involved in the morphological changes and tolerant/sensitive effects associated with the trade-off against biotic and abiotic stresses in many plant species, including *Arabidopsis*, rice, and maize [8,10,58,89,90]. Nevertheless, there is no direct evidence of a correlation between G protein signaling and trade-off modulators such as SnRKs and TOR. The only possible link is the RGS1-mediated sugar sensing and response. In addition to HEXOKINASE1 (HXK1) and SnRK1/TOR acting as cytoplasmic glucose sensors, RGS1 senses glucose as a plasma membrane receptor [35,91]. Recognition of glucose as a ligand triggers RGS1 endocytosis, which negatively regulates GPA1 activity [40]. Therefore, activated G protein signaling and TOR appear to influence glucose-mediated growth by sensing the available nutrient resources, including glucose, in response to stress conditions (Figure 3).

In contrast to plants, mammalian G protein signaling was reported to act as a positive or negative upstream regulator of mTORC1 by phosphorylating the TOR and Raptor components of the mTORC1 complex. These phosphorylations were mediated by the GPCR-mediated protein kinase A (PKA) pathway [92]. Although plants have a deficiency in GPCR-mediated cAMP and PKA signaling, this does not exclude the evolutionary scenario of the functional link between G protein signaling and trade-off modulators. Furthermore, G protein signaling is involved in regulating the life–death decision of cells in *Arabidopsis*, maize, and rice [9,63,93,94], similar to TOR [14], suggesting the relevance of G protein signaling in the trade-off regulation through crosstalk with nutrient sensing and sugar signaling.

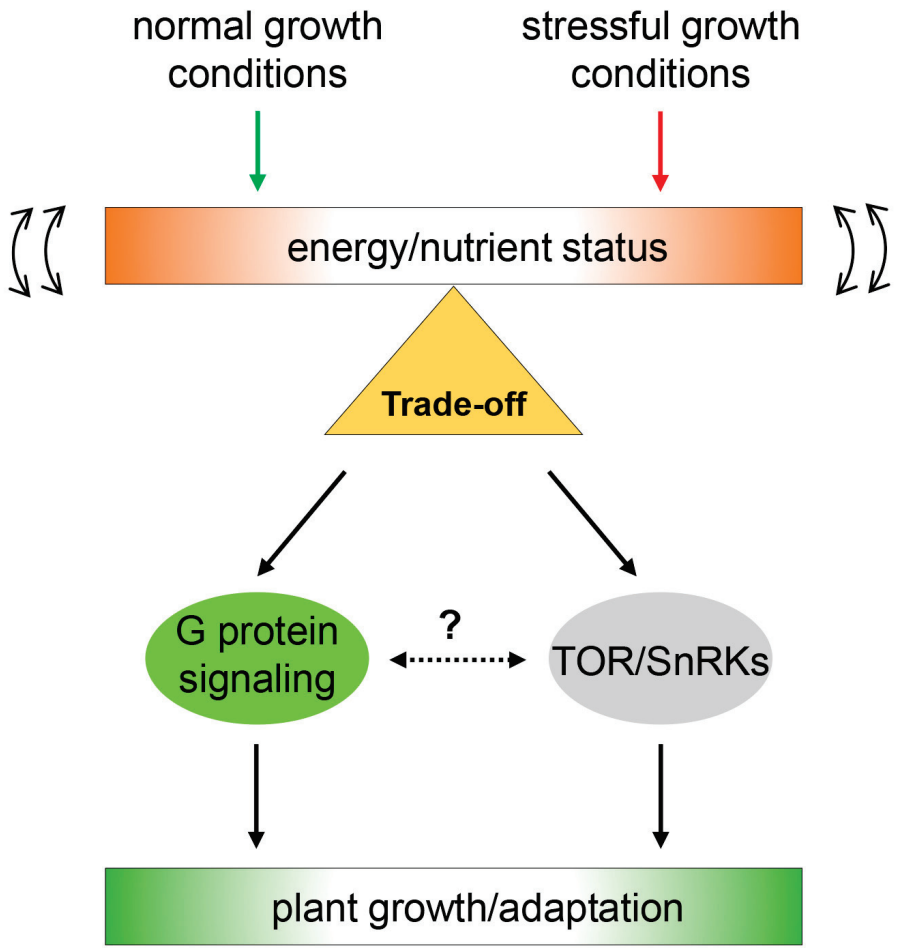

Figure 3. Hypothetical model of G protein signaling in the trade-off regulation. Energy status controlled by environmental conditions affects downstream signaling modules. Plant G protein signaling is involved in the regulation of plastic growth through RGS1, a putative glucose receptor. TOR and SnRKs as energy/nutrient sensors reciprocally act as trade-off modulators for plant growth and adaptation to environmental conditions. Open arrowheads indicate fluctuating energy and nutrient status controlled by normal and stressful growth conditions. Arrows indicate the involvement of downstream regulatory pathways for plant growth and adaptation to different environmental conditions. Dotted arrows indicate unidentified links between G-protein signaling and trade-off modulators.

3. Conclusions

In contrast to the molecular processes mediated by GPCR activation in animals, plant G protein signaling was recently reported to be activated by the G protein regulator 7TM-RGS1 or RLKs, which are relatively abundant in plants. Although the details of the signaling process are different due to the composition and corresponding receptors, the sensing and response of G protein signaling to environmental stimuli, including hormonal, olfactory, biotic and abiotic stress, and nutrient signals, is likely to have evolved in a similar manner in animals and plants in terms of function [15,95]. The relationship between G protein signaling and important trade-off modulators, such as SnRKs and TOR, that sense nutrient and energy status is known in animals but is currently unclear in plants (Figure 3). Therefore, further studies will examine whether plant G protein signaling is directly or indirectly associated with the trade-off modulators. These efforts, through a clearer understanding of the trade-off regulation mechanisms, may provide new strategies for designing and breeding stress-tolerant crops that can reset energy allocation to avoid the penalty of growth inhibition.

Funding: This study was supported by the National Research Foundation of Korea (NRF) funded by the Ministry of Education (2021R1F1A1047817).

Conflicts of Interest: The author declares no conflict of interest.

References

1. Janni, M.; Maestri, E.; Gulli, M.; Marmiroli, M.; Marmiroli, N. Plant responses to climate change, how global warming may impact on food security: A critical review. *Front. Plant Sci.* **2024**, *14*, 1297569. [CrossRef] [PubMed]
2. Schneider, H.M. Characterization, costs, cues and future perspectives of phenotypic plasticity. *Ann. Bot.* **2022**, *130*, 131–148. [CrossRef]
3. Li, Y.; Yang, Z.; Zhang, Y.; Guo, J.; Liu, L.; Wang, C.; Wang, B.; Han, G. The role of HD-ZIP proteins in plant abiotic stress tolerance. *Front. Plant Sci.* **2022**, *13*, 1027071. [CrossRef]
4. Zhang, H.; Zhao, Y.; Zhu, J.K. Thriving under Stress: How Plants Balance Growth and the Stress Response. *Dev. Cell* **2020**, *7*, 529–543. [CrossRef]
5. Zhou, Q.; Liu, D.; Wei, Y.; Ma, N.; Zhang, R.; Zhang, Z.; Jiang, C.; Yuan, H. Functional Characterization of Tea Plant (*Camellia sinensis* L.) *CsCBF2* Gene Involved in Multiple Abiotic Stress Response in Tobacco (*Nicotiana tabacum* L.). *Horticulturae* **2022**, *8*, 853. [CrossRef]
6. Kudo, M.; Kidokoro, S.; Yoshida, T.; Mizoi, J.; Kojima, M.; Takebayashi, Y.; Sakakibara, H.; Fernie, A.R.; Shinozaki, K.; Yamaguchi-Shinozaki, K. A gene-stacking approach to overcome the trade-off between drought stress tolerance and growth in Arabidopsis. *Plant J.* **2019**, *97*, 240–256. [CrossRef] [PubMed]
7. Leysen, H.; Walter, D.; Christiaenssen, B.; Vandoren, R.; Harputluoğlu, İ.; Van Loon, N.; Maudsley, S. GPCR Are Optimal Regulators of Complex Biological Systems and Orchestrate the Interface between Health and Disease. *Int. J. Mol. Sci.* **2021**, *22*, 13387. [CrossRef]
8. Urano, D.; Chen, J.G.; Botella, J.R.; Jones, A.M. Heterotrimeric G protein signalling in the plant kingdom. *Open Biol.* **2013**, *3*, 120186. [CrossRef]
9. Urano, D.; Jones, A.M. Heterotrimeric G Protein-Coupled Signaling in Plants. *Annu. Rev. Plant Biol.* **2014**, *65*, 365–384. [CrossRef]
10. Zhang, H.; Xie, P.; Xu, X.; Xie, Q.; Yu, F. Heterotrimeric G protein signalling in plant biotic and abiotic stress response. *Plant Biol.* **2021**, *23*, 20–30. [CrossRef]
11. Yang, S.; Jung, S.; Lee, H. Heterotrimeric G Protein-Mediated Signaling Is Involved in Stress-Mediated Growth Inhibition in *Arabidopsis thaliana*. *Int. J. Mol. Sci.* **2023**, *24*, 11027. [CrossRef] [PubMed]
12. Wang, Y.; Lv, Y.; Yu, H.; Hu, P.; Wen, Y.; Wang, J.; Tan, Y.; Wu, H.; Zhu, L.; Wu, K.; et al. GR5 acts in the G protein pathway to regulate grain size in rice. *Plant Commun.* **2024**, *5*, 100673. [CrossRef] [PubMed]
13. Karimian, P.; Trusov, Y.; Botella, J.R. Conserved Role of Heterotrimeric G Proteins in Plant Defense and Cell Death Progression. *Genes* **2024**, *15*, 115. [CrossRef] [PubMed]
14. Hung, C.M.; Garcia-Haro, L.; Sparks, C.A.; Guertin, D.A. mTOR-Dependent Cell Survival Mechanisms. *Cold Spring Harb. Perspect. Biol.* **2012**, *4*, a008771. [CrossRef]
15. Jones, A.M.; Assmann, S.M. Plants: The latest model system for G protein research. *EMBO Rep.* **2004**, *5*, 572–578. [CrossRef]
16. Ma, H.; Yanofsky, M.F.; Meyerowitz, E.M. Molecular cloning and characterization of *GPA1*, a G protein α subunit gene from *Arabidopsis thaliana*. *Proc. Natl. Acad. Sci. USA* **1990**, *87*, 3821–3825. [CrossRef]
17. Weiss, C.A.; Garnaat, C.W.; Mukai, K.; Hu, Y.; Ma, H. Isolation of cDNAs encoding guanine nucleotide-binding protein β-subunit homologues from maize (ZGB1) and *Arabidopsis* (AGB1). *Proc. Natl. Acad. Sci. USA* **1994**, *91*, 9554–9558. [CrossRef]
18. Mason, M.G.; Botella, J.R. Completing the heterotrimer: Isolation and characterization of an Arabidopsis thaliana G protein γ-subunit cDNA. *Proc. Natl. Acad. Sci. USA* **2000**, *97*, 14784–14788. [CrossRef]
19. Mason, M.G.; Botella, J.R. Isolation of a novel G protein γ-subunit from *Arabidopsis thaliana* and its interaction with Gβ. *Biochim. Biophys. Acta* **2001**, *1520*, 147–153. [CrossRef]
20. Chakravorty, D.; Trusov, Y.; Zhang, W.; Acharya, B.R.; Sheahan, M.B.; McCurdy, D.W.; Assmann, S.M.; Botella, J.R. An atypical heterotrimeric G protein γ-subunit is involved in guard cell K^+-channel regulation and morphological development in *Arabidopsis thaliana*. *Plant J.* **2011**, *67*, 840–851. [CrossRef]
21. Trusov, Y.; Chakravorty, D.; Botella, J.R. Diversity of heterotrimeric G protein γ-subunits in plants. *BMC Res. Notes* **2012**, *5*, 608. [CrossRef] [PubMed]
22. Miao, J.; Yang, Z.; Zhang, D.; Wang, Y.; Xu, M.; Zhou, L.; Wang, J.; Wu, S.; Yao, Y.; Du, X.; et al. Mutation of *RGG2*, which encodes a type B heterotrimeric G protein γ subunit, increases grain size and yield production in rice. *Plant Biotechnol. J.* **2019**, *17*, 650–664. [CrossRef] [PubMed]
23. Chakravorty, D.; Gookin, T.E.; Milner, M.J.; Yu, Y.; Assmann, S.M. Extra-Large G Proteins Expand the Repertorie of Subunits in Arabidopsis Heterotrimeric G Protein Signaling. *Plant Physiol.* **2015**, *169*, 512–529. [CrossRef] [PubMed]
24. Urano, D.; Maruta, N.; Trusov, Y.; Stoian, R.; Wu, Q.; Liang, Y.; Jaiswal, D.K.; Thung, L.; Jackson, D.; Botella, J.R.; et al. Saltational evolution of the heterotrimeric G protein signaling mechanisms in the plant kingdom. *Sci. Signal.* **2016**, *9*, ra93. [CrossRef]
25. Ding, L.; Pandey, S.; Assmann, S.M. Arabidopsis extra-large G proteins (XLGs) regulate root morphogenesis. *Plant J.* **2008**, *53*, 248–263. [CrossRef]

26. Pandey, S.; Monshausen, G.B.; Ding, L.; Assmann, S.M. Regulation of root-wave response by extra large and conventional G proteins in *Arabidopsis thaliana*. *Plant J.* **2008**, *55*, 311–322. [CrossRef]
27. Oka, Y.; Saraiva, L.R.; Kwan, Y.Y.; Korsching, S. The fifth class of Gα proteins. *Proc. Natl. Acad. Sci. USA* **2009**, *106*, 1484–1489. [CrossRef]
28. Pandey, S. Heterotrimeric G Protein Signaling in Plants: Conserved and Novel Mechanisms. *Annu. Rev. Plant Biol.* **2019**, *70*, 213–238. [CrossRef]
29. Oldham, W.M.; Hamm, H.E. Heterotrimeric G protein activation by G-protein-coupled receptors. *Nat. Rev. Mol. Cell Biol.* **2008**, *9*, 60–71. [CrossRef]
30. Ghosh, P.; Rangamani, P.; Kufareva, I. The GAPs, GEFs, GDIs and. . .now, GEMs: New kids on the heterotrimeric G protein signaling block. *Cell Cycle* **2017**, *16*, 607–612. [CrossRef]
31. Jones, J.C.; Duffy, J.W.; Machius, M.; Temple, B.R.S.; Dohlman, H.G.; Jones, A.M. The crystal structure of a self-activating G protein α subunit reveals its distinct mechanism of signal initiation. *Sci. Signal.* **2011**, *4*, ra8. [CrossRef] [PubMed]
32. Urano, D.; Jones, J.C.; Wang, H.; Matthews, M.; Bradford, W.; Bennetzen, J.L.; Jones, A.M. G Protein Activation without a GEF in the Plant Kingdom. *PLoS Genet.* **2012**, *8*, e1002756. [CrossRef] [PubMed]
33. Iiri, T.; Herzmark, P.; Nakamoto, J.M.; Van Dop, C.; Bourne, H.R. Rapid GDP release from Gsα in patients with gain and loss of endocrine function. *Nature* **1994**, *371*, 164–168. [CrossRef] [PubMed]
34. Johnston, C.A.; Taylor, J.P.; Gao, Y.; Kimple, A.J.; Grigston, J.C.; Chen, J.G.; Siderovski, D.P.; Jones, A.M.; Willard, F.S. GPTase acceleration as the rate-limiting step in *Arabidopsis* G protein-coupled sugar signaling. *Proc. Natl. Acad. Sci. USA* **2007**, *104*, 17317–17322. [CrossRef] [PubMed]
35. Chen, J.G.; Willard, F.S.; Huang, J.; Liang, J.; Chasse, S.A.; Jones, A.M.; Siderovsk, D.P. A Seven-Transmembrane RGS Protein That Modulates Plant Cell Proliferation. *Science* **2003**, *301*, 1728–1731. [CrossRef]
36. Hackenberg, D.; McKain, M.R.; Lee, S.G.; Choudhury, S.R.; McCann, T.; Schreier, S.; Harkess, A.; Pires, J.C.; Wong, G.K.S.; Jez, J.M.; et al. Gα and regulator of G-protein signaling (RGS) protein pairs maintain functional compatibility and conserved interaction interfaces throughout evolution despite frequent loss of RGS proteins in plants. *New Phytol.* **2017**, *216*, 562–575. [CrossRef]
37. Jones, J.C.; Temple, B.R.S.; Jones, A.M.; Dohlman, H.G. Functional Reconstitution of an Atypical G Protein Heterotrimer and Regulator of G Protein Signaling Protein (RGS1) from *Arabidopsis thaliana*. *J. Biol. Chem.* **2011**, *286*, 13143–13150. [CrossRef]
38. Huang, J.; Taylor, J.P.; Chen, J.G.; Uhrig, J.F.; Schnell, D.J.; Nakagawa, T.; Korth, K.L.; Jones, A.M. The Plastid Protein THYLAKOID FORMATION1 and the Plasma Membrane G-Protein GPA1 Interact in a Novel Sugar-Signaling Mechanism in *Arabidopsis*. *Plant Cell* **2006**, *18*, 1226–1238. [CrossRef]
39. Chen, Y.; Ji, F.; Xie, H.; Liang, J.; Zhang, J. The Regulator of G-Protein Signaling Proteins Involved in Sugar and Abscisic Acid Signaling in Arabidopsis Seed Germination. *Plant Physiol.* **2006**, *140*, 302–310. [CrossRef]
40. Urano, D.; Phan, N.; Jones, J.C.; Yang, J.; Huang, J.; Grigston, J.; Taylor, J.P.; Jones, A.M. Endocytosis of the seven-transmembrane RGS1 protein activates G-protein-coupled signalling in *Arabidopsis*. *Nat. Cell Biol.* **2012**, *14*, 1079–1088. [CrossRef]
41. Phan, N.; Urano, D.; Srba, M.; Fischer, L.; Jones, A.M. Sugar-induced endocytosis of plant 7TM-RGS proteins. *Plant Signal. Behav.* **2013**, *8*, e22814. [CrossRef] [PubMed]
42. Boller, T.; Felix, G. A Renaissance of Elicitors: Perception of Microbe-Associated Molecular Patterns and Danger Signals by Pattern-Recognition Receptors. *Annu. Rev. Plant Biol.* **2009**, *60*, 379–406. [CrossRef] [PubMed]
43. Nishad, R.; Ahmed, T.; Rahman, V.J.; Kareem, A. Modulation of Plant Defense System in Response to Microbial Interactions. *Front. Microbiol.* **2020**, *11*, 1298. [CrossRef]
44. Chinchilla, D.; Zipfel, C.; Robatzek, S.; Kemmerling, B.; Nürnberger, T.; Jones, J.D.G.; Felix, G.; Boller, T. A flagellin-induced complex of the receptor FLS2 and BAK1 initiates plant defense. *Nature* **2007**, *448*, 497–500. [CrossRef] [PubMed]
45. Lu, D.; Wu, S.; Gao, X.; Zhang, Y.; Shan, L.; He, P. A receptor-like cytoplasmic kinase, BIK1, associates with a flagellin receptor complex to initiate plant innate immunity. *Proc. Natl. Acad. Sci. USA* **2010**, *107*, 496–501. [CrossRef]
46. Liang, X.; Ding, P.; Lian, K.; Wang, J.; Ma, M.; Li, L.; Li, L.; Li, M.; Zhang, X.; Chen, S.; et al. Arabidopsis heterotrimeric G proteins regulate immunity by directly coupling to the FLS2 receptor. *eLife* **2016**, *5*, e13568. [CrossRef]
47. Liang, X.; Ma, M.; Zhou, Z.; Wang, J.; Yang, X.; Rao, S.; Bi, G.; Li, L.; Zhang, X.; Chai, J.; et al. Ligand-triggered de-repression of *Arabidopsis* heterotrimeric G proteins coupled to immune receptor kinases. *Cell Res.* **2018**, *28*, 529–543. [CrossRef]
48. Torres, M.A.; Morales, J.; Sánchez-Rodríguez, C.; Molina, A.; Dangl, J.L. Functional Interplay Between *Arabidopsis* NADPH Oxidases and Heterotrimeric G Protein. *Mol. Plant-Microbe Interact.* **2013**, *26*, 686–694. [CrossRef]
49. Liu, J.; Ding, P.; Sun, T.; Nitta, Y.; Dong, O.; Huang, X.; Yang, W.; Li, X.; Botella, J.R.; Zhang, Y. Heterotrimeric G Proteins Serve as a Converging Point in Plant Defense Signaling Activated by Multiple Receptor-Like Kinases. *Plant Physiol.* **2013**, *161*, 2146–2158. [CrossRef]
50. Zeng, W.; He, S.Y. A Prominent Role of the Flagellin Receptor FLAGELLIN-SENSING2 in Mediating Stomatal Response to *Pseudomonas syringae* pv *tomato* DC3000 in Arabidopsis. *Plant Physiol.* **2010**, *153*, 1188–1198. [CrossRef]
51. Melotto, M.; Underwood, W.; Koczan, J.; Nomura, K.; He, S.Y. Plant Stomata Function in Innate Immunity Against Bacterial Invasion. *Cell* **2006**, *126*, 969–980. [CrossRef] [PubMed]
52. Zhang, W.; He, S.Y.; Assmann, S.M. The plant innate immunity response in stomatal guard cells invokes G-protein-dependent ion channel regulation. *Plant J.* **2008**, *56*, 984–996. [CrossRef] [PubMed]

53. Aranda-Sicilia, M.N.; Trusov, Y.; Maruta, N.; Chakravorty, D.; Zhang, Y.; Botella, J.R. Heterotrimeric G proteins interact with defense-related receptor-like kinases in *Arabidopsis*. *J. Plant Physiol.* **2015**, *188*, 44–48. [CrossRef] [PubMed]
54. Xue, J.; Gong, B.Q.; Yao, X.; Huang, X.; Li, J.F. BAK1-mediated phosphorylation of canonical G protein alpha during flagellin signaling in *Arabidopsis*. *J. Integr. Plant Biol.* **2019**, *62*, 690–701. [CrossRef]
55. Lee, S.; Rojas, C.M.; Ishiga, Y.; Pandey, S.; Mysore, K.S. Arabidopsis Heterotrimeric G-Proteins Play a Critical Role in Host and Nonhost Resistance Against *Pseudomonas syringae* Pathogens. *PLoS ONE* **2013**, *8*, e82445. [CrossRef]
56. Tunc-Ozdemir, M.; Urano, D.; Jaiswal, D.K.; Clouse, S.D.; Jones, A.M. Direct Modulation of Heterotrimeric G Protein-Coupled Signaling by a Receptor Kinase Complex. *J. Biol. Chem.* **2016**, *291*, 13918–13925. [CrossRef]
57. Xu, L.; Yao, X.; Zhang, N.; Gong, B.Q.; Li, J.F. Dynamic G protein alpha signaling in Arabidopsis innate immunity. *Biochem. Biophys. Res. Commun.* **2019**, *516*, 1039–1045. [CrossRef]
58. Wang, J.; Long, X.; Chern, M.; Chen, X. Understanding the molecular mechanisms of trade-offs between plant growth and immunity. *Sci. China Life Sci.* **2021**, *64*, 234–241. [CrossRef]
59. Cheng, Z.; Li, J.F.; Niu, Y.; Zhang, X.C.; Woody, O.Z.; Xiong, Y.; Djonović, S.; Millet, Y.; Bush, J.; McConkey, B.J.; et al. Pathogen-secreted proteases activates a novel plant immune pathway. *Nature* **2015**, *521*, 213–216. [CrossRef]
60. Ishida, T.; Tabata, R.; Yamada, M.; Aida, M.; Mitsumasu, K.; Fujiwara, M.; Yamaguchi, K.; Shigenobu, S.; Higuchi, M.; Tsuji, H.; et al. Heterotrimeric G proteins control stem cell proliferation through CLAVATA signaling in *Arabidopsis*. *EMBO Rep.* **2014**, *15*, 1202–1209. [CrossRef]
61. Urano, D.; Miura, K.; Wu, Q.; Iwasaki, Y.; Jackson, D.; Jones, A.M. Plant Morphology of Heterotrimeric G Protein Mutants. *Plant Cell Physiol.* **2016**, *57*, 437–445. [CrossRef] [PubMed]
62. Bommert, P.; Je, B.I.; Goldshmidt, A.; Jackson, D. The maize Gα gene *COMPACT PLANT2* functions in CLAVATA signalling to control shoot meristem size. *Nature* **2013**, *502*, 555–558. [CrossRef] [PubMed]
63. Wu, Q.; Regan, M.; Furukawa, H.; Jackson, D. Role of heterotrimeric Gα proteins in maize development and enhancement of agronomic traits. *PLoS Genet.* **2018**, *14*, e1007374. [CrossRef] [PubMed]
64. Wu, Q.; Xu, F.; Liu, L.; Char, S.N.; Ding, Y.; Je, B.I.; Schmelz, E.; Yang, B.; Jackson, D. The maize heterotrimeric G protein β subunit controls shoot meristem development and immune response. *Proc. Natl. Acad. Sci. USA* **2020**, *117*, 1799–1805. [CrossRef] [PubMed]
65. Sun, S.; Wang, L.; Mao, H.; Shao, L.; Li, X.; Xiao, J.; Quyang, Y.; Zhang, Q. A G-protein pathway determines grain size in rice. *Nat. Commun.* **2018**, *9*, 851. [CrossRef]
66. Vu, L.D.; Xu, X.; Gevaert, K.; De Smet, I. Developmental Plasticity at High Temperature. *Plant Physiol.* **2019**, *181*, 399–411. [CrossRef]
67. Yeh, C.H.; Kaplinsky, N.J.; Hu, C.; Charng, Y.Y. Some like it hot, some like it warm: Phenotyping explore thermotolerance diversity. *Plant Sci.* **2012**, *195*, 10–23. [CrossRef]
68. Ling, Y.; Serrano, N.; Gao, G.; Atia, M.; Mokhtar, M.; Woo, Y.H.; Bazin, J.; Veluchamy, A.; Benhamed, M.; Crespi, M.; et al. Thermopriming triggers splicing memory in Arabidopsis. *J. Exp. Bot.* **2018**, *69*, 2659–2675. [CrossRef]
69. Sedaghatmehr, M.; Thirumalaikumar, V.P.; Kamranfar, I.; Marmagne, A.; Masclaux-Daubresse, C.; Balazadeh, S. A regulatory role of autophagy for resetting the memory of heat stress in plants. *Plant Cell Environ.* **2019**, *42*, 1054–1064. [CrossRef]
70. Zhao, Y.; Liu, S.; Yang, K.; Hu, X.; Jiang, H. Fine-control of growth and thermotolerance in plant response to heat stress. *J. Integr. Agric.* 2024; *in press*. [CrossRef]
71. Sharma, M.; Jamsheer, K.M.; Shukla, B.N.; Sharma, M.; Awasthi, P.; Mahtha, S.K.; Yadav, G.; Laxmi, A. Arabidopsis Target of Rapamycin Coordinates with Transcriptional and Epigenetic Machinery to Regulate Thermotolerance. *Front. Plant Sci.* **2021**, *12*, 741965. [CrossRef] [PubMed]
72. Casal, J.J.; Balasubramanian, S. Thermomorphogenesis. *Annu. Rev. Plant Biol.* **2019**, *70*, 321–346. [CrossRef]
73. Park, E.; Kim, Y.; Choi, G. Phytochrome B Requires PIF Degradation and Sequestration to Induce Light Responses across a Wide Range of Light Conditions. *Plant Cell* **2018**, *30*, 1277–1292. [CrossRef] [PubMed]
74. Franklin, K.A.; Lee, S.H.; Patel, D.; Kumar, S.V.; Spartz, A.K.; Gu, C.; Ye, S.; Yu, P.; Breen, G.; Cohen, J.D.; et al. PHYTOCHROME-INTERACTING FACTOR 4 (PIF4) regulates auxin biosynthesis at high temperature. *Proc. Natl. Acad. Sci. USA* **2011**, *108*, 20231–20235. [CrossRef]
75. Sun, J.; Qi, L.; Li, Y.; Chu, J.; Li, C. PIF4-Mediated Activation of *YUCCA8* Expression Integrates Temperature into the Auxin Pathway in Regulating *Arabidopsis* Hypocotyl Growth. *PLoS Genet.* **2012**, *8*, e1002594. [CrossRef]
76. Gaillochet, C.; Burko, Y.; Platre, M.P.; Zhang, L.; Simura, J.; Willige, B.; Kumar, S.V.; Ljung, K.; Chory, J.; Busch, W. HY5 and phytochrome activity modulate shoot to root coordination during thermomorphogenesis. *Development* **2020**, *147*, dev192625. [CrossRef]
77. Zhou, Y.; Xu, F.; Shao, Y.; He, J. Regulatory Mechanisms of Heat Stress Response and Thermomorphogenesis in Plants. *Plants* **2022**, *11*, 3410. [CrossRef] [PubMed]
78. Blázquez, M.A.; Ahn, J.H.; Weigel, D. A thermosensory pathway controlling flowering time in *Arabidopsis thaliana*. *Nat. Genet.* **2003**, *33*, 168–171. [CrossRef] [PubMed]
79. Lee, H.J.; Jung, J.H.; Llorca, L.C.; Kim, S.G.; Lee, S.; Baldwin, I.T.; Park, C.M. FCA mediates thermal adaptation of stem growth by attenuating auxin action in *Arabidopsis*. *Nat. Commun.* **2014**, *5*, 5473. [CrossRef]

80. Ha, J.H.; Lee, H.J.; Jung, J.H.; Park, C.M. Thermo-Induced Maintenance of Photo-oxidoreductases Underlies Plant Autotrophic Development. *Dev. Cell* **2017**, *41*, 170–179. [CrossRef]
81. Maregalha, L.; Confraria, A.; Baena-González, E. SnRK1 and TOR: Modulating growth-defense trade-offs in plant stress responses. *J. Exp. Bot.* **2019**, *70*, 2261–2274. [CrossRef] [PubMed]
82. Hrabak, E.M.; Chan, C.W.M.; Gribskov, M.; Harper, J.F.; Choi, J.H.; Halford, N.; Kudla, J.; Luan, S.; Nimmo, H.G.; Sussman, M.R.; et al. The Arabidopsis CDPK-SnRK Superfamily of Protein Kinases. *Plant Physiol.* **2003**, *132*, 666–680. [CrossRef] [PubMed]
83. Baena-González, E.; Rolland, F.; Sheen, J. A central integrator of transcription networks in plant stress and energy signalling. *Nature* **2007**, *448*, 938–942. [CrossRef]
84. Xiong, Y.; Sheen, J. The Role of Target of Rapamycin Signaling Networks in Plant Growth and Metabolism. *Plant Physiol.* **2014**, *164*, 499–512. [CrossRef]
85. Ren, M.; Qiu, S.; Venglat, P.; Xiang, D.; Feng, L.; Selvaraj, G.; Datla, R. Target of Rapamycin Regulates Development and Ribosomal RNA Expression Through Kinase Domain in Arabidopsis. *Plant Physiol.* **2011**, *155*, 1367–1382. [CrossRef] [PubMed]
86. Xiong, Y.; McCormack, M.; Li, L.; Hall, Q.; Xiang, C.; Sheen, J. Glucose-TOR signalling reprograms the transcriptome and activates meristems. *Nature* **2013**, *496*, 181–186. [CrossRef]
87. Mahfouz, M.M.; Kim, S.; Delauney, A.J.; Verma, D.P.S. *Arabidopsis* TARGET OF RAPAMYCIN Interacts with RAPTOR, Which Regulates the Activity of S6 Kinase in Response to Osmotic Stress Signals. *Plant Cell* **2006**, *18*, 477–490. [CrossRef]
88. Wang, L.; Li, H.; Zhao, C.; Li, S.; Kong, L.; Wu, W.; Kong, W.; Liu, Y.; Wei, Y.; Zhu, Z.K.; et al. The inhibition of protein translation mediated by AtGCN1 is essential for cold tolerance in *Arabidopsis thaliana*. *Plant Cell Environ.* **2017**, *40*, 56–68. [CrossRef]
89. Colaneri, A.C.; Tunc-Ozdemir, M.; Huang, J.P.; Jones, A.M. Growth attenuation under saline stress is mediated by the heterotrimeric G protein complex. *BMC Plant Biol.* **2014**, *14*, 129. [CrossRef]
90. Cui, Y.; Jiang, N.; Xu, Z.; Xu, Q. Heterotrimeric G protein are involved in the regulation of multiple agronomic traits and stress tolerance in rice. *BMC Plant Biol.* **2020**, *20*, 90. [CrossRef]
91. Zou, W.; Yu, Q.; Ma, Y.; Sun, G.; Feng, X.; Ge, L. Pivotal role of heterotrimeric G protein in the crosstalk between sugar signaling and abiotic stress response in plants. *Plant Physiol. Biochem.* **2024**, *210*, 108567. [CrossRef] [PubMed]
92. Melick, C.H.; Lama-Sherpa, T.D.; Curukovic, A.; Jewell, J.L. G-Protein Coupled Receptor Signaling and Mammalian Target of Rapamycin Complex 1 Regulation. *Mol. Pharmacol.* **2022**, *101*, 181–190. [CrossRef] [PubMed]
93. Wang, S.; Narendra, S.; Fedoroff, N. Heterotrimeric G protein signaling in the *Arabidopsis* unfolded protein response. *Proc. Natl. Acad. Sci. USA* **2007**, *104*, 3817–3822. [CrossRef] [PubMed]
94. Utsunomiya, Y.; Samejima, C.; Takayanagi, Y.; Izawa, Y.; Yoshida, T.; Sawada, Y.; Fujisawa, Y.; Kato, H.; Iwasaki, Y. Suppression of the rice heterotrimeric G protein β-subunit gene, *RGB1*, causes dwarfism and browning of internodes and lamina joint regions. *Plant J.* **2011**, *67*, 907–916. [CrossRef]
95. Chakravorty, D.; Assmann, S.M. G protein subunit phosphorylation as a regulatory mechanism in heterotrimeric G protein signaling in mammals, yeast, and plants. *Biochem. J.* **2018**, *475*, 3331–3357. [CrossRef]

plants

MDPI

Review

Plant Immunity: At the Crossroads of Pathogen Perception and Defense Response

Sajad Ali [1,*,†], Anshika Tyagi [1,†] and Zahoor Ahmad Mir [2,†]

[1] Department of Biotechnology, Yeungnam University, Gyeongsan 38541, Republic of Korea; anshikabio@yu.ac.kr
[2] Department of Plant Science and Agriculture, University of Manitoba, Winnipeg, MB R2M 0TB, Canada; zahoorbio@gmail.com
* Correspondence: sajadmicro@yu.ac.kr
† These authors contributed equally to this work.

Abstract: Plants are challenged by different microbial pathogens that affect their growth and productivity. However, to defend pathogen attack, plants use diverse immune responses, such as pattern-triggered immunity (PTI), effector-triggered immunity (ETI), RNA silencing and autophagy, which are intricate and regulated by diverse signaling cascades. Pattern-recognition receptors (PRRs) and nucleotide-binding leucine-rich repeat (NLR) receptors are the hallmarks of plant innate immunity because they can detect pathogen or related immunogenic signals and trigger series of immune signaling cascades at different cellular compartments. In plants, most commonly, PRRs are receptor-like kinases (RLKs) and receptor-like proteins (RLPs) that function as a first layer of inducible defense. In this review, we provide an update on how plants sense pathogens, microbe-associated molecular patterns (PAMPs or MAMPs), and effectors as a danger signals and activate different immune responses like PTI and ETI. Further, we discuss the role RNA silencing, autophagy, and systemic acquired resistance as a versatile host defense response against pathogens. We also discuss early biochemical signaling events such as calcium (Ca^{2+}), reactive oxygen species (ROS), and hormones that trigger the activation of different plant immune responses. This review also highlights the impact of climate-driven environmental factors on host–pathogen interactions.

Keywords: plant immunity; pathogens; receptors; signaling; calcium; reactive oxygen species; hormonal crosstalk; disease resistance

1. Introduction

Plants face different microbial pathogens, such as fungi, bacteria, oomycetes, and viruses, which affect their growth and reproduction [1]. Microbial diseases are one of the leading causes of crop yield losses in modern agriculture and have significant global repercussions on food security, economy, and environmental sustainability [2,3]. For example, they can reduce yield production by up to 16%, which is further increased during post harvesting [4]. Pathogens can spread to plants by different modes such as water, air, and transmission by insects, animals, and humans. They utilize diverse strategies to infect plants, including immune suppression and the secretion of toxins and degradative enzymes that aid in colonization and nutrient release [1,5]. Some pathogens may directly enter and infiltrate plant tissues, whereas others enter through wounds or natural openings. Fungal pathogens have different modes of nutritional lifestyles, such as biotrophic, hemi biotrophic, and necrotrophic, and they evolve different strategies to infect plants [3]. Necrotrophic fungal pathogens obtain their energy from dead or dying cells, whereas biotrophs obtain their nutrients and energy from living cells. In contrast, hemibiotrophs first infiltrate living cells before switching to a necrotrophic way of life in order to harvest nutrients from the dead tissues [3]. Oomycetes and fungal pathogens use special structures like appressoria and haustoria to penetrate host cells and to release effectors as well as to obtain

nutrients [5]. For instance, the smut disease-causing fungus *Ustilago maydis* secretes the Pep1 effector from fungal hyphae, which is necessary for host tissue penetration [6]. On the other hand, viruses are obligatory parasites that require a host cell to proliferate and infect plants. During plant virus interaction, viral pathogens hijack the host machinery system, leading to metabolic, physiological, molecular, and morphological alterations in plants [7]. Particularly, viral proteins play a major role in pathogenesis in addition to replication, encapsidation, and transmission [8]. Bacterial pathogens use different strategies to infect plants. For instance, they use different secretion systems to secrete effectors both within and outside of plant host cells. The type III secretion system (T3SS), which transports effectors within host cells and is essential for pathogenesis, is a well-studied secretory pathway for bacterial effectors [9]. For example, HopM1, an effector from *Pseudomonas syringae,* targets the *Arabidopsis* 14-3-3 protein GRF8/AtMIN10, suppressing stomatal defense [10]. Through their stylet secretions, insect pathogens like psyllids and aphids can also transfer effectors during feeding. Some of the typical signs of plant disease in plants are necrosis, wilting, rot, deformation, mold, discoloration, pustules, hypertrophy and hyperplasia (overgrowth), mummification, and destruction of infected tissue [11].

Primary pathogens in plants can also trigger host susceptibility to secondary infections by suppressing their immune system, which can further deteriorate their growth and survival. For instance, when the foliar bacteria *P. syringae* infects Arabidopsis, the plants become highly susceptible to the necrotrophic fungal pathogen *Alternaria brassicicola* [12]. Similarly, for biotrophic pathogen *Albugo candida*, infection in *Arabidopsis thaliana* suppresses the immune system, making them more susceptible to avirulent pathogens [13]. In some cases, various pathogen-produced molecules have been identified that suppress the plant immune system during co-infection. For example, in Arabidopsis, the natriuretic peptide receptor NPA produced by *P. syringae* downregulates a wide range of defense-related genes, enabling subsequent infection by the virulent *A. brassicicola* [13,14]. In a similar vein, fusaric acid released by *F. oxysporum* inhibits the expression of genes that control 2,4-diacetylphloroglucinol's antimicrobial action and makes wheat more susceptible to *Pseudomonas fluorescens* infection [15]. Pathogens can also alter the physiology, metabolism, and resource availability of their host plant, which can have a direct impact on plant development and fitness. As part of their virulence approach, they can control plant growth by manipulating plant hormone signaling or by mimicking phytohormones. For instance, bacterial pathogens can alter root growth by regulating auxin signaling [16]. Fascinatingly, lateral root development was greatly stimulated by *P. syringae* pv. tomato DC3000 infection. The development of lateral roots produced by *P. syringae* pv. tomato requires the presence of ARF19 and auxin response factor 7 (ARF7). However, salicylic acid (SA) inhibits lateral root formation and blocks the entry of *P. syringae* pv. tomato. On the other hand, a variety of developmental abnormalities, such as a thin lamina, a serrated leaf border, and an uneven leaf surface, were seen in *Arabidopsis* infected with the bacterial pathogen *Rhodococcus fascians* [17]. These developmental changes by *R. fascians* were due to the modulation of the host cytokinin (CK) metabolism, triggering cytokinin (CK) production through Arabidopsis response regulators 5/cytokinin 5 (ARR5/CK5) signaling [18]. For successful infection, pathogens can also utilize host nutritional resources that are required for normal plant growth and development [19]. Additionally, they produce diverse virulence factors that affect the plant primary metabolism, namely photosynthesis, which leads to growth retardation [20].

2. Impact of Climate Change or Environmental Factors on Plant–Pathogen Interaction

Plant pathogens are diverse in nature, and their interactions with their respective hosts are influenced by environmental factors [21]. In plant pathology, the well-known "disease triangle" concept emphasizes how pathogens and plants interact with their environment. Three main factors—pathogen virulence, host vulnerability, and ideal environmental conditions—determine the development of disease in plants [22]. Any alterations in favorable environmental conditions can affect disease development in plants. Environ-

mental factors like temperature, water availability, light, carbon dioxide, and nutrients in the soil directly affect plant–pathogen interactions, disease susceptibility, and pathogen distribution [23,24]. For example, drought stress affects plant–pathogen interactions and disease development in plants. Rice subjected to mild drought circumstances has increased *Magnaporthe grisea* susceptibility, which is due to the downregulation of plant defense marker genes such as pathogenesis-related genes [25]. In wheat, drought stress enhanced disease development caused by *Fusarium* spp. [26]. Plant fungal pathogens thrive at temperatures between 15 to 24 °C, and variations in the average global temperature will result in the establishment of increasingly pathogenic strains. According to Shakya et al. [27], variations in temperature have an impact on the development of the *Phytophthora infestans* that cause potato late blight disease. In wheat, the rising temperatures have led to the development of more virulent *Puccinia striiformis* race globally, which can have a more detrimental effect on crop productivity [28]. Similarly, in chestnut, increased winter temperatures have enhanced disease development and increased mortality [29]. On the other hand, higher levels of carbon dioxide have increased the *Fusarium graminearum*, virulence, and disease development in susceptible and resistant wheat cultivars [30]. Many studies have predicted that climate change will change temperature, water availability, and CO_2 concentration, which can have a dramatic impact on pathogen distribution, virulence, and host defense responses [23,27]. The recent events in climate change have evolved novel pathovars. For instance, the climate-driven shift towards heavier rainfall, elevated mean winter temperatures, and precipitation transition from summer to winter all contribute to an increased susceptibility to Phytophthora species [31]. It is anticipated that the global temperature increase will have a positive impact on pathogen evolution and disease distribution. One of the main abiotic drivers of climate change is temperature elevation, and models have indicated that this will lead to an increase in the frequency and intensity of disease epidemics [21]. Climate change, especially warming nights and reduced frost weather conditions, has led to the increase in pathogen virulence and disease occurrence [32]. Plant fungal pathogens thrive at temperatures between 15 to 24 °C, and variations in the average global temperature will result in the establishment of increasingly pathogenic strains. Similarly, a 10-degree temperature variation is ideal for soybean rust infection to cause maximum damage. As the climate shifts, new strains that are more adapted to survive will appear and take dominance. For instance, recent studies on the potato disease *P. infestans* and the wheat pathogen *Zymoseptoria tritici* have shown that both pathogens are well adapted to climatic fluctuations [33,34]. This adaptation is related to modifications in both genomic structure and gene expression. Further, we show the impact of climate change on plant–pathogen interactions in Figure 1. The recent development in statistical data-analyzing tools based on artificial intelligence prediction models have helped researchers to understand disease infestation and host specificity. However, future studies are required to develop new models to study how climate-change-driven factors can influence pathogen distribution, aggressiveness, and virulence and host specificity. Also, how they will affect host immune responses should be the top priority to tackle among researchers to combat future disease outbreaks.

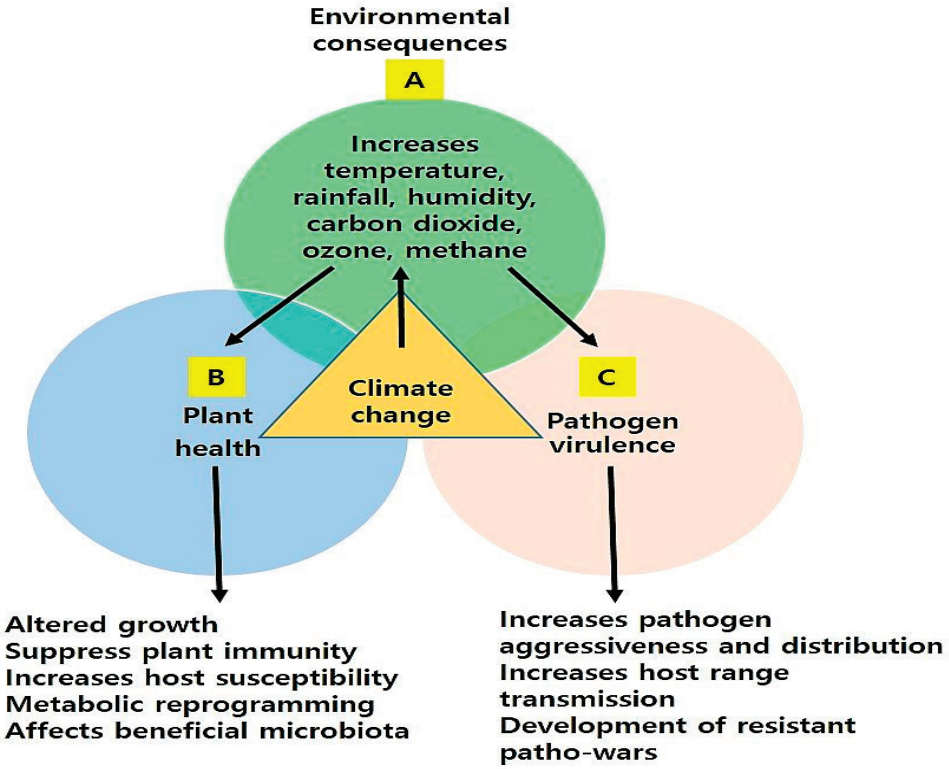

Figure 1. A schematic illustration showing the effect of climate change on environmental factors (A), pathogens (B), and the host defense system (C). Climate change increases temperature, rainfall, humidity, drought, carbon dioxide, and methane, which affects the plant health and immune system. These factors also change pathogen distribution, virulence, and resistance.

3. Pathogen Perception and Plant Immunity

The ability of plants to perceive and respond to pathogens governs the outcome of plant–pathogen interactions. It is well documented that plants have evolved many defense mechanisms to restrict pathogen invasion. The initial line of plant defense against pathogen attack is made up of preformed elements found on the surface of plant organs, such as the wax layer, cuticular lipids, hard cell walls, antimicrobial enzymes, or secondary metabolites [35,36]. Pathogens can overcome the preexisting defensive layer and are confronted by plants' inducible defense responses [37,38]. Generally, plants' extensive repertoire of immunological receptors that are able to identify any type of pathogen and their derived elicitors triggers the plant's inducible defense responses [38]. For successful infection, pathogens must overcome physical barriers, evade or suppress immune perception, and derive nutrients from plant tissues [38,39]. However, the plant immune system uses different strategies to defend from pathogen attack [40]. The first reaction is the pathogen or their derived molecule or effectors recognition by immune receptors like extracellular pattern-recognition receptors (PRRs) and nucleotide-binding leucine-rich repeat (NLR) receptors, which leads to the activation of diverse defense signaling pathways PTI and ETI to defend from the pathogen attack. The identification of R genes from plants and Avr genes from pathogens marked the beginning of the development of the molecular model of plant immunity [41–45]. Later, in 2000, the first plant receptor for a pathogen elicitor was discovered. Based on these findings, two tiers of plant immunity were proposed, namely pattern-triggered and effector-triggered immunity (PTI and ETI) [37]. Flagellin Sensing 2 (FLS2) was the first PAMP cell surface receptor identified in Arabidopsis that can recognize flg22 [46]. PRRs include receptor-like kinases or receptor-like proteins, which have different extracellular ligand-binding domains, including malectin-like domains, lectin domains, leucine-rich repeat (LRR) domains, and LysM domains, which function as mediators of the pathogen or pathogen-derived PAMPs and DAMPs recognition [47]. For example,

pathogen protein and peptide patterns or phytocytokines generated from plants are sensed by LRR ectodomain (ECD) receptors; pathogen oligosaccharides or carbohydrate structures are recognized by lysin-motif ECD receptors; and microbial lipids are preferentially bound by lectin ECD receptors. Both RlKs and RlPs have a single helical transmembrane domain, RKs feature an intracellular protein kinase domain for signaling, and RPs have a short cytoplasmic tail [47]. In addition to pathogen recognition, RLKs and RLPs also play important role in plant abiotic and mechanical stress perception as well as growth regulation. The two most common kinds of plant PRRs are cell surface leucine-rich repeat domain (LRR) receptor kinases (LRR-RKs) and LRR receptor proteins (LRR-RPs). Activation of RLKs leads to a series of biochemical changes, such as mitogen-activated protein kinase (MAPK) phosphorylation, which further triggers calcium burst, ROS wave formation, callose deposition, activation of hormonal signaling pathways, and transcriptional reprogramming of plant defense genes [48]. We display different PRRs identified in plants that act as key receptors for pathogen or MAPs/DAMPs recognition in Table 1.

Table 1. List of PRRs identified for pathogen or DAMPs/MAMPs perception in different plants.

Receptors	Family	Co-Receptor/Ligand	Host Plant	References
FLS2	LRR RLK/LLG1	Flg22	*A. thaliana*	[49,50]
EFR	LRR RLK	Elf18	*A. thaliana*	[51]
CERK1	LysM RLK	Chitin	*A. thaliana*, *Oryza sativa*	[52,53]
CEBiP	LysM RLP	Chitin	*O. sativa*	[54]
LYM1/LYM3	LysM RLP	PGNs	*A. thaliana*	[55]
LYP4/6	LysM RLP	PGNs/chitin	*O. sativa*	[56]
LeEix2	LRR RLP	Eix	*Solanum lycopersicum*	[57]
ReMax	LRR RLP	eMax	*A. thaliana*	[58]
PEPR1/2	LRR RLK	Peps	*A. thaliana*	[59–61]
Ve1	LRR RLP	Ave1	*S. lycopersicum*	[62]
Cf-2/4/5/9	LRR RLP	Avr2, Avr4, Avr9	*S. lycopersicum*	[63–66]
Cf-4E	LRR RLP	Avr4E	*S. lycopersicum*	[67,68]
Cf-9B	LRR RLP	Unknown	*S. lycopersicum*	[69]
PSKR1	LRR RLK	PSKα	*A. thaliana*	[70]
BIR1, SOBIR1, ERECTA, SRF3	LRR RLK	Unknown	*A. thaliana*	[71,72]
ds1	LRR RLK	Unknown	*Sorghum bicolor*	[73]
SISERK1	LRR RLK	Unknown	*S. lycopersicum*	[74]
NbSERK1	LRR RLK	Unknown	*Nicotiana benthamiana*	[75]
LYK4	LysM RLK	Unknown	*A. thaliana*	[76]
Bti9, SlLyk13	LysM RLK	Unknown	*S. lycopersicum*	[77]
THE1m, FER	CrRLK1L RLK	Unknown	*A. thaliana*	[78,79]
Pi-d2	LecRK	Unknown	*O. sativa*	[80]
OsWAK1	WAK	Unknown	*O. sativa*	[81]
TaRLK-R1, 2, 3	Other	Unknown	*Triticum aestivum*	[82]
SNC4	Other	Unknown	*A. thaliana*	[83]
LRK10	S-domain	Unknown	*T. aestivum*	[84]
BAK1	LRR RLK	Flg22, elf18, Peps, Eix	*A. thaliana*	[85–88]
LeEix1	LRR RLP	Eix	*S. lycopersicum*	[89]
SOBIR1	LRR RLK	Avr4, Ve1	*S. lycopersicum*	[90]

On the other hand, intracellular NLRs can recognize diverse effector proteins that are incorporated into plant cells during pathogen invasion, resulting in the activation of ETI. In plants, three types of NLRs, namely Toll-interleukin-1 receptor homology (TIR) domain containing NLRs (TNLs) and coiled-coil (CC) domain containing NLRs (CNLs) and resistance to powdery mildew 8 (RPW8)-like CC domain (CC-R)-containing NLR (RNL), have been identified that can sense pathogen effectors [91]. Different NLR subtypes oligomerize into resistosome structures upon activation, fulfilling dual functions in signal transduction and pathogen identification. ETI is associated with localized programmed cell death, also called hypersensitive response (HR-PCD). SA and ROS are two important signaling components that have been shown to activate ETI triggered PCD, which can

inhibit the spread of pathogens to neighboring cells [92]. However, PCD is regulated by SA-dependent non-expresser of pathogenesis-related protein 1 (NPR1) via the activation of plant defense genes and the forming of SA-induced NPR1 condensates (SINCs) in the cytoplasm, which sequester and degrade various signaling components involved in cell death, thereby turning on the pro-survival immune response [92]. How PPRs and NLRs triggers biochemical reprograming after pathogen or effector recognition, leading to the activation of inducible plant defense, is shown in Figure 2.

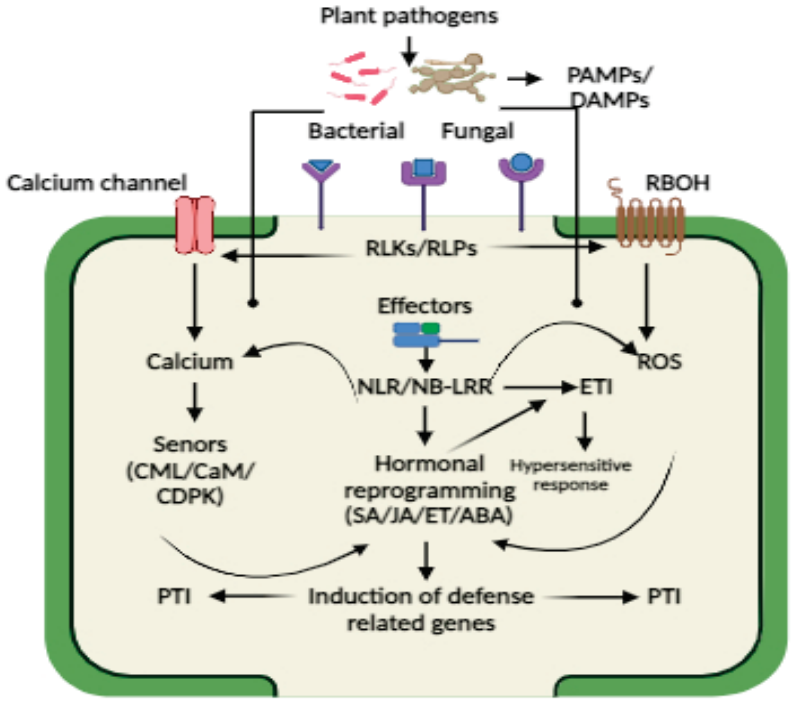

Figure 2. Schematic illustration showing the activation of two-tier plant immunity, namely PTI and ETI, in plants after pathogen, MAMPs/DAMPs, or effectors perception by PPRs and NLRs. Plants undergo biochemical reprogramming such as calcium burst, ROS production, and hormonal activation, which regulates diverse antimicrobial responses like hypersensitive response or programmed cell death or systemic acquired resistance.

In plants, both PTI and ETI elicit a systemic defensive response known as systemic acquired resistance (SAR), which provides a broad spectrum of disease resistance for a longer time [93]. SA accumulation is essential for the activation of SAR pathway in plants, and SA degradation by the bacterial SA hydroxylase *NahG* results in failure of SA-mediated resistance and SAR formation [94]. Despite the fact that SAR may be induced exogenously without the need for an ETI by applying SA and its synthetic analogs, how ETI triggers systemic SA accumulation is not fully understood. Recently, it was found that RBOHD produced H_2O_2, acting as a mobile signal for the formation of systemic SA by modulating the activity of its biosynthesis genes like *ICS1* via the sulfenylation of the CCA1 HIKING EXPEDITION (CHE) transcription factor (TF). It is noteworthy that plants with mutations in their H_2O_2-sensitive cysteine residue in CHE no longer produce SAR or accumulate SA systemically [95]. SAR in plants can persist for several weeks to months and can provide a broad spectrum of disease resistance without causing cell death. This is associated with massive transcriptional reprogramming and is dependent on *NPR1* and other transcription factors like TGAs. The accumulation of PR proteins is the hallmark of SAR, which possess diverse antimicrobial activity.

Autophagy has emerged as an important component of plant immune response, which regulates hormonal levels and hypersensitive response. In general, autophagy is catabolic process that transports damaged organelles or undesired proteins to vacuoles where they

are broken down and recycled [96]. It is crucial for the control of plants' cellular homeostasis, cell death, and stress adaption [96]. So far, 40 autophagy-related (ATG) genes have been found in plants, and they all have different but complementary functions in promoting autophagy [97]. In plant immunity, autophagy can have a dual function, supporting both pro-cell-death and pro-cell-survival processes [98]. For instance, autophagy can play key role in inhibiting the spread of PCD to surrounding cells during the ETI response [98]. Previous research has shown that the silencing of the autophagy-associated gene *ATG6/Beclin1* in tobacco plants results in a substantial spread of HR-PCD into nearby healthy tissue and systemic leaves during tobacco mosaic virus (TMV) infection. This study also reported that silencing other autophagy associated genes like *ATG3, ATG7*, and *VPS34* also showed the same results, which further supports that autophagy protects uninfected or healthy plant cells during HR response [98]. Autophagy can also protect uninfected plants from necrotrophic cell death. For instance, *Arabidopsis* ATG6 RNAi lines showed unconstrained spread of disease-induced cell death after infection with pathogenic Pst DC3000 [99]. Similarly, the silencing of autophagy genes such as *atg5-1*, *atg10-1*, and *atg18a-1* in Arabidopsis triggers disease-induced cell death during *A. brassicicola* infection [100]. These studies provide evidence on the involvement of autophagy in plant immunity; however, there remain many knowledge gaps on understanding the molecular underpinning of its regulatory mechanism during different plant–pathogen interactions. Therefore, future studies are required to identify potential molecular players that control autophagy during PCD and disease-induced cell death.

RNA silencing or RNA interference (RNAi) is also an important plant defense response that protects plants from pathogen infection [101]. It was initially shown that RNA silencing in plants occurs as a post-transcriptional process during viral infection and transgenesis [101]. There are two types: RNA transcriptional gene silencing (TGS) and post-transcriptional gene silencing (PTGS), and double-stranded (ds) or hairpin RNA substrates of dicer (DCL in plants) are important intermediary molecules that initiate RNA silencing to direct RNA degradation, DNA methylation, and translational repression [102]. Plant immunity is precisely regulated by small noncoding RNAs (sRNAs), which are important modulators of gene expression. The two main groups of plant sRNAs are small interfering RNAs (siRNA), which are recognized for their functions in silencing viral RNAs, and microRNAs, which modulate diverse immune and growth responses [103]. But unlike bacterial and fungal infections, viral genomes proliferate inside of their hosts, which is why RNA-silencing pathways are essential for anti-viral defense. Plants that are infected with any type of virus or subviral agent, such as viroids, satellites, or faulty RNAs, produce more viral siRNAs that may then be used to drive silencing against the viral genome [104]. Consequently, viruses are both targets and inducers of RNA silencing. Recent studies have shown that siRNA can also repress bacterial, fungal, and oomycete infection by targeting pathogen genes [105]. The identification of RNA-silencing suppressors in plant pathogens implies that host-silencing disruption is a common virulence tactic used by numerous phytopathogens [103]. Although there are many reports on the role of RNA silencing in combating pathogens, there remain many knowledge gaps on how pathogens suppress RNA silencing, therefore necessitating future investigation. In the future, it will be interesting to explore the how pathogens suppress RNA-silencing defense response in plants to promote disease and their multiplication. Also, identification of anti-RNA-silencing virulence factors in bacterial fungal and oomycetes pathogens can pave the way for improving disease resistance in plants.

4. Role of Calcium and ROS in Plant Immunity

After pathogen or effector recognition by different exterior and interior receptors, cells undergo biochemical reprograming like calcium burst, ROS wave formation, and defense hormonal activation, which modulate different immune responses (Figure 2). Both ETI and PTI activation triggers a variety of signaling events that are mostly similar, such as Ca^{2+} fluxes, ROS burst, transcriptional reprograming, and phytohormone production, with ETI

exhibiting a stronger response than PTI [106]. The early signaling events are an accumulation of secondary messengers like calcium and ROS that act as biochemical language codes that are sensed by different sensors that decode and elicit a series of downstream signaling cascades [106]. Previous studies have shown a mutual interplay between calcium and ROS, which has a positive influence on plant defense signaling [107,108].

Calcium signaling is reported to be essential for both layers of the plant immune system since alterations in intracellular Ca^{2+} levels have been well documented following both PRR and NLR activation [107,108]. However, plant cells need to maintain low cytosolic Ca^{2+} levels due to its cytotoxicity. Therefore, Ca^{2+} is sequestered in intracellular stores, such as the apoplast or the vacuole and endoplasmic reticulum in plants, but it can also be stored in vesicular compartments, mitochondria, and chloroplasts through active transport, which creates massive electrochemical potential gradients across membranes [109–111]. Ca^{2+} signals are produced by the coordinated activity of active transporters and channels, and they entail intracellular store release and apoplast inflow. Interestingly, various calcium channels, such as cyclic nucleotide-gated channels (CNGCs) [112], glutamate receptor-like (GLRs) [113], and hyperosmolality-induced channels (OSCAs) [114], have been identified to play a key role in PTI-mediated calcium-dependent signaling. In contrast, Ca^{2+} channels found in ETI require the formation of multimeric NLR resistosomes that form pore structures in the plasma membrane from the cytosolic side. We detail the roles of different calcium channels in plant immunity in Table 2.

Table 2. Roles of different types of calcium channels in plant immunity.

Calcium Channel	Family	Activation	Plants	References
CNGC2/4	CNGC family	Flg22, plant elicitor peptide pep3, or lipopolysaccharides (LPSs)	*A. thaliana*	[115–117]
OsCNGC9	CNGC family	Chitin	*O. sativa*	[118]
CNGC19	CNGC family	Pep1	*A. thaliana*	[119]
CNGC20	CNGC family	BAK-TO LIFE 2 (BTL2)	*A. thaliana*	[120]
OSCA1.3 and OSCA1.7	OSCA family	BIK1	*A. thaliana*	[114]
ANNEXIN1 (ANN1)	Annexin gene family	CERK1	*A. thaliana*	[121]
GLR2.7, GLR2.8, and GLR2.9	GLR family	Flg22-, elf18-, and pep1	*A. thaliana*	[122]

It is evident that Ca^{2+} influx across the plasma membrane is essential in both levels of immunity since Ca^{2+} channel blockers that stop Ca^{2+} entrance from the apoplast reduce Ca^{2+} signals and immunological responses in both PTI and ETI [97,98]. Also, gene-knockout studies have revealed that blockage of calcium channels directly affects the plant defense response's against pathogens [113,121]. However, there remain many knowledge gaps on how pathogens trigger calcium channel activation and the role of precise calcium sensors during immunity activation [123]. Future research is required to determine how RLKs and RLPs contribute to the activation of calcium channels during pathogen attack. It is well documented that RLKs can bind either rapid alkalinization factor (RALF) peptides or oligosaccharides that further activate calcium channels. Therefore, there is a need to underpin how pathogens induce RLKs-mediated calcium activation via RALF or oligosaccharide-based activation, and these need further investigation, which will provide novel insights not only for understanding cell wall-mediated plant immunity regulation but also for improving disease resistance [123].

Reactive oxygen species are important signaling molecules that regulate diverse plant growth and biotic and abiotic stress-adaptive responses [124]. In plants, members of the nicotinamide adenine dinucleotide phosphate (NADPH) oxidase family are responsible for ROS production during PTI. It is well known that one of plants' early responses towards pathogen attack is transient ROS burst, which plays a key role in regulating diverse plant defense responses [125]. During plant–pathogen interactions, the apoplast is a major route of ROS production. After pathogen sensing by RLKs and RLPs, a series of rapid

biochemical response occurs, which includes ROS generation. For example, RLKs like PBL1 and BIK1 are necessary for apoplastic ROS production [126] and cytosolic calcium burst [127] as well as for disease resistance to fungal and bacterial and pathogens [126]. ROS waves play a vital role in local and long-distance signaling during plant–pathogen interactions. Among RBOHs, the main contributor to the generation of ROS during innate immunity is RBOHD [128]. Pathogen pattern-induced cytosolic calcium burst is essential for the activation of RBOHD, as transient calcium burst causes conformational changes in RBOHD's N-terminal EF-hand motifs upon PAMP sensing, and CPK phosphorylation causes RBOHD to produce ROS [127,129]. ROS can also raise the intracellular calcium concentration and activate CPK5, even though calcium and CPKs function upstream of RBOHD activation in pattern-triggered immunity [129]. Interestingly, this reciprocal control between ROS and calcium most certainly plays a major part in the long-distance, cell-to-cell propagation of ROS and calcium known as ROS waves and calcium waves, which are thought to regulate systemic signaling during biotic and abiotic stressors [130]. Future studies are required to further explore calcium and ROS interplay during plant–pathogen interactions and defense activation and how they are regulated by cell wall receptors and other apoplastic signaling molecules, which will provide novel insights for understanding the complexity of the plant immune system. This will also help in improving disease resistance by identifying key players that modulate calcium/ROS-driven immune responses against diverse pathogens.

5. Revisiting the Role of Hormones in Plant Defense Response

Plants use sophisticated phytohormone signaling networks as a universal defensive mechanism against pathogen invasion [38,40]. It is well documented that plants undergo hormonal reprogramming to restrict disease progression, but it also plays a key role for plant survival, such as in the reallocation of resources, regulation of cell death, and modification of plant architecture [131]. In contrast, pathogens can also manipulate hormonal signaling pathways that support pathogen growth and disease development [131,132]. Based on the available literature, hormones such as SA, JA, and ET are recognized as primary plant defense hormones that provide disease resistance against diverse pathogens [105]. Recent studies have also reported the role of other hormones such as ABA, auxin, brassinosteroids (BL), auxins, cytokinins (CK), and gibberellins (GA), which play important roles in modulating plant responses to pathogen attack [38]. Interestingly, the interaction of different hormonal signaling pathways is critical for balancing growth–stress tradeoffs, which is crucial for plant survival and adaption.

SA plays a critical role in plant defense against biotrophic and semibiotrophic pathogens by triggering local and systemic resistance [38,39]. At the onset of a primary infection, SA levels rise in local leaves, which, along with other transportable signals, leads to the formation of SAR [133,134]. The SA receptors NPR1 and NPR3/NPR4 were identified, and they are crucial for SA-mediated systemic and local resistance [134]. Plants utilize two distinct routes to synthesize SA from chorismate: either through isochorismate synthase 1 (ICS1) in the chloroplast or via PAL in the cytoplasm [135]. The resultant gene network from the hormone-signaling pathways encompasses multiple transcription factor families; for example, WRKY proteins play a role in activating pathogenesis-related (PR) genes like *PR1*, while MYB factors are crucial in activating genes specific to flavonol biosynthesis within the phenylpropanoid pathway [38]. Phytoalexin-deficient 4 (PAD4) and enhanced disease susceptibility 1 (EDS1) genes are essential for the activation of SA pathways. PAD4 and EDS1 encode proteins that resemble triacyl-glycerol lipases, which are required for SA production [136]. SA is important for defense effector genes and systemic acquired resistance (SAR), as evidenced by *NahG* transgenic plants that break down SA with bacterial salicylate hydroxylase [137]. Furthermore, the SA–ABA interaction, as observed in the FLS2 receptor implicated in the PAMP response of *P. syringae*, activates SA and ABA responses, assisting in pathogen protection through stomatal closure [138].

In plants, JA provides defense response against necrotrophic fungal pathogens and pests [40]. On other hand, both biotrophic and hemi biotrophic viruses produce effectors that can manipulate the JA pathway, thereby increasing plants disease susceptibility [132]. JA and its derivatives, generally known as jasmonates, exhibit different functions and serve as a vital signal mediator in the defense against necrotrophic pathogens [40]. In terms of plant defense, JA not only activates the expression of PR genes [123] but also regulates the synthesis of secondary metabolites including glucosinolates, terpenoids, flavonoids, and phytoalexins [139,140]. In Arabidopsis, the *MYC2*, *MYC3*, and *MYC4* genes regulate the accumulation of JA in response to plant herbivory [141]. MYC2 positively regulates the expression of LOX2/3/4 after treatment with MeJA, and it also controls the expression of JAV1 and JAM1, which act as major regulators of JA biosynthesis and catabolism, respectively. After activation of JA signaling, defense responses are initiated near the wound site or SAR at the uninjured site far from the site of infection. Long-distance transport of JA occurs via vascular bundles from the place of initial synthesis to other parts of the plant. Recent investigations have demonstrated that the JA signaling pathway leads to the activated of downstream responsive genes such as *PR3*, chitinase, and lipoxygenase *LOXs* [142]. The MYC2 transcriptional activator regulates JA-mediated suppression of isochorismate synthase 1 (ICS1), a key enzyme in the isochorismate (IC) pathway, resulting in the induction of genes involved in salicylic acid (SA) metabolism via transcriptional regulation of SNAC-A transcription factors [143]. In *Arabidopsis*, genome-wide association mapping has revealed the role of genes involved in varied JA responses and hormonal interplay. The genes include nuclear-localized type B response regulators (RRB), also known as type B ARR in Arabidopsis, which function as a transcription factor and regulate the expression of CK-responsive genes [142]. According to recent studies, JA's volatile components, such as methyl-JA, are essential for the systemic wound signaling pathway. The bioactive form of jasmonoyl-L-isoleucine (JA-Ile) in Arabidopsis has also been observed to accumulate in distal leaves following pathogen infection [144]. Several studies have highlighted the role of JA and its related oxylipin metabolites in long-distance signaling [145]. Choi et al. [145] investigated the interconnectedness of microbe-associated molecular patterns (MAMPs) and damage-associated molecular patterns (DAMPs) with JA and oxylipin signaling. Recent studies have also implied the role of JA and oxylipins in the coordination of different defense signaling pathways, such as that of SA, to optimize a plant's response to a particular stress [146,147]. *JAZ9* and *NOG1-2* interact via a common binding domain and inhibit the interaction between *JAZ9* and *COI1* [121]. Effector-triggered immunity (ETI) is exemplified by the relationship between *JAZ9* and *NOG1-2*, wherein the effector reinstates stomata during bacterial infections, thereby decreasing the wound response.

The role of SA and JA in plant defense against viral pathogens is functionally validated in different plant systems. For example, SA signaling during plant–virus interaction is activated by effector *R* genes that cause the production of reactive oxygen species (ROS) and hypersensitive response (HR) and the expression of pathogenesis-related genes, which confers antiviral disease resistance [148]. After virus infection, the activation of SA-mediated defense response can inhibit intercellular trafficking, replication, and long-distance movement of viral pathogens. The RNA interference (RNAi) pathway is another antiviral defense response associated with the SA-mediated suppression of viral infection [149]. Similarly, the role of JA in plant antiviral defense has been reported in different plant–virus interactions. For instance, Han et al. [150] reported that rice stripe virus (RSV) induces the expression of JA pathway genes, which leads to RSV resistance in rice. Previous study has shown that exogenous treatment of JA decreased the DNA titer of beet curly top virus (BCTV), which further supports the role of JA in antiviral defense [151]. However, contradictory results were also reported that knockout of JA biosynthic genes reduced viral infection and its accumulation [132]. Apart from their respective roles, SA and JA crosstalk plays a crucial role in regulating antiviral defense responses [152]. According to Oka et al. [132], JA biosynthesis enzyme ALLENE OXIDE SYNTHASE (AOS) or JA receptor COI1 silencing boosted plant resistance to TMV and elevated SA levels in COI1- or AOS-silencing plants,

which decreased TMV accumulation in tobacco plants. Previous study has also shown the antagonistic interaction between SA and JA in tobacco and *Arabidopsis* plants after viral infection [153]. These findings emphasize the fact that changes in endogenous phytohormone levels are closely correlated with viral movement, replication, symptom development, and defense responses. New insights are being gained into the host manipulation theory and the changes that occur in phytohormones signaling networks during viral infection. Based on the available data, we show how SA and JA provide disease resistance against different types of pathogens in plants in Figure 3.

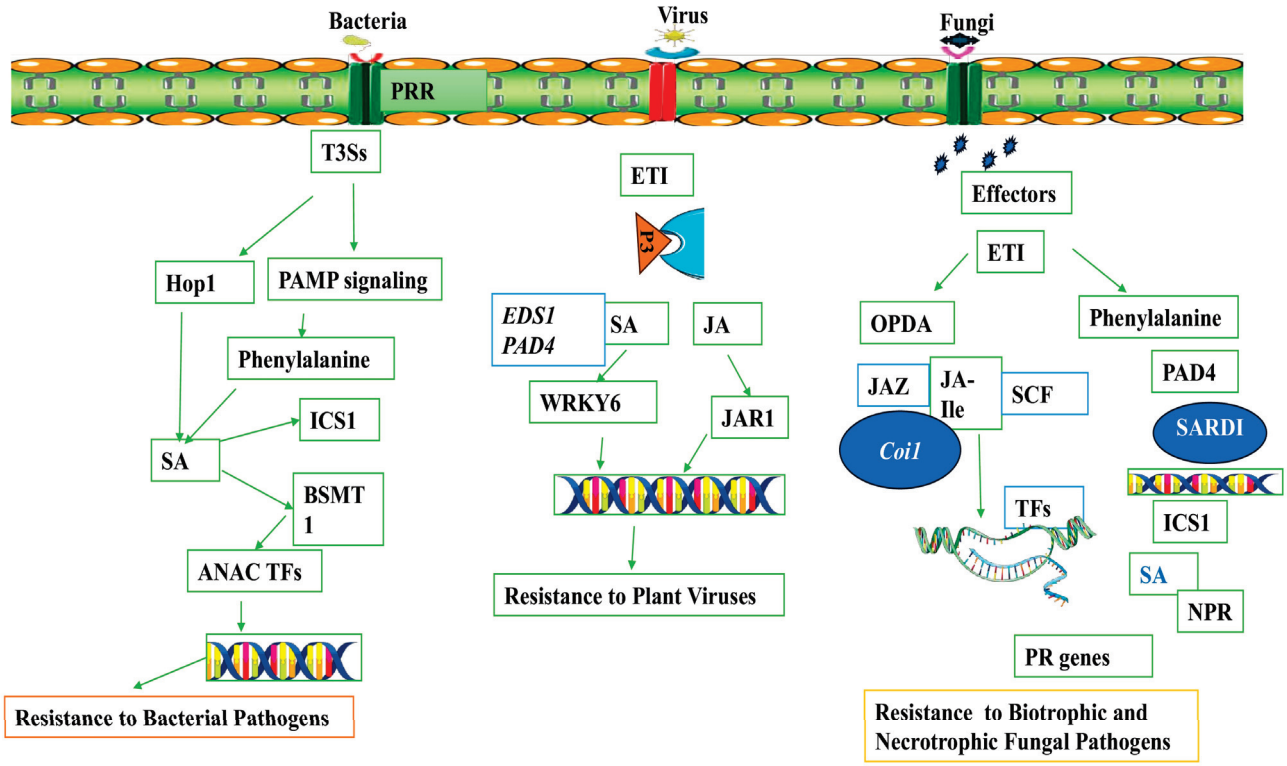

Figure 3. A schematic representation showing SA- and JA-dependent plant immunity against bacterial, viral, and fungal pathogens. This illustration also shows the roles of different players that modulate SA/JA-dependent immune responses.

Ethylene (ET) is a key component of plant immunity in addition to SA and JA. ET primarily confers resistance against necrotrophic fungal pathogens and participates in the induction of systemic resistance mediated by beneficial microbes [154]. Although ET and salicylic acid typically interact antagonistically, plant PRR perception of PAMPs causes ET, SA, and JA to accumulate as well. This trio is necessary for local PAMP-induced resistance to pathogens [155]. Early PTI responses include the production of ET, which regulates the synthesis of downstream defensive proteins and metabolites involved in plant immunity in combination with ROS and the activation of MAPK signaling cascades [156]. The perception of ethylene is initiated at the endoplasmic reticulum membrane. This triggers a signaling cascade that subsequently leads to the transcriptional regulation of ET-responsive genes in the nucleus via the participation of ETHYLENE RESPONSE FACTORs (ERFs) [157]. In response to pathogenic invasion, plants elicit the production of ET, which serves as a key regulator in inhibiting the growth of specific pathogens by modulating the transcriptional activity of genes involved in pathogen response. Plants exposed to a pathogen-associated molecular pattern known as bacterial flagellin peptide 22 (flg22) show the phosphorylation of rate-limiting enzymes involved in ET biosynthesis, ACS2, and ACS6, which is mediated by MAP kinases 3 and 6 (MPK3 and MPK6). Following this, EIN3 triggers the activation of many transcription factors, such as ERF1 and OCTADECANOID-

RESPONSIVE ARABIDOPSIS AP2/ERF 59 (ORA59), which are essential in regulating the expression of genes linked to immunity [158]. However, the role of ET in plant immunity is not fully understood. Previous studies have reported that bacterial pathogen *P. syringae* pv. infection in tomato leads to ET production during hypertensive response, which further supports the notion that ET plays a key role in modulating ETI [159]. However, there are major knowledge gaps regarding how ET modulates SA/JA crosstalk and systemic resistance against many pathogens.

Defense hormones have a well-established role in modulating a plant's response to external stimuli. Plants accumulate a wide range of chemical compounds in response to various stresses, including ABA, which can trigger stomatal closure and increase disease resistance [160]. ABA interacts both antagonistically and synergistically with the ET and SA signaling pathways, respectively, and is implicated in plant responses to a wide variety of diseases [161]. Due to the versatile nature of ABA in mediating plant response to both biotic and abiotic stresses, the role of ABA in mediating plant immunity is well understood. For example, ABA acts synergistically with JA but suppresses SA, which causes plants to be more vulnerable to biotrophic pathogens [162]. Increased levels of ABA in plants facilitate cross-adaptation against plant diseases and drought stress [160]. ABA also mediates the response of JA via the interaction with MYC2 transcription factors [163]. However, ABA also evokes JA responses via interaction with MYC2 transcription factors. JA has a positive interaction with ABA during plant response to multiple stresses and hence activates the MAP kinase signaling pathway in *A. thaliana* [164]. (Similarly, ABA-activated secondary messengers such as reactive oxygen species (ROS), nitric oxide (NO), and cytosolic free Ca^{2+} contribute to plant adaptation to both abiotic and biotic stresses [165]. Hormone crosstalk plays a critical role in regulating the plant immunological network for tailoring immune response to diverse plant pathogens. However, molecular interplay between hormonal cross talk dynamics is not fully understood and therefore warrants future investigation.

6. Conclusions

Application of pesticides has been a major driver to control microbial disease, but it has detrimental impact on ecology and human health in addition to the emergence of newly resistant pathogens. Pesticides can also alter soil physiochemical properties as well as soil-beneficial microbiota, which can have a negative impact on plant growth and stress adaptation. Hence, it is important to develop long-term crop disease-resistance cultivars in order to increase crop productivity for the growing population. In this regard, understanding the molecular dynamics of plant–pathogen interactions and identifying potential candidates are key for developing future disease-resistant crops. To increase plant resilience to microbial diseases, scientists are modifying plants' genetic makeup instead of using chemicals. Incredible discoveries have been made over the past few decades regarding how plants respond to pathogen attack, and a number of important players, including RLKs, calcium channels, RBOHs, and hormonal signatures, have been discovered. However, the details of their fundamental role in plant immunity and their biochemical complexity during plant–pathogen interactions remains largely unknown. Also, how climate change affects plant–pathogen interactions and plant immunity remains enigmatic and warrants future investigation. Because of their rapid natural adaptability to environmental extremes, shorter life cycles, and faster rates of multiplication, phytopathogens may become more common and lead to more severe diseases as a result of climate change. This could result in more catastrophic injury to crop plants. Therefore, understanding how plant immune systems will be affected by climate change and how it affects pathogen distribution and disease severity will help in developing climate- and disease-resistant crops in sustainable agriculture. In the near future, broad-spectrum resistance against pathogens infections is anticipated to be mostly produced by developments in targeted gene insertion by genome editing and molecular stacking. In the future, genome editing, more specifically, CRISPR-based technologies, will play a significant role in enhancing crop resistance to a wide range of pathogens, ensuring food safety and sustainable agriculture.

Author Contributions: Conceptualization, S.A., A.T. and Z.A.M.; methodology, S.A., A.T. and Z.A.M.; software, S.A., A.T. and Z.A.M.; validation, S.A., A.T. and Z.A.M.; formal analysis, S.A., A.T. and Z.A.M.; investigation, S.A., A.T. and Z.A.M.; resources, S.A., A.T. and Z.A.M.; data curation, S.A., A.T. and Z.A.M.; writing—original draft preparation, S.A., A.T. and Z.A.M.; writing—review and editing, S.A., A.T. and Z.A.M.; visualization, A.T. and Z.A.M.; supervision, S.A.; project administration, S.A. and A.T.; funding acquisition, S.A., A.T. and Z.A.M. All authors have read and agreed to the published version of the manuscript.

Funding: This research received no external funding.

Data Availability Statement: Not applicable.

Conflicts of Interest: The authors declare no conflicts of interest.

References

1. Ali, S.; Tyagi, A.; Bae, H. Plant microbiome: An ocean of possibilities for improving disease resistance in plants. *Microorganisms* **2023**, *11*, 392. [CrossRef] [PubMed]
2. Fones, H.N.; Bebber, D.P.; Chaloner, T.M.; Kay, W.T.; Steinberg, G.; Gurr, S.J. Threats to global food security from emerging fungal and oomycete crop pathogens. *Nat. Food* **2020**, *1*, 332–342. [CrossRef] [PubMed]
3. Ali, S.; Tyagi, A.; Rajarammohan, S.; Mir, Z.A.; Bae, H. Revisiting Alternaria-host interactions: New insights on its pathogenesis, defense mechanisms and control strategies. *Sci. Hortic.* **2023**, *322*, 112424. [CrossRef]
4. Oerke, E.C. Crop losses to pests. *J. Agric. Sci.* **2006**, *144*, 31–43. [CrossRef]
5. Petre, B.; Kamoun, S. How do filamentous pathogens deliver effector proteins into plant cells? *PLoS Biol.* **2014**, *12*, e1001801. [CrossRef] [PubMed]
6. Doehlemann, G.; Van Der Linde, K.; Aßmann, D.; Schwammbach, D.; Hof, A.; Mohanty, A.; Jackson, D.; Kahmann, R. Pep1, a secreted effector protein of *Ustilago maydis*, is required for successful invasion of plant cells. *PLoS Pathog.* **2009**, *5*, e1000290. [CrossRef]
7. Csorba, T.; Kontra, L.; Burgyan, J. Viral silencing suppressors: Tools forged to fine-tune host-pathogen coexistence. *Virology* **2015**, *479–480*, 85–103. [CrossRef]
8. Rubio, L.; Galipienso, L.; Ferriol, I. Detection of Plant Viruses and Disease Management: Relevance of Genetic Diversity and Evolution. *Front. Plant Sci.* **2020**, *11*, 1092. [CrossRef]
9. Cornelis, G.R. The type III secretion injectisome, a complex nanomachine for intracellular "toxin" delivery. *Biol. Chem.* **2010**, *391*, 745–751. [CrossRef]
10. Lozano-Durán, R.; Bourdais, G.; He, S.Y.; Robatzek, S. The bacterial effector HopM1 suppresses PAMP-triggered oxidative burst and stomatal immunity. *New Phytol.* **2014**, *202*, 259–269. [CrossRef]
11. Nazarov, T.; Chen, X.; Carter, A.; See, D. Fine mapping of high-temperature adult-plant resistance to stripe rust in wheat cultivar Louise. *J. Plant Prot. Res.* **2020**, *60*, 126–133.
12. Spoel, S.H.; Johnson, J.S.; Dong, X. Regulation of tradeoffs between plant defenses against pathogens with different lifestyles. *Proc. Natl. Acad. Sci. USA* **2007**, *104*, 18842–18847. [CrossRef] [PubMed]
13. Cooper, A.J.; Latunde-Dada, A.O.; Woods-Tör, A.; Lynn, J.; Lucas, J.A.; Crute, I.R.; Holub, E.B. Basic compatibility of Albugo candida in *Arabidopsis thaliana* and *Brassica juncea* causes broad-spectrum suppression of innate immunity. *Mol. Plant-Microbe Interact.* **2008**, *21*, 745–756. [CrossRef]
14. Spoel, S.H.; Koornneef, A.; Claessens, S.M.; Korzelius, J.P.; Van Pelt, J.A.; Mueller, M.J.; Buchala, A.J.; Métraux, J.P.; Brown, R.; Kazan, K.; et al. NPR1 modulates cross-talk between salicylate-and jasmonate-dependent defense pathways through a novel function in the cytosol. *Plant Cell* **2003**, *15*, 760–770. [CrossRef] [PubMed]
15. Notz, R.; Maurhofer, M.; Dubach, H.; Haas, D.; Défago, G. Fusaric acid-producing strains of Fusarium oxysporum alter 2, 4-diacetylphloroglucinol biosynthetic gene expression in Pseudomonas fluorescens CHA0 in vitro and in the rhizosphere of wheat. *Appl. Environ. Microbiol.* **2002**, *68*, 2229–2235. [CrossRef] [PubMed]
16. Kong, X.; Zhang, C.; Zheng, H.; Sun, M.; Zhang, F.; Zhang, M.; Cui, F.; Lv, D.; Liu, L.; Guo, S.; et al. Antagonistic interaction between auxin and SA signaling pathways regulates bacterial infection through lateral root in Arabidopsis. *Cell Rep.* **2020**, *32*, 108060. [CrossRef] [PubMed]
17. Depuydt, S.; De Veylder, L.; Holsters, M.; Vereecke, D. Eternal youth, the fate of developing Arabidopsis leaves upon *Rhodococcus fascians* infection. *Plant Physiol.* **2009**, *149*, 1387–1398. [CrossRef] [PubMed]
18. Depuydt, S.; Dolezal, K.; Van Lijsebettens, M.; Moritz, T.; Holsters, M.; Vereecke, D. Modulation of the hormone setting by *Rhodococcus fascians* results in ectopic KNOX activation in Arabidopsis. *Plant Physiol.* **2008**, *146*, 1267–1281. [CrossRef] [PubMed]
19. Denancé, N.; Sánchez-Vallet, A.; Goffner, D.; Molina, A. Disease resistance or growth: The role of plant hormones in balancing immune responses and fitness costs. *Front. Plant Sci.* **2013**, *4*, 44526. [CrossRef]
20. Garcia-Brugger, A.; Lamotte, O.; Vandelle, E.; Bourque, S.; Lecourieux, D.; Poinssot, B.; Wendehenne, D.; Pugin, A. Early signaling events induced by elicitors of plant defenses. *Mol. Plant-Microbe Interact.* **2006**, *19*, 711–724. [CrossRef]

21. Desaint, H.; Aoun, N.; Deslandes, L.; Vailleau, F.; Roux, F.; Berthomé, R. Fight hard or die trying: When plants face pathogens under heat stress. *New Phytol.* **2021**, *229*, 712–734. [CrossRef]
22. Roussin-Léveillée, C.; Rossi, C.A.; Castroverde, C.D.; Moffett, P. The plant disease triangle facing climate change: A molecular perspective. *Trends Plant Sci.* **2024**. [CrossRef] [PubMed]
23. Velásquez, A.C.; Castroverde, C.D.; He, S.Y. Plant–pathogen warfare under changing climate conditions. *Curr. Biol.* **2018**, *28*, R619–R634. [CrossRef]
24. Zarattini, M.; Farjad, M.; Launay, A.; Cannella, D.; Soulié, M.C.; Bernacchia, G.; Fagard, M. Every cloud has a silver lining: How abiotic stresses affect gene expression in plant-pathogen interactions. *J. Exp. Bot.* **2021**, *72*, 1020–1033. [CrossRef]
25. Bidzinski, P.; Ballini, E.; Ducasse, A.; Michel, C.; Zuluaga, P.; Genga, A.; Chiozzotto, R.; Morel, J.B. Transcriptional basis of drought-induced susceptibility to the rice blast fungus *Magnaporthe oryzae*. *Front. Plant Sci.* **2016**, *7*, 1558. [CrossRef]
26. Wakelin, S.A.; Gomez-Gallego, M.; Jones, E.; Smaill, S.; Lear, G.; Lambie, S. Climate change induced drought impacts on plant diseases in New Zealand. *Australas. Plant Pathol.* **2018**, *47*, 101–114. [CrossRef]
27. Shakya, S.K.; Goss, E.M.; Dufault, N.S.; Van Bruggen, A.H. Potential effects of diurnal temperature oscillations on potato late blight with special reference to climate change. *Phytopathology* **2015**, *105*, 230–238. [CrossRef] [PubMed]
28. Milus, E.A.; Kristensen, K.; Hovmøller, M.S. Evidence for increased aggressiveness in a recent widespread strain of *Puccinia striiformis* f. sp. tritici causing stripe rust of wheat. *Phytopathology* **2009**, *99*, 89–94.
29. Gustafson, E.J.; Miranda, B.R.; Dreaden, T.J.; Pinchot, C.C.; Jacobs, D.F. Beyond blight: Phytophthora root rot under climate change limits populations of reintroduced American chestnut. *Ecosphere* **2022**, *13*, e3917. [CrossRef]
30. Váry, Z.; Mullins, E.; McElwain, J.C.; Doohan, F.M. The severity of wheat diseases increases when plants and pathogens are acclimatized to elevated carbon dioxide. *Glob. Change Biol.* **2015**, *21*, 2661–2669. [CrossRef]
31. Serrano, M.S.; Romero, M.Á.; Homet, P.; Gómez-Aparicio, L. Climate change impact on the population dynamics of exotic pathogens: The case of the worldwide pathogen *Phytophthora cinnamomi*. *Agric. For. Meteorol.* **2022**, *322*, 109002. [CrossRef]
32. Hanson, M.C.; Petch, G.M.; Ottosen, T.B.; Skjøth, C.A. Climate change impact on fungi in the atmospheric microbiome. *Sci. Total Environ.* **2022**, *830*, 154491. [CrossRef] [PubMed]
33. Lehsten, V.; Wiik, L.; Hannukkala, A.; Andreasson, E.; Chen, D.; Ou, T.; Liljeroth, E.; Lankinen, Å.; Grenville-Briggs, L. Earlier occurrence and increased explanatory power of climate for the first incidence of potato late blight caused by *Phytophthora infestans* in Fennoscandia. *PLoS ONE* **2017**, *12*, e0177580. [CrossRef] [PubMed]
34. Francisco, C.S.; Ma, X.; Zwyssig, M.M.; McDonald, B.A.; Palma-Guerrero, J. Morphological changes in response to environmental stresses in the fungal plant pathogen *Zymoseptoria tritici*. *Sci. Rep.* **2019**, *9*, 9642. [CrossRef] [PubMed]
35. Reina-Pinto, J.J.; Yephremov, A. Surface lipids and plant defenses. *Plant Physiol. Biochem.* **2009**, *47*, 540–549. [CrossRef] [PubMed]
36. Piasecka, A.; Jedrzejczak-Rey, N.; Bednarek, P. Secondary metabolites in plant innate immunity: Conserved function of divergent chemicals. *New Phytol.* **2015**, *206*, 948–964. [CrossRef] [PubMed]
37. Jones, J.D.; Dangl, J.L. The plant immune system. *Nature* **2006**, *444*, 323–329. [CrossRef]
38. Ali, S.; Ganai, B.A.; Kamili, A.N.; Bhat, A.A.; Mir, Z.A.; Bhat, J.A.; Tyagi, A.; Islam, S.T.; Mushtaq, M.; Yadav, P.; et al. Pathogenesis-related proteins and peptides as promising tools for engineering plants with multiple stress tolerance. *Microbiol. Res.* **2018**, *212*, 29–37. [CrossRef] [PubMed]
39. Ali, S.; Mir, Z.A.; Bhat, J.A.; Tyagi, A.; Chandrashekar, N.; Yadav, P.; Rawat, S.; Sultana, M.; Grover, A. Isolation and characterization of systemic acquired resistance marker gene PR1 and its promoter from *Brassica juncea*. *3 Biotech* **2018**, *8*, 10. [CrossRef] [PubMed]
40. Ali, S.; Chandrashekar, N.; Rawat, S.; Nayanakantha, N.M.C.; Mir, Z.A.; Manoharan, A.; Sultana, M.; Grover, A. Isolation and molecular characterization of pathogenesis related PR2 gene and its promoter from *Brassica juncea*. *Biol. Plant* **2017**, *61*, 763–773. [CrossRef]
41. Staskawicz, B.; Dahlbeck, D.; Keen, N.T. Cloned avirulence gene of *Pseudomonas syringae* pv. glycinea determines race-specific incompatibility on *Glycine max* (L.) Merr. *Proc. Natl. Acad. Sci. USA* **1984**, *81*, 6024–6028. [CrossRef] [PubMed]
42. de Wit, P.J.G.M.; Hofman AEv Velthuis, G.C.M.; Kuc, J.A. Isolation and characterization of an elicitor of necrosis isolated from intercellular fluids of compatible interactions of *Cladosporium-Fulvum* (Syn Fulvia-Fulva) and tomato. *Plant Physiol.* **1985**, *77*, 642–647. [CrossRef]
43. Martin, G.B.; Brommonschenkel, S.H.; Chunwongse, J.; Frary, A.; Ganal, M.W.; Spivey, R.; Wu, T.; Earle, E.D.; Tanksley, S.D. Map-based cloning of a protein kinase gene conferring disease resistance in tomato. *Science* **1993**, *262*, 1432–1436. [CrossRef]
44. Bent, A.F.; Kunkel, B.N.; Dahlbeck, D.; Brown, K.L.; Schmidt, R.; Giraudat, J.; Leung, J.; Staskawicz, B.J. RPS2 of *Arabidopsis thaliana*: A leucine-rich repeat class of plant disease resistance genes. *Science* **1994**, *265*, 1856–1860. [CrossRef] [PubMed]
45. Jones, D.A.; Thomas, C.M.; Hammondkosack, K.E.; Balintkurti, P.J.; Jones, J.D.G. Isolation of the tomato Cf-9 gene for resistance to *Cladosporium-Fulvum* by transposon tagging. *Science* **1994**, *266*, 789–793. [CrossRef]
46. Chinchilla, D.; Bauer, Z.; Regenass, M.; Boller, T.; Felix, G. The Arabidopsis receptor kinase FLS2 binds flg22 and determines the specificity of flagellin perception. *Plant Cell* **2006**, *18*, 465–476. [CrossRef]
47. Dievart, A.; Gottin, C.; Périn, C.; Ranwez, V.; Chantret, N. Origin and diversity of plant receptor-like kinases. *Ann. Rev. Plant Biol.* **2020**, *71*, 131–156. [CrossRef] [PubMed]
48. DeFalco, T.A.; Zipfel, C. Molecular mechanisms of early plant pattern-triggered immune signaling. *Mol. Cell* **2021**, *81*, 3449–3467. [CrossRef]

49. Bauer, Z.; Gomez-Gomez, L.; Boller, T.; Felix, G. Sensitivity of different ecotypes and mutants of Arabidopsis thaliana toward the bacterial elicitor flagellin correlates with the presence of receptor-binding sites. *J. Biol. Chem.* **2001**, *276*, 45669–45676. [CrossRef]
50. Shen, Q.; Bourdais, G.; Pan, H.; Robatzek, S.; Tang, D. Arabidopsis glycosylphosphatidylinositol-anchored protein LLG1 associates with and modulates FLS2 to regulate innate immunity. *Proc. Natl. Acad. Sci. USA* **2017**, *114*, 5749–5754. [CrossRef]
51. Zipfel, C.; Kunze, G.; Chinchilla, D.; Caniard, A.; Jones, J.D.; Boller, T.; Felix, G. Perception of the bacterial PAMP EF-Tu by the receptor EFR restricts Agrobacterium-mediated transformation. *Cell* **2006**, *125*, 749–760. [CrossRef] [PubMed]
52. Liu, T.; Liu, Z.; Song, C.; Hu, Y.; Han, Z.; She, J.; Fan, F.; Wang, J.; Jin, C.; Chang, J.; et al. Chitin-induced dimerization activates a plant immune receptor. *Science* **2012**, *336*, 1160–1164. [CrossRef]
53. Shimizu, T.; Nakano, T.; Takamizawa, D.; Desaki, Y.; Ishii-Minami, N.; Nishizawa, Y.; Minami, E.; Okada, K.; Yamane, H.; Kaku, H.; et al. Two LysM receptor molecules, CEBiP and OsCERK1, cooperatively regulate chitin elicitor signaling in rice. *Plant J.* **2010**, *64*, 204–214. [CrossRef]
54. Kaku, H.; Nishizawa, Y.; Ishii-Minami, N.; Akimoto-Tomiyama, C.; Dohmae, N.; Takio, K.; Minami, E.; Shibuya, N. Plant cells recognize chitin fragments for defense signaling through a plasma membrane receptor. *Proc. Natl. Acad. Sci. USA* **2006**, *103*, 11086–11091. [CrossRef]
55. Willmann, R.; Lajunen, H.M.; Erbs, G.; Newman, M.A.; Kolb, D.; Tsuda, K.; Katagiri, F.; Fliegmann, J.; Bono, J.J.; Cullimore, J.V.; et al. Arabidopsis lysin-motif proteins LYM1 LYM3 CERK1 mediate bacterial peptidoglycan sensing and immunity to bacterial infection. *Proc. Natl. Acad. Sci. USA* **2011**, *108*, 19824–19829. [CrossRef]
56. Liu, B.; Li, J.F.; Ao, Y.; Qu, J.; Li, Z.; Su, J.; Zhang, Y.; Liu, J.; Feng, D.; Qi, K.; et al. Lysin motif-containing proteins LYP4 and LYP6 play dual roles in peptidoglycan and chitin perception in rice innate immunity. *Plant Cell* **2012**, *24*, 3406–3419. [CrossRef]
57. Ron, M.; Avni, A. The receptor for the fungal elicitor ethylene-inducing xylanase is a member of a resistance-like gene family in tomato. *Plant Cell* **2004**, *16*, 1604–1615. [CrossRef]
58. Jehle, A.K.; Lipschis, M.; Albert, M.; Fallahzadeh-Mamaghani, V.; Furst, U.; Mueller, K.; Felix, G. The receptor-like protein ReMAX of Arabidopsis detects the microbe-associated molecular pattern eMax from Xanthomonas. *Plant Cell* **2013**, *25*, 2330–2340. [CrossRef]
59. Huffaker, A.; Ryan, C.A. Endogenous peptide defense signals in Arabidopsis differentially amplify signaling for the innate immune response. *Proc. Natl. Acad. Sci. USA* **2007**, *104*, 10732–10736. [CrossRef]
60. Yamaguchi, Y.; Huffaker, A.; Bryan, A.C.; Tax, F.E.; Ryan, C.A. PEPR2 is a second receptor for the Pep1 and Pep2 peptides and contributes to defense responses in Arabidopsis. *Plant Cell* **2010**, *22*, 508–522. [CrossRef]
61. Krol, E.; Mentzel, T.; Chinchilla, D.; Boller, T.; Felix, G.; Kemmerling, B.; Postel, S.; Arents, M.; Jeworutzki, E.; Al-Rasheid, K.A.; et al. Perception of the Arabidopsis danger signal peptide 1 involves the pattern recognition receptor AtPEPR1 and its close homologue AtPEPR2. *J. Biol. Chem.* **2010**, *285*, 13471–13479. [CrossRef]
62. de Jonge, R.; van Esse, H.P.; Maruthachalam, K.; Bolton, M.D.; Santhanam, P.; Saber, M.K.; Zhang, Z.; Usami, T.; Lievens, B.; Subbarao, K.V.; et al. Tomato immune receptor Ve1 recognizes effector of multiple fungal pathogens uncovered by genome and RNA sequencing. *Proc. Natl. Acad. Sci. USA* **2012**, *109*, 5110–5115. [CrossRef] [PubMed]
63. Joosten, M.H.; Vogelsang, R.; Cozijnsen, T.J.; Verberne, M.C.; De Wit, P.J. The biotrophic fungus Cladosporium fulvum circumvents Cf-4-mediated resistance by producing unstable AVR4 elicitors. *Plant Cell* **1997**, *9*, 367–379.
64. Dixon, M.S.; Jones, D.A.; Keddie, J.S.; Thomas, C.M.; Harrison, K.; Jones, J.D. The tomato Cf-2 disease resistance locus comprises two functional genes encoding leucine-rich repeat proteins. *Cell* **1996**, *84*, 451–459. [CrossRef]
65. Kruger, J.; Thomas, C.M.; Golstein, C.; Dixon, M.S.; Smoker, M.; Tang, S.; Mulder, L.; Jones, J.D. A tomato cysteine protease required for Cf-2-dependent disease resistance and suppression of autonecrosis. *Science* **2002**, *296*, 744–747. [CrossRef]
66. Dixon, M.S.; Hatzixanthis, K.; Jones, D.A.; Harrison, K.; Jones, J.D. The tomato Cf-5 disease resistance gene and six homologs show pronounced allelic variation in leucine-rich repeat copy number. *Plant Cell* **1998**, *10*, 1915–1925. [CrossRef]
67. Takken, F.L.; Thomas, C.M.; Joosten, M.H.; Golstein, C.; Westerink, N.; Hille, J.; Nijkamp, H.J.; De Wit, P.J.; Jones, J.D. A second gene at the tomato Cf-4 locus confers resistance to cladosporium fulvum through recognition of a novel avirulence determinant. *Plant J.* **1999**, *20*, 279–288. [CrossRef] [PubMed]
68. Westerink, N.; Brandwagt, B.F.; de Wit, P.J.; Joosten, M.H. Cladosporium fulvum circumvents the second functional resistance gene homologue at the Cf-4 locus (Hcr9-4E) by secretion of a stable avr4E isoform. *Mol. Microbiol.* **2004**, *54*, 533–545. [CrossRef]
69. Panter, S.N.; Hammond-Kosack, K.E.; Harrison, K.; Jones, J.D.; Jones, D.A. Developmental control of promoter activity is not responsible for mature onset of Cf-9B-mediated resistance to leaf mold in tomato. *Mol. Plant Microbe Interact.* **2002**, *15*, 1099–1107. [CrossRef]
70. Mosher, S.; Seybold, H.; Rodriguez, P.; Stahl, M.; Davies, K.A.; Dayaratne, S.; Morillo, S.A.; Wierzba, M.; Favery, B.; Keller, H.; et al. The tyrosine-sulfated peptide receptors PSKR1 and PSY1R modify the immunity of Arabidopsis to biotrophic and necrotrophic pathogens in an antagonistic manner. *Plant J.* **2013**, *73*, 469–482. [CrossRef]
71. Llorente, F.; Alonso-Blanco, C.; Sanchez-Rodriguez, C.; Jorda, L.; Molina, A. ERECTA receptor-like kinase and heterotrimeric G protein from Arabidopsis are required for resistance to the necrotrophic fungus Plectosphaerella cucumerina. *Plant J.* **2005**, *43*, 165–180. [CrossRef] [PubMed]
72. Alcazar, R.; Garcia, A.V.; Kronholm, I.; de Meaux, J.; Koornneef, M.; Parker, J.E.; Reymond, M. Natural variation at Strubbelig Receptor Kinase 3 drives immune-triggered incompatibilities between Arabidopsis thaliana accessions. *Nat. Genet.* **2010**, *42*, 1135–1139. [CrossRef]

73. Kawahigashi, H.; Kasuga, S.; Ando, T.; Kanamori, H.; Wu, J.; Yonemaru, J.; Sazuka, T.; Matsumoto, T. Positional cloning of ds1, the target leaf spot resistance gene against Bipolaris sorghicola in sorghum. *Theor. Appl. Genet.* **2011**, *123*, 131–142. [CrossRef] [PubMed]
74. Mantelin, S.; Peng, H.C.; Li, B.; Atamian, H.S.; Takken, F.L.; Kaloshian, I. The receptor-like kinase SlSERK1 is required for Mi-1-mediated resistance to potato aphids in tomato. *Plant J.* **2011**, *67*, 459–471. [CrossRef] [PubMed]
75. Wan, J.; Tanaka, K.; Zhang, X.C.; Son, G.H.; Brechenmacher, L.; Nguyen, T.H.; Stacey, G. LYK4, a lysin motif receptor-like kinase, is important for chitin signaling and plant innate immunity in Arabidopsis. *Plant Physiol.* **2012**, *160*, 396–406. [CrossRef] [PubMed]
76. Zeng, L.; Velasquez, A.C.; Munkvold, K.R.; Zhang, J.; Martin, G.B. A tomato LysM receptor-like kinase promotes immunity and its kinase activity is inhibited by AvrPtoB. *Plant J.* **2012**, *69*, 92–103. [CrossRef] [PubMed]
77. Hematy, K.; Sado, P.E.; Van Tuinen, A.; Rochange, S.; Desnos, T.; Balzergue, S.; Pelletier, S.; Renou, J.P.; Hofte, H. A receptor-like kinase mediates the response of Arabidopsis cells to the inhibition of cellulose synthesis. *Curr. Biol.* **2007**, *17*, 922–931. [CrossRef] [PubMed]
78. Kessler, S.A.; Shimosato-Asano, H.; Keinath, N.F.; Wuest, S.E.; Ingram, G.; Panstruga, R.; Grossniklaus, U. Conserved molecular components for pollen tube reception and fungal invasion. *Science* **2010**, *330*, 968–971. [CrossRef] [PubMed]
79. Chen, X.; Shang, J.; Chen, D.; Lei, C.; Zou, Y.; Zhai, W.; Liu, G.; Xu, J.; Ling, Z.; Cao, G.; et al. A B-lectin receptor kinase gene conferring rice blast resistance. *Plant J.* **2006**, *46*, 794–804. [CrossRef]
80. Li, H.; Zhou, S.Y.; Zhao, W.S.; Su, S.C.; Peng, Y.L. A novel wall-associated receptor-like protein kinase gene, OsWAK1, plays important roles in rice blast disease resistance. *Plant Mol. Biol.* **2009**, *69*, 337–346. [CrossRef]
81. Zhou, H.; Li, S.; Deng, Z.; Wang, X.; Chen, T.; Zhang, J.; Chen, S.; Ling, H.; Zhang, A.; Wang, D.; et al. Molecular analysis of three new receptor-like kinase genes from hexaploid wheat and evidence for their participation in the wheat hypersensitive response to stripe rust fungus infection. *Plant J.* **2007**, *52*, 420–434. [CrossRef] [PubMed]
82. Bi, D.; Cheng, Y.T.; Li, X.; Zhang, Y. Activation of plant immune responses by a gain-of-function mutation in an atypical receptor-like kinase. *Plant Physiol.* **2010**, *153*, 1771–1779. [CrossRef] [PubMed]
83. Feuillet, C.; Schachermayr, G.; Keller, B. Molecular cloning of a new receptor-like kinase gene encoded at the Lr10 disease resistance locus of wheat. *Plant J.* **1997**, *11*, 4552. [CrossRef] [PubMed]
84. Chinchilla, D.; Zipfel, C.; Robatzek, S.; Kemmerling, B.; Nurnberger, T.; Jones, J.D.; Felix, G.; Boller, T. A flagellin-induced complex of the receptor FLS2 and BAK1 initiates plant defence. *Nature* **2007**, *448*, 497–500. [CrossRef] [PubMed]
85. Heese, A.; Hann, D.R.; Gimenez-Ibanez, S.; Jones, A.M.; He, K.; Li, J.; Schroeder, J.I.; Peck, S.C.; Rathjen, J.P. The receptor-like kinase SERK3/BAK1 is a central regulator of innate immunity in plants. *Proc. Natl. Acad. Sci. USA* **2007**, *104*, 12217–12222. [CrossRef]
86. Schulze, B.; Mentzel, T.; Jehle, A.K.; Mueller, K.; Beeler, S.; Boller, T.; Felix, G.; Chinchilla, D. Rapid heteromerization and phosphorylation of ligand-activated plant transmembrane receptors and their associated kinase BAK1. *J. Biol. Chem.* **2010**, *285*, 9444–9451. [CrossRef]
87. Postel, S.; Kufner, I.; Beuter, C.; Mazzotta, S.; Schwedt, A.; Borlotti, A.; Halter, T.; Kemmerling, B.; Nurnberger, T. The multifunctional leucine-rich repeat receptor kinase BAK1 is implicated in Arabidopsis development and immunity. *Eur. J. Cell Biol.* **2010**, *89*, 169–174. [CrossRef] [PubMed]
88. Roux, M.; Schwessinger, B.; Albrecht, C.; Chinchilla, D.; Jones, A.; Holton, N.; Malinovsky, F.G.; Tor, M.; de Vries, S.; Zipfel, C. The Arabidopsis leucine-rich repeat receptor-like kinases BAK1/SERK3 and BKK1/SERK4 are required for innate immunity to hemibiotrophic and biotrophic pathogens. *Plant Cell* **2011**, *23*, 2440–2455. [CrossRef] [PubMed]
89. Bar, M.; Sharfman, M.; Ron, M.; Avni, A. BAK1 is required for the attenuation of ethylene-inducing xylanase (Eix)-induced defense responses by the decoy receptor LeEix1. *Plant J.* **2010**, *63*, 791–800. [CrossRef]
90. Liebrand, T.W.; van den Berg, G.C.; Zhang, Z.; Smit, P.; Cordewener, J.H.; America, A.H.; Sklenar, J.; Jones, A.M.; Tameling, W.I.; Robatzek, S.; et al. Receptor-like kinase SOBIR1/EVR interacts with receptor-like proteins in plant immunity against fungal infection. *Proc. Natl. Acad. Sci. USA* **2013**, *110*, 10010–10015. [CrossRef]
91. Shao, Z.Q.; Wang, B.; Chen, J.Q. Tracking ancestral lineages and recent expansions of NBS-LRR genes in angiosperms. *Plant Signal. Behav.* **2016**, *11*, 2095–2109. [CrossRef]
92. Zhang, Y.; Yu, Q.; Gao, S.; Yu, N.; Zhao, L.; Wang, J.; Zhao, J.; Huang, P.; Yao, L.; Wang, M.; et al. Disruption of the primary salicylic acid hydroxylases in rice enhances broad-spectrum resistance against pathogens. *Plant Cell Environ.* **2022**, *45*, 2211–2225. [CrossRef] [PubMed]
93. Luna, E.; Bruce, T.J.; Roberts, M.R.; Flors, V.; Ton, J. Next-generation systemic acquired resistance. *Plant Physiol.* **2012**, *158*, 844–853. [CrossRef]
94. Vlot, A.C.; Dempsey, D.M.; Klessig, D.F. Salicylic acid, a multifaceted hormone to combat disease. *Annu. Rev. Phytopathol.* **2009**, *47*, 177–206. [CrossRef]
95. Cao, L.; Yoo, H.; Chen, T.; Mwimba, M.; Zhang, X.; Dong, X. H_2O_2 sulfenylates CHE linking local infection to establishment of systemic acquired resistance. *bioRxiv* **2023**. [CrossRef]
96. Leong, J.X.; Langin, G.; Üstün, S. Selective autophagy: Adding precision in plant immunity. *Essays Biochem.* **2022**, *66*, 189–206.
97. Marshall, R.S.; Vierstra, R.D. Autophagy: The master of bulk and selective recycling. *Annu. Rev. Plant Biol.* **2018**, *69*, 173–208. [CrossRef]

98. Liu, Y.; Schiff, M.; Czymmek, K.; Tallóczy, Z.; Levine, B.; Dinesh-Kumar, S.P. Autophagy regulates programmed cell death during the plant innate immune response. *Cell* **2005**, *121*, 567–577. [CrossRef]
99. Lenz, H.D.; Haller, E.; Melzer, E.; Kober, K.; Wurster, K.; Stahl, M.; Bassham, D.C.; Vierstra, R.D.; Parker, J.E.; Bautor, J.; et al. Autophagy differentially controls plant basal immunity to biotrophic and necrotrophic pathogens. *Plant J.* **2011**, *66*, 818–830. [CrossRef] [PubMed]
100. Patel, S.; Dinesh-Kumar, S.P. Arabidopsis ATG6 is required to limit the pathogen-associated cell death response. *Autophagy* **2008**, *4*, 20–27. [CrossRef] [PubMed]
101. Maksimov, I.V.; Shein, M.Y.; Burkhanova, G.F. RNA Interference in Plant Defense Systems. *Russ. J. Plant Physiol.* **2021**, *68*, 613–625. [CrossRef]
102. Vance, V.; Vaucheret, H. RNA silencing in plants--defense and counterdefense. *Science* **2001**, *292*, 2277–2280. [CrossRef] [PubMed]
103. Pumplin, N.; Voinnet, O. RNA silencing suppression by plant pathogens: Defence, counter-defence and counter-counter-defence. *Nat. Rev. Microbiol.* **2013**, *11*, 745–760. [CrossRef]
104. Ruiz-Ferrer, V.; Voinnet, O. Roles of plant small RNAs in biotic stress responses. *Annu. Rev. Plant Biol.* **2009**, *60*, 485–510. [CrossRef] [PubMed]
105. Lopez-Gomollon, S.; Baulcombe, D.C. Roles of RNA silencing in viral and non-viral plant immunity and in the crosstalk between disease resistance systems. *Nat. Rev. Mol. Cell Biol.* **2022**, *23*, 645–662. [CrossRef] [PubMed]
106. Marcec, M.J.; Gilroy, S.; Poovaiah, B.W.; Tanaka, K. Mutual interplay of Ca^{2+} and ROS signaling in plant immune response. *Plant Sci.* **2019**, *283*, 343–354. [CrossRef]
107. Seybold, H.; Trempel, F.; Ranf, S.; Scheel, D.; Romeis, T.; Lee, J. Ca^{2+} signalling in plant immune response: From pattern recognition receptors to Ca^{2+} decoding mechanisms. *New Phytol.* **2014**, *204*, 782–790. [CrossRef]
108. Moeder, W.; Phan, V.; Yoshioka, K. Ca^{2+} to the rescue– Ca^{2+} channels and signaling in plant immunity. *Plant Sci.* **2019**, *279*, 19–26. [CrossRef] [PubMed]
109. Clapham, D.E. Calcium signaling. *Cell* **2007**, *131*, 1047–1058. [CrossRef]
110. Edel, K.H.; Marchadier, E.; Brownlee, C.; Kudla, J.; Hetherington, A.M. The evolution of calcium-based signalling in plants. *Curr. Biol.* **2017**, *27*, R667–R679. [CrossRef]
111. Costa, A.; Navazio, L.; Szabo, I. The contribution of organelles to plant intracellular calcium signalling. *J. Exp. Bot.* **2018**, *69*, 4175–4193. [CrossRef]
112. Saand, M.A.; Xu, Y.P.; Munyampundu, J.P.; Li, W.; Zhang, X.R.; Cai, X.Z. Phylogeny and evolution of plant cyclic nucleotide-gated ion channel (CNGC) gene family and functional analyses of tomato CNGCs. *DNA Res.* **2015**, *22*, 471–483. [CrossRef]
113. Toyota, M. Conservation of Long-Range Signaling in Land Plants via Glutamate Receptor–Like Channels. *Plant Cell Physiol.* **2024**, *65*, 657–659. [CrossRef]
114. Thor, K.; Jiang, S.; Michard, E.; George, J.; Scherzer, S.; Huang, S.; Dindas, J.; Derbyshire, P.; Leitão, N.; DeFalco, T.A.; et al. The calcium-permeable channel OSCA1.3 regulates plant stomatal immunity. *Nature* **2020**, *585*, 569–573. [CrossRef]
115. Ali, R.; Ma, W.; Lemtiri-chlieh, F.; Tsaltas, D.; Leng, Q.; Bodman, S.; Berkowitz, G. Death don't have no mercy and neither does calcium: Arabidopsis CYCLIC NUCLEOTIDE GATED CHANNEL2 and innate immunity. *Plant Cell* **2007**, *19*, 1081–1095. [CrossRef]
116. Ma, Y.; Walker, R.; Zhao, Y.; Berkowitz, G. Linking ligand perception by PEPR pattern recognition receptors to cytosolic Ca^{2+} elevation and downstream immune signaling in plants. *Proc. Natl. Acad. Sci. USA* **2012**, *109*, 19852–19857. [CrossRef]
117. Tian, W.; Hou, C.; Ren, Z.; Wang, C.; Zhao, F.; Dahlbeck, D.; Hu, S.; Zhang, L.; Niu, Q.; Li, L.; et al. A calmodulin-gated calcium channel links pathogen patterns to plant immunity. *Nature* **2019**, *572*, 131–135. [CrossRef]
118. Wang, J.; Liu, X.; Zhang, A.; Ren, Y.; Wu, F.; Wang, G.; Xu, Y.; Lei, C.; Zhu, S.; Pan, T.; et al. A cyclic nucleotide-gated channel mediates cytoplasmic calcium elevation and disease resistance in rice. *Cell Res.* **2019**, *29*, 820–831. [CrossRef]
119. Meena, M.; Prajapati, R.; Krishna, D.; Divakaran, K.; Pandey, Y.; Reichelt, M.; Mathew, M.; Boland, W.; Mithöfer, A.; Vadassery, J. The Ca^{2+} channel CNGC19 regulates Arabidopsis defense against Spodoptera herbivory. *Plant Cell* **2019**, *31*, 1539–1562. [CrossRef]
120. Yu, X.; Xie, Y.; Luo, D.; Liu, H.; de Oliveira, M.; Qi, P.; Kim, S.; Ortiz-Morea, F.; Liu, J.; Chen, Y.; et al. A phospho-switch constrains BTL2-mediated phytocytokine signaling in plant immunity. *Cell* **2013**, *186*, 2329–2344. [CrossRef]
121. Espinoza, C.; Liang, Y.; Stacey, G. Chitin receptor CERK1 links salt stress and chitin-triggered innate immunity in Arabidopsis. *Plant J.* **2017**, *89*, 984–995. [CrossRef] [PubMed]
122. Bjornson, M.; Pimprikar, P.; Nürnberger, T.; Zipfel, C. The transcriptional landscape of Arabidopsis thaliana pattern-triggered immunity. *Nat. Plants* **2021**, *7*, 579–586. [CrossRef] [PubMed]
123. Tang, D.; Wang, G.; Zhou, J.M. Receptor kinases in plant-pathogen interactions: More than pattern recognition. *Plant Cell* **2017**, *29*, 618–637. [CrossRef] [PubMed]
124. Berrios, L.; Rentsch, J.D. Linking reactive oxygen species (ROS) to abiotic and biotic feedbacks in plant microbiomes: The dose makes the poison. *Inter. J. Mol. Sci.* **2022**, *23*, 4402. [CrossRef]
125. Lamb, C.; Dixon, R.A. The oxidative burst in plant disease resistance. *Annu. Rev. Plant Biol.* **1997**, *48*, 251–275. [CrossRef] [PubMed]
126. Zhang, J.; Li, W.; Xiang, T.; Liu, Z.; Laluk, K.; Ding, X.; Zou, Y.; Gao, M.; Zhang, X.; Chen, S.; et al. Receptor-like cytoplasmic kinases integrate signaling from multiple plant immune receptors and are targeted by a Pseudomonas syringae effector. *Cell Host Microbe* **2010**, *7*, 290–301. [CrossRef] [PubMed]

127. Ranf, S.; Eschen-Lippold, L.; Fröhlich, K.; Westphal, L.; Scheel, D.; Lee, J. Microbe-associated molecular pattern-induced calcium signaling requires the receptor-like cytoplasmic kinases, PBL1 and BIK1. *BMC Plant Biol.* **2014**, *14*, 374. [CrossRef]
128. Miller, G.; Schlauch, K.; Tam, R.; Cortes, D.; Torres, M.A.; Shulaev, V.; Dangl, J.L.; Mittler, R. The plant NADPH oxidase RBOHD mediates rapid systemic signaling in response to diverse stimuli. *Sci. Signal* **2009**, *2*, ra45. [CrossRef]
129. Dubiella, U.; Seybold, H.; Durian, G.; Komander, E.; Lassig, R.; Witte, C.P.; Schulze, W.X.; Romeis, T. Calcium-dependent protein kinase/NADPH oxidase activation circuit is required for rapid defense signal propagation. *Proc. Natl. Acad. Sci. USA* **2013**, *110*, 8744–8749. [CrossRef]
130. Gilroy, S.; Białasek, M.; Suzuki, N.; Górecka, M.; Devireddy, A.R.; Karpiński, S.; Mittler, R. ROS, calcium, and electric signals: Key mediators of rapid systemic signaling in plants. *Plant Physiol.* **2016**, *171*, 1606–1615. [CrossRef]
131. López, M.A.; Bannenberg, G.; Castresana, C. Controlling hormone signaling is a plant and pathogen challenge for growth and survival. *Curr. Opin. Plant Biol.* **2008**, *11*, 420–427. [CrossRef] [PubMed]
132. Oka, K.; Kobayashi, M.; Mitsuhara, I.; Seo, S. Jasmonic acid negatively regulates resistance to Tobacco mosaic virus in tobacco. *Plant Cell Physiol.* **2013**, *54*, 1999–2010. [CrossRef] [PubMed]
133. Xin, X.F.; He, S.Y. *Pseudomonas syringae* pv. tomato DC3000: A model pathogen for probing disease susceptibility and hormone signaling in plants. *Ann. Rev. Phytopathol.* **2013**, *51*, 473–498. [CrossRef] [PubMed]
134. Ali, S.; Mir, Z.A.; Tyagi, A.; Mehari, H.; Meena, R.P.; Bhat, J.A.; Yadav, P.; Papalou, P.; Rawat, S.; Grover, A. Overexpression of NPR1 in *Brassica juncea* confers broad-spectrum resistance to fungal pathogens. *Front. Plant Sci.* **2017**, *8*, 1693. [CrossRef] [PubMed]
135. Zavaliev, R.; Mohan, R.; Chen, T.; Dong, X. Formation of NPR1 condensates promotes cell survival during the plant immune response. *Cell* **2020**, *182*, 1093–1108. [CrossRef] [PubMed]
136. Lefevere, H.; Bauters, L.; Gheysen, G. Salicylic acid biosynthesis in plants. *Front. Plant Sci.* **2020**, *11*, 521987. [CrossRef]
137. Tandon, G.; Jaiswal, S.; Iquebal, M.A.; Kumar, S.; Kaur, S.; Rai, A.; Kumar, D. Evidence of salicylic acid pathway with EDS1 and PAD4 proteins by molecular dynamics simulation for grape improvement. *J. Biomol. Struct. Dyn.* **2015**, *33*, 2180–2191. [CrossRef] [PubMed]
138. Abreu, M.E.; Munné-Bosch, S. Salicylic acid deficiency in NahG transgenic lines and sid2 mutant's increases seed yield in the annual plant *Arabidopsis thaliana*. *J. Exp. Bot.* **2009**, *60*, 1261–1271. [CrossRef] [PubMed]
139. Schulze-Lefert, P.; Robatzek, S. Plant pathogens trick guard cells into opening the gates. *Cell* **2006**, *126*, 831–834. [CrossRef]
140. Wasternack, C.; Hause, B. The missing link in jasmonic acid biosynthesis. *Nat. Plants* **2019**, *5*, 776–777. [CrossRef]
141. Van Moerkercke, A.; Duncan, O.; Zander, M.; Šimura, J.; Broda, M.; Vanden Bossche, R.; Lewsey, M.G.; Lama, S.; Singh, K.B.; Ljung, K.; et al. A MYC2/MYC3/MYC4-dependent transcription factor network regulates water spray-responsive gene expression and jasmonate levels. *Proc. Natl. Acad. Sci. USA* **2019**, *116*, 23345–23356. [CrossRef] [PubMed]
142. Koo, A.J.K.; Gao, X.; Jones, A.D.; Howe, G.A. A rapid wound signal activates the systemic synthesis of bioactive jasmonates in Arabidopsis. *Plant J.* **2009**, *59*, 974–986. [CrossRef] [PubMed]
143. Boter, M.; Ruiz-Rivero, O.; Abdeen, A.; Prat, S. Conserved MYC transcription factors play a key role in jasmonate signaling both in tomato and Arabidopsis. *Genes. Dev.* **2004**, *18*, 1577–1591. [CrossRef]
144. Taylor, J.E.; Hatcher, P.E.; Paul, N.D. Crosstalk between plant responses to pathogens and herbivores: A view from the outside in. *J. Exp. Bot.* **2004**, *55*, 159–168. [CrossRef] [PubMed]
145. Choi, W.; Hilleary, R.; Swanson, S.J.; Kim, S.H.; Gilroy, S. Rapid, long-distance electrical and calcium signaling in plants. *Annu. Rev. Plant Biol.* **2016**, *67*, 287–310. [CrossRef] [PubMed]
146. Tripathi, D.; Raikhi, G.; Kumar, D. Chemical elicitors of systemic acquired resistance—Salicylic acid and its functional analogs. *Curr. Plant Biol.* **2019**, *17*, 48–59. [CrossRef]
147. Ramirez-Prado, J.S.; Abulfaraj, A.A.; Rayapuram, N.; Benhamed, M.; Hirt, H. Plant immunity: From signaling to epigenetic control of defense. *Trends Plant Sci.* **2018**, *23*, 833–844. [CrossRef]
148. Palukaitis, P.; Yoon, J.Y. R gene mediated defense against viruses. *Curr. Opin. Virol.* **2020**, *45*, 1–7. [CrossRef]
149. Campos, L.; Granell, P.; Tárraga, S.; López-Gresa, P.; Conejero, V.; Bellés, J.M.; Rodrigo, I.; Lisón, P. Salicylic acid and gentisic acid induce RNA silencing-related genes and plant resistance to RNA pathogens. *Plant Physiol. Biochem.* **2014**, *77*, 35–43. [CrossRef]
150. Han, K.; Huang, H.; Zheng, H.; Ji, M.; Yuan, Q.; Cui, W.; Zhang, H.; Peng, J.; Lu, Y.; Rao, S.; et al. Rice stripe virus coat protein induces the accumulation of jasmonic acid, activating plant defence against the virus while also attracting its vector to feed. *Mol. Plant Pathol.* **2020**, *21*, 1647–1653. [CrossRef]
151. Ji, M.; Zhao, J.; Han, K.; Cui, W.; Wu, X.; Chen, B.; Lu, Y.; Peng, J.; Zheng, H.; Rao, S.; et al. Turnip mosaic virus P1 suppresses JA biosynthesis by degrading cpSRP54 that delivers AOCs onto the thylakoid membrane to facilitate viral infection. *PLoS Pathog.* **2021**, *17*, e1010108. [CrossRef] [PubMed]
152. Syller, J.; Grupa, A. Antagonistic within-host interactions between plant viruses: Molecular basis and impact on viral and host fitness. *Mol. Plant Pathol.* **2016**, *17*, 769–782. [CrossRef] [PubMed]
153. Takahashi, H.; Kanayama, Y.; Zheng, M.S.; Kusano, T.; Hase, S.; Ikegami, M.; Shah, J. Antagonistic interactions between the SA and JA signaling pathways in Arabidopsis modulate expression of defense genes and gene-for-gene resistance to cucumber mosaic virus. *Plant Cell Physiol.* **2004**, *45*, 803–809. [CrossRef] [PubMed]
154. Pieterse, C.M.; Van der Does, D.; Zamioudis, C.; Leon-Reyes, A.; Van Wees, S.C. Hormonal modulation of plant immunity. *Annu. Rev. Cell Dev. Biol.* **2012**, *28*, 489–521. [CrossRef] [PubMed]

155. Boller, T.; Felix, G. A renaissance of elicitors: Perception of microbe-associated molecular patterns and danger signals by pattern-recognition receptors. *Annu. Rev. Plant Biol.* **2009**, *60*, 379–406. [CrossRef] [PubMed]
156. Wu, J.; Baldwin, I.T. New insights into plant responses to the attack from insect herbivores. *Annu. Rev. Genet.* **2010**, *44*, 1–24. [CrossRef] [PubMed]
157. Zhao, Z.X.; Feng, Q.; Liu, P.Q.; He, X.R.; Zhao, J.H.; Xu, Y.J.; Zhang, L.L.; Huang, Y.Y.; Zhao, J.Q.; Fan, J.; et al. RPW8.1 enhances the ethylene-signaling pathway to feedback-attenuate its mediated cell death and disease resistance in Arabidopsis. *New Phytol.* **2021**, *229*, 516. [CrossRef] [PubMed]
158. Pré, M.; Atallah, M.; Champion, A.; De Vos, M.; Pieterse, C.M.; Memelink, J. The AP2/ERF domain transcription factor ORA59 integrates jasmonic acid and ethylene signals in plant defense. *Plant Physiol.* **2008**, *147*, 1347–1357. [CrossRef]
159. Mur, L.A.; Lloyd, A.J.; Cristescu, S.M.; Harren, F.J.; Hall, M.; Smith, A. Biphasic ethylene production during the hypersensitive response in Arabidopsis: A window into defence priming mechanisms? *Plant Signal Behav.* **2009**, *4*, 610–613. [CrossRef] [PubMed]
160. Nguyen, D.; D'Agostino, N.; Tytgat, T.O.G.; Sun, P.; Lortzing, T.; Visser, E.J.W.; Cristescu, S.M.; Steppuhn, A.; Mariani, C.; van Dam, N.M.; et al. Drought and flooding have distinct effects on herbivore-induced responses and resistance in *Solanum dulcamara*. *Plant Cell Environ.* **2016**, *39*, 1485–1499. [CrossRef]
161. García-Andrade, J.; González, B.; Gonzalez-Guzman, M.; Rodriguez, P.L.; Vera, P. The Role of ABA in Plant Immunity is Mediated through the PYR1 Receptor. *Int. J. Mol. Sci.* **2020**, *21*, 5852. [CrossRef] [PubMed]
162. Mine, A.; Berens, M.L.; Nobori, T.; Anver, S.; Fukumoto, K.; Winkelmüller, T.M.; Takeda, A.; Becker, D.; Tsuda, K. Pathogen exploitation of an abscisic acid- and jasmonate-inducible MAPK phosphatase and its interception by Arabidopsis immunity. *Proc. Natl. Acad. Sci. USA* **2017**, *114*, 7456–7461. [CrossRef] [PubMed]
163. Dombrecht, B.; Xue, G.P.; Sprague, S.J.; Kirkegaard, J.A.; Ross, J.J.; Reid, J.B.; Fitt, G.P.; Sewelam, N.; Schenk, P.M.; Manners, J.M.; et al. MYC2 differentially modulates diverse jasmonate-dependent functions in Arabidopsis. *Plant Cell* **2007**, *19*, 2225–2245. [CrossRef]
164. Zheng, L.; Liu, G.; Meng, X.; Liu, Y.; Ji, X.; Li, Y.; Nie, X.; Wang, Y. A WRKY gene from *Tamarix hispida*, ThWRKY4, mediates abiotic stress responses by modulating reactive oxygen species and expression of stress-responsive genes. *Plant Mol. Biol.* **2013**, *82*, 303–320. [CrossRef] [PubMed]
165. Huang, H.; Ullah, F.; Zhou, D.X.; Yi, M.; Zhao, Y. Mechanisms of ROS regulation of plant development and stress responses. *Front. Plant Sci.* **2019**, *10*, 800. [CrossRef] [PubMed]

plants

MDPI

Review

Abiotic Stress in Rice: Visiting the Physiological Response and Its Tolerance Mechanisms

Bhaskar Sarma [1,†], Hamdy Kashtoh [2,†], Tensangmu Lama Tamang [2,†], Pranaba Nanda Bhattacharyya [3], Yugal Kishore Mohanta [4,5,*] and Kwang-Hyun Baek [2,*]

[1] Department of Botany, Dhemaji College, Dhemaji 787057, Assam, India; bhaskarsarma252@gmail.com
[2] Department of Biotechnology, Yeungnam University, Gyeongsan 38541, Gyeongbuk, Republic of Korea; hamdy_kashtoh@ynu.ac.kr (H.K.); orgchemtensa@ynu.ac.kr (T.L.T.)
[3] Department of Botany, Nanda Nath Saikia College, Titabar 785630, Assam, India; pranabananda_01@rediffmail.com
[4] Nano-Biotechnology and Translational Knowledge Laboratory, Department of Applied Biology, School of Biological Sciences, University of Science and Technology Meghalaya, Techno City, 9th Mile, Ri-Bhoi, Baridua 793101, Meghalaya, India
[5] Centre for Herbal Pharmacology and Environmental Sustainability, Chettinad Hospital and Research Institute, Chettinad Academy of Research and Education, Kelambakkam 603103, Tamil Nadu, India
* Correspondence: ykmohanta@gmail.com (Y.K.M.); khbaek@ynu.ac.kr (K.-H.B.); Tel.: +82-53-810-3029 (K.-H.B.)
† These authors contributed equally to this work.

Abstract: Rice (*Oryza sativa* L.) is one of the most significant staple foods worldwide. Carbohydrates, proteins, vitamins, and minerals are just a few of the many nutrients found in domesticated rice. Ensuring high and constant rice production is vital to facilitating human food supplies, as over three billion people around the globe rely on rice as their primary source of dietary intake. However, the world's rice production and grain quality have drastically declined in recent years due to the challenges posed by global climate change and abiotic stress-related aspects, especially drought, heat, cold, salt, submergence, and heavy metal toxicity. Rice's reduced photosynthetic efficiency results from insufficient stomatal conductance and natural damage to thylakoids and chloroplasts brought on by abiotic stressor-induced chlorosis and leaf wilting. Abiotic stress in rice farming can also cause complications with redox homeostasis, membrane peroxidation, lower seed germination, a drop in fresh and dry weight, necrosis, and tissue damage. Frequent stomatal movements, leaf rolling, generation of reactive oxygen radicals (RORs), antioxidant enzymes, induction of stress-responsive enzymes and protein-repair mechanisms, production of osmolytes, development of ion transporters, detoxifications, etc., are recorded as potent morphological, biochemical and physiological responses of rice plants under adverse abiotic stress. To develop cultivars that can withstand multiple abiotic challenges, it is necessary to understand the molecular and physiological mechanisms that contribute to the deterioration of rice quality under multiple abiotic stresses. The present review highlights the strategic defense mechanisms rice plants adopt to combat abiotic stressors that substantially affect the fundamental morphological, biochemical, and physiological mechanisms.

Keywords: abiotic stress; drought; physiology; rice; tolerance

1. Introduction

Rice (*Oryza sativa* L.), a species of Poaceae, is a ubiquitous staple food worldwide, offering vital nutrients, including carbohydrates, thiamin, folate, calcium, iron, pantothenic acid, and energy [1,2]. Due to the global significance of this economically essential crop in supporting growing human populations and meeting extensive nutritional needs, improving grain production and quality standards is becoming increasingly important [3,4]. Although yields have plateaued in the cultivation of most cereals, including rice, in recent decades, climate change is a significant challenge that greatly influences breeders' decisions

regarding productivity and quality issues [5]. In the coming decades, persistent negative impacts of climatic change and global warming can cause shifts in the severity, duration, and frequency of abiotic stress in rice farming, jeopardizing agricultural sustainability and global food security [6]. By 2050, it is anticipated that global warming and changes in the climate will lower irrigated rice production by 7%, while the yields of rainfed rice will likely decline by 6% and, more conservatively, up to 2.5%, respectively [7]. Various strategies have been adopted in climate-resilient agriculture to promote long-term sustainability. The Green Revolution brought a substantial increment in rice productivity across the globe through the usage of promising and high-yielding rice varieties and the implementation of modern farming techniques like drip irrigation, biofertilizers, biopesticides, and usage of recommended doses of plant protection formulations (PPFs) [8].

Rice farming is under continuous exposure to a broad category of biotic (pathogen invasion and insect infestations) and abiotic (extreme temperatures, drought, cold, heavy metal toxicity, and salinity) stress-related factors leading to serious agricultural issues like poor grain production and quality deterioration [9]. Figure 1 depicts different abiotic stress-related factors that negatively impact rice farming considerably.

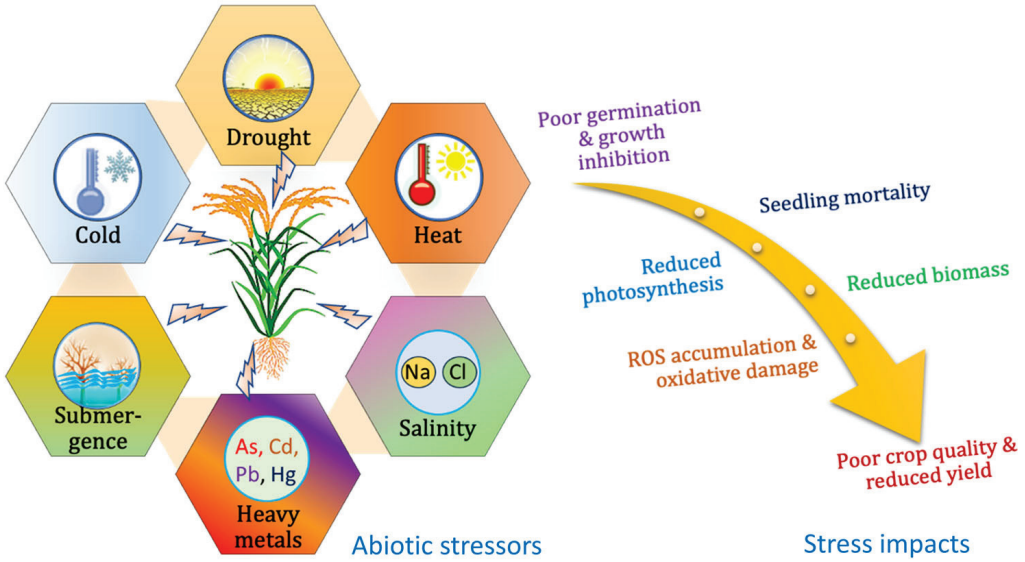

Figure 1. Effects of different abiotic stresses on rice.

Heat stress and drought are major abiotic stressors that interfere with rice's physiological, molecular, biochemical, and morphological responses, resulting in massive crop losses and compromises in quality [10]. It has become apparent that frequent exposure to high temperatures during rice cultivation appears to have detrimental effects in various tropical and subtropical countries, including India, China, Bangladesh, Pakistan, Thailand, and several African countries. This includes substantial declines in yield and quality, which can be attributed to the sudden occurrence of pollen sterility and loss of fertility [11]. According to Oladosu et al., frequent exposure to drought is detrimental to brown and milled rice, as it can drastically reduce the quality of grain production to a great extent [12]. On the other hand, a rise in temperature leads to a rise in humidity, making spikelets sterile [13]. The flower buds cannot mobilize essential nutrients like carbohydrates and derived products when subjected to extreme heat stress.

Chilling stress is another influential environmental stress that significantly impacts the rice plants' normal growth and development, including the percentage of seeds that successfully germinate, the vigor of seedlings, the formation of tillers, the reproductive capacity of plants, and the maturity of grains [14]. Similarly, under salinity stress, invasive apoplastic ion transport drives Na+ uptake into rice shoots [15]. Likewise, the submersion of plants can have detrimental effects on various physiological processes, including oxygen and carbon dioxide exchange, light availability, and nutrient absorption. These adverse con-

ditions can hinder the process of photosynthesis, exhaust energy reserves, and eventually lead to growth impairment or the mortality of plants [16]. According to Suwanmontri et al., rice farming under rainfed lowland ecosystems is severely affected by intense and rapid exposure to abiotic stressors, leading to significant damage both in terms of quality and quantity [17]. Furthermore, plants exposed to high amounts of heavy metals experience a decrease or complete halt in metabolic activities and exhibit morphological abnormalities, ultimately leading to a reduction in crop yield [18].

To adapt to these abrupt changes in environments, plants have established intricate response mechanisms for detecting environmental signals and displaying appropriate physiological, morphological, and biochemical adaptations. Abiotic stressors can trigger the up- or downregulation of various genes, activating or inhibiting multiple signaling pathways and enhancing the plant's tolerance to different environmental challenges [19]. Therefore, a complex interaction of signaling cascades is required at the molecular level to recognize external stimuli and the subsequent awakening of defense mechanisms [16]. In recent years, significant advancements have been made in our understanding of how plants respond to abiotic stresses. This progress can be attributed to contributions made in plant physiology, genetics, biotechnology, and molecular biology. By building upon the existing knowledge of stress tolerance mechanisms in rice cultivars, it is possible to develop novel gene pools that exhibit enhanced resistance to abiotic stresses [20]. In light of the preceding, this review aims to assess the biochemical, physiological, and morphological responses of rice to different abiotic stimuli and identify the process parameters used to generate rice varieties that are tolerant to abiotic stress.

2. Morphophysiological and Biochemical Impacts and Tolerance Mechanisms in Response to Different Abiotic Stressors

2.1. Drought Stress

The environment has witnessed several persistent repercussions from global climate change, like alterations to the growing season, patterns of rainfall, severe droughts, and soaring temperatures. A significant impact of these changes is the serious threat posed to global rice production by drought stress [21]. Statistics show that 42 million hectares of rice in Asia are occasionally or frequently vulnerable to drought, significantly reducing yield [22–24]. According to Lafitte et al., rice suffers economic losses of 48–94% during the reproductive stage due to water stress and another 60% during the grain-filling stage [25]. Reduced cell development, elongation, expansion, and the disruption of plant antioxidant activity triggered by the buildup of reactive oxygen species (ROS) are all ways that drought stress affects rice yield [26].

2.1.1. Morphophysiological and Biochemical Responses to Drought Stress

Plants have different strategies to deal with drought, which include escape, avoidance, and tolerance. Escape involves adapting to a shorter life cycle or growing seasonally to reproduce before the environment becomes dry [27]. Avoidance focuses on maintaining a high water potential in plants by reducing water loss through stomatal control and having a well-developed root system for water uptake [28]. Tolerance, on the other hand, involves limiting the number and size of leaves in response to water scarcity, but this strategy can result in reduced yield [29]. Rice production is particularly impacted by three typical types of droughts: early water stress, which delays the transplantation of seedlings; mild intermittent stress with cumulative impacts; and late stress, which affects late-maturing varieties [30]. The root–canopy ratio, plant height, and dry weight decrease upon water scarcity exposure. Especially at the flowering stage of rice, the rate of photosynthesis, stomatal conductance, rate of transpiration, water potential of leaves, and the air–leaf temperature gap all experience a substantial decline [23]. During the reproductive stage, rice is highly susceptible to water stress, significantly reducing grain production with a drastic decrease in the number of whole grains and spikelets per panicle [31]. The major plant part that detects changes in soil conditions are the roots, which also play a pivotal

role in how plants react to water stress. When studying rice root systems under drought stress, a significant positive association was observed between root diameter, depth, and overall plant health and vitality. In drought, plants lengthen their roots to use the water in the soil more efficiently [32]. In response to the drought, rice's root length increases, enabling the plants to access deeper water reserves in the soil. Additionally, there is a notable reduction in the diameter of nodal roots, leading to the development of relatively finer roots that aid in resource conservation [33]. Many upland *japonica* rice cultivars can withstand drought because of their vast and deep root systems. In contrast, the indica subspecies of rice often experience a reduction in their growth period [34]. Rice is less adapted to water-scarce circumstances than other cereal crops. Upland rice cultivars' deep root systems are considered good at sustaining yields under drought conditions. In contrast, lowland rain-fed rice crops are susceptible to fluctuating soil water levels, and specific genotypes have adapted to these circumstances by promoting root growth even before and throughout drought [35]. According to Banoc et al., rice plants with well-established root systems exhibit greater water stress resilience and can maintain productivity even under such conditions [36]. Root growth takes precedence over shoot growth when there is a water shortage. Notably, there is a significant disparity in the rate of sap leakage from the root network between rice genotypes that are tolerant to drought and those that are susceptible to it [37].

The rolling of leaves is an adaptive mechanism against water deficiency. This adaptation benefits plants in times of water scarcity and low soil moisture, as it effectively reduces transpiration rates and helps maintain a favorable water balance within plant tissues [38]. As the intensity of the drought stress increases, rice leaves often exhibit varying degrees of leaf rolling. Broader-leafed *indica* rice cultivars perform better in drought conditions than shorter, narrower-leafed varieties regarding biomass, stomatal conductance, and transpiration efficiency [39]. Furthermore, to sustain turgor conditions, plant cells subjected to drought attempt to regulate their osmotic potential by accumulating specific osmolytes. One of the most well-known osmolytes, proline, functions as a mediator in osmotic control to protect the cell against ROS while maintaining the integrity of the plasma membrane. Accumulation of proline is linked to increased resistance to stress [40].

Photosynthesis, a crucial metabolic process that regulates the growth and yield of crops, is influenced by drought and water stress. When water is scarce, the relative water content in plants is reduced. In response, plants employ water-saving strategies such as closing stomata, which reduces the intake of CO_2, transpiration rate, and gaseous exchange and impedes electron transport, leading to the accumulation of ROS [41–43]. Drought stress limits the efficient operation of photosystems I and II (PSI and PSII), disrupts the function of rubisco, and hinders the electron transport chain and ATP synthesis [26,44]. In drought conditions, the efficiency of photosynthetic pigments such as carotenoids, phycobilin, and chlorophyll is diminished. This leads to insufficient absorption of light, inadequate light harvesting, and ineffective photoprotection, eventually leading to limited photosynthesis and a decrease in the production of photosynthates [45,46]. Moreover, carotenoid also has a role in plant signaling during stress; thereby, a reduction in their content can detrimentally affect signal perception during drought stress [47]. Multiple studies have documented the effects of drought stress on the structural integrity of chloroplasts, chlorophyll production, and photosynthesis. When subjected to drought stress, chloroplasts change shape, transitioning from oval to nearly round. Additionally, they move from the cell wall toward the center of the cell, and the thylakoids within the chloroplasts become disorganized [48]. Another study observed irregularly shaped chloroplasts with swollen thylakoids in response to drought stress [49]. The severity and duration of the stress and the specific plant species or genotype determine the extent to which chloroplast integrity is affected [50]. Drought stress leads to the accumulation of ROS, predominantly in chloroplasts and to some extent in mitochondria, resulting in oxidative stress [51]. Furthermore, ROS produced in the chloroplasts of water-stressed plants can negatively regulate the expression of genes related to photosynthesis and chlorophyll production via retrograde signaling [52,53].

Direct or indirect oxidative stress in water scarcity conditions causes cell membrane lipid peroxidation in plants, which in turn stimulates a cascade of physiological and biochemical changes with the potential to disrupt metabolism and negatively impact crop yield and quality [54]. During drought stress, the plant's ROS overproduction causes an abnormal decrease in photosynthetic electron chains [55]. Various ROS, such as hydroxyl radical ($HO^{\cdot}$), hydrogen peroxide (H_2O_2), and superoxide anion (O_2^{-}), are generated by multiple cell organelles. These ROS trigger oxidative damage to cellular components, DNA fragmentation, the suppression of enzyme activity, and lead to lipid and protein peroxidation. They also initiate programmed cell death pathways, ultimately leading to cell death. Antioxidants are vital plant nutrients that scavenge ROS. Therefore, enhancing the expression of antioxidants boosts the rice plants' ability to withstand drought. Non-enzymatic antioxidants such as ascorbate (AsA), tocopherol, and glutathione (GSH), are different from catalase (CAT), glutathione reductase (GR), ascorbate peroxidase (APX), superoxide dismutase (SOD), and monodehydroascorbate reductase (MDHAR), which are enzymatic antioxidants. The metabolic processes of SOD, CAT, peroxidase (POD), and soluble sugars were elevated in drought-tolerant rice cultivars, whereas malondialdehyde (MDA) level was reduced [56]. At the time of the filling phase, the drought would swiftly increase the activities of POD and CAT while slightly decreasing SOD activity, reducing AsA and GSH contents, and maintaining low levels of H_2O_2 and MDA. It is commonly accepted that drought causes increased POD and CAT activities of leaves [33]. The removal of H_2O_2 is significantly aided by the use of ascorbic acid, which is an essential antioxidant. During the ascorbic acid-glutathione cycle, APX employs two of the ascorbic acid molecules to catalyze the breakdown of H_2O_2 into water. This reaction was followed by the synthesis of monodehydroascorbate. As rice's drought stress increases, the AsA content of functional leaves drops [57]. Enhancing the content of naturally occurring antioxidants (both enzymatic and non-enzymatic) could be a tactic to lessen or stop oxidative damage and boost plant resilience to drought. During drought, redox-sensitive flavonoids and phenolic acids are synthesized to counteract ROS and bind transition metal ions required for the Fenton reaction [58]. Redox-sensitive phenolic acids (protocatechuic acid, gentisic acid, syringic acid, gallic acid, caffeic acid, salicylic acid (SA), and p-coumaric acid) and flavonoids (rutin, catechin, kaempferol, quercetin, naringin, apigenin, and myricetin) provide drought-tolerant rice cultivars with the capacity to sustain redox homeostasis [59]. Polyamines, which are small molecules with a positive charge, affect rice's adaptation to stress from drought. Some polyamines identified in plants include putrescine, spermidine, and spermine [60]. They can interact with several signaling networks and control homeostasis, osmotic potential, and membrane stability. When rice plants are subjected to drought stress, there is an elevation in polyamine levels, which is associated with enhanced photosynthetic activity, decreased water loss, and improved ability to detoxify and adapt to osmotic stress [61]. Carotenoids are crucial members of the antioxidant defense system because they prevent the synthesis of singlet oxygen, stabilize triplet chlorophyll in tissues under stress, and shield plants from oxidative damage. As a result, rice's carotenoid content rises to counteract oxidative stress [62].

2.1.2. Molecular Response to Drought Stress

Rice plants have developed complex mechanisms to survive different abiotic stresses. These mechanisms allow them to adapt or avoid stress by responding optimally. Abiotic stressors are often interconnected and cause damage to plant cells, resulting in oxidative stress [63]. When plants encounter stress, membrane receptors detect the initial signals and transmit them to initiate transcription. This process is controlled by hormones, transcription factors (TFs), and transcription factor-binding proteins (TFBPs). These factors work together to activate stress-responsive mechanisms, repair damaged proteins and membranes, and restore homeostasis [64] (Figure 2). Inadequate response at any stage of the signaling and gene activation process can lead to permanent alterations in cellular equilibrium,

breakdown of functional and structural proteins and membranes, and ultimately, cell death [65].

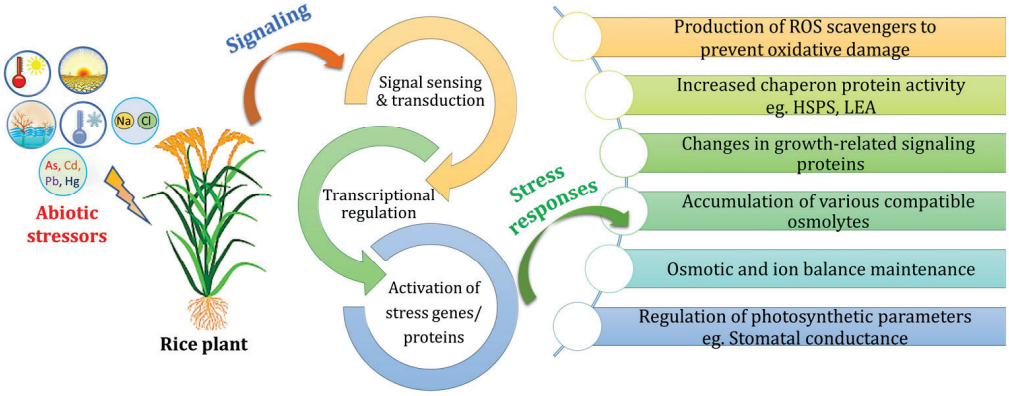

Figure 2. A simplified diagram illustrating how rice plants respond to various abiotic stresses. The overall signaling pathways in plants are triggered when they perceive signals related to abiotic stress, leading to the activation of stress responses.

To combat water scarcity, drought stress in rice activates both abscisic acid (ABA)-dependent and ABA-independent signaling pathways [66]. It works via extensive and intricate signaling pathways to regulate drought stress. This involves adjusting the physiological, biochemical, and molecular attributes of the rice to improve the root's ability to acquire more water and the stomata's ability to lose less water. This adaptation helps the plants cope with water scarcity stress. Plants respond to drought stress by narrowing their stomata to reduce water loss, improve water utilization efficiency, and enhance their chances of survival [67,68]. ABA governs the movement of stomata to lessen the transpiration rate under drought stress [69–71]. ABA receptor, OsPYL/RCAR5, has been demonstrated to exert a positive regulatory effect on the expression of genes that are responsive to abiotic stress, and overexpressing the *OsPYL/RCAR5* gene additionally enhanced transgenic rice's ability to withstand drought [72]. Research has demonstrated that rice *DREB* transcription factors are essential controllers of ABA-independent drought responses. Rice cultivars that overexpress *OsDREB1F* exhibited improved drought tolerance, indicating that this gene mediates the ABA-dependent pathway [73]. When rice undergoes drought stress, the root system improves cuticle resilience and boosts the number, density, and depth of root hairs [74]. One key component in achieving that is *DRO1*, a combined quantitative trait locus (QTL) linked to root depth, which is upregulated in response to drought stress, promotes deeper growth of roots, and enhances tolerance against drought [75]. It also regulates the elongation of cells of the root tip, asymmetric growth, and bending of the root tip. When transformed with *DRO1*, rice cultivars with shallow roots become drought tolerant by establishing a deeper root system [75]. Drought resistance also depends on genes related to osmotic adjustment, equilibrium of stomatal activity, water-use effectiveness, phytohormones, and root and shoot biomass. Various genes, like *OsPYL/RCAR5* and *EcNAC67*, cause delayed leaf rolling and increased root and shoot mass under drought stress [72,76]. Drought resistance in rice is improved by *EcNAC67* overexpression. When exposed to water stress, in comparison to non-transgenic *ASD16*, transgenic plants displayed delayed leaf rolling signs. Additionally, they revived quickly after re-watering, retained a 20% higher relative water content in the leaves, and experienced a less pronounced decline in plant height and yield [76]. Research studies revealed that the *DSM1* gene, a Raf-like MAPKKK, might modulate ROS scavenging to mediate drought responses in rice [77]. Table 1 presents a summary of key genes associated with drought resistance in rice.

Table 1. Identified genes linked to drought stress tolerance in rice.

Name of Genes	Function	Reference
DRO1	Stimulates the growth of roots, resulting in increased length and deeper penetration into the soil	[75]
EcNAC67	Enhances water content, postpones leaf curling, and increases the mass of roots and shoots	[78]
DsM1	Assists in removing reactive oxygen species and enhances drought resistance during the early growth (seedling) phase	[77]
OsPYL/RCAR5	Causes the closure of stomata and controls the weight of leaves	[33]
OsDREB2B	Length of roots and the amount of root growth	[73]
OsNAC5	Increases the size of the roots and improves the amount of grain produced	[79]
SNAC1	Enhances spikelet fertility	[80]
OsLEA3-1	Enhances grain yield	[81]
OsbZIP23	Increase grain yield	[82]
OsbZIP72	Enhancing tolerance to drought and increasing sensitivity to ABA (upregulating ABA)	[83]
AP37	Improves the process of seed filling and increases the weight of the grain	[84]
OsNAC10	Enhances resistance to drought during the vegetative phase, enhances root size, and enhances crop productivity	[79,85]
EDT1/HDG11	Increases water use efficiency, the buildup of compatible osmolytes, heightened antioxidant enzymatic activity, and improves photosynthesis	[86]
AtDREB1A	Osmolytes accumulation, maintenance of chlorophyll, increment in relative water content, and reduction in ion leakage	[87]
OsCPK9	Enhances drought tolerance in transgenics through improved stomatal closure and osmoregulation	[88]
ADC	Enhances resistance to drought by synthesis of polyamines such as putrescine and spermine	[61]
OsOAT	Enhances resistance to drought and promotes higher seed production	[89]
OsTPS1	Enhances rice seedling's tolerance to drought, cold, and salinity stress	[90]
P5CS	Enhances biomass production under salinity and drought stresses	[91]
HVA1	Plasma membrane stability, increases leaf relative water content (RWC) and growth under drought stress	[92]
Hrf1	Drought resistance via antioxidants generation, ABA signaling, and regulating stomata closure	[93]
JERF1	Enhances drought resistance	[94]
OsRDCP1	Improves drought stress tolerance	[95]
OsSDIR1	Regulates stomata under drought stress	[96]
OsSRO1c	Regulates stomatal closure and enhances oxidative stress tolerance	[97]

It has been noted that seed priming is an effective strategy to reinforce the antioxidative defense system and enhance plant stress responses. One study observed a notable increase in antioxidant activity, total phenolic content, and expression of *RD1* and *RD2*, rice drought-responsive genes belonging to the AP2/ERF family in two different rice genotypes, Nagina-22 (known for its drought tolerance), and Pusa Sugandh-5 (known for its drought sensitivity). This upregulation was observed when the seeds of these genotypes were primed with different plant hormonal or chemical elicitors, such as methyl jasmonate, SA, and paclobutrazol, under drought stress [98]. Rice that has been colonized by *Trichoderma harzianum* isolates is drought tolerant, grows faster, and experiences a delay in the effects of drought [99]. Colonization boosts rice's ability to acquire and store water and root growth. In colonized plants, there is a lesser increase in the concentration of stress-induced metabolites.

2.2. Heat Stress

Global food security is now seriously threatened by heat stress brought on by a fast-changing climate. When the temperature rises above a specific point and continues for a while, it is said to be under heat stress, which can permanently harm plant growth and development [100]. Without effective adaptability, CO_2 fertilization, and genetic development, it is predicted that every one-degree rise in the global mean temperature will result in lower worldwide yields of wheat, rice, maize, and soybeans [101]. Rice can grow normally at temperatures between 27 and 32 °C. Above 32 °C, all phases of growth and development of plants are negatively affected. The flowering stage, however, required a temperature of 33 °C. Heat damage occurs when rice is exposed to air temperatures above 35 °C [102].

2.2.1. Morphophysiological and Biochemical Responses to Heat Stress

Rice has three types of heat stress resistance: defense, avoidance, and tolerance. Heat defense is the mechanism of controlling morphological development and transpiration of leaves to lower the temperature of the panicles and avoid deterioration from scorching temperatures [103]. Heat avoidance includes adjusting spikelet flowering time by shortening the flowering period and early blooming, which is a desirable characteristic for developing heat-resistant rice cultivars [104]. Heat tolerance is the ability to continue generally living in hot temperatures. In response to heat stress, rice adjusts its physiochemical processes, which comprises growth retardation, leaf rolling, the senescence of leaves, and changes to fundamental physiological functions such as photosynthesis, respiration, the permeability of membranes, and ROS, that minimize the pollen sterility [105].

In addition to the hormone synthesis that influences the growth and development of shoots, the roots play essential roles in water intake and nutrients [106]. Although root systems are crucial in helping plants adapt to high temperatures, their thermotolerance mechanism has been less explored. Most of the research has focused on studying the aerial parts of plants [107,108]. Root growth is more susceptible to high temperatures than shoot growth, due to its lower optimal temperature [109]. Typically, when soil temperatures are elevated, a decrease in root growth and physiological activity occurs before the cessation of shoot growth [110]. A study showed that the rice plant roots failed to elongate and divide at a temperature of 43 °C [111]. Heat stress can affect rice plants during most of their vegetative growth stages. When temperatures are consistently high, the potential for seed germination decreases, resulting in a lower germination rate and weaker seedling growth [112]. When exposed to heat stress (42–45 °C), the seedlings experience increased water loss, wilting and yellowing of leaves, hindered growth of roots and seedlings, and in severe cases, death of the seedlings [102,113]. Similarly, rice seeds failed to germinate upon continuous exposure to a constant temperature of 43 °C [114]. In addition, another study found that rice plants died in the initial vegetative phase when exposed to a constant air temperature of 40 °C and high levels of CO_2 (700 ppm) [115]. Furthermore, when

a sequence of distinct heat stress treatments was applied to rice seeds, young seeds, in particular, were the most vulnerable in the initial two days following flowering [116].

Rice plants are more vulnerable to heat stress during the reproductive stage than the vegetative stage, including initiation of panicle, development of male and female gametophytes, anthesis, pollination, and fertilization [117,118]. Under heat stress (40 °C day/35 °C night) for 15 days, rice output per plant was 86% lower overall, and the panicle number was roughly 35% lower [119]. In *japonica* rice, compared to *indica* rice, heat stress significantly impacts the number of tillers and panicles [120]. When the rice plant enters the flowering stage, it becomes highly vulnerable to elevated temperatures. The second-most vulnerable stage appears around nine days before blossoming. Significant rises in temperatures during anthesis cause a high proportion of spikelets to be sterile. During the grain-filling stage, heat stress has been observed to impact the quality of rice negatively. This is evident through a decrease in palatability, an unfavorable grain appearance, and an increase in grain chalkiness [121–124]. The presence of chalky kernels is considered the most prominent indication of heat stress during this particular phase of rice development. During the panicle-initiation stage, heat-stressed plants experience a decrease in non-structural carbohydrates, underdeveloped vascular bundles, and smaller glumes, ultimately reducing grain weight [125]. The total grains and rice production percentage declines as nighttime temperatures rise. White immature kernels are formed when rice plants endure exposure to high temperatures at the ripening stage, disrupting the carbohydrate sink–source balance. The increased rhizosphere temperature causes the total dry weight of super rice to decrease by 16.26% [126].

A reduction in the stomatal aperture size, the xylem in the leaves, and an increase in the trichome density on both surfaces are additional examples of common adaptive responses to heat stress [127]. Photosynthesis is a crucial biochemical function in plants that is most susceptible to heat. The main sites of injury at high temperatures in chloroplast are light-dependent reactions in the thylakoid membrane and carbon fixation reactions in the stroma [128]. High temperature has a strong affinity for the thylakoid membrane. Significant changes in chloroplasts include changed thylakoid structural arrangement, loss of grana stacking, and grana swelling during heat stress. Heat shock decreases the number of photosynthetic pigments. At extreme temperatures, the enzymatic activities of invertase, ADP-glucose pyrophosphorylase, and sucrose phosphate synthase are diminished, leading to a substantial decrease or complete cessation of the function of PSII [129,130].

Heat stress-induced imbalance in metabolic activities, including photosynthesis and respiration, results in a rise in ROS or a fall in the cell's efficiency to scavenge oxygen radicals. When exposed to high temperatures, rice anthers produce much more ROS, decreasing floret fertility and pollen viability [131]. MDA, a reliable indication of free radical damage to cell membranes, is produced when membrane lipids under heat stress undergo peroxidation. Increased lipid peroxidation demonstrated that oxidative stress frequently developed in rice leaves following exposure to high temperatures [132]. Various enzymes and metabolites take part in the antioxidant defense framework. The antioxidant enzymes, such as SOD, APX, CAT, GR, glutathione peroxidase (GPX), and peroxiredoxins, assist in shielding the cells from an accumulation of ROS. Furthermore, Phenolic chemicals can remove ROS, neutralize singlet and triplet oxygen, or break down peroxides. Moreover, the GSH molecule has a crucial function in protecting the photosynthetic system [133].

2.2.2. Molecular Response to Heat Stress

Heat stress signals are sensed through numerous heat shock transcription factors (HSTFs) and proteins. Various genes related to Ca^{2+} homeostasis, ROS, lipid metabolism, and phytohormones are activated to trigger the response against heat stress [134]. In rice, a large number of high-temperature-related genes, including stress-related transcription factors (TFs), HSTFs, and heat shock proteins (HSPs), have been cloned. These genes are involved in heat stress-related temperature sensing and response [135] (Table 2). *OsHSP26.7*, for instance, encodes an HSP that shields chloroplasts from oxidative damage brought on

by extreme heat and ultraviolet radiation [136]. Similarly, under the *HSP101* promoter, *OsWRKY11* encodes a TF with a WRKY domain that can dramatically increase rice's tolerance towards heat and drought [137]. Furthermore, a NAC TF called *SNAC3* mediates ROS metabolism, and OsMYB55 TF in rice significantly improves tolerance to high-temperature and increases grain yield [138,139]. The *HYR* gene is a crucial regulator that can directly activate photosynthesis and can control downstream genes involved in carbon metabolism as well as morphology and physiology during drought and heat stress, maintaining the yield of rice [140]. The cytoskeleton plays a vital role in the ability of organisms to tolerate and adapt to stressful conditions. In the case of rice, a specific intermediate filament called *OsIF* has been identified as being particularly important in mitigating the implications of heat and salinity stress on the photosynthetic apparatus and overall crop yield [119]. Additionally, several enzymes, including glutamate decarboxylase and glutamine synthase, are some of the additional key factors that produce stress-related amino acids that aid rice in tolerating extreme heat [139,141]. A mitochondrial lipase known as EG1 can activate the expression of floral organ genes during high temperatures, thereby preserving the consistency of floral organ growth [142]. Table 2 presents a summary of key genes associated with heat stress tolerance in rice.

Table 2. Identified genes linked to heat stress tolerance in rice.

Name of Genes	Function	Reference
OsMYB55	Enhances amino acids' metabolic process, enhancing the ability to withstand high temperatures	[139]
OsAREB1	Controls abiotic stress-responsive gene expression utilizing an ABA-dependent mechanism	[143]
OsHSF7	Increases the expression of HSPs and other genes that protect against exposure to high temperatures, resulting in enhanced resistance to heat	[144]
HSP101	The effects of heat training in rice seedlings are prolonged by post-transcriptional interactions of *HSA32/HSP101* after heat treatment	[145]
GAD3	Participate in the ability to withstand high temperatures	[139]
OsHTAS	Improves rice's ability to withstand heat by mediating stomata closure caused by H_2O_2	[146]
TCM5	Plays a vital role in the development of chloroplasts and the maintenance of PSII function in high temperatures	[147]
EG1	Enhances homeostasis in floral organs and the ability to withstand temperature changes by activating a pathway involving mitochondrial lipase in response to high temperatures	[147]
OsTT1	Breaks down poisonous denatured proteins while preserving the high-temperature response process	[127]
TOGR1	Plays a role in the normal processing of rRNA precursors at high temperatures and acts as a chaperone for the nucleolar SSU complex, crucial for cell growth in high-temperature environments	[148]
OsHES1	Plays a crucial part in adjusting to heat stress and ensuring the proper functioning of chloroplasts.	[149]
OsAET1	Plays a dual function in regulating the response to high temperatures through tRNA modification and control of translation	[150]

Table 2. *Cont.*

Name of Genes	Function	Reference
OsNTL3	Plays a crucial role in thermotolerance by interacting with *OsbZIP74*	[151]
OsHsfA2c	Involved in regulating the transcription of the HSP100 gene in the cytoplasm of rice	[152]
OsHCI1	Facilitates the nuclear export of target proteins, and its heterologous expression enhanced thermotolerance	[141]
OsNSUN2	Controls the mRNA modification of 5-methylcytosine (m5C), which improves mRNA translation efficiency and sustains normal development at higher temperatures	[153]
OsTT3.1	TT3.2 is ubiquitinated by TT3.1 for vacuolar degradation, and TT3.1 may function as a thermosensor	[154]
OsTT3.2	Chloroplasts rely on mature TT3.2 proteins to protect thylakoids against the detrimental effects of heat stress	[154]
OsANN1	Enhances SOD and CAT activity, controls H_2O_2 content and redox homeostasis, to provide cell protection against abiotic stress	[155]

As a key defense against heat stress, plants accumulate soluble carbohydrates like glucose and fructose as well as non-soluble sugars like starch [156]. Under acute heat stress, the expression of OsSUT1, a sucrose transporter, is elevated, which results in increased sugar buildup and reduced photosynthesis [157]. Tolerance to high temperatures in plants is greatly influenced by the accumulation of certain metabolites. Under intense heat, the MYB55 TF in rice controls the expression of downstream glutamate dehydrogenases GAD3 and glutamine synthase OsGS1.2, thus promoting the buildup of stress-related amino acids like gamma-aminobutyric acid (GABA) and L-glutamic acid [139]. The analysis of the temporal transcriptome of germinating seeds subjected to heat stress at 35 °C reveals that the early response to heat stress is mediated by the Inositol-requiring enzyme 1 (IRE1)-mediated endoplasmic reticulum (ER) stress response and the jasmonic acid (JA) pathways. As JA promotes the spliced form of *OsbZIP50*, a gene marker linked to the IRE1-specific pathway, it is hypothesized that the rise in JA concentration levels during heat stress may happen before the ER stress response [116]. Numerous genes associated with high-temperature responses have been documented, leading to a better understanding of the signaling pathways in which they participate. Nevertheless, the precise molecular processes and regulatory systems underlying sensing of high-temperature signaling and transmission to downstream components remain inadequately recognized, thus necessitating further investigation as the critical area of prospective studies.

Ethylene, a crucial plant hormone, significantly regulates biotic or abiotic stress signaling. In the case of heat stress in rice seedlings, ethylene-mediated signaling has been found to mitigate oxidative damage, preserve chlorophyll levels, and enhance thermotolerance [158]. Specifically, under heat stress conditions, ethylene-mediated signaling controls the mRNA transcripts of certain heat stress transcription factors (HSFs) and genes related to ethylene signaling [125]. Phytohormones are also crucial in controlling how rice yield qualities react to heat stress. Specifically, cytokinin and abscisic acid (ABA) regulate the number of spikelets per panicle under high-temperature conditions. Additionally, gibberellin and indole-3-acetic acid may be associated with spikelet fertility, while indole-3-acetic acid, ABA, gibberellin, and cytokinin regulate grain weight [100].

When exposed to heat stress, foliar sprays of boric acid (25, 50, or 100 mg L^{-1}) or sodium borate (50 mg L^{-1}) substantially boosted net photosynthetic rates in comparison to untreated plants [159]. The use of foliar borate compounds on seedlings experiencing

heat stress led to a decrease in oxidative damage, as indicated by the reduction in the levels of leaf MDA and proline synthesis and an enhancement in the photochemical efficiency of PSII.

2.3. Cold or Low-Temperature Stress

Rice is sensitive to cold, especially during the germination process, which causes significant economic losses. The dynamics of the crop's growth are negatively impacted by cold stress in temperate and high-altitude rice-growing regions in the tropics and subtropics [160]. Cold stress has detrimental consequences on rice, such as decreased seedling growth, poor germination, constrained leaf expansion, chlorosis, and wilting. Necrosis, or tissue death, is the final impact of these factors [161].

2.3.1. Morphophysiological and Biochemical Responses to Cold or Low-Temperature Stress

In circumstances of cold stress, the growth of rice shoots and roots is hindered in terms of length, fresh and dry weight, and protein content [162]. A research study found that when exposed to cold stress, the root growth and developmental characteristics of various genotypes of rice decreased, ranging from 2% to 87% [163]. Furthermore, when rice is subjected to cold stress during the vegetative stage, the leaves begin to yellow, the plant grows shorter, and the number of tillers decreases [164]. Rice's ability to germinate, as well as its coleoptile and radicle growth, is significantly reduced by low temperatures. Inhibition of seed germination and growth retardation or death of the seedlings cause a decline in crop yield [165]. The reproductive phase of rice, specifically in the post-meiotic stages of anthers, has a pronounced impact on pollen production due to cold stress [166]. In addition, cold temperatures during the immature microspore stage of rice anthers lead to heightened protein degradation. Other effects of cold stress comprise damage to the photosynthetic apparatus, including modifications to the number of chloroplasts, ultrastructure, light-harvesting chlorophyll antenna complexes, modified grana arrangement, and lamellar structures [164,167]. Thus, there is a shortage of plant energy resources since cold temperatures generally slow photosynthetic processes. This is due to the reduced activity of several enzymes involved in tetrapyrrole metabolism and the down-regulation of gene expression, which affects chlorophyll production [164]. The circadian clock is crucial for rice's reaction to chilling stress. Night chilling stress affects leaf chlorophyll metabolism and PSII more severely than its daytime equivalent [168]. Additionally, nitrogen intake has often been found to be restricted by chilling stress in rice [169]. Numerous studies have shown that stress caused by low water temperature reduces nitrogen absorption [170,171]. This could be attributed to the decreased activity of enzymes and transporters in the roots under such conditions.

Plants have developed advanced mechanisms to prevent damage caused by cold temperatures. One such mechanism is cold acclimation, where plants exposed to mild cold temperatures for a short period become more resistant to following freezing stress [172,173]. During cold acclimation, various physiological, biochemical, and molecular transformations take place. These include the activation of antioxidant systems, the production and buildup of cryoprotectants, and the implementation of mechanisms that safeguard and stabilize cell membranes [174]. To keep the cell membrane stable, the content of unsaturated phospholipids in the membrane increases. Additionally, cells store osmotic molecules rich in sucrose and proline, as well as antifreeze proteins, which help to retain water molecules [175]. Plants synthesize various proteins such as late embryogenesis abundant (LEA), anti-freezing proteins (AFP), and cold shock proteins (CSP) to increase their tolerance to cold stress [176,177]. Lower molecular-weight solutes, soluble sugars, and proline act as osmoprotectants to shield plants from cold-induced damage. Similarly, the accumulation of protective proteins like LEA, AFPs, and CSPs during cold acclimation is crucial for enhancing cold tolerance in plants [178]. The acclimation mechanism is crucial for improving the ability of plants to withstand cold temperatures. Even plants that are

sensitive to cold, like rice, can adapt to chilling conditions [179,180]. Freezing-resistant plants also adapt through cold acclimation, where they are exposed to temperatures slightly above freezing. Under these conditions, aquaporins play a key role in regulating the water uptake mechanism and the permeability of cell membranes [181–184]. Various studies have shown that aquaporins are functionally important in controlling the hydraulic conductivity of roots (Lpr) [180,185,186]. It has also been demonstrated that the decrease in water uptake in rice under cold stress is associated with a decrease in aquaporin expression [187].

Furthermore, the presence of low temperatures can result in the buildup of ROS and H_2O_2. This accumulation can subsequently lead to leakage of electrolytes, lipid peroxidation, and damage to the cell membrane [188]. This can be observed through the rise in levels of MDA. The breakdown of polyunsaturated lipids to MDA is one possible way ROS can damage cells and tissues [188,189]. Plants contain a variety of antioxidant systems to prevent catastrophic breakdown of protein and lipid components when under stress. Antioxidants like CAT, POD, 2,2-diphenyl-1-picrylhydrazyl, and SOD can compete against ROS generation in rice under cold stress due to their high stability and pace of rising [164]. A study on rice cultivars under cold stress found that cultivars with a faster growth rate had greater H_2O_2 levels in the shoots but lower levels in the roots. However, this was reversed in the case of rice cultivars with a low growth rate. Moreover, the roots had higher MDA concentrations and electrolyte leakage due to cell damage than the shoots under cold stress. Cold stress boosts SOD and CAT activities in the rice roots [162]. These biochemical characteristics can be used as a selection marker for breeding and adjusting rice crops with enhanced cold tolerance.

Glutamic acid (Glu) is essential in the amino acid metabolism of plants and is involved in vital metabolic processes during abiotic stress [190]. These functions include the production of proline and gamma-aminobutyric acid (GABA), which are essential for plants' defense systems [191]. Under cold stress, GABA, proline, and soluble carbohydrates like glucose and sucrose buildup in rice and work as osmoprotectants to prevent damage from dehydration and freezing [192,193]. The findings suggest that GABA and proline could improve plants' ability to withstand cold temperatures.

2.3.2. Molecular Response to Cold or Low-Temperature Stress

Rice plants must maintain the stability of their cell membranes, their levels of chlorophyll and fluorescence, the initiation of ROS defense mechanisms, and the accumulation of osmolytes to withstand cold stress [194]. During cold stress, COLD1 and CIPK sense cold-related stress signals, and several genes relating to osmoprotectants and phytohormones are modulated. To facilitate cold sensing and extracellular Ca^{2+} influx at low temperatures, COLD1 has been demonstrated to interact with the rice G protein α subunit 1 (RGA1) [195]. Rice CBL-interacting protein kinase 7 (OsCIPK7), in addition to *COLD1*, is believed to recognize cold stress cues by controlling the configuration of its kinase domain and the influx of Ca^{2+} [196].

At low temperatures, endogenous ABA levels rise, and expression of ABA-responsive genes is activated, strengthening plant tolerance to cold stress. Overexpression of the *OsPYL9* (an ABA receptor), which positively modulates ABA signaling, can dramatically increase rice's ability to withstand low temperatures [197]. In addition to the fundamental component PYL-PP2C-SnRK2-ABF, the ABA signaling pathway also involves nitric oxide (NO), ROS, Ca^{2+}, phospholipid molecules, and other kinases, like MAPK [198]. The mitogen-activated protein kinase OsMAPK3 elevates trehalose content and strengthens rice adaptation against cold stress [199]. Table 3 presents a summary of key genes associated with cold stress tolerance. Although there has been a significant advancement in cold stress tolerance, little is known about single-cell responses in rice plants.

Table 3. Identified genes linked to cold stress tolerance in rice.

Name of Genes	Function	Reference
OsLTPL159	Reduces the toxic effects of ROS, increases cell wall's cellulose deposition, and increases osmolyte accumulation in rice, which increases the plant's ability to withstand cold temperatures in its early seedling stages	[200]
qPSST6	Long-chain fatty acid production, involved in rice's cold-tolerance during the booting stage	[201]
OsCOIN	Protein induced by cold enhances cold, drought, and salt tolerance	[202]
Osa-MIR319a	Increased leaf blade width	[203]
OsGH3-2	Regulates ABA and auxin levels during cold and drought stress	[204]
OsMYB3R-2	Regulates cell cycle (especially G2/M phase) to mediate cold tolerance in rice	[205]
SNAC2	Enhances cold and salt tolerance in rice	[206]
OsDREB1F	Enhances cold tolerance in rice	[207]
ASR3	Enhances cold/draught tolerance mediated by hormonal/sugar signaling	[208]
OsFAD2	An essential enzyme that raises grain yield and germination rate under LTS (low-temperature stress conditions)	[209]
OsLti6b	Produces hydrophobic protein in the ovaries and stamens of flowers undergoing cold treatment	[210]
OsWRKY45	Has a significant role in the signaling of ABA and serves as a means of communication between abiotic and biotic stresses	[211]
OsRAN2	GTPase that enhances cold tolerance through cell cycle regulation	[212]
OsSPX1	Participates in phosphate signaling as well as the interplay between the oxidative and cold stress tolerance mechanisms.	[213]
OsDEG10	Produces RNA-binding protein and has a key role in cold tolerance as well as response to other stresses (anoxia, photooxidative, and salinity)	[214]
Oscrr6	It has a key role in rice growth/photosynthesis at colder temperatures	[215]
OsPIP2	Participates in water homeostasis during cold stress tolerance	[216]
OsPRP3	Involved in the enhancement of cold tolerance in rice	[217]
OsAsr1	Involved in both vegetative and reproductive stages of cold tolerance	[218]
MYBS3	Modulates cold tolerance signaling pathways	[219]
OVP1	Involved in lowering malondialdehyde levels and increasing proline accumulation to increase tolerance to cold	[220]

Abiotic stressors can be effectively reduced using nanoparticles. Zinc oxide nanoparticles (ZnO NPs) applied topically considerably reduce the chilling stress experienced by rice seedlings, resulting in increased plant height and root length and enhanced dry biomass.

With the decreased concentration of H_2O_2 and MDA, in addition to higher activities of the key antioxidative enzymes like SOD, CAT, and POD, ZnO NPs further restore chlorophyll accumulation and markedly mitigate chilling-induced oxidative stress [221]. Plant melatonin, an organic molecule, has also been demonstrated to be crucial for plant stress adaptation. Melatonin pretreatments boost the non-enzymatic antioxidant content and upregulate the antioxidant enzyme activity in rice. The application of exogenous melatonin reduces rice seedling development inhibition, formation of ROS, MDA, inhibitions of photosynthesis and PSII activities, and cell death brought on by cold stress in rice [222]. Similarly, Teixeira et al. found that rice seed priming with carrot extract greatly speeds up germination and raises the final germination percentage while reducing the damage caused by cold [223].

2.4. Submergence Stress

Submergence is a major concern for rice cultivation in lowlands subjected to rainfall and flood-prone regions globally. It is expected to become more common as climate change increases flood threats, particularly in regions impacted by monsoon rains in Asia [224]. Rice plants possess a partially aquatic characteristic, enabling them to thrive in waterlogged or submerged environments for extended periods [225]. Nevertheless, prolonged submersion exposes rice plants to various stresses, such as reduced access to light, decreased gaseous exchange, physical damage, and increased vulnerability to pests. In addition, submergence typically lowers the photosynthesis process, depleting carbohydrate stores and eventually causing the death of the plant [226]. Rice usually comes to be affected by two different types of flooding. The initial type is flash flooding, which arises when the crop is flooded for 1–2 weeks due to a sudden rise in water levels. Another kind of flooding is stagnant flooding, in which the water level rises above 100 cm and stays there for several weeks [227].

2.4.1. Morphophysiological and Biochemical Responses to Submergence Stress

Rice is extremely sensitive to submersion during the germination and early seedling growth stages. When rice seeds are entirely submerged in water, they suffer from hypoxia or anoxia, resulting in poor germination and seedling mortality [228]. The rice plant undergoes numerous morphological and physiological changes as a result of submergence. Rice withstands submersion by growing longer leaf sheaths and blades during the seedling stage and internodes during the vegetative growth stage [229]. Even submergence-tolerant types attempt to expose their leaf tips above the water's surface if the flooding lasts longer than two to three weeks to ensure their survival [230,231]. When fully submerged, the leaves and stems of the rice plant grow moderately longer to reach the water's surface. However, there are negative effects from this elongation process that are necessary for post-submergence plant growth [232]. Turbid water reduces the amount of light that may pass through floodwater, which lowers photosynthesis and, as a result, the submerged plant uses its reserve carbohydrate to sustain its metabolism [233]. However, if the depth of flooding is significant and the duration of flooding is prolonged, the plant's limited ability to perform photosynthesis causes its energy reserves to deplete rapidly, ultimately leading to the plant's death [234]. The amount of carbohydrates found in plant sections determines a variety's capacity to withstand submersion [235]. Submergence-tolerant rice cultivators benefit from limited shoot elongation because they preserve carbohydrate reserves, which aid in resuming development after de-submergence. For recovery from submergence shock, carbohydrate availability following flooding is crucial [236]. During periods of flooding, plants are entirely or partially immersed in water. However, when the floodwater recedes, the plants are suddenly exposed to oxygen again. This reoxygenation process can harm plants after being submerged. MDA, O_{2-}, and H_2O_2 were found to increase in rice plants' leaves after being submerged for seven days as a sign of oxidative damage [237]. Rice leaves began to dry out when exposed to air oxygen again after being submerged for 7 to 10 days [238]. Due to conserving glucose metabolism during submersion, tolerant rice

cultivars on de-submergence exhibit an ascent in fresh biomass. On the other hand, the non-tolerant cultivars' reserves undergo hydrolysis and are incapable of regeneration. These findings suggest that resistance to several stresses, including submersion, re-oxygenation, and dehydration, is necessary for a plant to survive a flood [239]. Due to frequent oxygen deprivation and low light intensity, submerged plants develop ROS, which, if unchecked, can adversely harm the cellular structure and end in plant death. [240]. The antioxidant defense mechanism is crucial to detoxify ROS and lessen their harmful effects. SOD, APX, and GPX are the substances that are crucial in ROS detoxification [241].

To thrive in submerged environments, rice cultivars employ two growth control techniques: quiescence and escape strategies, both of which rely on ethylene-responsive transcription factors (ERFs). In the quiescence strategy, shoot prolongation is postponed for quite some time (10–14 days) during flash flooding to save carbohydrates [242]. Utilizing conserved carbohydrates, cultivars that can withstand submersion can resume their growth after de-submergence. The escape strategy is adopted by deepwater rice genotypes and involves rapid internode extension to climb above the water level [243]. To implement these strategies, rice has evolved specific anatomical and morphological characteristics. These include the development of adventitious roots, aerenchyma formation, radial oxygen loss (ROL) barrier, and the ability to create a thin film of gas on its leaves. Furthermore, rice plants generate ventilated tissues and ethylene to aid in gas exchange and regulate the programmed death of specific cells in the cortex and epidermis [244,245]. In addition, the growth of adventitious roots regulates the death of epidermal cells utilizing the mechanical energy they produce [246]. When submerged, rice plants rapidly accumulate gibberellic acid (GA), which leads to the elongation of internodes [247]. To protect their roots from oxygen loss, rice plants form an ROL barrier. This barrier extends from the base to the tip of the roots and is located outside the aerenchyma [248]. Various Asian rice cultivars have developed additional characteristics to adapt to prolonged submergence. These traits include aerobic germination and dormancy of leaf elongation during flash floods, and internode elongation during periodic flooding. Certain rice cultivars can withstand being submerged for around 15 days by limiting elongation growth, carbohydrate consumption, and chlorophyll degradation [249,250].

One of the significant regulators of rice's submergence reactions is ethylene. Owing to physical confinement and active production during stress, this gaseous phytohormone quickly builds up in tissues of submerged plants, inducing various acclimation reactions, such as shoot elongation, development of adventitious root, and glucose metabolism. Deep-water rice encourages internode growth during submersion to project the photosynthetic parts of the plant above the air–water contact [242]. High production rates of ethylene and sensitivity to the hormone mediate this flight response. Lowland rice that can withstand submersion, in contrast, limits the number of carbohydrates it consumes, which encourages underwater elongation and is used for cell division and elongation. Limited ethylene production and sensitivity are the causes of this tolerance [251]. Aerenchyma, which allows for relatively unimpeded movement of O_2 from well-aerated shoots to buried roots, is another way lowland rice adapts to soil waterlogging [252]. Inducing a barrier to radial O_2 loss (ROL) that reduces O_2 loss to the surroundings can further boost longitudinal O_2 diffusion along the root apex. Under flooded conditions, these characteristics are used by both lowland and upland different rice species [253].

Unlike flood-sensitive rice types, flood-tolerant rice cultivars utilize energy stores more effectively and maintain higher non-structural carbohydrate (NSC) concentrations in stems and leaves. Additionally, they use anaerobic respiration as a different energy-producing method. Submergence-tolerant rice cultivars decrease shoot prolongation to preserve energy for survival and recuperation following de-submergence. Complete submersion-tolerant rice genotypes maintain their chlorophyll and embrace a strategy of modest growth, shown by reduced elongation when submerged. Because of this, plants can save enough glucose reserves to maintain metabolism while submerged and after the floodwaters have receded [250].

2.4.2. Molecular Response to Submergence Stress

Rice plants implement passive approaches for adapting and avoiding recurring floods. *SUB1A* is a crucial modulator of submergence tolerance, which activates transcriptional modulation of other ERF response factors and *SLR1* [250]. In deepwater rice, the ERF OsEIL1 is stabilized by ethylene accumulation. OsEIL1 binds to the SD1 promoter to boost gene expression. SD1 participates in GA synthesis and affects internode elongation [254]. The GA then increases the expression of the Accelerator of Internode Elongation 1 (ACE1), while DEC1, a protein that prevents internode elongation, sees a decrease in expression [255]. In addition, OsEIL1 also activates the expression of other downstream genes as a result of submergence stress by binding to the promoter sites of *SNORKEL1* (SK1) and *SNORKEL2* (SK2) [247,256]. Table 4 presents a summary of key genes associated with submergence stress tolerance in rice.

Table 4. Identified genes linked to submergence stress tolerance in rice.

Name of Genes	Function	Reference
OsACS1	Involved in ethylene production and the rapid elongation of the stem in submerged rice	[257,258]
OsACS5	Involved in ethylene production and the rapid elongation of the stem in submerged rice	[257,258]
SNORKEL1 (SK1)	ERFs that modulate the internode elongation of deepwater rice during submergence	[247]
SNORKEL2 (SK2)	ERFs that regulate the internode elongation of deepwater rice during submergence	[247]
Submergence 1A (SUB1A)	Plant quiescence and plant survival under complete submergence	[249]
SDI	Involved in internode elongation	[254]
OsHSD1	Involved in underwater photosynthesis in submerged rice	[259]
OsTPP7	Involved in anaerobic germination	[260]
AGPPase	Promotes increased non-structural carbohydrate (NSC) buildup, which is accessible for a quick recovery after submersion	[261]
EREBP1	enhances resistance to submersion and facilitates better recovery from extended submersion	[262]
CIPK15	Involved in the regulation of sugar and energy production enabling growth of rice under floodwater	[263]

A study found that SK1 and SK2 respond during flood stress by encoding response factors associated with ethylene signaling [264]. During submergence, ethylene levels in rice rise, and the expression of SK1 and SK2 elevate, ultimately promoting internode elongation via GA [265–268]. Functional assessment of ERF-type TFs indicated that they play a role in regulating several physiological and morphological responses to submersion. SUBMERGENCE-1 (*Sub1*) and SK are TF genes that belong to the ERF class [247,249]. Three clusters of related genes, *SUB1A*, *SUB1B*, and *SUB1C*, expressing ERF-like TFs, are found in the Sub1 region of submergence-tolerant cultivars, with *SUB1A* being the most investigated. Systematic genetic analyses showed that *SUB1A* introgression with *SUB1B* and *SUB1C* imparts a strong endurance against submergence and does not alter rice grain quality or production [234,249,250,269]. Additionally, *SUB1A* prevents the development of proteins that loosen and expand cell walls in response to flooding stress, preserving high levels of chlorophyll a and b [270]. Furthermore, *SUB1A* also promotes resistance to oxidative stress by controlling genes that encode ROS-detoxifying enzymes [237].

In soil, silicon (Si) is the second most prevalent element. According to Debona et al., silicon significantly increases plant resilience to various biotic and abiotic stressors [271]. Si treatment improves rice root morphological features and chloroplast ultrastructure to counteract the inhibitory effect of submergence stress by boosting Si absorption, accumulation, and plant biomass. Si also lessens oxidase damage by increasing POD and CAT activity and decreasing MDA concentration, which helps rice recover from submersion stress-related damage [272,273].

2.5. Salinity Stress

Salinization is becoming an ever-worsening problem resulting from poor agricultural practices and environmental changes. Salinity is characterized by excessive levels of various salts in the soil, including sodium chloride, magnesium sulfates, magnesium bicarbonates, calcium sulfates, and calcium bicarbonates. When it is young, the rice crop is considered a salt-sensitive cereal, and as it matures, salinity limits the yield's efficiency [274,275]. Salt stress is particularly detrimental to rice during its early vegetative and reproductive phases. Water, along with toxic ions from the soil, enter the vascular section of the root system via two pathways: apoplastic and symplastic. Through the apoplastic pathway, salt stress causes shoots to accumulate more Na^+, primarily in mature leaves. A Na^+/K^+ symporter called the high-affinity potassium transporter (HKT) controls the movement of Na^+ and K^+ within plant cell membranes [276,277]. The potassium uptake is hampered by sodium ions overloading the root's surface. Na^+ interferes negatively with K^+ uptake because it shares the same molecular characteristics as K^+. When plants come under salt stress, a considerable quantity of Na^+ enters the plant, elevating the intracellular Na^+ levels. This has detrimental impacts since Na^+ competes with K^+ to activate enzymes and synthesize proteins [278].

2.5.1. Morphophysiological and Biochemical Responses to Salinity Stress

Rice plants exhibit various morphological, physiological, or biochemical changes and symptoms when exposed to high salinity. In extreme cases, they may even perish. Direct accumulated salts interfere with metabolic functions and all key morpho-physiological and yield-related traits, comprising photosynthesis, plant height, root length, tiller number, length of panicle, spikelet count per panicle, filling of grains, and plant biomass. As a result, yield is significantly reduced [279–281]. In a salt-sensitive plant, exposure to salinity stress results in pericycle shrinkage and physical damage. Salt stress exposure at the early seedling stage raises the mortality rate of rice leaves [282]. The productiveness of the rice crop under salt stress is greatly impacted by panicle sterility [283].

Salinity generally induces two types of stress in plants: osmotic and ionic stress. Osmotic stress arises when the salt concentration around the plant's roots exceeds the threshold tolerance level. On the other hand, ionic stress develops when there is a large Na+ inflow into the plant, which raises the salt concentration in older leaves to a toxic level. This leads to higher Na^+ concentrations in the vacuole and cytoplasm, disrupting metabolic processes and causing cell death [284]. In the beginning, osmotic stress caused by soil salinity restricts plant growth, and later, ionic stress follows. A significant amount of salt in the soil contributes to the first phase, characterized by reduced plant water intake and the subsequent induction of several cellular metabolic processes [285]. Enlargement of cells, cell wall protein synthesis, net photosynthesis, photosynthetically active radiation, stomatal conductance, relative water content, transpiration rate, and pigment degradation are all inhibited during the initial phase whereas the accumulation of compatible solutes and ABA increased [286]. According to research by Cha-umi et al., salt stress caused a significant drop in carotenoid and chlorophyll in rice leaves [287]. During the latter phase, the accumulation of ions (Na^+ and Cl^-) is linked to changes in the ions ratio of Na^+/K^+ and Na^+/Ca^{2+}. The subsequent increase in ions promotes the synthesis of ROS. The extra ROS generation increases cellular oxidative stress, which upsets the equilibrium between generating and eliminating ROS [288].

Like the majority of plants, rice has developed several defense strategies against salinity stress, such as (i) antioxidant generation for ROS detoxification (ii) ion homeostasis and compartmentation, (iii) osmoprotection through osmolyte regulation, and (iv) programmed cell death [289]. Plants have devised an exquisite antioxidant defense mechanism to scavenge and detoxify ROS to shield the cells from oxidative damage. According to studies, the salt-tolerant rice cultivar Pokkali performed better under salinity stress than the Pusa Basmati (salt-sensitive rice cultivar) in terms of ROS scavenging enzymes like CAT and content of antioxidants like AsA and GSH [290]. In rice plants, the basal area of the leaf can scavenge H_2O_2 by boosting the activity of CAT and maintaining higher constitutive levels of APX and GPX than those in the apical region under salinity. Under salt, the GR in the basal area might inhibit O_2 generation. The apical area can, however, scavenge O_2 by boosting SOD activity, whereas, under salinity, the activity of H_2O_2 scavenging enzymes, including APX and CAT reduced [291]. To prevent the rice from oxidative stress brought on by salt, both enzymatic and non-enzymatic ROS scavenging machinery must work together. A transcriptional cascade in rice roots, which is regulated by the transcription factor SERF1, is responsible for salt tolerance and is dependent on ROS [292].

To maintain ion homeostasis during salinity stress, plants employ different mechanisms. One of the mechanisms for tolerating salinity stress involves the transport of Na^+ and Cl^- in the roots to prevent their excessive accumulation in the leaves. This process includes removing Na^+ from the xylem and releasing ions back into the soil. If Na^+ exclusion fails, it can have toxic effects on older leaves, leading to their premature death [293]. The concentration of Na^+ in the rice leaves is linked with the salinity stress tolerance level in both *japonica* and *indica* rice varieties [294]. Maintaining a low cytosolic Na^+/K^+ ratio is important for maintaining ionic homeostasis and improving photosynthesis and overall plant growth [295,296]. During salinity stress, the accumulation of Na^+ in the leaves and shoots of salt-tolerant varieties of rice is lower compared to salt-sensitive varieties [297,298]. It was also reported that the salt-tolerant cultivar Pokkali can reduce Na+ uptake into the cytosol and maintain lower cytosolic Na^+ content by temporarily taking up Na^+ into the cytoplasm and quickly extruding it into vacuoles. However, the salt-sensitive rice variety BRRI Dhan29 was unable to perform this function [299].

Due to osmotic stress, most organisms, including bacteria and plants, accumulate specific organic solutes, especially proline and sugars which are referred to as osmoprotectants [300,301]. Trehalose, a non-reducing sugar, stands out for having a unique property that protects biological molecules from dehydration stress. According to Garg et al., the production and accumulation of trehalose in transgenic rice can give the grain some resistance to the negative impacts of salinity and drought [302]. Glycine betaine, a potent solute containing quaternary ammonium, is found in several organisms. Though rice plants generally do not store glycine betaine, it has been shown that they may absorb exogenously and store it in their leaves to aid in sustaining PSII quantum yield when subjected to salt stress [289,303]. If the plant's several defense strategies against salinity stress fail, it will implement programmed cell death (PCD) as a last-ditch effort to survive [304]. According to Liu et al.'s [305] findings, rice roots under salt stress had a well-regulated progression of cell death. This raised the possibility that the dead cells prevented salt exclusion by blocking the inflow of extra Na^+ ions into the interior of roots and shoots. Another possibility is that the plant sheds cells to avoid unregulated cell death and the release of toxins to safeguard and maintain the growth of other cells [306].

2.5.2. Molecular Response to Salinity Stress

Various proteins are involved in activating the tolerance mechanism against salt stress. They play different roles in the accumulation of MDA, antioxidants and osmoprotectants, ROS and Na^+ homeostasis, and electrolyte leakage [289]. Certain WRKY TFs restrict the expression of *DREB1B* and *OsNAC1*, contributing to salt susceptibility [307].

TFs influence salt tolerance positively or negatively. *OsCOIN*, *OsbZIP71*, *OsbZIP23*, *OsDREB2A*, and *OsMYB2* are some of the salt-responsive TFs that may cause a variety of

alterations in rice, such as a buildup of osmoprotectants and antioxidants and an upsurge in the activity of the Na^+ and K^+ transporters [308]. In rice, overexpression of these salt-responsive TFs promotes a higher survival rate of seedlings, reduces oxidative damage, and improves osmotic regulation [309,310]. On the contrary, *OsWRKY13*, one of the negative regulatory TFs, prevents the expression of the salt-responsive genes *SNAC1* and *ERD1*, thereby delaying the rice plants' growth and development [311]. The expression of genes including *SNAC1*, *NCED4*, *Rab16D*, and *DREB1B* was suppressed by the transcriptional repressor *OsWRKY45-2*, and as a consequence, overexpression of *OsWRKY45-2* drastically lowered the survivability of rice cultivars under salt stress [312]. Liu et al. revealed two newly discovered genes (*LOC Os02g49700*, *LOC Os03g28300*) and five known genes (*OsMYB6*, *OsGAMYB*, *OsHKT1;4*, *OsCTR3*, and *OsSUT1*) connected with grain production and its associated attributes in rice cultivars exposed to saline stress conditions [313].

According to Rahman et al., maintaining lower shoot Na^+ buildup is a standard method for preserving salt tolerance in rice [78]. These methods include sodium exclusion, effective toxic salt sequestration into older leaves and roots, compartmentalization of Na^+ into vacuoles, and extrusion from cells. According to Wang et al., *OsHKT1;1*, *OsHAK10*, and *OsHAK16* were shown to be elevated in the leaves of old rice under salt stress [314]. These genes are integral to Na^+ transport from the roots to the shoot. *OsHKT1;5* and *OsSOS1*, which promote Na^+ exclusion from xylem vessels of roots, thereby lowering accumulation in the shoot, were downregulated, resulting in large quantities of Na^+ in older leaves rather than young ones. Rice's class 1 HKT transporter eliminates extra Na^+ from the xylem, shielding the photosynthesis-dependent leaf tissues from the harmful effects of Na^+. By mediating K^+ absorption and transfer to sustain a high K^+/Na^+ ratio under salt stress, the K^+ transporter genes *OsHAK1* and *OsHAK5* are stimulated by salt stress in rice [315]. When there is a higher concentration of Na^+ in the cytosol, it is transported into the vacuole to prevent it from reaching toxic levels for enzyme reactions. Na^+/H^+ antiporters control this process. An increase in salt content activates the Na^+/H^+ antiporter action [316]. Two proton pumps, vacuolar H^+-ATPase, and vacuolar H^+-translocating pyrophosphatase, control the interchange of Na^+/H^+ in the vacuole. Modifying the vacuolar transporter levels can enhance rice's tolerance to salinity [317]. According to a study, elevated *CYP94C2b* expression and concurrent jasmonate inactivation in rice are associated with salt tolerance [318]. Table 5 summarizes the key genes associated with salt stress tolerance in rice.

Table 5. Identified genes linked to salt stress tolerance in rice.

Name of Genes	Function	Reference
OsCPK12	Increases resistance to high salt levels by decreasing ROS buildup	[319]
OsLOL5	Enhance ROS scavenging and rice tolerance under salinity stress	[320]
OsMAPK44	Participates in ion homeostasis under salinity stress	[321]
OsJRL40	Increases antioxidant enzymatic activities and maintains the balance of Na^+/K^+ during salinity stress. Manages rice's salt stress by regulating the expression of genes responsible for transporting Na^+/K^+, as well as genes involved in salt-responsive transcription factors and proteins	[322]
OsSAPK4	Modulates ion homeostasis as well as the growth and development of rice in a salinized environment	[323]
OsKAT1	Enhances rice's salinity tolerance by enhancing K^+ uptake and thus decreasing Na^+ accumulation	[324]

Table 5. *Cont.*

Name of Genes	Function	Reference
OsTPS8	Controls the ability of rice to tolerate salinity stress by managing the levels of soluble sugars and regulating the activity of genes related to ABA signaling through the regulation of *SAPK9*	[325]
OsBADH1	Enhances salinity stress tolerance by positively regulating osmoprotectant biosynthesis	[326]
OsMYB91	Manages the growth of rice and its ability to tolerate salt stress.	[327]
OsVP1 and OsNHX1	Enhances the tolerance of salt by decreasing the accumulation of Na^+ in leaves, photosynthesis activity, and increase root biomass	[328]
OsHKT1;1, OsHKT1;4 and OsHKT1;5	Enhance the tolerance of salt by decreasing the accumulation of Na^+ in shoots when exposed to salt stress	[329–331]
OsHAK5	Enhance rice's salinity tolerance by contributing to cation homeostasis	[332]

Arbuscular mycorrhizal fungus (AMF) symbionts aid the host plant development and ameliorate stress caused by abiotic factors. Under salt stress, the upland pigmented rice cv. Leum Pua (LP) infected with *Glomus etunicatum* produced total soluble sugars and free proline, which worked as osmolytes to preserve the flag leaf's photosynthetic capacities, chlorophyll pigments, Chla fluorescence, and stomatal function. Leum Pua rice infected with *Glomus etunicatum* maintained yield characteristics and showed high anthocyanin content in the pericarp [333].

2.6. Heavy Metal Stress

Heavy metal pollution is a major contributor to harmful effects on plants, ecosystems, soil, and water. It is a significant factor in reducing the quality and yield of crops. Rice grown in paddy soils contaminated with heavy metals like arsenic (As), cadmium (Cd), lead (Pb), and mercury (Hg) is a major source of heavy metal intake for humans in many countries. This gradual buildup of heavy metals in rice grains and their subsequent entry into the food chain poses a severe risk to agriculture and public health [334]. Heavy metals have the potency to modify reactions that aid in generating ROS, $^{\cdot}OH$, and H_2O_2 within living cells. Nevertheless, when highly reactive radicals come into contact with water, they produce $^{\cdot}OH$, which can harm essential biomolecules within cells such as carbohydrates, lipids, amino acids, and DNA [335–337]. Therefore, it is necessary to comprehend how heavy metals interact with rice crops at all levels, from the cellular to the entire plant, and to develop effective strategies to reduce these stress reactions [338,339].

2.6.1. Morphological and Physiological Responses to Heavy Metals

i. Arsenic

Arsenic can exist in various oxidation states in soil, the most prevalent of which are arsenides (As^{3-}), arsenites (As^{3+}), and arsenates (As^{5+}). Depending on the species, arsenic can harm rice, with inorganic species being far more toxic than organic ones. As^{5+} and As^{3+} are the most prevalent inorganic species found in the rice plant, whereas monomethylarsonic acid (MMA) and dimethylarsinic acid (DMA) are the most occurring organic species [340]. As^{3+} is thought to be more mobile and hazardous than As^{5+} among inorganic entities. It can react with methyl groups in any oxidation state to create organic arsenic species. However, compared to inorganic arsenic species, the presence of organic species in paddy soil is substantially lower. The reduced form (As^{3+}) predominates in anaerobic soil types, such as submerged rice fields, whereas As^{5+} (oxidized counterpart) predominates in

aerobic soil environments, such as highland rice fields [341]. An increase in arsenic absorption will have a detrimental impact on plant development. Poor and lower germination rates of seeds, impaired plant growth, lower photosynthetic rates, sterility-related yield loss, low biomass production, and a physiological condition known as straight head disease are just a few of the symptoms that are brought on by arsenic toxicity in rice plants [342]. Reduced floret/spikelet sterility, decreased grain production, and, in severe cases, the absence of panicles or heads are some signs of this disease. Arsenic toxicity damages the chloroplast and photosynthetic processes by deteriorating the membrane structure. Arsenic affects the metabolism of proteins, lipids, and carbohydrates. More crucially, arsenic can increase the production of ROS that is greater than what can be scavenged, damaging plants through oxidative stress. Exposure of rice seedlings to As^{5+} promotes the formation of H_2O_2, whereas As^{3+} was shown to induce the formation of O_2^- and H_2O_2, thereby causing lipid peroxidation [343]. When seedling roots are grown in an As^{5+} solution, APX activity is increased, reducing H_2O_2 through the ascorbate-glutathione cycle [344]. Similarly, the enzymatic antioxidants CAT, SOD, guaiacol peroxidase, chloroplastic ascorbate peroxidase, GR, and monodehydroascorbate reductase concentrations were raised for scavenging ROS developed in the presence of As^{3+} conditions [345].

ii. Cadmium

Cd is a trace element that is not necessary for plants but is widespread in the environment. Different anthropogenic operations such as smelting, mining, usage of synthetic phosphate fertilizers, and disposal of urban wastes lead to a rise in the levels of Cd in the environment that pose serious health risks to humans [346]. Recently, it has been found that Cd pollution in paddy soil poses a danger to rice quality [347]. Rice plants absorb Cd from the soil, eventually building up in the grains after several transit steps. Rice plant absorbs Cd from the ground through its roots, moves it to the shoots via xylem flow, reroutes it at nodes, and remobilizes it from the leaves. According to Huijie et al. [348], citrate, tartaric acid, and histidine were found to participate in root-to-shoot Cd transfer in the xylem actively. *Indica* cultivars often accumulate more significant amounts of Cd in their shoots and grains than *japonica* cultivars. Stomatal conductance, transpiration rate, leaf water content, vital minerals, water-soluble proteins, and enzyme- and non-enzyme-based antioxidants are all decreased due to Cd toxicity [349,350]. Cd poisoning reduced rice yield and grain quality by inducing changes in yield components (such as panicle number, spikelets per panicle, and spikelet setting percent). Excessive Cd has a deleterious impact on photosynthesis as it affects the photosynthetic pigments and disrupts electron transport mechanisms, interfering with chloroplast structure and Chl-protein complexes. This disruption causes a disturbance in Chl biosynthesis enzymes, the Calvin cycle, and water balance [351]. Cd prevents the formation of chlorophyll by inhibiting the enzyme δ-aminolevulinic acid dehydratase, which is present in rice seedlings. An increase in Cd concentration in the medium led to a higher accumulation of Cd in the seeds and the thiobarbituric acid reactive substance amount. It also caused a drastic decrease in the germination rate, shoot elongation, biomass, and water content of the rice [352].

Despite not being a direct cause, Cd can cause exorbitant accumulations of ROS when its concentration surpasses the plant tolerance level. This can occur through several mechanisms, comprising the exhaustion of ROS-scavenging enzymatic and non-enzymatic components, metabolic abnormalities during respiration, displacement of redox-active Fe from proteins, photorespiration, and CO_2 assimilation [351,353].

iii. Lead

Pb is a non-essential element that may disrupt plant metabolism if taken up by the plant. In addition to interfering with roots' ability to absorb minerals from the soil solution, Pb^{2+} ions also passively penetrate the roots of rice plants by following water streams that are moving through the soil. Pb is carried into the root epidermal cells from the soil and loaded into the root xylem vessels before being distributed to other plant organs [354]. In rice cultivars, a high Pb concentration (1.2 mM) results in a considerable decrease in plant

height, tiller count, panicle count, and spikelet count per panicle [355]. Lead poisoning negatively affects photosynthetic activity by altering chloroplast structure, slowing the production of carotenoid, plastoquinone, and chlorophyll, and breaking up the electron transport chain. Additionally, it causes a CO_2 shortage, which causes the stomata to close and Calvin cycle's enzymatic activity to decrease. According to a study by Khan et al. [356], Pb poisoning does not affect root development but drastically reduces shoot length and biomass of rice in nitrogen or phosphorus-deprived seedlings. ROS are overproduced, and antioxidant enzyme activity fluctuates due to Pb toxicity in plants.

iv. Mercury

One of the environment's most hazardous elements is Hg. Hg is a strong phytotoxin to plant cells at high concentrations and can cause injury and physiological disturbances. Hg preferentially accumulates on the roots of several plant species. As a result, the most toxic effects are observed at the roots. Under Hg stress, rice roots bind to proteins of 15–25 kDa, which results in irreparable harm to root development. Under Hg stress, rice roots altered the expression levels of the associated proteins [357]. When rice is grown on Hg-contaminated land, a significant amount of Hg is enriched into the grain, which is terrible for the rice's consumers [358]. There are three different types of mercury: methylmercury (MeHg), inorganic mercury (Hg^{2+}), and elemental mercury (Hg^0) [359]. Hg is most bio-accumulative in the form of methylmercury MeHg. MeHg is the most harmful type of Hg to human and animal health [358]. The generation of MeHg in the rhizosphere soil and its buildup in rice are greatly influenced by moderate soil Hg content (3 mg kg^{-1}). MeHg production in rhizosphere soil increases significantly at the blooming or filling stage, but rice leaves' antioxidant systems show little impact [273]. The bulk of an individual rice grain's Hg^{2+} by mass is found in the hull and bran. Conversely, white rice contains a large proportion of the more dangerous form of MeHg. Proteins contain MeHg, which is primarily coupled to cysteine in bran. This MeHg-cysteine relationship acts as a mobile nutrient during seed ripening and is actively transferred to the endosperm [360]. ROS, MDA content, and lipoxygenase activity are all considerably enhanced with increasing Hg levels in rice roots, which disturbs numerous cellular processes and hinders growth and development in rice plants [359].

2.6.2. Biochemical Responses to Heavy Metals

An increased quantity of heavy metals like As, Hg, Pb, and Cd triggers ROS generation, leading to oxidative stress. This stress damages the plasma membrane and disrupts rice plants' metabolism and physiological response. To combat oxidative stress, rice plants develop various defense strategies, such as activating the antioxidant defense system, ion homeostasis, osmolyte accumulation, osmoregulation, and excess production of signaling molecules [361,362]. In addition, in response to stress caused by heavy metals and metalloids, rice plants produce phytochelatins (PC), which are thiol-rich peptides [363]. For instance, rice leaves containing As-PC complexes reduce the amount of As^{3+} that may be transferred to the grain [364]. Similarly, under Cd stress, rice roots and leaves showed increased SOD, POD, CAT, GPX, and APX activity. Under Cd toxicity, rice also has higher levels of non-protein thiols like PCs and GSH to scavenge harmful free radicals [353]. In another experiment, rice showed an increase in the activity of CAT and POD under Pb poisoning. There was also an increase in the accumulation of proline and the content of sucrose with the rise in Pb concentration [355]

Recently, glutamate (Glu) has been found to participate in a signaling role in responses developed by plants toward abiotic stress [365]. In a study, glutamate supplementation was found to dramatically improve Cd-induced oxidative stress in rice with decreased levels of MDA, H_2O_2, O_2^-, proline, γ-aminobutyric acid, arginine, and higher activities of CAT, POD, and glutathione S-transferase. Roots of Cd-treated plants showed decreased expression of Cd-induced metal transporter genes OsNramp1, OsNramp5, OsIRT1, OsIRT2, OsHMA2, and OsHMA3 when supplemented with Glu [366]. According to Ahsan et al., 21 proteins were demonstrated to be engaged in defense and detoxification, antioxidant,

protein biosynthesis, and germination activities in rice under Cd toxicity [367]. Hg stress raises the free Phe and Trp content and upregulated numerous genes related to aromatic amino acids. Chen et al. found that applying Phe and Trp to rice roots exogenously increases their tolerance to Hg and significantly decreases the concentration of ROS that Hg induces [368]. Additionally, research has shown that the formation of iron plaque on the roots of rice may serve as a protective barrier, reducing the absorption of Cd and As into the roots of the rice plant [369,370].

2.6.3. Molecular Responses to Heavy Metals

Heavy metal stress-related signal transduction is triggered by the recognition of stress signals by receptors/ion channels and then carried on by non-protein messengers such as calcium, hydrogen ions, and cyclic nucleotides (Figure 3).

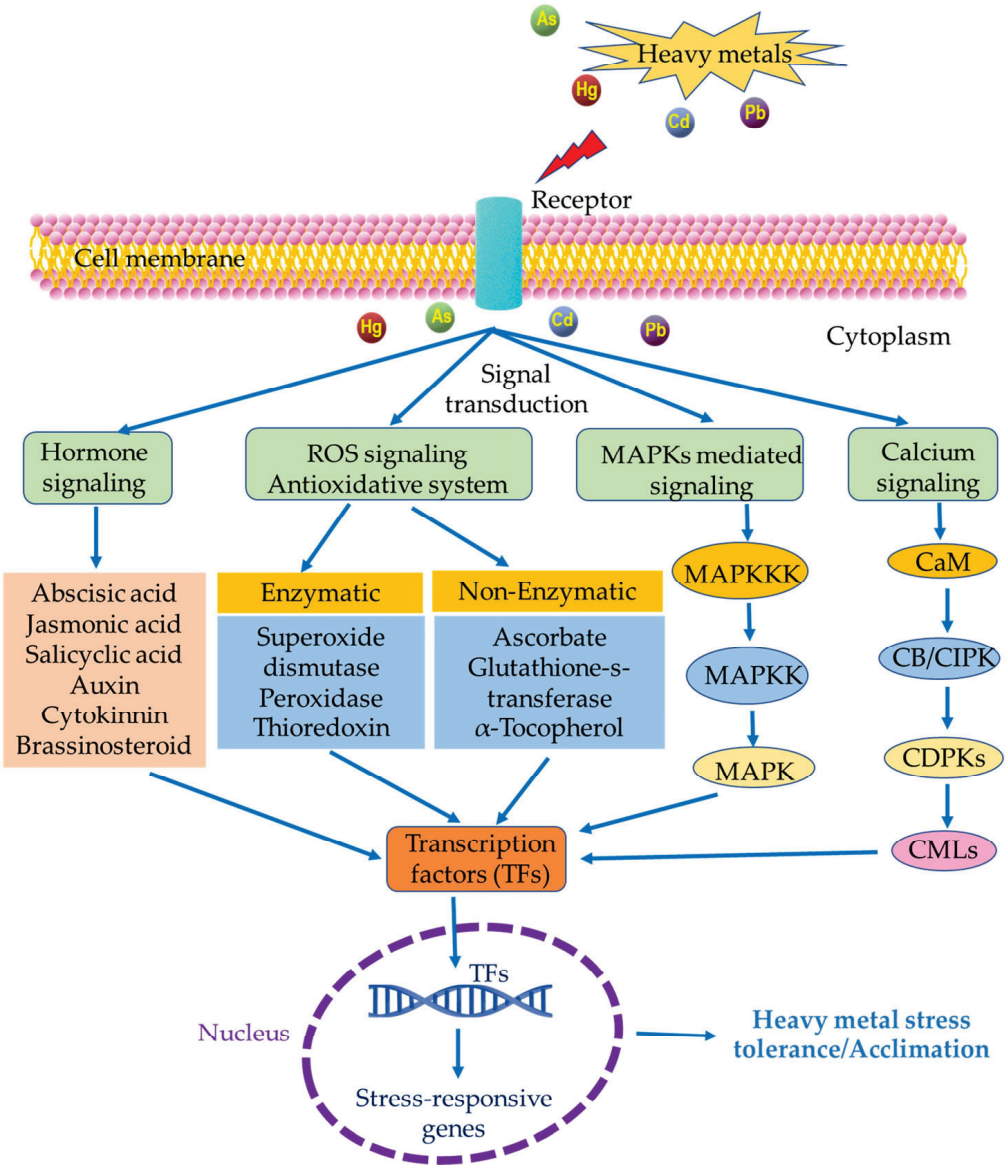

Figure 3. A schematic diagram showing a heavy metal stress signaling cascade that enhances stress-responsive gene expression in rice.

The stress signals are relayed by several kinases and phosphatases, which in turn cause the expression of multiple TFs and the generation of metal-detoxifying peptides [371–373]. Heavy metals initiate various distinctive signaling pathways in plants, which include

ROS signaling, calcium-dependent signaling, MAPK signaling, and hormone signaling that promote the expression of TFs and stress-responsive genes [344,372]. Calmodulins (CaM), calmodulin-like proteins, calcineurin B-like proteins, and CDPK are some of the calcium signaling sensors that monitor, process, and transmit changes in cytosolic Ca^{2+} content for the stress response. Individual sensors respond differently depending on the Ca^{2+} content [374,375]. Likewise, the MAPK signaling cascade also phosphorylates several TFs, including *NAC*, *MYC*, *MYB*, *bZIP, DREB*, and *ABRE*, which alters the expression of metal stress response genes [376,377]. For instance, Cd activates rice's myelin basic protein (MBP) kinase and *OsMAPK2* genes [378]. Additionally, numerous research studies have displayed that the activation of MAPKs by heavy metals in rice is caused by ROS production, accumulation, and modification [372,379]. Furthermore, several phytohormone signaling pathways, especially ethylene, auxin, and JA, are affected by ROS. According to Singh and Shah, JA treatment enhanced rice's ability to withstand Cd stress via improving antioxidant response [380]. When As^{3+} was applied to rice seedlings, comparative transcriptome analysis revealed modification in signal transduction, defensive responses, and hormonal signaling pathways, including ABA metabolism [381]. The results above strongly imply that changes in phytohormone levels alter how plants react to metal stress. Hence, it is crucial to comprehend the complex pathways through which metal stress is signaled in plants and the interconnections between them. This understanding is essential to unravelling the networks that plants employ to respond to stress. Numerous molecular research studies have examined how rice plants react to elevated levels of heavy metals. These research studies aim to enhance the ability of current rice cultivars to withstand heavy metal toxicity and offer valuable insights for incorporating these specific genes/traits into future breeding initiatives. Table 6 summarizes key genes associated with heavy metal tolerance in rice.

Table 6. Identified genes linked to heavy metals stress tolerance in rice.

Name of Genes	Function	Reference
OsHAC1;1 and *OsHAC1;2*	Drastically influence limiting the accumulation of As in both the shoots and grains of rice	[382]
OsNRAMP5	Enhances resistance to the toxicity of Cd	[383]
OsHMA3	Enhances resistance to the toxicity of Cd	[384]
OsABCG31	Enhances resistance to the toxicity of Cd and Pb	[385]
OsLCT1	Enhances resistance to the toxicity of Cd Al	[386]
OsSIZ	Enhances resistance to the toxicity of Cd	[387]
OsZIP1	Enhances resistance to the toxicity of Cd, Zn,	[388]
OsNAC5	Enhances resistance to the toxicity of Cd and Pb	[79]
OsMT1e	Encodes a metal-detoxifying protein	[389]
OsIRO2	TF that modulates the activity of genes related to Fe balance in rice	[390]
OsIRT1	Participates in Cd absorption in rice. It is involved in Cd stress tolerance	[391]
OsPCS1	It is involved in detoxifying heavy metals and involved in Cd stress tolerance	[392]
OsLCD	Involved in Cd compartmentation	[393]
OsSUV3	Improved Cd and Zn stress tolerance	[394]
OsSRK	Increases the uptake and transfer of Cd	[395]
OsHMA2	Improves transfer of Cd from roots to shoots	[395]
OsMYB45	Improves Cd stress tolerance	[396]
OsHB4	Improves Cd accumulation and tolerance	[397]

3. Conclusions

Abiotic stress is a significant factor restricting rice crop yield in many places of the world. Under the current climate change scenario, abiotic factors such as drought, heat, cold, submersion, salinity, and heavy metals are responsible for the sharp decline in rice yields. These abiotic stressors have a detrimental impact on various stages of plant growth and development, including germination, seedling establishment, lengths of root and shoot, plant height, blooming time, and ripening time. These stressors during both the vegetative and reproductive stages hinder the development of the plant's panicles and the filling of grains, decreasing overall grain production and posing a risk to global food security. The combined application of genomics and QTL-based techniques has aided in identifying genes and loci that contribute to adaptation to abiotic stress in rice. These recently discovered molecular candidates have the potential to enhance rice physiological growth, reproductive development, and crop yields in challenging environments. However, in the future, research employing high-throughput phenotype determination and next-generation sequencing technology will help identify innovative potential genes responsible for regulating grain development under varied stress situations, paving the way for the breeding of climate-ready crops. In this review, we have discussed the developments in the current understanding of the defense mechanisms that rice employs to counteract various environmental stresses. Despite our vast knowledge in this area, there are still gaps in our understanding. Bridging these gaps will allow researchers to design plants that respond better to environmental stimuli such as drought, heat, cold, submersion, salinity, heavy metals, etc.

Author Contributions: Conceptualization, B.S., H.K., T.L.T. and Y.K.M.; validation, P.N.B.; resources, B.S., H.K., T.L.T. and Y.K.M.; data curation, B.S., H.K. and T.L.T.; writing—original draft preparation, B.S., H.K., T.L.T. and Y.K.M.; writing—review and editing, P.N.B., Y.K.M. and K.-H.B.; supervision, Y.K.M. and K.-H.B.; All authors have read and agreed to the published version of the manuscript.

Funding: This research was supported by the Basic Science Research Program through the National Research Foundation of Korea (NRF), funded by the Ministry of Education (NRF-2021R1F1A1060297).

Conflicts of Interest: The authors declare no conflict of interest.

References

1. Yadav, G.S.; Lal, R.; Meena, R.S.; Babu, S.; Das, A.; Bhowmik, S.N.; Datta, M.; Layak, J.; Saha, P. Conservation tillage and nutrient management effects on productivity and soil carbon sequestration under double cropping of rice in north eastern region of India. *Ecol. Indic.* **2019**, *105*, 303–315. [CrossRef]
2. Mahanta, K.; Bhattacharyya, P.N.; Sharma, A.K.; Rajkhowa, D.; Lesueur, D.; Verma, H.; Parit, R.; Deka, J.; Medhi, B.K.; Kohli, A. Residue and soil dissipation kinetics of chloroacetanilide herbicides on rice (*Oryzae sativa* L.) and assessing the impact on soil microbial parameters and enzyme activity. *Environ. Monit. Assess.* **2023**, *195*, 910. [CrossRef] [PubMed]
3. Hanafiah, N.M.; Mispan, M.S.; Lim, P.E.; Baisakh, N.; Cheng, A. The 21st century agriculture: When rice research draws attention to climate variability and how weedy rice and underutilized grains come in handy. *Plants* **2020**, *9*, 365. [CrossRef] [PubMed]
4. Mohapatra, P.K.; Sahu, B.B. Diversity of Panicle Architecture and Traits Influencing Grain Filling. In *Panicle Architecture of Rice and Its Relationship with Grain Filling*; Springer International Publishing: Cham, Switzerland, 2022; pp. 107–128, ISBN 978-3-030-67897-5.
5. Pickson, R.B.; He, G.; Boateng, E. Impacts of climate change on rice production: Evidence from 30 Chinese provinces. *Environ. Dev. Sustain.* **2022**, *24*, 3907–3925. [CrossRef]
6. Dar, M.H.; Bano, D.A.; Waza, S.A.; Zaidi, N.W.; Majid, A.; Shikari, A.B.; Ahangar, M.A.; Hossain, M.; Kumar, A.; Singh, U.S. Abiotic Stress Tolerance-Progress and Pathways of Sustainable Rice Production. *Sustainability* **2021**, *13*, 2078. [CrossRef]
7. Saud, S.; Wang, D.; Fahad, S.; Alharby, H.F.; Bamagoos, A.A.; Mjrashi, A.; Alabdallah, N.M.; AlZahrani, S.S.; AbdElgawad, H.; Adnan, M.; et al. Comprehensive Impacts of Climate Change on Rice Production and Adaptive Strategies in China. *Front. Microbiol.* **2022**, *13*, 926059. [CrossRef] [PubMed]
8. Aguilar-Rivera, N.; Michel-Cuello, C.; Cárdenas-González, J.F. Green Revolution and Sustainable Development. In *Encyclopedia of Sustainability in Higher Education*; Leal Filho, W., Ed.; Springer International Publishing: Cham, Switzerland, 2019; pp. 833–850, ISBN 978-3-030-11352-0.
9. Iqbal, J.; Zia-ul-Qamar; Yousaf, U.; Asgher, A.; Dilshad, R.; Qamar, F.M.; Bibi, S.; Rehman, S.U.; Haroon, M. Sustainable Rice Production Under Biotic and Abiotic Stress Challenges. In *Sustainable Agriculture in the Era of the OMICs Revolution*; Prakash, C.S.,

Fiaz, S., Nadeem, M.A., Baloch, F.S., Qayyum, A., Eds.; Springer International Publishing: Cham, Switzerland, 2023; pp. 241–268, ISBN 978-3-031-15568-0.
10. Yang, Y.; Yu, J.; Qian, Q.; Shang, L. Enhancement of Heat and Drought Stress Tolerance in Rice by Genetic Manipulation: A Systematic Review. *Rice* **2022**, *15*, 67. [CrossRef]
11. Hussain, S.; Khaliq, A.; Ali, B.; Hussain, H.A. Temperature Extremes: Impact on Rice Growth and Development. In *Plant Abiotic Stress Tolerance*; Springer: Berlin/Heidelberg, Germany, 2019. [CrossRef]
12. Oladosu, Y.; Rafii, M.Y.; Samuel, C.; Fatai, A.; Magaji, U.; Kareem, I.; Kamarudin, Z.S.; Muhammad, I.; Kolapo, K. Drought Resistance in Rice from Conventional to Molecular Breeding: A Review. *Int. J. Mol. Sci.* **2019**, *20*, 3519. [CrossRef]
13. Fahad, S.; Adnan, M.; Hassan, S.; Saud, S.; Hussain, S.; Wu, C.; Wang, D.; Hakeem, K.R.; Alharby, H.F.; Turan, V.; et al. *Chapter 10—Rice Responses and Tolerance to High Temperature*; Hasanuzzaman, M., Fujita, M., Nahar, K., Biswas, J.K., Eds.; Woodhead Publishing: Sawston, UK, 2019; pp. 201–224, ISBN 978-0-12-814332-2.
14. Bhattacharya, A. *Effect of Low Temperature Stress on Photosynthesis and Allied Traits: A Review*; Springer: Singapore, 2022; ISBN 978-981-16-9037-2.
15. Horie, T.; Karahara, I.; Katsuhara, M. Salinity tolerance mechanisms in glycophytes: An overview with the central focus on rice plants. *Rice* **2012**, *5*, 11. [CrossRef]
16. Mahmood-ur-Rahman; Ijaz, M.; Qamar, S.; Bukhari, S.A.; Malik, K. *Chapter 27—Abiotic Stress Signaling in Rice Crop*; Hasanuzzaman, M., Fujita, M., Nahar, K., Biswas, J.K., Eds.; Woodhead Publishing: Sawston, UK, 2019; pp. 551–569, ISBN 978-0-12-814332-2.
17. Suwanmontri, P.; Kamoshita, A.; Fukai, S. Recent changes in rice production in rainfed lowland and irrigated ecosystems in Thailand. *Plant Prod. Sci.* **2020**, *24*, 15–28. [CrossRef]
18. Arif, N.; Sharma, N.C.; Yadav, V.; Ramawat, N.; Dubey, N.K.; Tripathi, D.K.; Chauhan, D.K.; Sahi, S. Understanding Heavy Metal Stress in a Rice Crop: Toxicity, Tolerance Mechanisms, and Amelioration Strategies. *J. Plant Biol.* **2019**, *62*, 239–253. [CrossRef]
19. Melo, F.V.; Oliveira, M.M.; Saibo, N.J.M.; Lourenço, T.F. Modulation of Abiotic Stress Responses in Rice by E3-Ubiquitin Ligases: A Promising Way to Develop Stress-Tolerant Crops. *Front. Plant Sci.* **2021**, *12*, 640193. [CrossRef]
20. Das, G.; Patra, J.K.; Baek, K.H. Insight into MAS: A Molecular Tool for Development of Stress Resistant and Quality of Rice through Gene Stacking. *Front. Plant Sci.* **2017**, *8*, 985. [CrossRef]
21. Pandey, V.; Shukla, A. Acclimation and Tolerance Strategies of Rice under Drought Stress. *Rice Sci.* **2015**, *22*, 147–161. [CrossRef]
22. Miyan, M.A. Droughts in asian least developed countries: Vulnerability and sustainability. *Weather Clim. Extrem.* **2015**, *7*, 8–23. [CrossRef]
23. Yang, X.; Wang, B.; Chen, L.; Li, P.; Cao, C. The Different Influences of Drought Stress at the Flowering Stage on Rice Physiological Traits, Grain Yield, and Quality. *Sci. Rep.* **2019**, *9*, 3742. [CrossRef]
24. Venuprasad, R.; Lafitte, H.R.; Atlin, G.N. Response to direct selection for grain yield under drought stress in rice. *Crop Sci.* **2007**, *47*, 285–293. [CrossRef]
25. Lafitte, H.; Ismail, A.; Bennett, J. Abiotic Stress Tolerance in Rice for Asia: Progress and the Future. In Proceedings of the 4th International Crop Science Congress, Brisbane, Australia, 26 September–1 October 2004.
26. Upadhyaya, H.; Panda, S.K. *Chapter 9—Drought Stress Responses and Its Management in Rice*; Hasanuzzaman, M., Fujita, M., Nahar, K., Biswas, J.K., Eds.; Woodhead Publishing: Sawston, UK, 2019; ISBN 978-0-12-814332-2.
27. Farooq, M.; Wahid, A.; Kobayashi, N.; Fujita, D.; Basra, S.M.A. Plant Drought Stress: Effects, Mechanisms and Management. In *Sustainable Agriculture*; Springer: Dordrecht, The Netherlands, 2009; pp. 153–188. [CrossRef]
28. Caine, R.S.; Yin, X.; Sloan, J.; Harrison, E.L.; Mohammed, U.; Fulton, T.; Biswal, A.K.; Dionora, J.; Chater, C.C.; Coe, R.A.; et al. Rice with reduced stomatal density conserves water and has improved drought tolerance under future climate conditions. *New Phytol.* **2019**, *221*, 371–384. [CrossRef] [PubMed]
29. Zampieri, E.; Pesenti, M.; Nocito, F.F.; Sacchi, G.A.; Valè, G. Rice Responses to Water Limiting Conditions: Improving Stress Management by Exploiting Genetics and Physiological Processes. *Agriculture* **2023**, *13*, 464. [CrossRef]
30. Fukai, S.; Cooper, M. Development of drought-resistant cultivars using physiomorphological traits in rice. *Field Crop. Res.* **1995**, *40*, 67–86. [CrossRef]
31. Moonmoon, S.; Islam, M. Effect of Drought Stress at Different Growth Stages on Yield and Yield Components of Six Rice (*Oryza sativa* L.) Genotypes. *Fundam. Appl. Agric.* **2017**, *2*, 285–289. [CrossRef]
32. Ranjan, A.; Sinha, R.; Singla-Pareek, S.L.; Pareek, A.; Singh, A.K. Shaping the root system architecture in plants for adaptation to drought stress. *Physiol. Plant.* **2022**, *174*, e13651. [CrossRef] [PubMed]
33. Kim, Y.; Chung, Y.S.; Lee, E.; Tripathi, P.; Heo, S.; Kim, K.-H.K.-H. Root Response to Drought Stress in Rice (*Oryza Sativa* L.). *Int. J. Mol. Sci* **2020**, *21*, 1513. [CrossRef] [PubMed]
34. Champoux, M.C.; Wang, G.; Sarkarung, S.; Mackill, D.J.; O'Toole, J.C.; Huang, N.; McCouch, S.R. Locating genes associated with root morphology and drought avoidance in rice via linkage to molecular markers. *Theor. Appl. Genet.* **1995**, *90*, 969–981. [CrossRef] [PubMed]
35. Bañoc, D.M.; Yamauchi, A.; Kamoshita, A.; Wade, L.J.; Pardales, J.R. Dry Matter Production and Root System Development of Rice Cultivars under Fluctuating Soil Moisture. *Plant Prod. Sci.* **2000**, *3*, 197–207. [CrossRef]
36. Bañoc, D.M.; Yamauchi, A.; Kamoshita, A.; Wade, L.J.; Pardales, J.R. Genotypic Variations in Response of Lateral Root Development to Fluctuating Soil Moisture in Rice. *Plant Prod. Sci.* **2000**, *3*, 335–343. [CrossRef]

37. Henry, A.; Cal, A.J.; Batoto, T.C.; Torres, R.O.; Serraj, R. Root attributes affecting water uptake of rice (*Oryza sativa*) under drought. *J. Exp. Bot.* **2012**, *63*, 4751–4763. [CrossRef]
38. Fang, Y.; Xiong, L. General mechanisms of drought response and their application in drought resistance improvement in plants. *Cell. Mol. Life Sci.* **2015**, *72*, 673–689. [CrossRef]
39. Farooq, M.; Kobayashi, N.; Ito, O.; Wahid, A.; Serraj, R. Broader leaves result in better performance of indica rice under drought stress. *J. Plant Physiol.* **2010**, *167*, 1066–1075. [CrossRef]
40. Kavi Kishor, P.B.; Sangam, S.; Amrutha, R.N.; Sri Laxmi, P.; Naidu, K.R.; Rao, K.R.S.S.; Rao, S.; Reddy, K.J.; Theriappan, P.; Sreenivasulu, N. Regulation of proline biosynthesis, degradation, uptake and transport in higher plants: Its implications in plant growth and abiotic stress tolerance. *Curr. Sci.* **2005**, *88*, 424–438.
41. Zhu, R.; Wu, F.; Zhou, S.; Hu, T.; Huang, J.; Gao, Y. Cumulative effects of drought–flood abrupt alternation on the photosynthetic characteristics of rice. *Environ. Exp. Bot.* **2020**, *169*, 103901. [CrossRef]
42. Mishra, S.S.; Behera, P.K.; Kumar, V.; Lenka, S.K.; Panda, D. Physiological characterization and allelic diversity of selected drought tolerant traditional rice (*Oryza sativa* L.) landraces of Koraput, India. *Physiol. Mol. Biol. Plants* **2018**, *24*, 1035–1046. [CrossRef] [PubMed]
43. Farooq, M.; Kobayashi, N.; Wahid, A.; Ito, O.; Basra, S.M.A. Strategies for Producing More Rice with Less Water. In *Advances in Agronomy*; Elsevier: San Diego, CA, USA, 2009; Volume 101, p. e1. [CrossRef]
44. Panda, D.; Mishra, S.S.; Behera, P.K. Drought Tolerance in Rice: Focus on Recent Mechanisms and Approaches. *Rice Sci.* **2021**, *28*, 119–132. [CrossRef]
45. Fahad, S.; Bajwa, A.A.; Nazir, U.; Anjum, S.A.; Farooq, A.; Zohaib, A.; Sadia, S.; Nasim, W.; Adkins, S.; Saud, S.; et al. Crop Production under Drought and Heat Stress: Plant Responses and Management Options. *Front. Plant Sci.* **2017**, *8*, 1147. [CrossRef]
46. Gupta, A.; Rico-Medina, A.; Caño-Delgado, A.I. The physiology of plant responses to drought. *Science* **2020**, *368*, 266–269. [CrossRef] [PubMed]
47. Ashraf, M.; Harris, P.J.C. Photosynthesis under stressful environments: An overview. *Photosynthetica* **2013**, *51*, 163–190. [CrossRef]
48. Zhang, F.-J.; Zhang, K.-K.; Du, C.-Z.; Li, J.; Xing, Y.-X.; Yang, L.-T.; Li, Y.-R. Effect of Drought Stress on Anatomical Structure and Chloroplast Ultrastructure in Leaves of Sugarcane. *Sugar Tech* **2015**, *17*, 41–48. [CrossRef]
49. Ayyaz, A.; Fang, R.; Ma, J.; Hannan, F.; Huang, Q.; Athar, H.-R.; Sun, Y.; Javed, M.; Ali, S.; Zhou, W.; et al. Calcium nanoparticles (Ca-NPs) improve drought stress tolerance in Brassica napus by modulating the photosystem II, nutrient acquisition and antioxidant performance. *NanoImpact* **2022**, *28*, 100423. [CrossRef]
50. Zahra, N.; Hafeez, M.B.; Kausar, A.; Al Zeidi, M.; Asekova, S.; Siddique, K.H.M.M.; Farooq, M.; Al Zeidi, M.; Asekova, S.; Siddique, K.H.M.M.; et al. Plant photosynthetic responses under drought stress: Effects and management. *J. Agron. Crop Sci.* **2023**, *209*, 651–672. [CrossRef]
51. Lum, M.S.; Hanafi, M.M.; Rafii, Y.M.; Akmar, A.S.N. Effect of drought stress on growth, proline and antioxidant enzyme activities of upland rice. *J. Anim. Plant Sci.* **2014**, *24*, 1487–1493.
52. Schlicke, H.; Hartwig, A.S.; Firtzlaff, V.; Richter, A.S.; Glässer, C.; Maier, K.; Finkemeier, I.; Grimm, B. Induced Deactivation of Genes Encoding Chlorophyll Biosynthesis Enzymes Disentangles Tetrapyrrole-Mediated Retrograde Signaling. *Mol. Plant* **2014**, *7*, 1211–1227. [CrossRef] [PubMed]
53. Busch, A.W.U.; Montgomery, B.L. Interdependence of tetrapyrrole metabolism, the generation of oxidative stress and the mitigative oxidative stress response. *Redox Biol.* **2015**, *4*, 260–271. [CrossRef] [PubMed]
54. Hasanuzzaman, M.; Hossain, M.A.; da Silva, J.A.T.; Fujita, M. Plant Response and Tolerance to Abiotic Oxidative Stress: Antioxidant Defense Is a Key Factor. In *Crop Stress and its Management: Perspectives and Strategies*; Springer: Dordrecht, The Netherlands, 2012; pp. 261–315. [CrossRef]
55. Asada, K. The Water-Water Cycle In Chloroplasts: Scavenging of Active Oxygens and Dissipation of Excess Photons. *Annu. Rev. Plant Physiol. Plant Mol. Biol.* **1999**, *50*, 601–639. [CrossRef] [PubMed]
56. Cruz de Carvalho, M.H. Drought stress and reactive oxygen species. *Plant Signal. Behav.* **2008**, *3*, 156–165. [CrossRef] [PubMed]
57. Wang, X.; Liu, H.; Yu, F.; Hu, B.; Jia, Y.; Sha, H.; Zhao, H. Differential Activity of the Antioxidant Defence System and Alterations in the Accumulation of Osmolyte and Reactive Oxygen Species under Drought Stress and Recovery in Rice (*Oryza Sativa* L.) Tillering. *Sci. Rep.* **2019**, *9*, 8543. [CrossRef] [PubMed]
58. Bhattacharjee, S.; Dey, N. Redox metabolic and molecular parameters for screening drought tolerant indigenous aromatic rice cultivars. *Physiol. Mol. Biol. Plants* **2018**, *24*, 7–23. [CrossRef] [PubMed]
59. Dey, N.; Bhattacharjee, S. Accumulation of Polyphenolic Compounds and Osmolytes under Dehydration Stress and Their Implication in Redox Regulation in Four Indigenous Aromatic Rice Cultivars. *Rice Sci.* **2020**, *27*, 329–344. [CrossRef]
60. Chen, D.; Shao, Q.; Yin, L.; Younis, A.; Zheng, B. Polyamine Function in Plants: Metabolism, Regulation on Development, and Roles in Abiotic Stress Responses. *Front. Plant Sci.* **2019**, *9*, 1945. [CrossRef]
61. Capell, T.; Bassie, L.; Christou, P. Modulation of the polyamine biosynthetic pathway in transgenic rice confers tolerance to drought stress. *Proc. Natl. Acad. Sci. USA* **2004**, *101*, 9909–9914. [CrossRef]
62. Kuru, İ.; Işıkalan, Ç.; Akbaş, F. Physiological and Biochemical Responses of Rice (*Oryza Sativa* L.) Varieties Against Drought Stress. *Bangladesh J. Bot.* **2021**, *50*, 335–342. [CrossRef]

63. Fujita, M.; Fujita, Y.; Noutoshi, Y.; Takahashi, F.; Narusaka, Y.; Yamaguchi-Shinozaki, K.; Shinozaki, K. Crosstalk between abiotic and biotic stress responses: A current view from the points of convergence in the stress signaling networks. *Curr. Opin. Plant Biol.* **2006**, *9*, 436–442. [CrossRef] [PubMed]
64. Hoang, X.L.T.; Nhi, D.N.H.; Thu, N.B.A.; Thao, N.P.; Tran, L.-S.P. Transcription Factors and Their Roles in Signal Transduction in Plants under Abiotic Stresses. *Curr. Genom.* **2017**, *18*, 483–497. [CrossRef] [PubMed]
65. Gao, J.-P.; Chao, D.-Y.; Lin, H.-X. Toward understanding molecular mechanisms of abiotic stress responses in rice. *Rice* **2008**, *1*, 36–51. [CrossRef]
66. Maruyama, K.; Todaka, D.; Mizoi, J.; Yoshida, T.; Kidokoro, S.; Matsukura, S.; Takasaki, H.; Sakurai, T.; Yamamoto, Y.Y.; Yoshiwara, K.; et al. Identification of Cis-Acting Promoter Elements in Cold- and Dehydration-Induced Transcriptional Pathways in Arabidopsis, Rice, and Soybean. *DNA Res.* **2012**, *19*, 37–49. [CrossRef] [PubMed]
67. Deng, Y.; Kashtoh, H.; Wang, Q.; Zhen, G.; Li, Q.; Tang, L.; Gao, H.; Zhang, C.; Qin, L.; Su, M.; et al. Structure and activity of SLAC1 channels for stomatal signaling in leaves. *Proc. Natl. Acad. Sci. USA* **2021**, *118*, e2015151118. [CrossRef] [PubMed]
68. Kashtoh, H.; Baek, K.-H. Structural and Functional Insights into the Role of Guard Cell Ion Channels in Abiotic Stress-Induced Stomatal Closure. *Plants* **2021**, *10*, 2774. [CrossRef] [PubMed]
69. Ma, Y.; Szostkiewicz, I.; Korte, A.; Moes, D.; Yang, Y.; Christmann, A.; Grill, E. Regulators of PP2C Phosphatase Activity Function as Abscisic Acid Sensors. *Science* **2009**, *324*, 1064–1068. [CrossRef]
70. Park, S.-Y.; Fung, P.; Nishimura, N.; Jensen, D.R.; Fujii, H.; Zhao, Y.; Lumba, S.; Santiago, J.; Rodrigues, A.; Chow, T.F.; et al. Abscisic Acid Inhibits Type 2C Protein Phosphatases via the PYR/PYL Family of START Proteins. *Science* **2009**, *324*, 1068–1071. [CrossRef]
71. Chen, X.; Ding, Y.; Yang, Y.; Song, C.; Wang, B.; Yang, S.; Guo, Y.; Gong, Z. Protein kinases in plant responses to drought, salt, and cold stress. *J. Integr. Plant Biol.* **2021**, *63*, 53–78. [CrossRef]
72. Kim, H.; Lee, K.; Hwang, H.; Bhatnagar, N.; Kim, D.-Y.; Yoon, I.S.; Byun, M.-O.; Kim, S.T.; Jung, K.-H.; Kim, B.-G. Overexpression of PYL5 in rice enhances drought tolerance, inhibits growth, and modulates gene expression. *J. Exp. Bot.* **2014**, *65*, 453–464. [CrossRef]
73. Matsukura, S.; Mizoi, J.; Yoshida, T.; Todaka, D.; Ito, Y.; Maruyama, K.; Shinozaki, K.; Yamaguchi-Shinozaki, K. Comprehensive analysis of rice DREB2-type genes that encode transcription factors involved in the expression of abiotic stress-responsive genes. *Mol. Genet. Genom.* **2010**, *283*, 185–196. [CrossRef] [PubMed]
74. Blum, A. Effective use of water (EUW) and not water-use efficiency (WUE) is the target of crop yield improvement under drought stress. *Field Crop. Res.* **2009**, *112*, 119–123. [CrossRef]
75. Uga, Y.; Sugimoto, K.; Ogawa, S.; Rane, J.; Ishitani, M.; Hara, N.; Kitomi, Y.; Inukai, Y.; Ono, K.; Kanno, N.; et al. Control of root system architecture by DEEPER ROOTING 1 increases rice yield under drought conditions. *Nat. Genet.* **2013**, *45*, 1097–1102. [CrossRef] [PubMed]
76. Rahman, H.; Ramanathan, V.; Nallathambi, J.; Duraialagaraja, S.; Muthurajan, R. Over-expression of a NAC 67 transcription factor from finger millet (*Eleusine coracana* L.) confers tolerance against salinity and drought stress in rice. *BMC Biotechnol.* **2016**, *16*, 35. [CrossRef] [PubMed]
77. Ning, J.; Li, X.; Hicks, L.M.; Xiong, L. A raf-like MAPKKK gene DSM1 mediates drought resistance through reactive oxygen species scavenging in rice. *Plant Physiol.* **2010**, *152*, 876–890. [CrossRef] [PubMed]
78. Rahman, A.; Nahar, K.; Hasanuzzaman, M.; Fujita, M. Calcium Supplementation Improves Na+/K+ Ratio, Antioxidant Defense and Glyoxalase Systems in Salt-Stressed Rice Seedlings. *Front. Plant Sci.* **2016**, *7*, 609. [CrossRef] [PubMed]
79. Jeong, J.S.; Kim, Y.S.; Redillas, M.C.F.R.; Jang, G.; Jung, H.; Bang, S.W.; Choi, Y.D.; Ha, S.H.; Reuzeau, C.; Kim, J.K. OsNAC5 overexpression enlarges root diameter in rice plants leading to enhanced drought tolerance and increased grain yield in the field. *Plant Biotechnol. J.* **2013**, *11*, 101–114. [CrossRef]
80. Hu, H.; Dai, M.; Yao, J.; Xiao, B.; Li, X.; Zhang, Q.; Xiong, L. Overexpressing a NAM, ATAF, and CUC (NAC) transcription factor enhances drought resistance and salt tolerance in rice. *Proc. Natl. Acad. Sci. USA* **2006**, *103*, 12987–12992. [CrossRef]
81. Xiao, B.; Huang, Y.; Tang, N.; Xiong, L. Over-expression of a LEA gene in rice improves drought resistance under the field conditions. *Theor. Appl. Genet.* **2007**, *115*, 35–46. [CrossRef]
82. Xiang, Y.; Tang, N.; Du, H.; Ye, H.; Xiong, L. Characterization of OsbZIP23 as a Key Player of the Basic Leucine Zipper Transcription Factor Family for Conferring Abscisic Acid Sensitivity and Salinity and Drought Tolerance in Rice. *Plant Physiol.* **2008**, *148*, 1938–1952. [CrossRef]
83. Lu, G.; Gao, C.; Zheng, X.; Han, B. Identification of OsbZIP72 as a positive regulator of ABA response and drought tolerance in rice. *Planta* **2009**, *229*, 605–615. [CrossRef] [PubMed]
84. Oh, S.J.; Kim, Y.S.; Kwon, C.W.; Park, H.K.; Jeong, J.S.; Kim, J.K. Overexpression of the Transcription Factor AP37 in Rice Improves Grain Yield under Drought Conditions. *Plant Physiol.* **2009**, *150*, 1368–1379. [CrossRef] [PubMed]
85. Jeong, J.S.; Kim, Y.S.; Baek, K.H.; Jung, H.; Ha, S.H.; Choi, Y.D.Y.D.; Kim, M.; Reuzeau, C.; Kim, J.K. Root-Specific Expression of OsNAC10 Improves Drought Tolerance and Grain Yield in Rice under Field Drought Conditions. *Plant Physiol.* **2010**, *153*, 185–197. [CrossRef] [PubMed]
86. Yu, L.; Chen, X.; Wang, Z.; Wang, S.; Wang, Y.; Zhu, Q.; Li, S.; Xiang, C. Arabidopsis Enhanced Drought Tolerance1/HOMEODOMAIN GLABROUS11 Confers Drought Tolerance in Transgenic Rice without Yield Penalty. *Plant Physiol.* **2013**, *162*, 1378–1391. [CrossRef] [PubMed]

87. Ravikumar, G.; Manimaran, P.; Voleti, S.R.; Subrahmanyam, D.; Sundaram, R.M.; Bansal, K.C.; Viraktamath, B.C.; Balachandran, S.M. Stress-inducible expression of AtDREB1A transcription factor greatly improves drought stress tolerance in transgenic indica rice. *Transgenic Res.* **2014**, *23*, 421–439. [CrossRef] [PubMed]
88. Wei, S.; Hu, W.; Deng, X.; Zhang, Y.; Liu, X.; Zhao, X.; Luo, Q.; Jin, Z.; Li, Y.; Zhou, S.; et al. A Rice Calcium-Dependent Protein Kinase OsCPK9 Positively Regulates Drought Stress Tolerance and Spikelet Fertility. *BMC Plant Biol.* **2014**, *14*, 133. [CrossRef]
89. You, J.; Hu, H.; Xiong, L. An ornithine δ-aminotransferase gene OsOAT confers drought and oxidative stress tolerance in rice. *Plant Sci.* **2012**, *197*, 59–69. [CrossRef] [PubMed]
90. Li, H.-W.; Zang, B.-S.; Deng, X.-W.; Wang, X.-P. Overexpression of the trehalose-6-phosphate synthase gene OsTPS1 enhances abiotic stress tolerance in rice. *Planta* **2011**, *234*, 1007–1018. [CrossRef]
91. Zhu, B.; Su, J.; Chang, M.; Verma, D.P.S.; Fan, Y.-L.; Wu, R. Overexpression of a Δ1-pyrroline-5-carboxylate synthetase gene and analysis of tolerance to water- and salt-stress in transgenic rice. *Plant Sci.* **1998**, *139*, 41–48. [CrossRef]
92. Chandra Babu, R.; Zhang, J.; Blum, A.; David Ho, T.-H.; Wu, R.; Nguyen, H. HVA1, a LEA gene from barley confers dehydration tolerance in transgenic rice (*Oryza sativa* L.) via cell membrane protection. *Plant Sci.* **2004**, *166*, 855–862. [CrossRef]
93. Zhang, L.; Xiao, S.; Li, W.; Feng, W.; Li, J.; Wu, Z.; Gao, X.; Liu, F.; Shao, M. Overexpression of a Harpin-encoding gene hrf1 in rice enhances drought tolerance. *J. Exp. Bot.* **2011**, *62*, 4229–4238. [CrossRef] [PubMed]
94. Zhang, Z.; Li, F.; Li, D.; Zhang, H.; Huang, R. Expression of ethylene response factor JERF1 in rice improves tolerance to drought. *Planta* **2010**, *232*, 765–774. [CrossRef] [PubMed]
95. Bae, H.; Kim, S.K.; Cho, S.K.; Kang, B.G.; Kim, W.T. Overexpression of OsRDCP1, a rice RING domain-containing E3 ubiquitin ligase, increased tolerance to drought stress in rice (*Oryza sativa* L.). *Plant Sci.* **2011**, *180*, 775–782. [CrossRef]
96. Gao, T.; Wu, Y.; Zhang, Y.; Liu, L.; Ning, Y.; Wang, D.; Tong, H.; Chen, S.; Chu, C.; Xie, Q. OsSDIR1 overexpression greatly improves drought tolerance in transgenic rice. *Plant Mol. Biol.* **2011**, *76*, 145–156. [CrossRef] [PubMed]
97. You, J.; Zong, W.; Li, X.; Ning, J.; Hu, H.; Li, X.; Xiao, J.; Xiong, L. The SNAC1-targeted gene OsSRO1c modulates stomatal closure and oxidative stress tolerance by regulating hydrogen peroxide in rice. *J. Exp. Bot.* **2013**, *64*, 569–583. [CrossRef] [PubMed]
98. Samota, M.K.; Sasi, M.; Awana, M.; Yadav, O.P.; Amitha Mithra, S.V.; Tyagi, A.; Kumar, S.; Singh, A. Elicitor-Induced Biochemical and Molecular Manifestations to Improve Drought Tolerance in Rice (*Oryza Sativa* L.) through Seed-Priming. *Front. Plant Sci.* **2017**, *8*, 934. [CrossRef]
99. Pandey, V.; Ansari, M.W.; Tula, S.; Yadav, S.; Sahoo, R.K.; Shukla, N.; Bains, G.; Badal, S.; Chandra, S.; Gaur, A.K.; et al. Dose-dependent response of Trichoderma harzianum in improving drought tolerance in rice genotypes. *Planta* **2016**, *243*, 1251–1264. [CrossRef]
100. Wu, C.; Cui, K.; Wang, W.; Li, Q.; Fahad, S.; Hu, Q.; Huang, J.; Nie, L.; Peng, S. Heat-Induced Phytohormone Changes Are Associated with Disrupted Early Reproductive Development and Reduced Yield in Rice. *Sci. Rep.* **2016**, *6*, 34978. [CrossRef]
101. Zhao, C.; Liu, B.; Piao, S.; Wang, X.; Lobell, D.B.; Huang, Y.; Huang, M.; Yao, Y.; Bassu, S.; Ciais, P.; et al. Temperature increase reduces global yields of major crops in four independent estimates. *Proc. Natl. Acad. Sci. USA* **2017**, *114*, 9326–9331. [CrossRef]
102. Kilasi, N.L.; Singh, J.; Vallejos, C.E.; Ye, C.; Jagadish, S.V.K.; Kusolwa, P.; Rathinasabapathi, B. Heat Stress Tolerance in Rice (*Oryza Sativa* L.): Identification of Quantitative Trait Loci and Candidate Genes for Seedling Growth Under Heat Stress. *Front. Plant Sci.* **2018**, *9*, 1578. [CrossRef]
103. Wang, Y.; Wang, L.; Zhou, J.; Hu, S.; Chen, H.; Xiang, J.; Zhang, Y.Y.Y.; Zeng, Y.; Shi, Q.; Zhu, D.; et al. Research Progress on Heat Stress of Rice at Flowering Stage. *Rice Sci.* **2019**, *26*, 1–10. [CrossRef]
104. Ishimaru, T.; Hirabayashi, H.; Kuwagata, T.; Ogawa, T.; Kondo, M. The Early-Morning Flowering Trait of Rice Reduces Spikelet Sterility under Windy and Elevated Temperature Conditions at Anthesis. *Plant Prod. Sci.* **2012**, *15*, 19–22. [CrossRef]
105. Fahad, S.; Ihsan, M.Z.; Khaliq, A.; Daur, I.; Saud, S.; Alzamanan, S.; Nasim, W.; Abdullah, M.; Khan, I.A.; Wu, C.; et al. Consequences of high temperature under changing climate optima for rice pollen characteristics-concepts and perspectives. *Arch. Agron. Soil Sci.* **2018**, *64*, 1473–1488. [CrossRef]
106. Ranathunge, K.; Steudle, E.; Lafitte, R. Control of water uptake by rice (*Oryza sativa* L.): Role of the outer part of the root. *Planta* **2003**, *217*, 193–205. [CrossRef]
107. Khan, S.; Anwar, S.; Ashraf, M.Y.; Khaliq, B.; Sun, M.; Hussain, S.; Gao, Z.; Noor, H.; Alam, S. Mechanisms and Adaptation Strategies to Improve Heat Tolerance in Rice. A Review. *Plants* **2019**, *8*, 508. [CrossRef] [PubMed]
108. Ren, H.; Bao, J.; Gao, Z.; Sun, D.; Zheng, S.; Bai, J. How rice adapts to high temperatures. *Front. Plant Sci.* **2023**, *14*, 1137923. [CrossRef] [PubMed]
109. González-García, M.P.; Conesa, C.M.; Lozano-Enguita, A.; Baca-González, V.; Simancas, B.; Navarro-Neila, S.; Sánchez-Bermúdez, M.; Salas-González, I.; Caro, E.; Castrillo, G.; et al. Temperature changes in the root ecosystem affect plant functionality. *Plant Commun.* **2023**, *4*, 100514. [CrossRef] [PubMed]
110. Arai-Sanoh, Y.; Ishimaru, T.; Ohsumi, A.; Kondo, M. Effects of Soil Temperature on Growth and Root Function in Rice. *Plant Prod. Sci.* **2010**, *13*, 235–242. [CrossRef]
111. Yamakawa, Y.; Kishikawa, H. On the Effect of Temperature upon the Division and Elongation of Cells in the Root of Rice Plant. *Jpn. J. Crop Sci.* **1957**, *26*, 94–95. [CrossRef]
112. Liu, J.; Hasanuzzaman, M.; Wen, H.; Zhang, J.; Peng, T.; Sun, H.; Zhao, Q. High temperature and drought stress cause abscisic acid and reactive oxygen species accumulation and suppress seed germination growth in rice. *Protoplasma* **2019**, *256*, 1217–1227. [CrossRef]

113. Liu, J.; Sun, X.; Xu, F.; Zhang, Y.; Zhang, Q.; Miao, R.; Zhang, J.; Liang, J.; Xu, W. Suppression of OsMDHAR4 Enhances Heat Tolerance by Mediating H_2O_2-Induced Stomatal Closure in Rice Plants. *Rice* **2018**, *11*, 38. [CrossRef] [PubMed]
114. Chaudhary, T.N.; Ghildyal, B.P. Germination Response of Rice Seeds to Constant and Alternating Temperatures. *Agron. J.* **1969**, *61*, 328–330. [CrossRef]
115. Baker, J.T. Yield responses of southern US rice cultivars to CO_2 and temperature. *Agric. For. Meteorol.* **2004**, *122*, 129–137. [CrossRef]
116. Sandhu, J.; Irvin, L.; Liu, K.; Staswick, P.; Zhang, C.; Walia, H. Endoplasmic Reticulum Stress Pathway Mediates the Early Heat Stress Response of Developing Rice Seeds. *Plant. Cell Environ.* **2021**, *44*, 2604–2624. [CrossRef] [PubMed]
117. Jagadish, S.V.K.; Murty, M.V.R.; Quick, W.P. Rice Responses to Rising Temperatures--Challenges, Perspectives and Future Directions. *Plant. Cell Environ.* **2015**, *38*, 1686–1698. [CrossRef] [PubMed]
118. Arshad, M.S.; Farooq, M.; Asch, F.; Krishna, J.S.V.; Prasad, P.V.V.; Siddique, K.H.M. Thermal stress impacts reproductive development and grain yield in rice. *Plant Physiol. Biochem.* **2017**, *115*, 57–72. [CrossRef] [PubMed]
119. Soda, N.; Gupta, B.K.; Anwar, K.; Sharan, A.; Govindjee, S.-P.L.S.; Pareek, A.; Govindjee; Singla-Pareek, S.L.; Pareek, A. Rice Intermediate Filament, OsIF, Stabilizes Photosynthetic Machinery and Yield under Salinity and Heat Stress. *Sci. Rep.* **2018**, *8*, 4072. [CrossRef] [PubMed]
120. Wang, H.H.; Wang, H.H.; Shao, H.; Tang, X. Recent Advances in Utilizing Transcription Factors to Improve Plant Abiotic Stress Tolerance by Transgenic Technology. *Front. Plant Sci.* **2016**, *7*, 67. [CrossRef]
121. Miyahara, K.; Wada, T.; Sonoda, J.-Y.; Tsukaguchi, T.; Miyazaki, M.; Tsubone, M.; Yamaguchi, O.; Ishibashi, M.; Iwasawa, N.; Umemoto, T.; et al. Detection and validation of QTLs for milky-white grains caused by high temperature during the ripening period in Japonica rice. *Breed. Sci.* **2017**, *67*, 333–339. [CrossRef]
122. Kaneko, K.; Sasaki, M.; Kuribayashi, N.; Suzuki, H.; Sasuga, Y.; Shiraya, T.; Inomata, T.; Itoh, K.; Baslam, M.; Mitsui, T. Proteomic and Glycomic Characterization of Rice Chalky Grains Produced Under Moderate and High-Temperature Conditions in Field System. *Rice* **2016**, *9*, 26. [CrossRef]
123. Nevame, A.Y.M.; Emon, R.M.; Malek, M.A.; Hasan, M.M.; Alam, M.A.; Muharam, F.M.; Aslani, F.; Rafii, M.Y.; Ismail, M.R. Relationship between High Temperature and Formation of Chalkiness and Their Effects on Quality of Rice. *Biomed Res. Int.* **2018**, *1653721*, 1653721. [CrossRef] [PubMed]
124. Wada, T.; Miyahara, K.; Sonoda, J.-Y.; Tsukaguchi, T.; Miyazaki, M.; Tsubone, M.; Ando, T.; Ebana, K.; Yamamoto, T.; Iwasawa, N.; et al. Detection of QTLs for white-back and basal-white grains caused by high temperature during ripening period in japonica rice. *Breed. Sci.* **2015**, *65*, 216–225. [CrossRef] [PubMed]
125. Wu, Y.S.; Yang, C.Y. Ethylene-Mediated Signaling Confers Thermotolerance and Regulates Transcript Levels of Heat Shock Factors in Rice Seedlings under Heat Stress. *Bot. Stud.* **2019**, *60*, 23. [CrossRef] [PubMed]
126. Li, S.; Jiang, H.; Wang, J.; Wang, Y.; Pan, S.; Tian, H.; Duan, M.; Wang, S.; Tang, X.; Mo, Z. Responses of Plant Growth, Physiological, Gas Exchange Parameters of Super and Non-Super Rice to Rhizosphere Temperature at the Tillering Stage. *Sci. Rep.* **2019**, *9*, 10618. [CrossRef] [PubMed]
127. Li, X.-M.; Chao, D.-Y.; Wu, Y.; Huang, X.; Chen, K.; Cui, L.-G.; Su, L.; Ye, W.-W.; Chen, H.; Chen, H.-C.; et al. Natural alleles of a proteasome α2 subunit gene contribute to thermotolerance and adaptation of African rice. *Nat. Genet.* **2015**, *47*, 827–833. [CrossRef] [PubMed]
128. Allakhverdiev, S.I.; Kreslavski, V.D.; Klimov, V.V.; Los, D.A.; Carpentier, R.; Mohanty, P. Heat stress: An overview of molecular responses in photosynthesis. *Photosynth. Res.* **2008**, *98*, 541–550. [CrossRef] [PubMed]
129. Rodriguez, M.; Canales, E.; Borras-Hidalgo, O. Molecular aspects of abiotic stress in plants. *Biotecnol. Apl.* **2005**, *22*, 1–10.
130. Djanaguiraman, M.; Annie Sheeba, J.; Durga Devi, D.; Bangarusamy, U. Cotton Leaf Senescence Can Be Delayed by Nitrophenolate Spray through Enhanced Antioxidant Defence System. *J. Agron. Crop Sci.* **2009**, *195*, 213–224. [CrossRef]
131. Zhao, Q.; Zhou, L.; Liu, J.; Du, X.; Asad, M.-A.-U.; Huang, F.; Pan, G.; Cheng, F. Relationship of ROS accumulation and superoxide dismutase isozymes in developing anther with floret fertility of rice under heat stress. *Plant Physiol. Biochem. PPB* **2018**, *122*, 90–101. [CrossRef]
132. Awasthi, R.; Bhandari, K.; Nayyar, H. Temperature stress and redox homeostasis in agricultural crops. *Front. Environ. Sci.* **2015**, *3*, 11. [CrossRef]
133. Soengas, P.; Rodríguez, V.M.; Velasco, P.; Cartea, M.E. Effect of Temperature Stress on Antioxidant Defenses in Brassica Oleracea. *ACS Omega* **2018**, *3*, 5237–5243. [CrossRef] [PubMed]
134. Hasanuzzaman, M.; Nahar, K.; Alam, M.; Roychowdhury, R.; Fujita, M. Physiological, Biochemical, and Molecular Mechanisms of Heat Stress Tolerance in Plants. *Int. J. Mol. Sci.* **2013**, *14*, 9643–9684. [CrossRef] [PubMed]
135. Zou, J.; Liu, C.; Chen, X. Proteomics of rice in response to heat stress and advances in genetic engineering for heat tolerance in rice. *Plant Cell Rep.* **2011**, *30*, 2155–2165. [CrossRef] [PubMed]
136. Lee, B.-H.; Won, S.-H.; Lee, H.-S.; Miyao, M.; Chung, W.-I.; Kim, I.-J.; Jo, J. Expression of the chloroplast-localized small heat shock protein by oxidative stress in rice. *Gene* **2000**, *245*, 283–290. [CrossRef]
137. Wu, X.; Shiroto, Y.; Kishitani, S.; Ito, Y.; Toriyama, K. Enhanced heat and drought tolerance in transgenic rice seedlings overexpressing OsWRKY11 under the control of HSP101 promoter. *Plant Cell Rep.* **2009**, *28*, 21–30. [CrossRef] [PubMed]
138. Fang, Y.; Liao, K.; Du, H.; Xu, Y.; Song, H.; Li, X.; Xiong, L. A stress-responsive NAC transcription factor SNAC3 confers heat and drought tolerance through modulation of reactive oxygen species in rice. *J. Exp. Bot.* **2015**, *66*, 6803–6817. [CrossRef] [PubMed]

139. El-kereamy, A.; Bi, Y.M.; Ranathunge, K.; Beatty, P.H.; Good, A.G.; Rothstein, S.J. The Rice R2R3-MYB Transcription Factor OsMYB55 Is Involved in the Tolerance to High Temperature and Modulates Amino Acid Metabolism. *PLoS ONE* **2012**, *7*, 52030. [CrossRef]
140. Ambavaram, M.M.R.; Basu, S.; Krishnan, A.; Ramegowda, V.; Batlang, U.; Rahman, L.; Baisakh, N.; Pereira, A. Coordinated regulation of photosynthesis in rice increases yield and tolerance to environmental stress. *Nat. Commun.* **2014**, *5*, 5302. [CrossRef]
141. Lim, S.D.; Cho, H.Y.; Park, Y.C.; Ham, D.J.; Lee, J.K.; Jang, C.S. The rice RING finger E3 ligase, OsHCI1, drives nuclear export of multiple substrate proteins and its heterogeneous overexpression enhances acquired thermotolerance. *J. Exp. Bot.* **2013**, *64*, 2899–2914. [CrossRef]
142. Zhang, B.; Wu, S.; Zhang, Y.; Xu, T.; Guo, F.; Tang, H.; Li, X.; Wang, P.; Qian, W.; Xue, Y. A High Temperature-Dependent Mitochondrial Lipase EXTRA GLUME1 Promotes Floral Phenotypic Robustness against Temperature Fluctuation in Rice (*Oryza sativa* L.). *PLOS Genet.* **2016**, *12*, e1006152. [CrossRef]
143. Hossain, M.A.; Cho, J.I.; Han, M.; Ahn, C.H.; Jeon, J.S.; An, G.; Park, P.B. The ABRE-binding bZIP transcription factor OsABF2 is a positive regulator of abiotic stress and ABA signaling in rice. *J. Plant Physiol.* **2010**, *167*, 1512–1520. [CrossRef]
144. Liu, J.G.; Qin, Q.-L.; Zhang, Z.; Peng, R.H.; Xiong, A.S.; Chen, J.M.; Yao, Q.H. OsHSF7 Gene in Rice, *Oryza Sativa* L., Encodes a Transcription Factor That Functions as a High Temperature Receptive and Responsive Factor. *BMB Rep.* **2009**, *42*, 16–21. [CrossRef]
145. Lin, M.Y.; Chai, K.H.; Ko, S.S.; Kuang, L.Y.; Lur, H.S.; Charng, Y.Y. A Positive Feedback Loop between Heat Shock Protein101 And Heat Stress-Associated 32-Kd Protein Modulates Long-Term Acquired Thermotolerance Illustrating Diverse Heat Stress Responses in Rice Varieties. *Plant Physiol.* **2014**, *164*, 2045–2053. [CrossRef] [PubMed]
146. Liu, J.; Zhang, C.; Wei, C.; Liu, X.; Wang, M.; Yu, F.; Xie, Q.; Tu, J. The RING Finger Ubiquitin E3 Ligase OsHTAS Enhances Heat Tolerance by Promoting H_2O_2-Induced Stomatal Closure in Rice. *Plant Physiol.* **2016**, *170*, 429–443. [CrossRef] [PubMed]
147. Zheng, K.; Zhao, J.; Lin, D.; Chen, J.; Xu, J.; Zhou, H.; Teng, S.; Dong, Y. The Rice TCM5 Gene Encoding a Novel Deg Protease Protein Is Essential for Chloroplast Development under High Temperatures. *Rice* **2016**, *9*, 13. [CrossRef] [PubMed]
148. Wang, D.; Qin, B.; Li, X.; Tang, D.; Zhang, Y.; Cheng, Z.; Xue, Y. Nucleolar DEAD-Box RNA Helicase TOGR1 Regulates Thermotolerant Growth as a Pre-rRNA Chaperone in Rice. *PLoS Genet.* **2016**, *12*, e1005844. [CrossRef] [PubMed]
149. Xia, S.; Liu, H.; Cui, Y.; Yu, H.; Rao, Y.; Yan, Y.; Zeng, D.; Hu, J.; Zhang, G.; Gao, Z.; et al. UDP-N-Acetylglucosamine Pyrophosphorylase Enhances Rice Survival at High Temperature. *New Phytol.* **2022**, *233*, 344–359. [CrossRef] [PubMed]
150. Chen, K.; Guo, T.; Li, X.M.; Zhang, Y.M.; Yang, Y.B.; Ye, W.W.; Dong, N.Q.; Shi, C.L.; Kan, Y.; Xiang, Y.H.; et al. Translational Regulation of Plant Response to High Temperature by a Dual-Function TRNAHis Guanylyltransferase in Rice. *Mol. Plant* **2019**, *12*, 1123–1142. [CrossRef] [PubMed]
151. Liu, X.; Lyu, Y.; Yang, W.; Yang, Z.; Lu, S.; Liu, J. A membrane-associated NAC transcription factor OsNTL3 is involved in thermotolerance in rice. *Plant Biotechnol. J.* **2020**, *18*, 1317–1329. [CrossRef]
152. Singh, A.; Mittal, D.; Lavania, D.; Agarwal, M.; Mishra, R.C.; Grover, A. OsHsfA2c and OsHsfB4b are involved in the transcriptional regulation of cytoplasmic OsClpB (Hsp100) gene in rice (*Oryza sativa* L.). *Cell Stress Chaperones* **2012**, *17*, 243–254. [CrossRef]
153. Tang, Y.; Gao, C.-C.; Gao, Y.; Yang, Y.; Shi, B.; Yu, J.-L.; Lyu, C.; Sun, B.-F.; Wang, H.-L.; Xu, Y.; et al. OsNSUN2-Mediated 5-Methylcytosine mRNA Modification Enhances Rice Adaptation to High Temperature. *Dev. Cell* **2020**, *53*, 272–286.e7. [CrossRef] [PubMed]
154. Zhang, H.; Zhou, J.-F.; Kan, Y.; Shan, J.-X.; Ye, W.-W.; Dong, N.-Q.; Guo, T.; Xiang, Y.-H.; Yang, Y.-B.; Li, Y.-C.; et al. A genetic module at one locus in rice protects chloroplasts to enhance thermotolerance. *Science* **2022**, *376*, 1293–1300. [CrossRef] [PubMed]
155. Qiao, B.; Zhang, Q.; Liu, D.; Wang, H.; Yin, J.; Wang, R.; He, M.; Cui, M.; Shang, Z.; Wang, D.; et al. A calcium-binding protein, rice annexin OsANN1, enhances heat stress tolerance by modulating the production of H_2O_2. *J. Exp. Bot.* **2015**, *66*, 5853–5866. [CrossRef] [PubMed]
156. Jeandet, P.; Formela-Luboińska, M.; Labudda, M.; Morkunas, I. The Role of Sugars in Plant Responses to Stress and Their Regulatory Function during Development. *Int. J. Mol. Sci.* **2022**, *23*, 5161. [CrossRef] [PubMed]
157. Miyazaki, M.; Araki, M.; Okamura, K.; Ishibashi, Y.; Yuasa, T.; Iwaya-Inoue, M. Assimilate translocation and expression of sucrose transporter, OsSUT1, contribute to high-performance ripening under heat stress in the heat-tolerant rice cultivar Genkitsukushi. *J. Plant Physiol.* **2013**, *170*, 1579–1584. [CrossRef] [PubMed]
158. Savada, R.P.; Ozga, J.A.; Jayasinghege, C.P.A.; Waduthanthri, K.D.; Reinecke, D.M. Heat stress differentially modifies ethylene biosynthesis and signaling in pea floral and fruit tissues. *Plant Mol. Biol.* **2017**, *95*, 313–331. [CrossRef] [PubMed]
159. Calderón-Páez, S.E.; Cueto-Niño, Y.A.; Sánchez-Reinoso, A.D.; Garces-Varon, G.; Chávez-Arias, C.C.; Restrepo-Díaz, H. Foliar boron compounds applications mitigate heat stress caused by high daytime temperatures in rice (*Oryza sativa* L.) Boron mitigates heat stress in rice. *J. Plant Nutr.* **2021**, *44*, 2514–2527. [CrossRef]
160. Li, J.; Zhang, Z.; Chong, K.; Xu, Y. Chilling tolerance in rice: Past and present. *J. Plant Physiol.* **2022**, *268*, 153576. [CrossRef]
161. Bhattacharya, A. Effect of Low-Temperature Stress on Germination, Growth, and Phenology of Plants: A Review. In *Physiological Processes in Plants Under Low Temperature Stress*; Springer: Singapore, 2022; pp. 1–106. [CrossRef]
162. Hsu, C.H.; Hsu, Y.T. Biochemical Responses of Rice Roots to Cold Stress. *Bot. Stud.* **2019**, *60*, 14. [CrossRef]

163. Reddy, K.R.; Seghal, A.; Jumaa, S.; Bheemanahalli, R.; Kakar, N.; Redoña, E.D.; Wijewardana, C.; Alsajri, F.A.; Chastain, D.; Gao, W.; et al. Morpho-Physiological Characterization of Diverse Rice Genotypes for Seedling Stage High- and Low-Temperature Tolerance. *Agronomy* **2021**, *11*, 112. [CrossRef]
164. Freitas, G.M.; Thomas, J.; Liyanage, R.; Lay, J.O.; Basu, S.; Ramegowda, V.; Amaral, M.N.; Benitez, L.C.; Bolacel Braga, E.J.; Pereira, A.; et al. Cold tolerance response mechanisms revealed through comparative analysis of gene and protein expression in multiple rice genotypes. *PLoS ONE* **2019**, *14*, e0218019. [CrossRef]
165. Baruah, A.R.; Ishigo-Oka, N.; Adachi, M.; Oguma, Y.; Tokizono, Y.; Onishi, K.; Sano, Y. Cold tolerance at the early growth stage in wild and cultivated rice. *Euphytica* **2009**, *165*, 459–470. [CrossRef]
166. González-Schain, N.; Roig-Villanova, I.; Kater, M.M. Early Cold Stress Responses in Post-Meiotic Anthers from Tolerant and Sensitive Rice Cultivars. *Rice* **2019**, *12*, 94. [CrossRef] [PubMed]
167. Nurhasanah Ritonga, F.; Chen, S. Physiological and Molecular Mechanism Involved in Cold Stress Tolerance in Plants. *Plants* **2020**, *9*, 560. [CrossRef] [PubMed]
168. Lu, X.; Song, S.; Xiao, Y.; Fan, F.; Zhou, Y.; Jia, G.; Tang, W.; Peng, J. Circadian Clock-Coordinated Response to Chilling Stress in Rice. *Environ. Exp. Bot.* **2021**, *185*, 104398. [CrossRef]
169. Shimono, H.; Fujimura, S.; Nishimura, T.; Hasegawa, T. Nitrogen Uptake by Rice (*Oryza sativa* L.) Exposed to Low Water Temperatures at Different Growth Stages. *J. Agron. Crop Sci.* **2012**, *198*, 145–151. [CrossRef]
170. Feng, H.; Yan, M.; Fan, X.; Li, B.; Shen, Q.; Miller, A.J.; Xu, G. Spatial expression and regulation of rice high-affinity nitrate transporters by nitrogen and carbon status. *J. Exp. Bot.* **2011**, *62*, 2319–2332. [CrossRef] [PubMed]
171. Lu, B.; Yuan, Y.; Zhang, C.; Ou, J.; Zhou, W.; Lin, Q. Modulation of key enzymes involved in ammonium assimilation and carbon metabolism by low temperature in rice (*Oryza sativa* L.) roots. *Plant Sci.* **2005**, *169*, 295–302. [CrossRef]
172. Guy, C.L. Cold Acclimation and Freezing Stress Tolerance: Role of Protein Metabolism. *Annu. Rev. Plant Physiol. Plant Mol. Biol.* **1990**, *41*, 187–223. [CrossRef]
173. Thomashow, M.F. Plant Cold Acclimation: Freezing Tolerance Genes and Regulatory Mechanisms. *Annu. Rev. Plant Physiol. Plant Mol. Biol.* **1999**, *50*, 571–599. [CrossRef]
174. Janmohammadi, M.; Zolla, L.; Rinalducci, S. Low temperature tolerance in plants: Changes at the protein level. *Phytochemistry* **2015**, *117*, 76–89. [CrossRef] [PubMed]
175. Dikilitas, M.; Karakas, S.; Simsek, E.; Yadav, A.N. Microbes from cold deserts and their applications in mitigation of cold stress in plants. In *Microbiomes of Extreme Environments*; CRC Press: Boca Raton, FL, USA, 2021; pp. 126–152, ISBN 9780429328633.
176. Steponkus, P.L.; Uemura, M.; Joseph, R.A.; Gilmour, S.J.; Thomashow, M.F. Mode of action of the COR15a gene on the freezing tolerance of Arabidopsis thaliana. *Proc. Natl. Acad. Sci. USA* **1998**, *95*, 14570–14575. [CrossRef] [PubMed]
177. Kaplan, F.; Kopka, J.; Sung, D.Y.; Zhao, W.; Popp, M.; Porat, R.; Guy, C.L. Transcript and metabolite profiling during cold acclimation of Arabidopsis reveals an intricate relationship of cold-regulated gene expression with modifications in metabolite content. *Plant J.* **2007**, *50*, 967–981. [CrossRef] [PubMed]
178. Ruelland, E.; Vaultier, M.-N.N.; Zachowski, A.; Hurry, V. Chapter 2 Cold Signalling and Cold Acclimation in Plants. In *Advances in Botanical Research*; Elsevier: Amsterdam, The Netherlands, 2009; Volume 49, pp. 35–150.
179. Yu, X.; Peng, Y.H.; Zhang, M.H.; Shao, Y.J.; Su, W.A.; Tang, Z.C. Water relations and an expression analysis of plasma membrane intrinsic proteins in sensitive and tolerant rice during chilling and recovery. *Cell Res.* **2006**, *16*, 599–608. [CrossRef] [PubMed]
180. Ahamed, A.; Murai-Hatano, M.; Ishikawa-Sakurai, J.; Hayashi, H.; Kawamura, Y.; Uemura, M. Cold Stress-Induced Acclimation in Rice is Mediated by Root-Specific Aquaporins. *Plant Cell Physiol.* **2012**, *53*, 1445–1456. [CrossRef] [PubMed]
181. Maurel, C.; Boursiac, Y.; Luu, D.-T.; Santoni, V.; Shahzad, Z.; Verdoucq, L. Aquaporins in Plants. *Physiol. Rev.* **2015**, *95*, 1321–1358. [CrossRef] [PubMed]
182. Maurel, C.; Javot, H.; Lauvergeat, V.; Gerbeau, P.; Tournaire, C.; Santoni, V.; Heyes, J. Molecular physiology of aquaporins in plants. In *International Review of Cytology*; Elsevier: Amsterdam, The Netherlands, 2002; Volume 215, pp. 105–148. [CrossRef]
183. Javot, H.; Lauvergeat, V.; Santoni, V.; Martin-Laurent, F.; Güçlü, J.; Vinh, J.; Heyes, J.; Franck, K.I.; Schäffner, A.R.; Bouchez, D.; et al. Role of a Single Aquaporin Isoform in Root Water Uptake. *Plant Cell* **2003**, *15*, 509–522. [CrossRef]
184. Postaire, O.; Tournaire-Roux, C.; Grondin, A.; Boursiac, Y.; Morillon, R.; Schäffner, A.R.; Maurel, C. A PIP1 Aquaporin Contributes to Hydrostatic Pressure-Induced Water Transport in Both the Root and Rosette of Arabidopsis. *Plant Physiol.* **2010**, *152*, 1418–1430. [CrossRef]
185. Murai-Hatano, M.; Kuwagata, T.; Sakurai, J.; Nonami, H.; Ahamed, A.; Nagasuga, K.; Matsunami, T.; Fukushi, K.; Maeshima, M.; Okada, M. Effect of Low Root Temperature on Hydraulic Conductivity of Rice Plants and the Possible Role of Aquaporins. *Plant Cell Physiol.* **2008**, *49*, 1294–1305. [CrossRef]
186. Aroca, R.; Amodeo, G.; Fernández-Illescas, S.; Herman, E.M.; Chaumont, F.; Chrispeels, M.J. The Role of Aquaporins and Membrane Damage in Chilling and Hydrogen Peroxide Induced Changes in the Hydraulic Conductance of Maize Roots. *Plant Physiol.* **2005**, *137*, 341–353. [CrossRef]
187. Sakurai, J.; Ishikawa, F.; Yamaguchi, T.; Uemura, M.; Maeshima, M. Identification of 33 Rice Aquaporin Genes and Analysis of Their Expression and Function. *Plant Cell Physiol.* **2005**, *46*, 1568–1577. [CrossRef] [PubMed]
188. Bhattacharjee, S. Heat and chilling induced disruption of redox homeostasis and its regulation by hydrogen peroxide in germinating rice seeds (*Oryza sativa* L., Cultivar Ratna). *Physiol. Mol. Biol. Plants* **2013**, *19*, 199–207. [CrossRef] [PubMed]

189. Hung, K.T.; Cheng, D.G.; Hsu, Y.T.; Kao, C.H. Abscisic acid-induced hydrogen peroxide is required for anthocyanin accumulation in leaves of rice seedlings. *J. Plant Physiol.* **2008**, *165*, 1280–1287. [CrossRef] [PubMed]
190. Seifi, H.S.; Van Bockhaven, J.; Angenon, G.; Höfte, M. Glutamate Metabolism in Plant Disease and Defense: Friend or Foe? *Mol. Plant-Microbe Interact.* **2013**, *26*, 475–485. [CrossRef] [PubMed]
191. Kavi Kishor, P.B.; Sreenivasulu, N. Is proline accumulation per se correlated with stress tolerance or is proline homeostasis a more critical issue? *Plant. Cell Environ.* **2014**, *37*, 300–311. [CrossRef] [PubMed]
192. Raza, A.; Charagh, S.; Abbas, S.; Hassan, M.U.; Saeed, F.; Haider, S.; Sharif, R.; Anand, A.; Corpas, F.J.; Jin, W.; et al. Assessment of proline function in higher plants under extreme temperatures. *Plant Biol.* **2023**, *25*, 379–395. [CrossRef] [PubMed]
193. da Cruz, R.P.; Sperotto, R.A.; Cargnelutti, D.; Adamski, J.M.; FreitasTerra, T.; Fett, J.P. Avoiding damage and achieving cold tolerance in rice plants. *Food Energy Secur.* **2013**, *2*, 96–119. [CrossRef]
194. Zhang, Q.; Chen, Q.; Wang, S.; Hong, Y.; Wang, Z. Rice and cold stress: Methods for its evaluation and summary of cold tolerance-related quantitative trait loci. *Rice* **2014**, *7*, 24. [CrossRef]
195. Ma, Y.; Dai, X.; Xu, Y.; Luo, W.; Zheng, X.; Zeng, D.; Pan, Y.; Lin, X.; Liu, H.; Zhang, D.; et al. COLD1 Confers Chilling Tolerance in Rice. *Cell* **2015**, *160*, 1209–1221. [CrossRef]
196. Deng, X.; Hu, W.; Wei, S.; Zhou, S.; Zhang, F.; Han, J.; Chen, L.; Li, Y.; Feng, J.; Fang, B.; et al. TaCIPK29, a CBL-Interacting Protein Kinase Gene from Wheat, Confers Salt Stress Tolerance in Transgenic Tobacco. *PLoS ONE* **2013**, *8*, e69881. [CrossRef]
197. Tian, X.; Wang, Z.; Li, X.; Lv, T.; Liu, H.; Wang, L.; Niu, H.; Bu, Q. Characterization and Functional Analysis of Pyrabactin Resistance-Like Abscisic Acid Receptor Family in Rice. *Rice* **2015**, *8*, 28. [CrossRef] [PubMed]
198. Zhu, J.-K. Abiotic Stress Signaling and Responses in Plants. *Cell* **2016**, *167*, 313–324. [CrossRef] [PubMed]
199. Zhang, Z.; Li, J.; Li, F.; Liu, H.; Yang, W.; Chong, K.; Xu, Y. OsMAPK3 Phosphorylates OsbHLH002/OsICE1 and Inhibits Its Ubiquitination to Activate OsTPP1 and Enhances Rice Chilling Tolerance. *Dev. Cell* **2017**, *43*, 731–743.e5. [CrossRef] [PubMed]
200. Zhao, J.; Wang, S.; Qin, J.; Sun, C.; Liu, F. The lipid transfer protein OsLTPL159 is involved in cold tolerance at the early seedling stage in rice. *Plant Biotechnol. J.* **2020**, *18*, 756–769. [CrossRef] [PubMed]
201. Sun, J.; Yang, L.; Wang, J.; Liu, H.; Zheng, H.; Xie, D.; Zhang, M.; Feng, M.; Jia, Y.; Zhao, H.; et al. Identification of a Cold-Tolerant Locus in Rice (*Oryza Sativa* L.) Using Bulked Segregant Analysis with a next-Generation Sequencing Strategy. *Rice* **2018**, *11*, 24. [CrossRef] [PubMed]
202. Liu, K.; Wang, L.; Xu, Y.; Chen, N.; Ma, Q.; Li, F.; Chong, K. Overexpression of OsCOIN, a Putative Cold Inducible Zinc Finger Protein, Increased Tolerance to Chilling, Salt and Drought, and Enhanced Proline Level in Rice. *Planta* **2007**, *226*, 1007–1016. [CrossRef] [PubMed]
203. Yang, C.; Li, D.; Mao, D.; Liu, X.; Ji, C.; Li, X.; Zhao, X.; Cheng, Z.; Chen, C.; Zhu, L. Overexpression of MicroRNA319 Impacts Leaf Morphogenesis and Leads to Enhanced Cold Tolerance in Rice (*Oryza Sativa* L.). *Plant Cell Environ.* **2013**, *36*, 2207–2218. [CrossRef] [PubMed]
204. Greco, M.; Chiappetta, A.; Bruno, L.; Bitonti, M.B. In Posidonia oceanica cadmium induces changes in DNA methylation and chromatin patterning. *J. Exp. Bot.* **2012**, *63*, 695–709. [CrossRef]
205. Ma, Q.; Dai, X.; Xu, Y.; Guo, J.; Liu, Y.; Chen, N.; Xiao, J.; Zhang, D.; Xu, Z.; Zhang, X.; et al. Enhanced Tolerance to Chilling Stress in OsMYB3R-2 Transgenic Rice Is Mediated by Alteration in Cell Cycle and Ectopic Expression of Stress Genes. *Plant Physiol.* **2009**, *150*, 244–256. [CrossRef]
206. Hu, H.; You, J.; Fang, Y.; Zhu, X.; Qi, Z.; Xiong, L. Characterization of transcription factor gene SNAC2 conferring cold and salt tolerance in rice. *Plant Mol. Biol.* **2008**, *67*, 169–181. [CrossRef]
207. Wang, Q.; Guan, Y.; Wu, Y.; Chen, H.; Chen, F.; Chu, C. Overexpression of a rice OsDREB1F gene increases salt, drought, and low temperature tolerance in both Arabidopsis and rice. *Plant Mol. Biol.* **2008**, *67*, 589–602. [CrossRef]
208. Joo, J.; Lee, Y.H.; Kim, Y.K.; Nahm, B.H.; Song, S.I. Abiotic stress responsive rice ASR1 and ASR3 exhibit different tissue-dependent sugar and hormone-sensitivities. *Mol. Cells* **2013**, *35*, 421–435. [CrossRef]
209. Shi, J.; Cao, Y.; Fan, X.; Li, M.; Wang, Y.; Ming, F. A rice microsomal delta-12 fatty acid desaturase can enhance resistance to cold stress in yeast and *Oryza sativa*. *Mol. Breed.* **2012**, *29*, 743–757. [CrossRef]
210. Kim, S.H.; Kim, J.Y.; Kim, S.J.; An, K.S.; An, G.; Kim, S.R. Isolation of Cold Stress-Responsive Genes in the Reproductive Organs, and Characterization of the OsLti6b Gene from Rice (*Oryza Sativa* L.). *Plant Cell Rep.* **2007**, *26*, 1097–1110. [CrossRef] [PubMed]
211. Tao, Z.; Kou, Y.; Liu, H.; Li, X.; Xiao, J.; Wang, S. OsWRKY45 alleles play different roles in abscisic acid signalling and salt stress tolerance but similar roles in drought and cold tolerance in rice. *J. Exp. Bot.* **2011**, *62*, 4863–4874. [CrossRef] [PubMed]
212. Chen, N.; Xu, Y.; Wang, X.; Du, C.; Du, J.; Yuan, M.; Xu, Z.; Chong, K. OsRAN2, essential for mitosis, enhances cold tolerance in rice by promoting export of intranuclear tubulin and maintaining cell division under cold stress. *Plant Cell Environ.* **2011**, *34*, 52–64. [CrossRef] [PubMed]
213. Wang, C.; Wei, Q.; Zhang, K.; Wang, L.; Liu, F.; Zhao, L.; Tan, Y.; Di, C.; Yan, H.; Yu, J.; et al. Down-Regulation of OsSPX1 Causes High Sensitivity to Cold and Oxidative Stresses in Rice Seedlings. *PLoS ONE* **2013**, *8*, 81849. [CrossRef] [PubMed]
214. Park, H.Y.; Kang, I.S.; Han, J.S.; Lee, C.H.; An, G.; Moon, Y.H. OsDEG10 encoding a small RNA-binding protein is involved in abiotic stress signaling. *Biochem. Biophys. Res. Commun.* **2009**, *380*, 597–602. [CrossRef] [PubMed]
215. Yamori, W.; Sakata, N.; Suzuki, Y.; Shikanai, T.; Makino, A. Cyclic Electron Flow around Photosystem i via Chloroplast NAD(P)H Dehydrogenase (NDH) Complex Performs a Significant Physiological Role during Photosynthesis and Plant Growth at Low Temperature in Rice. *Plant J.* **2011**, *68*, 966–976. [CrossRef] [PubMed]

216. Li, G.-W.G.-W.; Zhang, M.-H.M.-H.; Cai, W.-M.W.-M.; Sun, W.-N.W.-N.; Su, W.-A.W.-A. Characterization of OsPIP2: 7, a Water Channel Protein in Rice. *Plant Cell Physiol.* **2008**, *49*, 1851–1858. [CrossRef]
217. Gothandam, K.M.; Nalini, E.; Karthikeyan, S.; Shin, J.S. OsPRP3, a flower specific Proline-rich protein of rice, determines extracellular matrix structure of floral organs and its overexpression confers cold-tolerance. *Plant Mol. Biol.* **2010**, *72*, 125–135. [CrossRef]
218. Kim, S.-J.; Lee, S.-C.; Hong, S.K.; An, K.; An, G.; Kim, S.-R. Ectopic expression of a cold-responsive OsAsr1 cDNA gives enhanced cold tolerance in transgenic rice plants. *Mol. Cells* **2009**, *27*, 449–458. [CrossRef] [PubMed]
219. Su, C.-F.; Wang, Y.-C.; Hsieh, T.-H.; Lu, C.-A.; Tseng, T.-H.; Yu, S.-M. A Novel MYBS3-Dependent Pathway Confers Cold Tolerance in Rice. *Plant Physiol.* **2010**, *153*, 145–158. [CrossRef] [PubMed]
220. Zhang, J.; Li, J.; Wang, X.; Chen, J. OVP1, a Vacuolar H+-translocating inorganic pyrophosphatase (V-PPase), overexpression improved rice cold tolerance. *Plant Physiol. Biochem.* **2011**, *49*, 33–38. [CrossRef] [PubMed]
221. Song, Y.; Jiang, M.; Zhang, H.; Li, R. Zinc Oxide Nanoparticles Alleviate Chilling Stress in Rice (*Oryza Sativa* L.) by Regulating Antioxidative System and Chilling Response Transcription Factors. *Molecules* **2021**, *26*, 2196. [CrossRef] [PubMed]
222. Han, Q.H.; Huang, B.; Ding, C.B.; Zhang, Z.W.; Chen, Y.E.; Hu, C.; Zhou, L.J.; Huang, Y.; Liao, J.Q.; Yuan, S.; et al. Effects of Melatonin on Anti-Oxidative Systems and Photosystem II in Cold-Stressed Rice Seedlings. *Front. Plant Sci.* **2017**, *8*, 785. [CrossRef] [PubMed]
223. Teixeira, S.B.; Pires, S.N.; Ávila, G.E.; Silva, B.E.P.; Schmitz, V.N.; Deuner, C.; Silva Armesto, R.; Silva Moura, D.; Deuner, S.; da Silva Armesto, R.; et al. Application of Vigor Indexes to Evaluate the Cold Tolerance in Rice Seeds Germination Conditioned in Plant Extract. *Sci. Rep.* **2021**, *11*, 11038. [CrossRef]
224. Bui, L.T.; Ella, E.S.; Dionisio-Sese, M.L.; Ismail, A.M. Morpho-Physiological Changes in Roots of Rice Seedling upon Submergence. *Rice Sci.* **2019**, *26*, 167–177. [CrossRef]
225. Kumar, A.; Nayak, A.K.; Hanjagi, P.S.; Kumari, K.S.V.; Mohanty, S.; Tripathi, R.; Panneerselvam, P. Submergence stress in rice: Adaptive mechanisms, coping strategies and future research needs. *Environ. Exp. Bot.* **2021**, *186*, 104448. [CrossRef]
226. Nishiuchi, S.; Yamauchi, T.; Takahashi, H.; Kotula, L.; Nakazono, M. Mechanisms for coping with submergence and waterlogging in rice. *Rice* **2012**, *5*, 2. [CrossRef]
227. Kato, Y.; Collard, B.C.Y.; Septiningsih, E.M.; Ismail, A.M. Increasing flooding tolerance in rice: Combining tolerance of submergence and of stagnant flooding. *Ann. Bot.* **2019**, *124*, 1199–1209. [CrossRef] [PubMed]
228. Ismail, A.M.; Ella, E.S.; Vergara, G.V.; Mackill, D.J. Mechanisms associated with tolerance to flooding during germination and early seedling growth in rice (*Oryza sativa*). *Ann. Bot.* **2009**, *103*, 197–209. [CrossRef] [PubMed]
229. Jackson, M.B. Physiological and Molecular Basis of Susceptibility and Tolerance of Rice Plants to Complete Submergence. *Ann. Bot.* **2003**, *91*, 227–241. [CrossRef] [PubMed]
230. Sarkar, R.K.; Bhattacharjee, B. Rice Genotypes with SUB1 QTL Differ in Submergence Tolerance, Elongation Ability during Submergence and Re-generation Growth at Re-emergence. *Rice* **2011**, *5*, 7. [CrossRef]
231. Colmer, T.D.; Armstrong, W.; Greenway, H.; Ismail, A.M.; Kirk, G.J.D.; Atwell, B.J. Physiological Mechanisms of Flooding Tolerance in Rice: Transient Complete Submergence and Prolonged Standing Water. In *Progress in Botany*; Springer: Berlin/Heidelberg, Germany, 2014; Volume 75, pp. 255–307. [CrossRef]
232. Singh, H.P.; Singh, B.B.; Ram, P.C. Submergence tolerance of rainfed lowland rice: Search for physiological marker traits. *J. Plant Physiol.* **2001**, *158*, 883–889. [CrossRef]
233. Setter, T.L.; Ingram, K.T.; Tuong, T.P. Environmental characterization requirements for strategic research in rice grown under adverse conditions of drought, flooding and salinity. *Int. Rice Res. Inst.* **1995**, 3–18.
234. Bailey-Serres, J.; Fukao, T.; Ronald, P.; Ismail, A.; Heuer, S.; Mackill, D. Submergence Tolerant Rice: SUB1's Journey from Landrace to Modern Cultivar. *Rice* **2010**, *3*, 138–147. [CrossRef]
235. Sarkar, R.K.; Panda, D. Distinction and characterisation of submergence tolerant and sensitive rice cultivars, probed by the fluorescence OJIP rise kinetics. *Funct. Plant Biol.* **2009**, *36*, 222. [CrossRef]
236. Emes, M.J.; Wilkins, C.P.; Smith, P.A.; Kupkanchanakul, K.; Hawker, K.; Charlton, W.A.; Cutter, E.G. Starch utilization by deepwater rices during submergence. *Int. Deep. Rice Work.* **1988**, 26–30.
237. Fukao, T.; Yeung, E.; Bailey-Serres, J. The Submergence Tolerance Regulator SUB1A Mediates Crosstalk between Submergence and Drought Tolerance in Rice. *Plant Cell* **2011**, *23*, 412–427. [CrossRef]
238. Setter, T.L.; Bhekasut, P.; Greenway, H. Desiccation of leaves after de-submergence is one cause for intolerance to complete submergence of the rice cultivar IR 42. *Funct. Plant Biol.* **2010**, *37*, 1096. [CrossRef]
239. Upadhyay, R.; Panda, S.; Dutta, B. Growth, Chlorophyll and Electric Conductivity responses of rice cultivars to different levels of Submergence and Post-submergence Stress. *J. Phytol.* **2009**, *1*, 425–432.
240. Upadhyay, R.K. Oxidative Injury and Its Detoxification in Rice Plants after Submergence Stress. *Proc. Natl. Acad. Sci. India Sect. B Biol. Sci.* **2018**, *88*, 15–21. [CrossRef]
241. Ribeiro, C.W.; Korbes, A.P.; Garighan, J.A.; Jardim-Messeder, D.; Carvalho, F.E.L.L.; Sousa, R.H.V.V.; Caverzan, A.; Teixeira, F.K.; Silveira, J.A.G.G.; Margis-Pinheiro, M. Rice Peroxisomal Ascorbate Peroxidase Knockdown Affects ROS Signaling and Triggers Early Leaf Senescence. *Plant Sci.* **2017**, *263*, 55–65. [CrossRef] [PubMed]
242. Bailey-Serres, J.; Voesenek, L. Flooding Stress: Acclimations and Genetic Diversity. *Annu. Rev. Plant Biol.* **2008**, *59*, 313–339. [CrossRef] [PubMed]

243. Colmer, T.D.; Voesenek, L.A.C.J. Flooding tolerance: Suites of plant traits in variable environments. *Funct. Plant Biol.* **2009**, *36*, 665. [CrossRef] [PubMed]
244. Drew, M.C.; He, C.-J.; Morgan, P.W. Programmed cell death and aerenchyma formation in roots. *Trends Plant Sci.* **2000**, *5*, 123–127. [CrossRef]
245. Shiono, K.; Takahashi, H.; Colmer, T.D.; Nakazono, M. Role of ethylene in acclimations to promote oxygen transport in roots of plants in waterlogged soils. *Plant Sci.* **2008**, *175*, 52–58. [CrossRef]
246. Steffens, B.; Sauter, M. Epidermal Cell Death in Rice Is Confined to Cells with a Distinct Molecular Identity and Is Mediated by Ethylene and H_2O_2 through an Autoamplified Signal Pathway. *Plant Cell* **2009**, *21*, 184–196. [CrossRef]
247. Hattori, Y.; Hattori, Y.; Nagai, K.; Nagai, K.; Furukawa, S.; Furukawa, S.; Song, X.-J.X.-J.; Song, X.-J.X.-J.; Kawano, R.; Kawano, R.; et al. The Ethylene Response Factors SNORKEL1 and SNORKEL2 Allow Rice to Adapt to Deep Water. *Nature* **2009**, *460*, 1026. [CrossRef]
248. Colmer, T.D.; Pedersen, O. Oxygen dynamics in submerged rice (*Oryza sativa*). *New Phytol.* **2008**, *178*, 326–334. [CrossRef]
249. Xu, K.; Xu, X.; Fukao, T.; Canlas, P.; Maghirang-Rodriguez, R.; Heuer, S.; Ismail, A.M.; Bailey-Serres, J.; Ronald, P.C.; Mackill, D.J. Sub1A Is an Ethylene-Response-Factor-like Gene That Confers Submergence Tolerance to Rice. *Nature* **2006**, *442*, 705–708. [CrossRef] [PubMed]
250. Fukao, T.; Xu, K.; Ronald, P.; Bailey-Serres, J. A Variable Cluster of Ethylene Response Factor-like Genes Regulates Metabolic and Developmental Acclimation Responses to Submergence in Rice. *Plant Cell* **2006**, *18*, 2021–2034. [CrossRef] [PubMed]
251. Fukao, T.; Bailey-Serres, J. Ethylene—A key regulator of submergence responses in rice. *Plant Sci.* **2008**, *175*, 43–51. [CrossRef]
252. Jackson, M.; Armstrong, W. Formation of Aerenchyma and the Processes of Plant Ventilation in Relation to Soil Flooding and Submergence. *Plant Biol.* **1999**, *1*, 274–287. [CrossRef]
253. COLMER, T.D. Aerenchyma and an Inducible Barrier to Radial Oxygen Loss Facilitate Root Aeration in Upland, Paddy and Deep-water Rice (*Oryza sativa* L.). *Ann. Bot.* **2003**, *91*, 301–309. [CrossRef] [PubMed]
254. Kuroha, T.; Nagai, K.; Gamuyao, R.; Wang, D.R.; Furuta, T.; Nakamori, M.; Kitaoka, T.; Adachi, K.; Minami, A.; Mori, Y.; et al. Ethylene-gibberellin signaling underlies adaptation of rice to periodic flooding. *Science* **2018**, *361*, 181–186. [CrossRef] [PubMed]
255. Nagai, K.; Mori, Y.; Ishikawa, S.; Furuta, T.; Gamuyao, R.; Niimi, Y.; Hobo, T.; Fukuda, M.; Kojima, M.; Takebayashi, Y.; et al. Antagonistic regulation of the gibberellic acid response during stem growth in rice. *Nature* **2020**, *584*, 109–114. [CrossRef]
256. Reynoso, M.A.; Kajala, K.; Bajic, M.; West, D.A.; Pauluzzi, G.; Yao, A.I.; Hatch, K.; Zumstein, K.; Woodhouse, M.; Rodriguez-Medina, J.; et al. Evolutionary flexibility in flooding response circuitry in angiosperms. *Science* **2019**, *365*, 1291–1295. [CrossRef]
257. Straeten, D.; Zhou, Z.; Prinsen, E.; Onckelen, H.A.; Montagu, M.C.; Van Der Straeten, D.; Zhou, Z.; Prinsen, E.; Van Onckelen, H.A.; Van Montagu, M.C. A Comparative Molecular-Physiological Study of Submergence Response in Lowland and Deepwater Rice. *Plant Physiol.* **2001**, *125*, 955–968. [CrossRef]
258. Zarembinski, T.I.; Theologis, A. Expression characteristics of OS-ACS1 and OSACS2, two members of the 1-aminocyclopropane-1-carboxylate synthase gene family in rice (*Oryza sativa* L. Cv. Habiganj Aman II) during partial submergence. *Plant Mol. Biol* **1997**, *33*, 71–77. [CrossRef] [PubMed]
259. Kurokawa, Y.; Nagai, K.; Huan, P.D.; Shimazaki, K.; Qu, H.; Mori, Y.; Toda, Y.; Kuroha, T.; Hayashi, N.; Aiga, S.; et al. Rice leaf hydrophobicity and gas films are conferred by a wax synthesis gene (LGF 1) and contribute to flood tolerance. *New Phytol.* **2018**, *218*, 1558–1569. [CrossRef] [PubMed]
260. Kretzschmar, T.; Pelayo, M.A.F.; Trijatmiko, K.R.; Gabunada, L.F.M.; Alam, R.; Jimenez, R.; Mendioro, M.S.; Slamet-Loedin, I.H.; Sreenivasulu, N.; Bailey-Serres, J.; et al. A trehalose-6-phosphate phosphatase enhances anaerobic germination tolerance in rice. *Nat. Plants* **2015**, *1*, 15124. [CrossRef] [PubMed]
261. Panda, D.; Sarkar, R.K. Mechanism associated with nonstructural carbohydrate accumulation in submergence tolerant rice (*Oryza sativa* L.) cultivars. *J. Plant Interact.* **2014**, *9*, 62–68. [CrossRef]
262. Jisha, V.; Dampanaboina, L.; Vadassery, J.; Mithöfer, A.; Kappara, S.; Ramanan, R. Overexpression of an AP2/ERF Type Transcription Factor OsEREBP1 Confers Biotic and Abiotic Stress Tolerance in Rice. *PLoS ONE* **2015**, *10*, e0127831. [CrossRef]
263. Lee, K.-W.; Chen, P.-W.; Lu, C.-A.; Chen, S.; Ho, T.-H.D.; Yu, S.-M. Coordinated Responses to Oxygen and Sugar Deficiency Allow Rice Seedlings to Tolerate Flooding. *Sci. Signal.* **2009**, *2*, 61. [CrossRef] [PubMed]
264. Nagai, K.; Kurokawa, Y.; Mori, Y.; Minami, A.; Reuscher, S.; Wu, J.; Matsumoto, T.; Ashikari, M. SNORKEL Genes Relating to Flood Tolerance Were Pseudogenized in Normal Cultivated Rice. *Plants* **2022**, *11*, 376. [CrossRef]
265. Nemoto, K.; Ukai, Y.; Tang, D.-Q.; Kasai, Y.; Morita, M. Inheritance of early elongation ability in floating rice revealed by diallel and QTL analyses. *Theor. Appl. Genet.* **2004**, *109*, 42–47. [CrossRef]
266. Tang, D.-Q.; Kasai, Y.; Miyamoto, N.; Ukai, Y.; Nemoto, K. Comparison of QTLs for Early Elongation Ability between Two Floating Rice Cultivars with a Different Phylogenetic Origin. *Breed. Sci.* **2005**, *55*, 1–5. [CrossRef]
267. Hattori, Y.; Miura, K.; Asano, K.; Yamamoto, E.; Mori, H.; Kitano, H.; Matsuoka, M.; Ashikari, M. A Major QTL Confers Rapid Internode Elongation in Response to Water Rise in Deepwater Rice. *Breed. Sci.* **2007**, *57*, 305–314. [CrossRef]
268. Kawano, R.; Doi, K.; Yasui, H.; Mochizuki, T.; Yoshimura, A. Mapping of QTLs for floating ability in rice. *Breed. Sci.* **2008**, *58*, 47–53. [CrossRef]
269. Septiningsih, E.M.; Pamplona, A.M.; Sanchez, D.L.; Neeraja, C.N.; Vergara, G.V.; Heuer, S.; Ismail, A.M.; Mackill, D.J. Development of submergence-tolerant rice cultivars: The Sub1 locus and beyond. *Ann. Bot.* **2009**, *103*, 151–160. [CrossRef] [PubMed]

270. Fukao, T.; Yeung, E.; Bailey-Serres, J. The Submergence Tolerance Gene SUB1A Delays Leaf Senescence under Prolonged Darkness through Hormonal Regulation in Rice. *Plant Physiol.* **2012**, *160*, 1795–1807. [CrossRef] [PubMed]
271. Debona, D.; Rodrigues, F.A.; Datnoff, L.E. Silicon's Role in Abiotic and Biotic Plant Stresses. *Annu. Rev. Phytopathol.* **2017**, *55*, 85–107. [CrossRef] [PubMed]
272. Pan, T.; Zhang, J.; He, L.; Hafeez, A.; Ning, C.; Cai, K. Silicon Enhances Plant Resistance of Rice against Submergence Stress. *Plants* **2021**, *10*, 767. [CrossRef] [PubMed]
273. Guo, P.; Du, H.; Wang, D.; Ma, M. Effects of Mercury Stress on Methylmercury Production in Rice Rhizosphere, Methylmercury Uptake in Rice and Physiological Changes of Leaves. *Sci. Total Environ.* **2021**, *765*, 142682. [CrossRef] [PubMed]
274. Lutts, S.; Kinet, J.M.; Bouharmont, J. Changes in plant response to NaCl during development of rice (*Oryza sativa* L.) varieties differing in salinity resistance. *J. Exp. Bot.* **1995**, *46*, 1843–1852. [CrossRef]
275. Bundó, M.; Martín-Cardoso, H.; Pesenti, M.; Gómez-Ariza, J.; Castillo, L.; Frouin, J.; Serrat, X.; Nogués, S.; Courtois, B.; Grenier, C.; et al. Integrative Approach for Precise Genotyping and Transcriptomics of Salt Tolerant Introgression Rice Lines. *Front. Plant Sci.* **2022**, *12*, 797141. [CrossRef]
276. Rodríguez-Navarro, A.; Rubio, F. High-affinity potassium and sodium transport systems in plants. *J. Exp. Bot.* **2006**, *57*, 1149–1160. [CrossRef]
277. Ali, A.; Raddatz, N.; Pardo, J.M.; Yun, D. HKT sodium and potassium transporters in Arabidopsis thaliana and related halophyte species. *Physiol. Plant.* **2021**, *171*, 546–558. [CrossRef]
278. Assaha, D.V.M.; Ueda, A.; Saneoka, H.; Al-Yahyai, R.; Yaish, M.W. The Role of Na(+) and K(+) Transporters in Salt Stress Adaptation in Glycophytes. *Front. Physiol.* **2017**, *8*, 509. [CrossRef]
279. Khatun, S.; Rizzo, C.A.; Flowers, T.J. Genotypic variation in the effect of salinity on fertility in rice. *Plant Soil* **1995**, *173*, 239–250. [CrossRef]
280. Rao, P.S.; Mishra, B.; Gupta, S.R. Effects of Soil Salinity and Alkalinity on Grain Quality of Tolerant, Semi-Tolerant and Sensitive Rice Genotypes. *Rice Sci.* **2013**, *20*, 284–291. [CrossRef]
281. Zeng, Y.; Zhang, H.; Li, Z.; Shen, S.; Sun, J.; Wang, M.; Liao, D.; Liu, X.; Wang, X.; Xiao, F.; et al. Evaluation of Genetic Diversity of Rice Landraces (*Oryza sativa* L.) in Yunnan, China. *Breed. Sci.* **2007**, *57*, 91–99. [CrossRef]
282. Yeo, A.R.; Yeo, M.E.; Flowers, S.A.; Flowers, T.J. Screening of rice (*Oryza sativa* L.) genotypes for physiological characters contributing to salinity resistance, and their relationship to overall performance. *Theor. Appl. Genet.* **1990**, *79*, 377–384. [CrossRef] [PubMed]
283. Razzaq, A.; Ali, A.; Safdar, L.B.; Zafar, M.M.; Rui, Y.; Shakeel, A.; Shaukat, A.; Ashraf, M.; Gong, W.; Yuan, Y. Salt stress induces physiochemical alterations in rice grain composition and quality. *J. Food Sci.* **2020**, *85*, 14–20. [CrossRef] [PubMed]
284. Munns, R.; Tester, M. Mechanisms of Salinity Tolerance. *Annu. Rev. Plant Biol.* **2008**, *59*, 651–681. [CrossRef] [PubMed]
285. Xiao, F.; Zhou, H. Plant salt response: Perception, signaling, and tolerance. *Front. Plant Sci.* **2023**, *13*, 1053699. [CrossRef] [PubMed]
286. Hussain, S.; Zhang, J.; Hua, J.; Zhong, C.; Zhu, L.; Feng, L.F.; Cao, X.; Chuan, X.; Chuang, Y.S.; Miao, S.; et al. Effects of Salt Stress on Rice Growth, Development Characteristics, and the Regulating Ways: A Review. *J. Integr. Agric.* **2017**, *16*, 2357–2374. [CrossRef]
287. Cha-Um, S.; Supaibulwattana, K.; Kirdmanee, C. Comparative Effects of Salt Stress and Extreme pH Stress Combined on Glycinebetaine Accumulation, Photosynthetic Abilities and Growth Characters of Two Rice Genotypes. *Rice Sci.* **2009**, *16*, 274–282. [CrossRef]
288. Ran, X.; Wang, X.; Huang, X.; Ma, C.; Liang, H.; Liu, B. Study on the Relationship of Ions (Na, K, Ca) Absorption and Distribution to Photosynthetic Response of Salix matsudana Koidz Under Salt Stress. *Front. Plant Sci.* **2022**, *13*, 860111. [CrossRef] [PubMed]
289. Hoang, T.M.L.; Tran, T.N.; Nguyen, T.K.T.; Williams, B.; Wurm, P.; Bellairs, S.; Mundree, S. Improvement of Salinity Stress Tolerance in Rice: Challenges and Opportunities. *Agronomy* **2016**, *6*, 54. [CrossRef]
290. Vaidyanathan, H.; Sivakumar, P.; Chakrabarty, R.; Thomas, G. Scavenging of reactive oxygen species in NaCl-stressed rice (*Oryza sativa* L.)—Differential response in salt-tolerant and sensitive varieties. *Plant Sci.* **2003**, *165*, 1411–1418. [CrossRef]
291. Yamane, K.; Mitsuya, S.; Kawasaki, M.; Taniguchi, M.; Miyake, H. Antioxidant Capacity and Damages Caused by Salinity Stress in Apical and Basal Regions of Rice Leaf. *Plant Prod. Sci.* **2009**, *12*, 319–326. [CrossRef]
292. Schmidt, R.; Schippers, J.H.M.; Mieulet, D.; Watanabe, M.; Hoefgen, R.; Guiderdoni, E.; Mueller-Roeber, B. SALT-RESPONSIVE ERF1 Is a Negative Regulator of Grain Filling and Gibberellin-Mediated Seedling Establishment in Rice. *Mol. Plant* **2014**, *7*, 404–421. [CrossRef] [PubMed]
293. Rajendran, K.; Tester, M.; Roy, S.J. Quantifying the three main components of salinity tolerance in cereals. *Plant. Cell Environ.* **2009**, *32*, 237–249. [CrossRef] [PubMed]
294. Moradi, F.; Ismail, A.M. Responses of Photosynthesis, Chlorophyll Fluorescence and ROS-Scavenging Systems to Salt Stress During Seedling and Reproductive Stages in Rice. *Ann. Bot.* **2007**, *99*, 1161–1173. [CrossRef]
295. Maathuis, F. K + Nutrition and Na + Toxicity: The Basis of Cellular K+/Na+ Ratios. *Ann. Bot.* **1999**, *84*, 123–133. [CrossRef]
296. Rodrigues, C.R.F.; Silva, E.N.; Ferreira-Silva, S.L.; Voigt, E.L.; Viégas, R.A.; Silveira, J.A.G. High K + supply avoids Na + toxicity and improves photosynthesis by allowing favorable K + : Na + ratios through the inhibition of Na + uptake and transport to the shoots of Jatropha curcas plants. *J. Plant Nutr. Soil Sci.* **2013**, *176*, 157–164. [CrossRef]

297. Lee, K.-S.; Choi, W.-Y.; Ko, J.-C.; Kim, T.-S.; Gregorio, G.B. Salinity tolerance of japonica and indica rice (*Oryza sativa* L.) at the seedling stage. *Planta* **2003**, *216*, 1043–1046. [CrossRef]
298. Ghosh, N.; Adak, M.K.; Ghosh, P.D.; Gupta, S.; Sen Gupta, D.N.; Mandal, C. Differential responses of two rice varieties to salt stress. *Plant Biotechnol. Rep.* **2011**, *5*, 89–103. [CrossRef]
299. Kader, M.A.; Lindberg, S. Uptake of sodium in protoplasts of salt-sensitive and salt-tolerant cultivars of rice, *Oryza sativa* L. determined by the fluorescent dye SBFI. *J. Exp. Bot.* **2005**, *56*, 3149–3158. [CrossRef] [PubMed]
300. Johnson, M.K.; Johnson, E.J.; MacElroy, R.D.; Speer, H.L.; Bruff, B.S. Effects of Salts on the Halophilic Alga Dunaliella viridis. *J. Bacteriol.* **1968**, *95*, 1461–1468. [CrossRef] [PubMed]
301. Yancey, P.H.; Clark, M.E.; Hand, S.C.; Bowlus, R.D.; Somero, G.N. Living with Water Stress: Evolution of Osmolyte Systems. *Science* **1982**, *217*, 1214–1222. [CrossRef] [PubMed]
302. Garg, A.K.; Kim, J.; Owens, T.G.; Ranwala, A.P.; Choi, Y.D.; Kochian, L.V.; Wu, R.J. Trehalose accumulation in rice plants confers high tolerance levels to different abiotic stresses. *Proc. Natl. Acad. Sci. USA* **2002**, *99*, 15898–15903. [CrossRef] [PubMed]
303. Singh, P.; Choudhary, K.K.; Chaudhary, N.; Gupta, S.; Sahu, M.; Tejaswini, B.; Sarkar, S. Salt Stress Resilience in Plants Mediated through Osmolyte Accumulation and Its Crosstalk Mechanism with Phytohormones. *Front. Plant Sci.* **2022**, *13*, 1006617. [CrossRef] [PubMed]
304. Greenberg, J.T. Programmed cell death: A way of life for plants. *Proc. Natl. Acad. Sci. USA* **1996**, *93*, 12094–12097. [CrossRef]
305. Liu, S.-H.; Fu, B.-Y.; Xu, H.-X.; Zhu, L.-H.; Zhai, H.-Q.; Li, Z.-K. Cell death in response to osmotic and salt stresses in two rice (*Oryza sativa* L.) ecotypes. *Plant Sci.* **2007**, *172*, 897–902. [CrossRef]
306. Li, J.; Jiang, A.; Zhang, W. Salt Stress-induced Programmed Cell Death in Rice Root Tip Cells. *J. Integr. Plant Biol.* **2007**, *49*, 481–486. [CrossRef]
307. Khoso, M.A.; Hussain, A.; Ritonga, F.N.; Ali, Q.; Channa, M.M.; Alshegaihi, R.M.; Meng, Q.; Ali, M.; Zaman, W.; Brohi, R.D.; et al. WRKY transcription factors (TFs): Molecular switches to regulate drought, temperature, and salinity stresses in plants. *Front. Plant Sci.* **2022**, *13*, 1039329. [CrossRef]
308. Gumi, A.M.; Guha, P.K.; Mazumder, A.; Jayaswal, P.; Mondal, T.K. Characterization of OglDREB2A gene from African rice (*Oryza glaberrima*), comparative analysis and its transcriptional regulation under salinity stress. *Biotech* **2018**, *8*, 91. [CrossRef]
309. Liu, C.; Mao, B.; Ou, S.; Wang, W.; Liu, L.; Wu, Y.; Chu, C.; Wang, X. OsbZIP71, a bZIP transcription factor, confers salinity and drought tolerance in rice. *Plant Mol. Biol.* **2014**, *84*, 19–36. [CrossRef] [PubMed]
310. Jan, A.; Maruyama, K.; Todaka, D.; Kidokoro, S.; Abo, M.; Yoshimura, E.; Shinozaki, K.; Nakashima, K.; Yamaguchi-Shinozaki, K. OsTZF1, a CCCH-Tandem Zinc Finger Protein, Confers Delayed Senescence and Stress Tolerance in Rice by Regulating Stress-Related Genes. *Plant Physiol.* **2013**, *161*, 1202–1216. [CrossRef] [PubMed]
311. Qiu, D.; Xiao, J.; Xie, W.; Liu, H.; Li, X.; Xiong, L.; Wang, S. Rice Gene Network Inferred from Expression Profiling of Plants Overexpressing OsWRKY13, a Positive Regulator of Disease Resistance. *Mol. Plant* **2008**, *1*, 538–551. [CrossRef] [PubMed]
312. Qiu, D.; Xiao, J.; Ding, X.; Xiong, M.; Cai, M.; Cao, Y.; Li, X.; Xu, C.; Wang, S. OsWRKY13 Mediates Rice Disease Resistance by Regulating Defense-Related Genes in Salicylate- and Jasmonate-Dependent Signaling. *Mol. Plant-Microbe Interact.* **2007**, *20*, 492–499. [CrossRef]
313. Liu, C.; Chen, K.; Zhao, X.; Wang, X.; Shen, C.; Zhu, Y.; Dai, M.; Qiu, X.; Yang, R.; Xing, D.; et al. Identification of Genes for Salt Tolerance and Yield-Related Traits in Rice Plants Grown Hydroponically and under Saline Field Conditions by Genome-Wide Association Study. *Rice* **2019**, *12*, 88. [CrossRef]
314. Wang, H.; Zhang, M.; Guo, R.; Shi, D.; Liu, B.; Lin, X.; Yang, C. Effects of salt stress on ion balance and nitrogen metabolism of old and young leaves in rice (*Oryza sativa* L.). *BMC Plant Biol.* **2012**, *12*, 194. [CrossRef]
315. Chen, G.; Hu, Q.; Luo, L.; Yang, T.; Zhang, S.; Hu, Y.; Yu, L.; Xu, G. Rice Potassium Transporter OsHAK1 Is Essential for Maintaining Potassium-Mediated Growth and Functions in Salt Tolerance over Low and High Potassium Concentration Ranges. *Plant Cell Environ.* **2015**, *38*, 2747–2765. [CrossRef]
316. Blumwald, E. Sodium transport and salt tolerance in plants. *Curr. Opin. Cell Biol.* **2000**, *12*, 431–434. [CrossRef]
317. Bassil, E.; Coku, A.; Blumwald, E. Cellular ion homeostasis: Emerging roles of intracellular NHX Na+/H+ antiporters in plant growth and development. *J. Exp. Bot.* **2012**, *63*, 5727–5740. [CrossRef]
318. Kurotani, K.I.; Hayashi, K.; Hatanaka, S.; Toda, Y.; Ogawa, D.; Ichikawa, H.; Ishimaru, Y.; Tashita, R.; Suzuki, T.; Ueda, M.; et al. Elevated Levels of CYP94 Family Gene Expression Alleviate the Jasmonate Response and Enhance Salt Tolerance in Rice. *Plant Cell Physiol.* **2015**, *56*, 779–789. [CrossRef]
319. Asano, T.; Hayashi, N.; Kobayashi, M.; Aoki, N.; Miyao, A.; Mitsuhara, I.; Ichikawa, H.; Komatsu, S.; Hirochika, H.; Kikuchi, S.; et al. A Rice Calcium-Dependent Protein Kinase OsCPK12 Oppositely Modulates Salt-Stress Tolerance and Blast Disease Resistance. *Plant J.* **2012**, *69*, 26–36. [CrossRef]
320. Guan, Q.; Ma, H.; Wang, Z.Z.; Wang, Z.Z.; Bu, Q.; Liu, S. A rice LSD1-like-type ZFP gene OsLOL5 enhances saline-alkaline tolerance in transgenic Arabidopsis thaliana, yeast and rice. *BMC Genom.* **2016**, *17*, 142. [CrossRef] [PubMed]
321. Jeong, M.-J.; Lee, S.-K.; Kim, B.-G.; Kwon, T.-R.; Cho, W.-S.; Park, Y.-T.; Lee, J.-O.; Kwon, H.-B.; Byun, M.-O.; Park, S.-C. A rice (*Oryza sativa* L.) MAP kinase gene, OsMAPK44, is involved in response to abiotic stresses. *Plant Cell. Tissue Organ Cult.* **2006**, *85*, 151–160. [CrossRef]
322. Gao, Q.; Yin, X.; Wang, F.; Hu, S.; Liu, W.; Chen, L.; Dai, X.; Liang, M. OsJRL40, a Jacalin-Related Lectin Gene, Promotes Salt Stress Tolerance in Rice. *Int. J. Mol. Sci.* **2023**, *24*, 7441. [CrossRef] [PubMed]

323. Diédhiou, C.J.; Popova, O.V.; Dietz, K.-J.; Golldack, D. The SNF1-type serine-threonine protein kinase SAPK4regulates stress-responsive gene expression in rice. *BMC Plant Biol.* **2008**, *8*, 49. [CrossRef] [PubMed]
324. Obata, T.; Kitamoto, H.K.; Nakamura, A.; Fukuda, A.; Tanaka, Y. Rice Shaker Potassium Channel OsKAT1 Confers Tolerance to Salinity Stress on Yeast and Rice Cells. *Plant Physiol.* **2007**, *144*, 1978–1985. [CrossRef] [PubMed]
325. Vishal, B.; Krishnamurthy, P.; Ramamoorthy, R.; Kumar, P.P. OsTPS8 controls yield-related traits and confers salt stress tolerance in rice by enhancing suberin deposition. *New Phytol.* **2019**, *221*, 1369–1386. [CrossRef] [PubMed]
326. Hasthanasombut, S.; Ntui, V.; Supaibulwatana, K.; Mii, M.; Nakamura, I. Expression of Indica rice OsBADH1 gene under salinity stress in transgenic tobacco. *Plant Biotechnol. Rep.* **2010**, *4*, 75–83. [CrossRef]
327. Zhu, N.; Cheng, S.; Liu, X.; Du, H.; Dai, M.; Zhou, D.X.; Yang, W.; Zhao, Y. The R2R3-Type MYB Gene OsMYB91 Has a Function in Coordinating Plant Growth and Salt Stress Tolerance in Rice. *Plant Sci.* **2015**, *236*, 146–156. [CrossRef]
328. Liu, S.; Zheng, L.; Xue, Y.; Zhang, Q.; Wang, L.; Shou, H. Overexpression of OsVP1 and OsNHX1 Increases Tolerance to Drought and Salinity in Rice. *J. Plant Biol.* **2010**, *53*, 444–452. [CrossRef]
329. Ren, Z.H.; Gao, J.P.; Li, L.G.; Cai, X.L.; Huang, W.; Chao, D.Y.; Zhu, M.Z.; Wang, Z.Y.; Luan, S.; Lin, H.X. A rice quantitative trait locus for salt tolerance encodes a sodium transporter. *Nat. Genet.* **2005**, *37*, 1141–1146. [CrossRef] [PubMed]
330. Suzuki, K.; Yamaji, N.; Costa, A.; Okuma, E.; Kobayashi, N.I.; Kashiwagi, T.; Katsuhara, M.; Wang, C.; Tanoi, K.; Murata, Y.; et al. OsHKT1: 4-Mediated Na+ Transport in Stems Contributes to Na+ Exclusion from Leaf Blades of Rice at the Reproductive Growth Stage upon Salt Stress. *BMC Plant Biol.* **2016**, *16*, 22. [CrossRef] [PubMed]
331. Wang, R.; Jing, W.; Xiao, L.; Jin, Y.; Shen, L.; Zhang, W. The Rice High-Affinity Potassium Transporterl: L Is Involved in Salt Tolerance and Regulated by an MYB-Type Transcription Factor. *Plant Physiol.* **2015**, *168*, 1076–1090. [CrossRef] [PubMed]
332. Horie, T.; Sugawara, M.; Okada, T.; Taira, K.; Kaothien-Nakayama, P.; Katsuhara, M.; Shinmyo, A.; Nakayama, H. Rice sodium-insensitive potassium transporter, OsHAK5, confers increased salt tolerance in tobacco BY2 cells. *J. Biosci. Bioeng.* **2011**, *111*, 346–356. [CrossRef] [PubMed]
333. Tisarum, R.; Theerawitaya, C.; Samphumphuang, T.; Polispitak, K.; Thongpoem, P.; Singh, H.P.; Cha-um, S. Alleviation of Salt Stress in Upland Rice (*Oryza sativa* L. Ssp. Indica Cv. Leum Pua) Using Arbuscular Mycorrhizal Fungi Inoculation. *Front. Plant Sci.* **2020**, *11*, 348. [CrossRef] [PubMed]
334. Jallad, K.N. Heavy metal exposure from ingesting rice and its related potential hazardous health risks to humans. *Environ. Sci. Pollut. Res.* **2015**, *22*, 15449–15458. [CrossRef] [PubMed]
335. Wysocki, R.; Tamás, M.J. How Saccharomyces cerevisiae copes with toxic metals and metalloids. *FEMS Microbiol. Rev.* **2010**, *34*, 925–951. [CrossRef]
336. Sharma, S.K.; Goloubinoff, P.; Christen, P. Non-native Proteins as Newly-Identified Targets of Heavy Metals and Metalloids. In *Cellular Effects of Heavy Metals*; Springer: Dordrecht, The Netherlands, 2011; pp. 263–274. [CrossRef]
337. Hu, T.; Zhu, S.; Tan, L.; Qi, W.; He, S.; Wang, G. Overexpression of OsLEA4 enhances drought, high salt and heavy metal stress tolerance in transgenic rice (*Oryza sativa* L.). *Environ. Exp. Bot.* **2016**, *123*, 68–77. [CrossRef]
338. Liang, J.; Zhou, M.; Zhou, X.; Jin, Y.; Xu, M.; Lin, J. JcLEA, a Novel LEA-Like Protein from Jatropha curcas, Confers a High Level of Tolerance to Dehydration and Salinity in Arabidopsis thaliana. *PLoS ONE* **2013**, *8*, e83056. [CrossRef]
339. Mahajan, S.; Tuteja, N. Cold, salinity and drought stresses: An overview. *Arch. Biochem. Biophys.* **2005**, *444*, 139–158. [CrossRef] [PubMed]
340. Guillod-Magnin, R.; Brüschweiler, B.J.; Aubert, R.; Haldimann, M. Arsenic species in rice and rice-based products consumed by toddlers in Switzerland. *Food Addit. Contam. Part A* **2018**, *35*, 1164–1178. [CrossRef] [PubMed]
341. Murugaiyan, V.; Zeibig, F.; Anumalla, M.; Siddiq, S.A.; Frei, M.; Murugaiyan, J.; Ali, J. Arsenic Stress Responses and Accumulation in Rice. In *Rice Improvement*; Springer: Berlin/Heidelberg, Germany, 2021; pp. 281–313. [CrossRef]
342. Rahman, M.A.; Hasegawa, H.; Rahman, M.M.; Miah, M.A.M.; Tasmin, A. Straighthead disease of rice (*Oryza sativa* L.) induced by arsenic toxicity. *Environ. Exp. Bot.* **2008**, *62*, 54–59. [CrossRef]
343. Choudhury, B.; Chowdhury, S.; Biswas, A.K. Regulation of growth and metabolism in rice (*Oryza sativa* L.) by arsenic and its possible reversal by phosphate. *J. Plant Interact.* **2011**, *6*, 15–24. [CrossRef]
344. Dubey, S.; Shri, M.; Misra, P.; Lakhwani, D.; Bag, S.K.; Asif, M.H.; Trivedi, P.K.; Tripathi, R.D.; Chakrabarty, D. Heavy metals induce oxidative stress and genome-wide modulation in transcriptome of rice root. *Funct. Integr. Genom.* **2014**, *14*, 401–417. [CrossRef]
345. Mishra, S.; Jha, A.B.; Dubey, R.S. Arsenite treatment induces oxidative stress, upregulates antioxidant system, and causes phytochelatin synthesis in rice seedlings. *Protoplasma* **2011**, *248*, 565–577. [CrossRef] [PubMed]
346. Haider, F.U.; Liqun, C.; Coulter, J.A.; Cheema, S.A.; Wu, J.; Zhang, R.; Wenjun, M.; Farooq, M. Cadmium Toxicity in Plants: Impacts and Remediation Strategies. *Ecotoxicol. Environ. Saf.* **2021**, *211*, 111887. [CrossRef] [PubMed]
347. Sun, L.; Wang, J.; Song, K.; Sun, Y.; Qin, Q.; Xue, Y. Transcriptome Analysis of Rice (*Oryza Sativa* L.) Shoots Responsive to Cadmium Stress. *Sci. Rep.* **2019**, *9*, 10177. [CrossRef]
348. Fu, H.; Yu, H.; Li, T.; Wu, Y. Effect of Cadmium Stress on Inorganic and Organic Components in Xylem Sap of High Cadmium Accumulating Rice Line (*Oryza sativa* L.). *Ecotoxicol. Environ. Saf.* **2019**, *168*, 330–337. [CrossRef]
349. Yang, H.; Yu, H.; Tang, H.; Huang, H.; Zhang, X.; Zheng, Z.; Wang, Y.; Li, T. Physiological responses involved in cadmium tolerance in a high-cadmium-accumulating rice (*Oryza sativa* L.) line. *Environ. Sci. Pollut. Res.* **2021**, *28*, 41736–41745. [CrossRef]

350. Mostofa, M.G.; Hossain, M.A.; Fujita, M.; Tran, L.S.P. Physiological and Biochemical Mechanisms Associated with Trehalose-Induced Copper-Stress Tolerance in Rice. *Sci. Rep.* **2015**, *5*, 11433. [CrossRef] [PubMed]
351. Mostofa, M.G.; Rahman, M.M.; Ansary, M.M.U.; Fujita, M.; Tran, L.S.P. Interactive Effects of Salicylic Acid and Nitric Oxide in Enhancing Rice Tolerance to Cadmium Stress. *Int. J. Mol. Sci.* **2019**, *20*, 5798. [CrossRef] [PubMed]
352. Wang, Y.; Jiang, X.; Li, K.; Wu, M.; Zhang, R.; Zhang, L.; Chen, G. Photosynthetic responses of *Oryza sativa* L. seedlings to cadmium stress: Physiological, biochemical and ultrastructural analyses. *BioMetals* **2014**, *27*, 389–401. [CrossRef] [PubMed]
353. Rizwan, M.; Ali, S.; Adrees, M.; Rizvi, H.; Zia-ur-Rehman, M.; Hannan, F.; Qayyum, M.F.; Hafeez, F.; Ok, Y.S. Cadmium stress in rice: Toxic effects, tolerance mechanisms, and management: A critical review. *Environ. Sci. Pollut. Res.* **2016**, *23*, 17859–17879. [CrossRef] [PubMed]
354. Aslam, M.; Aslam, A.; Sheraz, M.; Ali, B.; Ulhassan, Z.; Najeeb, U.; Zhou, W.; Gill, R.A. Lead Toxicity in Cereals: Mechanistic Insight Into Toxicity, Mode of Action, and Management. *Front. Plant Sci.* **2021**, *11*, 2248. [CrossRef] [PubMed]
355. Khan, M.; Rolly, N.K.; Al Azzawi, T.N.I.; Imran, M.; Mun, B.G.; Lee, I.J.; Yun, B.W. Lead (Pb)-Induced Oxidative Stress Alters the Morphological and Physio-Biochemical Properties of Rice (*Oryza Sativa* L.). *Agronomy* **2021**, *11*, 409. [CrossRef]
356. Khan, F.; Hussain, S.; Tanveer, M.; Khan, S.; Hussain, H.A.; Iqbal, B.; Geng, M. Coordinated effects of lead toxicity and nutrient deprivation on growth, oxidative status, and elemental composition of primed and non-primed rice seedlings. *Environ. Sci. Pollut. Res.* **2018**, *25*, 21185–21194. [CrossRef]
357. Li, Y.F.; Zhao, J.; Li, Y.F.; Xu, X.; Zhang, B.; Liu, Y.; Cui, L.; Li, B.; Gao, Y.; Chai, Z. Comparative Metalloproteomic Approaches for the Investigation Proteins Involved in the Toxicity of Inorganic and Organic Forms of Mercury in Rice (*Oryza sativa* L.) Roots. *Metallomics* **2016**, *8*, 663–671. [CrossRef]
358. Mao, Q.; Tang, L.; Ji, W.; Rennenberg, H.; Hu, B.; Ma, M. Elevated CO_2 and Soil Mercury Stress Affect Photosynthetic Characteristics and Mercury Accumulation of Rice. *Ecotoxicol. Environ. Saf.* **2021**, *208*, 111605. [CrossRef]
359. Palmieri, J.; Rzigalinski, B.; Benjamin, B.; Collins, E.; Kaur, G.; Brunette, J.; Council-Troche, M.; Wilson, M.; Meacham, S.; Guthrie, T. Implications and Significance of Mercury in Rice. *J. Food Nutr. Metab.* **2020**, *3*, 1–5. [CrossRef]
360. Meng, B.; Feng, X.; Qiu, G.; Anderson, C.W.N.; Wang, J.; Zhao, L. Localization and Speciation of Mercury in Brown Rice with Implications for Pan-Asian Public Health. *Environ. Sci. Technol.* **2014**, *48*, 7974–7981. [CrossRef] [PubMed]
361. Rao, G.; Ashraf, U.; Huang, S.; Cheng, S.; Abrar, M.; Mo, Z.; Pan, S.; Tang, X. Ultrasonic seed treatment improved physiological and yield traits of rice under lead toxicity. *Environ. Sci. Pollut. Res.* **2018**, *25*, 33637–33644. [CrossRef] [PubMed]
362. Ashraf, U.; Tang, X. Yield and Quality Responses, Plant Metabolism and Metal Distribution Pattern in Aromatic Rice under Lead (Pb) Toxicity. *Chemosphere* **2017**, *176*, 141–155. [CrossRef] [PubMed]
363. Hartley-Whitaker, J.; Ainsworth, G.; Meharg, A.A. Copper- and Arsenate-Induced Oxidative Stress in *Holcus Lanatus* L. Clones with Differential Sensitivity. *Plant Cell Environ.* **2001**, *24*, 713–722. [CrossRef]
364. Duan, G.-L.; Hu, Y.; Liu, W.-J.; Kneer, R.; Zhao, F.-J.; Zhu, Y.-G. Evidence for a role of phytochelatins in regulating arsenic accumulation in rice grain. *Environ. Exp. Bot.* **2011**, *71*, 416–421. [CrossRef]
365. Kong, D.; Ju, C.; Parihar, A.; Kim, S.; Cho, D.; Kwak, J.M. Arabidopsis Glutamate Receptor Homolog3.5 Modulates Cytosolic Ca^{2+} Level to Counteract Effect of Abscisic Acid in Seed Germination. *Plant Physiol.* **2015**, *167*, 1630–1642. [CrossRef] [PubMed]
366. Jiang, M.; Jiang, J.; Li, S.; Li, M.; Tan, Y.; Song, S.; Shu, Q.; Huang, J. Glutamate Alleviates Cadmium Toxicity in Rice via Suppressing Cadmium Uptake and Translocation. *J. Hazard. Mater.* **2020**, *384*, 121319. [CrossRef]
367. Ahsan, N.; Lee, S.H.; Lee, D.G.; Lee, H.; Lee, S.W.; Bahk, J.D.; Lee, B.H. Physiological and protein profiles alternation of germinating rice seedlings exposed to acute cadmium toxicity. *Comptes Rendus Biol.* **2007**, *330*, 735–746. [CrossRef]
368. Chen, Y.-A.; Chi, W.-C.; Trinh, N.N.; Huang, L.-Y.; Chen, Y.-C.; Cheng, K.-T.; Huang, T.-L.; Lin, C.-Y.; Huang, H.-J. Transcriptome Profiling and Physiological Studies Reveal a Major Role for Aromatic Amino Acids in Mercury Stress Tolerance in Rice Seedlings. *PLoS ONE* **2014**, *9*, e95163. [CrossRef]
369. Kalita, J.; Pradhan, A.K.; Shandilya, Z.M.; Tanti, B. Arsenic Stress Responses and Tolerance in Rice: Physiological, Cellular and Molecular Approaches. *Rice Sci.* **2018**, *25*, 235–249. [CrossRef]
370. Liu, J.; Cao, C.; Wong, M.; Zhang, Z.; Chai, Y. Variations between rice cultivars in iron and manganese plaque on roots and the relation with plant cadmium uptake. *J. Environ. Sci.* **2010**, *22*, 1067–1072. [CrossRef] [PubMed]
371. Islam, E.; Khan, M.T.; Irem, S. Biochemical mechanisms of signalling: Perspectives in plant under arsenic stress. *Ecotoxicol. Environ. Saf.* **2015**, *114*, 126–133. [CrossRef] [PubMed]
372. Kumar, S.; Trivedi, P.K. Heavy Metal Stress Signaling in Plants. In *Plant Metal Interaction*; Ahmad, P., Ed.; Elsevier: Amsterdan, The Netherlands, 2016; pp. 585–603. [CrossRef]
373. Rao, K.P.; Vani, G.; Kumar, K.; Wankhede, D.P.; Misra, M.; Gupta, M. Arsenic stress activates MAP kinase in rice roots and leaves. *Arch. Biochem. Biophys.* **2011**, *506*, 73–82. [CrossRef] [PubMed]
374. Conde, A.; Chaves, M.M.; Geros, H. Membrane transport, sensing and signaling in plant adaptation to environmental stress. *Plant Cell Physiol.* **2011**, *52*, 1583–1602. [CrossRef] [PubMed]
375. Steinhorst, L.; Kudla, J. Calcium and reactive oxygen species rule the waves of signaling. *Plant Physiol.* **2013**, *163*, 471–485. [CrossRef] [PubMed]
376. Lin, Y.F.; Aarts, M.G. The molecular mechanism of zinc and cadmium stress response in plants. *Cell. Mol. Life Sci.* **2012**, *69*, 3187–3206. [CrossRef] [PubMed]

377. Tiwari, S.; Lata, C.; Singh Chauhan, P.; Prasad, V.; Prasad, M. A functional genomic perspective on drought signalling and its crosstalk with phytohormone-mediated signalling pathways in plants. *Curr. Genom.* **2017**, *18*, 469–482. [CrossRef] [PubMed]
378. Yeh, C.M.; Hsiao, L.J.; Huang, H.J. Cadmium activates a mitogen-activated protein kinase gene and MBP kinases in rice. *Plant Cell Physiol.* **2004**, *45*, 1306–1312. [CrossRef]
379. Liu, X.M.; Kim, K.E.C.; Kim, K.E.C.; Nguyen, X.C.; Han, H.J.; Jung, M.S. Cadmium activates Arabidopsis MPK3 and MPK6 via accumulation of reactive oxygen species. *Phytochemistry* **2010**, *71*, 614–618. [CrossRef]
380. Singh, I.; Shah, K. Exogenous application of methyl jasmonate lowers the effect of cadmium-induced oxidative injury in rice seedlings. *Phytochemistry* **2014**, *108*, 57–66. [CrossRef]
381. Chakrabarty, D.; Trivedi, P.K.; Misra, P.; Tiwari, M.; Shri, M.; Shukla, D. Comparative transcriptome analysis of arsenate and arsenite stresses in rice seedlings. *Chemosphere* **2009**, *74*, 688–702. [CrossRef] [PubMed]
382. Shi, S.; Wang, T.; Chen, Z.; Tang, Z.; Wu, Z.; Salt, D.E.; Chao, D.Y.; Zhao, F.J. OsHAC1;1 and OsHAC1;2 function as arsenate reductases and regulate arsenic accumulation. *Plant Physiol.* **2016**, *172*, 1708–1719. [CrossRef]
383. Tang, L.; Mao, B.; Li, Y.; Lv, Q.; Zhang, L.; Chen, C.; He, H.; Wang, W.; Zeng, X.; Shao, Y.; et al. Knockout of OsNramp5 Using the CRISPR/Cas9 System Produces Low Cd-Accumulating Indica Rice without Compromising Yield. *Sci. Rep.* **2017**, *7*, 14438. [CrossRef] [PubMed]
384. Lu, C.; Zhang, L.; Tang, Z.; Huang, X.Y.; Ma, J.F.; Zhao, F.J. Producing cadmium-free Indica rice by overexpressing OsHMA3. *Environ. Int.* **2019**, *126*, 619–626. [CrossRef]
385. Arya, G.C.; Sarkar, S.; Manasherova, E.; Aharoni, A.; Cohen, H. The Plant Cuticle: An Ancient Guardian Barrier Set Against Long-Standing Rivals. *Front. Plant Sci.* **2021**, *12*, 663165. [CrossRef] [PubMed]
386. Tang, L.; Dong, J.; Tan, L.; Ji, Z.; Li, Y.; Sun, Y.; Chen, C.; Lv, Q.; Mao, B.; Hu, Y.; et al. Overexpression of OsLCT2, a Low-Affinity Cation Transporter Gene, Reduces Cadmium Accumulation in Shoots and Grains of Rice. *Rice* **2021**, *14*, 89. [CrossRef]
387. Mishra, N.; Srivastava, A.P.; Esmaeili, N.; Hu, W.; Shen, G. Overexpression of the Rice Gene OsSIZ1 in Arabidopsis Improves Drought-, Heat-, and Salt-Tolerance Simultaneously. *PLoS ONE* **2018**, *13*, 201716. [CrossRef]
388. Liu, X.S.; Feng, S.J.; Zhang, B.Q.; Wang, M.Q.; Cao, H.W.; Rono, J.K.; Chen, X.; Yang, Z.M. OsZIP1 Functions as a Metal Efflux Transporter Limiting Excess Zinc, Copper and Cadmium Accumulation in Rice. *BMC Plant Biol.* **2019**, *19*, 283. [CrossRef]
389. Rono, J.K.; Le Wang, L.; Wu, X.C.; Cao, H.W.; Zhao, Y.N.; Khan, I.U.; Yang, Z.M. Identification of a New Function of Metallothionein-like Gene OsMT1e for Cadmium Detoxification and Potential Phytoremediation. *Chemosphere* **2021**, *265*, 129136. [CrossRef]
390. Ogo, Y.; Itai, R.N.; Kobayashi, T.; Aung, M.S.; Nakanishi, H.; Nishizawa, N.K. OsIRO2 is responsible for iron utilization in rice and improves growth and yield in calcareous soil. *Plant Mol. Biol.* **2011**, *75*, 593–605. [CrossRef]
391. Tao, J.; Lu, L. Advances in Genes-Encoding Transporters for Cadmium Uptake, Translocation, and Accumulation in Plants. *Toxics* **2022**, *10*, 411. [CrossRef] [PubMed]
392. Yamazaki, S.; Ueda, Y.; Mukai, A.; Ochiai, K.; Matoh, T. Rice Phytochelatin Synthases OsPCS1 and OsPCS2 Make Different Contributions to Cadmium and Arsenic Tolerance. *Plant Direct* **2018**, *2*, e00034. [CrossRef] [PubMed]
393. Shimo, H.; Ishimaru, Y.; An, G.; Yamakawa, T.; Nakanishi, H.; Nishizawa, N.K. Low cadmium (LCD), a novel gene related to cadmium tolerance and accumulation in rice. *J. Exp. Bot.* **2011**, *62*, 5727–5734. [CrossRef] [PubMed]
394. Sahoo, R.K.; Tuteja, N. OsSUV3 functions in cadmium and zinc stress tolerance in rice (*Oryza sativa* L. cv IR64). *Plant Signal. Behav.* **2014**, *9*, e27389. [CrossRef] [PubMed]
395. Ding, Y.; Ye, Y.; Jiang, Z.; Wang, Y.; Zhu, C. MicroRNA390 Is Involved in Cadmium Tolerance and Accumulation in Rice. *Front. Plant Sci.* **2016**, *7*, 235. [CrossRef] [PubMed]
396. Hu, S.; Yu, Y.; Chen, Q.; Mu, G.; Shen, Z.; Zheng, L. OsMYB45 plays an important role in rice resistance to cadmium stress. *Plant Sci.* **2017**, *264*, 1–8. [CrossRef] [PubMed]
397. Ding, Y.; Gong, S.; Wang, Y.; Wang, F.; Bao, H.; Sun, J.; Cai, C.; Yi, K.; Chen, Z.; Zhu, C. MicroRNA166 Modulates Cadmium Tolerance and Accumulation in Rice. *Plant Physiol.* **2018**, *177*, 1691–1703. [CrossRef]

MDPI AG
Grosspeteranlage 5
4052 Basel
Switzerland
Tel.: +41 61 683 77 34

Plants Editorial Office
E-mail: plants@mdpi.com
www.mdpi.com/journal/plants

Academic Open
Access Publishing

mdpi.com

ISBN 978-3-7258-5814-9